
ADENOMYOSIS
Diagnostic Features and
Clinical Impact
Connie O. Rees

ADENOMYOSIS:
Diagnostic Features and Clinical Impact

The work of this thesis was funded in part by a grant by GE Healthcare, the Catharina Onderzoeksfonds, Stichting Vrouw en Onderzoek Catharina Ziekenhuis.

Financial support for the printing of this thesis was kindly provided by Wetenschapsbureau Catharina Ziekenhuis, Endometriose Stichting, NVOG Werkgroep Gynaecologische Endoscopie, Erbe Nederland, Gedeon Richter Benelux, Medical Dynamics, Chipsoft and Goodlife Pharma.

Cover Design and Layout: Designed using DALL-E ® and Canva ®
Printing: Ridderprint Bv.

ISBN: 978-90-386-5991-6

A catalogue record is available in the Eindhoven University of Technology and Ghent University Library.

Adenomyosis:
Diagnostic Features and Clinical Impact

PROEFSCHRIFT

ter verkrijging van de graad van doctor aan de Technische Universiteit Eindhoven en de Universiteit Gent en de, op gezag van de rector magnificus prof.dr. S.K. Lenaerts en prof. dr. R. van de Walle voor een commissie aangewezen door het College voor Promoties, in het openbaar te verdedigen op
2 April, 2024 om **16 uur**

door

Connie O. Rees

geboren te Tokyo, Japan

Dit proefschrift is goedgekeurd door de promotoren en de samenstelling van de promotiecommissie is als volgt:

Voorzitter:	prof.dr.ir. M.C. Beurden (TU/e) prof. dr. B. Heindyrckx (Ghent University)
Promotoren:	prof.dr.ir. M. Mischi
	prof. dr. S. Weyers (Ghent University Hospital)
Copromotor:	prof.dr. B.C. Schoot
Promotiecommissieleden	dr. K. Isaacson (Harvard School of Medicine) prof.dr. V. Mijatovic (Amsterdam UMC) prof.dr.ir. H. Wijkstra prof. dr. T. Hamerlynck (Ghent University)
Adviseur:	prof.dr. H.A.A.M. Van Vliet (Catharina Ziekenhuis Eindhoven)

Het onderzoek of ontwerp dat in dit proefschrift wordt beschreven is uitgevoerd in overeenstemming met de TU/e Gedragscode Wetenschapsbeoefening

Table of Contents

GENERAL MESSAGES OF THIS THESIS:

- Adenomyosis can be reliably diagnosed on MRI when additionally taking clinical symptoms into account
- Adenomyosis disrupts uterine contractile function which may explain worse fertility and obstetric outcomes
- Adenomyosis is a subtype of endometriosis and functions as part of a spectrum of the same disease
- Severe adenomyosis in combination with endometriosis is associated with worse fertility outcomes
- Adenomyosis is associated with a higher risk of adverse obstetric outcomes

PART I

Summary and Introduction

SUMMARY:

Adenomyosis is a common and potentially debilitating benign gynaecological condition characterised by the infiltration of endometrial tissue and stroma into the uterine myometrium. Associated symptoms are dysmenorrhoea, heavy menstrual bleeding, and subfertility, which can greatly impact quality of life. Adenomyosis often occurs in conjunction with endometriosis and is considered part of the spectrum of the same disease. The reported prevalence of adenomyosis is still uncertain, with estimates ranging from as low as 5% up to 85%. The lack of uniform diagnostic criteria for adenomyosis, and the fact that up to a third of women are asymptomatic (or do not present themselves to a clinician), exacerbates this problem.

Historically, adenomyosis was only diagnosed on histopathology after hysterectomy at the end of a woman's fertile phase of life. However, modern advances in non-invasive imaging have shown that adenomyosis is present in younger nulliparous women. With this knowledge, adenomyosis is being linked not only to clinical symptoms, but also to infertility and obstetric complications. Non-invasive and accurate diagnosis, along with clarity into the impact adenomyosis has on fertility and pregnancy, is thus crucial. Hence, we assessed the effect of adenomyosis on uterine contractile and reproductive function, starting with an exploration into its non-invasive diagnosis by way of MRI, and ending with its influence on fertility and obstetric outcomes.

First, we conducted a literature study on the existing MRI-based diagnostic criteria for adenomyosis and carried out a meta-analysis into their reported diagnostic accuracy. We surmised that whilst a wide variety of MRI-based parameters have been used and reported, no uniformly applied criteria exist. Moreover, the individual diagnostic accuracy of each parameter is unclear. Based on the criteria described in the literature, we developed a multivariate diagnostic predictive tool for adenomyosis diagnosis using a retrospective cohort of patients with histologically confirmed adenomyosis. We also were able to validate this method using an external patient cohort.

One promising element of MRI-based diagnosis parameter is the uterine anatomical 'junctional zone', which coordinates rhythmic uterine contractions,

or peristalsis. Previous research has suggested that abnormal uterine contractility affects fertility, and may thus represent a causal link between adenomyosis and infertility. Therefore, we introduced a novel quantitative speckle-tracking method on trans-vaginal ultrasound for the quantitative analysis of the uterine contractile function and investigated its potential to predict the success of in-vitro fertilisation (IVF) treatment. We then suggested a set of reference values for normal uterine contractile function in a prospective cohort of healthy women using this dedicated speckle tracking algorithm. Next, we investigated existing literature for the reported effect that uterine abnormalities (including adenomyosis, leiomyomas and congenital uterine anomalies) have on uterine contractile function. We found that whilst knowledge is scarce, uterine contractile behaviour seems to be affected by uterine pathology. Finally, uterine contractility features of healthy women were compared to women with adenomyosis. We observed significant differences in uterine contractility across the menstrual cycle between women with adenomyosis versus those without.

To explore if fertility outcomes are significantly affected in women with adenomyosis, we investigated IVF/ICSI (intra-cytoplasmatic sperm injection) outcomes of a retrospective cohort of patients with MRI-diagnosed adenomyosis, endometriosis or both, compared to matched male infertility controls. We found that women with both adenomyosis and endometriosis have significantly fewer live births compared to the control group. We further report that adenomyosis patients with following characteristics have worse IVF/ICSI outcomes compared to male infertility controls: combined endometriosis, a larger (relative) junctional zone, and the presence of myometrial cysts.

Finally, we investigated if the presence of adenomyosis was associated with adverse obstetric outcomes. To do so, we carried out a retrospective analysis of Dutch population-level data looking at obstetric outcomes in women with histologically diagnosed adenomyosis over a period of 23 years. Women with proven adenomyosis demonstrated a higher prevalence of a wide range of adverse obstetric outcomes including: hypertensive disorders, a higher rate of caesarean sections, more small-for-gestational-age children and failure to progress in labour.

Overall, we show that adenomyosis can be reliably diagnosed non-invasively on MRI using a variety of parameters, and confirm its effect on the whole spectrum of uterine (reproductive) function.

Nederlandse Samenvatting

Adenomyose is een veel voorkomende en vaak invaliderende goedaardige gynaecologische aandoening. Het wordt gekenmerkt door infiltratie van endometriumweefsel en stroma in het myometrium van de baarmoeder. Geassocieerde symptomen zijn: dysmenorroe, hevige menstrueel bloedverlies en onvruchtbaarheid, die allen de kwaliteit van leven sterk kunnen beïnvloeden. Adenomyose komt vaak voor in combinatie met endometriose en wordt vaak beschouwd als onderdeel van het spectrum van dezelfde ziekte. De gerapporteerde prevalentie van adenomyose is nog steeds onzeker, met schattingen variërend van zo laag als 5% tot zelfs 85%. Het gebrek aan uniforme diagnostische criteria voor adenomyose, en het feit dat tot een derde van de vrouwen mogelijk asymptomatisch is (of zich niet meldt bij een arts), verergert dit probleem.

Historisch gezien werd adenomyose alleen gediagnosticeerd op histopathologie na hysterectomie aan het einde van de vruchtbare levensfase van een vrouw. Moderne ontwikkelingen op het gebied van niet-invasieve beeldvorming hebben echter aangetoond dat adenomyose ook aanwezig is bij jongere vrouwen. Met deze kennis wordt adenomyose niet alleen in verband gebracht met klinische symptomen zoals pijn en hevig bloedverlies, maar ook met onvruchtbaarheid en obstetrische complicaties. Niet-invasieve en nauwkeurige diagnose, samen met duidelijkheid over de impact die adenomyose heeft op vruchtbaarheid en zwangerschap, is dus cruciaal. Daarom onderzochten we het effect van adenomyose op de contractiele en reproductieve functie van de uterus, beginnend met een verkenning van de niet-invasieve diagnose door middel van MRI, en eindigend met de mogelijke invloed op vruchtbaarheid en obstetrische uitkomsten.

Allereerst hebben we een literatuurstudie uitgevoerd naar de bestaande (op MRI gebaseerde) diagnostische criteria voor adenomyose en een meta-analyse uitgevoerd naar hun gerapporteerde diagnostische nauwkeurigheid. We stelden vast dat er weliswaar een grote verscheidenheid aan MRI-gebaseerde parameters is gebruikt en gerapporteerd, maar dat er geen uniform toegepaste criteria bestaan. Bovendien is de individuele diagnostische nauwkeurigheid van elke parameter onduidelijk. Op basis van de in de literatuur beschreven criteria ontwikkelden we vervolgens een multivariaat

diagnostisch predictie model voor de diagnose van adenomyose met behulp van een retrospectief cohort van patiënten met histologisch bevestigde adenomyose. We konden dit model tevens extern valideren met behulp van een apart patiënten cohort.

Een veelbelovend diagnostische parameter op basis van MRI is de anatomische 'junctionele zone' van de baarmoeder, die de ritmische samentrekkingen van de baarmoeder, of peristaltiek, coördineert. Eerder onderzoek heeft suggereert dat abnormale contractiliteit van de baarmoeder de vruchtbaarheid beïnvloedt en dus een oorzakelijk verband kan vormen tussen adenomyose en onvruchtbaarheid. Daarom introduceerden we een nieuwe kwantitatieve speckle-tracking methode op transvaginale echografie voor de kwantitatieve analyse van de contractiliteit van de baarmoeder. We onderzochten we het potentieel van een nieuwe kwantitatieve speckle-tracking methode op transvaginale echografie om het succes van in-vitrofertilisatie (IVF) behandelsucces te voorspellen. We hebben daarbij een reeks referentiewaarden voorgesteld voor normale baarmoeder contractiliteit in een prospectief cohort van gezonde vrouwen met behulp van dit speckle tracking-algoritme. Vervolgens hebben we de bestaande literatuur onderzocht op het gerapporteerde effect dat afwijkingen aan de baarmoeder (waaronder adenomyose, leiomyomen en aangeboren baarmoederafwijkingen) hebben op de contractiele functie van de baarmoeder. Tot slot werden kenmerken van de uteruscontractiliteit van gezonde vrouwen vergeleken met die van vrouwen met adenomyose. We zagen significante verschillen in uteruscontractiliteit tijdens de menstruatiecyclus tussen vrouwen met adenomyose en vrouwen zonder adenomyose.

Om te onderzoeken of vruchtbaarheidsuitkomsten daadwerkelijk significant worden beïnvloed bij vrouwen met adenomyose, onderzochten we IVF/ICSI (intracytoplasmatische sperma-injectie) uitkomsten van een retrospectief cohort van patiënten. Deze patiënten hadden MRI-gediagnosticeerde adenomyose, endometriose of beide, en vergeleken deze met gematchte controle met mannelijke onvruchtbaarheid. We vonden dat vrouwen met zowel adenomyose als endometriose significant minder levendgeborenen hadden in vergelijking met de gezonde controlegroep van veronderstelde normale vrouwen. Vervolgens werden individuele MRI-kenmerken van adenomyose bij IVF/ICSI-patiënten in verband gebracht met de IVF/ICSI-uitkomsten. We

rapporteren dat adenomyose patiënten met de volgende kenmerken slechtere IVF/ICSI-uitkomsten hebben in vergelijking met mannelijke onvruchtbaarheidscontroles: gecombineerde endometriose, een (relatief) grotere junctionele zone, en de aanwezigheid van myometriale adenomyotische cysten.

Tot slot onderzochten we of de aanwezigheid van adenomyose geassocieerd was met ongunstigere obstetrische uitkomsten. Het aanwezig zijn van afwijkend spierweefsel van de baarmoeder zou immers ook effect op de zwangerschap en de bevalling kunnen hebben. Hiertoe voerden we een retrospectieve analyse uit van gegevens op Nederlands populatieniveau waarbij we keken naar obstetrische uitkomsten bij vrouwen met histologisch gediagnosticeerde adenomyose over een periode van 23 jaar. Vrouwen met bewezen adenomyose vertoonden een hogere prevalentie van een breed scala aan ongunstige obstetrische uitkomsten, waaronder: hypertensieve aandoeningen, een hoger percentage keizersneden, meer kleine kinderen voor de zwangerschapsduur en een langere duur van de bevalling.

Over het geheel genomen laten we zien dat adenomyose betrouwbaar op MRI beelden gediagnosticeerd kan worden aan de hand van verschillende parameters, en bevestigen we het negatieve effect van adenomyose op het hele spectrum van de baarmoeder(voortplantings)functie.

CHAPTER 1:
General Introduction

General Introduction to Adenomyosis

Adenomyosis is a prevalent and potentially debilitating benign gynaecological condition characterised by the infiltration of endometrial tissue and stroma into the uterine myometrium. The most commonly associated symptoms are dysmenorrhoea, heavy menstrual bleeding, and subfertility, which can greatly impact quality of life (1,2). The prevalence of adenomyosis as a whole remains unknown and debated, ranging from estimates as low as 5% (3) to as high as 85% (4). This uncertainty stems for a large part from the fact that there exists no consensus on the diagnostic criteria of adenomyosis, and that up to a third of women with adenomyosis are asymptomatic and/or may never present themselves to a clinician (5–7). It is thought that adenomyosis originates in the so-called 'junctional zone' (JZ) between the endometrial and myometrial layer of the uterus (see Figure 1.1), where subsequent thickening and irregularity of the JZ characterises adenomyosis. The identification and evaluation of the JZ hence plays a crucial role in the diagnosis and recognition of adenomyosis.

Whilst it is commonly accepted that irregularities in the JZ are indicative of adenomyosis, the exact pathophysiological mechanisms behind the disease are still open to discussion. Generally speaking, there are three theories as to the aetiology of adenomyosis:

- *De novo* metaplasia of Mullerian remnants in the myometrium
- Tissue injury and active repair (8–10), whereby chronic (micro-) trauma to the JZ and endometrium leads to invagination of endometrium into the myometrium, e.g. due to uterine surgery for example
- 'From outside to inside' invasion of endometriosis cells into the uterine myometrium (11,12)

Adenomyosis Subtypes and Classifications:

Adenomyosis is generally accepted to have three subtypes: focal, diffuse and cystic.

Focal adenomyosis is concentrated in one area of the myometrium, generally as a single lesion characterised by (heterogenous) thickening of the JZ. Diffuse adenomyosis affects most of the uterus, and results in an enlarged and globular uterus with generally irregular JZ borders.

Finally, cystic adenomyosis, widely regarded as the rarest subtype, involves cystic *adenomyomas* in the myometrium, which contain endometrial tissue (13). Figure 1.1 shows examples of these subtypes on MRI.

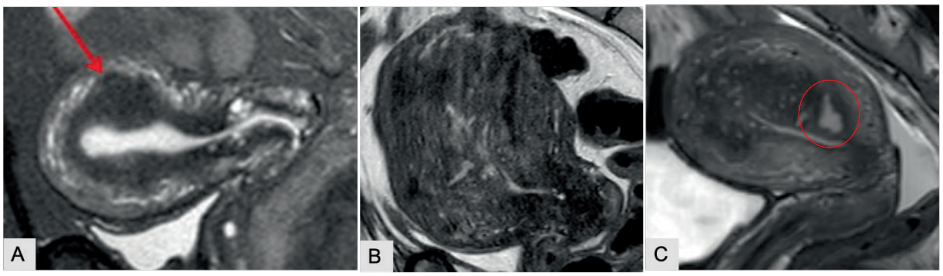

Figure 1.1: Examples of MRI subtypes (on MRI), **A.** Focal adenomyosis concentrated in the posterior wall (red arrow) **B.** Diffuse adenomyosis affecting the whole uterine wall **C.** Cystic adenomyosis with islands of endometrial tissue in the myometrium (largest cystic focus circled in red). (Images taken from own study populations).

Whilst the aforementioned subtypes are most commonly reported in the literature, some authors (14–18) have further made the distinction between adenomyosis of the inner myometrium (AIM) and adenomyosis of the outer myometrium (AOM). Here, the inner myometrium refers to the inner one third of the myometrium closest to the endometrium, and the outer myometrium refers to the outer two thirds (see Figure 1.2). Similarly, AIM can also be referred to as *adenomyosis interna*, and AOM as *adenomyosis externa*. This classification system can also be combined with the former, where an adenomyosis lesion could also be described as 'focal adenomyosis of the outer myometrium' (FAOM) (12) for example.

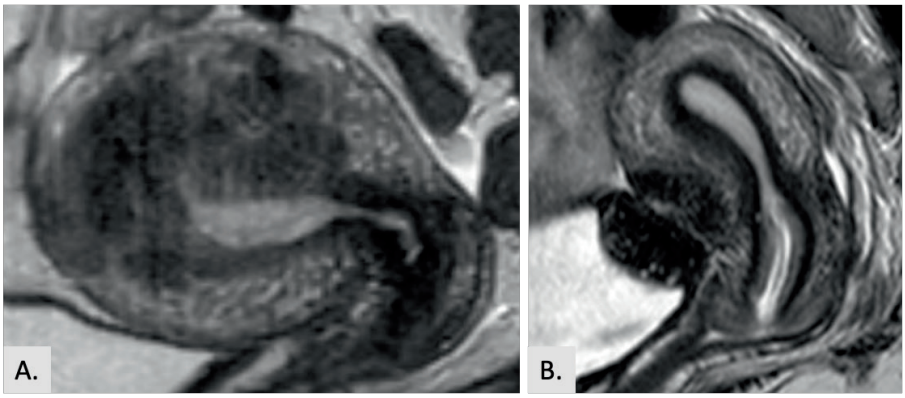

Figure 1.2: Examples of adenomyosis subtypes, **A.** Adenomyosis of the inner myometrium of the posterior wall (AIM), **B.** (Focal) Adenomyosis of the outer myometrium (FAOM) on the anterior wall, in continuum with an endometriosis lesion of the bladder. (Images taken from own study populations).

Diagnosing adenomyosis

Accurate adenomyosis diagnosis remains challenging as there is no consensus on diagnostic criteria, and it often differs between regions, hospitals and clinicians (19). In the associated condition endometriosis, it is known that the diagnostic delay is an average of nine years (20,21). It is unknown how long this is for adenomyosis, but it is likely to be similar, if not longer. Another element of the disease that impedes easy diagnosis is the fact that adenomyosis often coexists with other (benign) diseases; namely leiomyomas and endometriosis. Leiomyomas particularly can hamper accurate diagnosis as they are much easier to recognise on various imaging techniques (and thus may distract from adenomyosis lesions), and also are associated with similar clinical symptoms (22–24). In fact, concomitant leiomyomas are reported in up to 50% of adenomyosis patients (25). Similarly, adenomyosis and endometriosis are also often found together, with adenomyosis sometimes being referred to as '*endometriosis interna*'. Opinions are divided as to if adenomyosis and endometriosis are separate diseases, or subtypes of the same disease (8,10,19,26).

Histopathological diagnosis of adenomyosis

The gold standard for adenomyosis diagnosis remains histopathology. Indeed, adenomyosis was first identified in hysterectomy specimens by von Rokitansky in the 1860's as '*cystosarcoma adenoids uterinum*' or '*adenomyoma*', and eventually given its present name of '*uterine adenomyosis*' by Frankl in 1925 (27).

On histology, most often (and most accurately) after hysterectomy, adenomyosis is recognised as myometrial invasion of endometrial stroma, surrounded by myometrial hyperplasia. The minimum distance required for invasion into the myometrium to be considered as indicative of adenomyosis is debated (19). Some experts propose a range of 1-4mm, others at least one third of the total myometrial thickness. The common theme is that there must be recognisable endometrial tissue deeper than the endo-myometrial junction (7). An example of adenomyosis on histopathology is shown in Figure 1.3.

The aforementioned criteria for adenomyosis are thus not uniformly classified, and different pathologists and hospital tend towards different definitions (19). The most commonly reported definitions for adenomyosis lesions are however, as follows:

- At least one low power field from (an irregular) endo-myometrial junction, or
- 1 to 2.5 mm below the basal layer of endometrium, or
- Deeper than 25% of the overall myometrial thickness

Another limitation of histological diagnosis is that accurate diagnosis is highly reliant on the method of tissue sampling and the number of slices taken at hysterectomy, and subsequently the size of the lesion. There is thus a potential for small adenomyosis lesions to be missed (19).

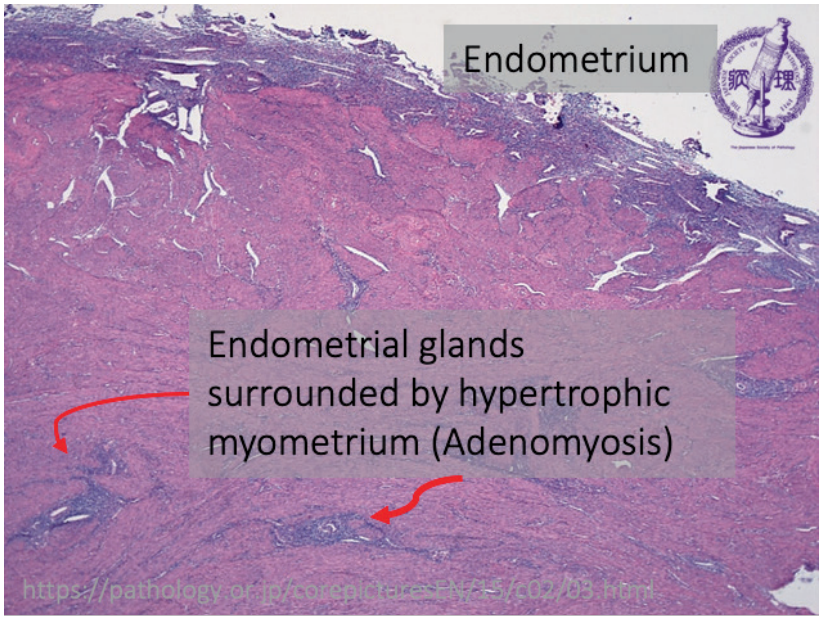

Figure 1.3. Example of adenomyosis on histology

Whilst hysterectomy is most commonly used as the standard for adenomyosis diagnosis, adenomyosis can also be diagnosed histologically using biopsy, generally in the context of hysteroscopy.

Biopsy diagnosis can be a useful alternative for histopathological diagnosis over hysterectomy, especially in the context of patients wishing to preserve their fertility, or otherwise wishing to avoid hysterectomy. The challenge of variable topographic distribution of adenomyosis across the uterus is multiplied in biopsy-driven adenomyosis diagnosis however. The hysteroscopist must biopsy exactly the correct area, and in cases without visibly suspect adenomyosis lesions during the procedure, a negative diagnosis by no means excludes the presence of adenomyosis.

Especially in women of fertile age, whereby hysterectomy would be preferable to avoid, there is thus still a need for an accurate diagnostic tool. The logical way in which to realise this, is by way of diagnosis via non-invasive imaging techniques.

Non-invasive diagnosis

- Ultrasound

In daily gynaecological practice, adenomyosis is often first suspected (alongside presence of corresponding symptoms) on the basis of the aspect of the uterus on trans-vaginal ultrasound (TVUS). Characteristics indicative of adenomyosis are generally described according to the MUSA (Morphological Uterus Sonographic Assessment (28)) criteria (see Figure 1.4). The reported sensitivity, specificity, and Area Under the Curve (AUC) of TVUS are (with 95% CI) 74% (SD 68%–79%), 76% (SD 71%–79%), and 0.7 respectively (29). See Figure 1.5 for illustrative examples on TVUS.

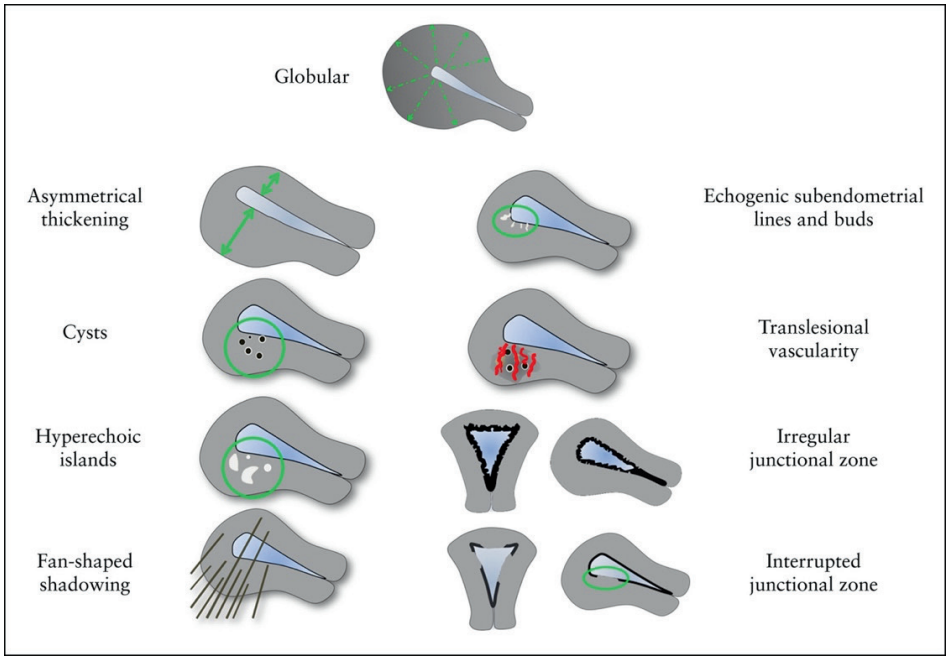

Figure 1.4. Sonographic characteristics of Adenomyosis according to the Morphological Uterine Sonographic Assessment (MUSA) Criteria of Van den Bosch et al. 2015 (30)

Despite the possibility to fairly accurately diagnose adenomyosis on standard TVUS, there are several limitations that should be considered. One problem posed by diagnosing adenomyosis by TVUS is in that it is susceptible to inter-observer variability (29,31–34), which often depends on the experience and expertise of the ultrasound technician or physician (35). As such, specifically in cases of mild or atypical adenomyosis, adenomyosis is easily overlooked. It

can also be difficult to distinguish between adenomyosis and other benign uterine pathologies such as leiomyomas. In fact, the sensitivity of TVUS for adenomyosis has been reported to be as low as 33% in the added presence of leiomyomas (36).

One form of TVUS diagnosis that is also in continuous development in the context of (benign) uterine disorders is 3-dimensional TVUS (3D-TVUS). 3D-TVUS is generally able to better assess the JZ and the overall structure of the endometrium in comparison to its 2-dimensional counterpart (19). Furthermore, due to being able to visualise several planes at once (coronal, sagittal and transverse), uterine asymmetry resulting from adenomyosis is more easily visualised. Because of these advances, 3D TVUS has a high reported sensitivity and specificity (95% CI), of 84% (77%–89%) and 84% (77%–89%) respectively (29).

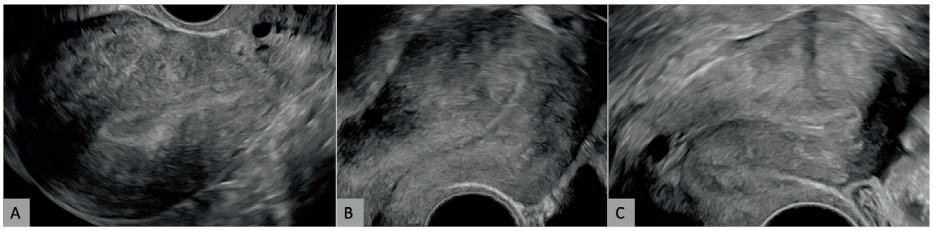

Figure 1.5. Adenomyosis examples on TVUS. **A.** Globular enlargement of the uterus with fan-shaped shadowing. **B.** Globular enlargement of the uterus with scattered hyperintense myometrial cystic foci. **C.** Uterus with asymmetric uterine wall thickening with scattered echogenic foci. (Images taken from own study populations).

- Magnetic Resonance Imaging (MRI)

Adenomyosis can be difficult to distinguish from other (benign or malignant) uterine disorders such as leiomyomas or carcinomas. For this reason, diagnosing adenomyosis using MRI has become preferred and is considered reliable, especially when the presentation is atypical on TVUS (29,32,37). MRI is not considered the first-in line diagnostic method however, due the higher associated cost and lesser availability than TVUS.

On imaging, the uterus is made up of three distinct layers (or 'zones'), each with slightly different imaging characteristics (i.e. signal intensity) on MRI (38).

The first is the inner lining of the uterus, or endometrial zone, followed by the junctional zone (JZ), and then the myometrial zone. On T2-weighted images, the endometrium normally exhibits high signal intensity, whereas the surrounding JZ exhibits relatively low signal intensity. The remainder of the myometrium is generally characterised by intermediate signal on T2 imaging (39,40). On T1 images, it is also possible to visualise potential haemorrhagic areas within the uterine structure, such as those sometimes seen in adenomyomas (41). As adenomyosis is thought to arise from the disruption and thickening of the JZ, the standard MRI imaging techniques used are thus T1- and T2- weighted MRI, which are most effective in identifying potential anomalies in the JZ.

Unlike with TVUS, which has the MUSA criteria, there are no accepted classification or diagnostic criteria when evaluating an MRI for presence of adenomyosis. While much has been reported about typical, atypical, direct and indirect MRI manifestations of adenomyosis (17,33,42), the recognition of these features often still depends on the professional analysing the images. Several different classifications of adenomyosis have been suggested based on these differing criteria (17,43), but few objective guidelines for adenomyosis exist.

The most widely reported objective measures are based on the appearance of JZ, with a thickness of over 12mm, a difference > 5mm between maximum and minimum JZ diameter, and a ratio of >40% of JZ to the full myometrium thickness thought to signify adenomyosis (34,36,40,44). These criteria are still not widely accepted however, with the 12mm cut-off value recently coming into question (45). This highlights the need for further characterisation of adenomyosis on MRI. Evaluation of the JZ can also be problematic as its thickness changes during the menstrual cycle and is affected by hormonal fluctuations, which can limits the ability to distinguish between 'normal' JZ and adenomyosis foci (42,46–48). Furthermore, uterine contractions during MRI can give a false impression of (focal) adenomyosis (42). Other examples of how adenomyosis can be objectified on MRI include uterine volume, uterine wall thickness or the volume or size of (suspected) adenomyotic foci (4,33,40,49,50). Some studies have also attempted to correlate MRI characteristics of adenomyosis with clinical outcomes, such as dysmenorrhoea, treatment response or obstetric outcomes (4,49,51–54), but it is unclear if

there is a direct relationship. This is a promising and clinically relevant query that needs further exploration as it would then become possible to predict (risk of) certain outcomes on the basis of non-invasive imaging.

There are thus a wide range of parameters on MRI that can be used to characterise and visualise adenomyosis, such as junctional zone thickness, myometrial signal intensity and uterine size (33). However, many of them have not been specifically investigated for diagnostic accuracy versus histopathology, and little is likewise known about how they may correlate to clinical outcomes (32). Despite attempts to create (imaging-based) classification systems for adenomyosis (16,17), there currently exists no widely used tool for prediction of adenomyosis diagnosis.

Adenomyosis treatment

Once accurately diagnosed, adenomyosis can be (symptomatically) treated fairly effectively using a variety of strategies. . The choice of strategy is the result of type of complaints and clinical issues (e.g. pain, dysmenorrhea, abnormal bleeding, dyspareunia, fertility, age, uterine preservation wishes). All treatment options have a reported positive effect on quality of life, uterine and lesion size, symptoms (e.g. dysmenorrhoea) and fertility to differing extents (7,55).

Medical treatment

In clinical practice, initial treatment options for adenomyosis often involve symptomatic (pain or bleeding) relief (NSAID's or tranexaminic acid) and/or hormonal therapy (56,57). Hormonal therapies range from systemic combined oral contraceptive pills (COCs) and progesterone-only pills (POPs) to more localised levonorgestrel intra-uterine devices (Lng-IUDs). All of these hormonal options have the goal of relative suppression of endometrium build-up and stimulation of endometrial atrophy, with subsequent reduction of adenomyosis-related symptoms. As with associated endometriosis, GnRH agonists or antagonists, selective oestrogen and/or progesterone modulators (SERMs and SPRMs) can also be employed in cases resistant to other forms of hormonal therapy (56,58).

Embolisation and radiofrequency ablation

In recent years, more focus is also being laid on minimally invasive treatments such as uterine artery embolisation (UAE) or high-frequency ultrasound (HiFU) ablation strategies (59,60). Both of these methods, though not available to, or suitable for, all adenomyosis patients, also show promise with regards to symptom and lesion reduction whilst being uterus-sparing (61).

Surgical treatment

If the patient wishes to avoid hormonal therapies, or there are relevant contraindications, surgical therapy by way of local excision of adenomyotic lesions, or a hysterectomy can be indicated. With the ongoing development of a wide array of medicinal therapies, hysterectomy is becoming seen as a last-resort option in women without an active child-wish. Surgical excision of smaller localised lesions can also be an option in women wishing to retain reproductive function (62), but is only feasible in certain cases, and is generally only done in centres with the relevant expertise. Without total hysterectomy, and especially without concomitant hormonal therapy, it is likely, however, that the disease will return over time (63).

Effect of adenomyosis on uterine (contractile function)

Embryologically, the uterine myometrium is made up two types of tissue: the neometrium and the archimetrium. The neometrium makes up the outer two layers of the myometrium, and is generally thought to be the driving force behind strong uterine contractions, as associated with contractions during labour and pregnancy. The archimetrium, the innermost layer of myometrium bordering on the endometrium (which includes the JZ), is linked to uterine peristaltic contractions outside of pregnancy (64).

In the 1990's and early 2000's, it was established that normal uterine contractile function follows a distinct pattern throughout the menstrual cycle (65–69). At the start of the cycle, during menstruation, uterine contractions travel mostly from the fundus-to-cervix direction with a relatively low frequency. Subsequently, in the follicular phase, uterine peristalsis travels from the cervix-to-fundus direction, with increasing contraction frequency until the periovulatory (late follicular) phase. After ovulation, during the luteal phase, the uterus enters a relatively quiescent state with the lowest frequency of uterine contractions. The characteristics of these contractions proved of

importance for fertility when examined in in-vitro fertilisation (IVF) populations (70,71).

One theory as to the aetiology of adenomyosis, and also the pathophysiological mechanism behind its symptoms, relates to how adenomyosis affects the JZ and thereby uterine contractile function. Chronic peristaltic contractions could induce repeated (micro) trauma to the JZ, causing inflammation which in turn leads to locally increased oestrogen production, which stimulates myometrial activity and inducing a vicious cycle of chronic hyperperistalsis (61). Over a lifetime, this cycle leads to gradually worsening adenomyosis with increasing age (63). This theory has been corroborated by longitudinal studies that have reported a directly proportional relationship between JZ width, adenomyosis severity and age. (46,72–74).

Several studies have investigated uterine contractility in endometriosis and adenomyosis, in an attempt to corroborate the theory that uterine contractions are abnormal in these diseases (75,76). It is theorised that with a disruption in the JZ, such as by adenomyosis, uterine contractility is likewise impaired, leading to so-called *dysperistalsis* (76,77) and consequently, adenomyosis-related symptoms. Despite these studies showing promising results, the methods used to assess uterine contractility have been subjective, complex, and/or relatively user- and patient-unfriendly. If uterine contractility (in normal and abnormal uteri) could be objectively and reliably assessed, a concrete conclusion could be made regarding how, and if, uterine contractility is affected in adenomyosis patients.

Effect of adenomyosis on fertility

In the previous sections, we have established how adenomyosis behaves, is diagnosed, and how it may disrupt uterine contractile function. One other crucial aspect of uterine function (arguably *the* uterine function) that adenomyosis has been reported to affect is fertility.

With the advent of improving imaging techniques, adenomyosis has also been more frequently diagnosed in younger, nulliparous women, and is being increasingly causally linked to sub- or in-fertility and adverse pregnancy outcomes (78–81). Adverse reproductive outcomes in adenomyosis could occur for several reasons. First, JZ disruption in adenomyosis is thought to cause dysfunction in uterine peristaltic movement, and thereby inhibits both sperm transport and embryo implantation (75,82,83). Further evidence exists showing a different expression of factors involved in embryo implantation such as osteopontin and HoxA10 in adenomyosis, as well as increased endometrial free radicals and inflammatory cytokines (84,85) which may impact embryo development.

In the context of infertility, several studies have investigated specifically how adenomyosis affects IVF outcomes. The majority of studies seem to show a negative influence of adenomyosis on IVF, with a recent retrospective study by Sharma et al. (86) showing a significantly reduced pregnancy rate after IVF in women with signs of adenomyosis on TVUS. A study by Ballester et al. (87) with endometriosis patients showed a particularly large contrast, with IVF pregnancy rates of 19% versus 82% respectively for patients with and without adenomyosis. A study examining adenomyosis characteristics on TVUS also reported a direct relationship between severity of adenomyosis and assisted reproductive technologies (ART) outcomes (80). These findings have been corroborated in meta-analyses (88,89), with Vercellini et al., reporting that adenomyosis reduces likelihood of pregnancy in ART by 28%. Conversely, studies have also been published that cannot show an association of adenomyosis with IVF failure (90–93), including in a meta-analysis (94). Thus, there still remains a lack of consensus regarding the extent to which adenomyosis affects fertility and IVF.

The junctional zone and infertility

As junctional zone dysfunction and changes are thought be associated with infertility, several studies have specifically investigated if changes in the JZ can be correlated with IVF outcomes. While these studies are heterogenous in design and study population, they all seem to show a potential link between thickened JZ and infertility. For instance, Meylaerts et al. (95) reported that infertile women have a thicker mean JZ on MRI than healthy nulliparous women. Similarly, El Gaber et al.(96) showed that women with recurrent implantation failure had a thicker JZ (on TVUS) than women with unexplained infertility. Kunz et al.(97) also linked a thickened JZ to reduced oocyte quality amongst IVF or intracytoplasmic sperm injection (ICSI) patients. Maubon et al. (98) and Piver et al. (99) suggested more specifically that a JZ of over 7mm can be used to predict IVF failure with 97% accuracy. Several of these studies included women with endometriosis, and suggested that a thicker junctional zone (and thereby potential adenomyosis) could also be independently related to IVF failure in the context of endometriosis (97,98,100).

Adenomyosis on MRI and infertility

Despite promising results separately suggesting a link between MRI characterisation of the JZ and infertility, and adenomyosis on MRI and infertility, few studies have investigated these two aspects in conjunction with each other. Some evidence does exist suggesting a link between adenomyosis severity and fertility, for instance that women with diffuse adenomyosis do seem to have worse fertility outcomes than those with focal adenomyosis (101). More detailed studies characterising adenomyosis on MRI in the context of infertility are needed. We thus propose to carry out a detailed exploration into the characterisation of adenomyosis and MRI in the context of infertility, and to attempt to correlate this concretely to IVF outcomes.

Effect of adenomyosis on pregnancy outcomes

In the foregoing section, we established that it is now becoming accepted that presence of adenomyosis affects a woman's chances of becoming pregnant, and increases her chance of miscarriage. More and more current literature also denotes however, that the risk of complications continue into later pregnancy as well.

Adenomyosis and pre-term birth and miscarriage

One of the most commonly reported adverse obstetric outcomes that has been associated with adenomyosis is pre-term birth (PTB, delivery prior to 37 weeks gestation). A recently published systematic review and meta-analysis based on 4 studies investigating pregnancies in women with adenomyosis calculated an odds ratio (OR) of 2.74 for PTB. The calculated OR for miscarriage was even higher at 3.40 (81). Taken individually, the reported OR's for PTB in women with adenomyosis have ranged from 1.96 (102) to as high as 24.53 (103). While most studies were conducted in women with and without adenomyosis, several investigated obstetric outcomes in women with endometriosis, stratified by the presence or absence of adenomyosis. These studies showed mixed results (86,104–106). A meta-analysis did however report higher OR's for PTB in adenomyosis compared to only endometriosis patients (1.47 vs. 3.09) (107).

Due to infertility often accompanying adenomyosis, a large proportion of women with adenomyosis end up going on to have pregnancies facilities with assisted reproductive technologies (ART). This is a potentially confounding factor in adverse obstetric outcomes as there is a higher risk of preterm birth in IVF pregnancies. Several studies did however correct for mode of conception, and still reported a statistically significant higher odds ratio for preterm birth in women with adenomyosis (101,103,104,108,109).

Adenomyosis and placental function

In addition to impacting fertility, recent studies also suggest that adenomyosis gives an increased risk for adverse obstetric outcomes (50,107,110). This is possibly due to altered trophoblast invasion and spiral artery remodelling (111,112), linking it to conditions such as placental disorders, hypertensive disorders of pregnancy (HDPs) and foetal growth restriction (FGR) and small-for-gestational age (SGA) infants. In accordance with this theory, significantly higher OR's have been reported by the majority of studies investigating obstetric outcomes in adenomyosis. A meta-analysis of eleven studies calculated a composite OR of 3.90 for SGA (81). The studies that did not report significant outcomes did still report a trend of a higher risk of SGA in adenomyosis (86,106). A few studies have also been published linking adenomyosis and hypertensive disorders such as preeclampsia (PE), with an OR of 7.87 being suggested in one meta-analysis (81). One study also

suggested that women with adenomyosis specifically have a higher risk of late-onset preeclampsia(4). Evidence also exists which introduces a correlation between adenomyosis and placental malposition (i.e. placenta praevia) and placental abruption (101,104,106,108).

Adenomyosis and neonatal outcomes
No studies thus far have been able to prove a significant association between adenomyosis and adverse neonatal outcomes (not including low birth weight, LBW). The few studies investigating outcomes such as low Apgar score or umbilical artery pH did not report significant results (50,105).

Despite most the published studies reporting evidence to associate adenomyosis with obstetric complications there are a few common weaknesses to these studies which may limit their generalisability. First, they all have relatively small sample sizes, with the largest study including 245 women with adenomyosis (101), and most studies including 50-60. Furthermore, all studies used trans-vaginal ultrasound diagnosis (or 2 only self-reported diagnosis (101,110)) as the diagnostic method of choice for adenomyosis, which is not considered the golden standard of adenomyosis diagnosis. It can be argued therefore that one cannot be certain that the previously carried out studies truly included the correct population. In addition, no studies have thus far been conducted investigating this question in a Dutch population, with very few being carried out in a large (European) population in general. Further common issues with these studies are heterogenous inclusion/exclusion criteria, and presence of various confounding factors such as most studies only investigating fertility outcomes in IVF/ICSI patients.

So, due to the scarce and still relatively conflicting evidence, women with adenomyosis are not generally considered to qualify as having high-risk pregnancies, and no guidelines exist for the management of pregnant women diagnosed with adenomyosis. More large-scale studies are needed to yield unambiguous results to inform clinical practice and management of these women.

Thesis Objectives:

In summary, there are a number of knowledge gaps inhibiting the complete understanding of the diagnosis and clinical impact of adenomyosis. Trans-vaginal ultrasound (TVUS) faces limiations in inter-observer variability and difficulty distinguishing adenomyosis from other uterine pathologies. MRI is preferred for atypical cases but lacks widely accepted criteria. The importance of accurate diagnosis is crucial, especially given adenomyosis's association with infertility. Studies and expert opinion does suggest a potential link between adenomyosis and aberrant uterine contractile function, fertility and adverse obstetric outcomes. Consensus on the extent of adenomyosis' impact on fertility and contractile function remains elusive however, emphasising the need for further research.

We have identified the following objectives for this thesis:

- What are the objective parameters of adenomyosis on MRI and what is their potential for the accurate diagnosis of adenomyosis on using MRI?
- How can we objectively assess uterine contractile function in the non-pregnant uterus, and is it affected by the presence of adenomyosis?
- To what extent does adenomyosis affect fertility outcomes in the context of IVF?
- Does adenomyosis affect obstetric and neonatal outcomes?

Thesis Outline:
In this thesis, we assess the effect of adenomyosis on the whole spectrum of uterine contractile and reproductive function, starting with an exploration into non-invasive diagnosis by way of MRI, and ending with its influence on obstetric outcomes. The thesis is divided into dedicated parts assessing each of the thesis objectives as described above.

Part II:
Chapter Two of this thesis focusses on the existing MRI-based diagnostic criteria for adenomyosis and their reported diagnostic accuracy from available literature. Based on the resultant described criteria, we then developed a multivariate diagnostic tool for adenomyosis diagnosis based on MRI and clinical parameters in **Chapter Three**. In **Chapter Four** we externally validate this prediction model using a separate patient cohort.

Part III:
In **Chapter Five** we develop a new 2D TVUS method employing speckle tracking and explore its use for assessing uterine contractile function and its potential for predicting IVF success. In **Chapter Six,** using this new method, we suggest a set of reference values for normal uterine contractile function in a prospective cohort of healthy women with normal uteri. In **Chapter Seven,** we then investigate existing literature for the effect that uterine abnormalities (including adenomyosis, leiomyomas and congenital uterine anomalies) have on uterine contractile function. We then used the same cohort of normal women to compare uterine contractility features to women with adenomyosis in **Chapter Eight** to assess how and if uterine contractility is affected.

Part IV:
Chapter Nine explores the IVF/ICSI outcomes of patients with adenomyosis, endometriosis or both compared to match male infertility controls. Subsequently, in **Chapter Ten** individual MRI characteristics of adenomyosis in IVF/ICSI patients are associated with IVF/ICSI outcomes.

Part V:
After assessing the effect of adenomyosis on fertility in the previous chapters, **Chapter Eleven** focusses on the association of adverse obstetric outcomes in histologically diagnosed adenomyosis patients at the Dutch population-level.

PART II

Diagnosis of Adenomyosis on MRI

CHAPTER 2:

Objective measures of adenomyosis on MRI and their diagnostic accuracy—a systematic review & meta-analysis

Authors:
Connie O. Rees
Joost Nederend
Massimo Mischi
Hubertus A. A. M. van Vliet
Benedictus C. Schoot

The content of this chapter has been published in *Acta Obstetrica et Gynecologica Scandinavica*, 2021; vol. 100: pages 1377–1391.
DOI: 10.1111/aogs.14139

ABSTRACT:

Objectives: To systematically review literature on how adenomyosis can be objectively quantified on MRI in a scoping manner, and review the diagnostic performance of these characteristics compared to histopathological diagnosis. Additionally, to summarize correlations between measures of adenomyosis on MRI and clinical outcomes.

Materials & Methods: We searched databases Pubmed, Embase and Cochrane for relevant literature up to April 2020 according to PRISMA guidelines. We included studies that objectively assessed adenomyosis on MRI, and separately assessed studies investigating the diagnostic performance of MRI versus histopathology for inclusion in a meta-analysis. The QUADAS-2 tool was used for risk of bias, with many studies showing an unclear or high risk of bias.

Results: 80 studies were included, of which 14 assessed the diagnostic performance of individual MRI parameters, with four included in the meta-analysis of diagnostic accuracy. Common MRI parameters were: junctional zone (JZ) characteristics such as maximal JZ thickness; pooled sensitivity 71.6 (95% CI 46.0 – 88.2), specificity 85.5% (52.3 – 97.0) , JZ differential; pooled sensitivity 58.9% (95% CI 44.3 – 72.1), specificity 83.2% (95% CI 71.3 – 90.8) and JZ to myometrial ratio; pooled sensitivity 63.3% (95% CI 51.9 – 73.4), specificity 79.4% (95% CI 42.0 – 95.4), adenomyosis lesion size , uterine morphology (pooled sensitivity 42.9% (95% CI 15.9 – 74.9), specificity 87.7%, (95%CI 37.9 – 98.8)) and changes in signal intensity (e.g. presence of myometrium cysts; pooled 59.6% (95% CI 41.6 – 75.4) and specificity of 96.1% (95% CI 80.7 – 99.3). Other MRI parameters have been used for adenomyosis diagnosis however their diagnostic performance is unknown. Few studies attempted to correlate adenomyosis MRI phenotype to clinical outcomes.

Conclusions: A wide range of objective parameters for adenomyosis exist on MRI; however, in many cases their individual diagnostic performance remains uncertain. JZ characteristics remain the most widely used and investigated with acceptable diagnostic accuracy. Specific research is needed into how these objective measures of adenomyosis can be correlated to clinical outcomes

KEYWORDS: Adenomyosis, Uterus, Endometriosis, Magnetic Resonance Imaging, Diagnosis, Non-invasive Imaging

ABBREVIATIONS:

MRI: magnetic resonance imaging; JZ: junctional zone; JZmax; maximal junctional zone; JZmin: minimal junctional zone; JZ Diff: junctional zone differential; TVUS: transvaginal ultrasound; SROC: summary receiver operator curve; SI: signal intensity; LSI: low signal intensity; HSI: high signal intensity; ADC: apparent diffusion coefficient; ; DWI: diffusion weighted imaging; DTI: diffusion tensor imaging;

INTRODUCTION:

Adenomyosis is a prevalent and potentially debilitating gynaecological condition characterized by dysmenorrhoea and heavy menstrual bleeding. Adenomyosis is thought to arise from and lead to disruptions in the uterine 'junctional zone' (JZ) between the uterine endometrium and myometrium. With the advent of improving imaging techniques, adenomyosis has been more frequently diagnosed in younger, nulliparous women. Along with greatly affecting their quality of life, it is also increasingly linked to sub- or in-fertility and adverse pregnancy outcomes (81,85,107). The relationship between (the extent of) adenomyosis and these clinical outcomes remains largely unknown.

One barrier to elucidating the relationship of adenomyosis (severity) to clinical outcomes is the accurate diagnosis of adenomyosis. Despite continuing advances in 2D and 3D transvaginal ultrasound imaging, MRI is generally considered to be the most consistently accurate in the diagnosis of adenomyosis (29,32); however, there is still no accepted classification system or a set of diagnostic criteria to evaluate adenomyosis on MRI. While much has been reported about typical, atypical, direct and indirect MRI manifestations of adenomyosis (33,42) , the recognition of these features often still depends on the experience and expertise of the radiologist and/or gynaecologist. Furthermore, it is still disputed which of the wide range of features reported is the most accurate. This makes it difficult to assess the true diagnostic accuracy of MRI for adenomyosis as different centres and physicians may use different criteria.

If adenomyosis could be noninvasively and objectively quantified (e.g. on MRI), the burden of disease could be correlated with various clinical outcomes, such as symptom severity, therapy response, or fertility outcomes. Similarly, potential changes in adenomyosis could be more easily followed over a patient's lifetime, or during their menstrual cycle (33,34,47,113). To the best of our knowledge, there is currently no comprehensive overview describing the quantitative analysis of adenomyosis on MRI imaging.

The objectives of this review are thus as follows: the primary objective is to evaluate the diagnostic accuracy of MRI features for adenomyosis versus histopathology, with secondary objectives being to (1) summarize in a

scoping manner how adenomyosis can be objectively quantified on MRI, (2) how objective measures of adenomyosis on MRI have been correlated to clinical outcomes.

METHODS:

The full review protocol can be found on the PROSPERO database, with protocol ID CRD42020163106.

Data Sources:

The search was conducted in online databases PubMed (MEDLINE), Embase and Cochrane, and relevant articles were also screened for additional references missed in the initial search. The search was conducted using synonyms and keywords relating to adenomyosis and MRI. Full search details can be found in the supplementary file.

Main outcome measures:

The outcomes of this review were the existing objective measures of adenomyosis on MRI, and their (if stated) individual diagnostic accuracy and relationship to clinical outcomes.

Study eligibility

We included studies investigating the diagnosis, evaluation or classification of adenomyosis objectively based on MRI. Studies were included regardless of study design, use of hormonal therapy, age, or clinical manifestation. Studies written in English, Dutch or French were considered for inclusion, published up to April 7th 2020.

Data reported in secondary analysis (reviews), case reports, letters to editors, conference abstracts, and protocols for ongoing studies were excluded. We also excluded studies that only reported subjective measures of adenomyosis on MRI, for instance: lesion localisation, subjective signal intensity i.e. 'dark' or 'low', or only noting 'JZ irregularity' without objectifying this (by measurement in mm).

Quality assessment and risk of bias:

A risk of bias assessment of included studies was only carried out for the studies investigating diagnostic accuracy, using the QUADAS-II tool (22, Tables 2.S8-2.S11). Risk of bias summary graphs and tables were constructed

using RevMan 5.3.0. It was not deemed relevant to assess the quality of the other studies investigating adenomyosis on MRI for risk of bias.

Data collection and analysis:

Study Selection

Study selection was conducted in Rayyan (rayyan.qcri.org) in a blinded fashion by two reviewers (CR & IR) based on title and abstract, followed by full-text assessment. If full-text was not available, contact was sought with the corresponding author of the article. The relevant articles were sorted into one or both of two groups upon full-text screening and data extraction done separately (Tables 2.S1 – 2.S4):

- Studies investigating diagnostic accuracy of adenomyosis on MRI versus histopathology
- Studies evaluating adenomyosis objectively on MRI without assessing diagnostic accuracy

Data collection and extraction

Data extraction was done independently by two reviewers (CR & IR). Data pertaining to study design, study population, the type of MRI conducted, definition of adenomyosis on MRI, the diagnostic performance (if reported) of MRI parameters, as well as if the MRI diagnosis was confirmed with histopathology was collected. All measured MRI characteristics of adenomyosis on MRI were extracted, with a focus on objective measures. Examples of objective measures include: JZ thickness (in mm), uterine volume or length, adenomyosis lesion size (in mm, or cm^3). If clinical or treatment outcomes were mentioned (in relation to MRI characteristics), these were also reported. See supplementary file for the full data extraction table (Tables 2.S1-2.S4).

Data synthesis and statistical analysis:

Data synthesis was done in two steps, dependent on the study design. For studies investigating diagnostic accuracy, data was synthesized narratively, and the diagnostic performance measures were summarized. We produced forest plots in Graphpad Prism 8.0 showing pairs of sensitivity and specificity together with 95% confidence intervals from each study (based on extracted data in 2 x 2 tables for each study). Summary receiver operating

characteristic (SROC) curves were constructed using MetaDTA. Separate forest plots and SROC curves were created for each diagnostic MRI parameter where the relevant diagnostic information was available. A pooled sensitivity and specificity for each parameter (if possible) was calculated using MetaDTA (115) using a bivariate model. Illustrative MRI images per objective parameter were taken from our centre.

RESULTS:

General characteristics of the studies

Search Results:

As shown in Figure 2.1, a total of 80 articles were ultimately deemed eligible for inclusion in this review. Fourteen were diagnostic accuracy studies which investigated MRI versus histopathology for adenomyosis, four of which reported diagnostic accuracy data for individual MRI parameters (e.g. JZ thickness >12mm) and could be included in the meta-analysis. The remaining 66 studies were of varying study designs and did not investigate the diagnostic performance of MRI specifically, but did describe objective measures of adenomyosis on MRI, and were included to satisfy the secondary objectives of this review.

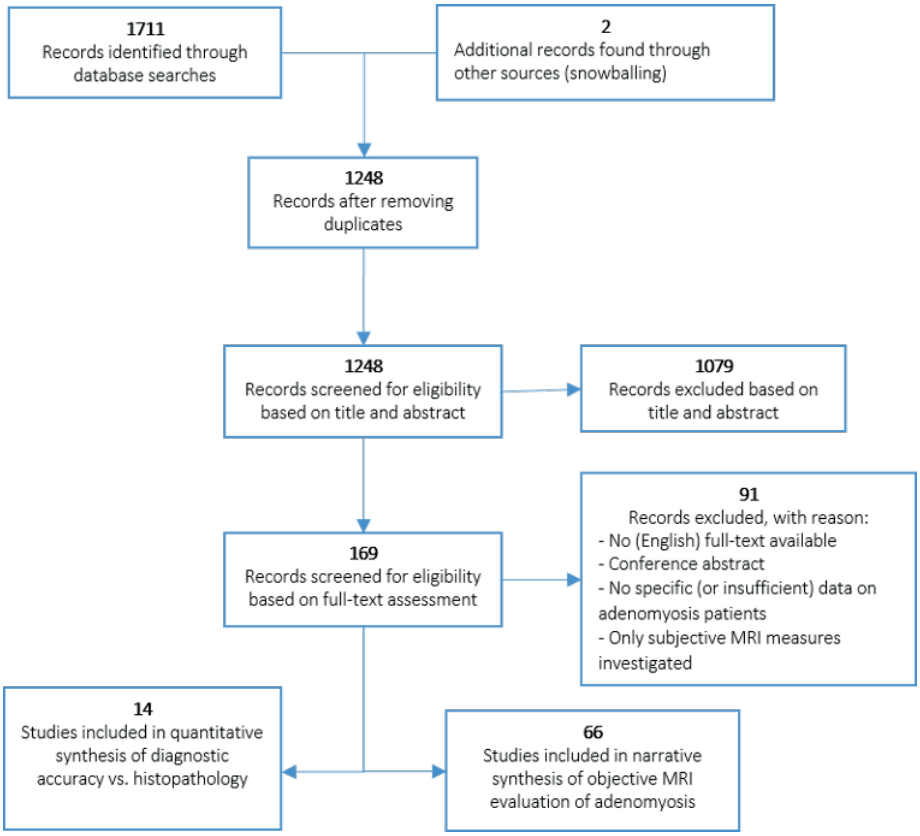

Figure 2.1: PRISMA Flow Diagram of Study Selection

Characteristics of Included Studies:

The study characteristics and outcomes for the included studies are summarized in Tables 2.S5 -2.S7 of the supplementary file. The MRI sequences most often implemented in order to assess adenomyosis on MRI were T1- and T2- weighted MRI. Eight studies reported using 3.0 Tesla coil MRI, the remaining studies used 1.0 or 1.5 Tesla coil MRI.

Methodological quality of included studies:

Only the studies investigating diagnostic accuracy were assessed for methodological quality. A graphical summary of the quality assessment is shown in Figure 2.2, as well as the assessment per included study in Figure 2.3. In the domain of patient selection, two studies were deemed to have a high risk of bias due to their retrospective design and/or unclear exclusion criteria (116,117). For the index test domain (MRI), two studies had a high risk of bias, as no definition of adenomyosis prior to MRI evaluation was reported (118,119). As for the reference standard domain, many studies did not clearly report if pathologists were blinded. Two studies were deemed to have a high risk of bias as in one (120) the assessment of the reference test was not blinded, and in the other (121) the reference diagnosis was only made based on myometrial biopsy instead of hysterectomy. For patient flow and timing, most studies did not provide enough information to assess this domain properly. Hamimi et al. (117) had a high risk of bias on this domain as not all patients received the same reference standard diagnosis. Two studies (117,121) were arguably less applicable with regards to the analysis of diagnostic accuracy. Hamimi et al. did not compare the index test to histopathological diagnosis in many cases, and Phillips et al. only investigated the diagnostic performance of MRI in relation to adenomyomas, and not adenomyosis generally. Because of their low applicability and quality, the results of these two studies were not included in the meta-analysis. Complete details per study can be found in the supplementary file (Tables 2.S8-2.S11).

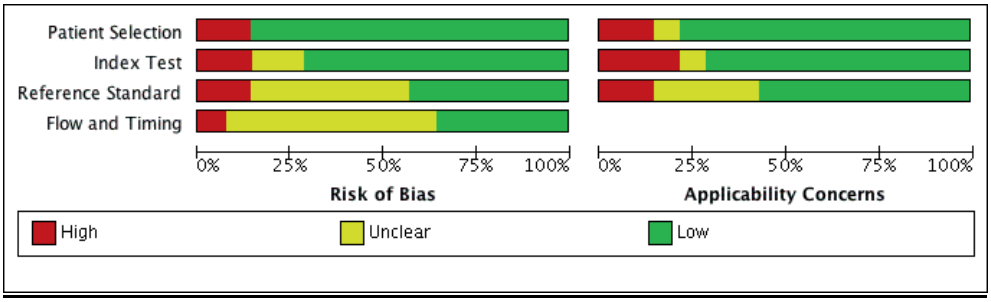

Figure 2.2: Summary Graph of Study Quality According to the QUADAS-II Tool

Figure 2.3: Quality Assessment per included study according to the QUADAS II Tool

Results synthesis:

We identified four common characteristics that have been used to diagnose and objectively visualize adenomyosis on MRI: junctional zone thickness and irregularity, adenomyosis lesion size, overall uterine morphology, and tissue signal intensity (see Table 2.1 for a full overview, and Table S12). The pooled diagnostic accuracy of MRI parameters can be seen in Table 2.2.

Table 2.1: Objective Measures of Adenomyosis on MRI

MRI Feature	Definition	Unit	Possible Stratification	Studies Mentioned (N)*
Junctional Zone Parameters				
Mean JZ	Average Junctional Zone diameter	Mm	<5mm, <7mm, <8mm, <10mm, <12mm >12mm, >15mm	N=56 (4,8,45,51–53,59,60,77,100,113,116–118,120,122–162)
JZ Max	Maximal diameter of Junctional Zone	Mm	<7mm, <10mm, <12mm >12mm, >15mm	N=18 (4,8,45,51–53,59,60,77,100,113,116–118,120,122–162)
JZ Min	Minimal diameter of Junctional Zone	Mm		N=5 (4,122,123,149)
JZ Diff	As a measure of JZ irregularity Difference between maximal and minimal JZ	Mm	<5mm difference and >5mm difference	N=7 (4,45,122,123,149,155,159)
JZ Asymmetry	Difference between anterior and posterior Junctional Zone	Mm	<2mm difference >2mm difference	N=1 (137)
Junctional Zone to Myometrium Ratio	Ratio of Junctional zone to full myometrium thickness at the same point of the uterine wall At maximal JZ, or as an average	%	>40% and <40%	N=16 (4,12,45,52,72,123,125,128,131,136,144,146,149,151,155,160)
Adenomyosis lesion size				
Adenomyotic foci volume	Volume of adenomyotic foci in 3 orientations	Mm^3	Diameter <40mm 40-60 mm >60mm	N=27 (4,12,49,52,118,121,122,126,131,133–135,140,141,151,154,158,162–168).
Uterine Parameters				
Uterine Volume	Uterine volume measured at mid-corpus in 3 orientations	Mm^3		N=28 (4,53,60,121,122,130,133,136–138,142,144–146,150,153,155,156,159,163,164,166–171)
Uterine Length	Measured from cervix to fundus in sagittal orientation	Mm		N=7 (23,29,32,57,71,78,80,89)
Average Uterine Wall Thickness	Uterine wall thickness measured from endometrium to myometrium	Mm		N=12 (8,51,151,160,77,100,136–138,143,148,149).
Uterine Asymmetry	Difference between anterior and posterior uterine wall	Mm		N=4 (8,113,137,149)
Tissue Signal Intensity				
Number of high signal intensity adenomyotic foci	Absolute number of visible high signal intensity myometrial foci (compared to normal myometrium) on T1 or T2 imaging	n		N=3 (49,126,163)

Adenomyosis Signal intensity ratio on T2 imaging	Signal intensity ratio of adenomyotic tissue compared to rectus muscle or normal myometrium (measured in ROI of the same size)	N=4 (52,140,141,163)
ADC Value	Apparent Diffusion Coefficient of adenomyotic tissue on DWI	N=5 (119,139,140,143,172)

*Reference numbers refer to the full reference list of the included studies as reported in the supplementary file

Junctional Zone Thickness

JZ thickness was the most widely reported objective measure of adenomyosis. Fifty-six studies (see Table 2.1 for details) reported the measurement of the thickness of the JZ in the assessment, or diagnosis, of adenomyosis. Studies reported differing threshold values of the JZ, with the cut-off ranging between 5 mm (113) and 15 mm (122), with 12mm being the most common (see Figure 2.4 for an example). The individual diagnostic accuracy of this value was reported in four studies, see Table 2.2, Figure 2.5 and Figures 2.S1 and 2.S2 for details. Most studies reported using the mean JZ diameter to assess adenomyosis, but several studies also separately noted the maximum (JZ Max, n= 1 and minimum (JZ Min, n=5) diameter.

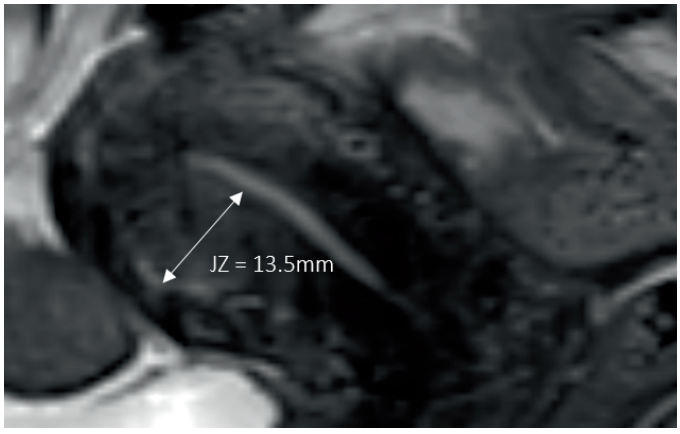

Figure 2.4: Sagittal T2W MRI showing the junctional zone (JZ) with a diameter of >12m

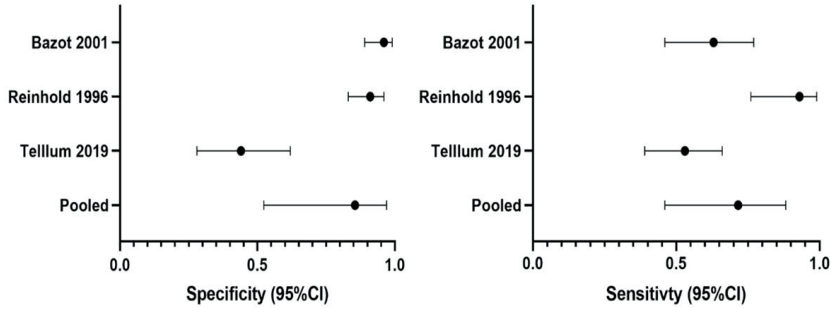

Figure 2.5: Diagnostic Performance of Junctional Zone > 12mm on MRI vs. Histopathology

Junctional Zone Differential / Junctional Zone Irregularity
Another frequently (n=7 studies) reported quantifiable measure of adenomyosis on MRI is the JZ differential (JZ Diff). This is calculated by subtracting the JZ Min from the JZ Max, and functions as an objective measure of the irregularity of the uterine JZ, which can be a diagnostic criterion for adenomyosis (see Figure 2.6 for an example). Two studies (45,122) investigated its diagnostic performance (see Table 2.2, Figure 2.7, Figure 2.S3 and 2.S4 for details). JZ asymmetry, measured as the difference between the anterior and posterior JZ at the same point of the uterus was only mentioned in one study (137).

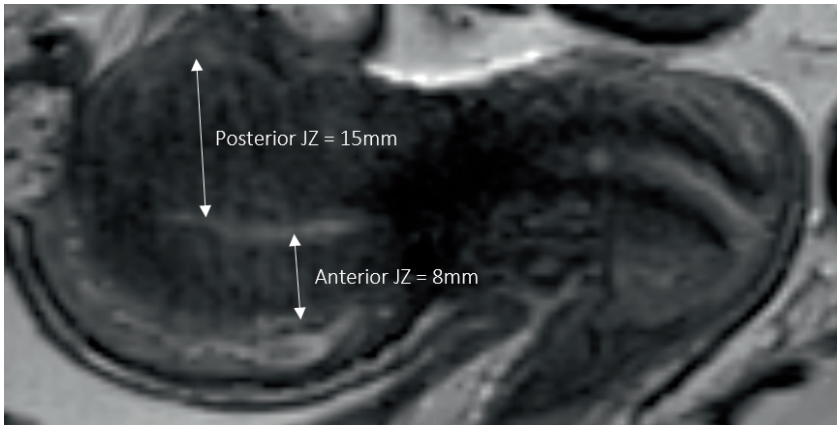

Figure. 2.6: Sagittal T2W MRI showing junctional zone (JZ) asymmetry of the anterior and posterior walls, with a JZ differential (JZ Diff) > 5mm

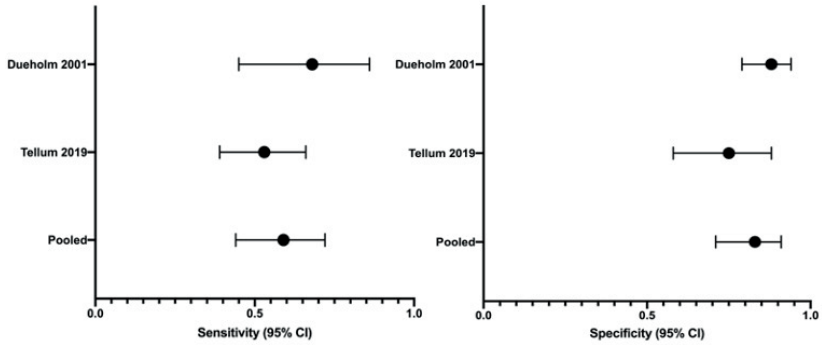

Figure 2.7: Diagnostic Performance of Junctional Zone Differential > 5mm on MRI vs. Histopathology

Junctional Zone to Myometrium Ratio / Extent of Myometrial Involvement
In order to quantify the extent of the invasion adenomyosis on MRI, several studies have investigated the (maximal) ratio of JZ to normal myometrium of the uterus (n=16 studies, see Table 2.1). This is thought to signify a relative increase in JZ thickness, and thereby myometrial tissue involvement. It is expressed as a percentage or ratio, with a value of 40-50% generally thought to indicate adenomyosis (see Figure 2.8 for an example).

Two studies investigated the diagnostic performance of this parameter (see Table 2.2, Figure 2.9 and supplementary file Figures 2.S5 and 2.S6 for details).

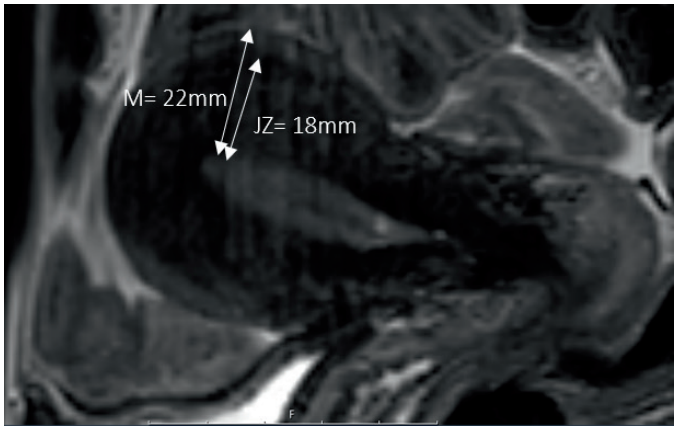

Figure 2.8: Sagittal T2W MRI showing junctional zone (JZ) and myometrial (M) thickness. The JZ to Myometrium Ratio here is 0.8 (80%)

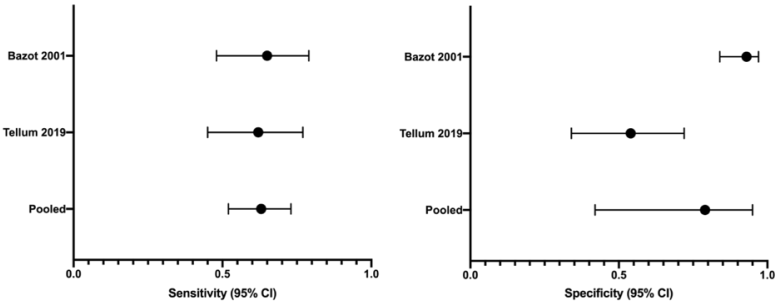

Figure 2.9: Diagnostic Performance of Junctional Zone to Myometrium Ratio > 40% on MRI vs. Histopathology

Adenomyosis Lesion Size:

Specifically for focal type adenomyosis, the lesion size or volume was often reported as a method to quantify the extent of adenomyosis (see Figure 2.10 for an example, n= 27 studies, see Table 2.1). The adenomyosis lesion was usually identified based on an 'ill-defined' low intensity area in the myometrium on T2-weighted imaging. No studies investigated this parameter in the context of diagnostic accuracy, with most studies assessing (reduction in) lesion size as a measure of treatment response. Only one study investigated lesion size with clinical outcome, and suggested that extent of lesion volume reduction after treatment may have a direct relationship with symptom reduction (52).

In addition to elements of the JZ, another widely reported measure of adenomyosis on MRI is how it affects the uterus as a whole.

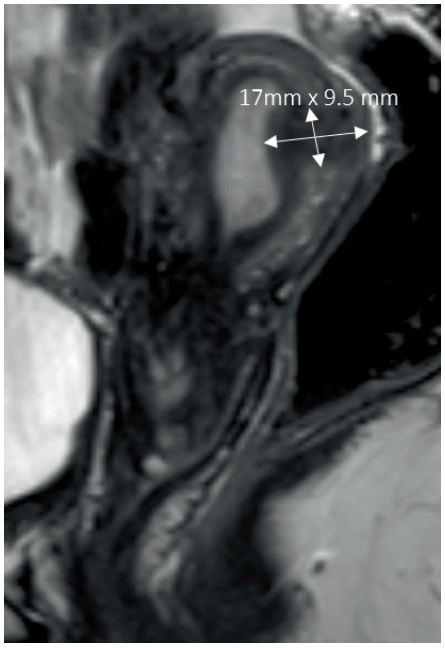

Figure 2.10: Sagittal T2W MRI showing a focal adenomyosis lesion in the posterior uterine wall

Uterine Morphology:

The volume or size (length) of the uterus (see Figure 2.11 for an illustrative example) was used as an indicator for the extent of adenomyosis in 27 studies (see Table 2.1).

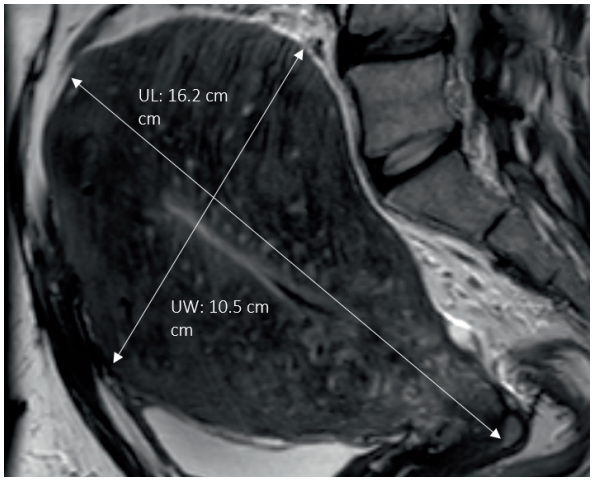

Figure 2.11: Sagittal T2W MRI showing an enlarged, diffusely adenomyotic uterus, with a uterine length (UL) of 16.2cm and a uterine width (UW) of 10.5cm

Only uterine enlargement was investigated for diagnostic accuracy, see Table 2.2, Figure 2.12, and Figures 2.S7 and 2.S8 for details).

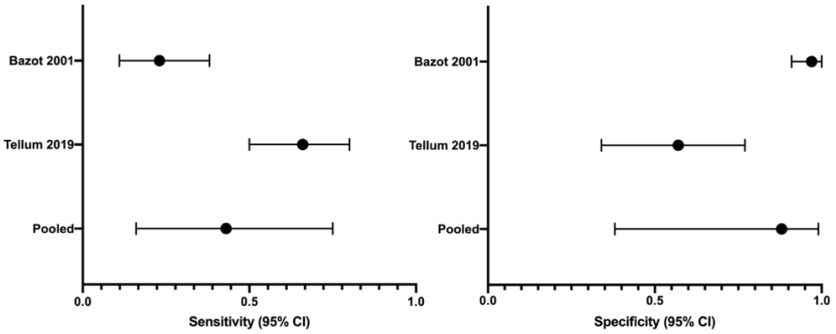

Figure 2.12: Diagnostic Performance of Uterine Enlargement on MRI vs. Histopathology

Uterine wall thickness (either as a mean, or the maximum thickness) has also been reported, with 12 studies reporting this as an outcome measure (Table 2.1). Most studies assessed this parameter in the context of high frequency ablation treatment. The shape of the uterus is an additional feature of adenomyosis that has been evaluated. Several studies reported homogenous or smooth enlargement of the uterus as a defining characteristic of adenomyosis, and others looked at uterine asymmetry (as in Figure 2.13). Most studies evaluated this subjectively, but four studies (8,113,137,149) quantified the extent of uterine asymmetry by measuring the difference between the width of the anterior and posterior walls in the context of adenomyosis.

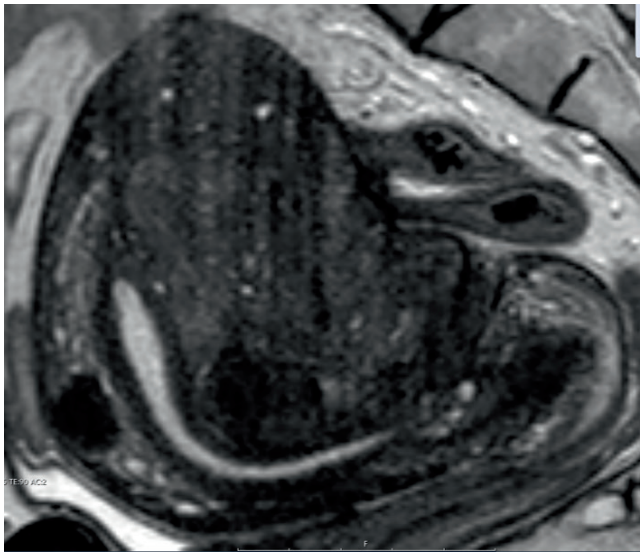

Figure 2.13: Sagittal T2W MRI showing clear posterior and anterior wall asymmetry due to focal adenomyosis (and several leiomyomas)

Tissue Signal Intensity

A third element of adenomyosis that can be objectively characterized on MRI is the signal intensity (SI) of the affected tissue. Most studies only reported this subjectively (i.e. low high SI (LSI or HSI) foci in the myometrium, without further quantification). Three studies investigated the presence of HSI cysts or foci in the myometrium for their diagnostic accuracy (See Table 2.2, Figure 2.14 and Figures 2.S9 and 2.S10). No other parameters related to tissue signal intensity were investigated for their diagnostic accuracy.

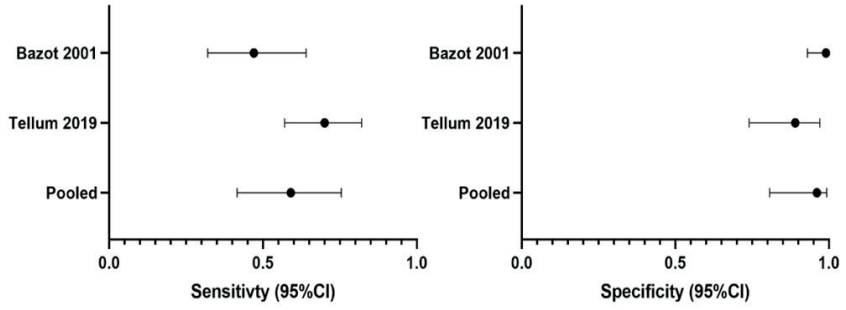

Figure 2.14: Diagnostic Performance of Presence of Myometrial Cysts on MRI vs. Histopathology

Three studies (49,126,163) attempted to quantify the extent of adenomyosis by reporting the absolute number of HSI foci (on T2 imaging) in the myometrium (as shown in Figure 2.15). No cut-off value regarding the number of HSI foci has been described, with the majority of studies denoting their presence as stand-alone evidence of adenomyosis.

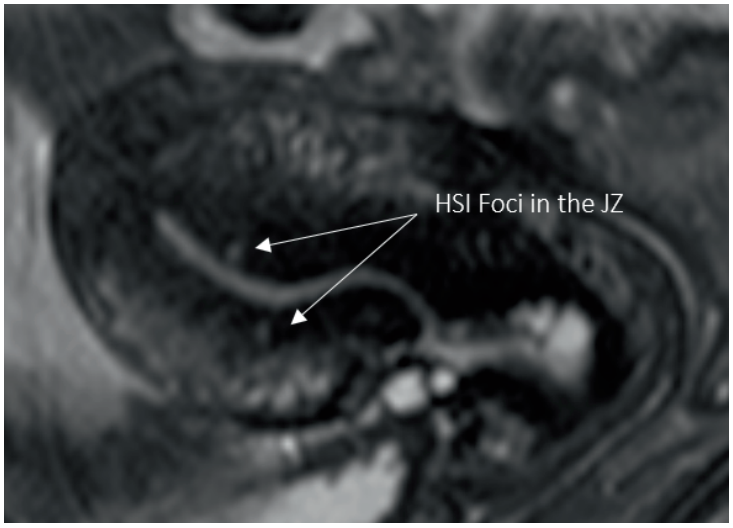

Figure 2.15: Sagittal T2W MRI showing subtle high signal intensity (HSI) foci in the junctional zone (JZ)

Four studies (52,140,141,163) described a method to quantify the SI of adenomyotic tissue further, on T2 imaging. In these studies the relative SI ratio of adenomyotic tissue was compared to that of apparently normal myometrium, or rectus muscle, and given an absolute value (see Figure 2.16 for a visualization). This ratio has not been investigated for diagnostic accuracy.

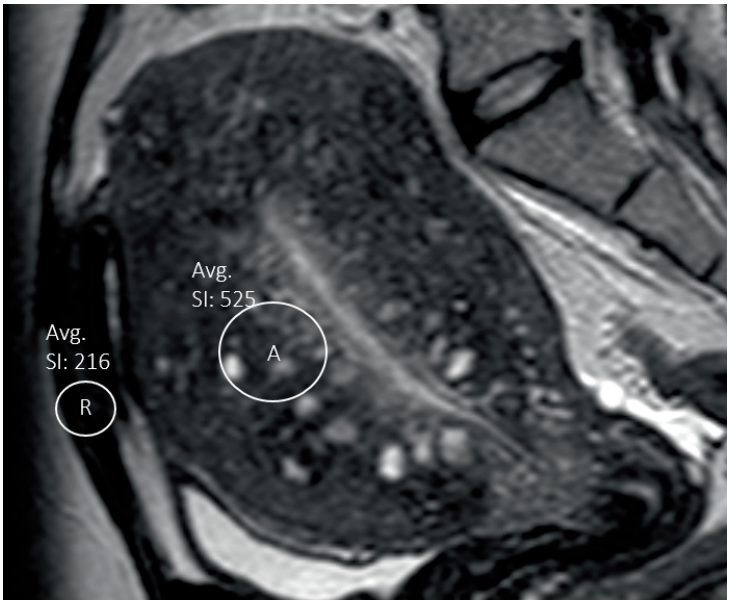

Figure 2.16: Sagittal T2W MRI showing an example of adenomyosis tissue (A) signal intensity (SI) versus that of the rectus muscle (R)

Tissue Diffusion Characteristics

Finally, five studies (see Table 2.1) used diffusion weighted imaging (DWI) to characterize adenomyosis, and attempted to quantify this. In these studies, the apparent diffusion coefficient (ADC) was measured for adenomyotic tissue compared to healthy uterus tissue, or other types of lesions (fibroids, sarcomas). DWI allows visualization of water diffusion characteristics of different types of tissue, of which ADC is a quantitative measure (173). Tian et al. (119) investigated the added value of adenomyosis DWI and ADC values, and found it significantly improved diagnostic accuracy compared to conventional MRI sequences (95.7% vs. 89.1% respectively). Similarly, Kilickesmez et al. (143) found that JZ tissue in adenomyosis patients had significantly different ADC values compared to JZ tissue in healthy patients (albeit not compared to histopathological diagnosis).

Table 2.2: Pooled Diagnostic Accuracy of Individual MRI Parameters for Adenomyosis

Adenomyosis MRI Feature	Studies investigating diagnostic accuracy (n)	Pooled Sensitivity (%, 95% CI)	Pooled Specificity (%, 95% CI)
JZ Thickness > 12mm	4	71.6 (46.0 – 88.2)	85.5 (52.3 – 97)
JZ Differential >5mm	2	58.2 (44.3-72.1)	83.2 (71.3 – 90.8)
JZ to Myometrium Ratio >40%	2	63.3 (51.9-73.4)	79.4 (42.0-95.4)
Enlarged Uterus	2	42.9 (15.9-74.9)	87.7 (37.9 – 98.8)
Myometrial Cysts	3	59.6 (41.6-75.4)	96.1 (80.7 – 99.3)

Correlation with Clinical outcomes:

JZ thickness was most often investigated as an in relation to clinical outcomes. Several studies (n= 8) used (reduction in) JZ thickness as a measure of therapy response, but relatively few studies investigated (change in) JZ thickness and other clinical outcomes. Those that did, reported conflicting results (51,59,72,152). Froeling et al. and Fukunishi et al. could not find a direct relationship between JZ thickness and symptom reduction or severity (53,136). Conversely, four other studies did report an direct association between duration and severity of dysmenorrhea and JZ thickness (59,60,77,152). An increase of average JZ thickness with age, suggesting a relationship to higher incidence of adenomyosis in older women has also been reported (72,77,100). Kunz et al. (100) and Kissler et al. (51) investigated JZ thickness in the context of uterine dysperistalsis-associated infertility but did not find a significant relationship. Further studies (8,12,149,151) evaluated JZ thickness in the context of endometriosis phenotypes, whereby Larsen et al. (149) reported an increased mean JZ in conjunction with endometriosis severity. Chapron et al. refuted this however (12).

Uterine size and morphology has also been somewhat correlated to clinical outcomes (see Table 1), with uterine volume sometimes used in the context of symptom reduction. Generally, uterine size was directly associated with severity of adenomyosis symptoms.

Furthermore, several attempted to correlate tissue signal intensity with therapy response (49,144,163). Keserci et al. (52) suggested that a lower

adenomyosis SI ratio vs normal myometrium was associated with more symptom reduction after therapy.

DISCUSSION:

Generally, adenomyosis can be diagnosed and quantified on MRI by looking at four characteristics: junctional zone thickness and (ir)regularity, adenomyosis lesion size, uterine morphology, and (relative) myometrial signal intensity. We are unable to suggest from our results which single MRI parameter is most accurate as a diagnostic criterion due a lack of data, however JZ thickness is the most widely used. Most reported diagnostic adenomyosis MRI parameters have in fact not been verified versus the gold standard of histopathology. Only a small number of studies investigated the correlation between MRI phenotype and clinical outcome, with conflicting results.

This is the first review to specifically investigate how adenomyosis can be *objectively* quantified on MRI and which summarizes the diagnostic potential of individual MRI parameters up to now. Previous similar reviews have looked at the use of MRI in the diagnosis and classification of adenomyosis in general, or the JZ separately (16,32). Munro et al. (32) and Kobayashi et al. (16) reviewed the existing classification systems for adenomyosis on imaging and histology and attempted to correlate MRI findings to clinical outcomes. As with our review, the classification systems and diagnostic criteria were shown to vary widely, and few studies correlated clinical outcomes in adenomyosis to MRI phenotype. This was also noted by Gordts et al. (43), highlighting a need for standardized classification and diagnosis of adenomyosis. It has been postulated that adenomyosis phenotype may not be able to be reliably correlated to clinical outcomes (32), and it should be noted that imaging alone may not be the final answer in defining adenomyosis phenotypes. More knowledge of the (epi)genetic profile of adenomyosis, in combination with well-defined and detailed imaging, will likely provide a definitive characterization of the disease in future. Several studies have summarized the relationship of JZ thickness generally to various clinical outcomes (46,98). These studies reported a significant relationship between JZ thickness and outcomes such as infertility, or menstrual phase; however, it is unknown how this may translate to adenomyosis patients. Of the studies included in this review, it could be suggested that JZ thickness is correlated to symptom severity, treatment response, infertility and age.

Imaging of the uterine anatomy and function has progressed rapidly over the last few decades, with sophisticated functional imaging of the uterus becoming more common. This is leading to new insights into different aspects of uterine function such as uterine movement, blood flow and structural and functional changes during the menstrual cycle (174,175). Techniques employed now include DWI, blood oxygenation function studies and cine MRI (176–178). More recently, the use of DTI has also been explored in uterine and gynaecological disorders like endometriosis, malignancies and uterine fibroids, suggesting great potential in the use of these techniques in gynaecological conditions (179,180). Their diagnostic potential remains to be definitively evaluated, however the one study which investigated DTI for its diagnostic potential showed superior accuracy over conventional MRI (119).

There are several limitations which may impact our results. First, despite their benefits, our broad inclusion criteria inevitably led to a heterogeneous selection of study designs and populations. This makes it difficult to apply the MRI parameters presented to specific patient groups (i.e. pre- or post-menopausal, symptomatic or asymptomatic, with or without concomitant fibroids or endometriosis etc.). Furthermore, many studies did not report on the specific diagnostic performance of individual parameters, meaning we could only include a small number of studies in our quantitative analysis. Studies which did report on individual MRI parameters also showed varied quality and results, leading to broad confidence intervals in our pooled analysis. As a result, we were not able to answer one of the objectives of our review; namely, which individual parameter is most accurate.

Few studies corrected for influence of the menstrual cycle. Evaluation of the JZ can be problematic as its thickness changes during the menstrual cycle and is affected by hormonal therapy, making it difficult to distinguish between 'normal' JZ and adenomyosis foci (42). This thought has been echoed in previous reviews bringing the reliability of only JZ evaluation as a diagnostic marker for adenomyosis into question (29,45). It is debatable how much adenomyotic tissue in the JZ responds to these hormonal stimuli (42), but it is accepted that MRI diagnosis should take place in the proliferative phase of the menstrual cycle to minimize hormonal influence. Furthermore, only eight studies used 3.0T MRI, with the majority using 1.5T coils, which impacts overall image quality and thus diagnostic potential.

Another noteworthy issue is that included studies used different definitions of adenomyosis. Whilst the definition used was often similar, exact criteria and cut-off values varied. This difference persisted in recent studies, which confirms a lack of consensus regarding diagnostic criteria for adenomyosis on MRI. The histopathological definition used for adenomyosis was similarly often unclearly defined.

Despite these limitations, we do believe the results of our review are clinically relevant and highlight future research opportunities. Our inability to comprehensively summarize the clinical impact of adenomyosis on MRI serves in highlighting the need for studies which specifically investigate this correlation. If the MRI phenotype of adenomyosis can be definitively linked to certain clinical outcomes (fertility, treatment response, symptom severity), this would be of great value for both clinicians and patients. The overview provided here can form the basis for such research, and thereby aid in the creation of an objective, accurate, clinically applicable, and commonly accepted classification system of adenomyosis. The development of a (patient-specific) diagnostic tool or predictive algorithm based on individual MRI parameters could also be facilitated by the results presented here.

CONCLUSION:

This review has identified three main characteristics that can be quantified on MRI in order to visualize the extent of adenomyosis. These characteristics are also of generally acceptable diagnostic accuracy and can be used to differentiate adenomyosis on MRI from other uterine lesions and disorders. Knowledge of these parameters can form the basis for much-needed research into how adenomyosis severity on MRI can be related to clinical outcomes and aid in the development of an objective diagnostic tool for adenomyosis. More research into the characterization of adenomyosis using MRI imaging techniques is needed in order be able to fully characterize adenomyosis objectively and be sure of the diagnostic accuracy of these imaging modalities.

ACKNOWLEDGEMENTS: We would like to thank bachelor student Iris Rupert for her help in the study screening and data extraction process.

CHAPTER 3:

Prediction of Adenomyosis Diagnosis based on MRI

Authors:
Connie O. Rees
Marloes van de Wiel
Joost Nederend
Aleida Huppelschoten
Massimo Mischi,
Hubertus A.A.M. van Vliet,
Benedictus C. Schoot

The content of this chapter has been published in the *Journal of Endometriosis and Uterine Disorders,* June 2023; vol. 2:
DOI: 10.1016/j.jeud.2023.100028

ABSTRACT

Objective: Development of a multivariate prediction model based on MRI and clinical parameters for histological adenomyosis diagnosis

Materials and Methods: This single centre retrospective cohort study took place in the gynaecological department of a referral hospital. 296 undergoing hysterectomy with preoperative pelvic MRI between 2007-2022 were included. MRI's were retrospectively assessed for adenomyosis markers (junctional zone (JZ) parameters, high signal intensity foci (HSI) foci) in a blinded fashion. A multivariate regression model for histopathological adenomyosis diagnosis was developed based on MRI and clinical variables from univariate analysis with p>0.10 and factors deemed clinically relevant.

Results: 131/296 women (44.3%) had histopathological adenomyosis. Patients were of comparable age at hysterectomy, BMI and clinical symptoms, p>0.05. Adenomyosis patients more often had undergone a curettage (22.1% vs. 8.9%, p=0.002), a higher mean JZ thickness (9.40 vs. 8.35mm, *p* <.001), maximal JZ thickness (16.00 vs. 13.40mm, p<.001), mean JZ/myometrium ratio (0.56 vs. 0.49, p=.040), and JZ differential (8.60 vs. 8.15mm, p=.003). Presence of HSI foci was the strongest predictor for adenomyosis (39.7% vs. 8.9%, *p*<.001). Based on the parameters age and BMI, history of curettage, dysmenorrhoea, abnormal uterine bleeding (AUB), mean JZ, JZ Differential ≥ 5mm, JZ/myometrium ratio >.40, and presence of HSI Foci, a predictive model was created with a good Area Under the Curve (AUC) of .776.

Conclusions: This is the first study to create a diagnostic tool based on MRI and clinical parameters for adenomyosis diagnosis. After sufficient external validation, this model could function as a useful clinical-decision making tool in women with suspected adenomyosis.

KEYWORDS: Adenomyosis; MRI; Hysterectomy; Pathology; Diagnosis;

ABBREVIATIONS:

MRI: Magnetic Resonance Imaging; **TVUS:** Transvaginal Ultrasound; **JZ:** Junctional Zone; **BMI:** Body Mass Index; **OR**: Odds Ratio; **AUB:** Abnormal Uterine Bleeding;

INTRODUCTION:

The gold standard for diagnosing adenomyosis is histopathological after hysterectomy. Adenomyosis can also be diagnosed using Magnetic Resonance Imaging (MRI) (29,31,181). Accurate diagnosis on MRI remains challenging as a consensus on diagnostic criteria is lacking (19). Clinically, adenomyosis can be suspected based on symptoms (dysmenorrhoea, abnormal uterine bleeding (AUB) and infertility (19,81)), but this can be difficult due to up to a third of patients being asymptomatic (5,19). Ultrasound (TVUS) diagnostic criteria do exist and are the most commonly used non-invasive diagnostic tool(182–184), but are dependent on experienced sonographers (125,185,186). Furthermore, TVUS is less reliable in cases of mild or atypical adenomyosis (24,182). Moreover, in cases with combined pathology (e.g. adenomyosis and fibroids, or adenomyosis and endometriosis) TVUS diagnosis can be extra challenging (182). In cases such as these, MRI can help lead to a more definitive diagnosis.

In the frequently associated condition endometriosis (187), reported diagnostic delay is up to nine years (20,21). The diagnostic delay for adenomyosis is unknown. The mental and physical toll on women suffering from either of these conditions is considerable (188). Especially in women of fertile age, there is a need for an accurate diagnostic tool so that appropriate management can be implemented swiftly. Early diagnosis is clinically relevant even in mild cases, due to a potential for reproductive sequelae (81). Such a tool could also be used to predict certain clinical outcomes such as treatment response, or fertility outcomes.

There are a wide range of MRI parameters that can be used to characterise adenomyosis, such as junctional zone (JZ) thickness, myometrial signal intensity and uterine size (33,181). Many of them have not been investigated for diagnostic accuracy, and little is likewise known about their correlation with clinical outcomes (32,181). Despite attempts to create (imaging-based) classification systems for adenomyosis (16,17), there exists no clinically applicable tool for prediction of adenomyosis diagnosis on MRI.

This study aims to create a multivariate prediction model for histopathological diagnosis of adenomyosis based on a combination of MRI parameters and clinical criteria prior to hysterectomy.

MATERIALS AND METHODS:

Study Objective:

To develop a multivariate prediction model for adenomyosis diagnosis on histopathology after hysterectomy based on MRI and clinical parameters.

Setting:

Gynaecological department of a Dutch regional referral teaching hospital.

Design:

Single centre retrospective observational cohort study

Patient Selection and Eligibility:

Patients were selected through screening of electronic hospital patient records in Healthcare Information eXchange (HiX) (ChipSoft BV, Amsterdam, the Netherlands), based on electronic search queries in CTcue (CTcue BV, Amsterdam, the Netherlands). Relevant search terms are presented in appendix 3A.

Women were eligible for inclusion if they underwent a hysterectomy due to benign pathology in our centre between 2007 and March 2022 and had pre-operative pelvic MRI available. Subjects were included regardless of symptoms. Subjects were excluded if: they did not have a pelvic MRI prior to hysterectomy, they had an unsuitable MRI protocol (see appendix 10B for further specification), they were post-menopausal (due to no longer active disease), had a gynaecological malignancy, or if no pathology report was available after hysterectomy. Patients were also excluded if they explicitly stated that they did not want their information to be used for research purposes.

Outcomes:

The primary outcome assessed in this study is the histopathological diagnosis of adenomyosis after hysterectomy. Secondary outcomes include clinical and MRI parameters of included patients.

Histopathology Diagnosis:

Adenomyosis was diagnosed based on histopathology if endometrial glands were seen in the myometrium:

- At least one low power field from (an irregular) endo-myometrial junction, or
- 1 to 2.5 mm below basal layer of endometrium, or
- Deeper than 25% of the overall myometrial thickness

Local MRI Protocol:
All pelvic MRIs were carried out with either a 1.5T or 3T MRI system (Philips, Ingenia, the Netherlands). Local protocol included a T2-weighted turbo spin echo (T2-TSE) sequence in the sagittal, axial, and coronal planes, and a T1-weighted turbo spin echo (T1-TSE) sequence in the axial plane. A slice thickness of 3 millimetres was generally used, with variations ranging from 3-5 millimetres. All patients were pre-treated with an antispasmodic agent (1 mL of 20 mg/mL Buscopan®, Sanofi, Paris, France) intravenously or intramuscularly to minimise the effects of uterine and bowel peristalsis on image interpretation. Some patients received multiple pelvic MRIs prior to hysterectomy. In those cases, the MRI closest to the hysterectomy was chosen for the assessment. See appendix 10B for full details.

MRI Assessment:
Two investigators (MvdW and CR) independently reviewed all pelvic MRIs for signs of adenomyosis blinded to the final histopathological diagnosis. Adenomyosis was suspected when one or more of the following features was present: (irregular) JZ >12mm, presence of myometrial high signal intensity (HSI) foci and/or asymmetric enlarged uterus (other than due to presence of leiomyoma's). Measurements were done using Spectra IDS7 version 21.1 (Linköping, Sweden). Table 3.S1 shows an overview and definition of the parameters that were measured. Consensus was reached if there was a difference of <2mm. If discrepancies existed between the assessments of the two investigators, expertise was sought from a pelvic radiologist (J.N.). The researchers independently concluded whether an MRI adenomyosis diagnosis was suspected, after which the pathology report was consulted to review the conclusive histopathological diagnosis. The influence of uterine contractions on JZ measurements was minimised by confirming (maximal) JZ thickness in more than one imaging plane. In the case of bad quality MRIs, or extremely abnormal uteri affecting the ability for assessment, only those MRI parameters that could be reliably measured were assessed.

Data Management:
To store patient data, protected software, Research Manager (Research Manager, Deventer, the Netherlands), was used. Data pertaining to patients were given a pseudonymised study ID and could therefore not be traced back to the individual patient.

Data Analysis and Model Development
The study was conducted conform both the STROBE (189) and the TRIPOD statements (190) (see appendices 10C and 10D for the appropriate checklists). All statistical analyses were conducted with IBM SPSS Statistics, version 28.0 (IBM Corp., Armonk, NY, USA). Flowcharts were created using Miro (Miro, Amsterdam, the Netherlands). Except for univariate logistic regression analysis, a p-value of <.05 was considered statistically significant for all variables.

Between-group differences were compared between patients with and without a histopathological adenomyosis diagnosis after hysterectomy. For clinical characteristics and primary MRI parameters, counts and frequencies were reported. For normally distributed continuous variables, means and standard deviations were calculated. For continuous variables that were not normally distributed, medians and inter-quartile ranges were given. To assess between-group differences for continuous variables, Student's t-Test and Mann-Whitney U test were used. For categorical variables, the Chi Squared test was used.

For all possible predictive factors, sensitivity, specificity, PPV, NPV, positive likelihood ratio (PLR), negative likelihood ratio (NLR), and accuracy were calculated. Potential threshold values of continuous variables were investigated using Receiver Operator Characteristics (ROC) curves and Area Under the Curve (AUC) to identify appropriate cut-off values, and to test the prognostic diagnostic potential for histopathological adenomyosis diagnosis.

For the development of the prediction model, the methodology as described by Grant et al. (191) and the TRIPOD guidelines were followed (190). For all individual potential predictors for a histopathological adenomyosis diagnosis, a univariate logistic regression analysis was first performed. The odds ratios (ORs) with their corresponding 95% confidence intervals (CIs) were reported. Missing values were dealt with by multiple imputation. Furthermore, interaction terms were used to test possible interaction between individual predictive

factors. Tests for multicollinearity were performed as well to assess potential correlation between predictors. Individual variables were used for inclusion into the multivariate logistic regression model if they had a *p*-value <.10 in the univariate logistic regression analysis, or if they were considered clinically relevant, and if they had a high diagnostic performance (sensitivity/specificity>70% or AUC >0.70). Overfitting of the model was avoided by reducing the number of variables included in the model and by using shrinkage factors. Model fit was further improved by including additional predictive power of continuous variables based on locally weighted smoothing (LOESS).

The final model was evaluated for discrimination and calibration performance. The AUC was obtained to discriminate between women with and without a histopathological adenomyosis diagnosis after hysterectomy. To assess the calibration of the predicted probabilities, and to show the relation between predicted and observed probabilities for the histopathological adenomyosis diagnosis, an observed to expected ratio was calculated and a Hosmer and Lemeshow Test was performed.

Ethics Statement:

This study was approved by the local medical ethical review board, with study number nWMO-2020.135. Informed consent was waived due to the retrospective study design.

RESULTS:

Patient selection

296 women out of 1,139 potentially eligible women, were included for analysis. See Figure 3.1 for detailed overview of the patient selection and exclusion procedure.

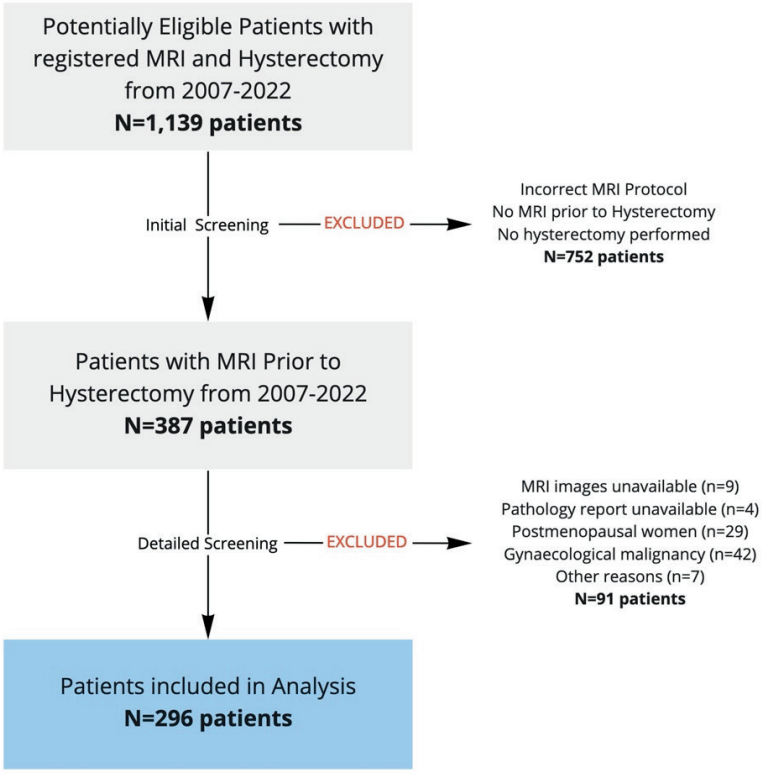

Figure 3.1. Flowchart of Patient Selection and Exclusion

Patient characteristics

Table 3.1 presents patient characteristics of patients with and without a histopathological adenomyosis diagnosis. Out of 296 patients undergoing hysterectomy, 131 (44.2%) received adenomyosis diagnosis based on histopathology. 34.4% (45/131) patients had concomitant uterine fibroids, and 53.4% (70/131) had concomitant endometriosis (as diagnosed by MRI or laparoscopy). In general, age, Body Mass Index (BMI), medical history, and clinical symptoms were comparable between patients with and without adenomyosis ($p>.05$). However, patients with a histopathological diagnosis of

adenomyosis more often had a history of curettage after miscarriage (22.1% vs. 8.9%, *p*=.002).

Table 3.1: Patient Characteristics

	Histopathology		
	Adenomyosis (n=131)	No Adenomyosis (n=165)	p-value
Demographics			
Age at MRI	42.24 ± 5.943	40.94 ± 6.019	.617
BMI	26.82 ± 5.539	26.38 ± 5.474	.416
Intoxications			
Smoking	35 (26.7%)	44 (28.0%)	.629
Medical History			
History of Curettage*	29 (22.1%)	14 (8.9%)	.002
Gravidity	3.0 ± 2.0	2.5 ± 2.0	.342
Parity	2.0 ± 2.0	2.0 ± 1.0	.814
History of Caesarean Section	33 (25.2%)	55 (35.0%)	.542
Irregular cycle†	30 (22.9%)	36 (22.9%)	.562
Hormonal medication‡	57 (43.5%)	62 (39.5%)	.426
Endometriosis§	70 (53.4%)	72 (45.9%)	.200
Uterine Fibroids	45 (34.4%)	65 (41.4%)	.220
Symptoms			
Dysmenorrhoea	96 (73.3%)	99 (63.1%)	.491
AUB	81 (61.8%)	88 (56.1%)	.201
Chronic pain	95 (72.5%)	110 (70.1%)	.779
Subfertility	26 (19.8%)	39 (24.8%)	.417
Dyschezia	18 (13.7%)	30 (19.1%)	.185
Dyspareunia	50 (38.2%)	66 (42.0%)	.903

MRI= Magnetic Resonance Imaging; BMI= Body Mass Index; AUB=Abnormal Uterine Bleeding; *in the context of miscarriage or termination of pregnancy

† defined as <21 days or >35 days in duration or cycle length that varied from month to month by >4 days

‡i.e. combined oral contraceptive pill (COC), progesterone only pill (POP), GnRH antagonist, levonorgestrel intra-uterine device (Ln-IUD)

§ as diagnosed on MRI or laparoscopy

MRI characteristics

Table 3.2 presents primary MRI characteristics of patients with and without a histopathological diagnosis of adenomyosis. 21 patients were not assessed on MRI due to a poor quality of the MRI, or the inability of the researchers to identify the endometrium or the JZ (e.g. due to disruption of the normal uterine anatomy in patients with severe uterine fibroids). Furthermore, 52 MRIs were re-assessed and discussed with a third investigator due to discrepancies between the two researchers. Most discrepancies related to the presence of

High Signal Intensity (HSI) foci (n=31) and individual JZ measurements (including JZ Max) (n=15) (see Table S2 for further details).

Table 3.2: MRI Characteristics for patients with adenomyosis diagnosis versus those without

	Histopathology		
	Adenomyosis (n=131)	No Adenomyosis (n=165)	p-value
MRI Features			
Mean JZ (mm)	9.40 ± 6.40	8.35 ± 4.60	<.001
JZ Max (mm)	16.0 ± 10.10	13.40 ± 6.20	<.001
JZ Diff (mm)	8.60 ± 7.20	8.15 ± 5.50	.003
Mean JZ/MYO	0.56 ± 0.29	0.49 ± 0.21	.040
Mean JZ Asymmetry (mm)	0.10 ± 3.50	0.35 ± 2.90	.518
Mean Wall Thickness (mm)	18.72 ± 6.50	17.12 ± 6.00	.069
Mean Wall Asymmetry (mm)	1.73 ± 6.50	1.02 ± 6.10	.295
Mean Uterine Length (mm)	88.80 ± 17.90	89.05 ± 18.70	.989
Mean Uterine Volume (mm^3)	240,774.63 ± 167,707.00	214,199.41 ± 160,215.50	.613
Adenomyosis Focus SI	402.00 ± 191.00	422.50 ± 213.80	.363
SI Ratio	2.18 ± 1.02	2.38 ± 1.15	.521
JZ Max ≥12 mm (n)	87 (66.4%)	73 (46.5%)	.004
JZ Diff ≥5 mm (n)	109 (83.2%)	99 (63.1%)	.024
JZ/MYO >.4 (n)	92 (70.2%)	98 (62.4%)	.021
HSI Foci (n)	52 (39.7%)	14 (8.9%)	<.001

MRI = Magnetic Resonance Imaging; JZ = Junctional Zone; Max = Maximum; JZ Diff = Junctional Zone Differential; JZ/MYO = Junctional Zone to Myometrium Ratio; SI = Signal Intensity; HSI = High Signal Intensity

Significant differences between groups were found for mean JZ thickness, maximal JZ thickness, and JZ differential (JZ Diff) (p<.001, <.001, and .003, respectively). Similar differences were observed for the cut-offs of JZ ≥12 mm, JZ Diff ≥5 mm, and JZ to myometrium ratio (JZ/MYO) >.4 (p=.004, .024, and .021, respectively). Compared to patients without adenomyosis, the MRIs of patients with adenomyosis more often showed HSI foci (39.7% vs. 8.9%, p<.001). Figure 3.2 shows illustrative examples of these MRI features in patients with and without a histopathological diagnosis of adenomyosis.

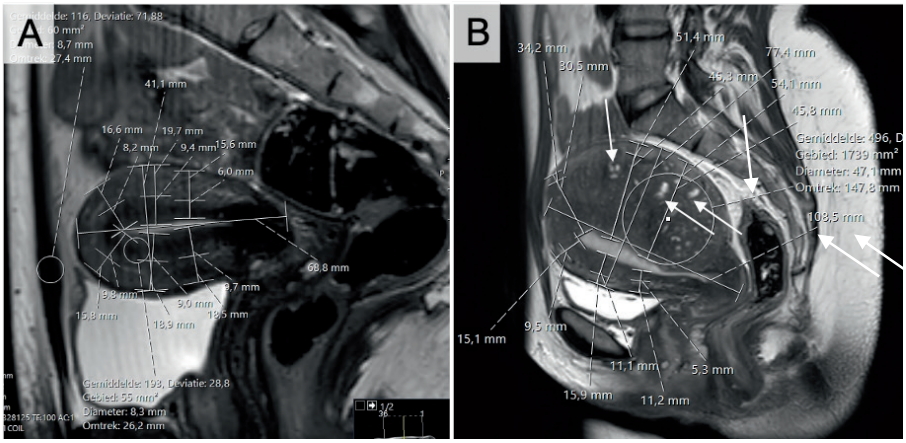

Figure 3.2. Illustrative examples of MRI's of two included patients. **A.** MRI measurements in a patient without histopathological diagnosis of adenomyosis. Mean JZ thickness was 8.7mm (<12mm), JZ Max was 9.8 mm (<12 mm), and JZ Diff was 3.8mm (<5 mm). JZ/MYO was .50 (>.40), and HSI foci were not present. **B.** MRI measurements in a patient with histopathological diagnosis of adenomyosis. Mean JZ thickness was 24.6 mm (≥12 mm), JZ Max was 45.8 mm (≥12 mm), and JZ Diff was 40.5 mm (≥5mm). JZ/MYO was 0.74 (>.40), and HSI foci were present (white arrows)

Diagnostic accuracy

Table 3.3 presents the diagnostic accuracy of MRI in general and the individual potential predictors of adenomyosis. MRI overall had a sensitivity of 50.4%, a specificity of 66.9%, a PPV of 55.9%, a NPV of 61.8%, a positive LR of 1.5, and a negative LR of 0.7. The overall accuracy was 59.4%. A history of curettage showed an overall accuracy of 59.7%, with a sensitivity of 22.1%, a specificity of 91.1%, a PPV of 67.4%, a NPV 58.4%, a positive LR 2.5, and a NLR of 0.9. Additionally, AUB had a sensitivity of 94.2%, a specificity of 11.1%, a PPV of 47.9%, and a NPV of 68.8%. The positive LR of AUB was 1.1, negative LR 0.5, and overall accuracy 49.7%. A JZ Diff $\geq$ 5 mm on MRI had an overall accuracy of 54.8%, with a sensitivity of 88.6%, a specificity of 22.0%, a PPV of 52.5%, a NPV of 66.7%, a positive LR of 1.1, and a negative LR of 0.5. The sensitivity of the presence of HSI foci was 40.3%, the specificity was 91.0%, the PPV was 48.4%, and the NPV was 52.6%. The positive LR was 4.8, the negative LR was 0.7, and the overall accuracy was 68.1%. Reader (CR and MvdW) detection versus initial radiologist diagnosis is shown in Table S3.

In tests for individual prognostic diagnostic potential using the ROC-curve, no continuous variables showed an AUC $\geq$0.7. Highest AUCs were found for mean JZ thickness and JZ Max (AUC .624) (data not shown).

Table 3.3: Diagnostic Accuracy of MRI and Clinical Parameters for Histopathological Adenomyosis Diagnosis

	Histopathological Adenomyosis Diagnosis						
	Sensitivity	Specificity	PPV	NPV	PLR	NLR	Overall accuracy
MRI Overall	50.4%	66.9%	55.9%	61.8%	1.5	0.7	59.4%
Intoxications							
Smoking	38.9%	57.7%	44.3%	52.2%	0.9	1.1	49.0%
Medical History							
History of Curettage	22.1%	91.1%	67.4%	58.4%	2.5	0.9	59.7%
History of Caesarean Section	91.7%	5.2%	37.5%	50.0%	0.9	1.6	70.2%
Irregular cycle	36.1%	59.6%	45.5%	50.0%	0.9	1.1	48.3%
Hormonal medication	53.3%	51.9%	47.9%	57.3%	1.1	0.9	52.5%
Symptoms							
Dysmenorrhoea	94.1%	8.3%	49.2%	60.0%	1.0	0.7	50.0%
AUB	94.2%	11.1%	47.9%	68.8%	1.1	0.5	49.7%
Chronic Pain	97.9%	2.7%	46.3%	60.0%	1.0	0.8	46.7%
Subfertility	19.8%	75.2%	40.0%	5.9%	0.8	1.1	50.0%
Dyschezia	23.4%	67.4%	37.5%	51.2%	0.7	1.1	47.3%
Dyspareunia	72.5%	26.7%	43.1%	55.8%	1.0	1.0	46.5%
Endometriosis	53.4%	54.1%	49.3%	50.7%	1.2	0.9	53.8%
Uterine Fibroids	34.4%	58.6%	40.9%	51.7%	0.8	1.1	47.6%
MRI Features							
Mean JZmax ≥12mm	71.9%	45.5%	54.4%	64.2%	1.3	0.6	58.0%
Mean JZdiff ≥5 mm	88.6%	22.0%	52.4%	66.7%	1.1	0.5	54.8%
Mean JZ/MYO ≥.4	71.3%	29.5%	48.4%	52.6%	1.0	1.0	49.6%
HSI Foci	40.3%	91.0%	78.8%	64.8%	4.8	0.7	68.1%

PPV = Positive Predictive Value; NPV = Negative Predictive Value; PLR = Positive Likelihood Ratio;
NLR = Negative Likelihood Ratio; AUB=Abnormal Uterine Bleeding; JZmax = Maximal Junctional Zone Thickness; JZdiff = Junctional Zone Differential; JZ/MYO = Junctional Zone to Myometrium Ratio; HSI = High Signal Intensity.

Prediction of histopathological adenomyosis

Table 3.4 presents the results of both univariate and multivariate logistic regression analysis. Univariate logistic regression analysis showed p-values <.10 for: age at MRI, history of curettage, mean JZ thickness, JZ Max, JZ Diff, JZ/MYO, mean uterine volume, JZ Max ≥12 mm, JZ Diff ≥5 mm, and the presence of HSI foci. The potential predictors showed no two-way interaction; however, mean JZ thickness, JZ Max, and JZ Diff did show multicollinearity. These variables were not included in the multivariate regression model to avoid overoptimism. Nevertheless, high diagnostic performance was found for dysmenorrhoea and AUB (sensitivity/specificity >70%). Additionally, due to clinical relevance, BMI was manually forced into the multivariate model. The final model included age at MRI, BMI, history of curettage, dysmenorrhoea, AUB, mean JZ thickness, JZ Diff ≥5 mm, JZ/MYO >.40, and the presence of HSI foci. In this model, mean JZ thickness, JZ/MYO >.40 and the presence of HSI foci reached statistical significance. Preference was given to variables with the most statistical significance in univariate analysis, and the number of included variables in the model was kept to a minimum. To further correct the model for overfitting, a shrinkage factor of .747 was applied. Since LOESS already showed a good model fit for the continuous variables of interest, no modifications were necessary. The formula for the final prediction model therefore is as follows:

$$Y = \frac{1}{1 + e^{-(-3.246 + (\text{age} * .032) + (\text{BMI} * .026) + (\text{history of curettage (yes=1 no=0)} * .633) + (\text{dysmenorrhoea (yes=1 no=0)} * .073) + (\text{AUB (yes=1 no=0)} * .028) + (\text{mean JZ} * .138) + (\text{JZ Diff} \geq 5 \text{ mm (yes=1 no=0)} * .320) - \left(\frac{\text{JZ}}{\text{MYO}} > .04 \text{ (yes=1 no=0)} * 1.226\right) + (\text{HSI Foci (yes=1 no=0)} * 1.148)}}$$

Discrimination performance evaluation of this prediction model showed an AUC of .776. A sub-analysis was conducted to assess whether the clinical query presented to the pathologist affected model diagnostic performance. The pathologist was directly asked to assess for the presence of adenomyosis in 142/296 patients. Model diagnostic performance did not improve significantly when adenomyosis was specifically evaluated for (data not shown).

Calibration performance evaluation showed an observed to expected ratio of 1.2, and the Hosmer and Lemeshow test that did not reach statistical significance (p=.688).

Table 3.4: Univariate and Multivariate Logistic Regression Analysis for Histopathological Adenomyosis Diagnosis.

	Univariate analysis			Multivariate analysis		
Variable	dOR	95% CI	p-value	dOR	95% CI	p-value
Age at MRI	1.037	.997-1.079	.070	1.044	.966-1.128	.275
BMI	1.015	.972-1.059	.506	1.036	.965-1.112	.327
Intoxications						
Smoking	.868	.488-1.543	.629			
Medical History						
History of Curettage	2.904	1.462-5.770	.002	2.332	.734-7.414	.151
Gravidity	1.074	.849-1.359	.551			
Parity	1.038	.821-1.313	.753			
History of Caesarean Section	.600	.114-3.148	.546			
Irregular Cycle	.833	.450-1.543	.562			
Hormonal Medication	1.232	.737-2.058	.426			
Endometriosis	1.355	.851-2.157	.201			
Uterine Fibroids	.741	.458-1.197	.221			
Symptoms						
Dysmenorrhoea	1.455	.499-4.243	.493	1.103	.210-5.787	.907
AUB	2.025	.674-6.080	.208	1.038	.260-4.139	.958
Chronic Pain	1.295	.212-7.917	.779			
Subfertility	.749	.427-1.314	.314			
Dyschezia	.631	.318-1.250	.187			
Dyspareunia	.957	.473-1.937	.903			
MRI Features						
Mean JZ	1.132	1.061-1.207	<.001	1.203	1.040-1.392	.013
JZ Max	1.083	1.039-1.128	<.001			
JZ Diff	1.089	1.035-1.146	<.001			
Mean JZ Asymmetry	1.031	.979-1.087	.250			
Mean Wall Thickness	.997	.972-1.023	.823			
Mean Wall Asymmetry	1.004	.988-1.021	.613			
Mean JZ/MYO	4.148	1.102-15.61	.035			
Mean Uterine Length	.995	.987-1.002	.173			
Mean Uterine Volume	1.000	1.000-1.000	.043			
Adenomyosis Focus SI	1.001	1.000-1.002	.162			
SI Ratio	.936	.774-1.131	.492			
JZ Max ≥12 mm	2.138	1.268-3.605	.004			

JZ Diff ≥5 mm	2.202	1.097-4.420	.026	1.535	.441-5.351	.501
JZ/MYO >.4	1.040	.614-1.763	.883	0.194	.060-.621	.006
HSI Foci	6.850	3.568-13.148	<.001	4.650	1.857-11.648	.001

dOR= Diagnostic Odds Ratio; CI = Confidence Interval; BMI = Body Mass Index; AUB: Abnormal Uterine Bleeding; JZ = Junctional Zone; JZ Max = Maximal Junctional Zone Thickness; JZ Diff = Junctional Zone Differential; JZ/MYO = Junctional Zone to Myometrium Ratio; SI = Signal Intensity; HSI = High Signal Intensity.

DISCUSSION:

We assessed clinical and MRI parameters for their potential to predict histopathological adenomyosis diagnosis prior to hysterectomy. The resultant multivariate prediction model discriminates well between patients with and without adenomyosis (AUC 0.776). Five clinical characteristics: age at MRI, BMI, history of curettage, dysmenorrhoea, and AUB, and four primary MRI parameters: mean JZ thickness, JZ Diff ≥5 mm, JZ/MYO >.40, and the presence of HSI foci are included.

To the best of our knowledge, no comparable models for histopathological adenomyosis diagnosis based on MRI exist. Previous studies have investigated prediction of adenomyosis diagnosis based on ultrasound, with comparable accuracy (37,184,185). However, it is known that ultrasound diagnosis is highly operator dependent, with varying inter- and intra-observer variability (183,192,193). An MRI prediction model such as developed in our study thus has clinical value especially in cases where adenomyosis co-exists with other pathology (as was the case in the majority of our included patients), or is mild, or atypical.

The parameters ultimately included in this model are unsurprising when considering reported adenomyosis clinical presentation and aetiology. Dysmenorrhoea and AUB are the most frequently reported symptoms of adenomyosis (19,194) and were thus logical (and statistically significant) additions to the model. Age at MRI was further included in the model due to the known physiological increase in JZ thickness with age (46,98,195). BMI was also manually entered into the model as, despite univariate analysis showing no significant association, increased body weight and obesity have been reported as strong risk factors for adenomyosis (196).

History of curettage (after miscarriage) established itself to be an important predictor and was thus included in our model. It is debatable as to if curettage is a cause or a consequence of adenomyosis, as adenomyosis is often associated with risk of miscarriage (81). Conversely, curettage as a risk factor for the development of adenomyosis could potentially be explained by iatrogenic trauma leading to the mechanical transport of endometrial cells into the myometrium (8,10).

None of the primary MRI parameters alone were sufficient to diagnose adenomyosis conclusively, which is in line with the literature (34) . The presence of HSI foci emerged as the strongest predictor of the assessed MRI parameters ($p < .001$). Bazot et al. indeed described these foci as the only direct diagnostic criterion and almost pathognomonic for adenomyosis on MRI, although they are only detected in about half the cases (34). We also find, in agreement with recent insights into the (lack of) of diagnostic potential of JZ markers (197–199), that JZ thickness alone is not specific enough to diagnose adenomyosis on MRI. Notably in our cohort for instance, the mean maximum JZ in the non-adenomyosis cohort was already over the often reported cut-off value of 12mm (see Table 2, (45)) for adenomyosis, illustrating how attaching (too) much weight to this as a diagnostic marker is not reliable. This is further reflected in the low accuracy of MRI diagnosis overall for adenomyosis of 59.4% (see Table 3) in our cohort, for which JZ thickness >12mm was a main criterion. However, our results do suggest that the likelihood of adenomyosis increases with a larger JZ, especially if it is also irregular or proportionally takes up a large part of the total myometrium (as reflected in the markers JZ Diff and JZ/MYO ratio, see Tables 2 and 4). For this reason, it still included our model as a diagnostic marker, but without attaching a cut-off value for its general (maximum) thickness.

This study has several strengths and limitations that merit consideration. One strength of our study is that two researchers independently reviewed all pelvic MRIs blinded to the histopathology outcome. Furthermore, the proposed model was built on data of 296 patients and data driven variable selection was avoided, along with corrections for potential overfitting. Additionally, the combination of both clinical and MRI parameters makes this model easily implementable into daily clinical practice.

The present study used broad inclusion criteria, which could be interpreted as both a strength and limitation. On the one hand, inclusion of patients with comorbidities like uterine fibroids might have prevented an overestimation of diagnostic performance of the individual potential predictors. Alternatively, severe distortion of the uterus due to fibroids or endometriosis can limit the ability for complete objective assessment of all MRI parameters.
One limitation of the current study is that it was not possible to correct for the influence of the menstrual cycle on MRI parameters. Although it is known that JZ thickness changes during the menstrual cycle (46), cycle phase at time of MRI

was not reported for most of our patients. Furthermore, the choice for histopathology after hysterectomy as a reference standard introduces an element of selection bias. Potentially, our group consisted of women with more severe adenomyosis and thus may have affected the general phenotype. The present study did not conduct a central review of pathology however, and (histological) adenomyosis severity was generally not reported in pathology reports. Therefore this remains hypothetical. Similarly, future validation is needed to confirm the applicability of this model in women without indication for hysterectomy.

In clinical practice, our model could be used to calculate the risk of adenomyosis in individual patients. For example, in a 31-year-old woman with a BMI of 19 kg/m^2, without history of curettage, with complaints of both dysmenorrhoea and AUB, and an MRI with mean JZ thickness of 8.3 millimetres, a JZ Diff <5 mm, a JZ/MYO >.40, but HSI Foci (Figure 2A), the probability of adenomyosis is 14.9%. In a 35-year-old woman with a BMI of 24 kg/m^2, without history of curettage, with complaints of both dysmenorrhoea and AUB, and an MRI with a mean JZ thickness of 24.6 millimetres, a JZ Diff ≥5 mm, a JZ/MYO >.40 and HSI Foci (Figure 2B), this probability increases to 90.3%.

In conclusion, we present an MRI-based clinical prediction model for histopathological adenomyosis diagnosis. In future, this tool can be useful for both patients and clinicians, with a potential to reduce morbidity and to contribute to shared decision making. Since patient management depends on several factors, such as age, symptoms, and comorbidity, the clinical use of the predicted risks from the proposed model should still be decided on an individual basis. Thus, before steps are made for use in clinical practice, external validation of the model is needed.

CHAPTER 4:

Prediction of Adenomyosis Diagnosis based on MRI: an external validation study

Authors:
Cynthia Klaassen
Connie O.Rees
Marloes van de Wiel
Laurens van Boven
Joost Nederend
Hubertus .A.A.M. van Vliet
Massimo Mischi.
Benedictus C. Schoot

This chapter is currently submitted for publication

ABSTRACT

Introduction: Non-invasive diagnosis of adenomyosis remains challenging as there is still no consensus on diagnostic criteria. This indicates a current need for a non-invasive diagnostic tool. This study aims to externally validate a previously developed prediction model by Rees et al. to predict likelihood of histopathological adenomyosis diagnosis based on MRI

Materials and methods: This single-centre, observational, retrospective cohort study took place in a non-academic teaching hospital in the Netherlands. Patients were included if they had undergone a hysterectomy on suspicion of benign pathology between 2014 and 2022 with a pre-operative pelvic MRI. The MRIs were retrospectively assessed for adenomyosis markers. The developed model was applied to the patients in this external dataset. The prediction model utilized several clinical factors and MRI factors such as mean junctional zone (JZ) thickness, JZ Dif->5mm, JZ/myometrium ratio >0.40, and presence of high signal intensity (HSI) foci. The predictive performance of the model was assessed using the receiver operating characteristic (ROC) curve analysis and its calibration and discrimination were evaluated.

Results: Out of 195 patients, 78 patients (40%) received a diagnosis of adenomyosis based on histopathology. The previously developed model showed good external validity in this population with an Area Under the Curve (AUC) of 0.831 (95%CI 0.761 – 0.901). As for calibration, the Hosmer-Lemeshow test did not show significant difference between the predicted and observed outcome (chi-square 4.398, p = 0.820).

Conclusions: The developed model showed good to excellent discriminative performance in this external cohort in predicting the adenomyosis diagnosis based on MRI in individual patients. Given the model's accurate performance after external validation, its implementation in daily clinical practice could be considered.

Introduction

Adenomyosis is a benign uterine disorder which is defined by the existence of endometrial glands and stroma within the myometrium, initiating hypertrophy and hyperplasia of the surrounding smooth muscle cells (200). This condition can lead to detrimental symptoms, such as dysmenorrhea and infertility. Besides, adenomyosis might influence reproductive outcomes and is linked to pregnancy complications such as placental insufficiency. Adenomyosis exists in approximately 10% of the women of reproductive age and in 30 to 50% of women with infertility (81). Alongside physical complaints, a higher risk of depression and anxiety and a poorer quality of life in patients with adenomyosis have been demonstrated .

Non-invasive diagnosis of adenomyosis remains challenging. Until relatively recently, adenomyosis could only be diagnosed through histology after hysterectomy (201). This can cause diagnostic delay, since this invasive procedure is commonly performed in women in their late reproductive years (200). Clinically, the diagnosis of adenomyosis can be presumed, however it is difficult to determine due to the nonspecific symptoms and a fraction of women being asymptomatic (202). Considering the physical and mental burden and consequences of adenomyosis on women, it is absolutely valuable to diagnose this condition in a timely fashion.

Previous studies have demonstrated that adenomyosis can be diagnosed using less invasive methods, such as Magnetic Resonance Imaging (MRI) and transvaginal ultrasound (TVUS) (33,181). Although, there are TVUS diagnostic criteria available for adenomyosis diagnosis, such as the MUSA criteria, the reliability is dependent on the experience of the sonographer (30,185). Compared to TVUS, MRI is considered to be the most accurate of these methods (34). Various parameters on MRI have been investigated that can be used to characterize adenomyosis, such as junctional zone thickness, myometrial signal intensity and uterine size (33). Despite great efforts to create a non-invasive classification system for adenomyosis on MRI, there is as yet no clinically implemented tool for the prediction of adenomyosis diagnosis (16,43,203). Nevertheless, reliable imaging diagnostic classification systems are lacking and the diagnostic process of adenomyosis therefore remains a challenge (19).

For this reason, a non-invasive, internally validated diagnostic prediction model was developed in the Netherlands (204). This model predicts the histopathological diagnosis of adenomyosis based on a combination of clinical characteristics and MRI parameters prior to hysterectomy. The prediction model describes five clinical characteristics: age at MRI, BMI, history of curettage, dysmenorrhea and hypermenorrhea. Additionally, four primary MRI parameters were included in the model: mean junctional zone (JZ) thickness, JZ Differential ≥ 5 mm, Junctional Zone to Myometrium Ratio (JZ/MYO) ≥ 0.40, and the presence of High Signal Intensity (HSI) foci. Presence of HSI foci was the strongest significant predictor for adenomyosis in this model. The performance of this model showed an Area Under the Curve (AUC) after internal validation of 0.776.

This internally validated model can be useful as a prediction tool in patients with suspected adenomyosis and thereafter optimize the management of adenomyosis. The management of the disease depends on various aspects, such as comorbidities, age, impact of the complaints on daily life. Therefore, this tool can assist in shared decision making for both patients and clinicians in this management. The aim of this study was to externally validate this prediction model by Rees et al., so that this model can be clinically implemented for diagnosis of adenomyosis in the general population.

Study Objectives

The primary objective of this study was hence to perform an external validation of the multivariate diagnostic tool previously constructed by Rees et al. to predict likelihood of histopathological adenomyosis diagnosis based on MRI.

Methods

Study Design

This study was designed to be a single-centre, observational, retrospective cohort study. This geographical external validation study used data from 'Medisch Spectrum Twente (MST)' located in Enschede, a regional non-academic teaching hospital in the Netherlands.

Patient selection and Data Sources

Patients were included if they had undergone a hysterectomy on suspicion of benign pathology with a pre-operative pelvic MRI. Patients without an available pre-operative pelvic MRI were excluded. This study also excluded patients if a different MRI protocol was used and if no pathology rapport was available after hysterectomy. Furthermore, patients were excluded if they had (suspicion of) a gynaecological malignancy or if they did not want their information to be used.

The developed model included data of patients who had undergone surgery between January 2007 and January 2022. The dataset of this external validation study provided by the MST hospital included data of patients who had undergone surgery between January 2014 and January 2022. Patients were selected through screening based on electronic search queries in CTcue (CTcue BV, Amsterdam, the Netherlands) (see appendix 4A for further specification). Clinical characteristics were collected from the electronic hospital information system Healthcare Information eXchange (HiX) (ChipSoft BV, Amsterdam, the Netherlands).

Study Outcomes

The primary outcome was the histopathological diagnosis of adenomyosis after hysterectomy. Secondary outcomes included the characterisation of various MRI parameters of confirmed adenomyosis patients. Also, clinical parameters such as age, BMI, associated conditions such as endometriosis and relevant symptoms were evaluated.

Data Extraction and MRI Assessment

The imaging data were independently examined by two investigators from the Catharina Hospital Eindhoven blinded to the outcome of the pathology reports. The following baseline characteristics were retrospectively extracted

from the patient files: age at MRI and hysterectomy, BMI at MRI, history of curettage, other gynaecological or uterine pathology, treatment and clinical symptoms such as dysmenorrhea and hypermenorrhea. The following primary MRI parameters were investigated: Mean Junctional Zone (JZ) thickness, JZ Differential, JZ/MYO ratio and myometrial high signal intensity (HSI) foci. Figure 4.1 shows an illustrative example of the measuring points of the Junctional Zone (JZ). The exact definition and stratification of all measured MRI parameters are provided in Appendix B.

The diagnosis of adenomyosis was considered if any of the following factors were present: presence of HSI foci, asymmetric enlarged uterus (other than due to the existence of leiomyomas) or JZ thickness greater than 12mm. The MRI parameters were measured with the use of Synapse® Mobility version 5.7 (FUJIFILM Medical Systems U.S.A).

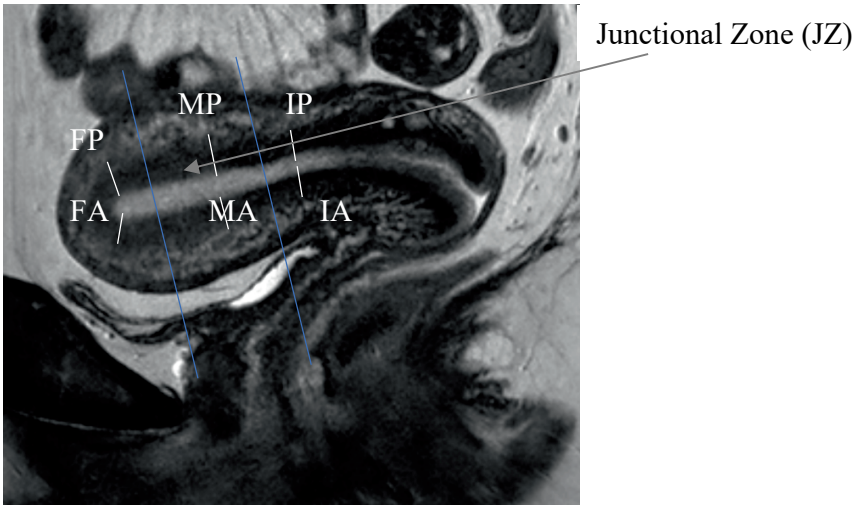

Figure 4.1. MRI of a patient in this external dataset without a histopathological diagnosis of adenomyosis. The Junctional Zone (JZ), the interface between the inner myometrium and the endometrium, was measured in six points of the uterus: fundus, mid-corpus, isthmus, measuring the anterior and posterior wall at each point.

Data management

The study utilised Research Manager (Research Manager, Deventer, the Netherlands), a secure software program, to securely store patient

information. Access to this software was restricted to only those researchers who were directly involved in the study. In order to maintain patient privacy and confidentiality, each patient was assigned an anonymised study ID, which ensured that their personal information could not be linked back to them.

MRI protocol

In the participating centre, all MRIs were carried out with a Philips 3T MRI system (Philips, Ingenia, the Netherlands). An MRI protocol other than 'cervix', 'endometriosis', 'abdomen' or 'pelvis' was excluded from this study. In almost all cases, the protocol involved acquiring T2-weighted turbo spin echo (T2-TSE) images in the sagittal, coronal and transverse planes. Also, the protocol involves acquiring a T1-weighted sequence, often using the Dixon method. In general, a slice thickness of 3-5 millimetres was used. At the MST hospital, patients did not receive any antispasmodic medication prior to MRI. When patients received multiple MRI scans prior to hysterectomy, the most recent MRI to hysterectomy was assessed.

Predictive model

A multivariate logistic regression model was developed to predict the probability of adenomyosis diagnosis (204). The final model included age and BMI at MRI, symptoms such as dysmenorrhea and abnormal uterine bleeding and several MRI features. The developed and internally validated formula for the likelihood of the histopathological diagnosis of adenomyosis was as follows:

$$Y = \frac{1}{\begin{array}{c}1+\mathrm{e}-(-3.246+(\mathrm{age}*.032)+(\mathrm{BMI}*.026)+(\mathrm{history\ of\ curettage\ (yes=1\ no=0)}*.633)+\\ (\mathrm{dysmenorrhoea\ (yes=1\ no=0)}*.073)+(\mathrm{AUB\ (yes=1\ no=0)}*.028)+(\mathrm{mean\ JZ}*.138)+\\ (\mathrm{JZ\ Diff} \geq 5\ \mathrm{mm\ (yes=1\ no=0)}*.320)-\left(\frac{\mathrm{JZ}}{\mathrm{MYO}}>.04\ \mathrm{(yes=1\ no=0)}*1.226\right)+\\ (\mathrm{HSI\ Foci\ (yes=1\ no=0)}*1.148)\end{array}}$$

Statistical analysis

The baseline characteristics of the patients with and without a histopathological adenomyosis diagnosis after hysterectomy were compared. These characteristics of the external dataset were compared with the characteristics of the original dataset. Categorical variables were reported as numbers and frequencies, and continuous variables as means with standard deviations. For group differences continuous variables were assessed using an independent t-test if they were normally distributed, and the Mann-Whitney U test if not. Categorical variables were analysed using the Chi-square test. Missing values

in the validation cohort were dealt by multiple imputation (205).

Additionally, for all possible predictive factors diagnostic accuracy was calculated to compare this with the measures of the initial study. Also, a logistic regression analysis was performed, presenting the corresponding odds ratios (OR) with their 95% confidence interval (CI). All analyses were conducted using SPSS Statistics version 28 (IBM Corp., Armonk, NY, USA). For all variables, a p-value $p < 0.05$ was considered as significant.

The model of Rees et al. was applied to the patients in the external dataset. The model performance was assessed using the receiver operating characteristic (ROC) curve and the area under the curve (AUC) (c-statistic) with their 95% CI. AUC ranges from 0.0 to 1.0. A value of >0.5 should be treated as the minimum value of AUC (206). The calibration of the model was assessed using a Hosmer and Lemeshow Test. Calibration of the models was assessed with calibration plots (207). The calibration demonstrates the relationship between the absolute predicted risks and the observed risks for the histopathological diagnosis of adenomyosis. The recommendations of both TRIPOD and STROBE guidelines were followed for reporting this external validation study (189,190). The methodology as described by Grant et al. (191) was also taken into consideration.

Ethical approval

This study was approved by the local medical ethical review board, with study number nWMO-K22-40. Due to the retrospective nature of this study, it was not deemed necessary to receive informed consent from the patients included in our study. However, if it was explicitly stated a patient medical file that they did not wish to have their information used for research purposes, they were excluded.

Results

Patient selection

Initially, 1439 potentially eligible patients were selected through screening based on electronic search queries in CTcue. Of these patients, 1244 patients were excluded after screening based on the exclusion criteria of this study. Ten patients were further excluded during the analysis of the data due to low quality of radiological imaging, only partial hysterectomy ,or pregnancy at time of MRI. The final analysis thus included data from 195 patients. The selection procedure is shown in Figure 4.2.

Figure 4.2. Study Flow Chart. MRI = Magnetic Resonance Imaging.

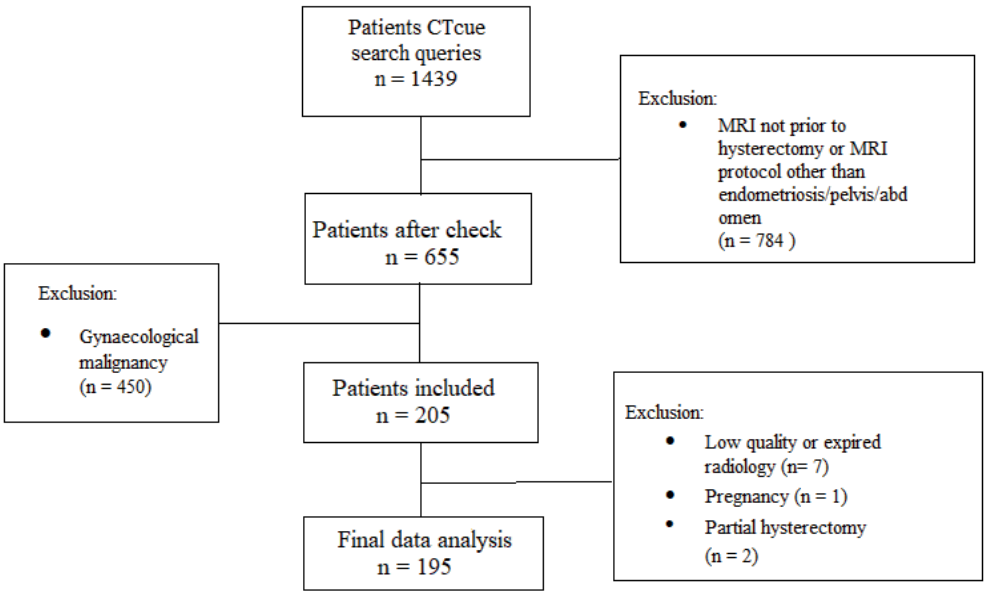

Baseline characteristics

Baseline characteristics of the external dataset are summarised in Table 4.1. Out of all included patients, 78 patients (40%) were diagnosed with adenomyosis based on histopathology. 117 patients (60%) did not receive the diagnosis of adenomyosis. In the adenomyosis group, mean age was 43.51 years (SD 7.771) and mean BMI was 27.70 kg/m2 (SD 4.715). In the patients without adenomyosis, mean age was 42.97 years (SD 9.724) and

mean BMI was 26.41 kg/m2 (SD 5.049). Patients with a histopathological diagnosis of adenomyosis more often had a history of endometriosis compared to patients without adenomyosis diagnosis (56.4% vs. 38.5%, p = 0.014). Patients with adenomyosis also had fibroids more often that patients without adenomyosis (54.7% vs. 34.6%, p = 0.006). Additionally, patients with adenomyosis were reported to have more dysmenorrhoea compared to patients without (66.2% vs. 44.3%, p = 0.011).

Table 4.1. Patient baseline characteristics.

	Histopathology: Adenomyosis (n=78)	*Histopathology: No adenomyosis (n=117)*	*P-value*
Demographics			
Age at MRI	43.51 ± 7.771	42.97 ± 9.724	0.357
BMI	27.70 ± 4.715	26.41 ± 5.049	0.076
Intoxications			
Smoking	11 (14.1%)	24 (20.5%)	0.487
Medical history			
History of curettage	10 (12.8%)	12 (10.3%)	0.579
Gravidity	2.34 ± 1.238	2.38 ± 1.237	0.816
Parity	1.61 ± 1.014	1.65 ± 1.107	0.827
History of caesarean section	17 (21.8%)	28 (23.9%)	0.889
Regular cycle	28 (35.9%)	41 (35.0%)	0.774
Hormonal medication*	35 (44.9%)	59 (50.4%)	0.447
Endometriosis ∞	44 (56.4%)	45 (38.5%)	0.014
Uterine Fibroids ∞	27 (34.6%)	64 (54.7%)	0.006
Symptoms			
Dysmenorrhea	51 (65.4%)	51 (43.6%)	0.011
AUB	27 (34.6%)	38 (32.5%)	0.932
Chronic pain	29 (37.2%)	41 (35.0%)	0.934
Subfertility	13 (16.7%)	9 (7.7%)	0.150
Dyschezia	17 (21.8%)	20 (17.1%)	0.702
Dyspareunia	23 (29.5%)	39 (33.3%)	0.818

BMI = Body Mass Index; MRI = Magnetic Resonance Imaging; AUB = Abnormal Uterine Bleeding;
*i.e., progesterone only pill, GnRH agonist, combined oral contraceptive pill, intra-uterine device with levonorgestrel.
∞ diagnosis based on MRI or laparoscopy.

MRI characteristics

MRI characteristics of the external dataset are summarised in Table 4.2. In 38 patients, it was not possible to assess the MRI features, as the researchers were unable to identify the junctional zone or the endometrium. The main reason for this was the presence of uterine fibroids, which distorted the uterine anatomy. Among the included patients, statistically significant differences were found between patients with adenomyosis versus without for mean JZ thickness (10.434 mm ±4.21 vs. 7.805mm ±2.18), maximal JZ thickness (17.765mm ± 8.57 vs. 11.553mm ±3.49), JZ differential (11.980 mm ±8.30 vs. 6.753mm ± 2.99) and mean JZ/MYO ratio (0.533 ±0.10 vs. 0.461 ± 0.11), all p <0.001. Patients with adenomyosis also more often had values above the cut-offs of maximal JZ ≥ 12 mm, JZ differential ≥ 5mm, JZ/MYO ratio >0.40, and the presence of HSI foci (all p <0.001 for each of these variables). An example of the assessment of the MRI features is shown in Figure 4.3.

Figure 4.3. Examples of the measurements of the MRI features.

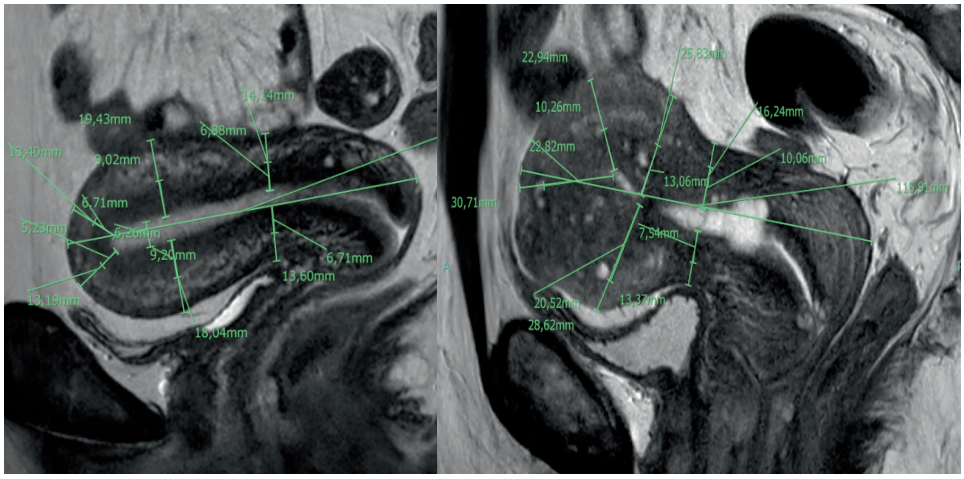

Left: a patient without the histopathological diagnosis of adenomyosis. The mean JZ was 7.3. JZ differential was 4.4, so <5mm. JZ/MYO ratio was 0.47, so >0.40. And no HSI foci were observed. **Right**: MRI measurements from the MRI of a patient with the histopathological diagnosis of adenomyosis. Mean JZ was 14.1. JZ differential was 23.4 (>5mm). JZ/MYO ratio was 0.60 (>0.40) and HSI foci were observed (white arrow shows

Table 4.2 MRI characteristics.

	Histopathology: Adenomyosis (n=78)	*Histopathology: No adenomyosis (n=117)*	*P-value*
Mean JZ (mm)	10.434 ± 4.21	7.805 ± 2.18	<0.001
JZ Max (mm)	17.765 ± 8.57	11.553 ± 3.49	<0.001
JZ Diff (mm)	11.980 ± 8.30	6.753 ± 2.99	<0.001
Mean JZ/MYO	0.533 ± 0.10	0.461 ± 0.11	<0.001
Mean JZ Asymmetry	1.290 ± 5.81	0.676 ± 1.37	0.314
Mean Wall Thickness (mm)	21.066 ± 8.87	19.448 ± 7.24	0.078
Mean Wall Asymmetry (mm)	8.563 ± 25.56	1.9352 ± 38.99	0.233
Mean Uterine Length (mm)	99.761 ± 28.30	99.680 ± 27.52	0.804
Mean Uterine Volume (mm^3)	304473.4 mm3 ± 317462.1	331939.1 ± 533134.7	0.807
Adenomyosis Focus SI	33.168 ± 27.13	19.947 ± 8.71	0.071
SI Ratio	1.9366 ± 0.87	1.809 ± 0.55	0.912
JZ Max ≥12 mm	61 (78.2%)	35 (29.9%)	<0.001
JZ Diff ≥5 mm	72 (92.3%)	67 (57.3%)	<0.001
JZ/MYO >.4	60 (76.9%)	58 (49.6%)	<0.001
HSI Foci	55 (70.5%)	6 (5.1%)	<0.001

MRI = Magnetic Resonance Imaging; JZ = Junctional Zone; JZ Max = Junctional Zone Maximum; JZ Diff = Junctional Zone Differential; JZ/MYO ratio = Junctional Zone to Myometrium Ratio; SI = Signal Intensity; HSI = High Signal Intensity;

Diagnostic accuracy

The diagnostic accuracy of various potential predictors of adenomyosis and MRI in general for the external validation group is summarized in Table 4.3. These measurements were done to compare these values of the potential predictors from both datasets. Radiology reports of MRI overall in this population had a sensitivity of 21.8%, a specificity of 91,5%, a PPV of 63.0%, a NPV of 63.7%, a positive LR of 2.6 and a negative LR of 0.9. The overall accuracy of MRI was 63.6%. The MRI feature with the best overall accuracy was presence of HSI foci (84.7%). HSI foci had a sensitivity of 70.5%, a specificity of 89.7%, a PPV of 90.2%, a NPV of 82.0%, a positive LR of 6.8 and a negative LR of 0.3.

Table 4.3. Diagnostic Accuracy of Individual Clinical and MRI variables

Histopathological adenomyosis diagnosis

	Sensitivity	*Specificity*	*PPV*	*NPV*	*PLR*	*NLR*	*Overall accuracy*
Radiology report	21.8%	91.5%	63.0%	63.7%	2.6	0.9	63.6%
Intoxications							
Smoking	14.1%	57.3%	31.4%	57.3%	0.3	1.5	51.3%
Medical history							
History of curettage	12.8%	89.7%	45.5%	60.7%	1.2	1.0	59.0%
History of caesarean section	21.8%	45.3%	37.8%	58.2%	0.4	1.7	51.5%
Regular cycle	35.9%	13.7%	40.6%	66.7%	0.4	4.7	47.3%
Hormonal medication	44.9%	49.6%	37.2%	57.4%	0.9	1.1	47.7%
Endometriosis	56.4%	61.5%	49.4%	67.9%	1.5	0.7	59.5%
Uterine Fibroids	34.6%	45.3%	29.7%	51.0%	0.6	1.4	41.0%
Symptoms							
Dysmenorrhoea	65.4%	54.7%	50.0%	71.1%	1.4	0.6	59.9%
AUB	34.6%	65.8%	41.5%	60.6%	1.0	1.0	54.2%
Chronic pain	37.2%	63.2%	41.4%	60.7%	1.0	1.0	53.6%
Subfertility	16.7%	90.6%	59.1%	62.4%	1.8	0.9	62.0%
Dyschezia	21.8%	81.2%	45.9%	61.3%	1.2	1.0	58.3%
Dyspareunia	29.5%	65.0%	37.1%	58.5%	0.8	1.1	51.6%
MRI Features							
Mean JZmax ≥12 mm	78.2%	56.4%	63.5%	82.5%	1.8	0.4	72.2%
Mean JZdiff ≥5 mm	92.3%	23.9%	51.8%	90.3%	1.2	0.3	58.8%
Mean JZ/MYO ≥0.4	76.9%	16.2%	50.8%	76.0%	0.9	1.4	55.2%
HSI foci	70.5%	89.7%	90.2%	82.0%	6.8	0.3	84.7%

MRI = Magnetic Resonance Imaging; PPV = Positive Predictive Value; NPV = Negative Predictive Value; PLR = Positive Likelihood Ratio; NLR = Negative Likelihood Ratio; AUB = Abnormal Uterine Bleeding; JZmax = Maximal Junctional Zone Thickness; JZdiff = Junctional Zone Differential; JZ/MYO = Junctional Zone to Myometrium Ratio; HSI foci = High Signal Intensity foci.

Logistic Regression Analysis

A univariate and multivariate logistic regression analysis was done to compare the predictive factors in the original study and external validation study. The results of both univariate and multivariate regression analysis are summarised in Table 4.4. In the univariate regression analysis the following variables showed p values <0.10: BMI, endometriosis, uterine fibroids, dysmenorrhea, subfertility, mean JZ, maximal JZ, JZ differential, adenomyosis focus signal

intensity (SI), maximal JZ ≥12 mm, JZ differential ≥5 mm, JZ to Myometrium ratio >0.4 and the presence of HSI foci. The multivariate logistic regression analysis of the variables included in the developed model showed statistical significance for dysmenorrhea (p=0.025), JZ Diff ≥5 mm (p=0.037) and the presence of HSI foci (p<0.001).

Table 4.4. Logistic regression analysis for histopathological adenomyosis diagnosis.

	Univariate logistic regression Odds ratio	**95% CI**	**P-value**	**Multivariate logistic regression Odds ratio**	**95% CI**	**P-value**
Demographics						
Age at MRI	1.007	0.975-1.039	0.676	1.010	0.929-1.098	0.820
BMI	1.054	0.994 – 1.117	0.079	1.036	0.937-1.146	0.486
Intoxications						
Smoking	1.000	0.999 - 1.001	0.943			
Medical history						
History of curettage	1.287	0.527-3.143	0.580	3.299	0.667-16.315	0.143
Gravidity	0.974	0.772-1.230	0.826			
Parity	0.968	0.740-1.267	0.815			
History of C-section	1.000	0.999-1.001	0.848			
Regular cycle	1.000	1.000-1.001	0.725			
Hormonal medication	0.800	0.450-1.422	0.447			
Endometriosis	2.071	1.157-3.706	0.014			
Uterine Fibroids	0.438	0.243-0.792	0.006			
Symptoms						
Dysmenorrhoea	2.462	1.353-4.479	0.003	5.927	1.250-28.097	0.025
AUB	1.094	0.596-2.010	0.772	0.576	0.167-1.982	0.381
Chronic pain	1.090	0.599-1.984	0.777			
Subfertility	2.392	0.968-5.912	0.059			
Dyschezia	1.346	0.653-2.773	0.421			

Dyspareunia	0.830	0.445-1.546	0.557			
MRI features						
Mean JZ	1.441	1.230-1.687	<0.001	1.089	0.810-1.463	0.573
JZ Max	1.352	1.218-1.500	<0.001			
JZ Diff	1.331	1.192-1.486	<0.001			
Mean JZ asymmetry	1.041	0.957-1.133	0.349			
Mean wall thickness	1.026	0.985-1.069	0.214			
Mean wall asymmetry	0.994	0.984-1.004	0.228			
Mean Uterine Length	1.000	0.990-1.011	0.984			
Mean Uterine Volume	1.000	1.000-1.000	0.696			
Adenomyosis Focus SI	1.050	0.992-1.111	0.090			
SI Ratio	1.244	0.560-2.763	0.591			
JZ Max ≥12 mm	8.216	4.036-16.726	<0.001			
JZ Diff ≥5 mm	10.030	2.913-34.530	<0.001	20.088	1.203-335.420	0.037
JZ/MYO >.4	3.276	1.222-8.783	0.018	2.801	0.303-25.875	0.364
HSI Foci	41.848	16.090-108.844	<0.001	150.644	21.627-1049.300	<0.001

CI = Confidence Interval; BMI = Body Mass Index; MRI = Magnetic Resonance Imaging; AUB = Abnormal Uterine Bleeding; JZ = Junctional Zone; JZ max = Maximal Junctional Zone; JZ diff = Junctional Zone Differential; JZ/MYO = Junctional Zone to Myometrium Ratio; SI = Signal Intensity; HSI = High Signal Intensity.

External validation

The original developed model was applied to all patients from the external dataset to evaluate the predictive performance. The predicted probabilities for the existence of adenomyosis in this external group varied from 0.14 to 0.99 (which corresponds to 14 and 99 percent respectively) and the mean of the predicted probabilities was 0.45.

The model's discriminative ability was assessed using the ROC curve, and the resulting AUC was 0.831 (95%CI 0.761 – 0.901) (see *Figure 4*). The Nagelkerke's R square for the overall performance of the model was 0.682. As for calibration, the Hosmer-Lemeshow goodness-of-fit test did not show significance (chi-square 4.398, p = 0.820).

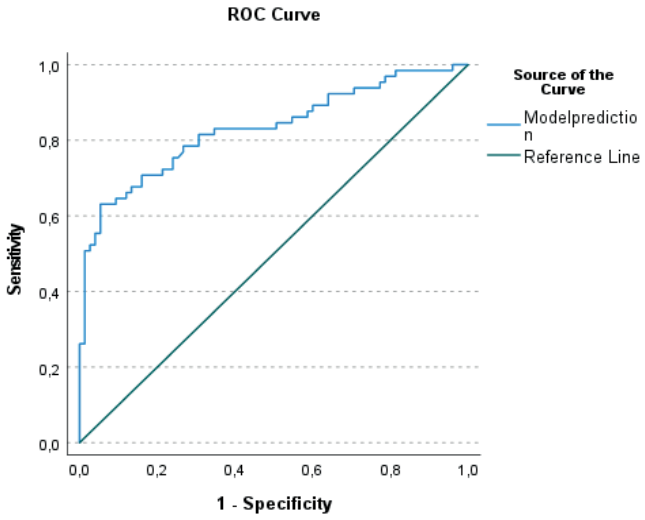

Figure 4.4. *ROC-curve external validation*. ROC-curve. The diagonal is the reference line, indicating an AUC of 0.50. A value less than 0.50 indicates the model is no better than random prediction. A value of 1.0 indicates perfect prediction. The AUC curve for this model was calculated at **0.831.**

Discussion

Non-invasive diagnosis of adenomyosis still remains challenging. Despite great efforts to create a non-invasive classification system for adenomyosis, there is as yet no clinically implemented prediction tool for MRI diagnosis and no external validation studies were performed as far as we know (16,43). Therefore, in this retrospective cohort study, we performed the first external validation of a promising developed prediction model by Rees et al. to make this model applicable for diagnosis and patient counselling in daily practice. The model was developed with a patient population from the Catharina Hospital Eindhoven in the Netherlands. An explanation for the chosen variables in this model is described in previous study (204). When applying the model to a comparable population from a different centre, the model showed good performance with an AUC of 0.831 (95%CI 0.761 – 0.901). The model was well-calibrated for our population. As in the initial study, presence of HSI foci was the most significant predictive variable.

To assess the generalisability of the developed prediction model, baseline characteristics of the external validation dataset were compared with the original dataset used in the development of the model. The age and BMI at MRI of both datasets do not show great difference, only one year or one point, which is arguably of little clinical relevance. In contrast to the initial study, this validation population did not show a statistically significant difference in a history of curettage between the groups of patients with and without a histopathological diagnosis of adenomyosis (12.8% vs. 10.3% respectively, p = 0.579). Only 22 patients in the entire external validation cohort had a history of curettage compared to 43 patients in the original dataset (22.1% in adenomyosis patients, p=0.002). A potential explanation for this difference in the prevalence of curettage could be that the surgery was completed elsewhere and thus not registered as clearly in the hospital database. The mean number of pregnancies was slightly higher in the adenomyosis group in the original dataset compared to the adenomyosis group in the external validation dataset (3.0 vs. 2.34 respectively). Despite the fact that this cohort did not show significance between the groups for history of curettage, adenomyosis has been associated with infertility and increased risk of miscarriage (81,85,208). Due to this increased miscarriage risk, women with adenomyosis may need to undergo curettage more often, which is why this was included in the model.

Additionally, in the external cohort, patients with adenomyosis more often had a history of endometriosis compared to patients without adenomyosis, as diagnosed on MRI or laparoscopy (56.4% vs. 38.5%, p=0.014). This difference was not statistically significant in the original dataset. Several studies have shown an association between adenomyosis and endometriosis. There is ongoing debate regarding if they should be seen as two separate conditions or as one disease spectrum with regard to their pathophysiological mechanisms (72,209–211). These differences in endometriosis prevalence between the datasets may have implications for the model's performance, given the clinical overlap in symptoms between endometriosis and adenomyosis, such as dysmenorrhoea.

Furthermore, in terms of symptoms, dysmenorrhoea was found to be statistically significantly between groups (66.2% vs. 44.3%, p = 0.011). Despite the fact this symptom was not significantly different in the original dataset, it was still included in the model, since dysmenorrhoea is the most commonly reported complaint in adenomyosis. The difference between the datasets can be explained by the subjective nature of this symptom. The fact that more patients had a history of endometriosis in the adenomyosis group may also contribute to this. Since the prevalence of dysmenorrhoea in the original dataset was higher in the adenomyosis group (73.3% vs. 63.1%, p = 0.491), despite not being significantly different, this may not significantly affect the model's performance however.

As for MRI characteristics, both datasets showed statistically significant differences for the same variables. It is important to note that the reliability of the JZ thickness on MRI as a predictor of adenomyosis is debatable. Several studies have reported a high reliability of the JZ thickness on MRI as predictor of adenomyosis, especially the use of a JZ thickness of >12 mm (33,47). However, recent studies suggest that JZ thickness may not be a reliable predictor for adenomyosis on its own and that symptoms and other MRI features should be weigh more heavily in adenomyosis (29,45,198). This was taken into account in the initial study. As a result, several factors were included in the model. Moreover, as in initial study, the presence of HSI foci was the strongest predictive MRI feature in this study. This is in accordance with previous studies that describe these HSI foci as main indicator for

adenomyosis (12,34,212). Overall, differences in baseline characteristics between the two datasets highlight the need for external validation studies to confirm the generalizability and reliability of the prediction model

Furthermore, the diagnostic accuracy of radiology reports of the MRIs in our population is warrants attention. In this external validation study, the diagnostic accuracy of radiology reports for MRIs was found to be 63.6%. Similarly, the internal validation study showed an overall diagnostic accuracy of 59.4% for the radiology reports (204). These percentages of diagnostic accuracy appear to be suboptimal compared to commonly reported values in literature (97). It is possible that the radiologists did not actively assess for adenomyosis if it was explicitly requested in the MRI application. A potential solution could be to involve gynaecologists in the assessment of the MRI parameters that are required for the model, and in the assessment of pelvic MRIs in general. This could enhance the efficiency of the process, as conducting the measurements required for this model can be learned and completed in a relatively short period of time.

The developed model showed good performance in the original dataset with an AUC of 0.776. After external validation, the performance of the model reached an AUC of 0.831, which indicates that the model has good to excellent discriminative ability. This means that the model is able to predict with high accuracy which patients are more likely to have histopathological adenomyosis (207). Typically, the performance of a logistic prediction model is better on the original dataset than the performance of this model on a new dataset . Patient selection for the developed dataset was between 2007 to 2022, while patient selection for the external dataset was between 2014 to 2022. This more recent patient cohort could be an explanation for the slightly better model performance in the external validation group. The general quality of the MRIs could have been better because they were more recent. Moreover, potentially the recognition of adenomyosis by the pathologist may have increased in recent years. This study also found a higher prevalence of uterine fibroids in the group without the diagnosis of adenomyosis compared to the adenomyosis group. This greater presence of uterine fibroids may have created a more homogenous group and contributed to the model's ability to better distinguish between these two groups. However, it is important to note that this is only a hypothesis.

As for calibration of the model, the Hosmer-Lemeshow goodness-of-fit test did not reach significance (chi-square 4.398, p = 0.820). This suggests that the model is a good fit for the data, and that the observed frequencies are not significantly different from the expected frequencies based on the model (Hosmer et al., 2013).

Since no clinically implemented tool for the diagnosis of adenomyosis on MRI is yet available, this study represents one of the first external validation studies. The fact that two investigators (one of them directly involved in the internally validation study) independently assessed all MRIs blinded to the outcome of the pathology reports, is a strength of this study. Besides, this external validation can be seen as a geographical validation, because the participating hospitals for both studies were in different regions of the country, which is considered a reliable approach for external validation (207). Also, the model is plausible to use in daily practice due to the straightforward clinical and MRI parameters.

A limitation of the study is the fact that it only consists of 195 included patients. 78 patients (40%) received the histopathological diagnosis of adenomyosis. Studies suggest that at least a number of 100 events (so in this case 100 patients with the diagnosis of adenomyosis) and 100 non-events are needed for reliable evaluation of a model's external performance (190,213). To detect smaller differences in performance of the model, larger sample sizes (at least 100 events) are needed. In small(er) datasets the model could be overoptimistic (213).

As in the initial cohort, in this cohort the phase of the menstrual cycle at the time of MRI was never reported. The thickness of the junctional zone changes during the menstrual cycle due to hormone levels (46,214). This is a limitation of the entire study, because both studies were unable to correct for the influence of the phase of the menstrual cycle due to it not being reported.

Another point of discussion could be that this model is tested only in patients who underwent hysterectomy. This may introduce selection bias, as it limits the generalisability of the model to patients undergoing a hysterectomy, and not

to all patient suspected of adenomyosis in general. Potentially, our study population consists of patients with more severe complaints who therefore undergo an MRI and hysterectomy.

This model could be used in clinical practice to predict the chance of adenomyosis in an individual patient. A notable issue with using the model is that the interpretation of outcome percentages varies by individual. Some patients may find a chance of 40 percent high, while another patient only desires to start a particular treatment at a 70 percent chance for example. Therefore, a cut-off value should be discussed.

Future research should perform an external validation in a larger cohort to confirm the model's generalisability and performance in different settings. Further investigation of the clinical usefulness and impact of the model in daily practice is also needed.

Conclusions

In conclusion, the developed model showed good to excellent discriminative performance in this external cohort for predicting the adenomyosis diagnosis based on MRI in individual patients. The model could be used in clinical practice and could aid in shared decision-making of the subsequent management of this disease, in conjunction with other tests and clinical information. It may be beneficial to involve gynaecologists in assessing the MRI parameters needed for the prediction model, given the suboptimal diagnostic accuracy of radiology reports in detecting adenomyosis. This could enhance the reliability of the diagnostic process. Larger (prospective) are needed before utilizing this model in daily practice.

PART III

Effect of Adenomyosis on Uterine Contractile Function

CHAPTER 5:

Characterisation of Uterine Peristaltic Waves by Ultrasound Strain Analysis

Authors:
Yizhou Huang
Connie O. Rees
Federica Sammali
Celine Blank
Benedictus C. Schoot
Massimo Mischi

The content of this chapter has been published in the *IEEE Transactions on Ultrasonics, Ferroelectrics, and Frequency Control*, issue 69 vol. 6, pages 2050-2060.
DOI: 10.1109/TUFFC.2022.3165688

Abstract:
Uterine peristalsis (UP) is a wavelike uterine motion that plays an important role in the generation of intrauterine streams for menstrual emptying and to support embryo implantation. Our understanding of uterine mechanical behaviour is hampered by a lack of quantitative analysis. Here, we propose a spatiotemporal analysis of UP by ultrasound speckle tracking and dedicated strain analysis. We aim at characterizing UP propagating around the endometrial cavity through the anterior and posterior walls of the uterus. To this end, velocity and coordination features are proposed in this study. We investigated a total of 11 healthy volunteers during their natural menstrual cycle and 81 patients undergoing in vitro fertilization (IVF) treatment. They all received multiple 4-minute 2-D transvaginal ultrasound scans. Significant differences in propagation velocity were found among different phases of the menstrual cycle, which are in line with the expected uterine behaviour. A significant difference in coordination was found between the group of women with successful (pregnancy at 11 weeks) and unsuccessful IVF. This result suggests that the ability to generate coordinated UP represents an important factor for IVF success. The proposed UP quantification may represent a valuable clinical tool for improved understanding of UP and improved decision-making in the context of IVF procedures.

INTRODUCTION:

Worldwide, approximately one in six couples experiences infertility during their reproductive ages (from 20 to 44 years old) [1]. Most women with (sub)fertility problems seek clinical support from assisted reproductive technologies, such as in vitro fertilization (IVF). In the last decade, the number of IVF cycles performed every year has increased by over 20% [2], [3]. However, the success rate of IVF treatment remains below 30%, with only a 4% increase [2], [3]. An IVF cycle consists of the preparation of the patient with exogenous hormones, after which the developed oocytes (eggs) are retrieved from the ovarian follicles and fertilized in vitro. The resulting embryos are then transferred back into the uterine cavity. Subsequent successful implantation of the embryo in the uterine wall leads to pregnancy. Several studies indicate that dysfunction of uterine contractility is one of the possible reasons hampering successful embryo implantation [4]–[7].

The uterine body consists of three parts: an outer serosal layer, an inner lining called endometrium, and an intermediate muscle layer called the myometrium (see Figure 5.1). Uterine contraction of a nonpregnant uterus, which refers to the shortening of the uterine muscle, was first mentioned in 1937 by Dickinson based on bimanual palpation [8]. Uterine contraction is reported to mostly occur around the endometrium, acting as a wave propagating alongside the endometrium. The resulting rhythmic uterine deformation (motion) is also known as uterine peristalsis (UP) [7]. Due to the influence of hormone levels, the UP patterns change in terms of direction, frequency, velocity, and amplitude during different phases of the menstrual cycle. In particular, during the luteal phase, when opposing contraction waves are often generated to keep the embryos inside the endometrial cavity and facilitate their implantation. Women suffering from infertility problems are also likely to suffer from uterine disorders, such as endometriosis and adenomyosis, or endocrine disbalances, which can affect UP and hamper embryo implantation. Therefore, a reliable assessment of the uterine activity outside pregnancy can be expected to provide valuable insight into the influence of UP on IVF failure.

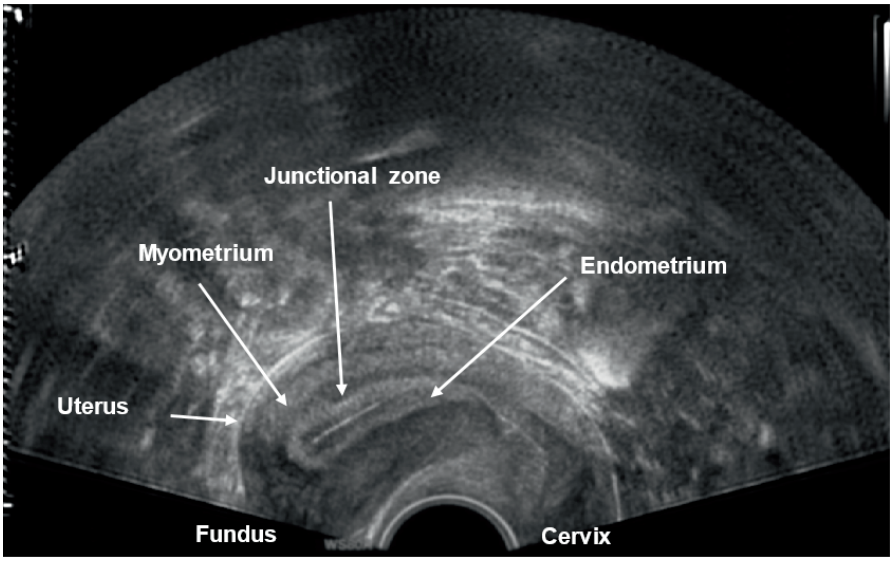

Figure 5.1: Example of acquired US frame from an in-vivo recording during the late follicular phase.

Currently, most studies on the assessment and characterization of UP are based on qualitative measurements by visual inspection of transvaginal ultrasound (TVUS) recordings [7], [9]–[11], [12]. Visual characterization of the uterine activity in this manner is rather challenging and subjective, especially during the late luteal (LL) phase of the menstrual cycle, or right before embryo transfer (ET) during IVF treatment, when the uterus is expected to be more quiet compared to the other phases. A recent study shows that three medical professionals share only mild agreement on the direction and timing of UP by visual inspection of 80 TVUS recordings [13]. The lack of an objective and quantitative analysis of uterine contractility thus limits the ability to characterize UP and improve the success of IVF treatment. Following up on our recent work on dedicated ultrasound (US) speckle tracking for quantitative analysis of uterine motion [14], this article presents a quantitative assessment of the uterine activity focusing on the propagation of UP during a natural menstrual cycle as well as during an IVF cycle. In particular, velocity, direction, and coordination of UP are assessed.

To quantify UP, uterine motion throughout the US recording must first be assessed. In the field of US-based speckle tracking, there are two major approaches to estimate motion, namely, block matching (BM) and optical flow

(OF). BM segments the image into blocks and seeks the best matches of these blocks in subsequent frames based on a chosen matching criterion. On the other hand, OF is a pixel-to-pixel gradient approach that estimates the velocity of the target object between two subsequent frames. In our study, OF is chosen over BM due to its higher sensitivity to subpixel motion [15]. Moreover, as introduced by Bouguet [16], the tracking accuracy of OF can be further improved by implementing iterative spatial warping. The adopted OF method was first optimized and validated in vitro using a dedicated setup with human ex vivo uteri [17].

For each TVUS recording, tracking markers (TMs) were manually placed along both the anterior and posterior walls of the endometrium (see Figure 5.2). The TMs were always positioned starting 5 mm from the fundal extremity of the endometrium and moving toward the cervix, spaced 2.5 mm from each other. Movements of these TMs were tracked over time. Radial strain rates (RSRs) were derived between each pair of TMs to generate a time–space representation of UP along the endometrium. Relevant features, such as UP velocity, direction, and coordination, were then extracted from the resulting time–space representation.

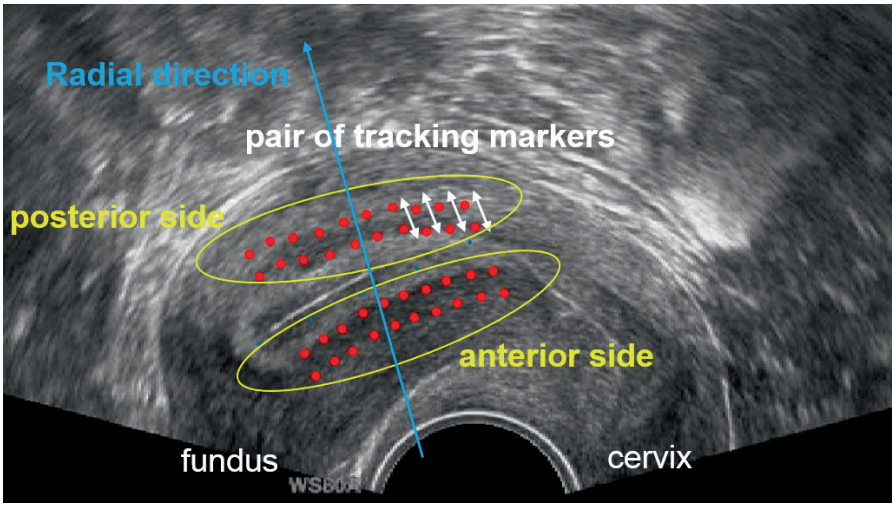

Figure 5.2 Tracking marker grid (red dots) positioning along the anterior and posterior walls of the endometrium. TVUS recording acquired from a healthy volunteer during the LF phase.

In vivo validation was carried out to test the feasibility of our proposed method. Healthy volunteers underwent four TVUS scans acquired during four selected phases of the natural menstrual cycle, namely, during menstruation (Menses), LF, early luteal (EL), and LL phases. The proposed method was evaluated for its ability to distinguish the peristaltic patterns among the selected phases.

The method was also evaluated in the context of IVF. TVUS recordings were performed on 81 patients during an IVF treatment cycle. Our validation aimed at testing the ability of the proposed UP features to predict the successful and unsuccessful pregnancy groups before ET into the uterine cavity.

Methodology

A. Data Acquisition

In this study, US acquisitions on 11 healthy volunteers (age: 31.2 ± 5.2 years; body mass index (BMI): 22.6 ± 2.3 kg/m2) were performed at the Catharina Hospital Eindhoven (Eindhoven, The Netherlands) [18]. These healthy volunteers underwent two subsequent 4-min TVUS B-mode scans using a Samsung-Medison WS80A scanner equipped with a V5-9 transvaginal probe during Menses, LF, EL, and LL phases.

In addition, US acquisitions in women undergoing IVF were collected from two studies. From the IMPLANT 1 study [19], aiming at testing inhibitors of the uterine activity, US recordings in 65 control patients (age: 31.4 ± 3.1 years; BMI: 23.4 ± 4.1 kg/m2) receiving placebo were collected. These patients underwent fresh day-3 ET with one or two embryos, one of which being of good quality according to the Istanbul conference Alpha criteria [20]. They had history of no more than one failed IVF cycle and used a gonadotropin-releasing hormone (GnRH) antagonist protocol with a single injection of human chorionic gonadotropin (HCG) for triggering ovulation. Being part of the control (placebo) group, the uterine activity was influenced by injected hormones only. For all patients, 4-min B-mode TVUS recordings were acquired 4 h before ET. Being a multi-centre study, various brands of ultrasound scanners and probes were used. More details on the patient enrolment and IVF protocol can be found in [19].

At Ghent University Hospital, 4-min B-mode TVUS recordings were acquired 1 h before ET in 16 patients (age: 32.1 ± 4.7 years; BMI: 25.9 ± 4.7 kg/m2) undergoing day 5 ET with the single ET based on the Istanbul conference definition [20]. The enrolled patients received GnRH for follicle stimulation and HCG injection 34–36 h before oocytes retrieval. The 4-min B-mode TVUS recordings were acquired 1 h before ET using Samsung-Medison WS80A scanner equipped with a V5-9 transvaginal probe. More details can be found in [21].

The IMPLANT 1 study was retrospective, while the Catharina Hospital and Ghent University Hospital studies were prospective, with the sonographers being properly instructed on the imaging requirements for this study.

The acquisition frame rate ranged from 25 to 30 frames/s. All the recordings were converted to audio video interleave (AVI) format for further analysis.

Due to motion artifacts during insertion and positioning of the probe in the uterine cavity as well as during its removal, the time length for all 2-D recordings was shortened to 3 min by cropping a certain part of the recording in the beginning and at the end.

B. Ultrasound Speckle Tracking

US speckle is caused by the interference of the backscatter US waves received by the transducer. Tissue forms a unique speckle pattern that can be tracked over time. Therefore, tissue motion can be assessed by tracking the movement of the speckle pattern. The highest endometrial wave velocity is less than 2 mm/s [10]. Therefore, with an acquisition frame rate and pixel size equal to 30 Hz and 0.065 mm, respectively, uterine motion between subsequent frames was smaller than one pixel. To deal with such subpixel motion and provide accurate tracking results, OF was employed to perform speckle tracking in this study. With I being the intensity of a certain pixel, the pixel velocities in the x - and y -directions, v_x and v_y , are thus represented by the intensity gradients in the spatial (x,y) and temporal (t) domains according to

$$v\_x \ \partial I/\partial x \ + v\_y \ \partial I/\partial y \ + \partial I/\partial t \ = 0$$

To solve the above ill-conditioned equation, Lukas and Kanade [22] proposed to estimate the motion of a block instead of a pixel under the assumption of constant flow within the block. The velocities in both directions are then obtained by least square estimation. After that, the pixel location in the target frame is updated according to the estimated velocities.

The accuracy of OF can be further improved by applying an iterative refinement approach under the assumption of small motion [16]. In this study, OF was first applied to track the motion of a selected speckle pattern between the reference frame and the target frame. Based on an initial estimation $\underline{v_1}$, the target frame was warped by the 2-D interpolation. In this way, the movement of the speckle pattern was partly retrieved between the reference and the target frames. In the following second iteration, a new estimation of residual motion, $\underline{v_2}$, was derived between the reference and the warped target frames. This process was applied iteratively until the residual motion $\underline{v_n}$ converged to a very small value or it reached the maximum number of

iterations M . The final estimation of the pixel motion, $\underline{v}_{end}$, was then calculated as the sum of the initial motion and all residual motions:

$$v_{end} = \sum_{iter=1}^{M} v_{iter}$$

Apart from applying this iterative refinement, the choice of the block size is also crucial for OF to obtain accurate tracking results. For small blocks, the tracking becomes sensitive to local motion and noise, while for large blocks, the hypothesis of constant flow may be violated. The optimization of the block size was carried out ex vivo using the dedicated experimental procedure proposed in [17]. The optimized block size resulted to be 41×41 pixels^2 (around 2.6×2.6 mm^2).

C. Anatomical Strain Framework

UP is often observed close to the endometrium, in the junctional zone, rather than in the myometrium [23]. TMs were therefore selected along both the anterior and posterior walls of the endometrial cavity at the first frame of each TVUS recording.

A semiautomatic approach was employed to maintain the same distance between each pair of neighbouring TMs both in the radial and longitudinal directions (see Figure 5.2). In this study, the distance was chosen corresponding to the optimal block size.

Out-of-plane (OOP) motion is a frequent phenomenon during in vivo 2-D TVUS acquisition. The occurrence of OOP motion is mainly caused by the movement of the imaged target in the 3-D perpendicular to the observation plane. Sometimes, it might also be caused by the influence of probe motion and patient movement. Once OOP motion occurs, the speckle pattern being tracked moves out of the observation plane. The resulting decorrelation of the speckle pattern will lead to speckle tracking errors. To mitigate the influence of OOP motion on the accuracy of 2-D speckle tracking with in vivo data, we proposed a two-step approach.

In the first step, the middle lining of the endometrium was manually drawn and ten *TMs* ($TMs_{midline}$) with isotropic distance were generated along the middle lining (see Figure 5.3a); speckle tracking was applied to the $TMs_{midline}$ through the entire recording. We estimated the global translation of the endometrium

(x_n, y_n) for each frame *n* by averaging the movement of $TMs_{midline}$ in the horizontal and vertical directions. After that, we estimated the rotation of the endometrium (θ_n) by linear fitting based on the coordinates of $TMs_{midline}$ [see Figure 5.3(b)]. In this way, even if part of the endometrium was affected by OOP motion, the global translation and rotation could still be recovered from the rest of $TMs_{midline}$, which were not affected by OOP motion.

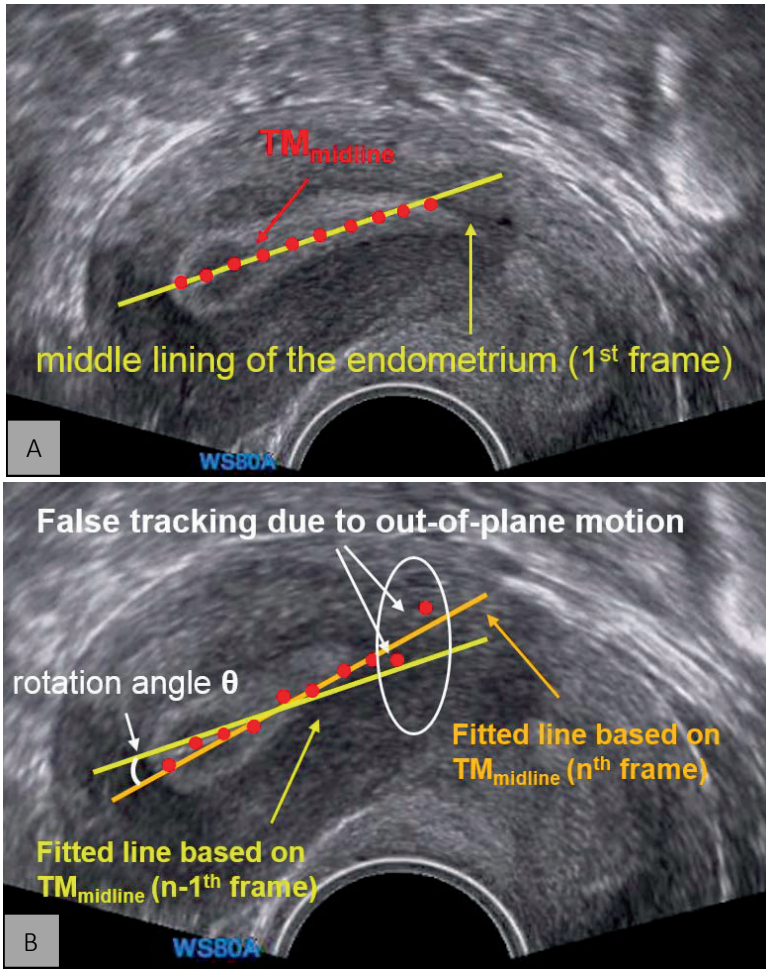

Figure 5.3. A. Ten $TMs_{midline}$ selected along the middle lining of the endometrium. **B.** OOP motion started from the nth frame. Although speckle tracking failed with two *TMs* (indicated with white arrow), the global rotation of the endometrium could still be recovered by the fit lines between the subsequent frames.

Once the global translation (x_n, y_n)and rotation (θ_n) of the endometrium were obtained through the entire recording, the coordinates of the TMs were updated for each frame *n* as:

$$\begin{bmatrix} X_n \\ Y_n \end{bmatrix} = \begin{bmatrix} \cos\theta_n & -\sin\theta_n \\ \sin\theta_n & \cos\theta_n \end{bmatrix} \times \begin{bmatrix} X_{n-1} \\ Y_{n-1} \end{bmatrix} + \begin{bmatrix} x_n \\ y_n \end{bmatrix}$$

$$n=2,\ldots\ldots, N \qquad (2)$$

where *N* is the total number of frames and (X_1, Y_1) represents the coordinates of the TMs selected in the first frame, relative to the uterine anatomy.

A quantitative measure was introduced to evaluate the quality of the TVUS recordings. Pierson correlation coefficient (PCC) was here used to test the similarity of the speckle patterns between the subsequent frames [24]. The quality of the recording was then determined by the average PCC over all TMs. Recordings with an average PCC >0.8, indicating negligible speckle decorrelation due to OOP motion in subsequent frames, were accepted for further analysis.

In the second step, speckle tracking was then applied to TMs. For example, to estimate motion between the $(n-1)$th and the *n*th frames, instead of updating the coordinates of TMs based on their displacements, the coordinates were updated to (X_n, Y_n) according to (2). As a result, speckle tracking is applied only between two subsequent frames. In this way, even if OOP motion caused decorrelation and poor tracking, the tracking error remains limited between two frames without further accumulation. With this approach, tracking is performed for TMs representing consistent anatomical regions, enabling further interpretation of the results as associated with the uterine anatomy and geometry.

The author was blinded to the acquisition characteristics, such as the success of IVF treatment and the menstrual phases when positioning the TMs.

D. Radial Strain Rate Analysis

Strain rate imaging is one of the most widely used approaches for measuring regional or global deformation of the muscle. Therefore, to characterize UP, RSR was derived from both the anterior and posterior walls of the endometrium.

RSR was calculated from the ratio between the variations in the distance between each pair of TMs in the radial direction (see Figure 2) and their original distance, which is given as:

$$RSR_n = \frac{\sqrt{(v_{x1} - v_{x2})^2 + (v_{y1} - v_{y2})^2}}{D_{n-1}} \qquad n=2,\ldots\ldots, N \qquad (3)$$

where (v_{x1}, v_{y1}) and (v_{x2}, v_{y2}) represent the estimated velocities in the *x*- and *y*-directions from the chosen pair of TMs between the $(n-1)$th and the nth frames, D_{n-1} represents the absolute distance between the chosen pair of TMs at the $(n-1)$th frame, and N is the total number of frames in the recording. Because of the framework introduced in (2), D_{n-1} remains equal to D_1 . As a result, (3) provides an estimate that is related to the Lagrangian strain.

From our observations, UP was not the only source of motion influencing the movement of the endometrium in TVUS recordings. Other motions, either coming from different organs, such as bowels and bladder, or caused by heartbeat, respiration, and probe movement during the acquisition, were all recorded during the US scan. Therefore, a bandpass filter was applied to the RSR signals to remove the interference from these undesired motion sources.

From the literature, UP during a normal menstrual cycle varies from 0.5 to 4.1 contractions per minute [25], while during IVF treatment, UP appears to show higher frequencies due to the ovarian stimulation, resulting in a range from 0.5 to 5 contractions per minute [12], [26]. The cut-off frequencies of the bandpass filter were therefore set according to the literature based on the application.

E. Feature Extraction

In this study, we focused on analysing the velocity, direction, and coordination of the UP, which might have a direct impact on the success of pregnancy.

Based on the RSR signals, we created a time–space representation of the UP waves propagating along with the endometrium, as shown in Figure 5.4A and B. The RSR signals are aligned in space from the cervix to fundus (y -axis) based on the distance between each pair of TMs. The x -axis represents the time evolution of RSR signals, and the colour code represents the value of the RSR signals. Positive RSR, shown in yellow, indicates uterine relaxation, while

negative RSR, shown in blue, indicates uterine contraction. Clear UP propagation from cervix to fundus (C2F) and from fundus to cervix (F2C) can be observed in Figure. 4A and B, respectively.

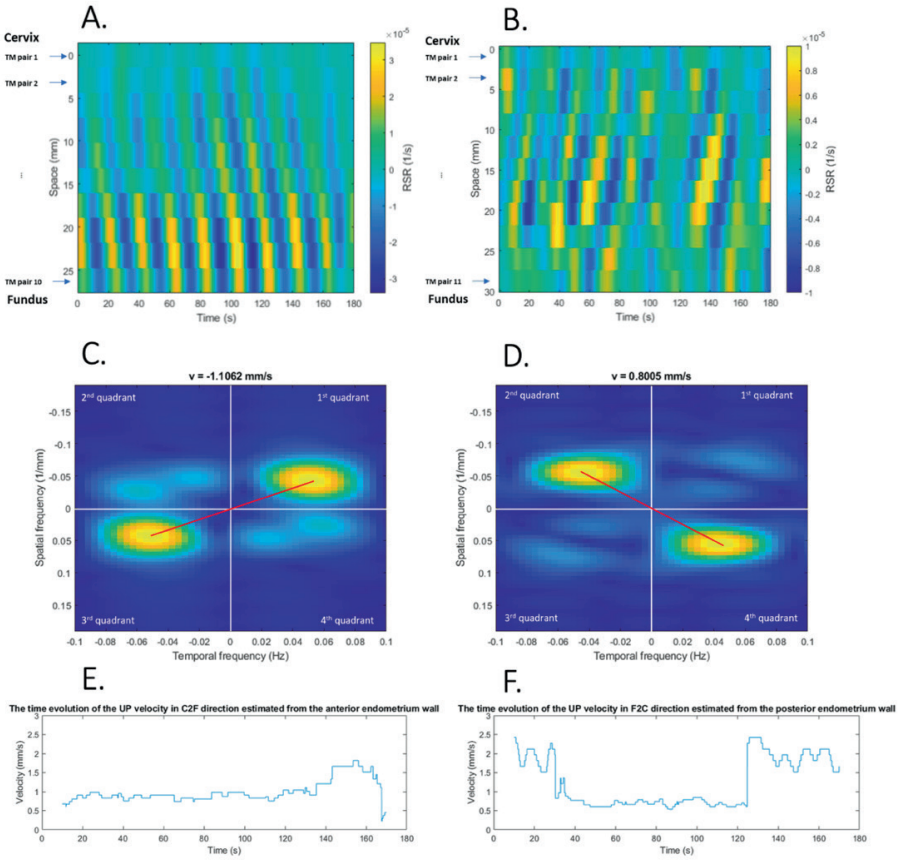

Figure 5.4.

A. UP time–space representation based on the RSR extracted from the anterior wall of the endometrium from a healthy volunteer. This plot shows clear propagation C2F. **B.** UP time–space representation based on the RSR extracted from the posterior wall of the endometrium from a healthy volunteer. This plot presents the F2C propagation. **C.** Corresponding k -space representation of (a): dominant spectral peaks (marked with red points) are present in the first and third quadrant representing C2F propagation. **D.** Corresponding k -space representation of B: dominant spectral peaks (marked with red points) are present in the second and fourth quadrant representing F2C propagation. **E.** Time evolution of the UP velocity in the C2F direction estimated from A. **F.** Time evolution of the UP velocity in the F2C direction estimated from B.

1) UP Velocity:

A moving window, including 600 frames (20s), was applied to segment the time–space representation over time. This duration allows including at least one full UP wave cycle in the time window. Within each segment, 2-D fast Fourier transform was applied to the time–space representation, providing a frequency representation in the *k* -space domain. UP velocities in both C2F and F2C directions can be explicitly estimated from the peaks in the first quadrant (representing C2F propagation) and the second quadrant (representing F2C propagation) of the *k* -space.

Figure 4A and B shows the frequency representations of Figure 4A and B within one of the moving windows (*t* = 40 –60s). The evolution of UP velocities in both directions is shown in Figure 4E and F.

The temporal and spatial frequencies of the dominant peristaltic motion were identified at the peaks of the spectrum. The corresponding UP velocity, v_{UP} , was then calculated as the ratio between the temporal frequency, f_t , and spatial frequency, f_x as:

$$v_{UP} = \frac{f_t}{f_x} \qquad (4)$$

2) UP Direction:

Theoretically, the direction of the propagation can be determined by the sign of v_{UP} . Propagation from C2F is here indicated by a positive sign, while propagation from F2C is indicated by a negative sign. However, as discussed in [9] and [11], more complex UP patterns can also be observed. Opposing propagation, which shows both C2F and F2C propagation, is often observed after ovulation to support embryo implantation; recoiling propagation, which consists of reflection and superposition of multiple peristaltic waves, can also be observed, as well as more complex propagation. Figure 5A shows an example of a complex propagation pattern during the EL phase.

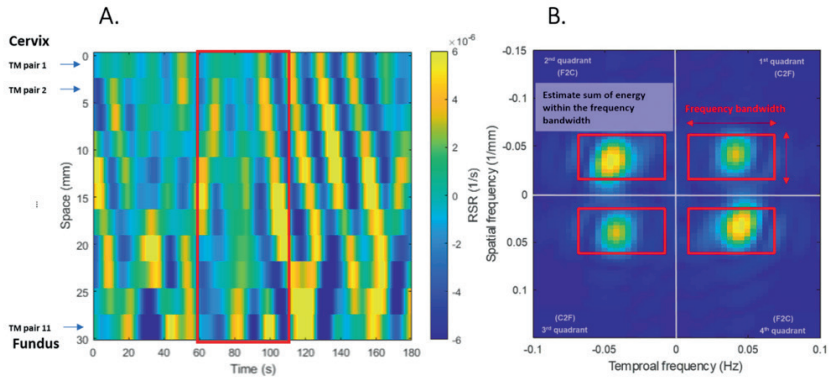

Figure 5.5. A. Time–space representation of a complex UP pattern. The direction of UP propagation changes from F2C to C2F during the acquisition (highlighted in the red area). **B.** *K*-space representation of the UP. The sum of the spectral energies estimated within the physiological bandwidth from the first and third quadrants represents the energy of C2F propagation; the sum of the spectral energies estimated within the physiological bandwidth from the second and fourth quadrants represents the energy of F2C propagation.

Simple binary classification based on the sign of v_{UP} is not suitable when a complex propagation pattern occurs. Therefore, we propose an energy ratio (ER) metrics, where the sum of spectral energies is estimated from the first quadrant ($E1$) and the second quadrant ($E2$), representing the energy of C2F and F2C propagation, respectively (see Figure 5.5B). This is given as:

$$ER = 2 \times \frac{E1}{E1 + E2} - 1 \quad (5)$$

The parameter ER is comprised between −1 and 1. In this study, we conventionally assumed ER > 0.1 to indicate C2F propagation and otherwise for ER <−0.1 . ER around zero indicates the presence of opposing or "standing" waves.

To estimate the global propagation direction, E1 and E2 were estimated on the full recording rather than within the moving window adopted for the estimation of the UP velocity.

F. UP Coordination

The fact that locally, e.g., along the anterior or posterior wall, UP shows a dominant direction, does not guarantee an effective peristaltic movement that is coordinated and generates microstreaming in the endometrial cavity. Simply focusing on the anterior and posterior walls, coordinated, effective peristalsis requires UP propagation on both sides of the endometrium to show the same direction at the same time. Especially before ovulation, muscles from both sides of the endometrium have to produce coordinated contractions to support sperm transport from the vagina to the fallopian tubes, where fertilization occurs [25], [27].

Similar time evolution of the ER is expected from both the anterior (ER_{ant}) and posterior (ER_{pos}) walls of the endometrium that are expected. Similarity measures, namely, cross correlation (CC), mean squared error (MSE), and Hausdorff distance (Hd) [17], [28], were therefore employed as cost functions to assess the spatiotemporal coordination of the UP.

Validation Strategy

In vitro and in vivo validations were performed to test the ability of the proposed method to measure and characterise UP. In vitro, we optimized the parameterization and verified the accuracy of the OF with the data acquired by a dedicated setup with an ex vivo uterus introduced in [17]. In vivo, the proposed method was validated with TVUS recordings acquired in healthy volunteers during their normal menstrual cycle and in patients undergoing IVF treatment.

A. Validation in Healthy Volunteers

According to previous studies [9], [25], the uterus presents different behaviour in different phases of the menstrual cycle, showing different contraction frequencies and velocities. Therefore, we validated our proposed method for its ability to characterize and distinguish different UP patterns along the natural menstrual cycle.

Feature Extraction:

After deriving the RSR from the tracking results, UP velocities in both C2F and F2C directions were calculated inside the moving window. After that, median velocities (MVs) in C2F and F2C directions were calculated by averaging velocities over time in the corresponding directions. The MSE, CC, and Hd between ER_{ant} and ER_{pos} were also estimated from each RSR signal to assess the UP coordination in each phase. The global propagation direction represented by ER metric was explicitly calculated on the full recording without the moving window.

Intra-observer and Inter-observer Study:

To validate the reproducibility of our method, we conducted an intra-observer study. The TMs were positioned by the same operator in two subsequent 4-min recordings acquired from the same healthy volunteer.

To further analyse the intra-observer variability, the TMs were positioned three times by the same operator in the same set of recordings. In addition, two clinicians were also asked to place the TMs on the same set of recordings to perform an interobserver variability test after a 10-min training.

Intraclass coefficient (ICC) was used to determine the agreement between the features extracted from different measurements.

ICC was calculated by using IBM SPSS Statistics 27. A two-way mixed model with index type of absolute agreement was employed to verify the reliability of our measures on UP velocities and coordination. ICC > 0.5 was considered as moderate agreement, ICC > 0.75 was considered a good agreement, and ICC > 0.9 was considered an excellent agreement [29].

Statistical Analysis:
It was performed using MATLAB 2018b. The Shapiro–Wilk test was first applied to test the normality of the distributions. A one-way analysis of variance test with Duncan test as post hoc (in case of Gaussian distribution) or Kruskal–Wallis test with Dunn–Sidak test as post hoc (in case of non-Gaussian distribution) was applied. MV, as well as the coordination features CC and MSE, was tested to discriminate among the four selected phases. A p -value < 0.05 was considered statistically significant.

B. Validation in IVF Patients

Validation in IVF patients aimed at testing the ability of the extracted features to distinguish between the successful and unsuccessful groups following IVF. Features that can establish significant differences between the two groups can be considered as predictors of successful IVF treatment. In all patients, only top-quality embryos, according to morphological analysis, were transferred.

Feature Extraction:
The MV of the UP in both C2F and F2C directions, as well as the coordination between ER_{ant} and ER_{pos} by CC, MSE, and Hd, was calculated from each RSR signal in each patient.

Statistical Analysis:
Double-tailed Student's t -test (in case of Gaussian distribution) or Wilcoxon rank-sum test (in case of non-Gaussian distribution) was used. A p-value < 0.05 was considered statistically significant.

Results

All results are reported in the format of median (quartiles 1–3).

A. Validation in Healthy Volunteers

Forty-four TVUS recordings from 11 healthy volunteers during the four different phases of the menstrual cycle were originally planned. However, due to drop-out of some subjects, two during Menses and one during LF, a total number of 41 TVUS recordings were eventually available for the analysis. These recordings underwent a quantitative quality check as introduced in Section II-C. Based on this, five additional recordings (two during Menses, one during EL, and two during LF) were excluded. Therefore, a total of 36 TVUS recordings (seven during Menses, eight during LF, ten during EL, and 11 during LL) were processed and contributed to our statistical analysis.

Figure 6A shows the MV in C2F and F2C direction extracted from the four selected phases of a normal menstrual cycle. From Menses to the LF phase, the MV in C2F direction increases from 0.72 (0.48–0.77) to 0.76 (0.63–0.96) mm/s, while it decreases to 0.71 (0.67–0.85) mm/s in the EL phase and 0.50 (0.49–0.61) mm/s in the LL phase. The MV in the F2C direction shows the same trend, with values of 0.66 (0.46–0.74) mm/s during Menses, 0.93 (0.56–1.31) mm/s in the LF phase, 0.75 (0.68–0.88) mm/s in the EL phase, and 0.52 (0.41–0.60) mm/s in the LF phase. In particular, the MV in the C2F direction shows a significant difference between the LF phase and the LL phase ($p = 0.0130$) and between the EL and the LL phases ($p = 0.0473$). Instead, the MV in the F2C direction shows a significant difference between the LF and the LL phases ($p = 0.0183$) and between the EL and the LL phases ($p = 0.0205$).

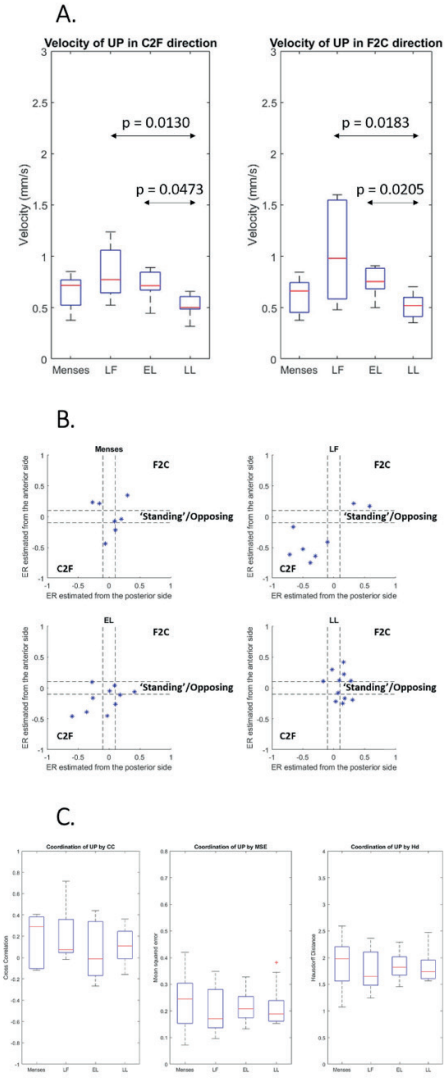

Figure 5.6.
Velocity, direction, and coordination results obtained from 36 TVUS recordings acquired during four phases of the menstrual cycle (seven during Menses, eight during LF, ten during EL, and 11 during LL) from healthy volunteers. **A.** Box plots reporting the statistical results for the UP MV extracted from the RSR signals along the C2F and F2C directions. The asterisk (*) indicates a significant difference ($p<0.05$) between different phases. **B.** Direction results based on the ER metrics estimated from the anterior (y -axis) and posterior (x -axis) walls of the endometrium. **C.** Coordination results based on CC, MSE, and Hd.

Figure 5.6B shows the direction of UP propagation among the selected four phases of the menstrual cycle. During Menses, UP propagation is mostly in the F2C direction. In the LF phase, dominant C2F or F2C propagation can be observed, and a similar behaviour also appears in the EL phase. Finally, in the LL phase, no F2C propagation but mostly "standing"/opposing propagation can be observed.

Considering the coordination feature, a trend toward higher CC [0.29 (−0.10 to 0.38)] was found in the Menses phase, and a trend toward lower MSE [0.17 (0.14–0.28)] and Hd [1.65 (1.48–2.10)] was both found in the LF phase [see Figure 5.6C].

In total, ten pairs of TVUS recordings (one during Menses, three during LF, one during EL, and five during LL) were available that passed the quantitative quality check. ICC and its 95% confidence interval of the extracted features are reported in Tables 5.1 and 5.2.

Table 5.1. Intra-observer Reproducibility Test: UP Velocity and Coordination Features Were Extracted From Two Subsequent TVUS Recordings Acquired From Ten Healthy Volunteers. ICC and Its 95% Confidence Interval of the Extracted Features Are Reported

Feature Name	ICC	95% Confidence Interval	
		Lower Bound	Upper Bound
Velocity C2F	0.918	0.689	0.979
Velocity F2C	0.961	0.798	0.991
Coordination by CC	0.950	0.771	0.988
Coordination by MSE	0.914	0.673	0.978
Coordination by Hd	0.899	0.602	0.975

Table 5.2. Intra-observer and Interobserver Variability Test: UP Velocity and Coordination Features Were Extracted From TVUS Recordings Acquired From Ten Healthy Volunteers. ICC (95% Confidence Interval) of the Extracted Features Is Calculated Among Three Trails (Intra-observer) and Three Operators (Inter-observer)

Feature Name	ICC	
	Intra-observer variability (95% CI)	Inter-observer variability (95% CI)
Velocity C2F	0.969 (0.910 – 0.992)	0.953 (0.866-0.987)
Velocity F2C	0.921 (0.762-0.979)	0.965 (0.899-0.990)
Coordination by CC	0.853 (0.589-0.960_	0.752 (0.318-0.931)
Coordination by MSE	0.841 (0.553-0.956)	0.762 (0.353-0.934)
Coordination by Hd	0.863 (0.616-0.963)	0.785 (0.409-0.940)

B. Validation in IVF Patients

In total, 81 TVUS recordings (65 from the IMPLANT 1 study and 16 from Ghent University Hospital) were acquired from IVF patients 1 h before ET; 20 TVUS recordings from the IMPLANT 1 study had to be excluded because of improper imaging windows. The remaining 61 TVUS recordings underwent the proposed quantitative quality check, by which additional 11 TVUS recordings from the IMPLANT 1 study were excluded. All 16 TVUS recordings acquired at Ghent University Hospital passed the quality check. In the end, in total, 50 TVUS recordings were included for further analysis. Sixteen out of the selected 50 patients got pregnant after the treatment, while the remaining 34 failed.

The UP MV in the C2F direction 1 h before ET was 0.51 (0.45 to 0.65) mm/s in the success group and 0.63 (0.57 to 0.74) mm/s in the failure group. When considering the C2F direction, the MV values were equal to 0.56 (0.52–0.65) mm/s in the successful group and 0.70 (0.61–0.74) mm/s in the unsuccessful group [see Figure5. 7A]. Significantly higher velocities in the C2F (p=0.0082) and F2C (p=0.0073) directions were found in the failure group compared to the success group.

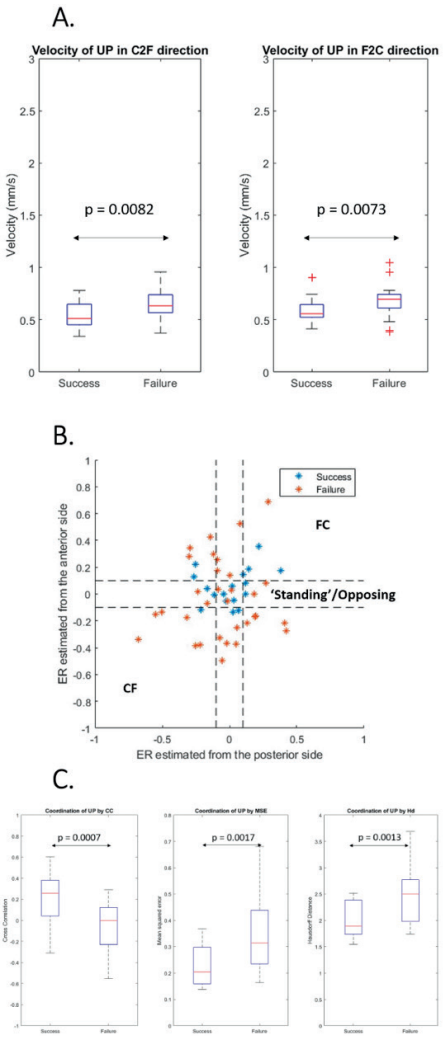

Figure 5.7. Velocity, direction, and coordination results obtained from 50 IVF patients are illustrated as follows: **A.** Box plots reporting the statistical results for the UP MV extracted from the RSR signals along the C2F and F2C directions. **B.** Direction results based on ER metrics estimated from the anterior (y -axis) and posterior (x -axis) walls of the endometrium. **C.** Coordination results based on CC, MSE, and Hd. The asterisk (*) indicates a significant difference ($p<0.05$) between successful and unsuccessful groups.

As shown in Figure 5.7B, the global direction features extracted from both the successful and unsuccessful pregnancy groups do not show different distributions and are scattered across all categories.

Considering the coordination features, higher CC [0.26 (0.04–0.38)], lower MSE [0.20 (0.16–0.30)], and lower Hd [1.89 (1.73–2.39)] were found in the success group compared to the failure group [CC = 0.00 (from −0.23 to 0.13), MSE = 0.31 (0.23–0.44), and Hd = 2.50 (1.98–2.77)] (see Figure 5.7B). The differences were statistically significant for all coordination features: CC ($p=0.0006$), MSE ($p=0.0017$), and Hd ($p=0.0013$).

Discussion

A. Validation in Healthy Volunteers

1) Estimation of UP Velocity, Direction, and Coordination:

The trend of the UP velocity changes across the selected menstrual phases is well aligned with the observation of Ijland et al. [10]. In the LL phase, which is the most quiescent phase during the entire menstrual cycle, the visualization of UP is challenging. Thus, from manual observation, no UP is reported. However, with our proposed method, the velocities of the UP in both directions could still be assessed. Besides, significant differences in the velocity of UP propagation were found between LF and LL phases and between EL and LL phases in both C2F and F2C directions. These findings are in agreement with previous literature reporting different behaviour of the uterus in the different phases of a natural menstrual cycle [9], [25].

Our findings on UP direction are in agreement with our clinical expectations and the findings from other qualitative studies [25], [30]. For instance, during Menses, intrauterine streams were expected to be generated mainly in the F2C direction for menstrual emptying, and in the LF phase, pure one-directional propagation was anticipated.

No significant difference was found based on the coordination features among the four selected phases during the menstrual cycle. However, a trend of higher UP coordination was found during the LF phase, which may correspond to the generation of coordinated contractions favouring sperm transport from the vagina to the orifices of the fallopian tubes, where fertilisation occurs [25], [27].

2) Intra-observer and Inter-observer Study:

According to the ICC results from the intra-observer reproducibility study (see Table I), excellent agreements were found for most of the features, indicating good reproducibility and robustness of our proposed method. We also observed excellent agreement for the velocity features, and good agreement for the coordination features from the intra-observer and interobserver variability studies. Since the coordination features required a good spatial alignment of the TMs positioned at both sides of the endometrium, posing extra challenge on the new users, the interobserver variability was slightly

worse than the intra-observer variability. This can be further improved by either conducting a more detailed TM positioning protocol for user guidance or investigating automatic segmentation techniques.

The ability to quantify and characterize the uterine activity with the proposed method can also aid the diagnosis of uterine dysfunction and diseases. This will be investigated in future dedicated studies.

B. Validation in IVF Patients

1) Estimation of UP Velocity, Direction, and Coordination:

Significantly higher velocities in both directions were found in the failure group compared to the success group. However, if we compare the velocities in the F2C direction extracted 1 h before ET and during the LF phase from healthy volunteers, the results are very similar. This finding suggest that, even though these patients are suffering from infertility problems and treated with hormones, the UP velocity is similar to that in healthy women in a comparable phase of the menstrual cycle.

Our findings also suggest UP direction to be a poor predictor of the success of embryo implantation. This result may be ascribed to the complex propagation patterns observed before embryo implantation in both the successful and unsuccessful pregnancy groups.

Significant differences in UP coordination were found between the success and failure groups from all metrics. Well-coordinated UP (higher CC and lower Hd and MSE) was found in the success group. This result suggests that proper coordination of uterine muscle contraction may be a relevant factor determining successful embryo implantation.

C. Study Limitations

This feasibility study was carried out with a limited dataset. To confirm the predictive value of the proposed features, larger datasets should be acquired and investigated in the future. The analysis of larger datasets would then benefit from automatic segmentation of the uterus, reported, e.g., in [31], enabling fully automatic positioning of the TMs rather than the semiautomatic approach employed in this study.

Twenty out of 81 TVUS recordings from IVF patients had to be excluded because of improper imaging window. These were all part of the retrospective IMPLANT 1 study, while no recording had to be excluded from the prospective Ghent study. This suggests the relevance of instructing the sonographers on the acquisition requirements.

The proposed speckle tracking method is based on TVUS B-mode images. This approach has the advantage of being easily transferred to different ultrasound scanners, However, more accurate results can in principle be obtained by the employment of the raw radio frequency (RF) signals, although conflicting results are reported [32]. In future work, when access to the RF signals is available, speckle tracking based on RF signals could be implemented and evaluated.

In this study, the TMs were positioned in the junctional zone close to the subendometrial line, which is the region where UP is mostly observed. However, from a physiological perspective, uterine motion should be mostly ascribed to myometrial cells [33]. Therefore, the initial positions of the TMs might have an impact on the UP characterization in relation to the physiological structure of the uterus. As we only investigated the UP characteristics close to the endometrium within the junctional zone, it would be interesting in the future to extend the investigation to the myometrium, where uterine motion originates, to obtain a more comprehensive analysis of UP.

D. Future Perspectives

Our proposed method for uterine strain analysis is designed to keep constant distances between the TMs over time and good alignment with the uterine anatomy while mitigating the effect of decorrelation due to OOP motion. These conditions enable our proposed spatial–temporal analysis. However, strong in-plane deformation of the endometrium might in principle lead to misalignment between the endometrial walls and the TM grid. To overcome these problems, automatic segmentation of the endometrial walls may be considered in the future [31], [34], possibly enabling improved grid placement and strain rate localization with respect to the uterine anatomy.

The promising novel features for the characterization of different uterine activity and associated UP patterns, such as UP velocity and coordination,

have been introduced in this study. In the future, these features can be integrated into a machine learning framework with additional standard features, such as contraction frequency and amplitude, to further improve the prediction of successful embryo implantation [18]. With this approach, clinicians could be supported with critical decision-making, such as whether to proceed with the ET or to freeze the embryo and wait for more favourable UP characteristics. In this way, increased IVF success rates may be possibly achieved. To test this hypothesis, dedicated clinical trials should be performed where predictive modelling and subsequent decisions are integrated into the clinical workflow. The mechanical activity of the uterus is not the only determinant of successful IVF. Extensive research has focused on the assessment of embryo quality as a predictor of successful embryo implantation [35]. Also, in this context, predictive models based on machine learning are being developed and investigated [36]. In addition, it is worth investigating the relationship between patient responses to hormone injection and related changes in UP characteristics. The combination of features reflecting embryo quality, hormone response, and UP characteristics can be envisaged to improve the prediction of IVF success throughout a machine learning model.

In this work, 2-D TVUS recordings were all acquired in the sagittal plane, and the main focus was on measuring the uterine contraction in the radial direction. However, with the advent of 3-D US options, complex UP patterns and OOP motion can be analysed and elucidated accounting for all spatial dimensions. This will also contribute to improve our knowledge of the uterine dynamics by exploring its longitudinal and circumferential deformation, opening up new possibilities for characterising UP and understanding the underlying physiological processes. Although this study focussed on IVF, UP assessment and characterization can represent a valuable diagnostic tool also in the context of widespread pathological conditions of the uterus, such as adenomyosis and endometriosis, which may be reflected in altered UP patterns. Dedicated clinical trials can be designed in the future to investigate the potential of the proposed features for the diagnosis of uterine diseases and dysfunctions.

Conclusion

A new method for quantitative analysis and characterization of UP based on ultrasound speckle tracking is proposed. Features related to the velocity,

direction, and coordination of the peristaltic waves are extracted and successfully evaluated for their ability to differentiate between the different phases of a natural menstrual cycle as well as to predict the success of in vitro fertilisation. Our promising results open up new possibilities for improving the success rates of in vitro fertilisation treatment as well as for improving our understanding of the physiological mechanisms underlying UP, which is still poorly comprehended.

References

[1] J. Boivin, L. Bunting, J. A. Collins, and K. G. Nygren, "International estimates of infertility prevalence and treatment-seeking: Potential need and demand for infertility medical care," Hum. Reprod., vol. 22, no. 6, pp. 1506–1512, Jun. 2007.

[2] A. Andersen et al., "Assisted reproductive technology in Europe, 2001. Results generated from European registers by ESHRE," Hum. Reproduction, vol. 20, no. 5, pp. 1158–1176, May 2005.

[3] C. De Geyter et al., "Corrigendum. ART in Europe, 2015: Results generated from European registries by ESHRE," Hum. Reproduction Open, vol. 2020, no. 3, pp. 1586–1601, Mar. 2020.

[4] R. Fanchin and J. M. Ayoubi, "Uterine dynamics: Impacton the human reproduction process," Reproductive Biomed. Online, vol. 8, no. Suppl. 2, pp. S57–S62, 2009, doi: 10.1016/S1472-6483(10)60450-6.

[5] L. Zhu, H. S. Che, L. Xiao, and Y. P. Li, "Uterine peristalsis before embryo transfer affects the chance of clinical pregnancy in fresh and frozen-thawed embryo transfer cycles," Hum. Reproduction, vol. 29, no. 6, pp. 1238–1243, Jun. 2014.

[6] N. P. M. Kuijsters, W. G. Methorst, M. S. Q. Kortenhorst, C. Rabotti, M. Mischi, and B. C. Schoot, "Uterine peristalsis and fertility: Current knowledge and future perspectives: A review and meta-analysis," Reproductive Biomed. Online, vol. 35, no. 1, pp. 50–71, 2017.

[7] M. M. Ijland, J. L. H. Evers, G. A. J. Dunselman, L. Volovics, and H. J. Hoogland, "Relation between endometrial wavelike activity and fecundability in spontaneous cycles," Fertility Sterility, vol. 67, no. 3, pp. 492–496, Mar. 1997.

[8] R. L. Dickinson, "The technic of timing human ovulation by palpablechanges in ovary, tube, and uterus," Amer. J. Obstetrics Gynecol., vol. 33, no. 6, pp. 1027–1033, 1937.

[9] I. van Gestel, M. M. Ijland, H. J. Hoogland, and J. L. H. Evers, "Endometrial wave-like activity in the non-pregnant uterus," Hum. Reproduction Update, vol. 9, no. 2, pp. 131–138, Mar. 2003, doi: 10.1093/humupd/dmg011.

[10] M. M. IJland, J. L. Evers, and H. J. Hoogland, "Velocity of endometrial wavelike activity in spontaneous cycles," Fertility Sterility, vol. 68, no. 1, pp. 72–75, Jul. 1997.

[11] J. C. Birnholz, "Ultrasonic visualization of endometrial movements," Fertility Sterility, vol. 41, no. 1, pp. 157–158, Jan. 1984.
[12] R. Fanchin, C. Righini, F. Olivennes, S. Taylor, D. de Ziegler, and R. Frydman, "Uterine contractions at the time of embryo transfer alter pregnancy rates after in vitro fertilization," Human Reproduction, vol. 13, no. 7, pp. 1968–1974, Jul. 1998.
[13] N. P. M. Kuijsters, F. Sammali, C. Rabotti, Y. Huang, M. Mischi, and B. C. Schoot, "Visual inspection of transvaginal ultrasound videos to characterize uterine peristalsis: An inter-observer agreement study," J. Ultrasound, vol. 23, no. 1, pp. 37–44, Feb. 2019.
[14] F. Sammali et al., "Dedicated ultrasound speckle tracking for quantitative analysis of uterine motion outside pregnancy," IEEE Trans. Ultrason., Ferroelectr., Freq. Control, vol. 66, no. 3, pp. 581–590, Mar. 2019.
[15] Y. Zhou and Y.-P. Zheng, "A motion estimation refinement framework for real-time tissue axial strain estimation with freehand ultrasound," IEEE Trans. Ultrason., Ferroelectr., Freq. Control, vol. 57, no. 9, pp. 1943–1951, Sep. 2010.
[16] J. Bouguet, "Pyramidal implementation of the affine Lucas Kanade feature tracker," Tech. Rep., 2001. [Online]. Available: http://robots.stanford.edu/cs223b04/algo_tracking.pdf
[17] F. Sammali et al., "Experimental setup for objective evaluation of uterine motion analysis by ultrasound speckle tracking," Biomed. Phys. Eng. Exp., vol. 4, no. 3, Mar. 2018, Art. no. 035012.
[18] F. Sammali et al., "Prediction of embryo implantation by machine learning based on ultrasound strain imaging," in Proc. IEEE Int. Ultrason. Symp. (IUS), Oct. 2019, pp. 1141–1144.
[19] G. Griesinger et al., "Effect of the oxytocin receptor antagonist nolasiban on pregnancy rates in women undergoing embryo transfer following IVF: Analysis of three randomised clinical trials," Hum. Reproduction, vol. 36, no. 4, pp. 1–14, Feb. 2021.
[20] B. Balaban et al., "The Istanbul consensus workshop on embryo assessment: Proceedings of an expert meeting," Hum. Reprod., vol. 26, no. 6, pp. 1270–1283, 2011.
[21] C. Blank et al., "Prediction of implantation after blastocyst transfer in in vitro fertilization: A machine-learning perspective," Fertility Sterility, vol. 111, no. 2, pp. 318–326, Feb. 2019.

[22] B. Lucas and T. Kanade, "An iterative image registration technique with an application to stereo vision," in Proc. Int. Joint Conf. Artif. Intell., vol. 2, 1981, pp. 674–679.
[23] S. Novellas et al., "MRI characteristics of the uterine junctional zone: From normal to the diagnosis of adenomyosis," Amer. J. Roentgenol., vol. 196, no. 5, pp. 1206–1213, May 2011.
[24] J. L. Rodgers and W. A. Nicewander, "Thirteen ways to look at the correlation coefficient," Amer. Statistician, vol. 42, no. 1, pp. 59–66, Feb. 1988, doi: 10.1080/00031305.1988.10475524.
[25] C. Bulletti, D. de Ziegler, V. Polli, L. Diotallevi, E. D. Ferro, and C. Flamigni, "Uterine contractility during the menstrual cycle," Hum. Reproduction, vol. 15, no. suppl. 1, pp. 81–89, Jun. 2000.
[26] R. Fanchin, "Uterine contractility decreases at the time of blastocyst transfers," Hum. Reproduction, vol. 16, no. 6, pp. 1115–1119, Jun. 2001.
[27] M. M. Ijland, G. A. Dunselman, H. Hoogland, and J. L. H. Evers, "Subendometrial contractions in the nonpregnant uterus: An ultrasound study," Eur. J. Obstetrics Gynecol. Reproductive Biol., vol. 70, no. 1, pp. 23–24, 1996.
[28] D. P. Huttenlocher, G. A. Klanderman, and W. J. Rucklidge, "Comparing images using the Hausdorff distance," IEEE Trans. Pattern Anal. Mach. Intell., vol. 15, no. 9, pp. 850–863, Sep. 1993.
[29] T. K. Koo and M. Y. Li, "A guideline of selecting and reporting intraclass correlation coefficients for reliability research," J. Chiropractic Med., vol. 15, no. 2, p. 155, Jun. 2016.
[30] G. Kunz and G. Leyendecker, "Uterine peristaltic activity during the menstrual cycle: Characterization, regulation, function and dysfunction," Reproductive Biomed. Online, vol. 4, pp. 5–9, Jan. 2002.
[31] R. Supriyanti, D. A. Putri, E. Murdyantoro, and H. B. Widodo, "Comparing edge detection methods to localize uterus area on ultrasound image," in Proc. 3rd Int. Conf. Instrum., Commun., Inf. Technol. Biomed. Eng. (ICICI-BME), Nov. 2013, pp. 152–155.
[32] J. Steinbuch, A. P. G. Hoeks, E. Hermeling, M. T. B. Truijman, F. H. B. M. Schreuder, and W. H. Mess, "Standard B-mode ultrasound measures local carotid artery characteristics as reliably as radiofrequency phase tracking in symptomatic carotid artery patients," Ultrasound Med. Biol., vol. 42, no. 2, pp. 586–595, Feb. 2016.

[33] R. Young, “Myocytes, myometrium, and uterine contractions,”in Annals of the New York Academy of Sciences, vol. 1101. Oxford, U.K.: Blackwell, Apr. 2007, pp. 72–84. [Online]. Available: ht.tp://ww.w.ncbi.nlm.nih.gov/pubmed/17442780
[34] N. Singhal, S. Mukherjee, and C. Perrey, “Automated assessment of endometrium from transvaginal ultrasound using deep learned snake,” in Proc. IEEE 14th Int. Symp. Biomed. Imag. (ISBI), Apr. 2017, pp. 283–286.
[35] T. Ebner, “Selection based on morphological assessment of oocytes and embryos at different stages of preimplantation development: A review,” Hum. Reproduction Update, vol. 9, no. 3, pp. 251 262, May 2003.
[36] C. Blank et al., “Assessment of uterine activity during IVF by quantitative ultrasound imaging: A pilot study,” Reproductive Biomed. Online, vol. 41, no. 6, pp. 1045–1053, Dec. 2020.

CHAPTER 6:

Uterine contractile activity in healthy women throughout the menstrual cycle measured using a novel quantitative two-dimensional transvaginal ultrasound speckle tracking method

Authors:
Connie O. Rees
Anna de Boer
Yizhou Huang
Blijke Wessels
Celine Blank
Nienke P.M. Kuijsters
Aleida D. Huppelschoten
Brunella Zizolfi
Virginia Foreste
Attilio Di Spiezio Sardo
Nikos Christoforidis
Hubertus A.A.M. van Vliet
Massimo Mischi
Benedictus C. Schoot

The content of this chapter has been published in *Reproductive Biomedicine Online*, 2021; vol 46:1 pages 115-122
DOI: 10.1016/j. rbmo.2022.08.104 1472-6483

ABSTRACT:

Objectives: To explore normal uterine contractile function across the menstrual cycle using a novel quantitative ultrasound method.

Materials and Methods: This multicentre prospective observational study took place in 3 European centres from 2014 - 2022. Uterine contraction frequency (contractions/minute), amplitude, direction (Cervix-to-fundus; C2F, Fundus-to-cervix; F2C), velocity, and coordination were investigated. Features were extracted from transvaginal ultrasound recordings (TVUS) using speckle tracking.

Women of ≥18 years of age, premenopausal with normal, natural menstrual cycles were included. A normal cycle was defined as: regular (duration 28 ± 2 days), no dysmenorrhea, no menometrorrhagia. 4-minute TVUS were performed during the menstrual phase (M), mid-follicular (MF), late follicular phase (LF), early luteal phase (EL) and/or late luteal phase (LL). Of the 96 recordings available from 64 women, 70 were suitable for inclusion in the analysis

Results: Contraction frequency (for the anterior wall) and velocity (for the anterior uterine wall in the F2C direction) were highest in the LF phase and lowest in the M and LL phases (1.61 vs. 1.31 and 1.35 contractions/min, $p<0.001$ and 0.81 vs. 0.67 and 0.62mm/sec, $p<0.001$ respectively).. No significant difference was found for contraction amplitude. Contraction coordination (simultaneous contraction of the anterior and posterior walls in the same direction) was least coordinated in the MF phase ($p=0.002$).

Conclusions: This is the first study that measures uterine contraction features in healthy women during the natural menstrual cycle on TVUS in an objective manner. Likewise, it introduces contraction coordination as a specific feature of uterine peristalsis. We confirm differences in uterine contractility across the menstrual cycle, with highest activity seen in the LF phase, and lowest in the LL phase.

Keywords: Uterine Peristalsis, TVUS, Menstrual Cycle, Speckle Tracking, Uterine Contractile Function

INTRODUCTION:

In a healthy uterus, rhythmic contractions change in rhythm and intensity during the menstrual cycle to support sperm propagation and embryo implantation (83,215–217). However, no study thus far has been able to comprehensively characterise all aspects of uterine contractions during the menstrual cycle; therefore, these characteristics remain largely speculative, based on heterogenous studies. Furthermore, research into its characteristics has been hampered by the subjectivity of the available measurement tools (83).

It has been suggested that aberrant uterine peristalsis or 'dysperistalsis' is associated with reduced fertility and/or symptoms such as dysmenorrhoea (218,219). Up to now, there exists no quantifiable marker for dysperistalsis, this being varyingly defined by previous investigators.
Multiple methods have been used to visualise and assess uterine contractions and their different characteristics, one of which is transvaginal ultrasound (TVUS). A recent study, however, showed that medical professionals shared only mild agreement on the direction and timing of uterine peristalsis by subjective visual inspection of TVUS recordings (220). Although visual inspection of TVUS can give a number of peristalsis parameters (frequency and direction), it is generally qualitative and unsuitable to quantify contraction amplitude or velocity. Furthermore, contraction coordination – being the synchronised movement of the anterior and posterior walls of the uterus – has never been investigated. There is thus a need for an objective, quantifiable method for uterine contraction assessment, preferably in a non-invasive, operator- and patient-friendly manner.

Recently published data by our group presented a novel method for assessing uterine contractility, using 2D TVUS and speckle tracking techniques (221–224). This has been tested and (externally) validated in IVF patients prior to embryo transfer (225,226). This method is able to quantitatively assess features such as contraction frequency and amplitude, in addition to a novel set of features: contraction coordination, direction, and velocity. Coordination is defined as the synchronised simultaneous movement of the anterior and posterior uterine walls; where the value reflects the degree of synchronicity of coordination. This aspect of uterine movement is potentially of clinical relevance for the assessment of (normal) uterine function.

Differences in uterine contractility have been shown to have a strong association with ongoing pregnancy in an IVF population (226). In this study, we explore the characteristics of normal uterine contractile function across the menstrual cycle in healthy, nulliparous women using this quantitative method, with a focus on the novel feature of coordination as a possible measure of dysperistalsis.

Materials and Methods:

Study objectives:

Evaluate uterine contraction features (frequency, amplitude, velocity, direction, and coordination) using a dedicated speckle-tracking algorithm by 2D transvaginal ultrasound measurement in healthy, women throughout the menstrual cycle.

Study design & setting:

Multi-centre observational prospective cohort study carried out in the outpatient gynaecology department of the Catharina Hospital in Eindhoven, the Netherlands, the University of Naples, Federico II Naples, Italy, and the Embryolab Fertility centre in Thessaloniki, Greece.

Participants:

Between September 2014 and January 2022, 74 healthy women were included from the gynaecological outpatient departments of the participating centres. Women were included if they were ≥18 years of age, premenopausal and had a normal, natural menstrual cycle. A normal cycle was defined as: regular (duration 28 ± 2 days), no dysmenorrhea, no menometrorrhagia. Exclusion criteria were: 1) pregnancy, 2) diagnosed with a mental disorder, 3) significant language barrier, 4) use of oral hormonal contraceptives or intrauterine device, 5) use of other (hormonal) medication affecting the uterus, or 6) uterine pathology (congenital or otherwise, e.g., leiomyomas, adenomyosis, based on (Morphological Uterine Sonographic Assessment (Morphological Uterine Sonographic Assessment, MUSA (183)) criteria. Ultrasound scans of the included women were also assessed retrospectively by experts to confirm the absence of uterine abnormalities.

Seventy-four women were enrolled in the study, of which 64 ultimately underwent TVUS recording at different phases of the menstrual cycle. This resulted in a total of 96 completed TVUS recordings across cycle phases. Eighteen recordings were subsequently excluded due to insufficient ultrasound quality for the analysis. Reasons for exclusion due to recording quality included: shadow across the endometrial lining, out-of-plane motion, or insufficient resolution of the images. Additionally, recordings of eight recordings were excluded due to suspicion of uterine abnormalities, or use of hormonal contraceptive methods. Figure 6.1 presents a flow diagram of

patient inclusion. Overall, 70 out of 96 conducted recordings from 64 women were included in the analysis.

Data sources and measurements:
TVUS measurement:
Transvaginal ultrasounds (TVUS) were performed during several phases of the menstrual cycle: the menstrual phase (M, cycle day (CD) 1-5), mid-follicular (MF, CD 6-10), late follicular phase (LF, CD 11-14), early luteal phase (EL, CD 15-20) and late luteal phase (LL, CD 21-28). During each session, four-minute video recordings of the uterus in the mid-sagittal section were made. The employed ultrasound machines were an Accuvix WA80S with Elite (Samsung Medison, Seoul, Korea) equipped with a V5-9 transvaginal probe (bandwidth 5-9 MHz) or a GE Voluson S10 Expert (GE Healthcare, Zipf, Austria) equipped with a RIC5-9W-RS probe (bandwidth 3.8-9.3MHz).

Feature Extraction:
Various uterine contractility features were extracted from the gathered ultrasound recordings using a quantitative dedicated speckle tracking algorithm previously developed and implemented in Matlab software (Mathworks, Natick, USA). The full details of the methodology of feature extraction have been described in detail in previously published works (221,224,226–229). Simply put, speckle tracking measures the displacement of image 'speckles' (such as those seen in various shades of grey on ultrasound images) over time. Speckle movement reflects movement of the imaged tissue, which in this case is movement of the uterine myometrium.

For each ultrasound recording, a grid of tracking markers was manually positioned over the uterine junctional zone along the endometrium, known to be the most contractile part of the uterus (see Figure 6.2 for an illustrative example). Grid markers were placed 5 mm from the fundus along the endometrial border. The grid markers were coupled in pairs, and distance and strain signals were derived between each pair in both the longitudinal and radial direction (See Figure 6.3). Several contraction features were extracted from the measured strain signals as described below. Previous analyses of inter and intra-observer variability in the placement of the grid markers showed a high level of correlation, making the method both reproducible and reliable (229), see appendix 6A.

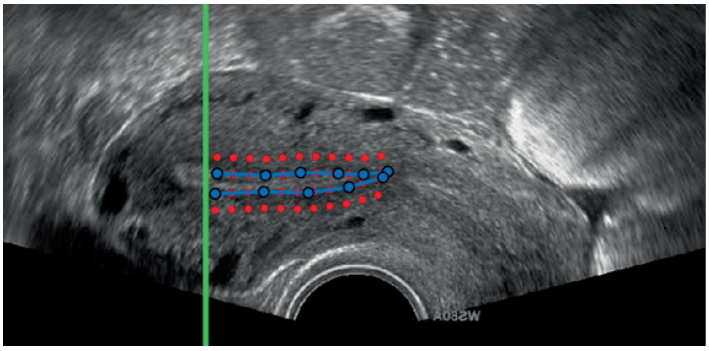

Figure 6.2: Ultrasound image of the uterus in the midsagittal section. Placement of the speckle tracking grid (red dots) along the endometrial border (blue line) at 5 mm (green line) from the apex of the fundus.

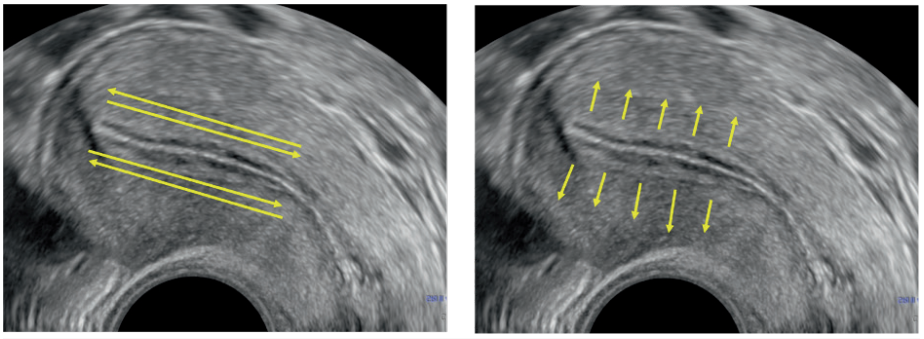

Figure 6.3: Ultrasound images of uterus in midsagittal section with depiction of contractions in the longitudinal (left) and radial (right) direction

Euclidean distance was used to derive the distance between each pair resulting in absolute motion estimates. The strain, $\in$, was defined as the relative variation of the distance, d, between the tracked blocks as: $\in=d(j)-d(j-1)/d(j-1)$, where d(j) and d(j - 1) indicate the distance between the tracked blocks at the current frame (j) and previous frame (j – 1), respectively.

Contraction Frequency:
Frequency features were analysed separately for the anterior and posterior wall of the uterus, in the longitudinal and radial direction. We will only present the longitudinal direction of contractions here. Frequency-related features are

reported as contractions per minute (221). Further technical details about feature extraction as well as pre-processing analysis can be found in Sammali *et al* . (2018) (224).

Contraction Amplitude:
Contraction amplitude features reflect the relative strength of uterine contraction. Amplitude of contraction was assessed by calculating the standard deviation of the strain signal in the longitudinal and radial directions from its frequency spectrum (Parseval's theorem) (230). A higher value reflected stronger uterine contractions. Results are reported for contractions in the longitudinal direction, separately for the anterior and posterior uterine walls.

Contraction Direction
Uterine peristalsis is thought to propagate mainly in one of two directions: either fundus-to-cervix (F2C) or cervix-to-fundus (C2F). The contraction direction was estimated by analysis of the radial strain signal representation in the spatiotemporal frequency domain, where the spatial domain is intended along the longitudinal direction of the uterus(229). The ratio between the strain signal energy in the quadrants corresponding to the two propagation directions (C2F and F2C) provided a global measure of the dominant propagation direction in each wall (posterior and anterior), separately (229). Basically, a more positive value represented movement predominantly in the F2C direction, whereas a more negative value represented movement predominantly in the C2F direction. A value around zero represented movement which did not show a predominant direction, being either circular movement, or standing or opposing contractions.

Contraction Velocity
Velocity, being propagation speed of the peristaltic waves in a certain direction (C2F or F2C, in mm/sec), was calculated for movement in the anterior and posterior walls. This was again done by analysing the radial strain signal representation in the spatiotemporal frequency domain, where the spatial domain is intended along the longitudinal direction of the uterus (224). The analysis was performed over a window of 20 seconds sliding over the full recording time. Subsequently, the median velocities (MV) in C2F and F2C directions were calculated by averaging velocities over time in the corresponding directions; a high value reflected increased velocity in the

reported direction. Results were reported separately for the anterior and posterior uterine walls.

Contraction Coordination:
In addition to the features described above, we also aimed to assess the coordination of uterine contraction. This is the first attempt at a quantifiable measurement of coordination of uterine movement up to now. In order to quantify this, we assessed whether the anterior and posterior wall of the uterus were moving synchronously or asynchronously. This was accomplished by estimating the time evolution of the estimated propagation direction over the anterior and posterior wall using a running window of 20 seconds. The two resulting evolutions were then compared using a similarity measure. This resulted in a feature defining the uterine contraction coordination depending on the adopted similarity measure: mean square error (MSE). Two additional coordination features (Hausdorff distance metric and cross correlation) were also investigated, and are shown in the appendix A. Again, full details on the technical background of these units has been published elsewhere (229). A higher value reflected decreased contraction coordination.

Study outcomes:
The primary outcomes investigated were the following uterine contraction features, compared between the four menstrual phases.

- Frequency, in contractions/minute
- Amplitude (unitless)
- Direction, (unitless, whereby >0.0 globally represents F2C movement, and <0.0 represents C2F movement)
- Median Velocity (mm/sec)
- Coordination, in Mean squared error

Statistical methods:
Statistical analysis was performed using IBM SPSS statistics version 27. The Shapiro-Wilk test was first employed to test the normality of the distributions. Comparison of the outcome measures (frequency, amplitude, direction, coordination and velocity) between the various phases was done using the Kruskal-Wallis test if abnormally distributed, and a one-way ANOVA if normally distributed (with Bonferroni correction). Statistical significance was defined as a p-value < 0.05. This study is reported according to STROBE guidelines (189)

Ethical approval:

This study received ethical approval from the local and regional ethical committees of participating centres, with study number NL52466.100.15 on July 15th, 2020 (Netherlands), May 12th, 2021 (Greece) and October 2021 (Italy) . All participants gave informed consent prior to study participation.

RESULTS:

Patient characteristics and recruitment:

Ultimately, (see Figure 6.1) 70 recordings from 64 women were available for analysis.

Table 6.1 presents an overview of the patient characteristics of the enrolled women (n=74).

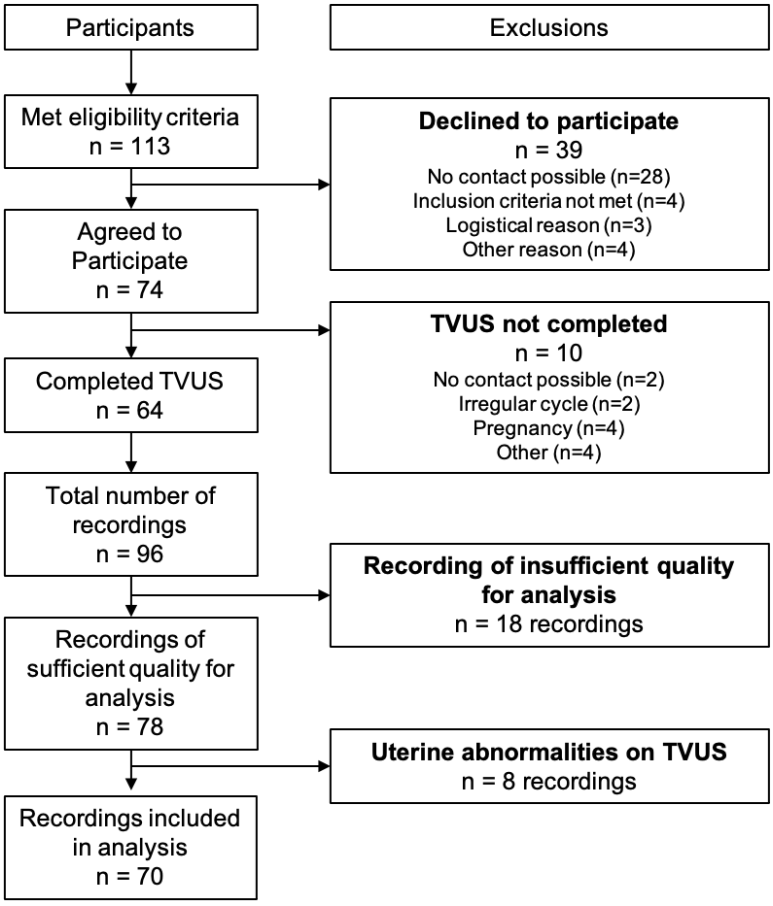

Figure 6.1: Flowchart of Patient Recruitment and Inclusion.

Table 6.1: Patient characteristics for analysed patients

Patient Characteristics	Total Analysed: 64 women
Patients per participating centre	
- **Netherlands**	33 (51.6%)
- **Italy**	24 (37.5%)
- **Greece**	7 (10.9%)
Age (years, Mean, SD)	34.1 (6.3)
BMI (median, IQR)	23.0 (3.75)
Parity (n, %)	
- **Nulliparous**	34 (53.1%)
- **Multiparous**	9 (14.1%)
- **Missing**	11 (17.2%)
Cycle duration (days, Mean, SD)	28.1 (1.7)
Cycle day menses measurement (Mean, SD)	2.42 (1.13)
Cycle day mid follicular measurement (Mean, SD)	8.33 (0.94)
Cycle day late follicular measurement (Mean, SD)	12.31 (0.85)
Cycle day early luteal measurement (Mean, SD)	16.33 (3.951)
Cycle day late luteal measurement (Mean, SD)	27.50 (1.00)
Uterine measurements	
- **Uterine length (mm (Mean, SD))**	71.44 (10.77)
- **Uterine Height (mm (Mean, SD))**	35.96 (6.18)
- **Uterine Width (mm Mean, SD))**	63.10 (1.06)
Endometrial thickness (mm (Median, IQR)) per Cycle Phase	Menses: 2.00 (0) Mid Follicular: 5.34 (1.52) Late Follicular: 7.46 (2.77) Early Luteal: 10.02 (3.92) Late Luteal: 6.60 (2.44)

Uterine contraction features:

Tables 6.2 – 6.6 present an overview of the values found per contraction feature across the menstrual cycle phases, for the features of frequency, direction, velocity, amplitude and coordination.

Contraction frequency, velocity and coordination differed significantly between menstrual phases. No significant differences were found between cycle phases for amplitude or direction.

Contraction frequency:

The overall values of contraction frequency per menstrual phase can be seen in Table 6.2. The highest mean contraction frequency (1.61 (SD 0.17), $p<0.001$) was found in the LF phase in the posterior wall. The phase with the lowest mean contraction frequency was the late luteal phase (1.28 (SD 0.12)

in the anterior wall, p=0.003). The early luteal and menstrual phases had comparable contraction frequencies(P>0.05).

Table 6.2. Contraction Frequency according to menstrual cycle phase

	Menstrual (n= 4)	**Mid follicular (n=11)**	**Late Follicular (n= 26)**	**Early Luteal (n=14)**	**Late Luteal (n=15)**	**p-value***
Contraction frequency, longitudinal, anterior wall (contractions/minute, Mean (SD))	1.31 (0.08)	1.46 (0.12)[a]	1.46 (0.14)[a]	1.40 (0.14)	1.28 (0.13)	0.003
Contraction frequency, longitudinal, posterior wall (contractions/minute, Mean (SD))	1.31 (0.13)	1.54 (0.14)[a, b]	1.61 (0.17)[a, b]	1.45 (0.17)	1.35 (0.19)	<0.001

[a] significant difference vs. LL; b: significant difference vs. M
*One-way ANOVA

Contraction Amplitude:

The overall values of contraction amplitude per cycle phase can be seen in Table 6.3. No significant differences were found between cycle phases. The mean contraction amplitude was 0.043-0.062 (SD 0.011-0.016) in the late follicular phase and 0.036-0.062 (SD 0.013-0.024) in the late luteal phase p>0.05.

Table 6.3. Amplitude of contractions according to menstrual cycle phase

	Menstrual (n= 4)	Mid follicular (n=11)	Late Follicular (n= 26)	Early Luteal (n=14)	Late Luteal (n=15)	p-value*
Standard deviation in strain longitudinal direction anterior (Mean, SD)	0.050 (0.015)	0.049 (0.010)	0.062 (0.016)	0.056 (0.013)	0.062 (0.024)	0.141
Standard deviation in strain longitudinal direction posterior (Mean, SD)	0.042 (0.006)	0.036 (0.010)	0.043 (0.012)	0.041 (0.014)	0.040 (0.014)	0.240
Standard deviation in strain radial direction anterior (Mean, SD)	0.041 (0.014)	0.038 (0.010)	0.045 (0.012)	0.047 (0.021)	0.038 (0.013)	0.266
Standard deviation in strain radial direction posterior (Mean, SD)	0.041 (0.011)	0.037 (0.010)	0.044 (0.011)	0.044 (0.023)	0.036 (0.013)	0.218

*One-way ANOVA

Contraction Direction and Velocity:

Contraction direction did not seem to differ significantly between menstrual phases (Table 6.4, $p>0.05$). During the menstrual phase, direction of contraction showed a trend towards F2C contractions. In other phases mainly C2F contractions were seen. Contraction velocity overall differed significantly across cycle phases. The velocity of contractions was significantly higher in the late follicular phase in all directions (see Table 6.5,$p<0.001$, $p=0.021$, 0.004 and 0.026 respectively), and lowest in the late luteal phase.

Table 6.4. Direction of contractions according to menstrual cycle phase

	Menstrual (n=4, Mean, SD)	Mid Follicular (n=11, Mean, SD)	Late Follicular (n=26, Mean, SD)	Early Luteal (n=14, Mean, SD)	Late Luteal (n=15, Mean, SD)	p-value*
Direction Anterior wall†	0.085 (0.288)	-0.100 (0.379)	-0.032 (0.396)	-0.054 (0.297)	0.084 (0.153)	0.669
Direction Posterior wall†	0.013 (0.279)	-0.270 (0.252)	-0.207 (0.180)	-0.206 (0.179)	-0.061 (0.242)	0.300
Predominant Direction	F2C	C2F	C2F	C2F	None	n/a

* one-way ANOVA

†A value under 0.0 reflects movements predominantly in the cervix-to-fundus direction, whereas a value higher than 0.0 reflects movement predominantly in the fundus-to-cervix direction. Values between -0.1 and 0.1 reflect no predominant direction, or standing/opposing contractions.

Table 6.5. Contraction velocity according to menstrual cycle phase

	Menstrual (n= 4)	Mid Follicular (n=11)	Late Follicular (n= 26)	Early Luteal (n=14)	Late Luteal (n=15)	p-value*
Fundus-to-Cervix Propagation Anterior (mm/sec, Median (IQR))	0.67 (0.10)	0.77 (0.26)	0.81 (0.31)[a]	0.71 (0.17)	0.62 (0.08)	<0.001
Fundus-to-Cervix Propagation Posterior (mm/sec, Median (IQR))	0.69 (0.09)	0.73 (0.23)	0.85 (0.21)	0.73 (0.12)	0.67 (0.16)	0.021
Cervix- to Fundus Propagation Anterior (mm/sec, Median (IQR))	0.68 (0.06)	0.80 (0.30)	0.82 (0.29)[a]	0.71 (0.14)	0.65 (0.13)	0.004
Cervix- to Fundus propagation Posterior (mm/sec, Median (IQR))	0.65 (0.11)	0.78 (0.31)	0.86 (0.33)[a]	0.74 (0.11)	0.66 (0.15)	0.026

a: significant difference vs. LL;

*Kruskal-Wallis

Contraction Coordination.

The contraction coordination values are shown for all cycle phases in Table 6.6. MSE showed a significant difference across the cycle phases, with a significantly (p=0.011) reduced coordination of contractions during the late follicular phase compared to the menstrual and late luteal phases. Further coordination parameters did not differ significantly between cycle phases (see appendix 6B).

Table 6.6. Coordination of contractions according to menstrual cycle phase

	Menstrual (n= 4)	**Mid Follicular (n=11)**	**Late Follicular (n= 26)**	**Early Luteal (n=10)**	**Late Luteal (n=10)**	**p-value***
MSE (Mean, SD)	0.15 (0.04)[b]	0.28 (0.75)[c]	0.24 (0.12)[a,c]	0.20 (0.08)	0.18 (0.07)	0.011

*One-way ANOVA

a: significant difference vs. LL; b: significant difference vs. late follicular; c: significant difference vs. M.

DISCUSSION:

The results of this exploratory study suggest a preliminary range of normal reference values in a healthy population of women without hormonal contraception and normal uteri. We present a novel, reproducible and objective method based on ultrasound speckle tracking. We are able to characterise uterine contraction amplitude and frequency, as well as coordination, direction, and velocity. Coordination, direction, and velocity of uterine contractions are features that have never before been quantified in this context. Our results show that contraction frequency and velocity are highest in the late follicular phase and lowest in the menstrual and late luteal phase. Coordination seems to be negatively affected by contractions with higher frequency and velocity in the late follicular phase compared to other phases. Amplitude and contraction direction in this population do not show significant variations across the menstrual cycle.

Our findings are generally in accordance with the existing literature concerning uterine contractile activity in the healthy uterus. Previously described methods to assess uterine contractility have assessed some subsets of the features that we present (226); however, this is the first study where all the presented features are quantified and evaluated (231). Our novel features for the characterization of different uterine activity and associated patterns - coordination, direction, and velocity - can form a new avenue for research and knowledge into uterine function. Our presented TVUS method for the quantitative analysis of uterine contractions is also easily reproducible (229), quick, objective, and patient-friendly. It is possible to potentially integrate into routine gynaecological practices (after sufficient training), and does not require extensive skill or expertise.

The main limitation of the results presented here is the small sample size of the study population. However, we do believe that the presented results are valid due to their general accordance with the currently accepted patterns of uterine peristalsis throughout the menstrual cycle. In addition, most patients received an ultrasound in only one phase of the menstrual cycle for a 4 minute time-frame, and therefore it was not possible to conduct a within-subjects comparison. It can be debated in how far this relatively short recording is representative of the behaviour of the uterus during this phase in general, however a sub-analysis with repeated recordings within subjects was

conducted in previous work (229), with comparable results. Additionally, the majority of ultrasounds were conducted in the late follicular phase which may influence the significance of results. Furthermore, due to the novel and still experimental nature of the quantitative analysis employed in this study, its clinical application in routine practice is not yet possible. It was also necessary to exclude a significant number of recordings from analysis (n=18) due to insufficient quality of the ultrasounds, which indicates that a learning curve is present which could (initially) affect clinical useability. In some cases this was avoidable (e.g. insufficient resolution or out-of-plane motion), but incidentally it is not possible to analyse contractions despite good ultrasound technique (for instance due to the orientation of the uterus, or shadows caused by intestinal contents for example). It is also not yet feasible to gain contraction feature results in real time while performing the ultrasound scan, as the implemented analysis still relies on offline, post-ultrasound data processing. In the future, steps need to be made in order to make our TVUS speckle tracking method for quantitative analysis of uterine contractions utilisable in daily clinical practice.

The results presented here are able to give us further insight into uterine behaviour at different phases of the menstrual cycle, whereby each cycle phase shows an individual contraction pattern. Our results clearly show that the late follicular phase is the most active with the highest contraction frequency and velocity. One could surmise that these features are thus of importance for the sperm transport and ovulation that occurs in this period of the menstrual cycle. Furthermore, the relatively reduced activity in the late luteal to menstrual phases suggest a relevance of these characteristics with regard to facilitation of embryo implantation and/or menstruation symptoms. The coordination feature has not before been investigated; however, our initial results show that increased contraction frequency and velocity seem to be accompanied by reduced coordination of contractions. The clinical importance of simultaneous (coordinated) anterior and posterior contractions and how it could relate to fertility outcomes or clinical symptoms for example merits further investigation. Potentially, this coordination feature could be seen as a measure of uterine dysperistalsis, which has been previously described in patients with infertility and endometriosis (77,219,232) with significant clinical consequences, especially with regards to fertility.

Now that we are able to suggest normal preliminary reference values for uterine peristalsis in a normal menstrual cycle, it is possible to better assess how and if uterine contractile activity is abnormal in different populations. Previous work by this research group has assessed uterine peristalsis in IVF patients, which showed great promise with regards to prediction of IVF treatment success (226). Future works will be able to compare how uterine contractions differ between fertile and infertile populations, also relative to the preliminary reference values in a normal menstrual cycle presented here, potentially identifying treatment target points, and perhaps uncovering a new facet of infertility aetiological mechanisms.

Although this study focused on healthy women with normal uteri, uterine peristalsis assessment and characterisation can also represent a valuable diagnostic tool in the context of common pathological conditions of the uterus, such as adenomyosis, endometriosis or uterine fibroids. The effect of these conditions on uterine function (and disease symptoms such as dysmenorrhoea and infertility) may in fact be reflected in altered uterine peristalsis patterns, such as coordination. Dedicated clinical trials can be designed to investigate the potential of the proposed features for the diagnosis of uterine diseases and dysfunctions. Differences in uterine contractions could be an explanatory factor for the symptomatology in certain uterine disorders, and thereby become a target for patient-tailored treatment.

In summary, we suggest preliminary reference values of uterine contraction features in healthy women during the natural menstrual cycle. Our study serves as a standard to which uterine peristalsis in infertile women or women with abnormal uteri can be compared, potentially identifying treatment targets and aetiological mechanisms yet unexplored. Furthermore, we hereby present novel uterine contraction features which can be used to assess the presence (or absence) of normal uterine contractility, namely coordination, direction, and velocity.

Funding:
Unrestricted grant GE Healthcare Austria

CHAPTER 7:

The influence of uterine abnormalities on uterine peristalsis in the non-pregnant uterus: a systematic review

Authors:
Anna de Boer
Connie O. Rees
Massimo Mischi
Hubertus A.A.M. van Vliet
Judith Huirne
Benedictus C. Schoot

The content of this chapter has been published in the *Journal of Endometriosis and Uterine Disorders*, 2023; vol: 2
DOI: 10.1016/j.jeud.2023.100038

Abstract

Uterine peristalsis is the rhythmic wave-like motion of the subendometrial layer of the uterus. These contractions change throughout the menstrual cycle in terms of direction, frequency and amplitude, and can be analysed with various methods. Not much is known about uterine peristalsis in patients with uterine abnormalities. To that end, we decided to systematically review the available studies for evidence on the influence of uterine abnormalities, including leiomyomas, endometriosis, adenomyosis and congenital uterine anomalies, on uterine peristalsis. After a systematic search of relevant databases, sixteen eligible studies were included in this review; eight case-control studies and eight controlled prospective cohort studies. The sample sizes ranged from twelve to 205 participants. Various methods of analysing uterine contractions were used, including transvaginal ultrasound, hysterosalpingo-radionuclide scintigraphy, cine MRI and intrauterine pressure measurement. Studies varied in their design, uterine contraction measurement method and patient groups. Generally however, uterine abnormalities do seem to have an influence on uterine peristalsis. Compared to healthy controls, the specific phase of the menstrual cycle (namely the periovulatory and luteal phases) seems to play a major role in the observed effect on uterine contractions. The included studies were difficult to compare directly due to heterogeneity however, and sample sizes were relatively small. Despite these limitations, it can be concluded that uterine abnormalities likely have a menstrual phase-dependent effect on uterine peristalsis and contraction features. These aberrant contractions potentially play a role in the relationship between (benign) uterine abnormalities and infertility, along with other associated symptoms (i.e., dysmenorrhoea, abnormal uterine bleeding). It is not yet possible to make a definite conclusion on the nature of this effect however. Further research is needed on objective measurement tools, treatment and clinical consequences of abnormal uterine peristalsis in patients with uterine abnormalities.

Keywords: Uterine peristalsis, Uterine abnormalities, Leiomyoma, Adenomyosis, Congenital uterine anomalies

Introduction

Contractions of the uterus during labour have been extensively studied and is basic knowledge amongst the population. On the contrary, knowledge of these wave-like motions (peristaltic contraction and relaxation of the subendometrial layer) outside pregnancy is relatively unknown and research into its characteristics has been hampered by the subjectivity of the available measurement tools (233). Today, no comprehensive and fully objective measurement tool is widely used.

Multiple methods have been used to visualise and analyse uterine contractions and its different characteristics (233). Intra-uterine pressure (IUP) measurement using a catheter is a precise method which is able to measure contraction frequency, direction and amplitude; however, the introduction of the catheter itself may influence the natural behaviour of the uterus. Measuring contraction direction is also not feasible when using one single(lumen) catheter (234). Transvaginal ultrasound (TVUS) is another method that can visualize uterine contractions (69). TVUS investigation, and the subsequent analysis of the imaging loops, can however be subjective due to a dependence on the observer's sonographic skills and ability to interpret the TVUS recordings. Furthermore, although several peristalsis parameters (e.g., frequency and direction) can be assessed on TVUS it is not possible to quantify the amplitude of the waves. Another way to visualize uterine contractions is hysterosalpingo-radionuclide scintigraphy (HSSG). It is excellent for demonstrating the contraction direction, however contraction amplitude and frequency cannot be assessed by HSSG. Recent studies have also used MRI to visualize and assess contractions (233). The so-called cine MRI is used to visualize peristalsis of the uterus in real-time (235). Similar to TVUS and HSSG, and despite its cost and sophistication, the evaluation of contraction amplitude is not possible by MRI (233).

In a healthy uterus, rhythmic contractions change in intensity as well as direction during the menstrual cycle to support sperm propagation and embryo implantation in response to hormonal variations (236). Other characteristics of uterine contractions - frequency and amplitude - are altered throughout the menstrual cycle as well (237). During menstruation for instance, uterine contractions are directed with high amplitude and low frequency from the uterine fundus to the cervix, whereas the periovulatory

phase is characterized by contractions directed towards the fundus at a high frequency. Uterine peristalsis is relatively quiescent during the luteal and early-to-mid follicular phases (238). If uterine contractile patterns differ significantly from the norm, dysperistalsis occurs, leading to uncoordinated and ineffective uterine contractions.

Relative consensus exists as to how uterine behaviour changes throughout the menstrual cycle; however, little is known about uterine activity in abnormal uteri, and if altered contractions are the intermediate for lower fertility outcomes and/or other symptomatology. It is well known that uterine abnormalities are associated with subfertility (239–242). We hypothesise that these uterine abnormalities such as uterine fibroids, adenomyosis and congenital uterine anomalies may disrupt uterine peristalsis thereby contributing to the associated symptoms of these disorders. In this systematic review we investigated the available literature to assess if uterine peristalsis is adversely affected in women with such uterine abnormalities. The primary objective of this review is to assess the influence of uterine abnormalities on uterine peristalsis, including leiomyomas, adenomyosis and congenital uterine anomalies.

Materials and methods

Review protocol:

The review protocol is available on PROSPERO under the ID CRD42021244280.

Study eligibility criteria

The researched population in this review were women with uterine abnormalities such as leiomyomas, adenomyosis, endometriosis and congenital uterine anomalies. Studies were only included if in vivo uteri were studied. Studies were included if uterine peristalsis was investigated in premenopausal women aged over 18 with regular menstrual cycles without hormonal therapy. The patients should not have received any surgical uterine treatment at baseline. Intervention studies, studying the effect of treatment of uterine abnormalities on uterine peristalsis were included if measurement of uterine peristalsis was also done prior to treatment. Cohort studies and case-control studies were deemed eligible for inclusion. Data reported in secondary analysis (reviews), case reports, letters to editors, conference abstracts, and protocols for ongoing studies were excluded. Due to the expected scarcity of relevant studies, studies were not excluded based on the method employed for the uterine contraction measurement. Articles were only included if published in English.

Data sources

Multiple databases were accessed on April 28th, 2022, in the search for relevant literature, namely: PubMed, the Cochrane Library and Embase. The search was repeated on June 17th, 2023, with no new relevant studies found.

Search strategy

Several key words were selected and included the terms “Uterine Contraction”, “Peristalsis”, “Uterus”, “Uterus/ abnormalities”, “Leiomyoma”, and “Adenomyosis”. Not only MeSH terms, but also free text terms [tiab] were used including “junctional zone contraction”, “endometrial wave”, “subendometrial contraction” and “congenital uterine anomaly”. Snowballing was also used to find further relevant articles. The full literature search including all used key words can be found in Appendix A.

Study screening and selection

The articles found during the initial literature search were assessed for relevance by one researcher (AB). The articles were first screened based on titles and abstracts, whereafter the remaining studies were evaluated based on the full text to assess final eligibility. The application Rayyan QCRI (243) was used to remove duplicates and support during study screening and selection. If more than one paper used same data, the publication with the largest included numbers was selected. Experts in the field (CR, BS) supported the study screening and selection process to confirm the literature search was sufficient to identify key publications on this topic, and to make sure that all relevant articles were included.

Data collection

Data was extracted by one researcher (AB) from the included articles using a pre-defined data-extraction table, see Table 7.3.

Data items

Outcomes of interest included the contraction presence, frequency, amplitude and direction. Secondary outcomes of interest were the influence of treatment of uterine abnormalities on uterine peristalsis. Other variables collected were relevant demographic patient characteristics (e.g., age, menstrual phases) and the specific method employed for measuring uterine peristalsis.

Risk of bias assessment

Due to anticipated heterogeneity of the studies, no one dedicated methodological quality assessment tool is available. For this reason, the Downs and Black checklist for measuring study quality was adjusted to suit the design of each included article (244). Question 27 of the original Downs and Black checklist was adjusted for all studies. A study was awarded a maximum of one point when a power calculation was done. If a question was not applicable to a study, it did not contribute to the final risk of bias evaluation. If due to missing information in a synthesis resulting from reporting bias a question from the Downs and Black checklist could not be answered, a question was awarded with zero points and put as unable to determine (UTD). Based on the risk of bias assessment, an overall quality score was awarded to the studies based on the percentage of points achieved, see Table 7.1.

Table 7.1: Definitions of the overall risk of bias quality scores

Percentage (%)	Overall quality score	Colour code
> 90	Excellent	☆
66.7 – 90	Good	●
50 – 66.7	Fair	●
< 50	Poor	●

Synthesis methods

A narrative approach was used to discuss the data extracted from the included studies. A meta-analysis was not carried out due to the expected heterogeneity of included studies.

Results

Study selection

The literature search provides us with 445 unique records. Four hundred and nineteen studies were excluded based on title and abstract. Reasons for exclusion include, but are not limited to inappropriate study design, animal-based studies or publication in a language other than English. A total of sixteen studies were eventually included in this systematic review. A schematic overview of the study screening and selection process can be seen in Figure 7.1.

Figure 7.1: PRISMA Flowchart for the selection of papers included in this systematic review

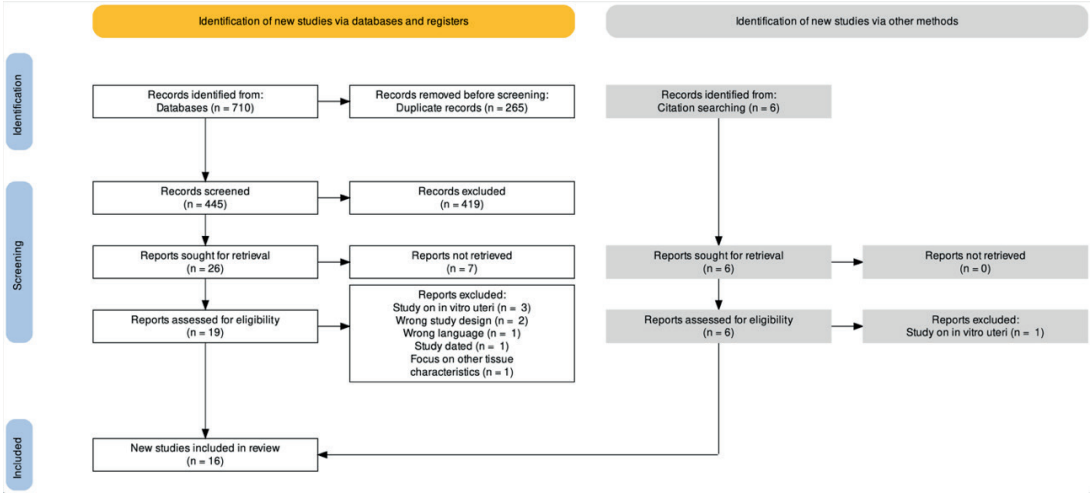

Study characteristics

Full details of the characteristics of the included studies are shown in Table 7.3. Of the sixteen included studies, nine studies assessed uterine peristalsis using Cine MRI, two using TVUS, one using HSSG and four using intrauterine pressure measurement. Table 7.4 shows an overview and definition of the measurement tools employed in the included studies. Eight studies assessed uterine peristalsis in patients with leiomyomas, five studies assessed uterine peristalsis in patients with endometriosis and/or adenomyosis and one study assessed uterine peristalsis in patients with congenital uterine anomalies, namely patients with a bicornuate uterus. One included study assessed uterine peristalsis in patients with leiomyomas and endometriosis. An additional paper on the influence of chronic endometritis on uterine peristalsis was identified and included, as chronic endometritis is classified as a uterine abnormality. No studies were identified that focussed solely on the influence of adenomyosis on uterine peristalsis. As described above, adenomyosis and endometriosis are associated and usually occur simultaneously to varying degrees however. Therefore, studies focussing on the influence of endometriosis on uterine peristalsis are included as well.

Table 7.3: Overview of study characteristics and main findings on leiomyomas, adenomyosis and endometriosis, congenital uterine anomalies and chronic endometritis.

Author (year)	Study design	Topic	Sample size	Inclusion/ exclusion criteria	Relevant patient demographics	Relevant control demographics	Method of measuring peristalsis	Assessed parameters	Moment of measurement	Intervention	Outcome measure	Results
Bulletti et al. (1997)	Case-control study	Endometriosis	16 patients, 12 controls	Patients: laparoscopically diagnosed endometriosis. Controls: normal menstruating, parous, no spontaneous abortion or symptoms of endometriosis	Age 30.55 years +/- 4.82	Age 35.50 years +/- 7.72	Intrauterine pressure measurement with two probes, one near the fundus and one near the cervix. For 20 minutes	Frequency, amplitude and basal pressure tone	/	/	Abnormal contractility	Fundus (patient vs control): frequency 28.40 +/- 8.96 vs 11.90 +/- 7.05 os/10min, amplitude 11.63 +/- 8.48 vs 6.41 +/- 4.29 mmHg, basal pressure tone 65.33 +/- 23.76 vs 25.28 +/- 19.94 mmHg.
Bulletti et al. (2002)	Controlled prospective case-control study	Endometriosis	22 patients, 22 controls	Both patients and controls: normal menstruation with unexplained fertility, nulliparous, no pelvic inflammatory disease, no severe adhesions and no adenomyosis. Patients: stage 2 or 3 endometriosis. Controls: no evidence of	Age 27.9 years +/- 5.5, 91% dysmenorrhea	Age 28.1 years +/- 6.2, 27% dysmenorrhea	Intrauterine pressure measurement with two probes, starting one near the fundus and one near the cervix. For 20 minutes while pulling out	Frequency, amplitude and basal pressure tone	Cycle day 2-4	Laparoscopic treatment	Uterine contractions, retrograde bleeding	Patient vs control: frequency 22.73 +/- 5.66 vs 11.09 +/- 3.26 os/10min, amplitude 20.82 +/- 3.94 vs 6.77 +/- 2.83 mmHg, baseline uterine pressure 50.14 +/- 16.30 vs 24.68 +/- 6.14 mmHg

				endometriosis								
Fornazari et al. (2019)	Controlled prospective study	Leiomyomas	26 patients	Symptomatic fibroids and indication for embolization with UFE, no hormonal blockade, premenopausal, not exclusively submucosal or subserosal fibroids, no current fertility therapies	Age 30 – 41 years (mean 36) 15 transmural, 5 submucosal, 5 intramural, 1 subserosal	/	Cine MRI, 4 min.	Presence, contraction pattern, fibroid location, uterine volume	Periovulatory phase	UFE	Uterine peristalsis	Cervix (patient vs control): frequency 25.90 +/- 10.21 vs 17.90 +/- 8.46 os/10min, amplitude 9.18 +/- 7.36 vs 6.95 +/- 4.07 mmHg, basal pressure tone 58.02 +/- 23.13 vs 42.41 +/- 14.18 mmHg
Kido et al. (2007)	Case-control study	Endometriosis	26 patients, 12 controls	Patients: pre-menopausal, diagnosed with endometrial cysts, no hormonal/ surgical treatment, no adenomyosis, no leiomyomas. Controls: no visible gynaecological anomalies, nulliparous, no gynaecological treatment, no fertility treatment, no hormonal treatment	Age 24-51 years (mean 35.1), 10 periovulatory, 13 luteal, 3 menstrual phases. 8 gravidities, 7 parous. 4 rights, 9 left, 13 bilateral cysts of the ovaries. Mean size cysts 4.2 +/- 2.2 cm	Age 23-32 years (mean 25.9)	Cine MRI, 2 min.	Presence, frequency, direction, sustained contractions	Periovulatory, luteal and menstrual phase	/	Uterine peristalsis	Patient vs control periovulatory phase: presence 30% vs 92%, <CF waves in patients, frequency 2.5 +/- 1.0 vs 4.4 +/- 1.6 per 2 min. Patient vs control luteal phase: presence 23% vs 25% Patient vs control menstrual phase: presence 100% vs 42%

Kido et al. (2011)	Controlled prospective study	Leiomyomas	20 patients	Symptomatic uterine leiomyomas, premenopausal, no hormone therapy, endometrium well visible, undergoing UAE	Age 39-53 years (mean 45.5 +/- 3.7)	/	Cine MRI, 3 min.	Presence, direction, frequency, uterine volume, index leiomyoma volume and location, number of leiomyomas	Periovulatory phase	UAE	Uterine peristalsis	After UAE: frequency increased ($p > 0,05$) direction remained mainly CF presence increased: 6 cases (3 intramural, 2 submucosal, 1 subserosal) with new UP
Kido et al. (2014)	Case-control study	Leiomyomas	20 patients, 20 controls	Patients: premenopausal, no hormone therapy, UP well assessed Controls: no pelvic abnormalities, no hormone therapy	Age 39-53 years (mean 45.5 +/- 3.7)	Age 19-46 years (mean 33.3)	Cine MRI, 3 min.	Presence, direction, frequency, index leiomyoma volume and location, number of leiomyomas	Periovulatory phase	/	Uterine peristalsis	Presence and frequency lower in patients directions in both mainly CF larger uterine volume and index fibroid (located intramurally) when UP No UP then fibroid submucosal, intracavitary or subserosal
Kissler et al. (2007)	Controlled prospective case-control study	Endometriosis and adenomyosis	80 patients, 24 controls	Patients: diagnosed with endometriosis. Controls: good health	Most rAFS-stages 1 and 2. 50 with peritoneal endometriosis of which 42 with additional adenomyosis of which 28 with focal spread of ≥1 adenomyotic lesions and 12 with diffuse adenomyosis	Not noted	HSSG, scans made up to 30 min. after application of marked microalbumin aggregates	Direction	Late follicular phase	/	Direction of utero-tubal transport	Patients(endometriosis) vs controls: 38.5% vs 67% intact utero-tubal transport capacity, 61.5% vs 33% pathologic transport. Endometriosis, no adenomyosis vs focal spread vs diffuse adenomyosis: 62.5% vs 46% vs 21.5% intact transport, 37.5% vs 54% vs 78.5% pathologic transport
Leyendecker et al. (1996)	Case-control study	Endometriosis	111 patients, 94	Patients: history of infertility, diagnosed	Age 21-38 years (mean 29), 1-7 years	Age 22-46 (mean 30)	TVUS, 5 min. and HSSG	Presence, frequency, direction	VSUP: menstrual and early, mid and	/	Uterine peristalsis	Patient vs control: doubling of frequencies during early, mid and late

			controls	endometriosis, tubal patency. Controls: regular cycles, history of fertility, tubal patency, no endometriosis.	of infertility (mean 4), 82 minimal - mild, 29 moderate - severe endometriosis. Most regular cycle, some prolonged proliferative and short luteal phase				late follicular, mid-luteal phase. HSSG: early, mid and late follicular phase			follicular and mid-luteal phase. Also increase in frequency during menses. Both decrease in FC contractions throughout cycle. Late follicular: patients show irregular contractions
Nishino et al. (2005)	Controlled prospective study	Leiomyomas	26 patients	Leiomyomas detected on TVUS; whole uterine cavity visible, able to visualize UP	Age 19-51 years (mean 41) 16 submucosal, 13 intramural/ subserosal leiomyomas, 3 both (included in submucosal). Leiomyoma size 1.5-10 x 1.5-8 cm. Submucosal: 1 menses, 3 follicular, 1 periovulatory, 10 luteal, 1 phase unclear. Intramural: 2 menses, 2 follicular, 2 periovulatory, 4 luteal phase	/	Cine MRI, 2 min.	Presence, direction, frequency, conduction, focal loss of waves and focal movements (direction and frequency)	Menstrual, follicular, periovulatory and luteal phase	/	Uterine peristalsis	Submucosal: UP present: 12/16, direction: 4/5 CF midcycle, 1/1 FC menstrual phase, frequency: 1-3x/2min luteal phase, 2-5x/2 min. remaining cycle, conduction of UP: 4/12 obscured, non-propagating movement adjacent to leiomyoma 9/16 with frequency of 5-14x/2 min. 4 showed loss of UP Intramural/ subserosal: UP present: 10/10, direction: 2/3 CF midcycle, 2/2 FC menstrual phase, frequency 1-4x/2 min luteal phase, 2-5x/2 min. remaining cycle. Conduction of UP good

Oliva et al. (1992)	Controlled prospective study	Bicornuate uterus	12 patients	Bicornuate uterus	7 symmetrical cavities, 5 asymmetrical cavities	/	Intrauterine pressure measurement with 2 balloon-closed catheters, 1 in each horn	Frequency, amplitude, basal pressure tone	Ovulation and premenstrual phase	Oxytocin and methyl ergobasine	Uterine motility	Before drugs: Symmetrical cavities: Ovulation: UP similar in horns, pressure: 5-12 mmHg, frequency: 3-5x/min. Premenstrual: UP similar in horns, pressure: 20-30 mmHg, frequency: 1/min. Asymmetrical cavities: Ovulation: UP dissimilar in horns. Premenstrual: UP in larger horn typical, smaller horn different
Orisaka et al. (2007)	Case-control study (pilot)	Leiomyomas	19 patients, 3 controls	Patients: premenopausal, normal menstrual cycles, diagnosed with leiomyomas Controls: healthy women	Age 24-42 years (mean 34.8) 15 intramural, 2 subserosal and 2 submucosal leiomyomas	Age 28-36 (mean 32), mean length cycle: 30.3 days	Cine MRI, 3-4 min.	Presence, direction, frequency	Menstruation, follicular, periovulatory and early, mid- and late luteal phase	/	Uterine peristalsis	UP present in all women. Direction: almost similar in both groups in follicular, periovulatory, early luteal and late luteal phase. Patient vs control: menstrual phase: FC + isthmical + opposing vs FC, midluteal phase: isthmical + CF + FC + opposing vs isthmical
Pinto et al. (2015)	Case-control study	Chronic endometritis	45 patients, 45 controls	Both patients and controls: no use of drugs (2 months), no smoking, no alcoholics, no uterine and adnexal pathology, no previous	Age 30.4 years +/- 4.5. Indication for hysteroscopy: infertility 42.3%, recurrent miscarriages 35.5%, abnormal uterine	Age 30.2 years +/- 3.5. Indication for hysteroscopy: infertility 56.3%, recurrent miscarriages 15.5%,	TVUS, 3 min.	Presence, direction, frequency	Periovulatory and midluteal phase	/	Direction and frequency of endometrial waves	Patient vs control: periovulatory phase: CF 26.7% vs 88%, FC 24% vs 0%, opposing 22.7% vs 12%, not propagated 13.3% vs 0%, absent 13.3% vs 0%. Frequency of UP higher in control group.

				pelvic surgery. Patients: diagnosis of chronic endometritis. Controls: No evidence of chronic endometritis	bleeding 22.2%	abnormal uterine bleeding 28.2%						
Qu et al. (2019)	Controlled prospective study	Leiomyomas	30 patients	> 18 years, premenopausal, planning to undergo USgHIFU treatment, diagnosed with non-malignant symptomatic leiomyomas, agreed to MRI, safe execution of MRI possible, myoma clearly visible with TVUS, no prior treatment of leiomyomas, no other pelvic/ systemic diseases and no scarring, no hormone therapy or IUD.	Age 24-47 years (mean 37)	/	Cine MRI, 2 min.	Presence, direction, frequency, uterine volume, index leiomyoma volume and location, number of leiomyomas	Periovulatory phase	USgHIFU	Uterine peristalsis	After USgHIFU: frequency: increased direction: remained CF presence: in 22-23 compared to 10-11 before intervention. Leiomyomas smaller and mainly intramural or submucosal and/or larger reduction rate of index leiomyoma when UP arose. No differences in uterine volume and reduction rate, location of largest fibroid, number of fibroids. Submucosal fibroids showed no UP
Szamatowicz et al. (1997)	Controlled	Leiomyomas	12 patients	Regularly menstruating women	Age 29 – 43 years	/	Intrauterine pressure measureme	Presence, amplitude,	Periovulatory phase	Myomectomy, oxytocin	Spontaneous uterine contractions	After myomectomy: presence: increased amplitude: increased

	prospecti ve study			undergoing myomectomy	Indication for myomectomy: 7 infertility, 5 dysmenorrhea/ menorrhagia		nt with one catheter in the tip of the fundus, 2-4 hours	deformatio n index	(day 10 – 15)	and vasopressin		deformation index: increased
Yoshino et al. (2010)	Controlle d prospecti ve study	Leiomyoma s (partially endometrio sis)	51 patient s	Solely Intramural leiomyomas, no other infertility factors (except endometriosi s), MRI during implantation window	Age 29-41 years, normal menstrual cycles with normal hormones (FSH, LH, prolactin, oestradiol and progesterone), tubal patency, normal BBT cycle.	/	Cine MRI, 3 min.	Presence, frequency, presence of endometrio sis, location and number of leiomyoma s	Implantatio n/ luteal phase (day 5-9)	Infertility treatment	Junctional zone movement	57% low frequency (0-1x/3 min.) and 43% high frequency (3-6x/3min.) UP Endometriosis morbidity same in both groups
Yoshino et al. (2012)	Controlle d prospecti ve study	Leiomyoma s	15 patient s	Infertility ≥ 24 months with intramural leiomyoma, ≥ 12 months when severe symptoms present, no other infertility factors, MRI before and after myomectomy at luteal day 5-9, high frequency (≥2x/3min.) UP before surgery.	Age 29-41 years, normal menstrual cycles with normal hormones (FSH, LH, prolactin, oestradiol and progesterone), tubal patency, normal BBT cycle.	/	Cine MRI, 3 min.	Presence, frequency	Luteal phase day 5-9	Myomecto my	Junctional zone movement	Frequency normalized in 14/15 patients from ≥ 2x/3 min. to 0-1x/3min. 1 patient from 5x/3min. to 3x/3min.

Abbreviations: UFE, uterine fibroid embolisation; UAE, uterine artery embolisation; CF, direction of uterine contractions cervix-to-fundus; UP, uterine peristalsis; rAFS-stage, revised American Fertility Society-stage; HSSG, hysterosalpingoscintigraphy; TVUS, transvaginal ultrasound; VSUP, video sonography of uterine peristalsis; FC, direction of uterine contractions fundus-to-cervix; USgHIFU, Ultrasound-Guided High-Intensify Focused Ultrasound; IUD, intra-uterine device; BBT, basal body temperature.

Risk of bias in studies

Table 7.2 shows the risk of bias per included study. Five studies were of good quality, seven studies of fair quality and four of the included studies of poor quality. No studies were of excellent quality. The extensive, non-simplified, quality assessment is included in appendix 7B.

Table 7.2: Simplified risk of bias assessment of the included studies

	Bulletti et al. (1997)	Bulletti et al. (2002)	Fornazari et al. (2019)	Kido et al. (2007)	Kido et al. (2011)	Kido et al. (2014)	Kissler et al. (2007)	Leyendecker et al. (1996)	Nishino et al. (2005)	Oliva et al. (1992)	Orisaka et al. (2007)	Pinto et al. (2015)	Qu et al. (2019)	Szamatowicz et al. (1997)	Yoshino et al. (2010)	Yoshino et al. (2012)
Reporting	5/8	6/11	9/11	7/8	7/11	5/8	2/9	6/8	5/7	2/10	5/7	4/8	9/11	7/11	7/9	10/11
External validity	0/2	2/3	1/3	0/2	1/3	0/2	0/2	0/2	2/2	0/2	0/2	0/2	0/3	1/3	2/3	1/3
Internal validity - bias	3/3	4/4	5/5	3/3	4/5	3/3	2/3	3/3	2/2	4/4	2/2	3/3	4/5	4/5	4/5	3/5
Internal validity - confounding (selection bias)	1/3	1/4	2/2	0/3	1/2	0/3	0/4	0/3	2/3	0/4	0/3	2/3	2/2	0/2	2/4	1/2
Power	0/1	0/1	0/1	0/1	0/1	0/1	0/1	0/1	0/1	0/1	0/1	0/1	0/1	0/1	0/1	0/1
Score	9/17	13/23	17/22	10/17	13/22	8/17	4/19	9/17	11/15	6/21	7/15	9/17	15/22	12/22	15/22	15/22
Overall quality assessment	●	●	●	●	●	●	●	●	●	●	●	●	●	●	●	●

Results of individual studies

An overview of the study characteristics and a summary of the extracted data is included in Table 7.3.

A summary of study findings per uterine contraction feature and uterine abnormality is shown in Table 7.4.

Table 7.4: Summary of Uterine Contractility Measurement Tools used in Included Studies

	Measurement Method	Contraction Features Assessed	Studies Used
Cine MRI	Subjective visualisation of contractions in the junctional zone of the uterus on 2D MRI	Frequency, Direction	(245–252)
IUP Catheter	Intra-uterine catheter with sensors at different points	Frequency, Amplitude, Direction	(253–256)
HSSG	Visualisation of displacement of vaginally administered radio-isotope over time using scintigraphy imaging	Direction	(219)
TVUS	Subjective visualisation of contractions in the junctional zone of the uterus on 2D ultrasound	Frequency, Direction	(219,232,257)

Leiomyomas and uterine peristalsis

Five out of six included studies investigating uterine contractility in leiomyoma patients used cine MRI, with one study investigating uterine contractility using an IUP catheter.

Presence of uterine contractions

In a case-control study by Orisaka et al. (2007), in all patients with leiomyomas (n= 19) and healthy controls (n= 3) uterine contractions were observed (252). Their conclusion that leiomyomas have no influence on the presence of uterine contractions was not confirmed by studies by Yoshino and Kido (246,249). Yoshino observed in a prospective study , an increased presence of uterine contractions in patients with leiomyomas (n= 15) during the midluteal phase (249). In the study by Kido et al fewer patients with leiomyomas (n= 20) showed uterine contractions compared to healthy controls (n=20) during the periovulatory phase (246). Nishino et al. (2005) reported that presence of uterine contractions may be correlated to the subtype of leiomyomas: patients with intramural leiomyomas (n=26) universally presented uterine peristalsis, whereas this was not seen in patients with submucosal leiomyoma's (250). Four controlled-prospective studies

observed an increase in presence of uterine contractions during the periovulatory phase after the treatment of leiomyomas by uterine artery embolisation (UAE), ultrasound-guided high-intensify focussed ultrasound treatment (USgHIFU), uterine fibroid embolisation (UFE) and myomectomy compared to before treatment (247,251,255,258).

Contraction frequency

The case-control study by Orisaka et al. observed almost identical peristaltic patterns regarding contraction frequency in patients with leiomyomas (n=19) versus healthy controls (n=3) during all phases of the menstrual cycle (252). Two studies, on the other hand, observed altered peristaltic patterns in patients with leiomyomas and suggested the influence of leiomyomas on contraction frequency seemed menstrual-phase dependent (246,249). A decreased contraction frequency in patients with leiomyomas (n=20) was reported during the periovulatory phase (246), whereas an increased frequency was noticed in some patients with leiomyomas (n=20) during the mid-luteal phase compared to controls (n= 20) (249). Leiomyoma localisation seemed to have no effect on the contraction frequency (250). In three controlled prospective studies, initially altered uterine peristalsis normalised after treatment of uterine leiomyomas, including myomectomy, UAE and USgHIFU (247,248,258). After treatment, a relatively decreased contraction frequency was noted during the mid-luteal phase (248), whereas an increase in frequency was observed during the periovulatory phase (247,258).

Contraction amplitude

The contraction amplitude in patients with leiomyomas has not been compared yet with the contraction amplitude in healthy controls. A study by Szamatowicz et al. reported a higher contraction amplitude after myomectomy however (255).

Contraction direction

In five studies, the contraction direction during the periovulatory phase was observed form cervix-to-fundus in both patients with leiomyomas and healthy controls (246,247,250,252,258). One of these case-control studies also concluded that contraction direction in the follicular and late luteal phase was almost identical in patients (n= and healthy women(n=. Differences in contraction direction between patients with leiomyomas (n=19) and healthy

women (n=3) were noted during menstruation and the mid-luteal phase (252). Nishino et al. (2005) showed a fundocervical contraction direction during menses in all patients with leiomyomas (n=26). The location of the leiomyomas seemed to be of no statistically significant influence (250). After treatment of uterine leiomyomas by either UAE or USgHIFU, the cervicalfundal movement during the periovulatory phase remained unchanged (247,258).

Additional peristaltic observations

A case-control study reported that 33% of the patients (n=9/16) with submucosal leiomyomas had disturbed uterine peristalsis. Specifically, higher frequency focal myometrial movements in the immediate vicinity of the leiomyoma were observed (250). After treatment of uterine leiomyomas with UFE, uterine contractions were noted to become more coordinated (251).

Adenomyosis/Endometriosis and uterine peristalsis

Five studies investigated uterine peristalsis in adenomyosis/endometriosis patients, with two studies using IUP catheter measurement, one TVUS and HSSG, one only HSSG, and one cine MRI.

Presence of uterine contractions

Uterine peristalsis was noted in both patients with endometriosis and healthy controls (253). Bulletti et al. (2002) confirmed the presence of uterine contractions during the menstrual phase in both patients with endometriosis (n=22) and controls (n=20) (254). In a case-control study by Kido et al. (2007), by contrast, a difference was found in the presence of uterine contractions throughout the entire menstruation cycle. During the periovulatory phase, statistically significantly fewer patients with endometriosis (n=26) had uterine contractions compared to controls (n=12). A trend towards a lower presence during the luteal phase and higher during the menstrual phase compared to controls was suggested but did not prove to be significant (245).

Contraction frequency

In three studies, the increase in frequency from early to late follicular phase in healthy controls was also observed amongst women with endometriosis (232,245,253,254). As reported in several studies, the contraction frequency

overall is different in the presence of endometriosis (232,245,253,254). When the menstrual phases are disregarded, a higher contraction frequency was observed in patients with endometriosis than in controls (253). Leyendecker et al. (1996) specifically investigated the contraction features through the menstrual cycle phases and found a higher contraction frequency in patients with endometriosis (n= 111) than in controls (n=94) across phases. Contraction frequency was especially increased in the follicular and mid-luteal phase (232). Contradictorily, Kido et al. (2007) found a decreased contraction frequency during the periovulatory phase in patients with endometrial cysts (n=26 vs. n=12) (245). A controlled prospective study contradicted these outcomes, showing that endometriosis had almost no influence on uterine contractions during the periovulatory phase. Endometriosis severity did not seem to affect contraction frequency (249).

Contraction amplitude

Bulletti et al. (1997) described a (non-significant) increased uterine amplitude in patients with endometriosis (n=16) compared to healthy women (n= 12) (253). Further research confirmed statistically significantly increased contraction amplitude in endometriosis patients (n=22 vs n=22) across menstrual cycle phases (254).

Contraction direction

Contraction direction in patients with endometriosis was only examined by two studies. One case-control study stated that patients with endometriosis (n=111) as well as healthy women (n=94) progressing through the menstrual cycle show a similar decrease in cervix-to-fundus directed contractions (232). A further case-control study focusing on the influence of endometriosis presenting as endometrioma's, did report a difference versus healthy women, with statistically significantly fewer uterine contractions from cervix-to-fundus in endometriosis patients during the periovulatory phase (245).

Additional peristaltic observations

During the follicular phase, patients with endometriosis (n=111) demonstrated more of these dysperistaltic contractions compared to controls (n= 94) (232). In patients with endometriosis and additional adenomyosis (n=24/80), hyperperistalsis is seen in patients with an focal adenomyosis (n=14/80)

whereas dysperistalsis was seen in patients with diffuse adenomyosis (n=11/80) (219).

Congenital uterine anomalies and uterine peristalsis

Contraction frequency

One small study investigated women with a bicornuate uterus (n=12). using an IUP catheter, these patients showed a similar contraction frequency when compared to what the literature reveals as normal in controls (256). In case of dissimilarity of the two parts of the uterus, differences in frequency, characterized by a disorganised pattern of contractions, were noticed in the smaller uterine horn especially in the late-luteal phase.

Chronic endometritis and uterine peristalsis

Contraction frequency

A case-control study using TVUS noticed a decreased contraction frequency in patients with chronic endometritis (n=45) compared to healthy controls (n=45), particularly during the periovulatory phase. No further differences were found (257).

Contraction direction

Pinto et al. (2015) reported a statistically significant influence by the presence of chronic endometritis on the contraction direction during the periovulatory and midluteal phase. During the periovulatory phase, patients with chronic endometritis presented less cervix-to-fundus contractions compared to healthy controls. During the midluteal phase patients showed general dysperistalsis (257).

Discussion

In summary, the available literature suggests that uterine abnormalities may indeed influence uterine peristalsis even though measurement methods differed across studies. Findings of included studies report that presence of leiomyomas generally lead to a decreased presence of uterine contractions in various menstrual phases, whereas endometriosis/adenomyosis lead to an increased frequency across menstrual phases. No changes in the presence of uterine contractions were noted in patients with a bicornuate uterus or chronic endometritis. Studies were contradictory on the influence of uterine abnormalities on contraction direction. Only patients with chronic endometritis exhibited clearly altered contraction direction was described. The influence of uterine abnormalities on contraction amplitude has not yet been studied extensively. Endometriosis, however, seems produce an increase in contraction amplitude. Dysperistalsis was noted in patients with leiomyomas, endometriosis, adenomyosis and an asymmetric bicornuate uterus. Another observation in patients with leiomyomas was that the treatment of leiomyomas re-established normal uterine contractions, which could confirm the effect of leiomyomas on uterine peristalsis.

Previously published systematic reviews have mainly focused on the influence of uterine contractions on fertility. Kuijsters et al. (2017) briefly described the influence of uterine abnormalities on peristalsis. The results of this systematic review supports their reported influence of uterine abnormalities on uterine contraction features (233). It was postulated that abnormal uterine contractions in patients with uterine abnormalities could be the cause of infertility (233), a hypothesis supported by Hunt et al. (2020). Effects of endometriosis, adenomyosis and leiomyomas on uterine peristalsis were also described by Hunt et al. (2020), with similar conclusions to this review. A clear influence of endometriosis on contraction direction was reported; however, this could not be confirmed in our review (259).

Even though more attention is being given to uterine peristalsis recently, few systematic reviews have been conducted on this subject. This review gives a clear summary of the published studies on the influence of uterine abnormalities on uterine peristalsis up to now. To give an overview of all gathered knowledge, it was chosen to include studies regardless of the

method used to assess uterine peristalsis. This, however, does make the results of the various studies difficult to compare. As seen in Tables 7.3 and 7.4, four techniques of visualising uterine peristalsis have been used, each with its own limitations. Few can assess all potential parameters and results are often based on subjective assessment of obtained images. To ensure comparability amongst studies, it would be better to eradicate this subjectivity by automating the analysis, as proposed by Sammali et al. (2019) (229,260).

Studies were also difficult to compare due to heterogeneity in study designs, populations and intervention. The moment of measurement in the menstrual cycle seemed to be of major influence on the observed contraction features, however not all studies reported this (253). Additionally, the sample size of most of the included studies was small. In three studies, participants were divided over the menstrual phases and uterine contractions were only assessed in that particular phase (245,250,252). As the result of this, only a few participants were assessed per menstrual phase. One might argue whether this is enough to draw conclusions. Furthermore, some included studies are relatively dated.

This results from a lack of recent literature on the influence of uterine abnormalities, specifically congenital uterine anomalies, on uterine peristalsis. Besides, reported differences in uterine contractions in endometriosis patients might be influenced by an unreported presence of adenomyosis. Since the sonographic diagnosis of adenomyosis can be difficult, an undiagnosed presence in this endometriosis group could have biased the outcome. Additionally, an article on the influence of endometriosis, presented as endometrial cysts, was included. It could be questioned if this has a comparable effect on uterine peristalsis as in (deep) endometriosis or adenomyosis.

Finally, the included studies use different definitions of uterine peristalsis. Non-propagating contractions were included in the definition of uterine peristalsis in some, and defined as dysperistalsis, but excluded or unmentioned in other studies. This calls for a standard definition for uterine peristalsis and its various features.

Conclusions

Despite the heterogeneity of the included studies, it can be concluded that uterine abnormalities influence uterine peristalsis, often leading to a, menstrual phase-dependent, altered frequency and decreased presence of uterine contractions. The presence of abnormal uterine peristalsis could indicate the presence of underlying uterine pathology. This knowledge could potentially aid in a better diagnosis of uterine abnormalities. More research is needed into objective measurement tools of uterine peristalsis, and into both treatment and clinical implications of abnormal uterine peristalsis in these patients.

CHAPTER 8:

Quantitative Ultrasound Measurement of Uterine Contractility in Adenomyotic Versus Normal Uteri: A multi-centre prospective study

Authors:
Connie O. Rees
Sophie Thomas
Anna de Boer
Yizhou Huang,
Brunella Zizolfi
Virginia Foreste
Attilio di Spiezio di Sardo
Nikos Christoforidis
Hubertus A.A.M. van Vliet
Massimo Mischi
Benedictus C. Schoot

The content of this chapter is currently accepted with revisions
Fertility & Sterility 2023

Abstract:

OBJECTIVES: To evaluate uterine contractility (UC) in adenomyosis patients compared to healthy controls using a quantitative two-dimensional transvaginal ultrasound (TVUS) speckle tracking method.

MATERIALS AND METHODS: This multi-centre prospective observational study took place in three European centres between 2014 and 2023. 46 women with a sonographic or MRI diagnosis of adenomyosis were included. 106 healthy controls without uterine pathologies were included. Four-minute TVUS recordings were performed and four UC features were extracted using a speckle tracking algorithm. The extracted features were: contraction frequency (CF) (contractions/minute), amplitude, velocity (mm/s) and coordination. Women with adenomyosis were compared to healthy controls according to the phase of the menstrual cycle.

RESULTS: Throughout the different phases of the menstrual cycle, trends of increased amplitude, decreased CF and velocity, and reduced contraction coordination were seen in adenomyosis patients compared to healthy controls. These were statistically significant in: the late follicular phase, with higher amplitude (0.087±0.042 vs. 0.050±0.018, p=0.001), lower CF and velocity (1.49±0.22 vs. 1.68±0.25 contractions/minute, p=0.021, and 0.65±0.18 vs. 0.88±0.29 mm/sec, p=0.014, respectively), and reduced contraction coordination (0.34±0.08 vs. 0.26±0.17, p=0.015), in the late luteal phase, with higher amplitude (0.050±0.022 vs 0.035±0.013, p=0.038), lower velocity (0.51±0.11 vs. 0.65±0.13 mm/sec, p=0.027), and reduced contraction coordination (0.027±0.06 vs. 0.18±0.07, p=0.011), and in the mid-follicular phase, with decreased CF (1.48±0.21 vs. 1.69±0.16 contractions/minute, p=0.013) in adenomyosis patients compared to controls. During menses, a higher pain score was significantly associated with lower CF and velocity and higher contraction amplitude ($P<0.05$).

CONCLUSION: UC differs in adenomyosis patient compared to healthy controls throughout the phases of the menstrual cycle. This suggests an etiological mechanism for the infertility and dysmenorrhea seen in adenomyosis patients. Moreover, it presents new potential therapeutic targets and diagnostic markers.

Keywords: Adenomyosis; Uterine Peristalsis; Transvaginal Ultrasound; Dysmenorrhoea

Introduction:

Uterine peristalsis (UP) occurs in the endo-myometrial layer of the non-pregnant uterus. On transvaginal ultrasound (TVUS) it can be visible in the junctional zone (JZ) and appears as wave-like movements (70,237). UP is thought to have physiological function and its behaviour is cycle-phase dependent (237,261,262). During menstruation, the peristalsis is directed from fundus-to-cervix (F2C), supporting the expulsion of endometrial lining, with a relatively low frequency. During the periovulatory phase, UP switches to cervix-to-fundus (C2F) contractions and has the highest frequency and velocity. It is thought that contractions in this phase are especially directed towards the ipsilateral side of the dominant follicle, supporting sperm transport (262,263). Disturbances herein may affect sperm transport and thus fertilization. After ovulation, contractions in the luteal phase are relatively quiescent in order to facilitate embryo implantation, with the lowest contraction frequency (CF) of all phases seen. During this phase, opposing contractions occur, directed toward the mid-corpus of the uterus from both the cervical and fundal regions. Similarly, disturbances in this phase of uterine contractility may affect the ability of an embryo to implant successfully. Recent work by our group has been able to measure this uterine peristaltic behaviour in an objective manner using a dedicated speckle tracking method on 2D-transvaginal ultrasound (263,264).

Adenomyosis is characterized by disruption of the uterine junctional zone (JZ). It is generally associated with abnormal uterine bleeding (AUB), dysmenorrhea, subfertility and chronic pain. As contractile function of the non-pregnant uterus is thought be concentrated in the JZ, this hypothetically leads to a disturbance of the uterine peristalsis (UP) in the context of adenomyosis (8,76,77). Aberrant uterine contractility has also been posited as an etiological mechanism for the development of adenomyosis and endometriosis (76,77,148), but evidence on this front is lacking (265).

Few studies have assessed differences in UP between non-pregnant women with adenomyosis and healthy women. The studies that do exist have been done using (subjective) methods which are not able to characterize all aspects of uterine motion in a quantitative manner (266). More knowledge on the physiological differences between these groups could contribute to a better understanding of adenomyosis, more accurate diagnosis, and potentially more

tailored treatment. In this multi-centre prospective study, we aimed to investigate the differences in uterine contractility in women with adenomyosis versus women with normal uteri throughout the menstrual cycle.

Materials and Methods:

Study objectives:

Evaluate uterine contraction features (frequency, amplitude, velocity, direction, and coordination) using a dedicated speckle-tracking algorithm by 2D transvaginal ultrasound measurement in women with adenomyosis versus women with normal uteri throughout the menstrual cycle.

Study design & setting:

This multi-centre observational prospective cohort study was carried out in the outpatient gynaecology departments of the Catharina Hospital in Eindhoven, the Netherlands, the University of Naples, Federico II Naples, Italy, and the Embryolab Fertility centre in Thessaloniki, Greece.

Participants:

Between September 2014 and January 2023, 179 women were included from of the participating centres. Women were included if they were ≥18 years of age, pre-menopausal and had a natural menstrual cycle (NMC). No power calculation was done due to lack of relevant published data on this topic.

Exclusion criteria were: 1) pregnancy, 2) unable to give informed consent, 3) significant language barrier, or 4) other benign uterine pathology (congenital or otherwise, e.g., leiomyomas, caesarean section scar, or other uterine surgery affecting the myometrial integrity) and 5) use of hormonal contraceptive methods or intra-uterine devices. Ultrasounds of included women were assessed retrospectively by two experts independently to confirm the presence or absence of uterine abnormalities. After enrolment, all TVUS recordings also were subjected to a quality check. Recordings could be considered of low quality due to several factors, including insufficient resolution, out-of-plane motion, intestinal shadowing, and suboptimal orientation of the uterus limiting the view of the endo-myometrium. In case of low quality, the recording was excluded from the study. Figure 2 presents a flow chart of patient inclusion.

Healthy women:

The control group consisted of healthy women with sonographically normal uteri. A normal cycle was defined as: regular (duration 28 (± 2) days), no dysmenorrhea (reported VAS <4 during menses), no menometrorrhagia.

Adenomyosis Patients

For the adenomyosis group, women were included if they had sonographic markers for adenomyosis, based on (Morphological Uterine Sonographic Assessment (Morphological Uterine Sonographic Assessment, MUSA (183)) criteria. Women were also included if they had signs of adenomyosis on MRI (if available), according to MRI criteria as described in literature (29,181,199). The added presence of endometriosis was not considered as an exclusion criteria.

Data sources and measurements:

TVUS measurement:

Transvaginal ultrasounds (TVUS) were performed during several phases of the menstrual cycle: the menstrual phase (M, cycle day (CD) 1-5), mid-follicular (MF, CD 6-10), late follicular phase (LF, CD 11-14), early luteal phase (EL, CD 15-20) and late luteal phase (LL, CD 21-28). Four-minute video recordings of the uterus in the mid-sagittal section were made. The ultrasound machines were: an Accuvix WA80S with Elite (Samsung Medison, Seoul, Korea) equipped with a V5-9 transvaginal probe (bandwidth 5-9 MHz) or a GE Voluson (GE Healthcare, Zipf, Austria) equipped with a RIC5-9W-RS probe (bandwidth 3.8-9.3MHz). Differences in speckle characteristics were corrected between both ultrasound platforms.

Feature Extraction:

Various uterine contractility features were extracted from the ultrasound recordings using a dedicated speckle tracking algorithm previously developed and implemented in Matlab software (Mathworks, Natick, USA). The full details of the methodology of feature extraction have been described in detail in previously published works (221,224,226–229). All contraction features were assessed separately for the anterior uterine wall (AW) and the posterior uterine wall (PW).

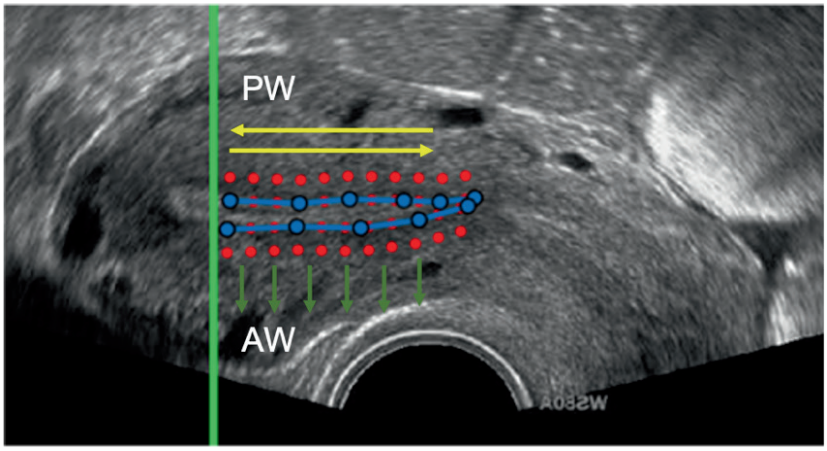

Figure 8.1: 2D Transvaginal ultrasound image of uterus in midsagittal section.

The region denoted by the blue and red markers is the junctional zone (JZ) where the uterine contraction features are observed and measured. The yellow arrows visualize movements in the longitudinal direction, and the green arrows illustrate movements in the radial direction. AW: Anterior Wall; PW: Posterior Wall.

Contraction Frequency:

Frequency features were analysed in the longitudinal and radial direction (see figure 8.1). Frequency-related features are reported as contractions per minute (221). Further technical details about feature extraction and analysis can be found in Sammali et al. (2019) (267).

Contraction Amplitude:

Contraction amplitude features reflect the relative strength of uterine contraction(221). Results are reported for contractions in the longitudinal direction.

Contraction Direction

Uterine contractions propagate in either the fundus-to-cervix (F2C) or the cervix-to-fundus (C2F) direction. The radial strain signal representation in the spatiotemporal frequency domain was analysed, where the spatial domain is intended along the longitudinal direction of the uterus (229). The ratio between the strain signal energy in the quadrants corresponding to the two propagation directions (C2F and F2C) provided a global measure of the dominant propagation direction in each wall (229). A more positive value

represented movement predominantly in the F2C direction, whereas a more negative value represented movement predominantly in the C2F direction. A value around zero represented movement without a predominant direction, that being opposing contractions.

Contraction Velocity:
Velocity, which is propagation speed of the peristaltic waves in a certain direction (C2F or F2C, in mm/sec), was calculated. This was again done by analysing the radial strain signal in the spatiotemporal frequency domain, along the longitudinal direction of the uterus (229). The analysis was performed over a window of 20 seconds sliding over the full recording time. Subsequently, the median velocities (MV) in C2F and F2C directions were calculated by averaging velocities over time in the corresponding directions. A high value reflected increased velocity in the reported direction.

Contraction Coordination:
We also assessed the coordination of uterine contractions. In order to quantify this, we assessed whether the anterior and posterior wall of the uterus were moving synchronously or asynchronously to each other. This resulted in a feature defining the uterine contraction coordination depending on the similarity in the dominant contraction direction between the anterior and posterior walls, denoted as: mean square error (MSE). Again, full details on the technical background of these units has been published elsewhere (229). A higher value reflected decreased contraction coordination.

Study outcomes:
The primary outcomes investigated were the following uterine contraction (UC) features:

- Frequency, in contractions/minute
- Amplitude (unitless)
- Direction, (unitless, whereby >0.0 globally represents F2C movement, and <0.0 represents C2F movement)
- Median Velocity (mm/sec)
- Coordination, in Mean squared error (MSE)

The UC features were compared between the adenomyosis and control group, according to the phase of the menstrual cycle. The UC features were then analysed in women with adenomyosis during the menstrual phase according to reported visual analogue scale (VAS) score.

Demographic and clinical characteristics were also gathered for participating women, such as age, BMI, parity, cycle duration, medical history, uterine morphology on TVUS and history of subfertility.

Statistical methods:
Statistical analysis was performed using IBM SPSS statistics version 28. Counts and frequencies were compared between groups for patient and demographic characteristics. Categorical variables were reported as frequencies and compared using the chi squared test. Continuous variables were reported as means (and standard deviation) if normally distributed, and medians (with interquartile range) if abnormally distributed. Comparison of the outcome measures (frequency, amplitude, direction, coordination and velocity) between patient groups per cycle phase was done using the Mann-Whitney U test if abnormally distributed, and independent T-test if normally distributed. The association between the UC features and dysmenorrhea (VAS score) in the adenomyosis group during M phase was measured using the Pearson correlation coefficient. Statistical significance was defined as a p-value < 0.05. This study is reported according to STROBE guidelines (189), see appendix 8A for the accompanying STROBE checklist.

Ethical approval:

This study received ethical approval from the local and regional ethical committees of participating centres, with study number NL52466.100.15. All participants gave informed consent prior to study participation. The WAVES study is registered in the Netherlands Trial Registry under number NL5035.

Results

Patient characteristics and recruitment

Forty-six women with adenomyosis and 106 women with healthy uteri were enrolled in our study. A total of 53 TVUS recordings were made of women with adenomyosis across the different phases of the menstrual cycle. Fourteen recordings were excluded after the quality check, leaving 39 recordings of adenomyosis patients included in analysis. These consisted of fourteen recordings during the M phase, seven during the MF phase, ten during the LF phase, one during the EL phase, nine during the LL phase. A total of 125 recordings were made of women with healthy uteri. Nineteen recordings were excluded during quality check, leaving 106 recordings of women with healthy uteri included in analysis. This resulted in eleven recordings during the M phase, eighteen during the MF phase, 48 during the LF phase, fourteen during the EL phase, fifteen during the LL phase. See Figure 8.2 for a detailed overview of patient and recording inclusion.

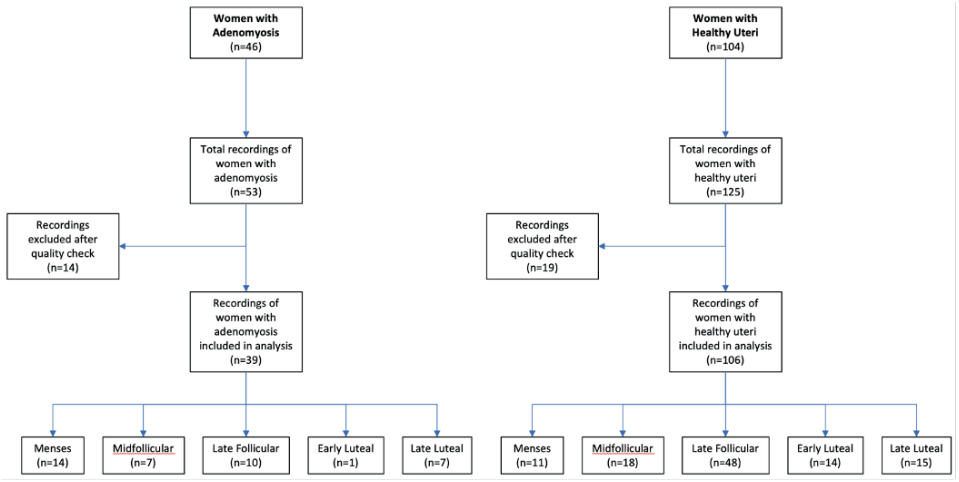

Figure 8.2: Flowchart of patient enrolment and inclusion for the adenomyosis and control groups.

Relevant patient characteristics are summarized in Table 8.1. Women with adenomyosis were older ($p<0.001$), had higher BMI ($p=0.003$), higher parity ($p=0.006$), and greater uterine lengths, heights, and widths ($p<0.001$, $p<0.001$, and 0.033, respectively) compared to healthy controls. Endometrial

thickness across phases of menstrual cycle did not differ significantly between women with adenomyosis and healthy controls (p>0.05).

Table 8.1: Patient Characteristics of Included Adenomyosis Patients and Healthy Controls

Clinical Parameters		Adenomyosis (n=39)	Control (n=106)	P-value*
Age (in years)		38.23 (7.46)	29.4 (6.74)	<0.001[1]
BMI (kg/m2)		26.2 (4.89)	23.0 (4.75)	0.003[1]
Parity	Median (n)	2	0	0.001[3]
	Multiparous (%)	28 (73.3)	43(40.7)	0.006[2]
Types of adenomyosis† (n (%))	Diffuse (%)	20 (51.3)	-	-
	Focal AW (%)	5 (12.8)		
	Focal PW (%)	5 (12.8)		
	Focal combination (%)	5 (12.8)		
	Adenomyoma (%)	4 (10.3)		
	Combination (%)	0 (0.0)		
Method of adenomyosis diagnosis	TVUS (%)	39 (100)	-	-
	MRI (%)	17 (43.6)		
Phase of menstrual cycle (n (%))	M	14 (35.9)	11 (10.4)	<0.005[2]
	MF	7 (17.9)	18 (17.0)	
	LF	10 (25.6)	48 (45.3)	
	EL	1 (2.6)	14 (13.2)	
	LL	7 (17.9)	15 (14.2)	
Uterine measurements (mm)	Uterine length	81.1 (14.1)	59.1 (21.5)	<0.001[1]
	Uterine height	49.1 (9.90)	31.7 (10.3)	<0.001[1]
	Uterine width (Median, IQR)	55.0 (13.4)	40.9 (19.9)	0.033[3]
Endometrial thickness per cycle phase (mm)	M	4.68 (2.68)	3.50 (0.71)	0.845[1]
	MF	5.23 (2.54)	6.50 (0.71)	0.564[1]
	LF	6.65 (3.56)	5.67 (2.08)	0.735[1]
	EL	10.0 (0.00)	8.67 (0.58)	0.157[1]
	LL	10.35 (3.43)	7.33 (0.58)	0.274[1]

Data are presented as n (%) or mean (SD) unless otherwise stated.
*p-value was considered significant at <0.05. † according to MUSA criteria for TVUS or on MRI imaging.
[1]T-test for independent samples [2]Chi-squared analysis [3]Mann-Whitney U test
AW: Anterior Wall; PW: Posterior wall; TVUS: Transvaginal Ultrasound; MRI: Magnetic resonance imaging; M: Menses; MF: Mid-follicular phase; LF: late follicular phase: EL: early luteal phase; LL: late luteal phase

Uterine contraction features

An overview of UC features across the different phases of the menstrual cycle in adenomyosis patients and healthy controls are presented in tables 8.2-8.6. A summary of significant differences of contraction features versus healthy uteri is shown in Figure 8.3. Table 8.3 shows UC features of adenomyosis patients according to VAS score of dysmenorrhea during the M phase.

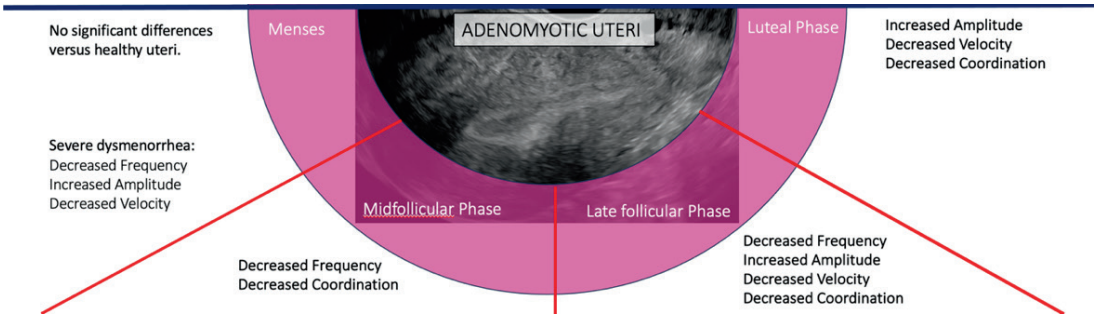

Figure 8.3: Summary figure of statistically significant (P<0.05) differences of uterine contractility features in healthy versus adenomyotic uteri per menstrual cycle phase.

Menses phase

Table 8.2 shows UC features of adenomyosis patients compared to controls during the menstrual (M) phase . There we no significant differences between the adenomyosis patients and the healthy controls.

Table 8.2. UC features in adenomyosis patients and healthy controls during the M phase of the menstrual cycle

UC feature	Direction of UC feature	Adenomyosis patients (n=14)	Healthy controls (n=11)	P-value*
CF (contractions/minute)	AW in radial direction	1.50 (0.17)	1.54 (0.17)	0.581[1]
	PW in radial direction	1.55 (0.24)	1.43 (0.11)	0.145[1]
Amplitude (SD)	AW in radial direction	0.046 (0.012)	0.039 (0.015)	0.208[1]
	PW in radial direction	0.040 (0.010)	0.037 (0.011)	0.248[2]
Velocity (mm/s)	F2C propagation, AW	0.65 (0.22)	0.70 (0.12)	0.477[1]
	C2F propagation, AW	0.71 (0.17)	0.71 (0.14)	0.903[1]
	F2C propagation, PW	0.68 (0.25)	0.68 (0.11)	0.843[1]
	C2F propagation, PW	0.72 (0.26)	0.68 (0.15)	0.743[2]
Coordination (MSE)		0.23 (0.14)	0.19 (0.08)	0.913[2]

All data are presented as mean (SD). *p-value was considered significant at <0.05. UC: uterine contractions; CF: contraction frequency; AW: anterior wall; PW: posterior wall; F2C; fundus-to-cervix; C2F: cervix-to-fundus
[1]T-test for independent samples [2] Mann-Whitney test

UC features of adenomyosis patients during M phase of the menstrual cycle were also analysed according to severity of dysmenorrhoea reflected by VAS scores (see Table 8.3). Increased dysmenorrhea severity was associated with lower CF in the PW ($p=0.012$), higher amplitude in the AW ($p=0.027$), and lower velocity in the C2F propagation direction of the PW ($p=0.028$). No significant results were found for contraction coordination.

Table 8.3. UC in adenomyosis patients according to VAS score of dysmenorrhoea during Menses

UC feature	Direction of UC feature	Reported VAS Score (n)						P-value*
		2 (n=1)	5 (n=1)	6 (n=2)	8 (n=5)	9 (n=1)	10 (n=1)	
CF (contractions/minute)	AW in radial direction	1.25	1.28	1.10 (0.25)	1.24 (0.18)	1.07	1.04	0.401
	PW in radial direction	1.83	1.30	1.41 (0.15)	1.20 (0.24)	1.07	1.07	0.012
Amplitude (SD)	AW in radial direction	0.040	0.032	0.039 (0.015)	0.056 (0.01)	0.050	0.061	0.027
	PW in radial direction	0.040	0.044	0.034 (0.009)	0.040 (0.01)	0.040	0.065	0.305
Velocity (mm/s)	F2C propagation, AW	0.90	0.61	0.90 (0.40)	0.64 (0.11)	0.63	0.49	0.109
	C2F propagation, AW	0.76	1.05	0.82 (0.06)	0.70 (0.14)	0.72	0.55	0.112
	F2C propagation, PW	0.90	0.50	0.78 (0.22)	0.78 (0.24)	0.79	0.40	0.493
	C2F propagation, PW	1.25	0.75	0.69 (0.01)	0.79 (0.20)	0.68	0.38	0.028
Coordination (MSE)		0.28	0.07	0.17 (0.08)	0.20 (0.06)	0.13	0.49	0.469

All data are presented as mean (SD). *p-value was considered significant at <0.05. The association between the UC features and dysmenorrhea (VAS score) in the adenomyosis group during M phase was measured using the Pearson correlation coefficient. VAS: visual analogue scale; UC: uterine contractions; CF: contraction frequency; AW: anterior wall; PW: posterior wall; F2C; fundus-to-cervix; C2F: cervix-to-fundus

Mid-follicular phase

UC features of adenomyosis patients were compared to those of healthy controls during the MF phase of the menstrual cycle (see Table 8.4). The CF was statistically significantly lower in the adenomyosis group compared to the healthy controls in the PW (1.48±0.21 vs. 1.69±0.16, p=0.013). Contraction coordination was statistically significantly worse in the adenomyosis group compared to the healthy controls (0.30±0.09 vs. 0.20±0.08, p=0.019). No other UC features differed statistically significantly.

Table 8.4. UC features in adenomyosis patients and healthy controls during the MF phase of the menstrual cycle

UC feature	Direction of UC feature	Adenomyosis patients (n=7)	Healthy controls (n=18)	P-value*
CF (contractions/minute)	AW in radial direction	1.54 (0.19)	1.62 (0.16)	0.297[1]
	PW in radial direction	1.48 (0.21)	1.69 (0.16)	0.013[1]
Amplitude (SD)	AW in radial direction	0.061 (0.050)	0.038 (0.011)	0.204[2]
	PW in radial direction	0.050 (0.034)	0.037 (0.011)	0.431[2]
Velocity (mm/s)	F2C propagation, AW	0.61 (0.16)	0.77 (0.22)	0.069[2]
	C2F propagation, AW	0.75 (0.28)	0.85 (0.23)	0.164[2]
	F2C propagation, PW	0.63 (0.12)	0.77 (0.29)	0.183[2]
	C2F propagation, PW	0.66 (0.16)	0.84 (0.29)	0.090[2]
Coordination (MSE)		0.20 (0.08)	0.30 (0.09)	0.019[1]

All data are presented as mean (SD). *p-value was considered significant at <0.05. UC: uterine contractions; CF: contraction frequency; AW: anterior wall; PW: posterior wall; F2C; fundus-to-cervix; C2F: cervix-to-fundus
[1]T-test for independent samples [2]Mann-Whitney test

Late follicular phase

UC features of adenomyosis patients versus healthy controls during the LF phase are presented in Table 8.5. The adenomyosis group shows statistically significantly lower CF in the AW (1.49±0.22 vs. 1.68±0.25, p=0.021), higher amplitude in both AW and PW (0.087±0.042 vs. 0.050±0.018, p=0.001 and 0.076±0.039 vs. 0.046±0.018, p=0.001), lower velocity in both F2C and C2F directions of the AW (0.65±0.18 vs 0.88±0.29, p=014 and 0.64±0.18 vs. 0.84±0.22, p=0.020, respectively) and F2C direction of the PW (0.64±0.20 vs. 0.82±0.21, p=0.014), and reduced contraction coordination (0.34±0.08 vs. 0.26±0.17, p=0.015) compared to healthy controls.

Table 8.5. UC features in adenomyosis patients and healthy controls during the LF phase of the menstrual cycle

UC feature	Direction of UC feature	Adenomyosis patients (n=10)	Healthy controls (n=48)	P-value*
CF (contractions/minute)	AW in radial direction	1.49 (0.22)	1.68 (0.25)	0.021[2]
	PW in radial direction	1.60 (0.29)	1.72 (0.27)	0.222[1]
Amplitude (SD)	AW in radial direction	0.087 (0.042)	0.050 (0.018)	0.001[2]
	PW in radial direction	0.076 (0.039)	0.046 (0.018)	0.001[2]
Velocity (mm/s)	F2C propagation, AW	0.65 (0.18)	0.88 (0.29)	0.014[2]
	C2F propagation, AW	0.64 (0.18)	0.84 (0.22)	0.020[2]
	F2C propagation, PW	0.64 (0.20)	0.82 (0.21)	0.014[2]
	C2F propagation, PW	0.77 (0.30)	0.90 (0.20)	0.128[2]
Coordination (MSE)		0.34 (0.08)	0.26 (0.17)	0.015[2]

All data are presented as mean (SD). *p-value was considered significant at <0.05. UC: uterine contractions; CF: contraction frequency; AW: anterior wall; PW: posterior wall; F2C; fundus-to-cervix; C2F: cervix-to-fundus
[1]T-test for independent samples [2] Mann-Whitney test

Early luteal phase

The analysis for this menstrual phase was not carried out due to only one adenomyosis patient being included.

Late luteal phase

Comparisons of UC features of adenomyosis patients and healthy controls during the LL phase are presented in Table 8.7. The adenomyosis patients showed statistically significantly higher amplitude in the PW (0.050±0.022 vs. 0.035±0.013, p=0.038), lower velocity in the C2F direction of the AW (0.51±0.11 vs. 0.65±0.13, p=0.027), and reduced contraction coordination (0.27±0.06 vs. 0.18±0.07, p=0.011) compared to healthy controls. No other statistically significant different results were found.

Table 8.6. UC features in adenomyosis patients and healthy controls during the LL phase of the menstrual cycle

UC feature	Direction of UC feature	Adenomyosis patients (n=7)	Healthy controls (n=15)	P-value*
CF (contractions/minute)	AW in radial direction	1.32 (0.14)	1.41 (0.14)	0.148[2]
	PW in radial direction	1.33 (0.20)	1.47 (0.15)	0.093[1]
Amplitude (SD)	AW in radial direction	0.059 (0.024)	0.038 (0.012)	0.148[2]
	PW in radial direction	0.050 (0.022)	0.035 (0.013)	0.038[2]
Velocity (mm/s)	F2C propagation, AW	0.55 (0.16)	0.62 (0.07)	0.184[1]
	C2F propagation, AW	0.51 (0.11)	0.65 (0.13)	0.027[1]
	F2C propagation, PW	0.56 (0.13)	0.67 (0.15)	0.130[2]
	C2F propagation, PW	0.54 (0.12)	0.68 (0.15)	0.055[1]
Coordination (MSE)		0.27 (0.06)	0.18 (0.07)	0.011[2]

All data are presented as mean (SD). *p-value was considered significant at <0.05. UC: uterine contractions; CF: contraction frequency; AW: anterior wall; PW: posterior wall; F2C; fundus-to-cervix; C2F: cervix-to-fundus
[1]T-test for independent samples [2]Mann-Whitney test

Discussion:

This multi-centre prospective study investigated the difference in uterine contractile features between women with adenomyotic versus normal uteri. Generally, adenomyosis patients had a lower CF and velocity, increased amplitude, and reduced contraction coordination compared to controls in most phases of the menstrual cycle, most significantly in the late follicular and late luteal phases.

Our findings confirm the hypotheses proffered in previous literature, that uterine (contractile) function is dysfunctional in women with adenomyosis. Several theories have been postulated in the literature to explain the dysfunction. An overexpression of oxytocin receptors in the myometrium of adenomyosis patients which can lead to hyperperistalsis and dysperistalsis has for instance been reported (259,268–270), reflecting increased contractile amplitude and more severe dysmenorrhea in adenomyosis patients. Studies have also reported that uterine oestrogen levels are raised in adenomyosis compared to healthy women (271,272). Oestrogen is known to stimulate uterine peristalsis and proliferation of the endometrium, and it is hence hypothesized that the hyper-estrogenic state may lead to (chronic) hyper-and dys-peristalsis (8). Dysperistalsis is associated with damage to the JZ, which is visible on TVUS and MRI imaging in adenomyosis. Our study supports these findings as amplitude was found to be increased in adenomyosis patients compared to healthy women throughout the menstrual cycle, potentially due to fibrotic changes in the JZ in adenomyosis.

Furthermore, our results similarly suggest that more severe dysmenorrhea is associated with more aberrant UC. However, the uterine hyperperistalsis that is described in adenomyosis patients in previous literature (76,77) was not reflected in our results, that is, if hyperperistalsis is to be interpreted as increased contraction frequency. Our findings instead show trends towards decreased CF in adenomyosis patients compared to healthy women, but with higher amplitude. We therefore cannot totally confirm the presence of *hyper*peristalsis in adenomyosis patients but do confirm fewer organized contractions (or less coordination of contractions) of higher amplitude, better encompassed by the word *dys*peristalsis. This finding is reflected in our results by way of universally decreased contraction coordination in adenomyosis patients compared to controls throughout the menstrual cycle.

Our results show the most statistically significant differences in UC between normal versus adenomyotic uteri during the LF and LL phases of the menstrual cycle. This might suggest an explanation for the link between subfertility and adenomyosis. With sperm transport and embryo implantation taking place during these menstrual phases, and being affected by aberrant UC in adenomyosis patients, subfertility seen in these patients could thereby be explained. The question of whether this dysperistalsis is a cause or effect of adenomyosis cannot be answered using our results and warrants further research.

Additionally, we attempted to investigate the increased prevalence of dysmenorrhea in adenomyosis patients. Despite our results not showing statistically significantly different UC behaviour during menses versus controls, we did find differences when assessing UC according to reported VAS score during menstruation. We report that increased dysmenorrhea severity was associated with relatively lower contraction frequency, higher amplitude and lower velocity compared to adenomyosis patients with less severe dysmenorrhea. Increased contractile amplitude and decreased velocity logically result in heavier and longer menstrual cramps, which is supported by our findings that more severe dysmenorrhea is reflected in more aberrant UC during menstruation. We hereby pave the way for the development of an objective tool to assess dysmenorrhea in adenomyosis patients.

The study has several strengths. Firstly, this is the first study to assess UC in adenomyosis patients compared to controls throughout the phases of menstrual cycle and therefore provides new insights into the condition for future clinical and research opportunities. Furthermore, as the method uses a TVUS, it is patient-friendly and easily accessible for future use in clinical practice. Moreover, the speckle tracking method of assessing uterine contractility is objective, reproducible and reliable (22,31). The study is a multi-centre study in an international setting, which allows for higher generalizability of the results. We also assessed uterine contraction features strictly according to menstrual cycle phase, which previous studies have not done in detail.

Nevertheless, the study also has a several limitations. The clearest limitation is the relatively small sample size of the study population (although it is generally larger than previous studies into uterine peristalsis (266)). Additionally, within-subject comparison was not possible in our groups as most women did not undergo TVUS in every phase of the menstrual cycle. Likewise, no sub-analysis was done to assess how different subtypes, locations and/or severity of adenomyosis may affect UC, as well as the added presence of endometriosis. These factors may all affect UC, as already shown by the significant differences in UC depending on degree of dysmenorrhea in this study. A barrier to carrying out this sub-analysis is the lack of uniform consensus on adenomyosis subtypes and how to define mild versus severe adenomyosis.

Another limitation is that the adenomyosis group was significantly older, had higher BMIs, greater uterus sizes, and higher parity than controls. As we do not yet know how age, uterus size, and BMI affect UC, their possible confounding effect cannot be discarded. It should be noted that adenomyosis itself leads to a higher uterine volume however. In addition, there was a relatively high number of recordings (n=33) that had to be excluded during the quality check. Within the adenomyosis group some recordings were excluded due to the severity of the adenomyosis which affected the imaging quality of the uterus. The ultimately analysed study group therefore consists of a higher number of relatively mild adenomyosis cases. Our results could therefore be an underestimation of the differences in UC between adenomyosis patients and healthy controls. Lastly, the TVUS speckle tracking method is not yet applicable for use in daily practice. Currently, contraction features are extracted through offline data processing, which does not allow them to be viewed in real time.

Our findings give new insights into the aetiology and clinical presentation of adenomyosis and may provide us with new diagnostic and therapeutic markers. In clinical practice, UC features can be used to objectively identify the initial extent of adenomyosis severity (and potentially its symptoms) and perhaps help to interpret the effect of treatment over time. Uterine contraction coordination especially provides a new avenue for future research to improve fertility in adenomyosis patients. Lastly, speckle tracking could also be used to identify aberrant UC features in other benign uterine disorders, such as

leiomyomas and congenital anomalies. Future research should also investigate how UC is affected in different types of adenomyosis and under different types of treatment.

Conclusions:
Our results confirm differences in uterine movement in adenomyotic versus healthy uteri. This could add to the etiological understanding of clinical symptoms of adenomyosis (i.e. dysmenorrhea and infertility). The notable difference between groups regarding frequency, velocity, amplitude and especially coordination, identifies these features as potential diagnostic or therapeutic targets. Further research into uterine contractility in women with (other) benign uterine disorders, and the effect of treatment on contractility, will hopefully lead to a better understanding of the clinical implications of abnormal uterine contractility.

Acknowledgements:
We would like to sincerely thank Liselot Wagenaar MD, Blijke Wessel MSc and Cynthia Klaassen MD for their (continued) help with patient inclusions and logistics of the project. Furthermore we continue to be grateful to GE Healthcare (Zipf, Austria) for their support of this research with regards to funding, and for facilitating the use of an ultrasound machine.

PART IV

Effect of Adenomyosis on Fertility Outcomes

CHAPTER 9:

Women with combined adenomyosis and endometriosis on MRI have worse IVF/ICSI outcomes compared to adenomyosis and endometriosis alone: A matched retrospective cohort study

Authors:
Connie O. Rees
Iris A.M. Rupert
Joost Nederend
Dimitri Consten
Massimo Mischi
Hubertus A.A.M. van Vliet
Benedictus C. Schoot

The content of this chapter has been published in the *European Journal of Obstetrics and Gynecology and Reproductive Biology*, 2022; vol 271 pages 223-234. DOI: 10.1016/j.ejogrb.2022.02.026

Abstract

Study objectives: To assess the effect of adenomyosis, endometriosis and combined adenomyosis and endometriosis, diagnosed on MRI, on IVF/ICSI outcomes versus male subfertility controls.

Study Design: This single-centre matched retrospective cohort study was carried out at Catharina Hospital in Eindhoven, The Netherlands. The study group consisted of infertile women undergoing their first, fresh embryo transfer during IVF/ICSI, with adenomyosis only (N=36), endometriosis only (N=61), and combined adenomyosis and endometriosis (N=93) based on MRI. The control group consisted of IVF/ICSI patients undergoing treatment due to male subfertility (N=889). 1:2 case-control matching based on age during IVF/ICSI, parity and number of embryos transferred was performed. Odds ratios were calculated for biochemical pregnancy, ongoing pregnancy and live birth rate versus matched male subfertility controls, and were corrected for embryo quality.

Results: Only the combined adenomyosis and endometriosis group showed a significantly reduced OR for biochemical pregnancy (p=0.004, OR 0.453 (95% CI 0.284 – 0.791)), ongoing pregnancy (p=0.001, OR 0.302 (95% CI: (0.167 – 0.608)) and live birth (p=0.001, OR 0.309 (95% CI: (0.168 – 0.644)) compared to matched male subfertility controls.

Conclusions: The lower (ongoing) pregnancy and live birth rates in the combined adenomyosis and endometriosis women can be attributed to more severe disease in these women, ultimately resulting in increased chances for failed implantation and miscarriage. This highlights the importance of screening for adenomyosis in endometriosis patients, and identifies these women target for additional (hormonal) treatment prior to IVF/ICSI.

Keywords: Adenomyosis, Endometriosis, Infertility, Magnetic Resonance Imaging, Assisted Reproductive Technologies

Introduction

Adenomyosis is a common benign uterine disorder characterised by invasion of the endometrium into the myometrium and is thought to arise from the junctional zone (JZ). Adenomyosis is often found in conjunction with endometriosis and may share aetiological mechanisms, such as metaplasia of mullerian remnants (10) .

Historically, adenomyosis was thought of as a disease affecting multiparous women, however with the advent of improved imaging techniques, it is also increasingly being linked to reproductive failure and infertility alongside endometriosis (80,98). Adenomyosis may have a higher prevalence in sub-fertile populations than expected, with a reported prevalence as high as 32% in infertile women (79,94,274).

Several theories exist to explain why women with adenomyosis may have reduced fertility. First, through disruption of the JZ, adenomyosis affects uterine contractions and thereby spermatozoa transport and embryo implantation due to the alterations in the JZ (77,275). The junctional zone is believed to be vital for uterine contraction initiation and modulation in the menstrual cycle (46,47). Alterations in the function and receptivity of the endometrium have also been reported in adenomyosis patients (84,160,276). Abnormal inflammatory responses have additionally been described, leading to embryo toxicity (277). Finally, anatomical changes of the uterine cavity are also thought to have an influence on embryo implantation (84).

Many women with adenomyosis also have (other forms of) endometriosis, which makes it difficult to assess whether the influence on infertility is due primarily to adenomyosis, endometriosis or a combination of both (278). It can be hypothesised, that when the two conditions occur together, the whole reproductive process is affected, with endometriosis affecting oocytes and fertilisation, and adenomyosis embryo implantation and the ongoing pregnancy (81). Few studies exist which have simultaneously investigated the separate *and* combined effect of endometriosis and adenomyosis on fertility outcomes. Moreover, despite magnetic resonance imaging (MRI) reported to be the most accurate and reproducible non-invasive diagnostic method for adenomyosis and endometriosis with a sensitivity of up to 88% and specificity of up to 91% (29,34), few studies have included patients diagnosed by this

method, favouring self-reported diagnosis or diagnosis by transvaginal ultrasound (TVUS, (81)).

We suggest that there is therefore a need to investigate how fertility outcomes are affected by the presence of only endometriosis, only adenomyosis or both, as visualized on MRI. As such, we carried out a retrospective cohort study comparing IVF/ICSI outcomes in women with MRI-diagnosed adenomyosis and/or endometriosis, compared to matched male infertility controls.

MATERIALS AND METHODS

Study design and setting

This single-centre retrospective cohort study was set at the Catharina Hospital in Eindhoven, The Netherlands, a regional referral centre between the years of 2008 and 2020.

Participants

Patients were women aged 18 to 42 years undergoing their first, fresh embryo transfer during IVF/ICSI. After meeting the local IVF/ICSI treatment eligibility requirements (see Appendix 10B), women in our centre received the same standard treatment. Pituitary downregulation was initiated with a recombinant GnRH agonist (Decapeptyl, Ferring Pharmaceuticals, Hoofddorp, the Netherlands), followed by ovarian stimulation using either recombinant follicle stimulating hormone (Gonal-F, Merck KGaA, Darmstadt, Germany) or human menopausal gonadotrophin (Menopur, Ferring Pharmaceuticals, Hoofddorp, the Netherlands; Fostimon, Goodlife Pharma, Lelystad, the Netherlands) at a standard starting dose of 150 IE/mL. Oocytes were fertilised on the same day as oocyte retrieval, either by IVF or ICSI (see Appendix 10B). Embryo transfer (single or double) took place three days after oocyte retrieval, after administration of human chorionic gonadotrophin (HCG, Pregnyl, *Merck KGaA, Darmstadt, Germany*) boost. Selection of the best quality (cleavage-stage) embryos was carried out according to local and alpha scoring criteria (see Appendix 10C). Luteal support was initiated with intravaginal progesterone (Utrogestan, *Besins Healthcare, Utrecht, the Netherlands*). See Appendix 10A for full details of local IVF/ICSI treatment protocol.

Study group

The study group included IVF/ICSI patients diagnosed with adenomyosis, endometriosis or both in the period of 2008 to 2020 on MRI. MRI consisted of T2-weighted images in axial, coronal and sagittal planes as well as axial T1-weighted images. Slight variations in protocol existed, however without significant implications for diagnostic quality. MRI criteria for the presence of adenomyosis were: focal or diffuse JZ thickening >12 mm, JZ/myometrium ratio >40%, and/or presence of high signal intensity myometrial foci on T1/T2 corresponding to an adenomyotic cyst (>2mm in diameter). MRI criteria for

endometriosis were any of the following: presence of a solid (invasive) hypointense lesion (with or without high signal intensity foci on T1/T2) outside the uterine cavity corresponding to adhesive endometriosis plaques; hyperintense (multiple) ovarian cysts on T1, or one or more cysts with high T1 signal intensity and shading on T2 corresponding to haemorrhagic endometriomas.
All pelvic MRIs carried out in women of a fertile age during the study period were re-evaluated by a study investigator (CR) and three pelvic radiologists, and were assigned to either an adenomyosis only, endometriosis only or combined endometriosis and adenomyosis sub-group. Subsequently, patient records of women with MRI-confirmed adenomyosis and/or endometriosis were assessed to identify women who underwent IVF or ICSI procedures in our centre. In the case of multiple MRIs, the one performed closest to IVF/ICSI treatment was assessed.

Women were excluded in case there was no MRI or IVF/ICSI data, if no embryo transfer took place, or if they objected to the use of their medical data.

Control group
For the control group, women between 18 and 42 years old who underwent their first, fresh IVF/ICSI cycle with embryo transfer between 2008 and 2020 due to confirmed male subfertility were included. Adenomyosis was assumed as not present if the patient had no reported uterine abnormalities and no reported history of symptoms associated with adenomyosis or endometriosis. Patients were excluded if no embryo transfer took place (e.g. freeze all, IVF cancellation), if there were signs of adenomyosis on TVUS or MRI (if available), or if they objected to use of their medical data.

Matching
Patients from the adenomyosis/endometriosis groups were automatically matched to the control group using SPSS Statistics to male subfertility controls. Matching was performed to account for various clinically significant confounders, namely: age during IVF, type of subfertility (i.e. primary or secondary) and number of embryos transferred (single or double embryo transfer). Since adenomyosis can be asymptomatic and often goes undiagnosed, total exclusion of adenomyosis from the control group could not

be guaranteed. Therefore, study group patients were matched to control group patients in a 1:2 ratio to reduce this influence on the outcome. A preference was given for exact matches.

Outcomes

The primary study outcomes were: biochemical pregnancy (positive serum HCG 16 days after embryo transfer (ET), ongoing pregnancy (a viable pregnancy 11 weeks after ET, with presence of foetal heartbeat on ultrasound) and live birth (delivery of a live foetus >24 weeks gestational age). Further patient characteristics collected included: age, BMI, indication for IVF/ICSI treatment, adenomyosis and/or endometriosis phenotypes, and IVF/ICSI treatment characteristics (type of subfertility (primary or secondary), infertility time (in months), treatment type (IVF or ICSI), fertilisation rate, embryo quality, number of transferred embryos). Full details and definitions of all outcomes can be found in Table A1 in Appendix A.

Data sources

Data regarding the IVF and ICSI cycles was taken from the Landelijk Specialistisch Fertiliteits Dossier (LSFD, Stichting Automatisering Fertiliteit (SAF), Utrecht, the Netherlands), the Dutch national electronic patient fertility database, and MRI data was taken from the local hospital patient records HiX (ChipSoft, Amsterdam, The Netherlands).

Statistical analysis

Data analysis was done using IBM SPSS Statistics Version 26. For normally distributed continuous variables, one-way ANOVA was used to evaluate differences between groups, the Kruskal-Wallis test was used in the case of abnormal distribution. A post-hoc test with Bonferroni correction was used to evaluate which groups showed significant differences. For categorical variables, differences between groups were evaluated using the Chi-square test using Bonferroni correction. Univariate and multivariate logistic regression (correcting for embryo quality) was carried out to calculate the odds ratio for primary outcomes for the study group(s) versus (matched) controls. A p-value <0.05 was considered statistically significant.

Ethical approval

Ethical approval was granted by the local institutional review board and the regional medical ethical committee, with study number nWMO-2020.005/W20.045.

RESULTS

Between the years of 2008 and 2020, 10.033 cycles of IVF/ICSI were performed at our institution. 2174 were fresh cycles carried out due to male subfertility in 938 patients. Forty-nine patients were excluded (see appendix G for full details and reasoning), ultimately leaving 889 patients for the control group undergoing their first, fresh cycle of IVF/ICSI due to male subfertility. Simultaneously, 255 women undergoing their first, fresh cycle of IVF/ICSI received a pelvic MRI in our centre, 190 of which showed signs of adenomyosis and/or endometriosis, and thereby met inclusion criteria for the study group. Ultimately, this yielded 36 patients for the adenomyosis only group, 61 for the endometriosis only group and 93 for the combined group. See Figure 9.1.

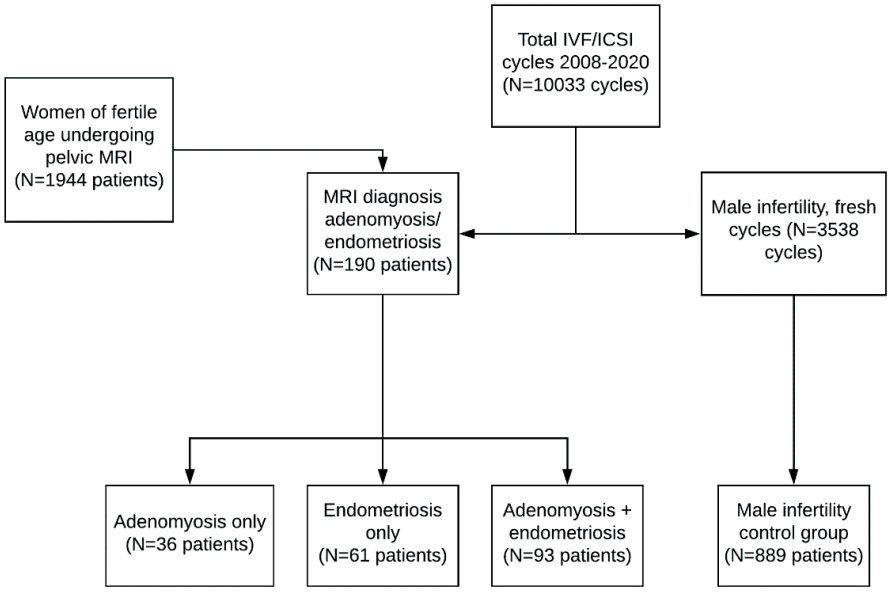

Figure 9.1 Flowchart of patient selection. Patients were recruited and assigned to either an adenomyosis only, endometriosis only, combined adenomyosis and endometriosis based on MRI. or male subfertility control

Patient characteristics before matching

Patient characteristics are summarised in Table 9.1. The adenomyosis group was on average 2.83 years older than the endometriosis group ($p=0.013$), 2.52 years older than the combined group ($p=0.021$) and 2.28 years older than the male subfertility controls ($p=0.014$) at the time of IVF treatment.

Additionally, women with only endometriosis had more primary subfertility compared to women with adenomyosis ($p<0.0005$). The age at the time of the MRI diagnosis was also different between the study subgroups, with the adenomyosis group having the highest mean age at MRI diagnosis (37.71 years, $p<0.0005$). Other characteristics were comparable between groups. Adenomyosis and endometriosis subtypes also did not differ significantly between groups ($p>0.05$). The number of patients receiving (hormonal or surgical) adenomyosis/endometriosis treatment prior to IVF was also not significant ($P>0.05$).

Table 9.1 Patient Characteristics before Matching

		Adenomyosis (N=36)	Endometriosis (N=61)	Combined (N=93)	Control (N=889)	P-value
BMI in kg/m² (Median, IQR)		23.59 IQR:7.76	23.03 IQR: 6.52	23.94 IQR: 6.21	23.63 IQR: 5.61	0.284[2]
Infertility time in months* (Mean, SD)		37.00 IQR:30	27.50 IQR: 28	31.00 IQR: 23	28.00 IQR: 22	0.236[2]
Age during IVF (Mean, SD)		33.75 (± 3.61)	30.92 (± 4.03)	31.23 (± 4.11)	31.47 (± 4.47)	0.012[1]
Cycle length (Median, IQR)		29.00 IQR:3	28.00 IQR: 3	28.00 IQR: 2	28.00 IQR: 2	0.260[2]
Age at MRI		37.71 (±4.32)	32.43 (± 4.94)	34.04 (± 5.71)	N/A	<0.0005
Type of subfertility*	Primary	18 (50.0%) a	46 (76.7%) b	65 (69.1 %) a, b	616 (69.4%) a, b	<0.0005[3]
	Secondary	15 (41.7%) a	13 (21.7%) a	23 (24.5 %) a	272 (30.6%) a	
	Unknown	3 (8.3%)	1 (1.7%)	6 (6.4%)	1	
Indication**	Male	11 (30.6%) a	9 (15.0%) a	12 (12.8 %) a	889 (100%) b	<0.0005[3]
	Female - Ovulatory disorder - Tubal factor	5 (13.9%) a 1 (3.0%) 1 (3.0%)	10 (16.7%) a 3 (5.0%) 7 (11.7%)	9 (9.6%) a 6 (7.1%) 7 (8.2%)	b	
	Combined Male and Female factor	4 (11.1%) a	21 (35.0 %) b	24 (25.5%) a, b	c	
	Endometriosis	5 (15.2%) a	22 (36.7 %) b	36 (38.3%) b	c	
	Idiopathic	7 (21.2%) a	5 (8.3 %) b	12 (12.8%) b	c	
Dysmenorrhoea	Yes	8 (22.2%)a, b	37 (61.7%) c	48(51.1%) b, c	165 (18.6%) a	<0.0005[3]
	No	15 (41.7%)a, b	13 (21.7%)c	25 (26.6%) b, c	584 (65.7%) a	
	Unknown	13 (36.1%)	10(16.7%)	21 (22.3%)	140 (15.7%)	
Endometriosis Treatment prior to IVF/ICSI	No treatment	15 (45.5%)	20 (33.3%)	29 (34.1%)	0 (0)	
	Oral contraceptive pill	4 (12.1%)	12 (20.0%)	7 (8.2%)	0 (0)	

	Hormonal Intra-uterine device	0 (0.0%)	3 (5.0%)	1 (1.2%)	0 (0)	
	GnRH Antagonist	3 (9.1%)	9 (15.0%)	12 (14.1%)	0 (0)	
	Endometriosis surgery	9 (27.3%)	30 (50.0%)	38 (44.7%)	0 (0)	0.080[3]
Endometriosis Type* **	Deep invasive Endometriosis	0 (0)	18 (30.0%)	23 (24.7%)	0 (0)	0.661[3]
	Endometriomas	0 (0)	32 (52.4%)	52 (55.9%)	0 (0)	0.364[3]
	Superficial Plaques	0 (0)	29 (47.5%)	50 (53.7%)	0 (0)	0.212[3]
Adenomyosis Type	Focal	16 (44.4%)	0 (0)	42 (45.1%)	0 (0)	0.162[3]
	Diffuse	5 (13.9%)	0 (0)	26 (27.9%)	0 (0)	
	Cystic	0 (0)	0 (0)	5 (5.5%)	0 (0)	
	Combined Focal + Cystic	5 (13.9%)	0(0)	12 (12.9%)	0 (0)	
	Combined Diffuse + Cystic	5 (13.9%)	0 (0)	5 (5.5%)	0 (0)	
	Unclear****	5 (13.9%)	0 (0)	3 (3.2%)	0(0)	

For normally distributed variables, values are depicted as Mean, standard deviation (SD) and for abnormally distributed variables as Median, Interquartile range (IQR). [1] = One-Way ANOVA, [2] = Kruskal-Wallis Test, [3] = Chi-square Test. Subscript letters denote significant differences between groups with different letters

* Primary subfertility are women/couples who are nulliparous, and secondary subfertility involves women/couples who are multiparous.

**Percentages can add up to >100% as patients could have multiple IVF/ICSI treatment indications simultaneously

***Total number of patients is greater than the group size as patients could have presence of different types of endometriosis simultaneously (i.e. endometriomas and superficial plaques)

**** Unclear adenomyosis type was assigned in cases whereby the imaging quality was insufficient, or the uterus was too abnormal to be able to accurately assess adenomyosis subtype

IVF/ICSI characteristics between groups before matching

Subsequently, IVF/ICSI characteristics were compared between groups (see Table 9.2). The control group had more patients undergoing ICSI (vs. IVF) compared to the study groups ($p<0.05$). Baseline endometrium thickness was higher in the adenomyosis only group compared to the other groups (5.0 vs. 3.0, $p=0.000$). Maximum endometrium thickness was comparable however. A difference in number of viable oocytes was also seen; the control group had 2.70 more viable oocytes than the combined group ($p<0.005$). The control group also had 1.23 more viable embryos than the combined group ($p<0.005$). The fertilisation rate was comparable between groups however ($p=0.215$). Embryo quality of the transferred embryos was not significantly different between groups ($p=0.295$ and $p=0.459$), nor was the number of embryos transferred ($p=0.113$).

Table 9.2 IVF/ICSI Treatment Characteristics between Groups

		Adenomyosis (n=36)	Endometriosis (n=61)	Combined (n= 93)	Control (n=889)	P-value
Type of treatment	IVF	27 (75%)$_a$	46 (75.4%) $_a$	70 (75.3%) $_a$	177 (19.9%) $_b$	<0.0005[3]
	ICSI	9 (25%)$_a$	15 (24.6%) $_a$	23 (24.7%) $_a$	712 (80.1%) $_b$	
Ovarian stimulation product	Gonal-F	22 (61.1%) $_{a, b}$	34 (56.7%) $_{b, c}$	39 (41.5%) $_c$	710 (85.4%) $_a$	<0.005[3]
	Menopur	4 (11.1%) $_{a, b}$	19 (31.7%)$_b$	34 (36.2%)$_b$	56 (6.7%)$_a$	
	Fostimon	0 $_a$	2 (3.3%) $_a$	5 (5.3%) $_a$	42 (5.1%) $_a$	
	Other	0	1 (1.7%)	0	23 (2.8%)	
Baseline Endometrial Thickness (mm, Median, IQR)		5.0 (4.0) $_{a. b.}$	3.0 (1.8) $_b$	3.3 (1.0)	3.0 (2.0) $_a$	0.000[2]
Maximum Endometrial Thickness (mm, Median, IQR)		10.3 (±1.8)	10.2 (±2.2)	10.3 (±2.05)	10.7 (2.97)	0.794[1]
Number of viable oocytes (Mean, SD)		8.69 (± 5.32)	9.44 (± 5.08)	7.42(± 4.35)	10.12 (± 5.73)	<0.0005[1]
Number of viable embryos (Mean, SD)		4.56 (±3.36)	5.61 (± 3.57)	4.30 (± 2.99)	5.53 (± 3.72)	0.009[1]
Fertilisation rate (Median, IQR)		0.56 IQR: 0.27	0.64 IQR: 0.32	0.60 IQR: 0.50	0.56 IQR: 0.33	0.215[2]
Embryos Transferred (N)	1	21 (58.3%)	47 (77%)	64 (70.3%)	570(64.2%)	0.113[3]
	2	15 (41.7%)	14 (23%)	27 (29.7%)	318(35.8%)	
Embryo quality 1*	Super	5 (14.7%)	14 (23.7%)	25 (27.8%)	298 (33.7%)	0.295[3]
	Good	6 (17.6%)	8 (13.6%)	12 (13.3%)	105 (11.9%)	
	Fair	15 (44.1%)	27 (45.8%)	36 (40%)	314 (35.6%)	
	Moderate	7 (20.6%)	10 (16.9%)	16 (17.8%)	133(15.1%)	
	Poor	1 (2.9%)	0	1 (3%)	33 (3.7%)	
Embryo quality 2*	Super	2 (15.4%)	2 (16.7%)	0	34 (10.8%)	0.459[3]
	Good	2 (15.4%)	3 (25%)	5 (20%)	40 (12.7%)	
	Fair	8 (61.5%)	4 (5.3%)	14 (56%)	134 (42.7%)	
	Moderate	1 (7.7%)	3 (25%)	5 (20%)	83 (26.4%)	
	Poor	0	0	1 (4%)	23 (7.3%)	

[1] = One-Way ANOVA, [2] = Kruskal-Wallis Test, [3] = Chi-square Test. Subscript letters denote significant differences between groups with different letters. For normally distributed variables, values are depicted as Mean, standard deviation (SD) and for abnormally distributed variables as Median, Interquartile range (IQR). * In some patients, 2 embryos are transferred. In those cases, embryo quality 2 indicates the quality of the second embryo according to alpha criteria .

Matching

Matching of the study group(s) based on age during IVF/ICSI, number of embryos transferred and type of subfertility (primary or secondary) was performed separately for each study subgroup. This resulted in 33 adenomyosis patients matched to 53 controls, with three unmatched patients in the adenomyosis group and one patient with only one match. For the endometriosis only group, 60 patients were matched to 118 controls, with one unmatched patient. In the combined group, 85 patients were matched to 164 controls, with eight unmatched patients. In total, 178 adenomyosis/endometriosis patients were matched to 354 male infertility controls. The resulting separate control groups had comparable characteristics, allowing for differences across the matching variables (see Appendix C). Matching based on embryo quality was not possible, due to the low number of exact matches (55 unmatched subjects).

IVF/ICSI outcomes after matching

IVF/ICSI outcomes after matching were compared between the different adenomyosis/endometriosis subgroups and the control group (see Table 9.3). Compared to their matched controls, the biochemical pregnancy rate was 33.3% for the adenomyosis group, 28.8% for the endometriosis group and 21.2% for the combined group. The ongoing pregnancy rate was 28.1% in the adenomyosis group, 25.4% in the endometriosis group and 12.9% in the combined group. Miscarriage rate (as the difference between biochemical and ongoing pregnancy, see Table 9.3) was not significantly different between groups. The live birth rate was 25% for both the adenomyosis and endometriosis group and was 11.9% in the combined group. Only the outcomes of the combined group differed significantly from their matched controls ($p<0.01$).

Table 9.3 IVF/ICSI Outcome after Matching

	Adenomyosis (N=33)	*Control (N=53)*	*P-value*
Biochemical pregnancy	*11 (33.3%)*	*19 (35.8%)*	*0.812*[1]
Ongoing pregnancy	*9 (28.1%)*	*15 (28.3%)*	*0.986*[1]
Miscarriage rate*	*2 (5.2%)*	*4 (7.5%)*	*1.000*[1]
Live birth	*8 (25.0 %)*	*14 (26.9%)*	*1.000* [1]
	Endometriosis (N=60)	***Control (N=118)***	***P-value***
Biochemical pregnancy	*17 (28.8%)*	*47 (39.8%)*	*0.267* [1]
Ongoing pregnancy	*15 (25.4%)*	*35 (29.7%)*	*0.690* [1]
Miscarriage Rate	*2 (3.4%)*	*12 (10.1%)*	*0.145*
Live birth	*15 (25.0%)*	*29 (24.6%)*	*0.353* [1]
	Combined (N=85)	***Control (N=164)***	***P-value***
Biochemical pregnancy	*18 (21.2%)*	*63 (37.8%)*	*0.010* [1]
Ongoing pregnancy	*11 (12.9%)*	*54 (33.1%)*	*0.000* [1]
Miscarriage rate	*7 (8.3%)*	*8 (4.7%)*	*0.216*[1]
Live birth	*10 (11.9%)*	*48 (30.4%)*	*0.001* [1]

Comparisons of IVF/ICSI outcome after matching for all study subgroups compared to their matched controls. [1] = Chi-square test.
*The difference between biochemical and ongoing pregnancy

Logistic regression after matching

After matching, the ORs were calculated using multivariate logistic regression (see Appendix D) and corrected for embryo quality (for full patient and IVF/ICSI characteristics after matching per study group, see Appendix C). ORs were not corrected for endometriosis surgery before IVF/ICSI, dysmenorrhoea or type of treatment (IVF or ICSI) since this did not have a significant effect on the outcome in the regression analysis ($p>0.05$). The aOR for biochemical pregnancy after matching was 0.895 for the adenomyosis group (95% CI (0.538; 2.236), 0.677 for the endometriosis group (95% CI (0.340; 1.348)) and 0.453 for the combined group (95% CI (0.241; 0.850) (see figure 5)). For ongoing pregnancy, the aOR for the adenomyosis group was 0.991 (95% CI (0.347; 2.629), for the endometriosis only group it was 0.945 (95% CI (0.455; 1.963)) and for the combined group 0.302 (95% CI (0.145; 0.628)). Similar results were found for live birth: the aOR was 0.905 for the adenomyosis group (95% CI (0.330; 2.479)), 0.843 for the endometriosis group (95% CI (0.398; 1.787)) and 0.309 for the combined group (95% CI (0.144; 0.662)) respectively.

DISCUSSION

Overall, infertile women with combined endometriosis and adenomyosis on MRI undergoing their first IVF/ICSI fresh embryo transfer had significantly worse fertility outcomes than matched male subfertility controls. These women had a 55% decreased chance of biochemical pregnancy (OR 0.453), a 70% decreased chance of ongoing pregnancy (OR 0.302) and a 69% decreased chance of a live birth (OR 0.309). Women with only adenomyosis or endometriosis did not appear to have significantly reduced chance of achieving pregnancy compared to male subfertility controls. This effect persisted after matching for age, parity and number of transferred embryos, and correcting for embryo quality.

Our results are largely in line with current literature. Sharma et al. looked at similar patient groups as this study, (albeit with a diagnosis based on TVUS). They reported a significantly reduced clinical pregnancy rate after IVF of 34.55% for the adenomyosis group, 36.62% in the endometriosis group and 22.72% for the combined group versus tubal factor controls. This is in accordance with our results, showing that a combined presence of adenomyosis and endometriosis results in the lowest clinical pregnancy rate in IVF/ICSI patients (86). Similarly, a study by Ballester et al. in colorectal endometriosis patients reported that an added presence of adenomyosis lead to significantly reduced cumulative clinical pregnancy rates (19% vs. 82.4%) (87). Not all studies have reported significant associations between the presence of adenomyosis in endometriosis patients and IVF/ICSI outcome however, with the topic still being contentious (93,274). It has been recently been suggested that the age-associated nature of adenomyosis forms an important confounder for worse fertility outcomes in this population (274). For this reason, we chose to match for maternal age during IVF, with our results still reaching statistical significance.

Based on our results therefore, we do suggest that patients with combined adenomyosis and endometriosis have a more severe form of the disease thus more impaired fertility compared to women with only one of the two disorders. The current data also seems to show that this is the case regardless of the individual adenomyosis or endometriosis phenotype. It is noteworthy also that the combined group constitute the largest proportion of infertile women undergoing IVF/ICSI treatment in our study: it suggests that these

women having more severely impaired fertility and thereby seek treatment in the first place. It is possible this is due to an added uterine or implantation factor in these women, as matching and correcting embryo quality did not diminish this effect.

In general clinical practice, when undergoing IVF/ICSI, arguably little attention is paid to whether a patient has adenomyosis, due to inconsistent diagnostic criteria and a lack of symptoms in many women. As a result, few clinical guidelines exist to tailor fertility treatments to women with adenomyosis (or endometriosis for that matter), and in many cases they simply follow the locally established IVF/ICSI protocols. The results presented here suggest that screening for adenomyosis in (infertile) endometriosis patients (on MRI) is clinically useful in an IVF/ICSI setting. Furthermore, due to the suspected severity of disease in the combined group, these patients represent a potential target group for additional hormonal therapy or surgery before undergoing IVF/ICSI, resulting in disease attenuation/regression (279)
.
Investigating this patient group separately, as done in this study, thus constitutes one of its strengths: it was possible to investigate the independent influence of adenomyosis and endometriosis on fertility. A further strength of this study is that only women with adenomyosis based on MRI were included, a more reliable method of diagnosing adenomyosis, as opposed to TVUS (29). Moreover, the extensive re-evaluation of the MRIs by three experienced pelvic radiologists in the context of this study also reduces the risk of bias that inevitably accompanies a retrospectively designed study. To the best of our knowledge, this is the first study which investigates fertility outcomes of adenomyosis and endometriosis separately and combined, based on MRI diagnosis.

This study does however have several limitations. First, the control group as a rule were healthy women, with no indication for MRI. This means no definitive assessment of adenomyosis presence in these women could be carried out. Hence, it is possible that some of these women had undiagnosed adenomyosis. To account for this eventuality, we chose to match the control group 1:2 with the study group. Second, although our study group was larger than many previously executed studies investigating the relationship between adenomyosis and infertility, the sample size was still relatively small, which

reduces the power of the results. This was reflected in the broad reported confidence intervals. Third, while the endometriosis and adenomyosis diagnosis was based on the MRI closest to the IVF/ICSI start date, in many cases the adenomyosis diagnosis was made after IVF/ICSI (see Table 1). Therefore, it is not known whether the adenomyosis was already present (to a similar extent) at the time of IVF/ICSI. However, when conducting a sensitivity analysis for only patients receiving an MRI prior to IVF, our results did not significantly differ. We believe this reflects the theory that adenomyosis is a disease which develops gradually over a life-time rather than representing a de novo diagnosis (63). Finally, there are some women (n=5, see Table 1) in the adenomyosis group that underwent assumed complete surgery for endometriosis before undergoing IVF, as the pelvic MRI showed no signs of endometriosis. Therefore, these patients were assigned to the adenomyosis only group, whilst they did show a history of endometriosis. Finally, several IVF/ICSI treatment parameters are not reported in our study population as part of standard treatment procedures, and thus could not be assessed for their potential confounding effect (e.g. baseline follicle count, AMH levels, (peak) serum oestradiol).

Overall, it can be said that adenomyosis negatively affect fertility outcomes, especially in conjunction with endometriosis. It is suspected that in IVF/ICSI patients with combined adenomyosis and endometriosis, the disease is more severe than in patients with only adenomyosis or endometriosis and thus has a greater impact on fertility. Accurate diagnosis of adenomyosis and endometriosis before undergoing IVF/ICSI is crucial. Therefore, making a pelvic MRI to diagnose or eliminate the presence of adenomyosis/endometriosis is recommended. More research is needed to further identify the relationship between adenomyosis and endometriosis and infertility. Especially large-scale studies with patient subdivision into adenomyosis only, endometriosis only and combined adenomyosis and endometriosis groups is valuable so as to tailor (pre) treatment per patient sub-type.

Acknowledgements
We would like to sincerely thank the team of pelvic radiologists at the Catharina Hospital for taking the time to revise the MRIs of the patients included in this study. Additionally we extend our thanks to Dr. M. van Rumste for providing us access to the IVF/ICSI treatment outcome data. Furthermore we would like to thank Catharina Hospital statistician Dr. Saskia Houterman for her support in analysis.

CHAPTER 10:

MRI Markers of Adenomyosis Severity Associated with Worse IVF/ICSI Outcomes

Authors:
Connie O. Rees
Sehriban Kocyigit
Joost Nederend
Massimo Mischi
Hubertus .A.A.M. van Vliet
Benedictus C. Schoot

The content of this chapter has been published in the *Journal of Endometriosis and Pelvic Pain Disorders*, 2023
DOI: 10.1177/22840265231195404

Abstract

Study Objective: The aim of this study was to characterise the severity of adenomyosis on MRI in infertile women, and to assess if MRI characteristics of adenomyosis severity are associated with worse IVF/ICSI pregnancy outcomes versus male infertility controls.

Materials & Methods: This single-centre retrospective study was carried out at Catharina Hospital in Eindhoven, The Netherlands. The MRIs of 124 infertile women undergoing their first, fresh embryo transfer during IVF/ICSI, diagnosed with adenomyosis only (N=31), or combined adenomyosis and endometriosis (N=93) were assessed. Measurements of MRI adenomyosis features were performed by two independent investigators. IVF/ICSI outcomes (biochemical pregnancy (BP), ongoing pregnancy (OP) and live birth (LB)) of adenomyosis patients were compared to those of 889 male infertility controls.

Results: Patients with adenomyosis had significantly worse IVF/ICSI outcomes compared to male infertility controls. When assessing individual MRI parameters, adenomyosis patients with a mean junctional zone (JZ) of >12mm, a JZ/Myometrium ratio of >40%, presence of myometrial cysts and presence of endometriosis (specifically deep invasive endometriosis(DIE)) showed statistically significantly worse outcomes compared to patients with milder disease.

Conclusion: The results of this retrospective study suggest that individual MRI markers for severe adenomyosis (mean JZ >12mm, myometrial cysts), especially when combined with (severe) endometriosis, may be associated with fewer pregnancies during IVF/ICSI when compared to male infertility controls. Future prospective studies should investigate the prognostic potential of these markers for prediction of IVF/ICSI success.

Keywords: Adenomyosis, Infertility, Assisted Reproductive Technologies, Magnetic Resonance Imaging, Pregnancy

Introduction

Adenomyosis is a benign gynaecological condition characterised by the infiltration of endometrial tissue and stroma into the myometrium of the uterus, causing disruption in the so-called junctional zone (JZ) (278). The prevalence of adenomyosis is unclear due to lack of consensus in diagnostic method and criteria, with reported prevalence varying widely from 5 to 70% (194,280). Younger nulliparous women are being more frequently diagnosed with adenomyosis and it is increasingly being linked to poor obstetric outcomes and infertility (80,81,94,107). A recent meta-analysis showed detrimental effects of adenomyosis on in vitro fertilisation (IVF) outcomes, with significantly reduced implantation, clinical pregnancy, ongoing pregnancy and live birth in adenomyosis patients (281).

Diagnosis of adenomyosis

Conventionally, the diagnosis of adenomyosis was obtained histologically from hysterectomy specimens, and this remains the gold standard (19). With the advent of improved imaging techniques, the diagnosis can also be made via trans-vaginal ultrasound (TVUS, sensitivity 78%, specificity 78%, positive likelihood ratio of 3.5 and a negative likelihood ratio of 0.28) and magnetic resonance imaging (MRI, sensitivity of 78%, specificity of 88%, a positive likelihood ratio of 6.8 (4.5%–10%), and a negative likelihood ratio of 0.25) (29,37). TVUS is arguably less reliable for diagnosing adenomyosis as it is relatively operator dependent (37). Furthermore, distinguishing adenomyosis from other uterine disorders such as leiomyomas or carcinomas can be difficult on TVUS. MRI is therefore often the preferred diagnostic method, specifically in atypical or mild cases of adenomyosis (19,61). Unfortunately, in contrast to TVUS, which has clear diagnostic criteria (the MUSA criteria (183)), there are no accepted diagnostic criteria for adenomyosis for MRI. The most widely reported MRI criteria are based on the appearance of the JZ, by looking at the following three features: (i) a JZ thickness ≥ 12 mm; (ii) a ratio of greater than 40% of JZ to myometrium and (iii) a difference greater than 5 mm between the maximum and minimum JZ diameter. There are further reported indirect and direct criteria for adenomyosis (with presence of myometrial cysts seeming most promising) on MRI but their diagnostic and clinical potential remains unclear (32,181).

Junctional zone & Infertility

Alterations in the JZ have been linked to fertility, as the JZ is influenced by cyclical hormonal changes in accordance with the endometrium (33,46). The JZ is believed to play an important in role in uterine contractions which are crucial for spermatozoa transport and embryo implantation (111). A handful studies have specifically investigated whether changes in the JZ could be linked with fertility outcomes (95,98). Limited studies have investigated the direct link of the type and the severity of adenomyosis to fertility outcomes however, with those that have showing conflicting results. A study by Tamura et al. showed that women with diffuse adenomyosis had worse fertility outcomes (101). Conversely, a study by Exacoustos et al. showed that focal adenomyosis was more often associated with infertility (106). By extensively characterising adenomyosis on MRI, the burden of disease could perhaps be definitively correlated with fertility outcomes and thereby inform clinical decision making.

Therefore, the aim of this study was to retrospectively quantify and characterise the extent of adenomyosis on MRI in infertile women undergoing IVF/ICSI, and to evaluate if certain MRI characteristics of adenomyosis severity show worse IVF/ICSI outcomes compared to controls.

Materials & Methods

Study design & Setting

This single-centre retrospective case-control study was conducted at the Catharina Hospital in Eindhoven, the Netherlands, a regional referral centre for fertility and endometriosis treatment. Patients were included between the years of 2007 and 2020. This study was ethically approved by the local institutional review board and the regional Medical Ethical Committee with study number nWMO-2020.005/W20.045, in March 2020.

Eligibility criteria:

IVF/ICSI Patients between the ages of 18 and 42 years, undergoing their first, fresh embryo transfer in our centre between 2008-2020 were eligible.

Study Population

IVF/ICSI patients that received an MRI at our hospital (according to local MRI protocol, see appendix 10A) on suspicion of adenomyosis and/or endometriosis were chosen as our study group. In order to confirm the initial diagnosis of adenomyosis and/or endometriosis of the MRI's that were conducted, a reassessment was made of these MRI's by pelvic radiologists and a study investigator (CR). The diagnosis of adenomyosis on MRI was made based on one of three criteria: (I) JZ thickness ≥ 12 mm on T2 either focally or diffusely, (II) the presence of high signal intensity foci (HSI) in the myometrium on T1 and/or T2 concordant with an adenomyotic cyst, (III) JZ/myometrium ratio of > 40% on T2. The diagnosis for endometriosis was based on the presence of one of the following criteria; (I) hyperintense (multiple) ovarian cysts on T1 and hypointense intensity on T2, (II) endometriosis plaques and (III) deep infiltrating endometriosis. Patient medical files were then assessed in order to identify which of these patients had undergone IVF/ICSI treatment and received their first fresh embryo transfer (ET) in our fertility department. Patients were included regardless of the timing of the MRI in relation to IVF/ICSI treatment.

Control Population:

The control group included women undergoing IVF/ICSI treatment due to a male factor only, with normal uteri on TVUS, or MRI where available. We chose only to include controls on the basis of normal uterus on imaging and

only a male factor to minimise the chance of including undiagnosed adenomyosis patients into the control group.

Exclusion criteria:
Patients who did not undergo ET, or only underwent frozen ET were excluded. Patients who explicitly objected to the usage of their medical data for research purposes were also excluded.

IVF/ICSI Treatment protocol
Included patients had to meet the local eligibility requirements of IVF/ICSI treatment protocol (see Appendix 10B). Patients first received pituitary downregulation with a recombinant GnRH agonist (Decapeptyl®, Ferring Gmbh, Germany), followed by ovarian stimulation. For ovarian stimulation either recombinant follicle stimulating hormone (Gonal-F®, Merck B.V. the Netherlands) or human menopausal gonadotrophin (Menopur® , Ferring B.V. the Netherlands, Fostimon®, Goodlife Fertility B.V. the Netherlands) was used. Fertilisation of the oocytes occurred the same day as oocyte retrieval, either by IVF or ICSI depending on the patients' medical indication. Three days after oocyte retrieval, ET (single or double) was carried out after administration of a human gonadotrophin (HCG, Pregnyl®, Merck Sharp & Dohme, Canada) boost. According to the local and alpha scoring criteria (see appendix 3) selection of the best quality embryos for transfer was carried out. Luteal support was maintained with intravaginal progesterone (Uterogestan®, Besins Healthcare, the Netherlands) and was initiated after ET.
Pelvic magnetic resonance imaging
The standard MRI protocol for pelvic examinations at this hospital included the following sequences; T2-weighted turbo spin echo (T2-TSE) sequences in the sagittal, axial and coronal planes, as well as T1-weighted turbo spin echo (T1-TSE) sequences in the axial plane. All scans were carried out with either a 1.5T or 3T MRI system (Phillips, Ingenia, the Netherlands). In order to minimise the effects of bowel motions/spasms and uterine peristalsis on image interpretation, all patients were administered an antispasmodic agent (1mL of 20mg/mL Buscopan®, Sanofi, Paris, France) intravenously or intramuscularly. The slice thickness used was generally 3 mm, with slight variations ranging from 3-5 mm. Minor changes existed in the protocol throughout the years, but had no significant impact on the diagnostic quality of the MRIs. In case of patients

receiving multiple MRI's, the MRI performed closest to IVF/ICSI treatment was chosen for measurements. Full details can be found in Appendix 10A.

MRI measurements

The MRI features assessed with a brief definition, unit, calculation and stratification can be found in Table 10.1, and an illustration of measurements taken shown in Figure 10.1. Measurements were performed independently by two study investigators (CR and SK) using Sectra IDS7 version 21.1 (Linköping, Sweden). The investigators' measurements were subsequently compared and measurements were considered equal when there was a difference ≤ 1 mm. A pelvic radiologist was consulted when doubts presented about the performed measurements. For all measurements, the junctional zone was defined as a low signal intensity region between the high signal intensity region of the endometrium and the intermediate signal intensity region of the outer myometrium on T2. In case of an ill-defined junctional zone which inhibited accurate measurement, the MRI was labelled as having 'poor JZ definition'. Focal adenomyosis was defined as focal widening of the JZ, or an ill-defined low signal intensity region of the uterine wall. In order to avoid mistaking uterine contractions for focal lesions, the precise location of the low signal intensity region was assessed in three directions (using a localisation cursor). When this low intensity region was not seen in other directions, it was categorised as a uterine contraction. Diffuse adenomyosis was defined in case of a diffuse thickening of the JZ of ≥ 12 mm showing a low T2 signal intensity with indistinct margins (Figure 10.1C).

Table 10.1 MRI characteristics of adenomyosis: Objective Adenomyosis MRI Features, based on (181):

MRI Feature	Definition	Unit	Stratification
Average Junctional Zone thickness (AJZ)	Mean of JZ measurement at 6 points of the uterus: Fundus, Mid-corpus, Isthmus, measuring the anterior and posterior wall at each point in the mid-sagittal plane.	Mm	>7mm, >10mm, >12mm
Maximal Junctional Zone Thickness (JZMax)	Maximal diameter of JZ from those measured at the 6 points as described above, with location	Mm	>7mm, >10mm, >12mm
Minimal Junctional Zone Thickness (JZMin)	Minimal diameter of JZ from those measured at the 6 points as described above	Mm	
Junctional Zone Differential (JZDiff)	As a measure of JZ irregularity Difference between maximal and minimal JZ	Mm	>5mm
Junctional Zone Asymmetry (JZAsymm)	Difference between anterior and posterior JZ (based on measurement at 6 points previously described)	Mm	
Junctional Zone to Myometrium Ratio (JZ/Myo Ratio)	Ratio of Junctional zone to full myometrium thickness (measured at 6 points previously described)	%	>40%
Uterine volume	Uterine length x width x height x 0.523 (146). The length of measured in the sagittal plane from the outer ostium of the cervix until the fundus. Width was measured in the axial plane, and height in the transverse plane at the mid-corpus.	Mm^3	
Average Uterine Wall Thickness	Uterine wall thickness measured from endometrium to myometrium, at 6 points previously described	Mm	
Adenomyotic foci volume	Volume of adenomyotic foci in 3 orientations Calculated using the formula of a sphere: $4/3.\pi.r\text{^}3$	Mm^3	<40mm^3, 40-60 mm^3, > 60 mm^3
(Number of) HSI adenomyotic foci (Myometrial Cysts)	Visible high signal intensity (HSI) myometrial foci (compared to normal myometrium) on T1 or T2-weighted imaging*		>5
Adenomyosis Signal intensity ratio (SIR)	Signal intensity ratio of adenomyotic tissue compared to that of the rectus muscle on T2 imaging (as measured using Region of Interest (ROI) circles).		

*on the total MRI scan, not per image slice. Duplicate counting foci in various slices was avoided by tracking lesions across slices using the localisation cursor.

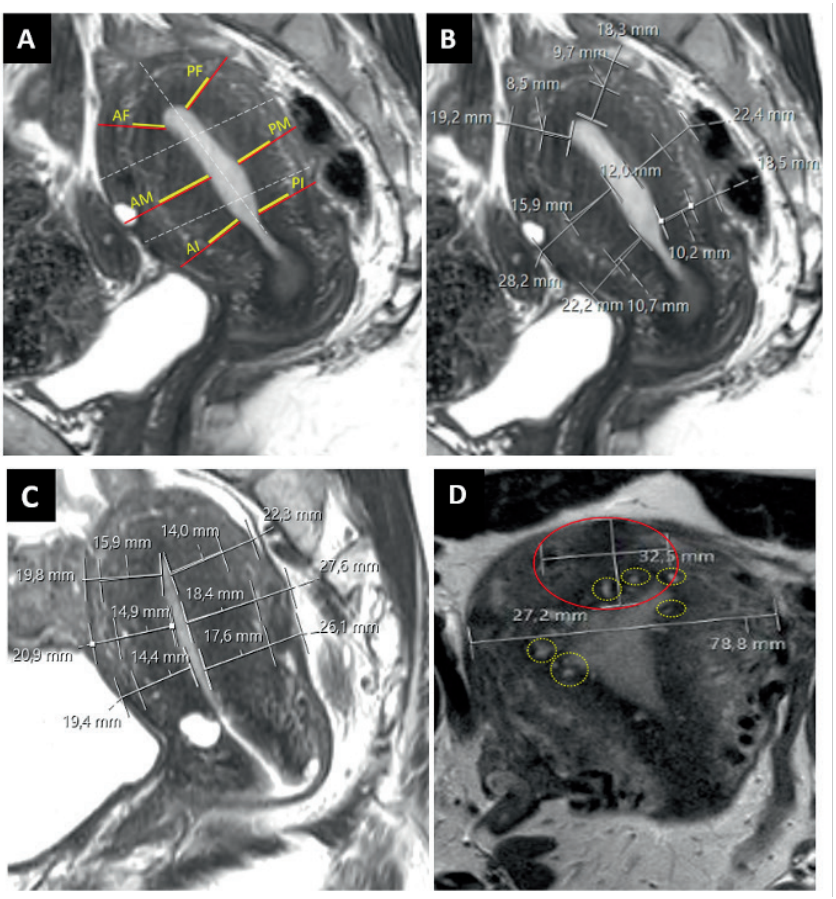

Figure 10.1 Measurements on MRI of Adenomyosis characteristics. All MRI images shown were performed on a T2-TSE. Figure A, B and C are shown in a sagittal plane, D in the transverse plane. A; The JZ thickness (yellow line) and the myometrium thickness (red line) measured at the level of fundus (F), mid-corpus (M) and isthmus (I) in the anterior (A) and posterior (P) wall of the uterus. B; The measurements of JZ thickness and myometrium thickness. C; A uterus with diffuse adenomyosis with a JZ ≥ 12 mm. D; Uterus volume determination using the width in the transverse plane (78.8 mm). JZ is showing high signal intensity foci's determined with dashed yellow circles. Volume of focal adenomyosis shown in the red circle

Outcomes

The primary outcomes of this study included: (I) biochemical pregnancy (BP, a positive HCG test on day 16 post- ET), (II) ongoing pregnancy (OP, presence of a foetal cardiac activity on ultrasound 11 weeks after ET), (III) live birth (LB, delivery of a viable foetus > 24 weeks of gestational age). Secondary outcomes included the MRI characteristics of adenomyosis as shown in Table 10.1.

Data sources & management

Patient characteristics, radiology reports and MRI data were retrieved from the electronic hospital patient records programme HIX (Chipsoft 6.1, Amsterdam, The Netherlands). Data concerning the IVF and ICSI cycles was retrieved from the Dutch national fertility database (Landelijk Specialistisch Fertiliteits Dossier, LFSD, Stichting Automatisering Fertiliteit (SAF), Utrecht, the Netherlands)). All patient data and MRI measurements were recorded in a secure electronic database (Research Manager version 5.53 (Cloud9 software, Deventer, the Netherlands)) and were later exported to IBM SPSS statistics (version 27) for data analysis.

Statistical analysis

The Shapiro-Wilk test was applied to assess normal distribution of data. Normally distributed data were presented as mean ± standard deviation (SD) and in case of non-normally distributed data as median (interquartile range). Between-group differences were assessed using the independent T-test or Mann-Whitney U test for the continuous variables, and for categorical variables a Chi-squared test or Fisher's exact test was performed (with Bonferroni correction). Subsequently, a multivariate logistic regression analysis for IVF/ICSI outcomes was carried out correcting for age at IVF, IVF or ICSI treatment, number of transferred embryos and embryo quality, leading to adjusted odds ratios (aOR). with 95% confidence interval (95% CI). Overall, a P-value of <0.05 was considered significant.

Results

Patient Inclusion and Characteristics

124 women with MRI-diagnosed adenomyosis were included (see Figure 10.2). 31 women had only adenomyosis and 93 women had both adenomyosis and endometriosis. 889 patients undergoing IVF/ICSI treatment due to male factor only were included in the control group. Table 10.2 shows demographic and IVF/ICSI treatment characteristics of both groups.

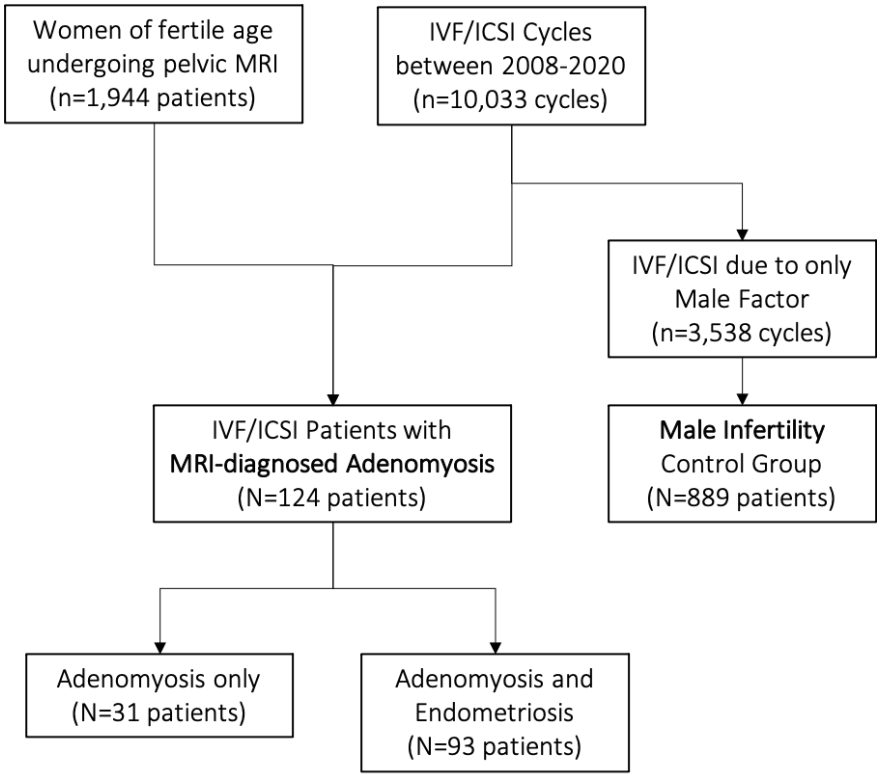

Figure 10.2 Flowchart of Patient Selection and Inclusion

Table 10.2 Patient Characteristics of IVF/ICSI Patients with MRI-Diagnosed Adenomyosis versus Male Infertility Controls

	Adenomyosis (N=124)	Control Group (N=889)	P-value
BMI in kg/m² (Median, IQR)	23.95 (21.30-28.33)	23.60 (21.44-27.04)	0.48
Infertility time in months (Median, IQR)	35.00 (23.50-53.50)	27.00 (20.00-41.00)	0.11
Age during 1st IVF cycle (Years, Median, IQR)	33.00 (30.00-35.50)	31.00 (28.00-35.00)	0.042
Year of IVF Treatment (Median, (IQR))	2011 (2008-2016)	2011 (2009-2014)	0.54
Cycle length (Days, Median, IQR)	28.00 (28.00-30.00)	28.00 (28.00-30.00)	0.43
Primary subfertility	79 (63.7%)	616 (69.4%)	0.92
Secondary subfertility	36 (29.0%)	272 (30.6%)	
Indication for fertility treatment			<0.001
- **Male Factor**	20 (16.3%)	889 (100%)	
- **Female Factor§**	13 (10.6%)		
- **Combined**	26 (21.1%)		
- **Endometriosis**	37 (30.1%)		
- **Idiopathic**	27 (22.0%)		
Type of treatment (N, (%))			<0.001
- IVF	93 (75.0)	177 (19.9)	
- ICSI	31 (25.0)	712 (80.1)	
Number of viable oocytes (Median, IQR)	7.0 (4.0-10.0)	8.0 (5.0-12.0)	0.015
Number of viable embryos (Median, IQR)	4.0 (2.0-6.0)	5.0 (3.0-8.0)	<0.001
Fertilisation rate (%, Median, IQR)	60.0 (45.0-75.0)	57.1 (40.0-72.0)	0.21
Number of Embryos Transferred (N, (%))			
- Single			0.42
- Double	83 (68.0)	570 (64.2)	
	39 (32.0)	318 (35.8)	
Embryo quality of First Transferred Embryo (N, (%)) [a]			0.11
- Super	28 (23.5)	298 (33.7)	
- Good	19 (16.0)	138 (15.6)	
- Fair	48 (40.3)*	314 (50.6)	
- Moderate	22 (18.5)	133 (14.9)	
- Poor	2 (1.7)	33 (3.7)	
Embryo quality of Second Transferred Embryo (N, (%)) [a]			
- Super	2 (5.7)*	0 (0.0)	<0.001
- Good	8 (22.9)	63 (20.1)	
- Fair	19 (54.3)	217 (69.1)	
- Moderate	5 (14.3)*	0 (0.0)	
- Poor	1 (2.9)*	34 (10.8)	

*an asterisk denotes statistically significant difference versus control. a: see Table 9.S3 for details on embryo quality criteria.

§ Female factor infertility included indications such as: ovulation disorders, tubal factor and cervical issues as IVF/ICSI indications. Controls more often underwent ICSI treatment (80.1% vs. 25.0%, p<0.001) and also had more viable oocytes (8.0 vs. 7.0, p=0.015) and embryos (5.0 vs. 4.0, p<0.001) versus adenomyosis patients. Embryo quality was similar between groups (p=0.112), but did differ (p<0.001) when looking only at the second transferred embryo where applicable.

MRI Characteristics:

A summary of all MRI characteristics can be seen in Table 10.3. Figure 10.3 shows several illustrative examples of adenomyosis. Thirty -six women received an MRI in advance of their first IVF/ICSI cycle, of which twelve women achieved pregnancy, and 24 did not. Seventy-eight women underwent MRI after fertility treatment, of which nineteen women became pregnant and 59 did not. There was no significant difference in terms of pregnancy observed between the group with MRI prior to fertility treatment and the group that had it afterwards (P=0.83, Table S4). Most women (83/124) had an MRI within five years of fertility treatment. No significant difference in terms of pregnancy rate was found when comparing these women to those received an MRI outside this time-frame (P= 0.91, Table S4) .

Table 10.3 MRI Characteristics of IVF/ICSI Patients with MRI-diagnosed Adenomyosis

		Adenomyosis Patients (n=124)
Age at MRI (Years, Mean, SD)		34.96 (5.46)
MRI conducted prior to IVF/ICSI treatment (N, (%))		46 (37.1)
MRI within 5 years of fertility treatment (N,(%))		83 (66.9)
Adenomyosis Type	Focal	58 (47.9)
	Diffuse	31 (25.6)
	Cystic	5 (4.1)
	Focal & Cystic	17 (14.0)
	Diffuse & Cystic	10 (8.3)
	Missing	3 (2.4%)
Average JZ (mm, Mean, SD)		8.68 mm (3.57)
	>7mm	89 (71.8)
	>10mm	41 (33.1)
	>12mm	20 (16.1)
	>15mm	9 (7.3)
Maximal JZ (mm, Mean, SD)		17.05 mm (8.70)
	>7mm	115 (92.7)
	>10mm	104 (83.4)
	>12mm	94 (77.4)
	>15mm	68 (54.8)
JZ Differential (mm, Mean, SD)		13.36 mm (8.68)
	>5mm	110 (88.7)
Average JZ/Myometrium Ratio (Mean, SD)		0.46 (0.14)
	>40%	92 (74.2)
JZ asymmetry (Mm, Mean, SD)		0.07 mm (0.81)
	>2mm	22 (17.7)
Presence of High Signal Intensity Foci (Myometrial Cysts)		60 (48.8)
	>5 HSI Foci	24 (19.4)
	T1-High signal HSI Foci	24 (19.4)
Uterine Length, in sagittal direction (Mm, Median, IQR)		78.90 (18.50)
Maximal Focal Lesion (Mm, Median, IQR)		23.30 (13.0)
Presence of endometriosis (N, (%))		93 (75.0)
	Presence of plaques	86 (69.4)
	Endometriomas	62 (50.0)

	Deep invasive endometriosis (DIE)	26 (21.0)
Presence of fibroids (N, (%))	Yes	5 (4.2)

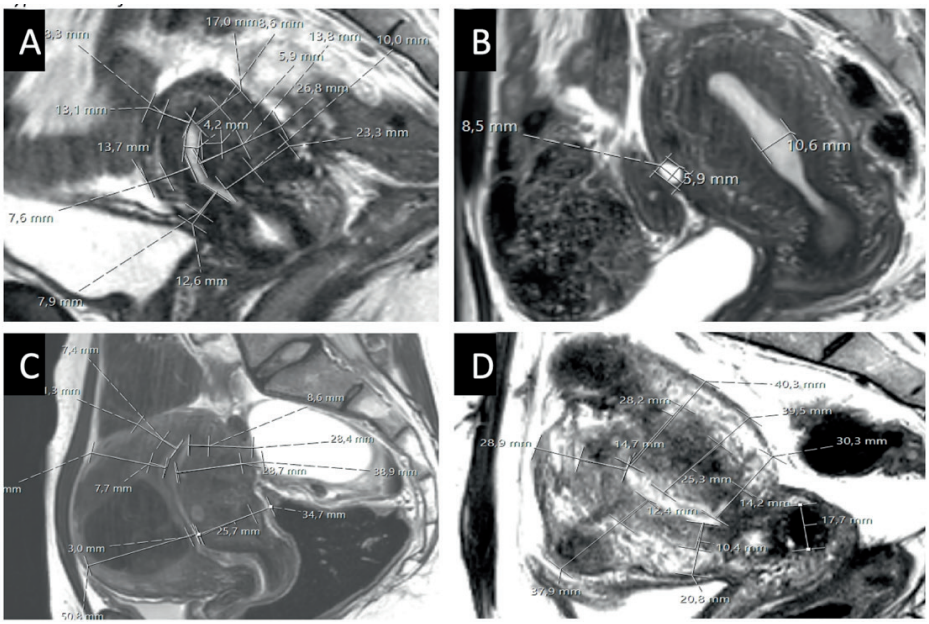

Figure 10.3 Examples of Adenomyotic Uteri in the Study Population. **A.** Uterus with focal adenomyosis in the posterior wall. **B.** Uterus with cystic adenomyosis in the anterior wall and a diffusely widened JZ. **C.** Enlarged uterus with a myoma in the anterior wall and diffuse adenomyosis with hyperintense foci in the JZ, and an ovarian endometrioma. **D.** Uterus with various myomas as well as a diffusely enlarged JZ with scattered hyperintense foci (myometrial cysts)

IVF/ICSI Outcomes:
A complete overview of IVF/ICSI outcomes for the adenomyosis versus controls is seen in Table 10.S6. Overall, patients with MRI-diagnosed adenomyosis showed significantly fewer biochemical and ongoing pregnancies and live births versus controls in crude analysis (25% vs. 36.3%, p=0.013, 15.6% vs. 29.4%, p=0.001, and 14.0% vs. 26.8%, p=0.009, respectively). A sub-analysis of patients with only fair-to-super quality embryos was also carried out (see supplementary file, Table S5), with comparable results (p=0.010 ,p=0.002 and p=0.014, respectively in crude analysis).

Subsequently, IVF/ICSI outcomes for patients with markers for adenomyosis or endometriosis severity were compared to controls (See Table 10.S6 for full results).

Table 10.4 presents a sub-analysis of adenomyosis MRI markers and reports the live birth rate (LBR) and adjusted odds ratio's for LB versus male infertility controls corrected for age at IVF, embryo quality, number of transferred embryos, and year of treatment. Results for BP and OP are shown in Table S7. Adenomyosis patients overall showed statistically significantly fewer LB compared to controls (aOR 0.560 (95% CI 0.318-0.988, p=0.045). The sub-analysis for patients with only fair-to-super quality embryos showed comparable results (aOR 0.457 (95% CI 0.239-0.877, p=0.018) Furthermore, the MRI markers of myometrial cysts, JZ-Diff >5mm, JZ/Myometrium ratio >40% and added presence of endometriosis remained statistically significantly associated with fewer LB versus controls.

Table 10.4: Live Birth Rate for Adenomyosis Severity MRI Markers versus Controls

Analysed Subgroup (N)	LBR Adenomyosis Cases (%)	LBR Control Group (N=889, %)	aOR (95% CI)*	p-value**
Adenomyosis Patients with Myometrial Cysts (n=60)	7 (12.1%)	233 (26.8%)	0.420 (0.177-0.997)	0.049
Adenomyosis Patients without Myometrial Cysts (n=63)	10 (16.1%)		0.556 (0.255-1.214)	0.14
Adenomyosis Patients with Mean JZ<12mm (N= 103)	15 (15.%)		0.510 (0.264-0.985)	0.045
Adenomyosis Patients with Mean JZ>12mm (N= 20)	2 (10.5%)		0.374 (0.082-1.700)	0.20
Adenomyosis Patients with JZ-Diff <5mm (N=13)	1 (7.7%)		0.255 (0.032-2.041)	0.20
Adenomyosis Patients with JZ-Diff>5mm (N= 110)	16 (15.0%)		0.519 (0.273-0.990)	0.046
Adenomyosis Patients with JZ-Myometrium <40% (N=31)	5 (16.7%)		0.598 (0.212-1.683)	0.33
Adenomyosis Patients with JZ-Myometrium Ratio >40% (N=92)	12 (13.3%)		0.453 (0.222-0.921)	0.029
Diffuse Adenomyosis (N=31)	5 (16.7%)		0.583 (0.209-1.201)	0.30
Focal Adenomyosis (N=58)	9 (15.5%)		0.525 (0.230-1.626)	0.13
Adenomyosis Alone (n=31)	5 (17.2%)		0.652 (0.225-1.889)	0.43
Adenomyosis and Endometriosis (n=93)	12 (14.1%)§		0.440 (0.219-0.886)	0.021
Adenomyosis without DIE (n=98)	15 (15.8%)		0.542 (0.280-1.050)	0.070
Adenomyosis with DIE (n=26)	2 (7.7%)§		0.272 (0.061-1.212)	0.088

LBR: live birth rate; aOR: adjusted Odds Ratio; DIE: Deep Invasive Endometriosis
*Multivariate logistic regression adjusted for: age at time of IVF, IVF or ICSI treatment, embryo quality, year of IVF treatment and number of transferred embryos,
**p-value for logistic regression analysis
§ denotes $p<0.05$ versus controls in crude analysis

Discussion

Previous studies have suggested that adenomyosis negatively affects reproductive outcomes, however, a lack of consensus in diagnostic criteria on MRI makes the relationship between disease severity and IVF/ICSI outcomes unclear. Hence, we investigated known MRI markers of adenomyosis severity in relation to IVF/ICSI outcomes. Our study showed a wide range of adenomyosis characteristics in infertile women, reflecting the varied nature of the disease, and highlighting the challenges in its diagnosis and clinical presentation. Results showed that within adenomyosis (and endometriosis) patients, patients with certain MRI markers (namely concomitant endometriosis, myometrial cysts, JZ Diff>5mm, and/or a JZ/Myometrium ratio >40%) exhibited significantly worse IVF/ICSI versus male infertility controls ($p<0.05$). These findings were confirmed when correcting for confounders in multivariate analysis.

Despite the fact that there are limited comparable studies, it can be said that our results are consistent with the current literature. In a study by Meylaerts et al., a thickened AJZ and JZmax on MRI were associated with infertility (95). A similar study by Maubon et al. examined the influence of JZ thickness in infertile women on implantation rates during IVF, and showed that a thickened JZ was a negative predictor for embryo implantation (98). This study also investigated JZ cut-offs and showed a implantation failure rate of 95.8% for patients with an AJZ> 7 mm and a JZmax > 10 mm compared to patients with a smaller JZ ($p < 0.0001$). In our study on the other hand, a higher JZ cut-off of 12mm was significantly associated with worse IVF/ICSI outcomes. The majority of women in our population already had a relatively thickened junctional zone due to the presence of adenomyosis, so the threshold proffered in the aforementioned study may well not be applicable to our population.

A handful of recent studies have investigated individual adenomyosis MRI characteristics and IVF/ICSI outcomes (15,142,282). A study by Iwasawa et al. found that patients with the extrinsic adenomyosis subtype had better fertility outcomes compared to other adenomyosis subtypes (15). Our study did not find a clear difference in IVF/ICSI outcomes between adenomyosis subtypes however. A possible explanation for this lies in the diverse categorisations of adenomyosis that exist, making consensus of certain MRI markers difficult (19). Our finding that the added presence of (deep invasive) endometriosis affects

IVF/ICSI pregnancy outcomes has been described before (106,283,284). One recent study also found that women with combined adenomyosis (irrespective of subtype) and endometriosis on MRI had fewer live births compared to endometriosis alone (282). Bourdon et al. additionally reported a significantly lower live birth rate in women with adenomyosis and endometriosis exhibiting myometrial cysts (282). Our study showed a similar relationship between live birth rate in relation to myometrial cysts (aOR 0.420, p=0.049). Overall therefore, our results support that adenomyosis in combination with (extensive) endometriosis could be seen as a more severe form of disease, and that these patients may form a specific subgroup potentially needing specific treatment protocols.

Strength & limitations

Our study has several strengths. First, the fact that the measurements were performed by two independent study investigators, reduces information bias. We also re-assessed all included MRIs during the study instead of relying on radiology report, accounting for differences in adenomyosis diagnosis over time and thereby increasing the internal consistency of our data. Correcting our results for relevant IVF/ICSI confounders also increases the reliability of our findings.

This study admittedly has limitations. First, despite our sample size being comparable to previous studies, the number of absolute pregnancies achieved in our study group is low (only 14% live births in patients with adenomyosis), reducing the power of the results. This is also reflected in the larger confidence intervals in the multivariate logistic regression analysis. It is possible that our study population represents a group of women with more severe disease (due to their infertility and indication for MRI in the first place), introducing an element of selection bias, and adding to the low pregnancy rate. Additionally, most MRI diagnoses of adenomyosis were made after IVF/ICSI treatment (78/124 patients). One could question whether the adenomyosis was present to a similar extent at the time of fertility treatment. We do not believe this to be a relevant issue however, as a sub-analysis based on the timing of the MRI in relation to IVF/ICSI treatment did not affect the results. Moreover, adenomyosis is known to be a disorder that develops over a lifetime, and can be assumed to be present throughout the reproductive life-phase (63). Another element of our

study to consider when interpreting our findings is the choice of control group. The majority of our control group did not undergo MRI, which means that the presence of adenomyosis in this group cannot be completely excluded, despite normal TVUS findings and lack of clinical adenomyosis symptoms. It is possible therefore that there are some undiagnosed adenomyosis patients in the control group, which may affect the final analysis. Furthermore, patients in our study cohort could have had other indications for infertility treatment in addition to endometriosis/adenomyosis, whereas our control group in theory only had male infertility. This inevitably introduces a further element of bias into our case group.

Clinical & future implications:

Our results support that specific MRI markers of adenomyosis and endometriosis severity may be associated with worse IVF/ICSI outcomes compared to male infertility controls. In this context, there is arguably value in thoroughly assessing severity and extent of adenomyosis pre-conceptionally, especially when in combination with endometriosis. Detailed mapping of adenomyosis on MRI may improve clinical counselling and management of adenomyosis and/or endometriosis patients considering IVF/ICSI. Our data shows that the lower IVF/ICSI pregnancy rates are mainly seen in patients with combined adenomyosis and endometriosis, with adenomyosis alone seemingly not enough to cause convincingly worse fertility outcomes in our study population. If adenomyosis and endometriosis are seen as a spectrum of the same disease, the combined diseases constitute more severe disease, and thus have a greater impact on reproductive ability. We did not include patients with only endometriosis so could not assess its potentially confounding effect here. However, previous work by our group has shown that endometriosis alone has less effect on IVF/ICSI outcomes than combined disease (283). Larger future studies with a prospective design should confirm these results, and aid in creating more personalised management and treatments for (infertile) adenomyosis patients.

Conclusion

This study assessed a number of MRI parameters (added presence of endometriosis (DIE), mean JZ >12mm, mean JZ/Myometrium ratio of >40% and presence of myometrial cysts) that could function as markers for IVF/ICSI outcomes and aid in counselling patients prior to starting treatment. We believe further (prospective) research should be encouraged. Mapping out the severity and the extent of adenomyosis and endometriosis in correlation to further clinical (fertility) outcomes could aid in clinical management of (infertile) women with the disease.

PART V

Effect of Adenomyosis on Obstetric Outcomes

CHAPTER 11:

The ADENO Study: Adenomyosis and its Effect on Neonatal and Obstetric Outcomes

Authors:
Connie O. Rees
Hubertus A.A.M. van Vliet
Albertus Siebers
Johan Bulten
Aleida G. Huppelschoten
Michelle E.M.H. Westerhuis
Massimo Mischi
Benedictus C. Schoot

The content of this chapter has been published in the A*merican Journal of Obstetrics and Gynecology*, 2023, Volume 229, Issue 1, Pages 49.e1-49.e12
DOI: /10.1016/j.ajog.2022.12.013

ABSTRACT:
Objectives: To investigate the prevalence of adverse obstetric and neonatal outcomes in women with histopathological adenomyosis compared to that of that of the general (Dutch) population
Study Design: This retrospective population-based study used two Dutch national databases (Perined, the perinatal registry, and the nationwide pathology databank (PALGA), from 1995-2018) to compare obstetric outcomes in women prior to histopathological adenomyosis diagnosis to the general Dutch population without registered histopathological adenomyosis. Odds Ratios (aOR, 95% CI) were calculated for adverse obstetric outcomes. Outcomes were corrected for: maternal age, parity, ethnicity, year of registered birth, induction of labour, hypertensive disorders in previous pregnancies, multiple gestation and low socioeconomic status.
Results: Pregnancy outcomes of 7,925 women with histopathological adenomyosis were compared to 4,615,803 women without registered adenomyosis. When corrected for confounders, women with adenomyosis had an aOR 1.37 (95% CI 1.25-1.50) for hypertensive disorders, an aOR of 1.37 (95% CI 1.25-1.51) for preeclampsia, aOR of 1.15 (95% CI 1.07-1.25) for a small-for-gestational-age infants. Women with adenomyosis had an aOR of 1.54 (95% CI 1.41-1.68) for emergency caesarean delivery, an aOR of 1.24 (95% CI 1.12-1.37) for failure to progress, an aOR of 1.29 (95% CI 1.10-1.48) for placental retention and an aOR of 1.23 (95% CI 1.10-1.38) for postpartum haemorrhage. No increased risk for HELLP, placental abruption, operative vaginal delivery or need for oxytocin stimulation was found.
Conclusions: Women with a histopathological diagnosis of adenomyosis show an increased prevalence of hypertensive disorders of pregnancy and small-for-gestational-age infants, failure to progress in labour and placental retention compared to the general population in prior pregnancies. This suggests uterine (contractile) function in labour and during pregnancy is impaired in women with adenomyosis.
Keywords: Adenomyosis; Adverse Obstetric Outcomes; Foetal Growth Restriction; Histopathology; Hypertensive disorders; Neonatal outcomes; Obstetric Complications; Placental abnormalities; Population study; Preeclampsia; Progress of Labour; SGA

Introduction:

Adenomyosis is a uterine condition closely linked to endometriosis, characterized by myometrial invasion of endometrial tissue. It is associated with dysmenorrhea, abnormal uterine bleeding, and chronic pelvic pain. Further evidence is gathering which identifies it as a cause for adverse reproductive outcomes (81,88,281). Its prevalence is debated, with some estimates as high as 20% of women in the fertile phase of life (7). While most studies have investigated the relationship between adenomyosis and fertility, recent literature also proposes that presence of adenomyosis may lead to a higher risk of obstetric complications such as preterm birth (PTB), foetal growth restriction (FGR) and hypertensive disorders of pregnancy (HDP) (103–105,108) .

Elements of the pathophysiology of adenomyosis – namely its disruption of the uterine junctional zone and thereby uterine contractility – have been hypothesized to influence the obstetric function of the uterus. HDP are thought to arise from impaired spiral artery development and placentation in this same junctional zone. Furthermore, the junctional zone has an important role in uterine contractile function (111,259,285), which is arguably most well-known in the onset and progress of labour. Common obstetric complications such as failure to progress, uterine hyperstimulation and atony, and placental retention are likewise associated with aberrant uterine contractility.

Part of the problem in gaining consensus regarding the (obstetric) consequences of adenomyosis lies in its diagnosis in the first place. Adenomyosis is often underdiagnosed due up to one third of women remaining asymptomatic (or not consulting a gynaecologist for their symptoms), alongside a lack of uniform diagnostic criteria (19,182). Whilst adenomyosis can be relatively accurately diagnosed using imaging techniques such as transvaginal ultrasound (TVUS) and magnetic resonance imaging (MRI), the diagnostic criteria vary, and there is a high level of inter-observer variability (29,31–34,181,192). For this reason, the gold standard for adenomyosis diagnosis remains histopathology. With biopsy also not being sufficiently accurate (286), adenomyosis is most reliably diagnosed after hysterectomy in women after having completed their childbearing wish. This poses a clinical challenge as it is now commonly accepted that adenomyosis may be highly prevalent in younger, nulliparous women (7,19,78,287).

Despite most of the published studies reporting convincing evidence associating adenomyosis with obstetric complications, common weaknesses of these studies limit their generalizability. First, they have relatively small sample sizes, with the largest study including 245 women with adenomyosis (101,110). Previous studies have made use of less reliable diagnostic methods such as TVUS (105) and MRI (4,102), with the larger published studies relying on self-reported diagnosis (104,110). Nevertheless, no studies exist on obstetric outcomes in combination with histopathological adenomyosis diagnosis. Hence, women with adenomyosis are not generally considered as having high-risk or complicated pregnancies.

Consequently, no guidelines exist for the management of pregnant women diagnosed with adenomyosis. Large-scale studies are needed to yield unambiguous results that can impact the clinical practice and (obstetric) management of women, preferably using the diagnostic gold standard of histopathology.

MATERIALS AND METHODS:

Study Objective:

To investigate the prevalence of adverse obstetric and neonatal outcomes in women with histopathological adenomyosis compared to that of that of the general (Dutch) population

Study Design:

Retrospective observational population-based cohort study
Setting: Dutch population-level data from 1995-2018.

Population:

Inclusion criteria
Study Group: Women between the ages of 18-50 histologically diagnosed with adenomyosis, from the Dutch nationwide pathology databank (PALGA) between the years of 1995 to 2018, with pregnancy outcomes registered in the Dutch national perinatal registry (Perined).
Control group: Women between the ages of 18-50 with registered pregnancy outcomes in the Perined registry between the years 1995 to 2018, *without* reported histopathological adenomyosis diagnosis.
Exclusion criteria
No pseudonymised personal identifier in the perinatal registry, meaning that data linkage could not be facilitated.

Sample Size calculation:
Due to the still disputed prevalence of adenomyosis (288) and risk of adverse pregnancy outcomes in women with adenomyosis, a sample size calculation was not conducted. However, due to this study using population-level data is assumed that the power of the results is sufficient to yield clinically significant results.

Study Outcomes:

The prevalence of adverse obstetric outcomes in women with adenomyosis was compared to the women without reported histopathological adenomyosis from the general Dutch population.

The primary outcomes of this study are summarised in Table 11.S1. Primary outcomes for this study included a variety of adverse obstetric outcomes: mode of delivery, preterm birth (PTB, delivery <37 weeks gestational age), failure to progress, placental retention, postpartum haemorrhage (PPH), hypertensive disorders of pregnancy (HDP), foetal growth restriction (FGR, biometry < 10^{th} percentile), and small for gestational age (SGA, birthweight <10^{th} percentile). Neonatal outcomes assessed included: perinatal mortality, low (<7) Apgar scores, neonatal asphyxia (umbilical artery pH (<7.00)) and need for NICU admission.

A full list of patient and obstetric characteristics as secondary outcomes is summarized in Tables 11.S1 and 11.S2. In the context of this study, we extracted the following information from the pathological reports: patient age at time of hysterectomy, year of hysterectomy, and previous diagnosis of endometriosis.

Data Sources:

PALGA – Dutch nationwide pathology databank

The PALGA (*Pathologisch Anatomisch Landelijk Geautomiseerd Archief*, Houten, the Netherlands) database has existed since 1971, functioning as a data- and biobank for histopathological material collected from Dutch pathology laboratories. Since 1991, it has achieved national coverage and currently holds the data of approximately 12 million patients. All women who received a diagnosis of adenomyosis based on histopathology were collected from this database. These women were selected by conducting a systematic search, with support from a pathologist. See Appendix 11B for the search strategy used.

Perined – Dutch National Perinatal Database

Perined (Utrecht, the Netherlands) is the Dutch national perinatal database which records pregnancy outcomes of all women giving birth under

supervision of a registered midwife or gynaecologist in the home, outpatient, or clinical setting (generally from 22 weeks gestational age). Perined has achieved national coverage of pregnancy outcome registration since 2000 and holds details over 5 million pregnancies. The relevant characteristics of *all* women who gave birth within the study period (1995-2018) were requested. A full list of the pregnancy and patient outcomes available from the database are shown in Appendix 11D.

Data linkage between PALGA and Perined

The women identified in the PALGA database with adenomyosis who have reported pregnancy outcomes in the Perined database were matched based on identification number. The combination and linkage of these two databases was facilitated using a Trusted Third Party (TTP) at Statistics Netherlands (CBS, Centraal Bureau voor de Statistiek). All data was fully anonymised with each individual woman assigned a pseudonymized ID. The study had to adhere stringently to the privacy guidelines of the CBS to avoid reporting revealing data. This meant that we were unable to report absolute values in certain situations, namely: for outcomes occurring in fewer than ten women, and any outcomes occurring with a prevalence of under 10% and/or more than 90%. We were also unable to report minimum or maximum values. Consequently a large fraction of the results are reported as a relative difference in prevalence (%) between groups, rather than their absolute values (e.g., +2%, as opposed to 6% and 8%).

Statistical Analysis:

Statistical analysis was carried out using SPSS Version 26. Outcomes were compared between women diagnosed with adenomyosis versus those without registered adenomyosis diagnosis. Dichotomous outcomes were compared using chi-squared analysis. For continuous variables, the independent T-test was used if normally distributed, and the Mann-Whitney-U test if abnormally distributed. A multivariate regression analysis was conducted to calculate adjusted Odds Ratios (aORs) for relevant outcomes and a 95% confidence interval. Outcomes were corrected for potential confounders: maternal age (at time of delivery), parity (at time of delivery), ethnicity, year of registered birth, induction of labour, multiple gestation and low socioeconomic status. Women who gave birth multiple times in the study period could be included more than once in the analysis. Bonferroni correction was applied where

appropriate to account for multiple comparisons and repeated measures. A p-value of <0.05 was considered as statistically significant for all variables. This study is reported according to the STROBE guidelines (189) (see Appendix 11G for the STROBE checklist). Figures were created using Miro and SPSS.

Ethical Considerations:

No informed consent was requested from the patients included as only anonymized data that is already publicly available was used. For the correlation between databases, a TTP was used de-anonymize and link the databases. Ethical approval from the regional ethical committee was obtained with local study number nWMO-2020.0015.

RESULTS:

Our initial search in the PALGA registry resulted in a total of 36,168 women between the ages of 18 and 50 who received the histopathological diagnosis of adenomyosis after hysterectomy between the years of 1995-2018. Out of this pool of women, 7,925 women could be linked to obstetric outcomes in the Perined registry. Table 11.1 gives an overview of the demographic characteristics of adenomyosis patients with pregnancy outcomes compared to the general population. The Perined registry was subsequently consulted to identify the obstetric outcomes of the general Dutch population in the same period, giving outcomes of 4,615,803 pregnancies of women without histologically confirmed adenomyosis. 548,852 Patients were excluded due to insufficient data to facilitate linkage between databases (for example due to missing patient identifiers). Patient selection is visualized in Figure 11.1.

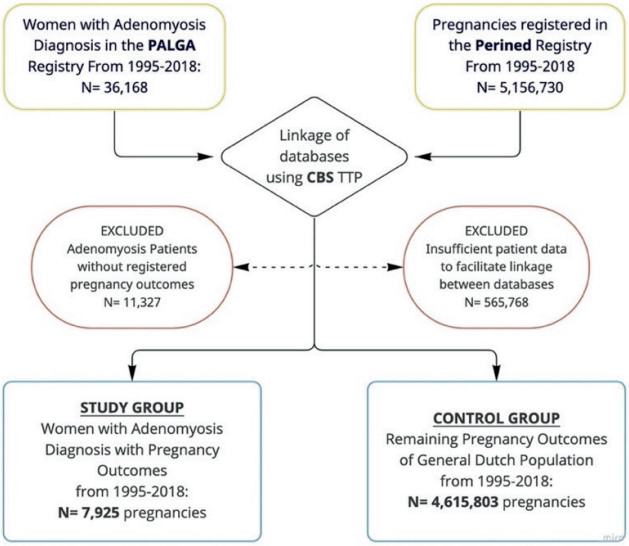

Figure 11.1 Flowchart of Patient Selection from the PALGA (Pathologisch Anatomisch Landelijk Geautomatiseerd Archief) and Perined Dutch National Databases. Linkage of the anonymized databases was carried out using the services of a trusted third party (TTP) via de Dutch Central Bureau of Statistics (CBS).

Relevant demographic obstetric characteristics and outcomes available were compared between the pregnancies in women with histologically diagnosed adenomyosis and those of the general Dutch population. Obstetric characteristics are summarised in Table 11.1, maternal and obstetric outcomes in Table 11.2, and neonatal outcomes in Table 11.3.

Table 11.1 Demographic and Obstetric characteristics of Adenomyosis patients versus the general Dutch population

Characteristic	Total Dutch Population (n=4,615,803)	Adenomyosis Patients (n=7,925)	p-value*
Low-income area (%)	587,058 (12.8%)	959 (12.1%)	P=0.078
Age of women at time of pregnancy (in Years, Mean (SD))	30.42 (4.87)	Mean 29.15 (4.43)	P<0.001
Registered year of pregnancy (Mean (SD))	2006 (6.80)	1999 (4.35)	P<0.001
Ethnicity			P<0.001
- Dutch/Caucasian	3,056,539 (79.6%)	5,024 (87.1%)	
- Mediterranean	431,571 (11.3%)	<10%	
Creole/Hindustani/Asian			
- Other	<10%	2,158 (37.4%)	
- Unknown	776,448 (20.2%)		
Obstetric Characteristics			
Gravidity (Median, (IQR))	2 (2)	2 (2)	P<0.001
Multiple gestation		-0.9%**	P<0.001
History of Miscarriage/Abortion (N, (%))	1,226,139 (26.4%)	2,420 (30.4%)	P<0.001
Number of previous miscarriages (Median, (IQR))	0 (1)	0 (1)	
Parity			P<0.001
- Median (IQR)	1 (1)	0 (1)	
- Primiparous	2,098,078 (45.7%)	4,928 (62.2%)	
- Multiparous		2,997 (37.8%)	
- Grande multiparity (>5)		-0.4%	
Mode of Conception (N, (%))			P<0.001
- Spontaneous	2,536,563 (55.0%)	5,217 (65.8%)	
- Ovulation induction		+1.1%	
- Intra-uterine insemination		+0.3%	
- IVF/ICSI		+1.4%	
- Other	1,921,094 (41.6%)	+0.1%	
- Unknown		2,201 (27.8%)	
Reported subfertility		+4.7%	P<0.001
Gestational age at time of first consultation (in Weeks, Median (IQR))	10 (5)	11 (4)	P<0.001
Diagnosis of uterine fibroids prior to pregnancy		+0.4%	P<0.001
Pregnancy setting at the start of pregnancy (N, (%))			P<0.001
- Midwife	3,955,220 (85.7%)	6,040 (76.2%)	
- Hospital/Clinical	638,368 (13.8%)	1,834 (23.1%)	
- Unknown		-0.3%	

History of HDP	+0.1%	P=0.444
Hyperemesis gravidarum	+0.3%	P<0.001

IVF: In-vitro Fertilization, ICSI: Intracytoplasmic sperm injection; HDP: Hypertensive disorders of Pregnancy, PIH: Pregnancy-Induced Hypertension
*P-value calculated using Chi^2 analysis for dichotomous outcomes, Independent T-test for normally distributed continuous variables and Mann-Whitney U test for abnormally distributed continuous variables.
**Some outcomes are reported only as a relative percentage difference between patient groups instead of absolute values, due to CBS data privacy restrictions. In some cases, this leads to percentages not adding up to 100%.

Obstetric characteristics were compared between groups (Table 11.1). Several significant differences were found between the adenomyosis patient pregnancies and those of the general Dutch population. Women with histopathological adenomyosis were more often primiparous (65.8% vs. 55.0%), and had more reported subfertility (+4.7%) and subsequently were more often pregnant after undergoing ART.

Table 11.2 shows descriptive analysis of all obstetric and maternal outcomes. Multivariate binary logistic regression analysis was performed for obstetric and neonatal outcomes. All outcomes were corrected for potential confounders: parity, age, year of birth, multiple gestation, induction of labour, low-income area, ethnicity, gestational diabetes, history of hypertensive disorder. Univariate analysis for relevant outcomes can be found in Table 11.S6. Table 11.S7 shows the full outcomes of multivariate regression analysis.

Table 11.2 Obstetric Outcomes for Adenomyosis Patients vs. Dutch General Population

Outcomes	Total Dutch Population (n=4,615,803)	Adenomyosis Patients (n=7,925)	p-value*
Gestational age in days at birth (Median (IQR))	279 (14)	277 (15)	P<0.001
Gestational age (in weeks) at birth (Median (IQR))	39 (2)	39 (2)	P<0.001
Gestational diabetes		-0.1%	P=0.593
Antepartum Haemorrhage		-1.5%	P<0.001
Preterm Premature Rupture of Membranes (PPROM)		+0.5%	P<0.001
Threatened prematurity***		+2.2%	P<0.001
Cervical insufficiency		+0.1%	P=0.113
HDP in current pregnancy (N, (%))		+3.8%	P<0.001
- Gestational Hypertension/PIH		+3.7%	
- Pre-eclampsia		+0.6%	
- HELLP/Eclampsia		+0.1%	
Proteinuria		+1.0%	P<0.001
Degree of Proteinuria (mg/L, Median (IQR))	581.00 (IQR 1190)	600.00 (IQR 1360)	P=0.124
Mode of start of labour (N, (%))			P<0.001
- Spontaneous	3,145,799 (68.2%)	5,556 (70.1%)	
- Induction of labor	790,130 (17.0%)	1,698 (21.4%)	
- Elective Caesarean		-1.3%	
Pregnancy setting at start of labour (N, (%))			P<0.001
- Midwife	2,248,806 (48.7%)	3,509 (44.3%)	
- Hospital/Clinical	2,067,261 (44.8%)	4,353 (54.9%)	
- Unknown		-0.8%	
- N/a		-4.9%	
Delivery Setting (N(%))			P<0.001
- Home delivery	855,114 (18.5%)	1,222 (15.4%)	
- Birthing centre		-0.6%	
- Hospital delivery under supervision of midwife		-1.3%	
- Hospital delivery under supervision of a gynaecologist	98,489 (64.7%)	5,991 (75.6%)	
- Unknown		-0.1%	

Mode of Delivery (N(%))			P<0.001
- **Vaginal**	3,114,932 (67.5%)	5,677 (71.6%)	
- **Spontaneous vaginal**		5,243 (66.2%)	
- **Instrumental delivery**		+2.8%	
- **Cesarean Section (CS)**	628,496 (13.6%)	1,567 (19.8%)	
- **Elective CS**		+1.9%	
- **Emergency CS**		+4.4%	
- **Unknown**		-7.2%	
Indication for labour induction/Elective CS (N, (%))	1,025,775 (22.2%)	2,324 (29.3%)	P<0.001
- **Elective**	419,887 (40.9%)	1,016 (43.7%)	
- **Foetal condition**	256,783 (25.0%)	464 (20.0%)	
- **Maternal condition**	199,489 (19.4%)	511 (22.0%)	
- **Maternal & Foetal Condition**	149,616 (14.6%)	333 (14.3%)	
Indication for Instrumental delivery/Emergency CS (N, (%))	842,981 (18.3%)	2,083 (26.2%)	P<0.001
- Foetal distress	234,881 (27.9%)	479 (23.0%)	
- Failure to progress	454,012 (53.9%)	1,248 (59.9%)	
- Foetal Distress and failure to progress		-0.5%	
- Other		-0.8%	
Postpartum Haemorrhage (>1 L)		+0.4%	P=0.194
Placental issues (composite)		+0.4%	P=0.028
Placental Abruption		+0.1%	P=0.082
Placental Retention		+0.3%	P=0.135
Placenta Previa		+0.1%	P=0.152
Meconium stained amniotic fluid (N(%))	496,331 (10.8%)	842 (10.6%)	P=0.729
Non-vertex lie (N(%))	536,804 (11.6%)	1,248 (15.7%)	P<0.001
Cephalopelvic disproportion		+0.7%	P<0.001
Foetal distress		+1.6%	P<0.001
Duration of ruptured membranes until delivery (hours, Median (IQR))	2.00 (7)	3.00 (8)	P<0.001
Prolonged rupture of membranes (>24h, (N(%)))	318,453 (6.9%)	733 (9.2%)	P<0.001
Duration of second stage of labour (minutes, Median (IQR))	18 (37)	27 (46)	P<0.001
Failure to progress in second stage of labour		+0.7%	P<0.001
Failure to progress in first stage of labour		+1.3%	P<0.001
Need for oxytocin stimulation	933,786 (39.9%)	1,029 (37.8%)	P<0.001

Pain relief during labour (Epidural or Morphinomimetics)	1,081,218 (23.4%)	2,044 (25.8%)	P<0.001
Episiotomy	1,084,463 (23.5%)	2,357 (29.7%)	P<0.001
Hospital Admission	2,498,476 (53.9%)	5,350 (67.5%)	P<0.001
Duration of hospital stay (days, Median (IQR))	1.00 (IQR 2)	2.00 (IQR 3)	
Maternal Mortality		+/- 0.0%	P<0.001
Uterine Rupture		+/- 0.0%	P=0.544
Endometritis/Puerperal Fever		+0.1%	P=0.002

*Calculated using chi-squared analysis for dichotomous outcomes, T-test for normally distributed continuous variables, and the Mann-Whitney U test for abnormally distributed continuous variables

** In some cases, no absolute values are reported due to data privacy restrictions. Instead the relative difference in percentages is shown between the adenomyosis population versus the general population. . In some cases, this leads to percentages not adding up to 100%.

***Threatened prematurity: admittance due to suspicion of threatened premature delivery due to either cervical insufficiency, premature contractions, or preterm premature rupture of membranes.

No significant differences were found for maternal mortality between groups. Outcomes of multivariate logistic regression are summarised in Figure 11.2 (as aOR's with 95% CI) for the majority of obstetric and neonatal outcomes.

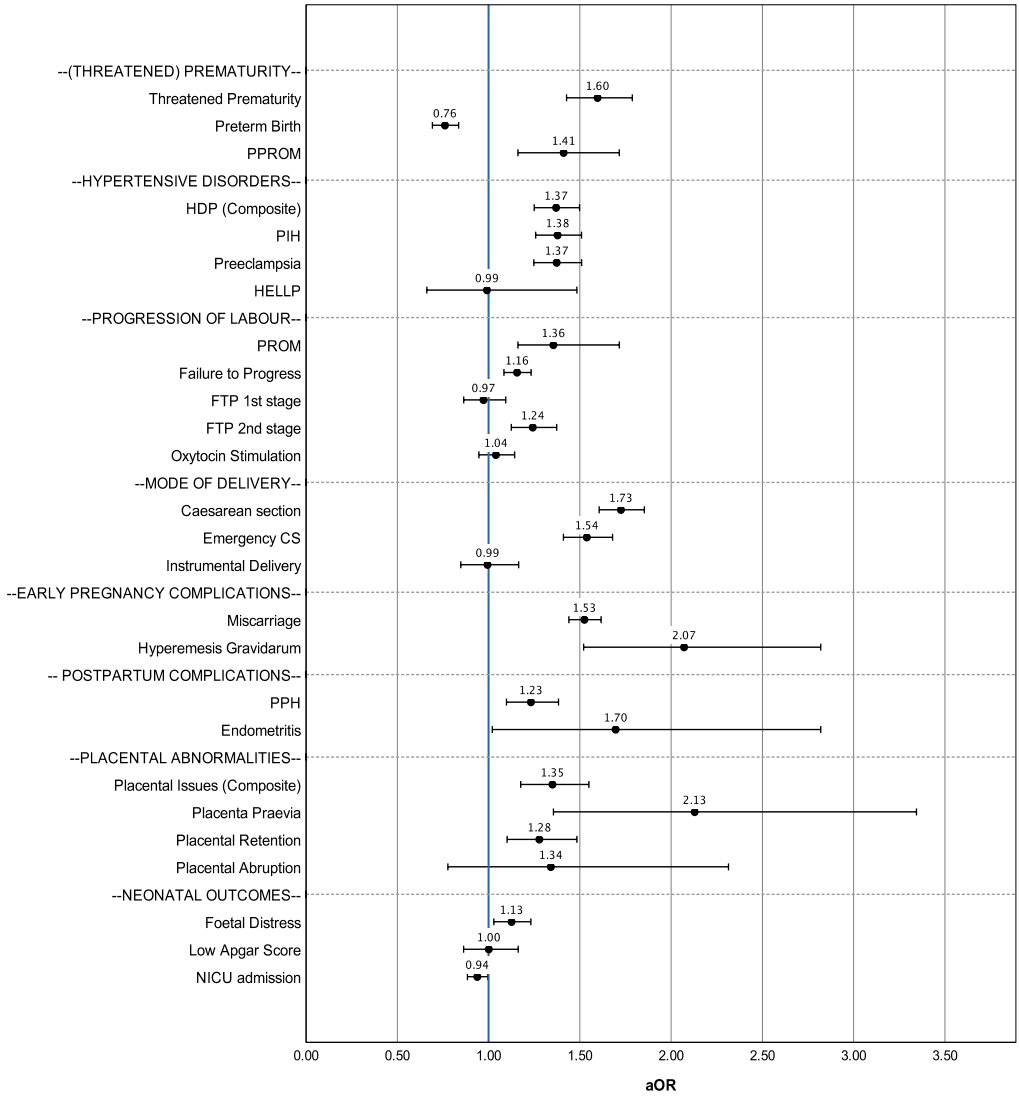

Figure 11.2 Forest plot of adjusted Odds Ratio (aOR's, with error bars signifying 95% CI) for relevant obstetric and neonatal outcomes for patients with histologically proven adenomyosis (n=7,925) versus women without histologically proven adenomyosis from the Dutch population (n=4,615,803). aOR's were corrected for: maternal age, parity, ethnicity, year of registered birth, induction of labour, multiple gestation and low socioeconomic status. PPROM: preterm premature rupture of membranes; HDP: hypertensive disorders of pregnancy; PIH: pregnancy-induced hypertension; HELLP: haemolysis, elevated liver enzymes, lowered platelets; FTP: Failure to Progress; PROM: Premature Rupture of Membranes; CS: Caesarean Section; PPH: Postpartum Haemorrhage; NICU: Neonatal Intensive Care Unit

Adenomyosis was found to have an increased prevalence of signs of premature labour (including cervical insufficiency, PPROM, and premature contractions) during pregnancy with 2.2% more women in the adenomyosis group diagnosed with premature labour or threatened prematurity compared to the general Dutch population. Likewise, there was a higher incidence (+0.5%) of PPROM and cervical insufficiency (increase of 0.5%; all $p<0.001$). However, prevalence of cervical insufficiency did not differ statistically significantly. When adjusting for confounders, we found an aOR of 1.47 (95% CI 1.33-1.63) for an episode of premature labour in general, and an aOR 1.41 (95% CI 1.16-1.72) for PPROM. Unexpectedly, women with adenomyosis showed lower prevalence of preterm birth (GA <37wk) with an aOR of 0.76 (95%CI 0.69-0.84) for PTB versus the general Dutch population.

There was a significantly ($P<0.001$) higher prevalence of HDP in the adenomyosis groups versus the general Dutch population. Adenomyosis patients had a higher prevalence of all forms of HDP, including PIH, PE and HELLP/Eclampsia. The aOR for all HDP combined was1.37 (95% CI 1.25-1.50).

Women with adenomyosis showed a higher prevalence of FGR (0.5% more prevalent in the adenomyosis groups, $p<0.001$) and SGA infants (14.3% versus 10.8% respectively, $p<0.001$) versus the general Dutch population. An aOR of 1.15 (95% CI 1.07-1.25) was found for an SGA foetus.

Women with adenomyosis showed significantly different outcomes with regards to progress of labour and mode of delivery. Women with adenomyosis had an aOR of 1.24 (95% CI 1.12-1.37) for failure to progress in labour in general when corrected for confounders. When stratifying this by stage of labour, specifically failure to progress in the second stage of labour remained statistically significant with an aOR of 1.24 (95% CI 1.12-1.37). Similarly, women with adenomyosis had a higher prevalence of PROM (>24 hours) compared to the general population (aOR 1.35 (95% CI 1.23-1.48). No significantly higher prevalence for need for oxytocin stimulation was found, with similarly insignificant results for failure to progress in the first stage of labour.

Mode of delivery also differed significantly between groups. Women with adenomyosis diagnosis had an aOR of 1.73 (95% CI 1.61-1.85) for caesarean delivery in general, and aOR of 1.54 (95% CI 1.41-1.70) for emergency caesarean delivery. The majority of emergency caesarean deliveries (59.9% vs 53.4% for adenomyosis and the general population respectively) were carried out due to failure to progress. No significant difference was found for instrumental delivery.

There was a lower prevalence of antepartum haemorrhage in the adenomyosis group versus the general Dutch population (1.5% lower in prevalence, $p<0.001$). Women with adenomyosis showed an increased risk of hyperemesis gravidarum (aOR 2.07 (95% CI 1.52-2.82)). Women with adenomyosis also experienced more miscarriages (30.4% vs. 26.4%, aOR 1.53 (95% CI 1.44-1.62)).

When looking at absolute values, no significantly increased prevalence of PPH could be found in the adenomyosis group ($p= 0.194$). When correcting for confounders however, a slightly increased risk for PPH was found in adenomyosis patients: aOR 1.23 (95% CI 1.10-1.38). Prevalence of endometritis was also increased in the adenomyosis group (aOR 1.70 (95% CI 1.02-2.82)).

Women with adenomyosis showed an increased prevalence of placental retention, placenta previa, and placental abruption (see Table 2), however, only placenta previa and placental retention showed statistically significantly increased aORs when adjusting for confounders (aOR 2.13 (95% CI 1.36 – 3.34) and aOR 1.28 (95% CI 1.10 -1.48) respectively). When combining placental issues into a composite outcome, statistical significance remained, with a reported aOR 1.35 (95% CI 1.18-1.55),

Several additional statistically significant differences were found between groups for other obstetric outcomes. An increased prevalence of foetal malposition (i.e. non-vertex lie) was seen in the adenomyosis group versus the general population (aOR 1.37 (95% CI 1.27-1.47)). Likewise, women with adenomyosis showed a higher prevalence for pain relief during labour (aOR 1.38 (95% CI 1.30-1.47)).

Several significant differences between the adenomyosis group and the general population were also found with regards to neonatal outcomes (see Table 3, and Figure 2). Children born from women with adenomyosis diagnosis showed a slightly lower birthweight (3308g (±670g) vs. 3372g (for adenomyosis versus general population respectively, $p<0.001$); however, the median birthweight percentile was still within normal range (p50.06 vs p50.67. $p<0.001$).

Women with adenomyosis showed a slightly increased prevalence of foetal distress during labour with an aOR of 1.13 (95% CI 1.03-1.23). No significant difference was found for presence of meconium-stained amniotic fluid ($p=0.729$). Likewise, no increased prevalence was found for neonatal mortality or low Apgar scores at birth ($p>0.05$), with neonates of women with adenomyosis also showing a lower prevalence of neonatal asphyxia ($p=0.036$). NICU admission was more common in the general population versus adenomyosis patients (17.2% versus 16.3% respectively, $p=0.037$).

DISCUSSION:

In our study, prior pregnancy outcomes of 7,925 women with a histopathological diagnosis of adenomyosis were compared to 4,615,803 women of the general Dutch population without adenomyosis. When corrected for common confounders, women with histopathological adenomyosis had an increased prevalence of HDP and SGA infants. Furthermore, women with adenomyosis more often had an emergency caesarean delivery, failure to progress and placental retention. There was no significantly increased risk for HELLP, eclampsia, placental abruption, operative vaginal delivery, or need for oxytocin stimulation.

No previous studies have investigated progress of labour in women with histologically-proven adenomyosis. Adenomyosis is thought to affect uterine contractile function due to the associated disruption of the junctional zone, leading to symptoms such as dysmenorrhea and infertility (77,289) . Uterine contractile function is arguably most well-known in the context of the onset and progress of labour, where common obstetric complications may be associated with ineffectual contractions. It can therefore be hypothesized that adenomyosis in pregnancy leads to a higher risk of these obstetric outcomes.

Aberrant (specifically, premature) uterine contractile function during pregnancy can also be related to premature birth (PTB). Past reported OR's for PTB in women with adenomyosis have ranged from 1.96 (102) to as high as 24.53 (103). Strikingly, our study cannot confirm this finding, with a lower risk of preterm birth in the adenomyosis group as compared to the general population (aOR 0.76 (95% CI 0.69-0.84). The adenomyosis group did however show an increased risk for threatened preterm birth including PPROM and cervical insufficiency. Potentially, this discrepancy lies in differences in (past) Dutch management protocols of PPROM and premature labour compared to previously published studies, leading to a later gestational age at birth. Another potential explanation for the difference in the results, is that most existing studies included mainly assisted reproductive technology (ART) patients in their populations (290,291), in contrast to our study. This may be a confounding factor leading to higher incidence of PTB in previous studies (although most studies did correct for mode of conception).

Hypertensive disorders of pregnancy are thought to arise from impaired implantation and placentation due to defective spiral artery development and

remodelling in this same junctional zone. Recent studies have suggested a link between adenomyosis and hypertensive disorders of pregnancy (4,81,281,291). Our study confirms this finding, with consistently higher aOR's for most HDPs compared to the general population. Additionally, we report a higher prevalence of FGR and SGA infants in the adenomyosis population. This could be simultaneously attributed to impaired placental implantation in adenomyotic uteri, with subsequent placental insufficiency affecting foetal growth.

Indeed, our results show a significantly increased prevalence of placental issues overall, be it malposition (i.e. previa) or problems with adherence (i.e. retention/abruption). The clearly higher prevalence of placenta previa (aOR 2.129 (95% CI 1.355 - 3.344)) may be explained by placental implantation being impaired at the site of adenomyotic lesions (most often in the corpus of the uterus), leading to aberrant localization of placental tissue. Interestingly however, despite the increased prevalence of placenta previa, women with adenomyosis did not show increased prevalence of antepartum haemorrhage. Possibly this was underreported. Alternatively, aberrant placental localization and implantation could also have formed the impetus for adenomyosis development in conjunction with the Tissue Injury and Active Repair (TIAR) theory as proposed by Leyendecker et al (9).

Previous studies also support our results for neonatal outcomes, with comparable studies investigating neonatal outcomes reporting mildly significant or statistically insignificant results (81,94). It seems therefore that adenomyosis affects mostly the maternal and obstetric outcomes, without a clinically relevant effect on neonatal outcome.

The results of our study support that women with subsequent proven adenomyosis more often experienced (prior) adverse obstetric outcomes. The diagnostic method referred to in this study – histopathological diagnosis mostly after hysterectomy – of course cannot be applied to pregnant women prospectively. However, the non-invasive diagnostic methods of transvaginal ultrasound and MRI can fairly accurately diagnose adenomyosis in the non-pregnant uterus (29,34,45,182). Whether adenomyosis is present at the time of the pregnancy is not proven by our study, and warrants future studies using MRI and ultrasound to shed light on directionality and causality of these

relationships. Nevertheless, if clear signs of adenomyosis are present, it is worth contemplating high-risk obstetric management of these patients. One could advocate for these patients needing more frequent foetal growth monitoring, or aspirin use from the first trimester for instance.

Further studies should investigate the effect of severity and type of adenomyosis on obstetric outcomes. Our study has confirmed that women with adenomyosis experience more obstetric and neonatal adverse outcomes, but this needs to be confirmed in prospective clinical studies. Subsequently, appropriate follow-up and adenomyosis treatments (hormonal, surgical or otherwise) can be assessed for their effect on obstetric complications.

Our study has several important strengths. First, the use of large population-based cohorts spanning a number of years, enabled us to conduct the largest study investigating this topic up to now. Moreover, this is the first study to use the gold standard of histologically confirmed adenomyosis. This gives our study a clear advantage due to the undisputed presence of adenomyosis in our study population. Third, contrary to the majority of existing studies, our study population includes both women who conceived naturally and used ART, making our conclusions more widely generalizable.

Despite its strengths, this study does have important limitations which should be considered. First, when conducting studies with a large (imbalanced) population, there is a higher chance of receiving statistically significant results. One then has to consider whether this statistical significance immediately translates to clinical significance. Nevertheless, as our results are generally in line with the existing literature, and remain significant after correction for a large number of confounders, they should be taken as clinically relevant.

Second, as only women with histologically confirmed adenomyosis were included, a potential bias may have been introduced. It is possible that women with more severe adenomyosis (symptoms) opt for operative over hormonal treatment, and are thereby able to receive histologically-confirmed diagnosis. Moreover, as not all women with adenomyosis undergo histological examination, the control group likely contains a substantial proportion of women with imaging-diagnosed adenomyosis. Hence, our results could be an over- (or under-) estimation of adenomyosis' true

association with (adverse) pregnancy outcomes. We are however of the opinion that due to the (much) larger size of our control group versus the adenomyosis group, this effect will have been sufficiently minimized however. We purposefully selected a broad control group in order to as far as possible reflect obstetric outcomes in the general population versus those with certain adenomyosis (as opposed to for example controls without adenomyosis at hysterectomy, as this group would represent a selected population with an indication for hysterectomy in the first place).

Despite the obvious benefits to using large and anonymized national databases, their use did introduce several constraints to the amount of patient information available. First, as visible in Figure 1, a large proportion of women with adenomyosis could not be linked to pregnancy outcomes. This is most likely due to limits regarding the years of available data and missing patient information. It is plausible that many women did experience pregnancies, but fell outside the study period. One could also hypothesize that as adenomyosis is linked to infertility (84,88,281), a large number of women with adenomyosis may not have been able to become pregnant in the first place, although this is purely speculative.

Additionally, pathological reports gave little to no information on the type of adenomyosis, making it difficult to draw conclusions regarding the effect of adenomyosis severity on obstetric outcomes. Likewise, in the Perined registry, certain potential confounding factors such as BMI and smoking were not (well) reported. We attempted to correct for these confounders by using the proxy of low- socio-economic background. Other potentially relevant patient characteristics such as miscarriages and mode of conception were also not well reported.

Conclusions:

This is the largest study to assess adverse obstetric outcomes in women with adenomyosis diagnosis based on histopathology. Our results confirm that women with histologically proven adenomyosis exhibit a higher prevalence of adverse obstetric outcomes, particularly for hypertensive disorders, failure to progress in labour and placental issues. Future prospective studies should investigate the extent to which non-invasive methods of adenomyosis

diagnosis can be associated with adverse obstetric outcomes, and which treatments of adenomyosis adequately reduce the risk of obstetric complications.

Acknowledgements:

We would like to thank Lisa Broeders at Perined and Fatima el Messlaki at CBS for their enthusiastic support and advice in gaining access to the data for this study.

PART VI

Discussion

CHAPTER 12:
General Discussion

In this thesis, we attempted to offer a wide view of the impact of adenomyosis on the uterine contractile and reproductive function. Starting with an exploration into its non-invasive diagnosis by way of MRI, we then continued to explore its possible effect on uterine contractility function, and end with its influence on fertility and obstetric outcomes.

SUMMARY OF THE RESULTS OF THIS THESIS

In **Chapters 2 and 3**, the diagnosis of adenomyosis using multiparametric MRI was explored. First, the existing literature of objective parameters used to diagnose MRI were summarised and assessed for their accuracy in diagnosing adenomyosis versus the golden standard of histopathology. A wide variety of classification systems and parameters have been used in the diagnosis of adenomyosis, with an overarching lack of uniformity. Overall, the most commonly used parameters involved the junctional zone (JZ), with cut-off values for its maximum diameter varying, but with 12 mm being most often used. When looking at the diagnostic accuracy of each parameter in a meta-analysis, the parameters that performed best were a JZ over 12 mm (sensitivity 71.6%, specificity 85.5%) and the presence of myometrial cysts or high signal intensity foci (sensitivity 59.6% and specificity 96.1%). No one single parameter performed well across the board. Subsequently, in **Chapter 3** we developed a multivariate prediction model for adenomyosis diagnosis by MRI, based on the MRI parameters as described in **Chapter 2** and using retrospective MRI and pathology data from a single centre. The final model performed well (AUC of 0.78), using a combination of five clinical and four MRI parameters. An external validation study using the same developed predictive model was conducted in **Chapter 4**, confirming good to excellent performance of the model in a different dataset (AUC 0.83). We concluded that it is most advisable to consider both patient and imaging characteristics for an accurate diagnosis of adenomyosis on MRI.

After investigating the non-invasive diagnosis of adenomyosis, we looked further into how, and if, adenomyosis indeed affects the uterine function in terms of uterine contractility. **Chapter 5** introduces a method to measure uterine peristalsis on 2D transvaginal ultrasound using speckle-tracking, showing its potential for clinical applicability in IVF patients. In **Chapter** 6, we attempted to define 'normal' uterine contractile function using a novel quantitative 2D speckle tracking method on TVUS in women with healthy, sonographically normal uteri. Here, we found that uterine contraction features

change according to menstrual cycle phase, and defined reference value ranges for all contraction features. Next, in **Chapter 7**, we evaluated the relevant literature to assess the existing evidence for if uterine contractility has been found to be affected by uterine abnormalities. The few available studies tended to be small, and used subjective and difficult to compare measurement tools. The majority of the studies did suggest that uterine contractile function is impaired in abnormal versus normal uteri in the natural menstrual cycle. Having established a baseline for healthy uterine contractile function, and examining the existing evidence for aberrant uterine contractility in abnormal uteri, we conducted a prospective observational cohort study in **Chapter 8**. We used the aforementioned 2D TVUS-based speckle tracking analysis method to evaluate uterine contractility features in women with adenomyotic uteri versus healthy controls throughout the menstrual cycle. Study results showed that uterine contractility shows most significant differences from healthy uteri in the periovulatory and luteal phases of the menstrual cycle for a variety of contractility features. In addition, specifically uterine contraction *coordination* seems most significantly impaired in adenomyosis patients compared to healthy controls, identifying this feature as a promising marker of normal uterine function.

Chapters 9 and 10 examine if patients with adenomyosis on MRI have worse IVF/ICSI outcomes compared to male infertility controls. In **Chapter 9**, it is shown that women with combined endometriosis and adenomyosis disease have statistically significantly worse IVF/ICSI outcomes than controls. This can suggest that more severe disease has a proportionally more severe effect on IVF/ICSI success rates. **Chapter 10** then delves deeper into which MRI markers may be specifically associated with the worst fertility outcomes. We observed that the added presence of (deep invasive) endometriosis and especially the presence of myometrial cysts is associated with fewer successful IVF/ICSI pregnancies.

Finally, in **Chapter 11**, the association of adenomyosis with adverse obstetric outcomes is explored. In this retrospective population-based cohort study, the obstetric and neonatal outcomes of patients with histologically proven adenomyosis (based on hysterectomy) are compared to that of the general Dutch population. After correcting for relevant confounders, we found that

women with adenomyosis show an increased prevalence of a wide range of adverse obstetric outcomes, namely: hypertensive disorders of pregnancy, foetal growth restriction, placental issues, and labour progression issues leading to a higher number of caesarean sections.

CLINICAL IMPLICATIONS AND RELEVANCE

- *Objective 1: Accurate and objective MRI diagnosis for adenomyosis*

The diagnostic modality focussed on within this thesis has been the MRI diagnosis of adenomyosis. It should be said that we do not hereby mean to suggest that all patients with suspected adenomyosis should be referred for an MRI. The primary first line diagnostic method used in clinical practice still is, and should be, TVUS diagnosis. TVUS is more widely available, quicker, and cheaper than MRI, and should form the basis of initial clinical work-up. Due to the widely used and accepted MUSA criteria, TVUS has been shown to be reliable for adenomyosis diagnosis in many cases, especially with improving ultrasound quality and the availability of 3D transvaginal ultrasound (29). There also exists a recently developed multivariate prediction model for TVUS adenomyosis diagnosis showing a similar performance to our developed model (184). It cannot go unmentioned however, that the literature that has been published regarding TVUS diagnosis generally relates mainly to TVUS carried out by expert observers in specialised clinics. The diagnostic accuracy here likely does not reflect the accuracy of TVUS diagnosis by every general gynaecologist in daily practice. This leaves room for further improvement and investigation into objective and reproducible diagnostic modalities. .

We hence chose to concentrate our research on MRI diagnosis as there are cases where ultrasound remains unclear, for example due to combined pathology, a (relatively) inexperienced observer, or need for extensive pre-operative work-up (199,292). In cases such as these, MRIs are often performed, but adenomyosis diagnosis then becomes difficult due to the current lack of accepted diagnostic criteria. For this reason, we chose to attempt to close this knowledge gap by summarising the diagnostic criteria available. Moreover, we also investigated which of these criteria (with symptoms) were most promising for facilitating accurate MRI diagnosis with our multivariate prediction model. Future (prospective) studies should focus on the further validation and implementation of this model for adenomyosis diagnosis. It may also be possible to further improve upon the model, with the addition of further developing diagnostic markers in future, like texture analysis or elastography (293,294). Improving the useability of the model could also involve exploration the use of automated MRI measurement using AI tools for example.

One element of adenomyosis MRI diagnosis in particular, and imaging diagnosis in general, that has recently come into the debate is the (un)importance of the JZ. JZ thickness is by far the most often reported diagnostic criteria for adenomyosis on MRI (33,47), albeit with a variety of cut-off values. It is also an important feature assessed as a part of the MUSA criteria on TVUS (197). Yet, in recent years, the concept of the uterine junctional zone as a physiological and anatomical entity has been put into question (45,198). We know that is a distinct visible element of uterine anatomy on both transvaginal ultrasound (TVUS) and MRI; however, it cannot be defined as such on histopathology (198). The junctional zone also appears differently on TVUS and MRI begging the question which of the phenotypes is most clinically relevant. In addition, the reported cut-off values are repeatedly brought into question in the literature (45,95,98). It is generally accepted that the junctional zone or 'endo-myometrial unit' has a physiological function, especially in terms of uterine contractility, and hence most probably affects uterine reproductive function (46,73,111,148). Clinically, it is therefore arguably important to be able identify when it is (functioning) abnormal(ly), for example in the context of adenomyosis. As adenomyosis is known to invade or inhabit this region, it is thus logical that this is the area is where most imaging abnormalities are found. In this thesis, we did confirm that the junctional zone is an important diagnostic marker for adenomyosis (**Chapters 3** and **4**) with irregularities and widening hereof showing a significant relationship with eventual histopathological adenomyosis diagnosis. Crucially however, we did not define a specific cut-off value for the JZ, finding instead that the *relative* irregularity and JZ thickness are of more importance than an absolute value.

One overarching aspect that should be addressed in the context of adenomyosis diagnosis in general is the reliability of the gold standard of adenomyosis diagnosis – histopathology. As mentioned prior, diagnostic criteria for adenomyosis on histology in fact can also vary, and can differ depending on the pathologist. The eye of the pathologist, much like that of the radiologist, is also often (at least in part) lead by the indication and query supplied by the treating gynaecologist when examining tissue. If the gynaecologist does not ask the pathologist directly to look for adenomyosis, or does not supply them with the right clinical context for them to suspect its possible presence there is a risk for underreporting the diagnosis. The very

same can be said for radiologists when assessing MRIs for adenomyosis (295). The problem of underreporting in MRI diagnosis was baldly present in the results seen in **Chapters 2** and **3**, where accuracy of initial radiologist reported diagnosis of adenomyosis was much lower at approximately 60% rather than 78-80% touted in the literature. These facts should serve as the impetus for further standardisation of diagnostic criteria across the board in adenomyosis, and highlight the road that still needs to be travelled for accurate multi-modal diagnosis.

- *Objective Two: Measuring uterine contractility, and how adenomyosis affects it – proof of JZ involvement?*

The potential physiological function of the JZ in both healthy and adenomyotic uteri was investigated in **Chapters 5**, **6** and **8** by way of the objective assessment of uterine contractility. The novel 2D TVUS speckle tracking method employed in these studies both provides novel insights into the intricacies of the uterine function, and proves that it tends to follow a standard pattern of behaviour throughout the natural menstrual cycle. Our method assesses uterine movement specifically in the junctional zone area between the endometrium and myometrium. **Chapter 8** goes further and supports that uterine abnormalities like adenomyosis may affect its integrity.

Previous studies have suggested potential mechanisms as to how adenomyosis may affect uterine contractility in the JZ, but these aberrant contractions have not been visualised as such until our study (8,294). Uterine movement in adenomyosis is potentially disrupted due to a possible combination of anatomical, inflammatory and physiological changes in the junctional zone. It is as of yet unclear if these changes are a cause or an effect of the adenomyosis present, but they undoubtedly have an effect on the structure and function of the uterus as a whole. Anatomical changes of the JZ occur due to the proliferation of smooth muscle cells around adenomyosis implants (as seen on histology). Where present, these muscle fibre bundles, due to their disorganised structure, are not able to contract in as coordinated a fashion as in normal myometrium (297). It stands to reason that the more of the JZ and myometrial tissue that is affected (by adenomyosis), the more uncoordinated and aberrant uterine contractions then become, leading to dysperistalsis. Once the integral structure of the JZ is affected, a vicious cycle ensues, leading to disruption of the basilar membrane between the

endometrium and myometrium and increase in intracellular space, which then facilitates further infiltration of adenomyosis into the myometrium (297). The dysperistalsis is also thought to lead to a chronic local inflammatory reaction (298). What is not yet clear however, and is not yet specifically investigated in our reported studies, is which threshold of JZ involvement will lead to objectifiable aberrant contraction activity, and if it is indeed the case that more severe adenomyosis shows equally severely affected contraction activity.

The two phases of the menstrual cycle showing the most significant differences in uterine contractility were the late follicular (or periovulatory) phase and the luteal phases. These two phases are arguably the most essential in terms of fertility, and aberrant uterine contractions here may well be an important aetiological mechanism behind sub- and in-fertility seen in adenomyosis patients.

Potential can also be seen for using the specific uterine contractile profile observed in adenomyosis patients versus normal patients to be further developed for clinical use as a diagnostic tool (for example in patients with symptoms suggestive of adenomyosis but with inconclusive imaging). We also hypothesise that uterine contractility most likely is affected by hormonal therapeutic agents used to treat adenomyosis symptoms. We then could take this method further and perhaps be able to assess changes in uterine contractility over time, and provide a therapeutic assessment tool. These applications are however still speculative - the speckle-tracking method employed is not yet useable for daily practice as additional validation and implementation studies should be carried out. As shown in **Chapter 5**, the method has proven to be reliable in terms of inter and intra-observer variability. Strides do still need to be made regarding the ease of the speckle tracking analysis, with real-time analysis during the TVUS procedure not yet feasible. Future (external) studies with larger populations should validate the results of the TVUS speckle-tracking method in the currently investigated patient groups.

The speckle tracking method could also be easily applied to other uterine abnormalities. As seen in **Chapter 7**, uterine leiomyoma's, endometritis, and congenital uterine anomalies are also most likely associated with aberrant

uterine contractility compared to healthy controls (albeit using different measurement methods). It remains to be researched how the uterine contractions associated with these different uterine abnormalities compare to those affected by adenomyosis versus healthy controls. We thus open up an avenue into the quantification of uterine contractility as an added marker of (ab)normal uterine function in the domain of gynaecological research and, perhaps one day, in gynaecological standard examinations.

- *Objectives Three and Four: Adenomyosis and its effect on fertility and obstetric outcomes*

Having established that adenomyosis can be diagnosed reliably and non-invasively, and that adenomyosis seems to affect a core element of uterine function by way of its effect on the uterine myometrial activity, we then assessed if this is indeed reflected in terms of reproductive outcomes.

When looking at adenomyosis-specific imaging markers, only the presence of myometrial cysts was significantly associated with worse IVF/ICSI outcomes in **Chapter 10**. A specific adenomyosis subtype as such could not be significantly associated with worse IVF/ICSI outcomes in our study. A variety of recent studies have suggested certain subtypes of adenomyosis to be associated with worse outcomes, but these studies are conflicting, with some suggesting an association with focal and others with diffuse adenomyosis. However, answering this query is not easy as there is still no uniform consensus on adenomyosis subtypes in general, and MRI diagnostic criteria in particular. This makes comparing and summarising the available literature difficult, as available studies often use different diagnostic criteria and categorisations. More attention is being given to the probable importance of adenomyosis and fertility outcomes. The hope is that, in time, a consensus will be reached as to not only which MRI diagnostic markers are most leading, but also what their clinical consequences could be. A consensus meeting with Delphi procedure of relevant experts is something which could aid and streamline this process. This has in fact already been done for adenomyosis ultrasound criteria (197), and for outcome reporting in uterus-sparing adenomyosis treatments (299), and paves the way for further strides in the field regarding adenomyosis on MRI and fertility outcome reporting.

In **Chapters 9** and **10,** results showed that it was women with both adenomyosis and endometriosis that had worse IVF/ICSI outcomes compared to women with only adenomyosis or endometriosis (also compared to male factor controls). As endometriosis and adenomyosis are often found together (50%-70% prevalence of combined disease in our study populations alone) it is difficult to separate the influence of adenomyosis from that of endometriosis. It is also still debated whether adenomyosis affecting the outer myometrium should be seen as external endometriosis invading the uterine wall, or as adenomyosis with a more atypical location. The challenge in answering this question is compounded by the fact that histologically both entities are similar (300). It is difficult, if not impossible, in the absence of hysterectomy, to absolutely exclude the presence of one disease in the presence of the other. Adenomyosis is in fact seen by many as an entity sharing physiological mechanisms with endometriosis (194,296,301), and should and could be seen as a subtype of endometriosis rather than a separate disease in and of itself. Having combined disease represents a patient population with a more widely affected reproductive system by the same disease process (ovarian function being affected by endometrioma's and uterine function by adenomyosis), and this logically leads to worse reproductive outcomes overall. It is also possible that these patients may exhibit characteristics that lead them to be more susceptible to severe endometriosis/adenomyosis in the first place (i.e. immune or genetic factors) which may in turn also affect their fertility. The two diseases should therefore be seen as part of a continuum or spectrum of disease, where their impact is assessed together.

We hence advocate that clinicians should be aware that when (sub-fertile) patients are diagnosed with one of the two diseases, conscious effort should be made to exclude or confirm that presence of either concomitant endometriosis or adenomyosis. Our results are in line with the theory that these patients constitute a group of with a high IVF/ICSI failure rate, and they should be appropriately counselled for this eventuality. Individualised (medical or surgery) treatment protocols could also be a possibility in this group. Research up to now has not yet convincingly shown which (pre-) ART treatment protocol is most effective in adenomyosis patients (302). Further prospective studies should be conducted, and specific guidelines for this group of patients do not yet exist.

Finally, the higher rate of adverse obstetric outcomes in adenomyosis patients as reported in **Chapter 11** should not be ignored. Further research of a prospective nature is warranted to confirm that adenomyosis patients could be seen as ones with high(er) risk pregnancies. If our findings are confirmed, one could argue for women with (suspicion) of adenomyosis qualifying for additional (foetal growth) monitoring during pregnancy for instance, or having an indication for aspirin use. In the Dutch context specifically, women with adenomyosis or endometriosis may also be advised against home births.

STRENGTHS AND LIMITATIONS

We are of the opinion that the research conducted as a part of this thesis has several strengths which make its results valuable and of interest for gynaecological practice. The majority of the studies conducted in the context of this thesis included patient data from a regional referral centre of expertise for endometriosis care, meaning access to a wide range of (complex) patient data and a larger than average eligible patient population. Additionally, regarding the diagnosis of adenomyosis, the developed prediction model was based on an exhaustive and expansive investigation of the available literature, using valid statistical methods. A preference was also given to objective measurements (excepting patient-reported symptoms) of adenomyosis on MRI, to make the diagnosis as reproducible and accurate as possible. The resultant prediction model then showed good performance in the patient population used, and shows promise for clinical applicability.

The broad scope of this thesis regarding not only the diagnosis but also the potential reproductive clinical impact of adenomyosis, means that we give a clear indication of the wide-ranging effect adenomyosis may have on the women that suffer from it. We also offer a new method for the assessment of how adenomyosis could affect uterine function in terms of an ultrasound-based quantitative assessment of uterine contractile function. We thus present an innovative and promising new measurement tool which has the potential to become a relevant assessment method of normal and abnormal uterine function in the context of fertility, but also symptomatology and treatment success.

- *Limitations*

The studies presented in this thesis admittedly have several limitations that should be considered when interpreting their results. First and foremost, the majority of chapters include retrospective analysis of patient data. This research design is classically considered more prone to forms of bias such as selection bias. Furthermore, there is a higher level of missing data as we are dependent on what has been reported in the patient files. MRI is not (always) part of standard work up procedures in (Dutch) endometriosis care, meaning that the conclusions drawn here based on MRI data cannot necessarily be extrapolated to the general (suspected) endometriosis patient visiting any outpatient clinic. In this vein, many of the patients included in the studies

reported in this thesis may constitute patients that have a long(er) history of complex combined disease, which may influence our results in general. Moreover, it is arguably not always necessary to conduct an MRI where adenomyosis is clearly able to be diagnosed on ultrasound. Which patient populations would ideally be suited to undergoing MRI diagnosis, and would most benefit from the clinical prediction model presented in this thesis, was not explored here.

Chapters 5, 6 and **8**, investigating uterine contractility in women with healthy and adenomyotic uteri, have relatively small study populations due to the use of a new analysis method of uterine contractility. This means that generalising the results garnered here, and the hypothesis as to their clinical relevance, to adenomyosis patients in general is still theoretical and needs to be validated. Similarly, the review in Chapter 5 also includes studies with small numbers and heterogenous study design, due to the topic of uterine contractility still being a developing field.

In **Chapters 9** and **10** looking into IVF/ICSI outcomes, it is a possibility that the control group may contain (some) women with undiagnosed adenomyosis or endometriosis. Almost none of the women in the control group underwent MRI due to there not being an indication; therefore, we cannot discard the possibility that some of these women may have had (mild) adenomyosis or endometriosis present. This could mean that the results could be an underestimation of the true difference in outcomes. It should also be noted that it is not standard procedure for women with suspected endometriosis or adenomyosis to undergo an MRI. This introduces the possibility that the women in the study groups might have had more severe symptoms and adds element of selection bias in our study group. Our results could then alternatively potentially overestimate the true effect of adenomyosis/endometriosis on IVF/ICSI outcomes. Another relevant aspect that should be considered is the inclusion of only patients undergoing their first, fresh embryo transfer. The fact that worse outcomes are seen at this stage of the treatment does not necessarily mean that these patients could not achieve pregnancy at all. In fact, some studies suggest that frozen embryo transfer in the natural cycle (303–305) may lead to more clinical pregnancies in endometriosis and/or adenomyosis patients, something which we did not investigate.

CONCLUSIONS

Overall, the results of this thesis support that adenomyosis can be diagnosed accurately on MRI, but also that it is important to do so as adenomyosis may well affect the whole reproductive process and function of the uterus. Uterine function first seems impaired in terms of fertility and obstetric outcomes, with a higher risk of miscarriage, infertility, and complications during pregnancy. In addition, the muscular function of the uterus as a whole is affected with aberrant contractile activity seen. Furthermore, we proffer that adenomyosis and endometriosis are part of a spectrum of the same disease, and patients with signs of both diseases are also the patients with the worst reproductive outcomes.

REFERENCES

1. Alcalde AM, Martínez-Zamora MÁ, Gracia M, Ros C, Rius M, Castelo-Branco C, et al. Assessment of Quality of Life, Sexual Quality of Life, and Pain Symptoms in Deep Infiltrating Endometriosis Patients With or Without Associated Adenomyosis and the Influence of a Flexible Extended Combined Oral Contraceptive Regimen: Results of a Prospective, Observational Study. J Sex Med. 2022;19(2).
2. Alcalde AM, Martínez-Zamora MÁ, Gracia M, Ros C, Rius M, Nicolás I, et al. Impact of Adenomyosis on Women's Psychological Health and Work Productivity: A Comparative Cross-Sectional Study. J Women's Heal. 2021;30(11).
3. Benagiano G, Brosens I, Carrara S. Adenomyosis: new knowledge is generating new treatment strategies. Womens Health (Lond Engl) [Internet]. 2009 May;5(3):297–311. Available from: https://www.ncbi.nlm.nih.gov/pubmed/19392615
4. Hasdemir PS, Farasat M, Aydin C, Ozyurt BC, Guvenal T, Pekindil G. The Role of Adenomyosis in the Pathogenesis of Preeclampsia. Geburtshilfe Frauenheilkd. 2016;
5. Protopapas A, Grimbizis G, Athanasiou S, Loutradis D. Adenomyosis: Disease, uterine aging process leading to symptoms, or both? Facts, Views Vis ObGyn [Internet]. 2020 Aug 5 [cited 2022 Jun 28];12(2):91. Available from: /pmc/articles/PMC7431194/
6. Peric H, Fraser IS. The symptomatology of adenomyosis. Best Pract Res Clin Obstet Gynaecol [Internet]. 2006 Aug;20(4):547–55. Available from: https://www.ncbi.nlm.nih.gov/pubmed/16515888
7. Struble J, Reid S, Bedaiwy MA. Adenomyosis: A Clinical Review of a Challenging Gynecologic Condition. Journal of Minimally Invasive Gynecology. 2016.
8. Leyendecker G, Bilgicyildirim A, Inacker M, Stalf T, Huppert P, Mall G, et al. Adenomyosis and endometriosis. Re-visiting their association and further insights into the mechanisms of auto-traumatisation. An MRI study. Arch Gynecol Obstet. 2015;
9. Leyendecker G, Wildt L, Mall G. The pathophysiology of endometriosis and adenomyosis: Tissue injury and repair. Arch Gynecol Obstet. 2009;
10. Guo SW. The Pathogenesis of Adenomyosis vis-à-vis Endometriosis. J Clin Med [Internet]. 2020 Feb 10 [cited 2020 Aug 3];9(2):485. Available from: https://www.mdpi.com/2077-0383/9/2/485
11. Marcellin L, Santulli P, Bourdon M, Maignien C, Campin L, Lafay-Pillet

MC, et al. Focal adenomyosis of the outer myometrium and deep infiltrating endometriosis severity. Fertil Steril. 2020;114(4).
12. Chapron C, Tosti C, Marcellin L, Bourdon M, Lafay-Pillet MC, Millischer AE, et al. Relationship between the magnetic resonance imaging appearance of adenomyosis and endometriosis phenotypes. Hum Reprod. 2017;
13. Brosens I, Gordts S, Habiba M, Benagiano G. Uterine Cystic Adenomyosis: A Disease of Younger Women. Vol. 28, Journal of Pediatric and Adolescent Gynecology. 2015.
14. Bourdon M, Oliveira J, Marcellin L, Santulli P, Bordonne C, Maitrot Mantelet L, et al. Adenomyosis of the inner and outer myometrium are associated with different clinical profiles. Hum Reprod. 2021;36(2).
15. Iwasawa T, Takahashi T, Maeda E, Ishiyama K, Takahashi S, Suganuma R, et al. Effects of localisation of uterine adenomyosis on outcome of in vitro fertilisation/intracytoplasmic sperm injection fresh and frozen-thawed embryo transfer cycles: a multicentre retrospective cohort study. Reprod Biol Endocrinol [Internet]. 2021 Dec 1 [cited 2022 Aug 3];19(1):1–11. Available from: https://rbej.biomedcentral.com/articles/10.1186/s12958-021-00764-7
16. Kobayashi H, Matsubara S. A Classification Proposal for Adenomyosis Based on Magnetic Resonance Imaging. Gynecol Obstet Invest. 2020;85(2):118–26.
17. Kishi Y, Suginami H, Kuramori R, Yabuta M, Suginami R, Taniguchi F. Four subtypes of adenomyosis assessed by magnetic resonance imaging and their specification. Am J Obstet Gynecol [Internet]. 2012 Aug;207(2):114.e1-7. Available from: https://www.ncbi.nlm.nih.gov/pubmed/22840719
18. Exacoustos C, Morosetti G, Conway F, Camilli S, Martire FG, Lazzeri L, et al. New Sonographic Classification of Adenomyosis: Do Type and Degree of Adenomyosis Correlate to Severity of Symptoms? J Minim Invasive Gynecol. 2020;27(6).
19. Chapron C, Vannuccini S, Santulli P, Abrão MS, Carmona F, Fraser IS, et al. Diagnosing adenomyosis: An integrated clinical and imaging approach. Hum Reprod Update. 2020;
20. Agarwal SK, Chapron C, Giudice LC, Laufer MR, Leyland N, Missmer SA, et al. Clinical diagnosis of endometriosis: a call to action. Am J Obstet Gynecol. 2019 Apr 1;220(4):354.e1-354.e12.
21. Staal AHJ, Van Der Zanden M, Nap AW. Diagnostic Delay of Endometriosis in the Netherlands. Gynecol Obstet Invest. 2016 Jul 1;81(4):321–4.
22. Tan N, McClure TD, Tarnay C, Johnson MT, Lu DS, Raman SS. Women

seeking second opinion for symptomatic uterine leiomyoma: role of comprehensive fibroid center. J Ther ultrasound [Internet]. 2014;2:3. Available from: https://www.ncbi.nlm.nih.gov/pubmed/25512867
23. Kassam Z, Petkovska I, Wang CL, Trinh AM, Kamaya A. Benign Gynecologic Conditions of the Uterus. Magn Reson Imaging Clin N Am [Internet]. 2017 Aug;25(3):577–600. Available from: https://www.ncbi.nlm.nih.gov/pubmed/28668161
24. Valentini AL, Speca S, Gui B, Soglia BG, Miccò M, Bonomo L. Adenomyosis: From the sign to the diagnosis. Imaging, diagnostic pitfalls and differential diagnosis: A pictorial review. Radiologia Medica. 2011.
25. Brucker SY, Huebner M, Wallwiener M, Stewart EA, Ebersoll S, Schoenfisch B, et al. Clinical characteristics indicating adenomyosis coexisting with leiomyomas: A retrospective, questionnaire-based study. Fertil Steril. 2014;101(1).
26. Bourdon M, Santulli P, Marcellin L, Maignien C, Maitrot-Mantelet L, Chapron C. Adenomyosis pathophysiology: An unresolved enigma. Vol. 50, Gynecologie Obstetrique Fertilite et Senologie. 2022.
27. Benagiano G, Brosens I. History of adenomyosis. Vol. 20, Best Practice and Research: Clinical Obstetrics and Gynaecology. 2006.
28. Van Den Bosch T, Dueholm M, Leone FPG, Valentin L, Rasmussen CK, Votino A, et al. Terms, definitions and measurements to describe sonographic features of myometrium and uterine masses: A consensus opinion from the Morphological Uterus Sonographic Assessment (MUSA) group. Ultrasound Obstet Gynecol. 2015;46(3).
29. Tellum T, Nygaard S, Lieng M. Noninvasive Diagnosis of Adenomyosis: A Structured Review and Meta-Analysis of Diagnostic Accuracy in Imaging. J Minim Invasive Gynecol [Internet]. 2019 Nov; Available from: https://www.ncbi.nlm.nih.gov/pubmed/31712162
30. Van den Bosch T, de Bruijn AM, de Leeuw RA, Dueholm M, Exacoustos C, Valentin L, et al. Sonographic classification and reporting system for diagnosing adenomyosis. Ultrasound Obstet Gynecol. 2019 May 1;53(5):576–82.
31. Dueholm M, Hjorth IMD. Structured imaging technique in the gynecologic office for the diagnosis of abnormal uterine bleeding. Best Pract Res Clin Obstet Gynaecol [Internet]. 2017 Apr;40:23–43. Available from: https://www.ncbi.nlm.nih.gov/pubmed/27818130
32. Munro MG. Classification Systems for Adenomyosis. J Minim Invasive Gynecol [Internet]. 2019 Nov; Available from: https://www.ncbi.nlm.nih.gov/pubmed/31785418
33. Agostinho L, Cruz R, Osório F, Alves J, Setúbal A, Guerra A. MRI for adenomyosis: a pictorial review. Insights Imaging [Internet]. 2017

Dec;8(6):549–56. Available from: https://www.ncbi.nlm.nih.gov/pubmed/28980163
34. Bazot M, Daraï E. Role of transvaginal sonography and magnetic resonance imaging in the diagnosis of uterine adenomyosis. Fertility and Sterility. 2018.
35. Dueholm M. Transvaginal ultrasound for diagnosis of adenomyosis: a review. Best Pract Res Clin Obstet Gynaecol [Internet]. 2006 Aug;20(4):569–82. Available from: https://www.ncbi.nlm.nih.gov/pubmed/16545618
36. Dueholm M, Lundorf E, Hansen ES, Sorensen JS, Ledertoug S, Olesen F. Magnetic resonance imaging and transvaginal ultrasonography for the diagnosis of adenomyosis. 2001;76(3):588-594. Available from: https://www.cochranelibrary.com/central/doi/10.1002/central/CN-00424865/full
37. Champaneria R, Abedin P, Daniels J, Balogun M, Khan KS. Ultrasound scan and magnetic resonance imaging for the diagnosis of adenomyosis: Systematic review comparing test accuracy. Acta Obstetricia et Gynecologica Scandinavica. 2010.
38. Mark AS, Hricak H, Heinrichs LW, Hendrickson MR, Winkler ML, Bachica JA, et al. Adenomyosis and leiomyoma: Differential diagnosis with MR imaging. Radiology. 1987;
39. Vitiello D, McCarthy S. Diagnostic imaging of myomas. Obstetrics and Gynecology Clinics of North America. 2006.
40. Exacoustos C, Manganaro L, Zupi E. Imaging for the evaluation of endometriosis and adenomyosis. Best Pract Res Clin Obstet Gynaecol. 2014;
41. Örs F, Lev-Toaff AS, Bergin D. Cystic adenomyoma: Transvaginal ultrasound and MRI findings. Anatol J Clin Investig. 2009;
42. Takeuchi M, Matsuzaki K. Adenomyosis: Usual and unusual imaging manifestations, pitfalls, and problem-solving MR imaging techniques. Radiographics. 2011;
43. Gordts S, Brosens JJ, Fusi L, Benagiano G, Brosens I. Uterine adenomyosis: A need for uniform terminology and consensus classification. Reprod Biomed Online. 2008;
44. Reinhold C, Tafazoli F, Wang L. Imaging features of adenomyosis. Hum Reprod Update [Internet]. 1998 Jul;4(4):337–49. Available from: https://www.ncbi.nlm.nih.gov/pubmed/9825849
45. Tellum T, Matic G V, Dormagen JB, Nygaard S, Viktil E, Qvigstad E, et al. Diagnosing adenomyosis with MRI: a prospective study revisiting the junctional zone thickness cutoff of 12 mm as a diagnostic marker. Eur Radiol [Internet]. 2019 Dec;29(12):6971–81. Available from: https://www.ncbi.nlm.nih.gov/pubmed/31264010

46. Meylaerts LJ, Wijnen L, Grieten M, Palmers Y, Ombelet W, Vandersteen M. Junctional zone thickness in young nulliparous women according to menstrual cycle and hormonal contraception use. Reprod Biomed Online. 2017;
47. Novellas S, Chassang M, Delotte J, Toullalan O, Chevallier A, Bouaziz J, et al. MRI characteristics of the uterine junctional zone: From normal to the diagnosis of adenomyosis. American Journal of Roentgenology. 2011.
48. Kido A, Togashi K, Koyama T, Yamaoka T, Fujiwara T, Fujii S. Diffusely enlarged uterus: evaluation with MR imaging. Radiographics [Internet]. 2003 Nov;23(6):1423–39. Available from: https://www.ncbi.nlm.nih.gov/pubmed/14615554
49. Gong C, Yang B, Shi Y, Liu Z, Wan L, Zhang H, et al. Factors influencing the ablative efficiency of high intensity focused ultrasound (HIFU) treatment for adenomyosis: A retrospective study. Int J Hyperth. 2016;
50. Mochimaru A, Aoki S, Oba MS, Kurasawa K, Takahashi T, Hirahara F. Adverse pregnancy outcomes associated with adenomyosis with uterine enlargement. J Obstet Gynaecol Res. 2015;
51. Kissler S, Zangos S, Kohl J, Wiegratz I, Rody A, Gätje R, et al. Duration of dysmenorrhoea and extent of adenomyosis visualised by magnetic resonance imaging. Eur J Obstet Gynecol Reprod Biol. 2008;
52. Keserci B, Duc NM. Magnetic resonance imaging features influencing high-intensity focused ultrasound ablation of adenomyosis with a nonperfused volume ratio of ≥90% as a measure of clinical treatment success: retrospective multivariate analysis. Int J Hyperth. 2018;
53. Froeling V, Scheurig-Muenkler C, Hamm B, Kroencke TJ. Uterine artery embolization to treat uterine adenomyosis with or without uterine leiomyomata: Results of symptom control and health-related quality of life 40 months after treatment. Cardiovasc Intervent Radiol. 2012;
54. Dashottar S, Singh AK, Debnath J, Muralidharan CG, Singh RK, Kumar S. Comparative analysis of changes in MR imaging of pre and post intrauterine progesterone implants in adenomyosis cases. Med journal, Armed Forces India [Internet]. 2015 Apr;71(2):145–51. Available from: https://www.ncbi.nlm.nih.gov/pubmed/25859077
55. Marnach ML, Laughlin-Tommaso SK. Evaluation and Management of Abnormal Uterine Bleeding. Mayo Clin Proc [Internet]. 2019;94(2):326–35. Available from: https://www.ncbi.nlm.nih.gov/pubmed/30711128
56. Pontis A, D'Alterio MN, Pirarba S, de Angelis C, Tinelli R, Angioni S. Adenomyosis: a systematic review of medical treatment. Gynecol Endocrinol [Internet]. 2016 Sep;32(9):696–700. Available from:

https://www.ncbi.nlm.nih.gov/pubmed/27379972
57. Streuli I, Dubuisson J, Santulli P, De Ziegler D, Batteux F, Chapron C. An update on the pharmacological management of adenomyosis. Vol. 15, Expert Opinion on Pharmacotherapy. 2014.
58. Benetti-Pinto CL, Mira TAA de, Yela DA, Teatin-Juliato CR, Brito LGO. Pharmacological Treatment for Symptomatic Adenomyosis: A Systematic Review. Rev Bras Ginecol Obstet [Internet]. 2019 Sep;41(9):564–74. Available from: https://www.ncbi.nlm.nih.gov/pubmed/31546278
59. Smeets AJ, Nijenhuis RJ, Boekkooi PF, Vervest HAM, Van Rooij WJ, Lohle PNM. Long-term follow-up of uterine artery embolization for symptomatic adenomyosis. Cardiovasc Intervent Radiol. 2012;
60. Nijenhuis RJ, Smeets AJ, Morpurgo M, Boekkooi PF, Reuwer PJHM, Smink M, et al. Uterine Artery Embolisation for Symptomatic Adenomyosis with Polyzene F-Coated Hydrogel Microspheres: Three-Year Clinical Follow-Up Using UFS–QoL Questionnaire. Cardiovasc Intervent Radiol. 2015;
61. Vannuccini S, Petraglia F. Recent advances in understanding and managing adenomyosis. F1000Research [Internet]. 2019;8. Available from: https://www.ncbi.nlm.nih.gov/pubmed/30918629
62. Osada H, Silber S, Kakinuma T, Nagaishi M, Kato K, Kato O. Surgical procedure to conserve the uterus for future pregnancy in patients suffering from massive adenomyosis. Reprod Biomed Online [Internet]. 2011 Jan;22(1):94–9. Available from: https://www.ncbi.nlm.nih.gov/pubmed/21118751
63. Benagiano G, Brosens I, Habiba M. Adenomyosis: A life-cycle approach. Reproductive BioMedicine Online. 2015.
64. Kunz G, Leyendecker G. Uterine peristaltic activity during the menstrual cycle: characterization, regulation, function and dysfunction. Reprod Biomed Online [Internet]. 2002;4:5–9. Available from: https://www.ncbi.nlm.nih.gov/pubmed/12470555
65. Kunz G, Noe M, Herbertz M, Leyendecker G. Uterine peristalsis during the follicular phase of the menstrual cycle: Effects of oestrogen, antioestrogen and oxytocin. Hum Reprod Update. 1998 Sep;4(5):647–54.
66. De Ziegler D, Bulletti C, Fanchin R, Epiney M, Brioschi PA. Contractility of the nonpregnant uterus: The follicular phase. In: Annals of the New York Academy of Sciences. 2001.
67. Bulletti C, De Ziegler D, Setti PL, Cicinelli E, Polli V, Flamigni C. The patterns of uterine contractility in normal menstruating women: From physiology to pathology. In: Annals of the New York Academy of Sciences. 2004.

68. Ijland MM, Evers JLH, Dunselman GAJ, Hoogland HJ. Subendometrial contractions in the nonpregnant uterus: An ultrasound study. Eur J Obstet Gynecol Reprod Biol. 1996;70(1):23–4.
69. Ijland MM, H Evers JL, J Dunselman GA, van Katwijk C, Lo Henk J Hoogland CR. Endometrial wavelike movements during the menstrual cycle. Am Soc Reprod Med. 1996;65(4).
70. van Gestel I, IJland MM, Evers JLH, Hoogland HJ. Complex endometrial wave-patterns in IVF. Fertil Steril. 2007;
71. Ijland MM, Hoogland HJ, Dunselman GAJ, Lo CR, Evers JLH. Endometrial wave direction switch and the outcome of in vitro fertilization. Fertil Steril. 1999 Mar;71(3):476–81.
72. Kunz G, Herbertz M, Beil D, Huppert P, Leyendecker G. Adenomyosis as a disorder of the early and late human reproductive period. Reprod Biomed Online [Internet]. 2007 Dec;15(6):681–5. Available from: https://www.ncbi.nlm.nih.gov/pubmed/18062865
73. Kido A, Koyama T, Kataoka M, Yamamoto A, Saga T, Turner R, et al. Physiological changes of the human uterine myometrium during menstrual cycle: Preliminary evaluation using BOLD MR imaging. J Magn Reson Imaging. 2007;
74. Shaked S, Jaffa AJ, Grisaru D, Elad D. Uterine peristalsis-induced stresses within the uterine wall may sprout adenomyosis. Biomech Model Mechanobiol. 2015;14(3).
75. Kissler S, Hamscho N, Zangos S, Wiegratz I, Schlichter S, Menzel C, et al. Uterotubal transport disorder in adenomyosis and endometriosis–a cause for infertility. BJOG. 2006 Aug;113(8):902–8.
76. Leyendecker G, Kunz G, Herbertz M, Beil D, Huppert P, Mall G, et al. Uterine peristaltic activity and the development of endometriosis. In: Annals of the New York Academy of Sciences. 2004.
77. Kissler S, Hamscho N, Zangos S, Wiegratz I, Schlichter S, Menzel C, et al. Uterotubal transport disorder in adenomyosis and endometriosis - A cause for infertility. BJOG An Int J Obstet Gynaecol. 2006;
78. Naftalin J, Hoo W, Pateman K, Mavrelos D, Holland T, Jurkovic D. How common is adenomyosis? A prospective study of prevalence using transvaginal ultrasound in a gynaecology clinic. Hum Reprod. 2012;27(12).
79. J. PA, I. O, J. M-S, L. C, C. I, J.A. G-V. High prevalence of adenomyosis in recurrent pregnancy loss and previous ART failure. Hum Reprod. 2014;
80. Puente JM, Fabris A, Patel J, Patel A, Cerrillo M, Requena A, et al. Adenomyosis in infertile women: Prevalence and the role of 3D ultrasound as a marker of severity of the disease. Reprod Biol Endocrinol. 2016;

81. Horton J, Sterrenburg M, Lane S, Maheshwari A, Li TC, Cheong Y. Reproductive, obstetric, and perinatal outcomes of women with adenomyosis and endometriosis: A systematic review and meta-analysis. Hum Reprod Update. 2019;
82. Campo S, Campo V, Benagiano G. Adenomyosis and infertility. Reprod Biomed Online. 2012 Jan;24(1):35–46.
83. Kuijsters NPM, Methorst WG, Kortenhorst MSQ, Rabotti C, Mischi M, Schoot BC. Uterine peristalsis and fertility: current knowledge and future perspectives: a review and meta-analysis. Reproductive BioMedicine Online. 2017.
84. Harada T, Khine YM, Kaponis A, Nikellis T, Decavalas G, Taniguchi F. The Impact of Adenomyosis on Women's Fertility. Obstet Gynecol Surv. 2016;
85. Vlahos NF, Theodoridis TD, Partsinevelos GA. Myomas and Adenomyosis: Impact on Reproductive Outcome. BioMed Research International. 2017.
86. Sharma S, Bathwal S, Agarwal N, Chattopadhyay R, Saha I, Chakravarty B. Does presence of adenomyosis affect reproductive outcome in IVF cycles? A retrospective analysis of 973 patients. Reprod Biomed Online. 2019;
87. Ballester M, Roman H, Mathieu E, Touleimat S, Belghiti J, Daraï E. Prior colorectal surgery for endometriosis-associated infertility improves ICSI-IVF outcomes: results from two expert centres. Eur J Obstet Gynecol Reprod Biol. 2017;
88. Younes G, Tulandi T. Effects of adenomyosis on in vitro fertilization treatment outcomes: a meta-analysis. Fertil Steril [Internet]. 2017;108(3):483-490.e3. Available from: https://www.ncbi.nlm.nih.gov/pubmed/28865548
89. Vercellini P, Consonni D, Dridi D, Bracco B, Frattaruolo MP, Somigliana E. Uterine adenomyosis and in vitro fertilization outcome: a systematic review and meta-analysis. Hum Reprod [Internet]. 2014 May;29(5):964–77. Available from: https://www.ncbi.nlm.nih.gov/pubmed/24622619
90. Benaglia L, Cardellicchio L, Paffoni A, Leonardi M, Faulisi S, Somigliana E. Adenomyosis does not influence pregnancy rate in women undergoing IVF. Fertil Steril. 2013;
91. Benaglia L, Cardellicchio L, Leonardi M, Faulisi S, Vercellini P, Paffoni A, et al. Asymptomatic adenomyosis and embryo implantation in IVF cycles. Reprod Biomed Online. 2014;
92. Costello MF, Lindsay K, McNally G. The effect of adenomyosis on in vitro fertilisation and intra-cytoplasmic sperm injection treatment outcome. Eur J Obstet Gynecol Reprod Biol. 2011;

93. Mijatovic V, Florijn E, Halim N, Schats R, Hompes P. Adenomyosis has no adverse effects on IVF/ICSI outcomes in women with endometriosis treated with long-term pituitary down-regulation before IVF/ICSI. Eur J Obstet Gynecol Reprod Biol. 2010;
94. Maheshwari A, Gurunath S, Fatima F, Bhattacharya S. Adenomyosis and subfertility: A systematic review of prevalence, diagnosis, treatment and fertility outcomes. Human Reproduction Update. 2012.
95. Meylaerts LJ, Wijnen L, Ombelet W, Bazot M, Vandersteen M. Uterine junctional zone thickness in infertile women evaluated by MRI. J Magn Reson Imaging. 2017;
96. Maged AM, Ramzy AM, Ghar MA, El Shenoufy H, Gad Allah SH, Wahba AH, et al. 3D ultrasound assessment of endometrial junctional zone anatomy as a predictor of the outcome of ICSI cycles. Eur J Obstet Gynecol Reprod Biol. 2017;
97. Kunz G, Beil D. Characterization of the uterine junctional zone prior to IVF/ICSI: An observational study. Arch Gynecol Obstet. 2010;
98. Maubon A, Faury A, Kapella M, Pouquet M, Piver P. Uterine junctional zone at magnetic resonance imaging: A predictor of in vitro fertilization implantation failure. J Obstet Gynaecol Res. 2010;
99. Piver P. Uterine factors limiting ART coverage. J Gynecol Obstet Biol la Reprod. 2005;
100. Kunz G, Beil D, Huppert P, Noe M, Kissler S, Leyendecker G. Adenomyosis in endometriosis - Prevalence and impact on fertility. Evidence from magnetic resonance imaging. Hum Reprod. 2005;
101. Tamura H, Kishi H, Kitade M, Asai-Sato M, Tanaka A, Murakami T, et al. Clinical outcomes of infertility treatment for women with adenomyosis in Japan. Reprod Med Biol. 2017;
102. Juang CM, Chou P, Yen MS, Twu NF, Horng HC, Hsu WL. Adenomyosis and risk of preterm delivery. BJOG An Int J Obstet Gynaecol. 2007;
103. Shin YJ, Kwak DW, Chung JH, Kim MY, Lee SW, Han YJ. The risk of preterm births among pregnant women with adenomyosis. J Ultrasound Med. 2018;
104. Harada T, Taniguchi F, Amano H, Kurozawa Y, Ideno Y, Hayashi K, et al. Adverse obstetrical outcomes for women with endometriosis and adenomyosis: A large cohort of the Japan Environment and Children's Study. PLoS One. 2019;
105. Scala C, Maggiore ULR, Racca A, Barra F, Vellone VG, Venturini PL, et al. Influence of adenomyosis on pregnancy and perinatal outcomes in women with endometriosis. Ultrasound Obstet Gynecol. 2018;
106. Exacoustos C, Lauriola I, Lazzeri L, De Felice G, Zupi E. Complications during pregnancy and delivery in women with untreated rectovaginal

deep infiltrating endometriosis. Fertil Steril. 2016;
107. Bruun MR, Arendt LH, Forman A, Ramlau-Hansen CH. Endometriosis and adenomyosis are associated with increased risk of preterm delivery and a small-for-gestational-age child: a systematic review and meta-analysis. Acta Obstetricia et Gynecologica Scandinavica. 2018.
108. Hashimoto A, Iriyama T, Sayama S, Nakayama T, Komatsu A, Miyauchi A, et al. Adenomyosis and adverse perinatal outcomes: increased risk of second trimester miscarriage, preeclampsia, and placental malposition. J Matern Neonatal Med. 2018;
109. Kim YM, Kim SH, Kim JH, Sung JH, Choi SJ, Oh S young, et al. Uterine wall thickness at the second trimester can predict subsequent preterm delivery in pregnancies with adenomyosis. Taiwan J Obstet Gynecol. 2019;
110. Yamaguchi A, Kyozuka H, Fujimori K, Hosoya M, Yasumura S, Yokoyama T, et al. Risk of preterm birth, low birthweight and small-for-gestational-age infants in pregnancies with adenomyosis: A cohort study of the Japan Environment and Children's Study. Acta Obstet Gynecol Scand. 2019;
111. Brosens I, Derwig I, Brosens J, Fusi L, Benagiano G, Pijnenborg R. The enigmatic uterine junctional zone: the missing link between reproductive disorders and major obstetrical disorders? Hum Reprod [Internet]. 2010 Mar;25(3):569–74. Available from: https://www.ncbi.nlm.nih.gov/pubmed/20085913
112. Brosens I, Pijnenborg R, Benagiano G. Defective myometrial spiral artery remodelling as a cause of major obstetrical syndromes in endometriosis and adenomyosis. Placenta [Internet]. 2013 Feb;34(2):100–5. Available from: https://www.ncbi.nlm.nih.gov/pubmed/23232321
113. Kang S, Turner DA, Foster GS, Rapoport MI, Spencer SA, Wang JZ. Adenomyosis: specificity of 5 mm as the maximum normal uterine junctional zone thickness in MR images. AJR Am J Roentgenol [Internet]. 1996 May;166(5):1145–50. Available from: https://www.ncbi.nlm.nih.gov/pubmed/8615259
114. Whiting PF, Rutjes AWS, Westwood ME, Mallett S, Deeks JJ, Reitsma JB, et al. Quadas-2: A revised tool for the quality assessment of diagnostic accuracy studies. Annals of Internal Medicine. 2011.
115. Freeman SC, Kerby CR, Patel A, Cooper NJ, Quinn T, Sutton AJ. Development of an interactive web-based tool to conduct and interrogate meta-analysis of diagnostic test accuracy studies: MetaDTA. BMC Med Res Methodol. 2019;
116. Moghadam R, Lathi RB, Shahmohamady B, Saberi NS, Nezhat CH, Nezhat F, et al. Predictive value of magnetic resonance imaging in

differentiating between leiomyoma and adenomyosis. JSLS J Soc Laparoendosc Surg [Internet]. 2006 Apr;10(2):216–9. Available from: https://www.ncbi.nlm.nih.gov/pubmed/16882423
117. Hamimi A. What are the most reliable signs for the radiologic diagnosis of uterine adenomyosis? An ultrasound and MRI prospective. Egypt J Radiol Nucl Med. 2015;
118. Badawy ME, Elkholi DGEY, Sherif MF, Hefedah MAE. Magnetic resonance imaging of uterovaginal lesions associated with female infertility. Middle East Fertil Soc J. 2015;
119. Tian T, Zhang G-F, Zhang H, Liu H. Intravoxel incoherent motion diffusion-weighted imaging in differentiating uterine fibroid from focal adenomyosis: initial results. Springerplus [Internet]. 2016;5:9. Available from: https://www.ncbi.nlm.nih.gov/pubmed/26759748
120. Ascher SM, Arnold LL, Patt RH, Schruefer JJ, Bagley AS, Semelka RCR, et al. Adenomyosis: Prospective comparison of MR imaging and transvaginal sonography. Radiology. 1994;
121. Phillips DR, Nathanson HG, Milim SJ, Haselkorn JS. Magnetic resonance imaging for diagnosing adenomyomata. J Am Assoc Gynecol Laparosc [Internet]. 1996 Feb;3(2):245–50. Available from: https://www.ncbi.nlm.nih.gov/pubmed/9050634
122. Dueholm M, Lundorf E, Hansen ES, Sorensen JS, Ledertoug S, Olesen F. Magnetic resonance imaging and transvaginal ultrasonography for the diagnosis of adenomyosis. Fertil Steril. 2001;
123. Andersson J, Khan Z, Gemzell-Danielsson K, Weaver A, Vaughan L, Stewart E. Vaginal Bromocriptine Improves Pain and Bleeding in Women with Adenomyosis. J Minim Invasive Gynecol. 2016;
124. Bazot M, Daraï E, De Givry SC, Boudghène F, Uzan S, Le Blanche AF. Fast breath-hold T2-weighted MR imaging reduces interobserver variability in the diagnosis of adenomyosis. Am J Roentgenol. 2003;
125. Bazot M, Cortez A, Darai E, Rouger J, Chopier J, Antoine JM, et al. Ultrasonography compared with magnetic resonance imaging for the diagnosis of adenomyosis: Correlation with histopathology. Hum Reprod. 2001;
126. Hricak H, Finck S, Honda G, Goranson H. MR imaging in the evaluation of benign uterine masses: Value of gadopentetate dimeglumine-enhanced T1-weighted images. Am J Roentgenol. 1992;
127. Masui T, Katayama M, Kobayashi S, Shimizu S, Nozaki A, Sakahara H. Pseudolesions related to uterine contraction: Characterization with multiphase-multisection T2-weighted MR imaging. Radiology. 2003;
128. Reinhold C, McCarthy S, Bret PM, Mehio A, Atri M, Zakarian R, et al. Diffuse adenomyosis: Comparison of endovaginal US and MR imaging with histopathologic correlation. Radiology. 1996;

129. Stamatopoulos CP, Mikos T, Grimbizis GF, Dimitriadis AS, Efstratiou I, Stamatopoulos P, et al. Value of Magnetic Resonance Imaging in Diagnosis of Adenomyosis and Myomas of the Uterus. J Minim Invasive Gynecol. 2012;
130. Bae SH, Kim MD, Kim GM, Lee SJ, Park S Il, Won JY, et al. Uterine Artery Embolization for Adenomyosis: Percentage of Necrosis Predicts Midterm Clinical Recurrence. J Vasc Interv Radiol. 2015;
131. Bourdon M, Santulli P, Chouzenoux S, Maignien C, Bailly K, Andrieu M, et al. The Disease Phenotype of Adenomyosis-Affected Women Correlates With Specific Serum Cytokine Profiles. Reprod Sci. 2019;
132. Bragheto AM, Caserta N, Bahamondes L, Petta CA. Effectiveness of the levonorgestrel-releasing intrauterine system in the treatment of adenomyosis diagnosed and monitored by magnetic resonance imaging. Contraception. 2007;
133. Bratby MJ, Walker WJ. Uterine artery embolisation for symptomatic adenomyosis-Mid-term results. Eur J Radiol. 2009;
134. Byun JY, Kim SE, Choi BG, Ko GY, Jung SE, Choi KH. Diffuse and focal adenomyosis: MR imaging findings. Radiographics. 1999;
135. Ferrari F, Arrigoni F, Miccoli A, Mascaretti S, Fascetti E, Mascaretti G, et al. Effectiveness of Magnetic Resonance-guided Focused Ultrasound Surgery (MRgFUS) in the uterine adenomyosis treatment: technical approach and MRI evaluation. Radiol Medica. 2016;
136. Fukunishi H, Funaki K, Sawada K, Yamaguchi K, Maeda T, Kaji Y. Early Results of Magnetic Resonance-guided Focused Ultrasound Surgery of Adenomyosis: Analysis of 20 Cases. J Minim Invasive Gynecol. 2008;
137. Imaoka I, Ascher SM, Sugimura K, Takahashi K, Li H, Cuomo F, et al. MR imaging of diffuse adenomyosis changes after GnRH analog therapy. J Magn Reson Imaging. 2002;
138. Jha RC, Takahama J, Imaoka I, Korangy SJ, Spies JB, Cooper C, et al. Adenomyosis: MRI of the uterus treated with uterine artery embolization. Am J Roentgenol. 2003;
139. Jha RC, Zanello PA, Ascher SM, Rajan S. Diffusion-weighted imaging (DWI) of adenomyosis and fibroids of the uterus. Abdom Imaging. 2014;
140. Jung DC, Kim MD, Oh YT, Won JY, Lee DY. Prediction of early response to uterine arterial embolisation of adenomyosis: Value of T2 signal intensity ratio of adenomyosis. Eur Radiol. 2012;
141. Keserci B, Duc NM. The role of T1 perfusion-based classification in predicting the outcome of magnetic resonance-guided high-intensity focused ultrasound treatment of adenomyosis. Int J Hyperthermia [Internet]. 2018;34(3):306–14. Available from:

https://www.ncbi.nlm.nih.gov/pubmed/28540825
142. Khandeparker MS, Jalkote S, Panpalia M, Nellore S, Mehta T, Ganesan K, et al. High-resolution magnetic resonance imaging in the detection of subtle nuances of uterine adenomyosis in infertility. Glob Reprod Heal. 2018;3(14).
143. Kilickesmez O, Bayramoglu S, Inci E, Cimilli T, Kayhan A. Quantitative diffusion-weighted magnetic resonance imaging of normal and diseased uterine zones. Acta radiol. 2009;
144. Kim KA, Yoon SW, Lee C, Seong SJ, Yoon BS, Park H. Short-term results of magnetic resonance imaging-guided focused ultrasound surgery for patients with adenomyosis: Symptomatic relief and pain reduction. Fertil Steril. 2011;
145. Kim MD, Won JW, Lee DY, Ahn CS. Uterine artery embolization for adenomyosis without fibroids. Clin Radiol. 2004;
146. Kitamura Y, Allison SJ, Jha RC, Spies JB, Flick PA, Ascher SM. MRI of adenomyosis: Changes with uterine artery embolization. Am J Roentgenol. 2006;
147. Krinsky G, DeCorato DR, Rofsky NM, Flyer M, Earls JP, Ambrosino M, et al. Rapid T2-weighted MR imaging of uterine leiomyoma and adenomyosis. Abdom Imaging. 1997;
148. Kunz G, Herbertz M, Beil D, Huppert G, Leyendecker G. Adenomyosis as a disorder of the early and late human reproductive period. Reprod Biomed Online. 2007;
149. Larsen SB, Lundorf E, Forman A, Dueholm M. Adenomyosis and junctional zone changes in patients with endometriosis. Eur J Obstet Gynecol Reprod Biol. 2011;
150. Lohle PNM, De Vries J, Klazen CAH, Boekkooi PF, Vervest HAM, Smeets AJ, et al. Uterine Artery Embolization for Symptomatic Adenomyosis with or without Uterine Leiomyomas with the Use of Calibrated Tris-acryl Gelatin Microspheres: Midterm Clinical and MR Imaging Follow-up. J Vasc Interv Radiol. 2007;
151. Marcellin L, Santulli P, Bortolato S, Morin C, Millischer AE, Borghese B, et al. Anterior Focal Adenomyosis and Bladder Deep Infiltrating Endometriosis: Is There a Link? J Minim Invasive Gynecol. 2018;
152. Parker JD, Leondires M, Sinaii N, Premkumar A, Nieman LK, Stratton P. Persistence of dysmenorrhea and nonmenstrual pain after optimal endometriosis surgery may indicate adenomyosis. Fertil Steril. 2006;
153. Park Y, Kim MD, Jung DC, Lee SJ, Kim G, Park S Il, et al. Can measurement of apparent diffusion coefficient before treatment predict the response to uterine artery embolization for adenomyosis? Eur Radiol. 2015;
154. Pelage J-P, Jacob D, Fazel A, Namur J, Laurent A, Rymer R, et al.

Midterm results of uterine artery embolization for symptomatic adenomyosis: initial experience. Radiology [Internet]. 2005 Mar;234(3):948–53. Available from: https://www.ncbi.nlm.nih.gov/pubmed/15681687
155. Sam M, Raubenheimer M, Manolea F, Aguilar H, Mathew RP, Patel VH, et al. Accuracy of findings in the diagnosis of uterine adenomyosis on ultrasound. Abdom Radiol (New York) [Internet]. 2019 Sep; Available from: https://www.ncbi.nlm.nih.gov/pubmed/31552462
156. Siskin GP, Tublin ME, Stainken BF, Dowling K, Dolen EG. Uterine artery embolization for the treatment of adenomyosis: Clinical response and evaluation with MR imaging. Am J Roentgenol. 2001;
157. Sofic A, Husic-Selimovic A, Carovac A, Jahic E, Smailbegovic V, Kupusovic J. The significance of MRI evaluation of the uterine Junctional zone in the early diagnosis of adenomyosis. Acta Inform Medica. 2016;
158. Song SE, Sung DJ, Park BJ, Kim MJ, Cho SB, Kim KA. MR imaging features of uterine adenomyomas. Abdom Imaging. 2011;
159. Stoelinga B, Hehenkamp WJK, Brölmann HAM, Huirne JAF. Real-time elastography for assessment of uterine disorders. Ultrasound Obstet Gynecol. 2014;
160. Streuli I, Santulli P, Chouzenoux S, Chapron C, Batteux F. Serum Osteopontin Levels Are Decreased in Focal Adenomyosis. Reprod Sci. 2017;
161. Verma SK, Lev-Toaff AS, Baltarowich OH, Bergin D, Verma M, Mitchell DG. Adenomyosis: Sonohysterography with MRI correlation. Am J Roentgenol. 2009;
162. Xia M, Jing Z, Zhi-Yu H, Jian-Ming C, Hong-Yu Z, Rui-Fang X, et al. Feasibility study on energy prediction of microwave ablation upon uterine adenomyosis and leiomyomas by MRI. Br J Radiol. 2014;
163. Gong C, Setzen R, Liu Z, Liu Y, Xie B, Aili A, et al. High intensity focused ultrasound treatment of adenomyosis: The relationship between the features of magnetic resonance imaging on T2 weighted images and the therapeutic efficacy. Eur J Radiol. 2017;
164. Guo Y, Duan H, Cheng J, Zhang Y. Gonadotrophin-releasing hormone agonist combined with high-intensity focused ultrasound ablation for adenomyosis: a clinical study. BJOG An Int J Obstet Gynaecol. 2017;
165. Lee JS, Hong GY, Lee KH, Kim TE. Changes in anti-müllerian hormone levels as a biomarker for ovarian reserve after ultrasound-guided high-intensity focused ultrasound treatment of adenomyosis and uterine fibroid. BJOG An Int J Obstet Gynaecol. 2017;
166. Long L, Chen J, Xiong Y, Zou M, Deng Y, Chen L, et al. Efficacy of high-intensity focused ultrasound ablation for adenomyosis therapy

and sexual life quality. Int J Clin Exp Med. 2015;
167. Xiong Y, Yue Y, Shui L, Orsi F, He J, Zhang L. Ultrasound-guided high-intensity focused ultrasound (USgHIFU) ablation for the treatment of patients with adenomyosis and prior abdominal surgical scars: A retrospective study. Int J Hyperth. 2015;
168. Zhang X, Li K, Xie B, He M, He J, Zhang L. Effective ablation therapy of adenomyosis with ultrasound-guided high-intensity focused ultrasound. Int J Gynecol Obstet. 2014;
169. Kim MD, Kim YM, Kim HC, Cho JH, Kang HG, Lee C, et al. Uterine artery embolization for symptomatic adenomyosis: A new technical development of the 1-2-3 protocol and predictive factors of MR imaging affecting outcomes. J Vasc Interv Radiol. 2011;
170. Wang S, Meng X, Dong Y. The evaluation of uterine artery embolization as a nonsurgical treatment option for adenomyosis. Int J Gynaecol Obstet [Internet]. 2016 May;133(2):202–5. Available from: https://www.ncbi.nlm.nih.gov/pubmed/26868068
171. Yang X, Zhang X, Lin B, Feng X, Aili A. Combined therapeutic effects of HIFU, GnRH-a and LNG-IUS for the treatment of severe adenomyosis. Int J Hyperth. 2019;
172. Yang Q, Zhang LH, Su J, Liu J. The utility of diffusion-weighted MR imaging in differentiation of uterine adenomyosis and leiomyoma. Eur J Radiol. 2011;
173. Takeuchi M, Matsuzaki K, Nishitani H. Diffusion-weighted magnetic resonance imaging of endometrial cancer: differentiation from benign endometrial lesions and preoperative assessment of myometrial invasion. Acta Radiol [Internet]. 2009 Oct;50(8):947–53. Available from: https://www.ncbi.nlm.nih.gov/pubmed/19724949
174. Thum MY, Saso S, Clancy N, Smith JR. Imaging of organ viability during uterine transplantation surgery. Hum Reprod. 2015;30:34–34.
175. He Y, Ding N, Li Y, Li Z, Xiang Y, Jin Z, et al. 3-T diffusion tensor imaging (DTI) of normal uterus in young and middle-aged females during the menstrual cycle: Evaluation of the cyclic changes of fractional anisotropy (FA) and apparent diffusion coefficient (ADC) values. Br J Radiol. 2015;
176. Nakagawa M, Nakaura T, Namimoto T, Iyama Y, Kidoh M, Hirata K, et al. A multiparametric MRI-based machine learning to distinguish between uterine sarcoma and benign leiomyoma: comparison with 18F-FDG PET/CT. Clin Radiol. 2019;
177. Fornazari VAV, Vayego SA, Szejnfeld D, Szejnfeld J, Goldman SM. Functional magnetic resonance imaging for clinical evaluation of uterine contractility. Einstein (Sao Paulo) [Internet]. 2018;16(1):eMD3863. Available from:

https://www.ncbi.nlm.nih.gov/pubmed/29694619
178. Nakashima A, Komesu I, Sakumoto T, Hamakawa H, Terada Y, Takayama H, et al. Study of uterine kinetics in nonpregnant women using cine-mode magnetic resonance imaging. Reprod Med Biol. 2019;
179. Bozkurt DK. Diffusion-weighted and diffusion-tensor imaging of normal and diseased uterus. World J Radiol. 2015;
180. Porpora MG, Vinci V, De Vito C, Migliara G, Anastasi E, Ticino A, et al. The Role of Magnetic Resonance Imaging-Diffusion Tensor Imaging in Predicting Pain Related to Endometriosis: A Preliminary Study. J Minim Invasive Gynecol [Internet]. 2018 Jun;25(4):661–9. Available from: https://www.ncbi.nlm.nih.gov/pubmed/29126882
181. Rees CO, Nederend J, Mischi M, van Vliet HAAM, Schoot BC. Objective measures of adenomyosis on MRI and their diagnostic accuracy—a systematic review & meta-analysis. Acta Obstetricia et Gynecologica Scandinavica. 2021.
182. Van den Bosch T, Van Schoubroeck D. Ultrasound diagnosis of endometriosis and adenomyosis: State of the art. Best Pract Res Clin Obstet Gynaecol [Internet]. 2018 Aug;51:16–24. Available from: https://www.ncbi.nlm.nih.gov/pubmed/29506961
183. Van den Bosch T, de Bruijn AM, de Leeuw RA, Dueholm M, Exacoustos C, Valentin L, et al. Sonographic classification and reporting system for diagnosing adenomyosis. Ultrasound in Obstetrics and Gynecology. 2019.
184. Tellum T, Nygaard S, Skovholt EK, Qvigstad E, Lieng M. Development of a clinical prediction model for diagnosing adenomyosis. Fertil Steril. 2018 Oct 1;110(5):957-964.e3.
185. Andres MP, Borrelli GM, Ribeiro J, Baracat EC, Abrão MS, Kho RM. Transvaginal Ultrasound for the Diagnosis of Adenomyosis: Systematic Review and Meta-Analysis. J Minim Invasive Gynecol. 2018 Feb 1;25(2):257–64.
186. Lazzeri L, Giovanni A Di, Exacoustos C, Tosti C, Pinzauti S, Malzoni M, et al. Preoperative and Postoperative Clinical and Transvaginal Ultrasound Findings of Adenomyosis in Patients With Deep Infiltrating Endometriosis.
187. Gonzales M, Accardo De Matos L, Orlando Da Costa Gonçalves M, Blasbalg R, João A, Dias J, et al. Patients with adenomyosis are more likely to have deep endometriosis.
188. Gambadauro P, Carli V, Hadlaczky G. Depressive symptoms among women with endometriosis: a systematic review and meta-analysis. Vol. 220, American Journal of Obstetrics and Gynecology. Mosby Inc.; 2019. p. 230–41.

189. Von Elm E, Altman DG, Egger M, Pocock SJ, Gøtzsche PC, Vandenbrouckef JP. The Strengthening the Reporting of Observational Studies in Epidemiology (STROBE) Statement: Guidelines for reporting observational studies. Bull World Health Organ. 2007 Nov;85(11):867–72.
190. Collins GS, Reitsma JB, Altman DG, Moons KGM. Transparent Reporting of a multivariable prediction model for Individual Prognosis Or Diagnosis (TRIPOD): the TRIPOD Statement. 2015; Available from: http://www.annals.org
191. Grant SW, Collins GS, Nashef SAM. Statistical Primer: developing and validating a risk prediction model †. Cardiothorac Surg [Internet]. 2018;54:203–11. Available from: https://academic.oup.com/ejcts/article/54/2/203/4993384
192. Rasmussen CK, Hansen ES, Dueholm M. Inter-rater agreement in the diagnosis of adenomyosis by 2- and 3-dimensional transvaginal ultrasonography. J Ultrasound Med [Internet]. 2019 Mar 1 [cited 2022 Aug 1];38(3):657–66. Available from: https://onlinelibrary.wiley.com/doi/full/10.1002/jum.14735
193. Habiba M, Gordts S, Bazot M, Brosens I, Benagiano G. Exploring the challenges for a new classification of adenomyosis. Reprod Biomed Online. 2020 Apr 1;40(4):569–81.
194. Aleksandrovych V, Basta P, Gil K. Current facts constituting an understanding of the nature of adenomyosis. Advances in Clinical and Experimental Medicine. 2019.
195. Hauth EAM, Jaeger HJ, Libera H, Lange S, Forsting M. MR imaging of the uterus and cervix in healthy women: determination of normal values. Eur Radiol [Internet]. 2007 Mar;17(3):734–42. Available from: https://www.ncbi.nlm.nih.gov/pubmed/16703306
196. Templeman C, Marshall SF, Ursin G, Horn-Ross PL, Clarke CA, Allen M, et al. Adenomyosis and endometriosis in the California Teachers Study. Fertil Steril. 2008 Aug 1;90(2):415–24.
197. Harmsen MJ, Van den Bosch T, Leeuw RA, Dueholm M, Exacoustos C, Valentin L, et al. Consensus on revised definitions of morphological uterus sonographic assessment (MUSA) features of adenomyosis: results of a modified Delphi procedure . Ultrasound Obstet Gynecol. 2021;
198. Harmsen MJ, Trommelen LM, de Leeuw RA, Tellum T, Juffermans LJM, Griffioen AW, et al. Multidisciplinary view on uterine junctional zone in uteri affected by adenomyosis: explaining discrepancies between MRI and transvaginal ultrasound images on a microscopic level . Ultrasound in Obstetrics & Gynecology. 2022. 0–3 p.
199. Tellum T, Munro MG. Classifications of Adenomyosis and Correlation

of Phenotypes in Imaging and Histopathology to Clinical Outcomes: a Review. Curr Obstet Gynecol Rep [Internet]. 2022;11(1):1–11. Available from: https://doi.org/10.1007/s13669-021-00320-5
200. Garcia L, Isaacson K. Adenomyosis: Review of the Literature. J Minim Invasive Gynecol. 2011 Jul 1;18(4):428–37.
201. Abbott JA. Adenomyosis and Abnormal Uterine Bleeding (AUB-A)-Pathogenesis, diagnosis, and management. Best Pract Res Clin Obstet Gynaecol [Internet]. 2017 Apr;40:68–81. Available from: https://www.ncbi.nlm.nih.gov/pubmed/27810281
202. Levy G, Dehaene A, Laurent N, Lernout M, Collinet P, Lucot J-P, et al. An update on adenomyosis. Diagn Interv Imaging [Internet]. 2013 Jan;94(1):3–25. Available from: https://www.ncbi.nlm.nih.gov/pubmed/23246186
203. Kishi Y, Shimada K, Fujii T, Uchiyama T, Yoshimoto C, Konishi N, et al. Phenotypic characterization of adenomyosis occurring at the inner and outer myometrium. PLoS One [Internet]. 2017;12(12):e0189522. Available from: https://www.ncbi.nlm.nih.gov/pubmed/29253010
204. Rees CO, van de Wiel M, Nederend J, Huppelschoten A, Mischi M, van Vliet HAAM, et al. Prediction of adenomyosis diagnosis based on MRI. J Endometr Uterine Disord. 2023 Jun 1;2:100028.
205. Donders ART, van der Heijden GJMG, Stijnen T, Moons KGM. Review: A gentle introduction to imputation of missing values. J Clin Epidemiol. 2006 Oct 1;59(10):1087–91.
206. Hajian-Tilaki K. Receiver operating characteristic (ROC) curve analysis for medical diagnostic test evaluation. Casp J Intern Med. 2013;4(2):627–35.
207. Ramspek CL, Jager KJ, Dekker FW, Zoccali C, Van DIepen M. External validation of prognostic models: what, why, how, when and where? Clin Kidney J [Internet]. 2021 Feb 3 [cited 2023 Nov 19];14(1):49–58. Available from: https://dx.doi.org/10.1093/ckj/sfaa188
208. Martínez-Conejero JA, Morgan M, Montesinos M, Fortuño S, Meseguer M, Simón C, et al. Adenomyosis does not affect implantation, but is associated with miscarriage in patients undergoing oocyte donation. Fertil Steril. 2011;
209. Eisenberg VH, Arbib N, Schiff E, Goldenberg M, Seidman DS, Soriano D. Sonographic Signs of Adenomyosis Are Prevalent in Women Undergoing Surgery for Endometriosis and May Suggest a Higher Risk of Infertility. Biomed Res Int. 2017;2017.
210. Vannuccini S, Tosti C, Carmona F, Huang SJ, Chapron C, Guo SW, et al. Pathogenesis of adenomyosis: an update on molecular mechanisms. Reproductive BioMedicine Online. 2017.
211. Maruyama S, Imanaka S, Nagayasu M, Kimura M, Kobayashi H.

Relationship between adenomyosis and endometriosis; Different phenotypes of a single disease? Vol. 253, European Journal of Obstetrics and Gynecology and Reproductive Biology. 2020.
212. Imaoka I, Wada A, Matsuo M, Yoshida M, Kitagaki H, Sugimura K. MR Imaging of Disorders Associated with Female Infertility: Use in Diagnosis, Treatment, and Management. Radiographics. 2003.
213. Vergouwe Y, Steyerberg EW, Eijkemans MJC, Habbema JDF. Substantial effective sample sizes were required for external validation studies of predictive logistic regression models. J Clin Epidemiol. 2005 May 1;58(5):475–83.
214. He YL, Ding N, Li Y, Li Z, Xiang Y, Jin ZY, et al. Cyclic changes of the junctional zone on 3 T MRI images in young and middle-aged females during the menstrual cycle. Clin Radiol. 2016 Apr 1;71(4):341–8.
215. Fanchin R, Ayoubi JM. Uterine dynamics: Impacton the human reproduction process. Reproductive BioMedicine Online. 2009.
216. van Gestel I, Ijland MM, Hoogland HJ, Evers JLH. Endometrial wave-like activity in the non-pregnant uterus. Human Reproduction Update. 2003.
217. Bulletti C, De Ziegler D. Uterine contractility and embryo implantation. Current Opinion in Obstetrics and Gynecology. 2006.
218. Kissler S, Zangos S, Vogl TJ, Hamscho N, Gruenwald F, Kohl J, et al. Impaired utero-tubal sperm transport in adenomyosis and endometriosis—a cause for infertility. Int Congr Ser. 2004;
219. Kissler S, Zangos S, Wiegratz I, Kohl J, Rody A, Gaetje R, et al. Utero-tubal sperm transport and its impairment in endometriosis and adenomyosis. In: Annals of the New York Academy of Sciences. 2007.
220. Kuijsters NPM, Sammali F, Rabotti C, Huang Y, Mischi M, Schoot BC. Visual inspection of transvaginal ultrasound videos to characterize uterine peristalsis: an inter-observer agreement study. J Ultrasound. 2020;
221. Sammali F, Kuijsters NPM, Huang Y, Blank C, Rabotti C, Schoot BC, et al. Dedicated Ultrasound Speckle Tracking for Quantitative Analysis of Uterine Motion Outside Pregnancy. IEEE Trans Ultrason Ferroelectr Freq Control. 2019;
222. Huang Y, Sammali F, Kuijsters NPM, Blank C, Schoot BC, Mischi M. Quantitative Motion Analysis of the Uterus by Optical Flow and Two-dimensional Strain Mapping. In: MeMeA 2018 - 2018 IEEE International Symposium on Medical Measurements and Applications, Proceedings. 2018.
223. Sammali F, Blank C, Xu L, Huang Y, Kuijsters NPM, Schoot BC, et al. Experimental setup for objective evaluation of uterine motion analysis by ultrasound speckle tracking. Biomed Phys Eng Express. 2018;

224. Sammali F, Blank C, Huang Y, Kuijsters NPM, Rabotti C, Schoot BC, et al. Quantitative Analysis of Uterine Motion Outside Pregnancy by Dedicated Ultrasound Speckle Tracking. In: IEEE International Ultrasonics Symposium, IUS. 2018.
225. Sammali F, Blank C, Bakkes TGH, Huang Y, Rabotti C, Schoot BC, et al. Multi-Modal Uterine-Activity Measurements for Prediction of Embryo Implantation by Machine Learning. IEEE Access. 2021;9:47096–111.
226. Blank C, Sammali F, Kuijsters N, Huang Y, Rabotti C, de Sutter P, et al. Assessment of uterine activity during IVF by quantitative ultrasound imaging: a pilot study [Internet]. Reproductive BioMedicine Online. 2020 [cited 2021 Oct 19]. p. 1045–53. Available from: https://www.sciencedirect.com/science/article/pii/S1472648320304399?casa_token=xEVdHOVluqMAAAAA:8nsb2PSMYxuUeR2w1rxl_W0OZwYZVprwug1uz8r3QUKcWQoY2FgH8kL5AIBDgBUE1wHWsSYFId0
227. Sammali F, Blank C, Bakkes THGF, Huang Y, Rabotti C, Schoot BC, et al. Prediction of embryo implantation by machine learning based on ultrasound strain imaging. In: IEEE International Ultrasonics Symposium, IUS. 2019.
228. Huang Y, Sammali F, Blank C, Kuijsters N, Rabotti C, Schoot BC, et al. Quantitative Ultrasound Imaging and Characterization of Uterine Peristaltic Waves. In: IEEE International Ultrasonics Symposium, IUS. 2018.
229. Huang Y, Rees C, Sammali F, Blank C, Schoot D, Mischi M. Characterization of uterine peristaltic waves by ultrasound strain analysis; Characterization of uterine peristaltic waves by ultrasound strain analysis. IEEE Trans Ultrason Ferroelectr Freq Control [Internet]. 2022;PP. Available from: http://www.ieee.org/publications_standards/publications/rights/index.html
230. Hu LY, Fan HY. Inversion formula and Parseval theorem for complex continuous wavelet transforms studied by entangled state representation. Chinese Phys B. 2010;19(7).
231. Kuijsters NPM, Methorst WG, Kortenhorst MSQ, Rabotti C, Mischi M, Schoot BC. Uterine peristalsis and fertility: current knowledge and future perspectives: a review and meta-analysis. Reprod Biomed Online. 2017 Jul 1;35(1):50–71.
232. Leyendecker, Kunz G, Wildt L, Beil D, Deininger H. Uterine hyperperistalsis and dysperistalsis as dysfunctions of the mechanism of rapid sperm transport in patients with endometriosis and infertility [Internet]. Vol. 11, Human Reproduction. 1996. Available from:

https://academic.oup.com/humrep/article/11/7/1542/636603
233. Kuijsters NPM, Methorst WG, Kortenhorst MSQ, Rabotti C, Mischi M, Schoot BC. Uterine peristalsis and fertility: current knowledge and future perspectives: a review and meta-analysis. Reprod Biomed Online. 2017 Jul 1;35(1):50–71.
234. Martinez-Gaudio M, Yoshida T, Bengtsson LP. Propagated and nonpropagated myometrial contractions in normal menstrual cycles. Am J Obstet Gynecol. 1973;
235. Togashi K. Uterine Contractility Evaluated on Cine Magnetic Resonance Imaging. Ann N Y Acad Sci [Internet]. 2007 Apr 1 [cited 2022 Jun 15];1101(1):62–71. Available from: https://onlinelibrary.wiley.com/doi/full/10.1196/annals.1389.030
236. Zhang Y, Qian J, Zaltzhendler O, Bshara M, Jaffa AJ, Grisaru D, et al. Analysis of *in vivo* uterine peristalsis in the non-pregnant female mouse. Interface Focus. 2019 Aug;9(4):20180082.
237. Bulletti C, De Ziegler D, Polli V, Diotallevi L, Del Ferro E, Flamigni C. Uterine contractility during the menstrual cycle. Hum Reprod. 2000;15(SUPPL. 1):81–9.
238. Oki T, Douchi T, Maruta K, Nakamura S, Nagata Y. Changes in endometrial wave-like movements in accordance with the phases of menstrual cycle. J Obstet Gynaecol Res. 2002 Jun;28(3):176–81.
239. Pritts EA, Parker WH, Olive DL. Fibroids and infertility: an updated systematic review of the evidence. Fertil Steril. 2009 Apr 1;91(4):1215–23.
240. Schenken RS, Guzick DS. Revised endometriosis classification: 1996. Fertil Steril. 1997;67(5):815–6.
241. Venetis CA, Papadopoulos SP, Campo R, Gordts S, Tarlatzis BC, Grimbizis GF. Clinical implications of congenital uterine anomalies: a meta-analysis of comparative studies. Reprod Biomed Online. 2014 Dec 1;29(6):665–83.
242. Taylor E, Gomel V. The uterus and fertility. Fertil Steril. 2008 Jan 1;89(1):1–16.
243. Rayyan – Intelligent Systematic Review - [Internet]. [cited 2022 Jun 15]. Available from: https://www.rayyan.ai/
244. Downs SH, Black N. The feasibility of creating a checklist for the assessment of the methodological quality both of randomised and non-randomised studies of health care interventions. J Epidemiol Community Heal [Internet]. 1998;52:377–84. Available from: http://jech.bmj.com/
245. Kido A, Togashi K, Nishino M, Miyake K, Koyama T, Fujimoto R, et al. Cine MR imaging of uterine peristalsis in patients with endometriosis. Eur Radiol. 2007;

246. Kido A, Ascher SM, Hahn W, Kishimoto K, Kashitani N, Jha RC, et al. 3 T MRI uterine peristalsis: Comparison of symptomatic fibroid patients versus controls. Clin Radiol. 2014 May 1;69(5):468–72.
247. Kido A, Ascher SM, Kishimoto K, Hahn W, Jha RC, Togashi K, et al. Comparison of Uterine Peristalsis Before and After Uterine Artery Embolization at 3-T MRI. http://dx.doi.org/102214/AJR105349 [Internet]. 2012 Nov 23 [cited 2022 Jun 15];196(6):1431–5. Available from: www.ajronline.org
248. Yoshino O, Nishii O, Osuga Y, Asada H, Okuda S, Orisaka M, et al. Myomectomy Decreases Abnormal Uterine Peristalsis and Increases Pregnancy Rate. J Minim Invasive Gynecol. 2012 Jan 1;19(1):63–7.
249. Yoshino O, Hayashi T, Osuga Y, Orisaka M, Asada H, Okuda S, et al. Decreased pregnancy rate is linked to abnormal uterine peristalsis caused by intramural fibroids. Hum Reprod [Internet]. 2010; Available from: https://academic.oup.com/humrep/article/25/10/2475/2385697
250. Nishino M, Togashi K, Nakai A, Hayakawa K, Kanao S, Iwasaku K, et al. Uterine contractions evaluated on cine MR imaging in patients with uterine leiomyomas. Eur J Radiol. 2005 Jan 1;53(1):142–6.
251. Adami Vayego Fornazari V, Szejnfeld D, Szejnfeld J, dio Emilio Bonduki C, Adami Vayego S, Menasce Goldman S, et al. Evaluation of Uterine Contractility by Magnetic Resonance Imaging in Women Undergoing Embolization of Uterine Fibroids. Cardiovasc Interv Radiol. 2018;42:186–94.
252. Orisaka M, Kurokawa T, Shukunami KI, Orisaka S, Fukuda MT, Shinagawa A, et al. A comparison of uterine peristalsis in women with normal uteri and uterine leiomyoma by cine magnetic resonance imaging. Eur J Obstet Gynecol Reprod Biol. 2007 Nov;135(1):111–5.
253. Bulletti C, De Ziegler D, Rossi S, Polli V, Massoneau M, Rossi E, et al. Abnormal uterine contractility in nonpregnant women. Ann N Y Acad Sci. 1997;828:223–9.
254. Bulletti C, Ziegler D De, Polli V, Del Ferro E, Palini S, Flamigni C. Characteristics of uterine contractility during menses in women with mild to moderate endometriosis. Fertil Steril. 2002 Jun 1;77(6):1156–61.
255. Szamatowicz J, Laudaǹski T, Bulkszas B, Åkerlund M. Fibromyomas and uterine contractions. Acta Obstet Gynecol Scand [Internet]. 1997 Oct 1 [cited 2022 Jun 15];76(10):973–6. Available from: https://onlinelibrary.wiley.com/doi/full/10.3109/00016349709034912
256. Oliva GC, Fratoni A, Genova M, Romanini C. Uterine motility in patients with bicornuate uterus. Int J Gynecol Obstet [Internet]. 1992

Jan 1 [cited 2022 Jun 15];37(1):7–12. Available from: https://onlinelibrary.wiley.com/doi/full/10.1016/0020-7292%2892%2990971-K
257. Pinto V, Matteo M, Tinelli R, Mitola PC, De Ziegler D, Cicinelli E. Altered uterine contractility in women with chronic endometritis. Fertil Steril. 2015 Apr 1;103(4):1049–52.
258. Qu Y, Xiao Z, Liu LA, Lv FF, Sheng BG, Li J, et al. Uterine Peristalsis Before and After Ultrasound-Guided High-Intensify Focused Ultrasound (USgHIFU) Treatment for Symptomatic Uterine Fibroids. 2019; Available from: https://www.medscimonit.com/abstract/index/idArt/913392
259. Hunt S, Abdallah KS, Ng E, Rombauts L, Vollenhoven B, Mol BW. Impairment of Uterine Contractility Is Associated with Unexplained Infertility. Semin Reprod Med [Internet]. 2020 Jan 1 [cited 2022 Jun 15];38(1):61–73. Available from: http://www.thieme-connect.com/products/ejournals/html/10.1055/s-0040-1716409
260. Sammali F, Kuijsters NPM, Huang Y, Blank C, Rabotti C, Schoot BC, et al. Dedicated Ultrasound Speckle Tracking for Quantitative Analysis of Uterine Motion Outside Pregnancy. IEEE Trans Ultrason Ferroelectr Freq Control. 2019 Mar 1;66(3):581–90.
261. Bulletti C, De Ziegler D. Uterine contractility and embryo implantation. Curr Opin Obstet Gynecol. 2006 Aug;18(4):473–84.
262. Kunz G, Noe M, Herbertz M, Leyendecker G. Uterine peristalsis during the follicular phase of the menstrual cycle: Effects of oestrogen, antioestrogen and oxytocin. In: Human Reproduction Update. 1998.
263. Rees CO, de Boer A, Huang Y, Wessels B, Blank C, Kuijsters N, et al. Uterine contractile activity in healthy women throughout the menstrual cycle measured using a novel quantitative two-dimensional transvaginal ultrasound speckle tracking method. Reprod Biomed Online. 2023 Jan 1;46(1):115–22.
264. Huang Y, Rees C, Sammali F, Blank C, Schoot D, Mischi M. Characterization of Uterine Peristaltic Waves by Ultrasound Strain Analysis. IEEE Trans Ultrason Ferroelectr Freq Control. 2022 Jun 1;69(6):2050–60.
265. Habiba M, Benagiano G, Guo S-W. An Appraisal of the Tissue Injury and Repair (TIAR) Theory on the Pathogenesis of Endometriosis and Adenomyosis. Biomolecules. 2023 Jun 11;13(6):975.
266. de Boer A, Rees CO, Mischi M, Van Vliet H, Huirne J, Schoot BC. The influence of uterine abnormalities on uterine peristalsis in the non-pregnant uterus: A systematic review. J Endometr Uterine Disord [Internet]. 2023;3(June):100038. Available from: https://doi.org/10.1016/j.jeud.2023.100038

267. Sammali F, Kuijsters NPM, Huang Y, Blank C, Rabotti C, Schoot BC, et al. Dedicated Ultrasound Speckle Tracking for Quantitative Analysis of Uterine Motion Outside Pregnancy. IEEE Trans Ultrason Ferroelectr Freq Control. 2019 Mar 1;66(3):581–90.
268. Lymperi S, Neofytou E, Vaitsopoulou C, Bazioti MG, Kalyvianaki K, Chatzimeletiou K, et al. Oxytocin preprotein and oxytocin receptor mRNA expression is altered in semen samples with abnormal semen parameters. Reprod Biomed Online. 2023 Feb 1;46(2):363–70.
269. Guo SW, Mao X, Ma Q, Liu X. Dysmenorrhea and its severity are associated with increased uterine contractility and overexpression of oxytocin receptor (OTR) in women with symptomatic adenomyosis. Fertil Steril. 2013 Jan 1;99(1):231–40.
270. Zhang Y, Yu P, Sun F, Li TC, Cheng JM, Duan H. Expression of oxytocin receptors in the uterine junctional zone in women with adenomyosis. Acta Obstet Gynecol Scand. 2015;94(4):412–8.
271. Mehasseb MK, Panchal R, Taylor AH, Brown L, Bell SC, Habiba M. Estrogen and progesterone receptor isoform distribution through the menstrual cycle in uteri with and without adenomyosis. Fertil Steril. 2011 Jun 1;95(7):2228-2235.e1.
272. Macer ML, Taylor HS. Endometriosis and Infertility. A Review of the Pathogenesis and Treatment of Endometriosis-associated Infertility. Obstetrics and Gynecology Clinics of North America. 2012.
273. Sammali F, Blank C, Xu L, Huang Y, Kuijsters NPM, Schoot BC, et al. Experimental setup for objective evaluation of uterine motion analysis by ultrasound speckle tracking. Biomed Phys Eng Express. 2018 Mar 13;4(3).
274. Higgins C, Fernandes H, Da Silva Costa F, Martins WP, Vollenhoven B, Healey M. The impact of adenomyosis on IVF outcomes: a prospective cohort study. Hum Reprod Open. 2021;
275. Buggio L, Monti E, Gattei U, Dridi D, Vercellini P. Adenomyosis: Fertility and obstetric outcome. A comprehensive literature review. Minerva Ginecologica. 2018.
276. Brosens J, Verhoeven H, Campo R, Gianaroli L, Gordts S, Hazekamp J, et al. High endometrial aromatase P450 mRNA expression is associated with poor IVF outcome. Hum Reprod. 2004;
277. Tremellen KP, Russell P. The distribution of immune cells and macrophages in the endometrium of women with recurrent reproductive failure. II: adenomyosis and macrophages. J Reprod Immunol [Internet]. 2012 Jan;93(1):58–63. Available from: https://www.ncbi.nlm.nih.gov/pubmed/22209314
278. Campo S, Campo V, Benagiano G. Adenomyosis and infertility. Reproductive BioMedicine Online. 2012.

279. van der Houwen LEE, Lier MCI, Schreurs AMF, van Wely M, Hompes PGA, Cantineau AEP, et al. Continuous oral contraceptives versus long-term pituitary desensitization prior to IVF/ICSI in moderate to severe endometriosis: study protocol of a non-inferiority randomized controlled trial. Hum Reprod Open. 2019;
280. Graziano A, Lo Monte G, Piva I, Caserta D, Karner M, Engl B, et al. Diagnostic findings in adenomyosis: a pictorial review on the major concerns. Eur Rev Med Pharmacol Sci [Internet]. 2015 Apr;19(7):1146–54. Available from: https://www.ncbi.nlm.nih.gov/pubmed/25912572
281. Nirgianakis K, Kalaitzopoulos DR, Schwartz ASK, Spaanderman M, Kramer BW, Mueller MD, et al. Fertility, pregnancy and neonatal outcomes of patients with adenomyosis: a systematic review and meta-analysis. Reprod Biomed Online. 2021;42(1):185–206.
282. Bourdon M, Santulli P, Bordonne C, Millisher AE, Maitrot-Mantelet L, Maignien C, et al. Presence of adenomyosis at MRI reduces live birth rates in ART cycles for endometriosis. Hum Reprod [Internet]. 2022 Jun 30 [cited 2022 Aug 3];37(7):1470–9. Available from: https://academic.oup.com/humrep/article/37/7/1470/6573229
283. Rees CO, Rupert IAM, Nederend J, Consten D, Mischi M, A.A.M. van Vliet H, et al. Women with combined adenomyosis and endometriosis on MRI have worse IVF/ICSI outcomes compared to adenomyosis and endometriosis alone: A matched retrospective cohort study. Eur J Obstet Gynecol Reprod Biol. 2022 Apr;271:223–34.
284. Coccia ME, Rizzello F, Mariani G, Bulletti C, Palagiano A, Scarselli G. Impact of endometriosis on IVF-ET cycles in young women: a stage dependent interference. Acta Obstet Gynecol Scand. 2011;
285. Brosens JJ, de Souza NM, Barker FG. Uterine junctional zone: function and disease. Lancet (London, England) [Internet]. 1995 Aug;346(8974):558–60. Available from: https://www.ncbi.nlm.nih.gov/pubmed/7658784
286. Dakhly DMR, Abdel Moety GAF, Saber W, Gad Allah SH, Hashem AT, Abdel Salam LOE. Accuracy of Hysteroscopic Endomyometrial Biopsy in Diagnosis of Adenomyosis. J Minim Invasive Gynecol. 2016 Mar 1;23(3):364–71.
287. Pinzauti S, Lazzeri L, Tosti C, Centini G, Orlandini C, Luisi S, et al. Transvaginal sonographic features of diffuse adenomyosis in 18-30-year-old nulligravid women without endometriosis: association with symptoms. Ultrasound Obs Gynecol [Internet]. 2015 [cited 2022 Nov 14];46:730–6. Available from: https://obgyn.onlinelibrary.wiley.com/doi/10.1002/uog.14834
288. Loring M, Chen TY, Isaacson KB. A Systematic Review of

Adenomyosis: It Is Time to Reassess What We Thought We Knew about the Disease. J Minim Invasive Gynecol. 2021 Mar 1;28(3):644–55.
289. Leyendecker G, Kunz G, Kissler S, Wildt L. Adenomyosis and reproduction. Best Practice and Research: Clinical Obstetrics and Gynaecology. 2006.
290. Berlanda N, Donati A, Fedele F, Lepri M, Vercellini P. Adenomyosis and Obstetrical Outcome: a Narrative Mini-Review of the Latest Evidence. Curr Obstet Gynecol Reports 2022 [Internet]. 2022 Apr 8 [cited 2022 Aug 3];1–12. Available from: https://link.springer.com/article/10.1007/s13669-021-00316-1
291. Harada T, Taniguchi F, Harada T. Increased risk of obstetric complications in patients with adenomyosis: A narrative literature review. Reprod Med Biol [Internet]. 2022 Jan 1 [cited 2022 Aug 3];21(1):e12473. Available from: https://onlinelibrary.wiley.com/doi/full/10.1002/rmb2.12473
292. Zhang M, Bazot M, Tsatoumas M, Munro MG, Reinhold C. MRI of Adenomyosis: Where Are We Today? https://doi.org/101177/08465371221114197 [Internet]. 2022 Jul 20 [cited 2023 Nov 21];74(1):58–68. Available from: https://journals.sagepub.com/doi/abs/10.1177/08465371221114197
293. Guo SW, Benagiano G, Bazot M. In Search of an Imaging Classification of Adenomyosis: A Role for Elastography? J Clin Med 2023, Vol 12, Page 287 [Internet]. 2022 Dec 30 [cited 2023 Dec 17];12(1):287. Available from: https://www.mdpi.com/2077-0383/12/1/287/htm
294. Chou SY, Chan C, Lee YC, Yu TN, Tzeng CR, Chen CH. Evaluation of adenomyosis after gonadotrophin-releasing hormone agonist therapy using ultrasound post-processing imaging: a pilot study. J Int Med Res [Internet]. 2020 Jun 1 [cited 2023 Dec 17];48(6). Available from: https://journals.sagepub.com/doi/full/10.1177/0300060520920056
295. Zanolli NC, Cline BC, Befera NT, Martin JG. Diagnostic accuracy of clinically reported adenomyosis on pelvic ultrasound and MRI compared to surgical pathology. Clin Imaging. 2022;82.
296. Leyendecker G, Kunz G, Wildt L, Beil D, Deininger H. Uterine hyperperistalsis and dysperistalsis as dysfunctions of the mechanism of rapid sperm transport in patients with endometriosis and infertility. Hum Reprod. 1996;11(7):1542–51.
297. Xie T, Xu X, Yang Y, Wu C, Liu X, Zhou L, et al. The Role of Abnormal Uterine Junction Zone in the Occurrence and Development of Adenomyosis. Reprod Sci [Internet]. 2022 Oct 1 [cited 2023 Dec

12];29(10):2719–30. Available from: https://link.springer.com/article/10.1007/s43032-021-00684-2
298. Barbanti C, Centini G, Lazzeri L, Habib N, Labanca L, Zupi E, et al. Adenomyosis and infertility: the role of the junctional zone. Gynecol Endocrinol [Internet]. 2021 [cited 2023 Dec 13];37(7):577–83. Available from: https://www.tandfonline.com/doi/abs/10.1080/09513590.2021.1878131
299. Tellum T, Naftalin J, Chapron C, Dueholm M, Guo SW, Hirsch M, et al. Development of a core outcome set and outcome definitions for studies on uterus-sparing treatments of adenomyosis (COSAR): an international multistakeholder-modified Delphi consensus study. Hum Reprod [Internet]. 2022 Aug 25 [cited 2023 Dec 13];37(9):2012–31. Available from: https://dx.doi.org/10.1093/humrep/deac166
300. Benagiano G, Brosens I, Habiba M. Structural and molecular features of the endomyometrium in endometriosis and adenomyosis. Hum Reprod Update [Internet]. 2014 May 1 [cited 2023 Nov 21];20(3):386–402. Available from: https://dx.doi.org/10.1093/humupd/dmt052
301. Maruyama S, Imanaka S, Nagayasu M, Kimura M, Kobayashi H. Relationship between adenomyosis and endometriosis; Different phenotypes of a single disease? Eur J Obstet Gynecol Reprod Biol. 2020 Oct 1;253:191–7.
302. Cozzolino M, Tartaglia S, Pellegrini L, Troiano G, Rizzo G, Petraglia F. The Effect of Uterine Adenomyosis on IVF Outcomes: a Systematic Review and Meta-analysis. Reprod Sci [Internet]. 2022 Nov 1 [cited 2023 Nov 21];29(11):3177–93. Available from: https://link.springer.com/article/10.1007/s43032-021-00818-6
303. Moayed ME, Moini A, Kashani L, Mojtahedi MF, Rezaee T, Tabasizadeh H, et al. Pregnancy outcomes in women with adenomyosis, undergoing artificial endometrial preparation with and without gonadotropin-releasing hormone agonist pretreatment in frozen embryo transfer cycles: An RCT. Int J Reprod Biomed [Internet]. 2023 Jun 1 [cited 2023 Nov 21];21(6):481. Available from: /pmc/articles/PMC10407916/
304. Wu Y, Huang J, Zhong G, Lan J, Lin H, Zhang Q. Long-term GnRH agonist pretreatment before frozen embryo transfer improves pregnancy outcomes in women with adenomyosis. Reprod Biomed Online. 2022 Feb 1;44(2):380–8.
305. Wang Y, Yi YC, Guu HF, Chen YF, Kung HF, Chang JC, et al. Impact of adenomyosis and endometriosis on IVF/ICSI pregnancy outcome in patients undergoing gonadotropin-releasing hormone agonist

treatment and frozen embryo transfer. Sci Reports 2023 131 [Internet]. 2023 Apr 25 [cited 2023 Nov 21];13(1):1–8. Available from: https://www.nature.com/articles/s41598-023-34045-7
306. Dashottar S, Singh AK, Debnath J, Muralidharan CG, Singh RK, Kumar S. Comparative analysis of changes in MR imaging of pre and post intrauterine progesterone implants in adenomyosis cases. Med J Armed Forces India. 2015;
307. Kang S, Turner DA, Foster GS, Rapoport MI, Spencer SA, Wang JZ. Adenomyosis: Specificity of 5 mm as the maximum normal uterine junctional zone thickness in MR images. Am J Roentgenol. 1996;

PART VII

Supplementary Material

APPENDICES PER CHAPTER:

The appendices per chapter can be found online using the QR code below.

LIST OF AUTHOR'S PUBLICATIONS:

Rees, C. O., Nederend, J., Mischi, M., van Vliet, H. A., & Schoot, B. C. (2021). Objective measures of adenomyosis on MRI and their diagnostic accuracy—a systematic review & meta-analysis. *Acta Obstetricia et Gynecologica Scandinavica*, *100*(8), 1377-1391.

Rees, C. O., Rupert, I. A., Nederend, J., Consten, D., Mischi, M., van Vliet, H. A., & Schoot, B. C. (2022). Women with combined adenomyosis and endometriosis on MRI have worse IVF/ICSI outcomes compared to adenomyosis and endometriosis alone: A matched retrospective cohort study. *European Journal of Obstetrics & Gynecology and Reproductive Biology*, *271*, 223-234.

Huang, Y., **Rees, C.O.,** Sammali, F., Blank, C., Schoot, D., & Mischi, M. (2022). Characterization of uterine peristaltic waves by ultrasound strain analysis. *IEEE Transactions on Ultrasonics, Ferroelectrics, and Frequency Control*.

Rees, C. O., Rupert, I. A., Nederend, J., Consten, D., Mischi, M., van Vliet, H. A., & Schoot, B. C. (2022). Vrouwen met gecombineerde adenomyose/endometrioses hebben slechtere IVF/ICSI uitkomsten dan adenomyose of endometrioses alleen. *NTOG March 2022*

Rees C.O, de Boer A, Huang Y, Wessels B, Blank C, Kuijsters N, Huppelschoten A, Zizolfi B, Foreste V, Sardo AD, Christoforidis N. Uterine contractile activity in healthy women throughout the menstrual cycle measured using a novel quantitative two-dimensional transvaginal ultrasound speckle tracking method. Reproductive BioMedicine Online. 2023 Jan 1;46(1):115-22.

Rees CO, van Vliet H, Siebers A, Bulten J, Huppelschoten A, Westerhuis M, Mischi M, Schoot B. The ADENO study: ADenomyosis and its Effect on Neonatal and Obstetric outcomes: a retrospective population-based study. American Journal of Obstetrics and Gynecology. 2023 Jul 1;229(1):49-e1.

Rees, C. O., van Vliet, H. A., & Schoot, B. C. (2023). Dysmenorrhea and uterine innervation in adenomyosis and endometriosis: the role of the sacrouterine ligament: reply. American Journal of Obstetrics & Gynecology. DOI: 10.1016/j.ajog.2023.02.006

C.O. Rees ADENO-studie: effect van adenomyose op obstetrische en neonatale uitkomsten *Nederlands Tijdschrift voor Obstetrie en Gynaecologie* vol. 136, april 2023

C.O. Rees, M. van de Wiel, J. Nederend, A. Huppelschoten, M. Mischi, H.A.A.M. van Vliet, B.C. Schoot, Prediction of adenomyosis diagnosis based on MRI, *Journal of Endometriosis and Uterine Disorders*, Volume 2, 2023 DOI: 10.1016/j.jeud.2023.100028

Rees C.O., Kocyigit S, Nederend J, Mischi M, van Vliet HA, Schoot BC. MRI markers of adenomyosis severity associated with worse IVF/ICSI outcomes. Journal of Endometriosis and Pelvic Pain Disorders. 2023 Aug 28:22840265231195404.

de Boer, A., **Rees, C. O**., Mischi, M., Van Vliet, H., Huirne, J., & Schoot, B. C. (2023). The influence of uterine abnormalities on uterine peristalsis in the non-pregnant uterus: A systematic review. Journal of Endometriosis and Uterine Disorders, 100038.
DOI: 10.1016/j.jeud.2023.100038

Presentations at International and Regional conferences

International Conferences:

2020:

International Society of Ultrasound in Obstetrics and Gynaecology (ISUOG) World Congress Virtual, October 2020:

Virtual Poster:
Rees, C. O., Blank, C., Kuijsters, N. P., Huang, Y., Sammali, F., Mischi, M., ... & Schoot, B. C. (2020). VP62. 05: Quantitative ultrasound measurement of endometrial waves in abnormal uteri: interim results of the WAVES study. *Ultrasound in Obstetrics & Gynecology*, *56*, 337-338.

European Society of Gynaecological Endoscopy (ESGE) Virtual Congress, October 2020:
Best Oral Abstract Session:
Rees, C. O., Blank, C., Kuijsters, N. P., Huang, Y., Sammali, F., Mischi, M., ... & Schoot, B. C. (2020). Quantitative ultrasound measurement of endometrial waves in adenomyosis.
*** Winner Young Endoscopist Award*

2021:

European Society of Human Reproduction and Embryology (ESHRE) Virtual Congress,
July 2021:

Poster:
Rees, C., Huang, Y., Akhtar, M., Mischi, M., Humberstone, A., & Schoot, B. (2021). P–362 The effect of nolasiban on uterine contractility at the time of embryo transfer in in vitro fertilisation patients. *Human Reproduction*, *36*(Supplement_1), deab130-361.

Poster:
Schoot, B., Rees, C., Huang, Y., De Boer, A., Wessels, B., Huppelschoten, D., ... & Mischi, M. (2022). P-305 Uterine contractile function across the menstrual cycle in healthy women: an exploration of objective reference values of sub-endometrial motion using speckle tracking. *Human Reproduction*, *37*(Supplement_1), deac107-291.

International Society of Ultrasound in Obstetrics and Gynaecology (ISUOG) World Congress Virtual, September 2021:

Poster:
Rees, C. O., Huang, Y., Akhtar, M., Mischi, M., Humberstone, A., & Schoot, B. C. (2021). OC16. 01: Quantitative analysis of uterine peristalsis for prediction of pregnancy in IVF patients: external validation of the WAVES method. *Ultrasound in Obstetrics & Gynecology*, *58*, 46-46.

European Society of Gynaecological Endoscopy (ESGE) Congress, Rome, Italy, October 2021:
Best Oral Session:
Rees C.O., van Vliet H.A.A.M., Siebers, B., Huppelschoten, A., Bulten, H., Westerhuis, M., Mischi, M., Schoot, B.C, The ADENO Study: Adenomyosis in Dutch women and its effect on Hypertensive Disorders

Free communication Oral Session:
Rees C.O., van Vliet H.A.A.M., Siebers, B., Huppelschoten, A., Bulten, H., Westerhuis, M., Mischi, M., Schoot, B.C, The ADENO Study: Adenomyosis in Dutch women and its effect on Progression of Labour

American Society of Reproductive Medicine (ASRM) Congress Virtual, October 2021:
Oral Abstract:
Rees, C. O., Rupert, I. A., Nederend, J., Consten, D., Mischi, M., van Vliet, H. A., & Schoot, B. C. Women with combined adenomyosis and endometriosis on MRI have worse IVF/ICSI outcomes compared to adenomyosis and endometriosis alone: A matched retrospective cohort study.

Virtual Poster:
Rees, C. O., Huang, Y., Akhtar, M., Mischi, M., Humberstone, A., & Schoot, B. C. (2021). QUANTITATIVE ANALYSIS OF UTERINE PERISTALSIS FOR PREDICTION OF PREGNANCY IN IVF PATIENTS: EXTERNAL VALIDATION OF THE WAVES METHOD. *Fertility and Sterility*, *116*(3), e329.

Virtual Poster:
Rees, C., Huang, Y., Akhtar, M., Mischi, M., Humberstone, A., & Schoot, B.The effect of nolasiban on uterine contractility at the time of embryo transfer in in vitro fertilisation patients. *Fertility and Sterility*, *116*(3), e329.

American Association of Gynecological Laparoscopy (AAGL) Congress Virtual,
December 2021:
Poster:
de Boer, A., Rees, C. O., Huirne, J. A. F., & Schoot, B. C. (2021). The Influence of Uterine Abnormalities on Uterine Peristalsis in the Non-Pregnant Uterus: A Systematic Review. *Journal of Minimally Invasive Gynecology*, *28*(11), S146.

2022:

European Federation for Ultrasound in Medicine and Biology (EFSUMB),
Timisoara, Romania, May 2022
"Quantitative ultrasound imaging of uterine peristalsis and machine learning for prediction of successful fertilization", Yizhou Huang, Connie Rees, Anna de Boer, Dick Schoot, and Massimo Mischi.
***Winner Young Investigator Award

European Society of Human Reproduction and Embryology (ESHRE), Milan, Italy,
July 2022:
Poster:
Schoot, B., Rees, C., Huang, Y., De Boer, A., Wessels, B., Huppelschoten, D., ... & Mischi, M. (2022). P-305 Uterine contractile function across the menstrual cycle in healthy women: an exploration of objective reference

values of sub-endometrial motion using speckle tracking. *Human Reproduction*, *37*(Supplement_1), deac107-291.
Poster:
De Boer, A., Rees, C., Blank, C., Huang, Y., Wessels, B., Wagenaar, L., ... & Schoot, B. C. (2022). P-333 The influence of hormonal stimulation on uterine peristalsis measured by ultrasound speckle tracking in women with IVF/ICSI treatment compared to normal ovulating women. *Human Reproduction*, *37*(Supplement_1), deac107-317.

International Society of Ultrasound in Obstetrics and Gynaecology (ISUOG) World Congress,
London, UK, September 2022:

Poster:
Rees, C., Huang, Y., De Boer, A., Wessels, B., Huppelschoten, D., ... & Schoot, B.C. Uterine contractile function across the menstrual cycle in healthy women: an exploration of objective reference values of sub-endometrial motion using speckle tracking.

Oral Poster:
Rees, C. O., Blank, C., Kuijsters, N. P., Huang, Y., Sammali, F., Mischi, M., ... & Schoot, B. C. WAVES Study: Uterine contractile function in normal vs. abnormal uteri.

Point of Care Ultrasound Conference (POCUS) Eindhoven, the Netherlands,
September 2022

Oral presentation:
"Quantitaive ultrasound imaging of uterine peristalsis for prediction of successful fertilization", Yizhou Huang, Connie Rees, Anna de Boer, Iva Milojkovic, Dick Schoot, and Massimo Mischi.

American Society of Reproductive Medicine (ASRM) Congress, Anaheim, California,
October 2022:
Oral Abstract:
Rees, C., Huang, Y., De Boer, A., Wessels, B., Huppelschoten, D., ... & Schoot, B.C. Uterine contractile function across the menstrual cycle in healthy women: an exploration of objective reference values of sub-endometrial motion using speckle tracking.

Oral Abstract:
Rees, C. O., Blank, C., Kuijsters, N. P., Huang, Y., Sammali, F., Mischi, M., ... & Schoot, B. C. WAVES Study: Uterine contractile function in normal vs. abnormal uteri.
*** *Winner Best Abstract by an In-Training Researcher*

Oral Abstract:
Rees C.O., van Vliet H.A.A.M., Siebers, B., Huppelschoten, A., Bulten, H., Westerhuis, M., Mischi, M., Schoot, B.C, The ADENO Study: Adenomyosis in Dutch women and its effect on Obstetric and Neonatal Outcomes: a population-based cohort study

European Society of Gynaecological Endoscopy (ESGE) Congress Lisbon, Portugal;
October 2022:
Poster:
Rees, C. O., Blank, C., Kuijsters, N. P., Huang, Y., Sammali, F., Mischi, M., ... & Schoot, B. C. WAVES Study: Uterine contractile function in normal vs. abnormal uteri.

Free Communication Oral:
Rees, C., Huang, Y., De Boer, A., Wessels, B., Huppelschoten, D., ... & Schoot, B.C. (2022). Uterine contractile function across the menstrual cycle in healthy women: an exploration of objective reference values of sub-endometrial motion using speckle tracking.

Free Communication Oral:
De Boer, A., Rees, C., Blank, C., Huang, Y., Wessels, B., Wagenaar, L., ... & Schoot, B. C. (2022). P-333 The influence of hormonal stimulation on uterine peristalsis measured by ultrasound speckle tracking in women with IVF/ICSI treatment compared to normal ovulating women.

Best Selected Oral Session:
Rees C.O., van de Wiel, M., Nederend, J., Huppelschoten A., Mischi, M., van Vliet. H.A.A.M., Schoot, B.C, Predicting Adenomyosis Diagnosis on MRI.

American Association of Gynecological Laparoscopy (AAGL) Congress, Denver, Colorado, December 2022
Oral Abstract:
WAVES Study: Uterine contractile function in normal vs. abnormal uteri.
Rees, C. O., Blank, C., Kuijsters, N. P., Huang, Y., Sammali, F., Mischi, M., ... & Schoot, B. C.

Oral Abstract:
Predicting Adenomyosis Diagnosis on MRI.
Rees C.O., van de Wiel, M., Nederend, J., Huppelschoten A., Mischi, M., van Vliet. H.A.A.M., Schoot, B.C,

2023

World Endometriosis Congress – Edinburgh, UK, April 2023

Free Communication Oral

FC6.P6 : The Adeno Study: Adenomyosis in Dutch Women and Its Effect of Neonatal and Obstetric Outcomes - a Retrospective Population-Based Study
Rees C.O., van Vliet H.A.A.M., Siebers, B., Huppelschoten, A., Bulten, H., Westerhuis, M., Mischi, M., Schoot, B.C,
*** Winner Best Oral Presentation by an Early Career Clinician*

Poster

P-318: Prediction of Pathological Adenomyosis Diagnosis based on MRI
Rees C.O., van de Wiel, M., Nederend, J., Huppelschoten A., Mischi, M., van Vliet. H.A.A.M., Schoot, B.C,

European Society of Human Reproduction and Embryology (ESHRE) Congress –
Copenhagen, Denmark – June 2023

Oral Poster Presentation

Thomas S, Rees C, Huang Y, Klaassen C, De Boer A, Zizolfi B, DiForeste V, Di Spiezio Sardo A, Christoforidis N, Van Vliet H, Mischi M. O-267 Uterine contractility in women with adenomyosis differs significantly from healthy control women-the waves study. Human Reproduction. 2023 Jun 1;38(Supplement_1):dead093-321.

Oral Presentation:

Thomas S, Rees C, Huang Y, Klaassen C, De Boer A, Zizolfi B, DiForeste V, Di Spiezio Sardo A, Christoforidis N, Van Vliet H, Mischi M. O-267 Uterine contractility in women with adenomyosis differs significantly from healthy control women-the waves study. Human Reproduction. 2023 Jun 1;38(Supplement_1):dead093-321.

Poster:

Rees C, Huang Y, Thomas S, Klaassen C, De Boer A, Blank C, Christoforidis N, Humberstone A, Mischi M, Schoot B. P-514 Uterine Contractility during Follicle Aspiration and Embryo Transfer and IVF/ICSI Outcomes: the WAVES study. Human Reproduction. 2023 Jun 1;38(Supplement_1):dead093-857.

European Society of Gynaecological Endoscopy (ESGE) Congress – Brussels, Belgium
October 2023

Oral Presentation (Invited Speaker) Belgian Day
Adenomyosis Diagnosis on MRI.
Rees CO.

Oral Presentation:
Rees CO, Klaassen C, van de Wiel M, van Boven L, Nederend J, Huppelschoten A, van Vliet HA, Schoot BC. Prediction of Adenomyosis Diagnosis Based on MRI: An External Validation Study. Journal of Minimally Invasive Gynecology
***Selected for Presentation in Plenary Session*

Poster:
Rees CO. Gabriel EMA, Westerhuis MW, Huppelschoten A, van Vliet HA, Schoot BC
Endometriosis and obstetric outcomes: a Dutch population-based cohort study

Poster:
Rees CO, Thomas S, Huang Y, Klaassen C, Wagenaar L, van Vliet H, Mischi M, Schoot BC. Uterine contractility during intrauterine device insertion and patient pain experience. Ultrasound

International Society of Ultrasound in Obstetrics and Gynaecology (ISUOG) World Congress,
Seoul, South Korea – October 2023

Oral Presentation:
Rees CO, Thomas S, Huang Y, Klaassen C, Christophoridis N, di Spiezio A, Mischi M, Schoot BC, Zizolfi B, van Vliet H. OC09. 04: Uterine contractility of adenomyosis patients normalises under hormonal contraception use. Ultrasound in Obstetrics & Gynecology. 2023 Oct;62:21-.

Poster:
Rees CO, Thomas S, Huang Y, Klaassen C, Wagenaar L, van Vliet H, Mischi M, Schoot BC. EP31. 17: Uterine contractility during intrauterine device insertion and patient pain experience. Ultrasound in Obstetrics & Gynecology. 2023 Oct;62:301-.

American Association of Gynecological Laparoscopy (AAGL) Congress, Nashville, Tennessee – November 2023

Oral presentation:
Rees CO, Klaassen C, van de Wiel M, van Boven L, Nederend J, Huppelschoten A, van Vliet HA, Schoot BC. Prediction of Adenomyosis Diagnosis Based on MRI: An External Validation Study. Journal of Minimally Invasive Gynecology. 2023 Nov 1;30(11):S18.

Oral presentation:
Rees CO, Thomas S, Huang Y, Klaassen C, Christoforidis N, Zizolfi B, van Vliet HA, Mischi M, Schoot BC. Uterine Contractility of Adenomyosis Patients Normalises Under Hormonal Contraception Use. Journal of Minimally Invasive Gynecology. 2023 Nov 1;30(11):S20.

Poster:
Rees CO, Thomas S, Huang Y, Klaassen C, Wagenaar LP, van Vliet HA, Mischi M, Schoot BC. 10484 Uterine Contractility during Intra-Uterine Device (IUD) Insertion and Patient Pain Experience. Journal of Minimally Invasive Gynecology. 2023 Nov 1;30(11):S125.

Regional Conferences

Witte Raaf Congress 2020 –April 2nd, Virtual, Dutch Working Group for Gynaecological Endoscopy
Oral presentation:
WAVES Study – Quantitative Ultrasound Measurement of Endometrial Waves in morphologically abnormal uteri
Rees, C. O., Blank, C., Kuijsters, N. P., Huang, Y., Sammali, F., Mischi, M., ... & Schoot, B.

Research Night Catharina Hospital, April 2021:
Eindhoven, the Netherlands
Rees, C. O., Rupert, I. A., Nederend, J., Consten, D., Mischi, M., van Vliet, H. A., & Schoot, B. C. Women with combined adenomyosis and endometriosis on MRI have worse IVF/ICSI outcomes compared to adenomyosis and endometriosis alone: A matched retrospective cohort study.
***Winner Best Poster Presentation*

IGO Doelencongres, Virtual, March 2021:
Dagprogramma: Echoscopie in de gynaecologische praktijk en hysteroscopie anno 2021
Presentatie: Adenomyose, classificatie volgens MRI: wat is de meerwaarde?
Rees CO, Nederend J, Huppelschoten A, van Vliet HA, Schoot BC.

Research Night Catharina Hospital, April, 2022:
Eindhoven, the Netherlands
Rees C.O., van Vliet H.A.A.M., Siebers, B., Huppelschoten, A., Bulten, H., Westerhuis, M., Mischi, M., Schoot, B.C, The ADENO Study: Adenomyosis in Dutch women and its effect on Obstetric and Neonatal Outcomes: a population-based cohort study

Witte Raaf Congress 2023 - Dutch Working Group for Gynaecological Endoscopy
April 2023, Epe, the Netherlqnds
Prediction of Adenomyosis Diagnosis on MRI
Rees CO, van de Wiel M, Nederend J, Huppelschoten A, van Vliet HA, Schoot BC.
** *Winner Young Researcher Prize*

ACKNOWLEDGEMENTS

Geachte Prof. dr. Schoot en Prof. dr. van Vliet, Lieve **Dick** en **Huib,** mijn dankwoord moet natuurlijk met jullie beginnen. Ik weet nog heel goed dat ik voor het eerst in het Catharina aankwam voor mijn sollicitatie gesprek in oktober 2019. Ik ging weg zonder echt te weten waar we het precies over hebben gehad, maar ik wist wel dat ik weg liep met een goed gevoel. Dat gevoel is nooit weg gegaan, en ik heb dankzij jullie een fantastische tijd gehad de afgelopen jaren en ongelooflijk veel Ivan de wereld!) gezien en geleerd. Ik ben jullie beide zo dankbaar voor jullie vertrouwen, steun, kritische blik, gulheid, en de kansen die ik heb mogen krijgen om ook onze resultaten te delen om de diverse congressen. Vooral bedankt voor mij zo welkom en gewaardeerd te laten voelen, en mij op mijn weg te helpen als toekomstige gynaecoloog en onderzoeker, en misschien ooit ook als PSV-fan. Ik kan mij werkelijk geen betere begeleiders voorstellen, en als ik ooit de kans krijg een promovendus te begeleiden, ga ik mijn uiterste best doen om jullie voorbeeld te volgen.

Dear Prof. ir. Mischi, dear **Massimo**, thank you so much for these past years of your support and continuously useful feedback! It doesn't fail to amaze me to see how many projects you are involved in, and yet you always responded to every one of my emails within 24 hours. I am so grateful for it to have been possible to work with you at the TU/e!

Geachte Prof. dr **Steven Weyers**, u wil ik natuurlijk bedanken als mijn promotor vanuit het UGent op te treden en deel uit te maken van mijn commissie. Ik wil u ook specifiek ook als opleider aan het UZ Gent bedanken om mij de kans te hebben gegeven om in opleiding tot gynaeoloog te komen.

Dear **Prof. K. Isaacson**, I would like to express my sincere appreciation for you having made the substantial effort and long journey from the United States to act as one of my committee members. It is an honour to have such an expert in the field be a part of this

Prof. dr. V. Mijatovic, hartelijke dank om deel uit te maken van mijn promotiecomissie. Het is een eer dat u uw expertise en visie wilde delen en hier tijd voor vrij kon maken.

Prof. dr. H. Wijkstra, ook aan u mijn oprechte dank voor het deelnemen aan mijn manuscript commissie en het delen van uw expertise.

Professor T. Hamerlynck, heel hartelijk dank voor de flexibiliteit en bereidheid deel te maken van mijn commissie in Gent, ik kijk er naar uit binnenkort meer samen te werken in het UZ!

Professor B. Heindryckx, dank voor het opnemen van het voorzitterschap in Gent, en vooral bedankt voor uw flexibiliteit en begrip.

Aan **Kim de Keyser** en **Gry Ulstein** van de UGent, heel hartelijk dank voor al jullie administratieve ondersteuning in de laatste fase van mijn doctoraat traject. Het was zonder jullie inzet en begrip een onmogelijkeheid geweest.

Beste Dr Nederend, Beste **Joost**, heel hartelijk dank voor jouw steun en expertise met betrekking tot het leren van MRIs interpreteren. Zonder jouw, en de andere betrokken radiologen, uitleg, tijd, en geduld was een groot deel van mijn promotieonderzoek niet mogelijk geweest. Ik hoop in de toekomst nog veel samen te kunnen werken!

Dr Christoforidis, dear **Nikos**, a sincere thank you to you and the team at Embryolab Fertility Clinic for you continuing massive contribution to the WAVES study inclusions! Without your tireless efforts this project would not have been anywhere near as successful. I very much look forward to our continued collaboration in the future!

Prof. di Spiezio di Sardo and Dr Zizolfi, Dear **Attilio** and **Brunella**, I am so grateful for the opportunity to work with you together on the WAVES project. Thanks to your enthusiasm for the project and your work on inclusions we have quickly been able to achieve a lot more than we would have been able to otherwise! I hope we will continue to expand the project even further in future!

Dear **Yizhou**, the WAVES study would never been as productive and long-lived if it wasn't for your constant enthusiasm, patience and support in the analysis! Our first meeting together really made me so excited to start the project, and your infectious cheerfulness and readiness to help has made carrying out this project so much easier. Your impressive ability to explain the complex technical processes involved in an accessible and patient way is really something you should be very proud of. I am also still very happy to be able to profit from your excelling food and restaurant tips!

Aan mijn allerliefste paranimfen **Ianthe en Liselot,** ik ben zo blij dat jullie naast mij staan in deze fase, ook al hield ik jullie niet altijd even veel op de hoogte.

Ianthe, Plaint, vanaf SUMMA dag 1 was het eigenlijk al duidelijk dat we voor altijd vriendinnen gingen zijn. Ik had dan ook natuurlijk niemand anders kunnen vragen om naast mij te staan voor mijn promotie. Ik weet zeker dat jij heel veel gaat bereiken in het leven, en ik kijk er naar uit om het mee te maken.

Lieve **Liselot**, wat een geluk dat jij bent begonnen het Cathrien! Huib en Dick hebben toch echt wel goede smaak. Ik kan mij geen betere mede promovendus bedenken. Ik sta ook vol verwondering hoe jij alles in je leven met passie en zo veel liefde doet, en iedereen behalce jezelf op een zet. Mijn bankrekening gaat wel blij zijn dat we niet zo vaak meer koffie kunnen drinken aan de koffiebar (of in Lissabon or Brussel), maar ik weet dat we dat vervangen op een andere manier.

Aan alle mede-assistenten, verloskundigen, verpleegkundigen en poli-medewerkers tijdens mijn tijd in het **Catharina**. Dank zij jullie heb ik tijdens mijn onderzoeks- en assistenten tijd met heel plezier kunnen werken in het CZE. Sommige hebben een actieve bijdrage geleverd aan het onderzoek met patienten informeren over de studie, maar vooral ben ik heel dankbaar voor de gezelligheid op de werkvloer! Jullie hebben al het werk duizend keer makkelijker gemaakt.

Lieve echoscopisten van het Catharina, lieve **Peggy**, **Esmee**, **Anke**, **Manita**, **Jeanine**, jullie hebben mij in het hele begin leren de gynaecologische echo's maken om een heel groot deel van de studies te kunnen doen! Ik ben jullie allemaal ook heel erg dankbaar dat jullie de diverse studenten ook hebben kunnen opleiden! Tegenwoordig is het minder echo's, maar vooral meer koffies (en wijntjes). Jullie maakte een poli-dag altijd gezelliger!

Aan alle gynaecologen in het Cathrien, ik ben jullie een voor een allemaal zo dankbaar voor een leerzame, waardevolle en ook hele gezellige onderzoeks- en opleidingstijd in het CZE. Dank jullie wel allemaal om mij zo thuis te laten voelen, en mij te helpen ontwikkelen tot gynaecoloog. Ik ben heel erg blij dat ik voorlopig toch nog net geen definitief afscheid hoef te nemen.

Lieve **Celine, Kelly** en **Nienke**, als mijn voorgangers als promovendi van Dick en/of het WAVES project, ben ik jullie zo dankbaar ten

eerste voor al het werk wat jullie al gedaan hadden. Dank zij jullie voorwerk was er zo'n goede basis om op te bouwen om mijn promotie voor te zetten. Dank jullie wel dat jullie altijd bereidt waren om mijn vragen te beantwoorden en ervaringen te delen!

Zo veel dank aan alle de studenten die in de afgelopen jaren mee hebben gedaan aan het onderzoek dat deel uitmaakt van dit proefschrift. **Iris Rupert en Sehriban Kocyigit,** als mijn eerste studenten ben ik heel dankbaar voor jullie ongelooflijk harde werk and mooie prestaties in zo'n korte tijd! **Anna de Boer, Blijke Wessels. Marloes van de Wiel, Cynthia Klaassens** en **Sophie Thomas,** al was het honderden MRIs bekijken, of het WAVES project in leven houden, ben ik jullie allemaal zo dankbaar voor jullie gezelligheid en flexibiliteit. Ik zou geen leukere club dames kunnen bedenken om uren in de kelder (of op congres) mee door te brengen! Dit proefschrift is ook van jullie!

Malou, inmiddels dr. Gelderblom (!), vanaf dag 1 klikte het, ik kan altijd op jouw rekenen voor eerlijke feedback en een vrolijk gezicht. Je bent een topper!

Marjolein en **Phyllis**, beste dr Hermens en dr van de Ploeg, wij zijn in 2019 samen in het noodgebouw begonnen en dank zij jullie heb ik mij (ondanks de lockdown) mij meteen thuis kunnen voelen als nieuwe arts-onderzoeker in het CZE. Inmiddels zijn we alledrie klaar met onze promoties, en AIOS, wie had dat gedacht! We hebben het gered!

Kelder dames: **Cynthia, Caroline, Annelouke, Anne, Charlotte,** het is altijd zo fijn geweest om op mijn compensatiedagen de kelder in te komen en bekende gezichten te zien! Het is zo inspirerend en motiverend om samen te zitten met mensen die zulk gepassioneerd werk verrichten.

Lieve cat ladies: **Sterre, Laura** en **Astrid,** ik kan altijd op jullie rekenen voor een afleiding van het werk middels de zeer productieve katten foto uitwisseling! Ik hoop dat onze app groep nog vele jaren zal bestaan. Op nog vele memes en nog veel meer wijntjes!

Beste gynaecologen, en vroedvrouwen van het **ZOL Genk**. Ik heb bij jullie in mijn eerste jaar als assistent zo veel mogen leren en groeien als arts, en ben heel dankbaar voor jullie geduld, feedback en steun. Ik ben heel blij dat ik dit jaar weer naar Genk mocht terugkomen om verder als assistent te kunnen werken.

Lieve **mede-assistenten van het ZOL** van beide lichtingen. Een deel van jullie heeft mij als groene assistent opgeleidt en ondersteund, en het andere deel zijn mijn heerlijke huidige collega's. Ik heb zo veel geluk gehad met zulke fijne mensen, waar we altijd op elkaar kunnen steunen.

Dr Browne, Lieve **Joyce**. Jou wil ik specifiek bedanken voor mij als bachelor student zo snel enthousiast te maken voor onderzoek doen binnen de gynaecologie en obstetrie. Het is dankzij jouw enthousiasme en toewijding dat ik wist dat ik wilde gaan promoveren. Zonder jou als voorbeeld was ik nooit tot dit punt geraakt. Ik hoop nu, en in de toekomst jouw voorbeeld te blijven volgen als wetenschapper en als (stage)begeleider!

Al mijn mede-**SUMMA's**, in het bijzonder **Irene, Lyanne, Lisanne, Lars, Me Julie, Noor**, **Amanda**, ik ben zo trots op waar iedereen nu staat! Wij zijn begonnen als over-ijverige SUMMA studenten, en nu is iedereen bezig met hun dromen waar maken. Op naar de volgende!

To all of my teachers at the **International School of the Sacred Heart** in Tokyo, you gave me a thirst for learning and also allowed me to enjoy the process. Without all of your guidance and example I would never have achieved any of the things I have up to now.

Dear **Harry,** I'm so glad we found each other right at the beginning of this PhD journey in Eindhoven for both of us, just in time for lockdown to begin. Apparently we've actually managed? Maybe now I'll finally have more time to get a proper hobby. In any case we can now work through the whole Grand Designs back-catalogue.

Joos, my tamago, my sister (pronounced as Ms Santa Maria would), you're the reason I became interested in researching endometriosis in the first place. I'm so proud of everything you've gotten through, and even though I'm taller than you, you really are the stronger twin.

Mam, Mother, nu mag je me echt Dr Connie gaan noemen als je wilt, want ik ga ook op niks anders reageren. Dank je dat je er altijd voor me bent geweest. Je bent altijd een inspiratie voor mij geweest om met humor en kracht door het leven te gaan, en altijd 'calm and assertive' te blijven. Ik hou van je.

Papa, thanks for always being there to give me advice, even when I don't want to hear it. You've taught me that you get furthest just by trying to be a decent person, and shown me that working hard with honesty and integrity pays off. Love you.

Als laatste wil ik alle vrouwen die mee hebben gedaan met de diverse studies in dit proefschrift bedanken voor hun bereidheid voor deelname. Ik hoop dat de resultaten van dit proefschrift er voor zorgen dat de kennis en zorg voor vrouwen met adenomyose en endometriose alleen maar verbeterd.

ABOUT THE AUTHOR

Connie Rees was born on October 10th, 1993 in Tokyo, Japan to a Dutch mother and British father. She and her twin sister Josephine, grew up internationally in Sint Pancras, the Netherlands, Tokyo, Japan and Moscow, Russia. She graduated from the Anglo-American School in Moscow, Russia in 2012, and afterwards received her bachelor's degree in Pre-medicine from University College Utrecht (UCU) in Utrecht, the Netherlands. During her bachelor's degree, she also spent a semester abroad at Nanyang Technological University in Singapore. After finishing her bachelor's degree, she started her medical degree at Utrecht University, completing the Selective Utrecht Medical Masters (SUMMA) programme with an MD and MSc degree. As part of her master's thesis, she conducted research for the SPOT Study at five hospitals in Accra, Ghana. Upon receiving her medical degree, she starting her PhD research at the Catharina Hospital in Eindhoven in late 2019 under the supervision of Prof. dr Dick Schoot (Eindhoven University of Technology, Ghent University), Prof. dr Huib van Vliet (Ghent University) and Prof. Massimo Mischi (Eindhoven University of Technology). In 2020, she also started her obstetrics and gynaecology training at Ghent University Hospital. As part of her residency she has worked at the Ziekenhuis Oost Limburg, in Genk, Belgium, and the Catharina Hospital in Eindhoven, the Netherlands. She lives together with her boyfriend, Harry, and their two cats, Barry and Neville.

APPENDICES PER CHAPTER:

CHAPTER 2

2A. Search Strategy:
((adenomyosis OR 'uterine adenomyosis' OR adenomyoma* OR
'endometriosis interna' OR adenomyosis [MeSH Terms/EmTree]))
AND
(MRI OR MR OR magnetic resonance imag* OR MRI [MeSH Terms/Emtree])
NOT
(Gallbladder)
Filters: Human

2B. Data extraction tables

The following data was extracted from the included relevant studies.

Table 2.S1 Data Extraction Table

Studies Investigating Diagnostic Accuracy of MRI vs Histopathology	
Authors, year	
Study design	e.g. retrospective/prospective cohort, pilot, feasibility, interventional, observational
Study objective	e.g. diagnostic accuracy, treatment evaluation, differentiating adenomyosis vs fibroids
Study population (N)	
Study inclusion criteria	e.g. symptomatic women receiving surgery,
Study exclusion criteria	e.g. using hormonal therapy, post-menopausal
Comparison groups	e.g. with adenomyosis vs. without adenomyosis (if applicable) (MRI vs. TVUS etc.)
Adenomyosis definition used on MRI	e.g. JZ >12mm on MRI, histopathological diagnosis, TVUS MUSA criteria, clinical symptoms
MRI slice thickness (mm)	e.g. 3mm, 4mm
MRI systems used and manufacturer	e.g. 1.5T, 3T
MRI sequences/techniques/settings used	e.g. T1/T2/DWI/DTI/T1-contrast-enhanced
All MRI features investigated	Signal intensity, JZ irregularity, JZ thickness etc.
Objectified MRI features	e.g. JZ thickness, JZ diff, JZ-Myometrium ratio etc., uterine size, lesion size, apparent diffusion coefficient
Evaluation by experienced radiologist?	Y/N
MRI (re-)evaluated during the study or previous evaluation used?	e.g. MRI evaluated during study, MRI conclusion used retrospectively (not validated)
Multiple (blinded) radiologist evaluation?	Y/N
Menstrual cycle accounted for?	e.g. MRI only conducted in proliferative phase
Histopathological Reference diagnosis made	Y/N
Pathological definition of Adenomyosis	e.g. 1/3 myometrial invasion, 2 fields invasion etc.
Type of tissue sampled	Hysterectomy or biopsy?
Experienced (multiple) pathologists evaluating tissue?	
Diagnostic accuracy investigated	Which element most accurate?
Outcomes measured	e.g. Symptom severity, menstrual blood volume, pain, change in uterine volume
Results of Adenomyosis characteristics on MRI	e.g. mean JZ thickness, mean uterine volume, # diffuse cases, # focal cases,
Adenomyosis-related Results	E.g. correlation with symptom reduction y/n, reduction in JZ thickness, degree of uterine volume reduction, diagnostic accuracy/specificity/sensitivity
Number of adenomyosis diagnosis on MRI	N=
Number of adenomyosis diagnosed on histopathology	N=
Comments	If any
QUADAS-II Quality Assessment	
a. Patient selection	

Method of patient selection	Random, consecutive, retrospective, prospective
Included patients	Inclusion criteria
Consecutive of random patients enrolled?	Yes/no/unclear
Case-control design avoided?	Yes/no/unclear
Inappropriate exclusion avoided?	Yes/no/unclear
Bias in patient selection process?	High, low, unclear (bias type?)
Do the included patients match the review question?	High, low, unclear
b. Index Test (i.e. MRI)	
MRI method	MRI sequences used
MRI interpretation	Multiple radiologists? Experienced radiologists?
Blinded to result of histopathology?	Yes/no/unclear
Pre-specified definition for adenomyosis on MRI?	Yes/no/unclear
Potential for bias in MRI interpretation?	High, low, unclear (bias type?)
Does the application of the MRI match the research question?	High, low, unclear
c. Reference Standard	
Histopathological adenomyosis definition	Which cut-off/definition used?
Interpretation of histopathology	Multiple pathologists? Experienced pathologists?
Likely to have correctly identify adenomyosis using this method?	Yes/no/unclear
Blinded to MRI diagnosis?	Yes/no/unclear
Potential for bias in histopathological diagnosis?	High, low, unclear (bias type?)
Does the application of the histopathological diagnosis match the research question?	High/low/unclear
d. Patient Flow and Timing	
Any patients that did not receive MRI or pathology or excluded from 2 x 2 table?	Yes/no, with number and reason(s)
Interval/intervention between MRI and histopathological diagnosis	If specified, months/days
Appropriate interval between MRI and histopathology?	Yes/no/unclear
All patients received (the same) histopathology diagnosis?	Yes/no/unclear
All patients included in analysis?	Yes/no/unclear
Potential for bias in patient flow?	High/low/unclear

For the studies investigating diagnostic accuracy 2 x 2 Tables were constructed in RevMan extracting the following information:

Table 2.S2 Empty 2 x2 Tables

	Histopathology+	**Histopathology-**
MRI+	n	n
MRI-	n	n

Table 2.S3 Empty Diagnostic Accuracy Parameters Table

Article	Sensitivity (%)	Specificity (%)	NPV (%)	PPV (%)
Author, Year				

Table 2.S4 Data Extracted for Studies not investigating Diagnostic Accuracy

Studies not investigating Diagnostic Accuracy	
Authors, year	
Study design	e.g. retrospective/prospective cohort, pilot, feasibility, interventional, observational
Study objective	e.g. diagnostic accuracy, treatment evaluation, differentiating adenomyosis vs fibroids
Study population (N)	
Study inclusion criteria	e.g. symptomatic women receiving surgery
Study exclusion criteria	e.g. using hormonal therapy, post-menopausal
Comparison groups	e.g. with adenomyosis vs. without adenomyosis (if applicable) (MRI vs. TVUS etc.)
Adenomyosis definition used	e.g. JZ >12mm on MRI, histopathological diagnosis, TVUS MUSA criteria, clinical symptoms
MRI slice thickness (mm)	e.g. 3mm, 4mm
MRI systems used	e.g. 1.5T, 3T
MRI sequences/techniques/settings used	e.g. T1/T2/DWI/DTI/T1-contrast-enhanced
All MRI features investigated	Signal intensity, JZ irregularity, JZ thickness etc.
Objectified MRI features	JZ thickness, JZ diff, JZ-Myometrium ratio etc., Apparent Diffusion Coefficient
Outcomes measured	e.g. Symptom severity, menstrual blood volume, pain, change in uterine volume
Results of Adenomyosis characteristics on MRI	e.g. mean JZ thickness, mean uterine volume, # diffuse cases, # focal cases,
Adenomyosis-related Results	E.g. correlation with symptom reduction y/n, reduction in JZ thickness, degree of uterine volume reduction, diagnostic accuracy/specificity/sensitivity
Comments	

2C Study Characteristics of Included Studies

Table 2.S5 Study Characteristics of Diagnostic Accuracy Studies

Authors, Year	**Study Design**	**Study objective**	**Study population (N)**	**Study Setting**	**Study inclusion criteria**	**Study exclusion criteria**	**MRI Adenomyosis definition used**	**MRI Manufacturer, Settings and Parameters**	**MRI features investigated**	**Histopathological definition of adenomyosis used**
Ascher et al. 1994(120)	Prospective diagnostic study	To compare conventional spin-echo MRI and TVUS for the diagnosis of adenomyosis	20 women with clinically suspected adenomyosis	University Hospital (USA)	Adenomyosis suspected on the basis of unexplained pelvic pain, menorrhagia	Evidence of leiomyoma at physical examination	A myometrial mass with indistinct margins of primarily LSI with all sequences OR diffuse or focal widening of the JZ (>5mm) on T2W, fast T2W SE images, and CE T1W images. Presence of HSI foci was used as an ancillary finding	Manufacturer: Siemens Impact or SP4000 System: 1.0T or 1.5T Slice Thickness: 5mm Sequences: T2W, T1W, T1 gadolinium CE	JZ thickness, HSI foci 2(unclear if on T2 or T1), JZ irregularity, adenomyosis type	Endometrial glands and stroma > 2.5 mm below the endometrial surface

Badawy et al. 2014 (118)	Prospective cross-sectional study	To study the mandatory indications and accuracy of MRI for the diagnosis of uterovaginal lesions associated with female infertility	54 infertile women with inconclusive uterovaginal lesions of TVUS/HSG	University Hospital (Egypt)	All infertile patients with uterovaginal lesions, except intracavitary lesions, that were not conclusively diagnosed by HSG and TVUS were included in the study.	Chronic renal impairment, allergy to the contrast medium. pacemakers, cochlea implants, jewellery of any kind and certain metallic objects	No clear definition of adenomyosis on MRI prior to diagnosis	Manufacturer: GE Signa System: 1.5T Slice Thickness: 5mm Sequences: T1W, T2W, STIR, T1 gadolinium CE	Signal intensity, shape, site, size, pattern of enhancement of lesions and their relations to surrounding structures. Adenomyosis: JZ thickness, uterine enlargement, presence of HSI foci (on T1 and T2), irregular LSI mass	NR
Bazot et al. 2001 (125)	Prospective diagnostic study	To compare accuracy of TVUS to MRI for diagnosis of adenomyosis, and to correlate imaging with histological findings	120 patients referred for hysterectomy	Regional hospital (France)	Referred for hysterectomy	Lack of TVUS/MRI for technical or pain reasons, cancelled surgery, conservative surgery instead of hysterectomy, endometrial resection	(i)large, regular, asymmetric uterus without leiomyoma, (ii) JZ max>12mm and/or ill-defined LSI myometrial area, (iii) JZ/Myometrium ratio >40%, (iv) HSI foci on T1/T2	Manufacturer: Phillips Gyroscan, Phillips Or Siemens Magnetom Vision System: 1.5T Slice Thickness: 5mm Sequences: T2W, T1W	JZ thickness, JZ/Myometrium ratio, JZ irregularity, HSI foci (on T1 and/or T2), adenomyosis localisation, type, uterus size, presence of fibroids or other uterine abnormalities	Macroscopic: Enlarged uterus and a dense anarchically fasciculated unlimited myometrium with small cavities (5-10mm) Microscopic: Presence of ectopic endometrial tissue within myometrium 2.5mm beyond the endometrial/

										myometrial junction.
Bazot et al. 2003 (124)	Prospective inter-observer variability study	To evaluate, in addition to turbo spin-echo (TSE) T2W sequences, the accuracy of breath-hold fast sequences using turbo inversion recovery and true fast imaging with steady-state free precession (FISP) for the diagnosis of adenomyosis, and	56 patients who underwent hysterectomy	University Hospital (France)	Women that underwent MRI with TSE T2W, turbo inversion recovery and true FISP sequences. Patients undergoing hysterectomy due to menorrhagia, post-menopausal bleeding, adnexal masses, genital prolapse and cervical intraepithelial neoplasia	Patients not undergoing hysterectomy, cases involving MRI without turbo spin-echo T2W, turbo inversion recovery and true FISP sequences	JZ > 12 mm or an ill-defined LSI area of myometrium or punctate HSI myometrial foci.	Manufacturer: Siemens Magnetom Vision System: 1.5T Slice Thickness: 5mm Sequences: T2W TSE	JZ thickness, uterine location and size, cavities in myometrium, presence of punctate HSI myometrial foci (on T2)	Macroscopic: Enlarged uterus and a dense anarchically fasciculated unlimited myometrium with small cavities (5-10mm) Microscopic: Presence of ectopic endometrial tissue in the myometrium located 2.5 mm beyond the endometrial–myometrial junction

		intra- and inter-observer variability								
Dueholm et al. 2001 (122)	Prospective diagnostic study	To compare the diagnostic potential of MRI and TVS in the diagnosis of adenomyosis	106 pre-menopausal patients undergoing hysterectomy for benign disease	University Hospital (Denmark)	Pre-menopausal patients undergoing hysterectomy for benign disease	Previous trans-cervical endometrial resection, malignant diagnosis, and acute or subacute indication for hysterectomy	Diffuse Adenomyosis: JZ Max >15 mm OR JZ of 12–15 mm with non-uniform, thickened JZ or focal not well-demarcated HSI or LSI areas in the myometrium	Manufacturer GE Signa, or Phillips Gyroscan System: 1.5T Slice Thickness: 4mm Sequences: T2	JZ uniformity, JZ Min, JZ Max, JZ Diff, Uterus volume, adenomyosis lesion size, presence of HSI foci on T2	Presence of endometrial glands or stroma >2mm deep in the endometrial–myometrial junction
Hamimi et al. 2015 (117)	Retrospective diagnostic cohort study	To define the most accurate signs for diagnosis of uterine adenomyosis using TVUS and MRI	60 women referred for MRI with suspicion of adenomyosis	University Hospital (Egypt)	Female patients with abnormal uterine bleeding in the fertile period	Recent abortion, pregnancy, malignant gynaecological disease, or under hormonal therapy	Intramyometrial cyst(s) Heterogeneous myometrium JZ thickness >12mm	Manufacturer Siemens, Avanto System: 1.5T Slice Thickness: 13mm Sequences: T1, T2, T1 gadolinium CE	JZ thickness, JZ irregularity, adenomyosis type, presence of myometrial cysts (unclear if on T1 or T2), heterogeneity of myometrium	NR

Hricak et al. 1992 (126)	Retrospective diagnostic study	To determine the role of gadopentetate CE T1W MRI in detection/ characterisation of benign uterine tumours	46 patients with surgically proven benign uterine disease (115 fibroid, 19 adenomyosis, 14 endometrial polyps)	University Hospital (USA)	Women >18 years, with a surgical diagnosis of benign uterine lesion, with pelvic MRI < 30 days prior to surgery	MRI >30 days before surgery	Enlarged uterus with smooth border, presence of HSI foci	Manufacturer GE Signa System: 1.5T Slice Thickness: 5mm Sequences: T1W, T2W, T1 gadolinium CE	Tissue SI (subjective), lesion margin, lesion size, uterus size, number of lesions, lesion border, JZ thickness, presence of HSI foci on T2	NR
Masui et al. 2003 (127)	Prospective observational study	To evaluate whether multiphase-multisection T2-weighted MRI help exclude pseudolesions mimicking leiomyoma and adenomyosis on static T2-weighted fast spin-echo	43 patients (adenomyosis n=18) undergoing pre-procedural MRI before hysterectomy	Referral hospital (Japan)	Female patients undergoing hysterectomy suspected of pelvic disease	No MRI prior to hysterectomy	ill-defined LSI lesions with or without HSI spots or having focal or diffuse thickening of the JZ >12 mm	Manufacturer GE Horizon LX Echo Speed System: 1.5T Slice Thickness: 5-6mm Sequences: T2W, T2-FSE, T2-SSFSE	JZ thickness at 6 points of the uterus, presence of leiomyoma, presence of HSI spots (on T2), adenomyosis type	NR

		(FSE) MR images								
Moghadam et al. 2006 (116)	Retrospective diagnostic study	To evaluate the role of MRI as a preoperative diagnostic tool for leiomyoma and adenomyosis	153 women with preoperative MRI before hysterectomy or myomectomy	University hospital (USA)	Women undergoing hysterectomy or myomectomy with a preoperative MRI	Not specified	Focal or diffuse widening of JZ> 12 mm, uterine enlargement, focal or diffuse LSI myometrial area in T2-weighted images, on CE T1 small HSI myometrial spots	Manufacturer Phillips Gyroscan System: 1.5T Slice thickness: NR Sequences: T2, T1	JZ thickness, Uterine enlargement, adenomyosis type, presence of HSI foci (on T1)	NR
Phillips et al. 1996 (121)	Prospective observational study	To evaluate the accuracy of MRI for diagnosing nodular adenomyosis By percutaneous myometrial biopsies	20 women with severe dysmenorrhea, chronic menorrhagia, and an MRI diagnosis of adenomyomas	Community hospitals (USA)	Women with enlarged uteri, chronic menorrhagia, and severe dysmenorrhea thought to have adenomyoma on MRI prior to conservative surgery	Endometrial cancer, premalignant lesions, leiomyoma, uterine cavity over 12cm, endometrial polyps	<u>Diffuse adenomyosis:</u> diffuse non-uniform widening of the JZ. <u>Adenomyoma:</u> localized, ill-defined, LSI mass, poorly marginated from the adjacent myometrium	Manufacturer NR System: NR Slice thickness: NR Sequences: T2W, T1W	JZ irregularity, uterine volume, lesion volume, LSI masses	Endometrial tissue, glands, and stroma present within the myometrium, at least one low power field from the endomyometrial junction. After myometrial biopsy.

Reinhold et al. 1996 (128)	Prospective cohort study	To compare accuracy of TVUS to MRI in adenomyosis diagnosis with histopathologic correlation	119 patients undergoing hysterectomy	University Hospital (Canada)	Women undergoing hysterectomy	Inadequate assessment of myometrium, endometrial carcinoma, technically inadequate TVUS due to large fibroids, refusal to undergo MRI	Subjective impression of localized or diffuse thickening of the uterine JZ (with or without the presence of HSI foci in the JZ) or the presence of a LSI myometrial mass with ill-defined borders	Manufacturer GE, Signa System: 1.5T Slice Thickness: 5mm Sequences: T2W	Uterine size, JZ Max, and Maximal JZ/Myometrial ratio, Adenomyosis type and localisation	Presence of endometrial glands and/or stroma > 1 high power field deep to the endometrial myometrial junction
Stamatopoulos et al. 2012 (129)	Prospective observational cohort study	To estimate the diagnostic performance of MRI in detection of fibroids and adenomyosis	153 women with an enlarged uterus and symptoms	University Hospital (Greece)	Heavy menstrual bleeding, pelvic mass, bulky uterus (larger than 10 weeks' gestational size) with no history of previous histologic investigation; no desire for further childbearing; and consent for total abdominal hysterectomy	Pregnancy; desire to retain fertility; preoperative diagnosis of malignant disease requiring hysterectomy; history of minimally invasive treatment of menorrhagia; need for uterine morcellation during surgery, medical contraindications to surgery	JZ > 12 mm, focal not well-demarcated areas were present in the myometrium, and non-uniform JZ	Manufacturer Siemens, Magnetom Impact System: 1.0T Slice Thickness: NR Sequences: T1W, T2W	JZ thickness, JZ irregularity, adenomyosis type, presence/size of fibroids, presence/size of leiomyosarcoma	Ectopic endometrium was recognized >2 mm deep in the myometrium; Diffuse: When endometrial glands or stroma were diffusely distributed in the myometrium. Focal: When circumscribed nodular aggregates of glands or stroma were found within the myometrium. Adenomyomas: When a

										circumscribed mass was found, composed of more than rare glands, predominantly of the endometrial type, and a stromal component that consisted primarily of smooth muscle
Tellum et al. 2019 (45)	Single-centre prospective observational cohort study	To assess the diagnostic accuracy of JZ thickness ≥ 12mm and morphological features of the JZ in MRI in diagnosing adenomyosis in a pre-menopausal study population	93 pre-menopausal women with a benign gynaecological condition	University Hospital (Norway)	Aged 30–50 years, having a benign condition, and hysterectomy being recommended as the appropriate treatment by a gynaecologist	Presence of malignancy, the use of any hormonal medication 3 months prior to the ultrasound examination and hysterectomy, or the need to morcellate the uterus during the hysterectomy.	One or more of: JZ Max ≥ 12 mm, myometrial cysts, or adenomyoma	Manufacturer: Phillips Ingenia or Achieva System: 3.0T or 1.5T Slice Thickness: NR Sequences: T1W, T2W	JZ thickness (Avg, Max, Min, Diff), myometrial cysts (on T1/T2), adenomyoma, JZ appearance, JZ/Myometrium ratio, Uterine shape, Fibroids (number), Size of largest fibroid	Presence of ectopic endometrial glands and stroma at 2.5 mm below the endometrial-myometrial junction

Tian et al. 2016 (119)	Prospective cohort study	To evaluate the performance of intra-voxel incoherent motion (IVIM)-DWI in differentiating uterine fibroids from focal adenomyoses	Women with fibroids (n=25) or focal adenomyosis (n=21) prior to surgery	University Hospital (China)	(1) newly suspected uterine diseases; (2) no previous treatment history	(1) contraindication for MRI; (2) uncooperative patients or no consent	NR	Manufacturer: Siemens Magnetom Avanto System: NR Slice Thickness: 5mm Sequences: T1W, T2W, DWI	Apparent diffusion coefficient total values (ADCtot), True diffusion coefficient (D), Pseudodiffusion coefficient (D*) and perfusion fraction (f), Signal-muscle ratio (SMR) for each lesion at both T1WI and T2WI sequence, and the Signal–noise ratio (SNR)	NR

NR: not reported, MRI: magnetic resonance imaging, TVUS: transvaginal ultrasound, SI: signal intensity, LSI: low signal intensity, HSI: high signal intensity, DWI: diffusion weighted imaging,

Table 2.S5 Study Results of Diagnostic Accuracy Studies

Author, Year	Outcomes Measured	Adenomyosis MRI Results for the population	Number of positive MRI diagnoses	Number of positive histopathology diagnoses	Diagnostic Accuracy Results
Ascher et al. 1994	Presence adenomyosis, type of adenomyosis	NR	15	17	NR. Calculated by reviewer after constructing 2 x 2 tables based on information provided in the paper. Can be found in the RevMan forest plots from page 43 onwards.
Badawy et al. 2014	Diagnostic accuracy of MRI for various uterine lesions after unclear TVUS/HSG	Diffuse: n= 14 Adenomyomas: n= 3	17	17	Accuracy: 100%, Sensitivity 100%, Specificity 100%, PPV 100%, NPV 100%
Bazot et al. 2001	Presence of adenomyosis, adenomyosis type	NR	NR	40	**Homogenous uterine enlargement**: Accuracy 72.5%. Sensitivity 22.5%, Specificity 97.5%, PPV 81.8%, NPV 72.5%, **HSI foci:** Accuracy: 81.7% Sensitivity 47.5%, Specificity 98.8%, PPV 95.0%, NPV 79.0% **JZ>12mm**: Accuracy 85.0% Sensitivity 62.5%, Specificity 96.3%, PPV 89.3%, NPV 83.7%, **JZ/Myometrium ratio**: Accuracy 83.3% Sensitivity 65.0%, Specificity 92.5%, PPV 81.3%, NPV 84.0%, **Combination**: Accuracy 87.5% Sensitivity 77.5%, Specificity 92.5%, PPV 83.8%, NPV 89.2%,
Bazot et al. 2003*	Accuracy of diagnosis using different MRI techniques and reviewers	16.7% adenomyoma 62.5% diffuse adenomyosis, 37.5% focal adenomyosis	NR	24 (42.9%)	Accuracy 83.9%. Sensitivity 75%, Specificity 90.6%, PPV 85.7%, NPV 82.8%,

Dueholm et al. 2001	Presence of adenomyosis on histopathology	No adenomyosis: Mean JZ Max: 10mm	14	22	Sensitivity 70%, Specificity 86% PPV 58%, NPV 91%. Higher JZ associated with more accurate MRI diagnosis (Cut-off: Max 12mm, Diff: 5-7mm)
Hamimi et al. 2015	Confirmed diagnosis of adenomyosis after imaging	NR	**Myometrial Cysts**: 20 TP, 5 FP, 15 TN, 20 FN **Heterogeneous myometrium:** 38 TP, 5 FP, 15 TN, 2 FN, **JZ >12mm:** 42 TP, 1 FP, 15 TN, 2 FN	45 TP, but seemingly only 5 based on histopathology	**Myometrial cysts**: Accuracy 58% Sensitivity 80%, Specificity 50% PPV 80%, NPV 43% **Heterogeneous myometrium**: Accuracy 88% Sensitivity 95%, Specificity 75% PPV 88%, NPV 88% **JZ>12mm**: Accuracy 95% Sensitivity 95%, Specificity 94% PPV 98%, NPV 88%
Hricak et al. 1992	Correct diagnosis of adenomyosis in different MRI sequences vs. histopathology	NR specifically	17	19	NR in study, 2 x 2 tables constructed by reviewer based on information provided in the paper. See from page 43 of the supplementary file for details.
Masui et al. 2003**	Diagnosis of adenomyosis (or leiomyoma) per different MRI method	No difference in detection for different MRI techniques	NR, calculated by reviewer See from page 43 of the supplementary file for details.	18	Accuracy: 82% Sensitivity: 69% Specificity: 67% PPV: 59% NPV: 90%
Moghadam et al. 2006	Accurate diagnosis of leiomyoma/adenomyosis vs. histopathology	NR	12 TP, 11 FP, 19 FN, 111 TN	31	Sensitivity 38%, Specificity 91% PPV 52% NPV 85%
Phillips et al. 1996***	Diagnosis of adenomyoma on MRI vs. myometrial biopsy	Mean adenomyoma volume: 125 +/- 12 cm^3 Mean uterine volume:	18TP, 2FP	18	Sensitivity: 100% Other diagnostic performance values NR.

		433+/29 cm^3			
Reinhold et al. 1996	Diagnostic accuracy of MRI vs TVUS, JZ max on MRI as cut-off	**Adenomyosis:** Diffuse: n=11 Mean JZ Max 15.0mm, Mean JZ/Myometrium ratio 0.69 **No adenomyosis:** Mean JZ max 7.7mm Mean JZ/Myometrium ratio 0.44	24TP, 13 FP, 4 FN	28	**Overall:** Sensitivity 86%, Specificity 86% PPV 65%, NPV 95%. **JZ >12 mm**: Sensitivity 93%, Specificity 91% PPV 79%, NPV 98% **JZ/Myometrium ratio** higher in adenomyosis patients (P<0.001) (no specific information on diagnostic performance).
Stamatopoulos et al. 2012	Histopathological diagnosis after hysterectomy	NR	13	26	Sensitivity 46.15%, Specificity 99.08%, PPV 92.31%, NPV 88.52% PLR 50.31%, NLR 0.54,
Tellum et al. 2019	Presence of adenomyosis on histopathology	JZ Max: 11.1mm, Mean JZ diff: 8.4mm, Mean JZ max: 15.8mm	**Combined**: 41 TP, 12FP, 19 TN, 13 FN, 8 undefined. **JZ>12mm**: 30 TP, 16 TN. **Myometrial cysts**: TP 40, TN 4. **Adenomyoma**: 18 TP, 2 TN **JZ diff >5mm**: TP 30, FP 9 **Irregular JZ:** TP 42 TN 6 **JZ/Myometrium ratio > 50%:** TP 24/39 TN 15/28.	*57*	**Combined**: Accuracy 70% Sensitivity 72% Specificity 67% PPV 77%, NPV 60% **JZ>12mm:** Accuracy 54% Sensitivity 53%, Specificity 56%, PPV 65%, NPV 43% **Myometrial cysts**: Accuracy 77% Sensitivity 70%, Specificity 89% PPV 91%, NPV 65% **Adenomyoma:** Accuracy 56%. Sensitivity 32%, Specificity 94% PPV 90%, NPV 47% **JZ diff>5.5mm:** Accuracy 61% Sensitivity 53%. Specificity 75% PPV 77%, NPV 50% **Irregular JZ:**

			Enlarged uterus: TP 29/44, TN 13/23		Accuracy 77% Sensitivity 74%, Specificity 74%, PPV 88%, NPV 67% **JZ/Myometrium ratio > 50%**: Accuracy 48% Sensitivity 42%. Specificity 58% PPV 50%, NPV 39% **Enlarged uterus:** Accuracy 56% Sensitivity 51%, Specificity 64% PPV 69%, NPV 45%
Tian et al. 2016	Difference in accuracy between conventional MRI and MRI + IVIM	NR	Focal adenomyosis: 18TP, TN 23	21	**Conventional MRI:** Accuracy 89.1% Sensitivity 90%, Specificity 88.5%, PPV 85.7%, NPV 92.0%, **MRI + IVIM:** Accuracy: 95.7% Sensitivity 100%, Specificity 92.6% PPV 90.5%, NPV 100.0%

NR: not reported, JZ: junctional zone, MRI: magnetic resonance imaging, TVUS: Transvaginal Ultrasound, HSG: Hysterosalpingography, TP: true positive, FP: false positive, TN: true negative, FN: false negative, PPV: positive predictive value, NPV: negative predictive value, PLR: positive likelihood ratio, NLR: negative likelihood ratio,

*only the diagnostic performance for the most experienced reviewer is reported here, as well as only the diagnostic data for the T2W TSE MRI sequence as this is more standardly used in clinical practice than the others investigated in this study

**only the diagnostic data for the standard T2W-FSE MRI was reported here, as results were the same for both methods.

***only investigated adenomyoma, not adenomyosis in general

Table 2.S6 Study Characteristics of Studies investigating Objective Measures of Adenomyosis on MRI

Authors, Year	Study Design	Study objective	Study population (N)	Study Setting	Study inclusion criteria	Study exclusion criteria	MRI Adenomyosis definition used	MRI Manufacturer, Settings and Parameters	MRI features investigated	Quantifiable MRI Characteristics investigated	Clinical Outcomes correlated with MRI Parameters ?
Andersson et al, 2016 (123)	Multi-centre, Prospective Pilot Study	Evaluate vaginal bromocriptine as treatment for symptoms of adenomyosis	23 women with diffuse adenomyosis	University hospital (Sweden), and Tertiary Hospital (USA)	Women aged 35-50 with regular heavy menstrual bleeding, with adenomyosis diagnosed by TVUS and MRI	Women actively pursuing pregnancy, <6 months post-partum, breastfeeding) , Enlarged uterus over umbilical level, Contraindications to bromocriptine, MRI suggestive for endometriosis or prolactinoma, IUD, antidepressants, opioid medication, suspected (gynaecological) malignancy	JZ > 12mm, JZ diff >5mm and ratio JZ/ myometrium >40%, presence of myometrial cystic changes	Manufacturer: NR System: NR Slice Thickness: NR Sequences: NR	Uterus size, JZ thickness, Cystic changes in JZ (unclear if on T1 or T2), Adenomyosis type, Presence of Fibroids, Fibroid size	Uterus size (length, Anterior Myometrium width, Posterior myometrium width) JZ Max, JZ Min, JZ Diff, JZ/Myometrium Ratio	No
Bae et al. 2015 (130)	Single-centre, Retrospective Interventional Cohort study	To evaluate the effect of degree of necrosis after UAE on symptom recurrence at midterm	50 Women with symptomatic pure adenomyosis (no fibroids)	University Hospital (Korea)	Women with pure adenomyosis who had UAE treatment, and received MRI 3 months prior to and post-	NR	JZ >12mm with or without punctate HSI foci	Manufacturer: NR System: NR	JZ thickness, Presence of HSI foci (on T1/T2), Necrosis percentage on CE MRI after	JZ thickness, Uterine volume,	Larger uterine volume associated with more symptom recurrence after

		clinical follow-up in patients with adenomyosis.			treatment with follow-up > 18 months after treatment			Slice Thickness: 4mm Sequences: T2W, T1W, T1-gadolinium CE	treatment, Adenomyosis type, Uterine volume		treatment. Adenomyosis subtype no association with degree of symptom recurrence.
Bourdon et al. 2018 (131)	Prospective cohort study	To compare serum cytokine profiles for the various adenomyosis phenotypes vs. disease-free women	80 women who had a pelvic MRI performed by the senior radiologist during pre-operative workup	University Hospital (France)	Non-pregnant patients <42 years who underwent surgical exploration by operative laparoscopy or laparotomy for benign gynaecological conditions	Cancer or borderline tumours, no consent to participate	<u>Diffuse adenomyosis</u>: JZ-max > 12 mm, JZ-myometrium ratio max > 40%. <u>Focal adenomyosis:</u> adenomyotic foci located in the outer shell of the uterus, separated from the JZ	Manufacturer: NR System: NR Slice Thickness: NR Sequences: T2W, T1W	JZ thickness, JZ max, JZ/Myometrium ratio, presence of HSI spots in myometrium (on T2), adenomyosis lesion size, adenomyosis type, adenomyosis lesion localisation	JZ thickness, JZ max, JZ/Myometrium ratio, adenomyosis lesion size	Mixed subtypes of adenomyosis associated with lower pro-inflammatory cytokine levels
Braghetto et al.	Prospective descriptive study	To evaluate the effect of the LNG-IUS on	29 Women with symptomatic	University Hospital (Brazil)	Diagnosis of adenomyosis on MRI with dysmenorrhoea	Endometrial polyps, Ovarian tumour/cyst, uterine	>12mm JZ diameter <u>OR</u>	Manufacturer: Elscint	JZ uniformity. JZ Max (at 3 points, the anterior,	JZ Max, Endometrial thickness,	Significant reduction in JZ thickness, and lesion

2007 (132)		adenomyotic lesions diagnosed and monitored by MRI	adenomyosis		and/or menorrhagia	malformation, cervical stenosis, history of cancer, postmenopausal status, history of pelvic infection, desire for pregnancy, addition hormone therapy, MRI contraindication	JZ diameter 8-12mm + ill-demarcated or focal thickening JZ with HIS foci	System: 2.0T Slice Thickness: 4.0mm Sequences T2W, T1W	posterior and fundal walls), Endometrial thickness, Uterine volume, presence of HSI foci (on T2)	Uterine volume	size after treatment. Also a concomitant significant reduction in dysmenorrhoea. No direct correlation investigated.
Bratby et al. 2009 (133)	Retrospective observational study (interim results)	Evaluate role of UAE in treating adenomyosis	27 Women with adenomyosis within cohort of women with fibroids	Local hospital (UK)	Women with symptomatic fibroids and adenomyosis on biopsy and MRI	NR	Focal or diffuse JZ >11 mm, HSI foci corresponding to myometrial cysts, poor definition of the JZ and poor definition of the lesion borders	Manufacturer: NR System: NR Slice Thickness: NR Sequences: NR	JZ thickness, Uterine/Adenomyoma volume, presence of HSI foci (unclear if T1 or T2), poor definition of JZ, presence of fibroids	JZ thickness, Uterine volume, Adenomyoma volume	Women with only adenomyosis (vs. adenomyosis and fibroids) showed more lesion reduction after treatment, but had a higher recurrence of menorrhagia.
Byun et al. 1999 (134)	Retrospective observational study	To review and illustrate the spectrum of MRI findings in diffuse and focal	308 patients undergoing hysterectomy	University Hospital (Korea)	Women undergoing hysterectomy that underwent pre-operative MRI because of vaginal spotting,	NR	<u>Diffuse adenomyosis</u>: diffuse ectopic growth of endometrium into myometriu	Manufacturer: GE Signa Advantage System:	JZ thickness, areas of HSI in lesion (on T1/T2), lesion size, shape, location, margin, pseudo-	JZ thickness, lesion size	No

		adenomyosis			premenstrual pelvic pain, dysmenorrhea, suspicion uterine mass or fibroid or other findings.		m with diffuse or focal widening of JZ. Focal adenomyosis: circumscribed mass in the myometrium.	1.5T Slice Thickness: 5 mm Sequences T1W, T2W	capsule and relation to endometrium		
Chapron et al. 2017 (12)	Prospective, observational, cross-sectional study	To investigate the relationship between endometriosis phenotypes (superficial peritoneal, deep infiltrating, ovarian endometrioma) and MRI appearance of adenomyosis	292 patients who underwent uterine surgery	University Hospital (France)	Non-pregnant patients between 18 -42 years of age, and who underwent surgery for symptomatic benign gynaecological conditions, with pre-operative MRI	Visually diagnosed as having endometriosis but lacking histological confirmation	Diffuse adenomyosis: JZ-max > 12 mm, JZ-myometrium ratio max > 40%. Focal adenomyosis: adenomyotic foci located in the outer shell of the uterus, separated from the JZ	Manufacturer: Siemens Sonata System: 1.5T Slice Thickness: 5 mm Sequences T2W, T1W	JZ max, JZ-myometrium ratio, HSI spots within myometrium (on T2), focal lesion size, focal lesion location	JZ max, JZ-myometrium ratio, Focal lesion size	No
Dashottar et al.	Prospective, diagnostic,	To evaluate the MRI findings of suspected	60 women with MRI-confirmed	Tertiary Teaching Hospital (India)	Patients with menorrhagia and MRI findings	(1) Patients with normal sized uterus on USG with normal echo	1) JZ thickness >14mm 2) Poor	Manufacturer: Siemens Magnet	JZ Max, JZ definition, presence of HSI foci (on	JZ Max, Uterus length	MRI phenotype of adenomyosi

2015 (306)	analytical study	cases of adenomyosis, and a comparative analysis of changes in the MRI findings in the pre & post LNG-IUD patients	adenomyosis		suggestive of adenomyosis	texture of the myometrium. (2) JZ< 10mm on MRI (3) Patients who were claustrophobic (4) Patients lost to follow-up/ operated/expulsion of IUD during the study and follow-up period.	definition/ indistinct margins JZ 3) HSI foci in myometrium. 4) JZ thickness 11-13mm and poor definition borders	om Harmony System: 1.0T Slice Thickness: 3-5mm Sequences T1, T2	T1/T2), uterus length, associated uterine lesions		s did not change significantly after treatment, however there was a significant reduction in symptoms.
Fan et al. 2012	Prospective interventional feasibility study	To test the feasibility of MRgHIFUS for treatment of adenomyosis.	10 Patients with symptomatic adenomyosis	University Hospital (China)	(1) Clinical and MRI diagnosis of adenomyosis (2) > 18 years of age, in pre-menopausal status with lesions between 3 and 10 cm in diameter (3) Symptomatic adenomyosis requiring treatment (4) Able to communicate with the nurse or physician during the procedure; (5) Consent for pre/post MRI	(1) Menstruating, pregnant or breastfeeding (2) MRI contraindication (3) Suspected or confirmed uterine malignancy	NR	Manufacturer: GE Omnisc an System: 1.5T Slice Thickness: 4 mm Sequences T2W, T1W, T1-gadolinium CE	Lesion volume, lesion size, localisation, NPV	Lesion volume, Lesion size	Lesion and uterine volume decreased after treatment, alongside symptom reduction. No specific analysis evaluating a correlation between the two outcomes.

Ferrari et al. 2015 (135)	Prospective cohort study	To evaluate the treatment efficacy of uterine adenomyosis using MRgFUS as a mini-invasive therapy	18 patients with symptomatic adenomyosis	University Hospital (Italy)	Premenopausal women affected by adenomyosis, diagnosed on MRI	Contraindications to treatment	JZ >12mm	Manufacturer: GE Signa Excite System: 1.5T Slice Thickness: 4 mm Sequences T1W, T2W	Lesion volume, JZ thickness, Lesion localisation	Lesion volume, JZ thickness	Symptoms reduced, and JZ thickness decreased to <12mm for almost all patients. No direct correlation investigated.
Froeling et al. 2012 (53)	Retrospective cohort study	To evaluate clinical outcome and HRQoL of women with UAE for uterine adenomyosis	40 women with symptomatic adenomyosis	University Hospital (Germany)	Premenopausal women with dominant menorrhagia, dysmenorrhea with or without bulk symptoms, MRI diagnosis of adenomyosis (with fibroids)	Postmenopausal women, active inflammatory disease, undiagnosed pelvic mass, pregnancy, renal insufficiency	JZ>12mm, with or without HSI foci	Manufacturer: Siemens Magnetom Vision or Symphony System: 1.5T Slice Thickness: NR	JZ thickness, presence of HSI foci (unclear if on T1 or T2), adenomyosis type, presence of fibroids	JZ thickness, Uterine volume	Degree of symptom improvement seemingly independent of JZ thickness or adenomyosis type.

								Sequences T2			
Fukunishi et al. 2008 (136)	Prospective cohort study	To evaluate the thermal ablative effects of MRgFUS on adenomyosis and to assess improvement in clinical parameters	20 patients with adenomyosis, with or without fibroids	General Hospital (Japan)	Premenopausal women >18y/o with symptomatic adenomyosis	Submucosal fibroid, Abnormal PAP smear, Pregnant/lactating, Non-accessible lesion, Dialysis patients, Under anti-coagulative therapy, active pelvic infection, Haemolytic anaemia, Cerebrovascular disease, Unstable cardiac status, Pelvic mass outside uterus, Contraindication to MRI, Intolerance to MRI contrast agents, <35% Hematocrit, Extensive abdominal scars anterior to treatment area	JZ>12mm	Manufacturer: GE Signa Excite System: 1.5T Slice Thickness: NR Sequences T1W, T2W, T1 gadolinium CE	JZ thickness, Myometrium diameter, JZ/Myometrium ratio, Uterine volume, post-treatment NPV volume	JZ thickness, JZ/Myometrium ratio, Myometrium thickness, Uterine volume	Degree of symptom improvement seemingly independent of JZ thickness or adenomyosis type.
Gong et al. 2017 (163)	Retrospective cohort study	To investigate the relationship between the features of MRI on T2WI and	428 patients with symptomatic adenomyosis undergoing HIFU ablation	University Hospital (China)	Clinical adenomyosis symptoms, aged over 18 years	Adenomyotic lesion could not be reached or visualised, Suspected/confirmed uterine malignancy, MRI contraindications	Focal/diffuse thickening JZ OR Presence LSI myometrial	Manufacturer: Siemens Magnetom Symphony	Size/location uterus, Size/location adenomyotic lesion, Signal intensity lesion vs normal	Uterine size, Lesion size, Number of HSI foci	No significant difference between treatment response based on

		the therapeutic efficacy of HIFU on adenomyosis.					mass with ill-defined borders	System: 1.5T Slice Thickness: 4 mm Sequences T1W, T2W, gadolinium CE	myometrium, Number of HSI foci on T2, NPV after therapy		MRI phenotype
Gong et al. 2016 (49)	Retrospective cohort study	To investigate factors affecting ablative efficiency of HIFU for adenomyosis	245 patients with symptomatic adenomyosis treated with USgHIFU ablation	University Hospital (China)	Menorrhagia/dysmenorrhoea symptoms, No systemic diseases	Adenomyotic lesion could not be reached or visualised, Pregnancy, Lactation or menstruation, Suspected/confirmed uterine malignancy, MRI contraindications	Focal/diffuse thickening JZ OR Presence LSI myometrial mass with ill-define borders	Manufacturer: Siemens, Magnetom Symphony System: 1.5T Slice Thickness: 4 mm Sequences T1W, T2W, gadolinium CE	Volume of adenomyotic lesion, Location adenomyosis, Uterus location, Number of HSI foci on T2, SI on T2, Enhancement type on T1	Lesion volume, Number of HSI foci	No correlation between symptom reduction and lesion volume, or number of HSI foci

Guo et al. 2017 (164)	Non-randomized prospective study	Investigate clinical efficacy of GnRH-a and HIFU ablation for adenomyosis treatment	79 patients with adenomyosis (55 only HIFU, 24 HIFU+GnRH)	Non-academic Hospital (China)	>18 years, premenopausal, diagnosis of adenomyosis based on MRI, menorrhagia/ dysmenorrhoea, JZ>30mm, unwilling to have hysterectomy/adenomyoectomy, no treatment for 1 year	Menstruation, Pregnancy, lactation, suspected or confirmed endometriosis, Pelvic adhesions, Confirmed or suspected uterine malignancy	Single layer of JZ >30mm	Manufacturer: NR System: NR Slice Thickness: NR Sequences T2	Uterus volume , Adenomyotic lesion volume	Uterus volume , Adenomyotic lesion volume	Severity of dysmenorrhoea no direct correlation with uterine or lesion volume
Hasdemir et al. 2016 (4)	Prospective, randomised study	To compare the presence of adenomyosis on MRI in patients with and without history of preeclampsia	69 women, with PE (n=34) and without (n=35)	University Hospital (Turkey)	Study group: diagnosis of preeclampsia Control: >1 pregnancy without preeclampsia	Control group: History of infertility, Endometriosis, Fibroid, Uterine surgery (except CS), Hydatiform mole	Any one of the following: <u>Direct:</u> Submucosal microcysts, adenomyoma/ cystic adenomyoma. <u>Indirect</u>: JZ >12mm, JZ diff >5mm, JZ/Myometrium Ratio>40%, enlarged uterus, indistinct JZ borders	Manufacturer: GE, Signa System: 1.5T Slice Thickness: 7 mm Sequences T2	Presence of submucosal microcysts (on T2), adenomyoma/ cystic adenomyoma location, lesion size, JZ max, JZ min, JZ diff, JZ/Myometrium ratio	JZ Max, JZ Min, JZ Diff, Mean JZ thickness, JZ-Myometrium ratio, Uterus volume, Lesion volume	Higher mean JZ seen in women with late-onset preeclampsia, More intrauterine growth restriction in women with adenomyomas

Imaoka et al. 2002 (137)	Prospective interventional cohort study	Evaluate uterine changes on MRI before and after GnRH analogue treatment in diffuse adenomyosis	31 patients with MRI features suggestive for diffuse adenomyosis	University Hospital (USA)	Adenomyosis diagnosis based on pelvic pain/menorrhagia symptoms, and MRI imaging	NR	JZ >10mm with indistinct margins	Manufacturer: GE, Signa System: 1.5T Slice Thickness: 5-7 mm Sequences T2, T1	JZ thickness, distinction of JZ margins, uterus location, adenomyosis type, uterine asymmetry, presence of HSI foci on T2, uterine volume, myometrial thickness	JZ thickness, Myometrium thickness, Uterus volume, Uterine asymmetry	All MRI parameters reduced after treatment, no correlation investigated between this and clinical symptoms.
Jha et al. 2003 (138)	Prospective interventional cohort study	To determine the MRI features seen after UAE and to evaluate the clinical response in patients with adenomyosis	Patients with adenomyosis treated with UAE	University Hospital (USA)	Adenomyosis diagnosis based on MRI treated with UAE	NR	JZ >12mm	Manufacturer: Siemens, Magnetom Vision System: 1.5T Slice Thickness: NR Sequences T2W, T1W, T1 CE	Uterus volume, Fibroid volume, JZ thickness, Myometrial thickness, adenomyosis type, presence of HSI foci (on T1 or T2)	Uterus volume, JZ thickness, Myometrial thickness	More symptoms reduction seen in women with pure adenomyosis.

Jha et al. 2014 (139)	Retrospective imaging study	To evaluate differences, if any, in the ADC values of fibroids and adenomyosis	93 patients, 50 with fibroids, 43 with adenomyosis	University Hospital (USA)	Patients with DWI MRI diagnosis of fibroids and adenomyosis	NR	JZ >12mm	Manufacturer: NR System: 1.5T Slice Thickness: NR Sequences T2W, T1W, DWI	ADC values of fibroids and adenomyosis, JZ thickness	ADC values of adenomyosis, JZ thickness	No
Jung et al. 2012 (140)	Retrospective cohort study	To identify imaging predictors for complete necrosis after UAE via quantitative measurement of the SI obtained from MRI of patients with adenomyosis	119 adenomyosis patients who underwent UAE	University Hospital (Korea)	Adenomyosis diagnosed by MRI who underwent UAE, pre-procedural MRI, UAE by same interventionist using the same embolisation protocol, with follow-up MRI 3 months after UAE	Concomitant uterine fibroids	Thickening JZ >12mm, ill-defined LSI on T2 area myometrium, or T2 HSI foci in myometrium	Manufacturer: GE, Signa System: 1.5T Slice Thickness: 5 mm Sequences T2W, T1W, T1-gadolinium CE	Adenomyosis type, Adenomyosis localisation, Adenomyosis lesion size, SI in adenomyosis lesion and rectus muscle (on T2), SI ratio necrosis percentage after UAE	JZ thickness, relative SI ratio, adenomyosis lesion size	A higher T2 SI ratio associated with better therapy response

Kang et al. 1996 (307)	Prospective cohort study	To investigate the specificity of the criterion stating that a diagnosis of adenomyosis can be made confidently from MRI of the uterus when the JZ is > 5 mm	20 women undergoing MRI of the pelvis	University Hospital (USA)	Women, 18-25 years old, nulliparous, no menorrhagia, metrorrhagia, dysmenorrhea, dyspareunia or other symptoms of pelvic disorders, no surgical procedure of the pelvis	Not meeting inclusion criteria	NR	Manufacturer: GE, Signa System: 1.5T Slice Thickness: 4 mm Sequences NR	Uterus length, Anteroposterior and transverse uterine diameter, Maximum thickness of endometrium, JZ Max, JZ thickness anterior/posterior/fundus/right wall/left uterine wall	JZ Max, JZ thickness of anterior/posterior uterine wall, right/left uterine wall and fundus	No
Keserci et al. 2018 (141)	Retrospective cohort study	To assess the relationship between MRI T1 perfusion-based classification and the outcome of MRgHIFU of adenomyosis, defined as NPV ratio	31 women who underwent HIFU treatment for adenomyosis	University Hospital (Malaysia, Vietnam)	18-56 years, with symptomatic adenomyosis	Endometrial disease, pelvic endometriosis, Uncontrolled systemic disease, Menstrual cycle, pregnant, Contraindication for MRI, Suspected malignancy	NR	Manufacturer: Phillips, Ingenia System: 1.5T Slice Thickness: 5 mm Sequences T1W, T2W, T1 dynamic CE	SI-curves vs normal myometrium on T1 CE, JZ thickness, adenomyosis type, adenomyosis volume, NPV ratio	JZ thickness, Adenomyosis volume	More symptom reduction associated with lower SI ratio

Keserci et al. 2018 (52)	Retrospective cohort study	To investigate the MRI features influencing: an immediate NPVr of 90% after HIFU ablation of adenomyosis, clinical efficacy, defined as adenomyosis volume reduction and the symptom severity score improvement of 6 months' follow-up,	66 women who underwent HIFU treatment for adenomyosis	University Hospital (Vietnam)	Symptomatic women with adenomyosis undergoing HIFU ablation	Adenomyosis too deep in pelvis for ablation, Ovarian tumour, Endometriosis, Systematic disease, Cancer disease, Preference for alternative treatment	NR	Manufacturer: Phillips, Ingenia System: 1.5T Slice Thickness: 5 mm Sequences T1W, T2W, T1 dynamic CE	Adenomyosis volume, Adenomyosis location, Adenomyosis type, Uterus position, SI of adenomyosis, Number of HSI foci (on T1), JZ/Myometrium ratio, Volume transfer constant, Reverse reflux rate constant, Volume fraction of extravascular extracellular space, Volume fraction of plasma	Adenomyosis volume, JZ thickness, JZ/Myometrium Ratio, Number of HSI foci	Lesion volume reduction may correlate with symptom reduction
Khandeparkar et al. 2018 (142)	Retrospective cohort study	To assess the impact of high-resolution MRI to detect the subtle nuances of uterine adenomyosis and its	114 primarily infertile patients	Referral Hospital (India)	(a) Clinically diagnosed cases of primary infertility; (b) Suspicion of adenomyosis on TAUS/TVUS; (c) Non-visualization/	(a) Other causes of primary infertility including: Mullerian ductal anomalies, ovulation factors, and, hormonal factors such as hypothalamic-	NR	Manufacturer: Siemens, Magnetom Skyra System: 3.0T	Uterine size, Uterine morphology, Endometrium thickness, Endometrium sharpness, JZ thickness, JZ SI, presence of HSI foci in JZ (on T2),	Uterine size, Endometrium thickness, JZ thickness	No

		associations, and, identify its key mimics prevailing in a subset of sub-fertile or infertile women, and create a structured reporting template which will contain standardized lexicon as well as comprehensive and accurate information			obscuration of the JZ; (d) Multi-parametric MRI performed at 3.0 T	pituitary axis abnormalities; (b) Secondary infertility		Slice Thickness: 3-5 mm Sequences T2W, T1W	JZ/myometrium border sharpness, Adenomyosis type, Presence of fibroids, Presence of endometriosis, Presence of myometrial contractions		
Kissler et al. 2008 (51)	Prospective observational study	To examine whether hyperperistalsis and dysperistalsis are caused by the endometriosis itself or by the adenomyotic component of the disease	41 women with infertility and laparoscopically proven endometriosis, 35 of them with signs of adenomyosis	University Hospital (Germany)	History of infertility and endometriosis diagnosed at laparoscopy with patent fallopian tubes	NR	JZ > 9 mm <u>OR</u> JZ < 9 mm with localised thickening of the JZ, poor definition of borders or HSI foci	Manufacturer: Siemens, Magnetom Symphony System: 1.5T Slice Thickness:	Adenomyosis type, JZ thickness, Myometrial thickness	JZ thickness, Myometrial thickness	More dysperistalsis in diffuse adenomyosis vs. focal, no significant relationship with JZ thickness

								5.5 mm Sequences T1W, T2W			
Kissler et al. 2006 (77)	Prospective observational cohort study	To analyse the extent of adenomyosis using MRI and relate it to the duration of dysmenorrhoea	70 patients with severe dysmenorrhoea	University Hospital (Germany)	Patients with severe dysmenorrhoea with or without infertility	NR	JZ >9mm	Manufacturer: Siemens, Magnetom Symphony System: 1.5T Slice Thickness: 5.5 mm Sequences T1W, T2W	Adenomyosis type, JZ thickness, Myometrial thickness	JZ thickness, Myometrial thickness	Higher JZ associated with longer-term dysmenorrhoea
Kilicksmez et al. 2009 (143)	Prospective observational study	To calculate the normal and diseased ADC values of the uterine zones, and to determine a threshold ADC value	87 patients (35 fibroid, 26 nabothian cysts, 14 endometrial carcinoma, 12 adenomyosis, 10 cervical	University Hospital (Turkey)	Malignant/benign uterine lesion	NR	NR	Manufacturer: Siemens, Avanto System: 1.5T	JZ thickness, Myometrium thickness, ADC values	ADC values per uterine zone (benign, normal, malignant), JZ Thickness, Myometriu	No

		for the detection of uterine malignancies	carcinoma, 10 endometrial polyps), 50 healthy controls (5 perimenopausal, 4 postmenopausal, 41 premenopausal)					Slice Thickness: 6.0 mm Sequences T1W, T2W, DWI, T1-CE		m Thickness	
Kim et al. 2011 (144)	Retrospective observational study (interim results)	To evaluate the degree of symptomatic relief as well as alterations in pain levels after MRgFUS treatment	35 women with adenomyosis that underwent MRgFUS	University Hospital (South Korea)	Women with adenomyosis undergoing MrgFUS treatment with dysmenorrhoea / hypermenorrhoea	Not completing treatment	NR	Manufacturer: NR System: 1.5T Slice Thickness: NR Sequences NR	Adenomyosis type, Presence of fibroids, Uterine volume, JZ/Myometrium ratio, JZ Thickness	Uterine volume, JZ/Myometrium ratio, JZ Thickness	More symptom reduction in diffuse group,
Kim et al. 2011 (169)	Prospective interventional study	To evaluate the safety and effectiveness of a new embolisation technique to achieve complete necrosis of	40 patients with adenomyosis diagnosed on MRI	University Hospital (South Korea)	Adenomyosis diagnosed on MRI without fibroids	Presence of fibroids, Incomplete treatment	JZ >12mm, ill-defined SI, HSI foci	Manufacturer: GE, Signa System: 1.5T	Adenomyosis type, SI on T2, degree of necrosis after UAE, Uterine volume	Uterine volume	Low initial SI associated with better therapy response

		adenomyosis after UAE and to determine predictive factors on MRI						Slice Thickness: 5 mm Sequences T2W T1W			
Kim et al. 2004 (145)	Retrospective interventional cohort study	To evaluate the therapeutic effectiveness of UAE for the treatment of symptomatic pure adenomyosis of the uterus without fibroids	43 women with symptomatic adenomyosis	University Hospital (South Korea)	Symptomatic women with pure adenomyosis undergoing UAE	Presence of fibroids	Poorly defined, low SI mass with or without HSI foci on T2-weighted imaging and thickening of JZ > 12 mm	Manufacturer: Siemens, Magnetom Vision System: NR Slice Thickness: 6 mm Sequences T2W, T1W, T1 CE	Degree of necrosis, Uterine volume, Adenomyosis type, JZ thickness	Uterine volume, JZ thickness	Focal adenomyosis showed a better therapy response. Symptoms and uterine volume significantly decreased after treatment. No direct correlation investigated.
Kitamura et al. 2006 (146)	Prospective observational study	To describe the MRI features of patients with pure or dominant adenomyosis treated	31 women with adenomyosis	University Hospital (USA)	Symptomatic women with clinical suspected adenomyosis	Adenomyosis not being the dominant abnormality	JZ > 12 mm, dominant adenomyosis was diagnosed when coexisting	Manufacturer: Siemens, Magnetom Vision	Uterine volume, JZ thickness, JZ/Myometrium ratio, Adenomyosis distribution	Uterine volume, JZ thickness, JZ/Myometrium ratio	Uterine volume, JZ and JZ/Myo ratio significantly decreased after therapy. No

		with UAE and to correlate imaging features with symptoms					fibroids < 4 cm.	System: 1.5T Slice Thickness: NR Sequences T1W, T2W, T1-Dynamic CE			correlation between MRI parameters and degree of symptom reduction investigated.
Krinsky et al. 1997 (147)	Prospective observational study	To compare images obtained with three different rapid T2-weighted pulse sequences with images from a standard high-resolution MRI of uterine leiomyoma and adenomyosis TSE sequence	18 women referred for MRI with adenomyosis or leiomyoma	University hospital (USA)	Women referred for MRI of the uterus	NR	Diffuse or focal low SI myometrial mass, with indistinct margins, which blended imperceptibly with surrounding myometrium, or as diffuse thickening of the JZ >12mm	Manufacturer: Siemens, Magnetom Vision System: 1.5T Slice Thickness: 4-7 mm Sequences T2W	JZ thickness, Presence of HSI foci (on T2), Adenomyosis type, Presence of fibroids	JZ thickness, Adenomyosis lesion volume, Uterine volume	JZ thickness, and lesion size decreased after therapy. No correlation with symptom reduction investigated.

Kunz et al. 2007 (148)	Prospective observational study	To present a comprehensive view of adenomyosis as a disease possibly affecting women all of ages during the reproductive phase of life	160 women with infertility due to endometriosis, 67 healthy controls	University hospital (Germany)	History of infertility with endometriosis diagnosed by laparoscopy, with a regular menstrual cycle	Irregular menstrual cycle, Bleeding disorder, Uterine anomalies (fibroids, congenital)	NR	Manufacturer: Siemens, Magnetom Impact System: 1.0T Slice Thickness: 3-4mm Sequences T2W	JZ thickness, Myometrium thickness, JZ/Myometrium ratio	JZ thickness, Myometrium thickness, JZ/Myometrium ratio	Larger posterior JZ in women with concomitant endometriosis.
Kunz et al. 2005 (100)	Prospective observational study	To substantiate role of adenomyosis in infertility	160 women with infertility due to endometriosis, 67 healthy controls	University hospital (Germany)	History of infertility with endometriosis diagnosed by laparoscopy, with a regular menstrual cycle	Irregular menstrual cycle, Bleeding disorder, Uterine anomalies (fibroids, congenital)	NR	Manufacturer: Siemens Magnetom Impact System: 1.0T Slice Thickness: 3-4mm Sequences T2W	JZ thickness, Endometrium length, Uterine length, Total myometrium thickness	Endometrium length, JZ thickness, Myometrium thickness, Uterine length	Women with endometriosis also had the most extensive adenomyosis. No correlation with degree of endometriosis infiltration.

Larsen et al. 2011 (149)	Prospective observational study	To evaluate image findings in the JZ in patients with endometriosis and correlate with image findings of adenomyosis. To attempt a correlation of the degree of adenomyotic infiltration with the degree of infiltration and stage of endometriosis	Group 1: Patients with suspected DIE (n= 153), Group 2: Cervical cancer patients (n=29), Group 3: Patients undergoing hysterectomy for benign conditions (n=100)	University Hospital (Denmark)	153 Patients with suspected DIE about to undergo surgery, and 129 without endometriosis before hysterectomy	NR	(a) In the presence of focal poorly demarcated LSI areas in the myometrium with HSI myometrial spots arising from the JZ, OR (b) JZ >15 mm OR (c) when a JZ-diff of >5 mm was present.	Manufacturer: GE, Signor Phillips, Achieva System: 1.5T Slice Thickness: 4mm Sequences T2W	JZ min, JZ max, JZ Diff, Poor JZ definition, JZ/Myometrium ratio, Presence of HSI foci (on T2), Uterine wall thickness	JZ Min, JZ Max, JZ Diff, Anterior/ posterior uterine wall thickness, JZ/Myometrium ratio	Higher mean JZ in women with (more severe) endometriosis
Lee et al. 2017 (165)	Prospective interventional cohort study	To assess the changes in AMH levels after ablation for symptomatic uterine fibroids and adenomyosis using USgHIFU	79 Patients with uterus fibroids and adenomyosis (fibroid n=45, adenomyosis n=34)	University hospital (South Korea)	Symptomatic uterine fibroids and adenomyosis	(1) Pedunculated uterine fibroids, Asymptomatic uterine fibroids <5 cm in diameter; (2) Asymptomatic focal adenomyosis; (3) Abdominal wall thickness of > 5 cm;	NR	Manufacturer: NR System: NR Slice Thickness: NR	Adenomyosis lesion volume	Adenomyosis lesion volume	No

						(4) Suspected malignancy; (5) Evidence of known or suspected extensive pelvic adhesions such as a history of acute pelvic inflammatory disease and severe pelvic endometriosis; (6) BMI > 25, a history of smoking, alcohol, endocrine disease, polycystic ovarian disease, lower abdominal surgery including ovarian surgery, and chemotherapy prior to this treatment		Sequences T2W, T1W			
Leyendecker et al. 2015 (8)	Retrospective observational study	(1) To corroborate the concept of auto-traumatisation by re-visiting, in view of discrepant results in the literature,	143 women with suspected adenomyosis on the basis of TVUS and symptoms	Referral Hospital (Germany)	Age 18-42, TVUS MUSA criteria; Optional: with endometriosis, dysmenorrhoea	Fibroids	JZ > 12 mm <u>OR</u> JZ <12mm, with: cystic structures within the JZ, focal thickening of the JZ that could	Manufacturer: Siemens, Magnetom Impact System: 1.0T	JZ thickness, Anterior/Posterior max uterine wall diameter, Lesion localisation, Adenomyosis type, Presence of cystic	JZ thickness, Maximum uterine wall thickness (anterior vs. posterior)	More endometriosis is in group with higher mean JZ.

		the association of adenomyosis with endometriosis and (2) to extend our views concerning the mechanisms of uterine auto-traumatization.					not be related to functional alterations	Slice Thickness: 3 mm Sequences T2W, T1W	structures (on T2)		
Lohle et al. 2007 (150)	Multi-centre Retrospective study	To evaluate clinical and MRI results after UAE in women with symptomatic adenomyosis with or without uterine leiomyoma	38 women with symptomatic adenomyosis treated with UAE (adenomyosis only n=12, adenomyosis dominance with fibroids, n=12, fibroid dominance n=8)	2 public hospitals (Netherlands & Germany)	Women having undergone UAE	NR	Diffuse or focal broadening of the JZ >12mm with LSI on T2W images, with or without punctate HSI myometrial foci corresponding to myometrial cysts	Manufacturer: Siemens, Magnetom Vision/ Symphony System: 1.5T Slice Thickness: 5 mm Sequences	Uterine volume, Fibroid volume, JZ thickness, Contrast enhancement, Adenomyosis type	Uterine volume, JZ thickness	More JZ decrease in fibroid group. Significant uterine volume reduction after treatment. No specific correlation between these parameters and symptom reduction investigated.

								T2W, T1W, T1-CE			
Long et al. 2015 (166)	Prospective interventional study	To evaluate the efficacy, safety and sexual life quality outcomes of ultrasound-guided HIFU ablations for the treatment of patients with symptomatic adenomyosis and uterine volumes >200 cm3	51 adenomyosis patients with a uterine volume >200 cm3	University Hospital (China)	Adenomyosis diagnosis confirmed by at least two gynaecologists and HIFU physicians according to clinical manifestations and MRI. >18 years, no medical treatments at 3 months before surgery. Patients with adenomyosis >3 cm diameter, located at unilateral uterine muscle walls with surgical indications, had desire to receive treatments and complied with 12 month follow-up. Accurate communication with physicians	Acute pelvic inflammation or acute episodes of chronic pelvic inflammation, patients during menstruation, pregnancy and lactation periods. Connective tissue illnesses or received abdominal radiotherapy with a large dosage. Patients which had undergone enhanced MRI and had anaesthetic contraindications	NR	Manufacturer: SIemens, Magnetom Vision System: 1.5T Slice Thickness: NR Sequences: T1W spin-echo, T2W spin-echo, T1W gradient-echo	Size and location of lesions (anterior or posterior wall). Lesion and uterus volume	Uterus volume, adenomyosis lesion volume	Uterine and lesion volume reduced after therapy. No specific correlation investigated between volume reduction and degree of symptom reduction.

					and nurses, no other complications, <51 years, partners alive						
Marcellin et al. 2018 (151)	Prospective observational cross-sectional study	To evaluate the association between bladder DIE and anterior focal adenomyosis of the outer myometrium (aFAOM) diagnosed by preoperative MRI.	Women undergoing surgical excision of endometriosis	University hospital (France)	<42 years, non-pregnant, with surgery of endometriosis lesions	No pre-operative MRI, Women with cancer, Infectious disease, No consent	<u>Diffuse adenomyosis:</u> JZ Max> 12 mm and maximal JZ/myometrial ratio > 40%. FAOM: presence of HSI foci within the myometrium on axial and sagittal T2 planes. <u>Focal adenomyosis:</u> corresponds to subtype II (extrinsic) according to the Kishi classification and must be considered	Manufacturer: Siemens, Sonata System: 1.5T Slice Thickness: 5mm Sequences T2W, T1W	Adenomyosis type, localisation, JZ thickness, JZ Max, JZ/myometrium ratio, myometrium thickness. Adenomyosis volume, HSI foci (on T2), posterior FAOM	Adenomyosis volume, JZ thickness, JZ Max, Myometrium thickness, JZ/Myometrium ratio	No correlation between symptoms and adenomyosis (subtype) on MRI.

							as focal adenomyosis is located in the outer myometrium (FAOM).				
Nijenhuis et al. 2015 (60)	Prospective observational study	To assess midterm outcome of UAE for women with therapy resistant adenomyosis using polyzene F-coated hydrogel microspheres	29 women with adenomyosis (15 in combination with fibroids)	University Hospital (Netherlands)	Women with therapy-resistant adenomyosis with or without fibroids, suffering from heavy menstrual pain or bulk related symptoms or a combination	Pregnancy, Suspicion or presence of a malignancy or infection, Already infarcted fibroids, Post-menopausal status, Asymptomatology and women who wished to conceive	LSI of the myometrium on T2W images, Diffuse or focal thickening of JZ >12 mm with or without HSI foci corresponding to myometrial cysts	Manufacturer: NR System: NR Slice Thickness: NR Sequences T2W,, T1W, T1-CE	JZ thickness, Uterine volume, Infarction percentage of fibroids and uterus	JZ thickness, Uterus volume	JZ thickness could predict therapy response. Higher baseline JZ associated with symptom recurrence.
Parker et al. 2006 (152)	Prospective clinical trial	To evaluate whether persistence of pelvic pain after excision of endometriosis was associated with adenomyosis as defined by a	53 women with chronic pelvic pain	Government research hospital (USA)	Reproductive aged women with chronic pelvic pain.	NR	JZ > 11 mm	Manufacturer: NR System: NR Slice Thickness: NR Sequences	JZ thickness, Presence of endometriosis	JZ thickness	Higher mean JZ associated with less symptom reduction, higher baseline pain levels, age and parity. Endometriosis stage not associated

		thickened JZ on MRI						T2W			with JZ thickness.
Park et al. 2015 (153)	Prospective cohort study	To determine the usefulness of the ADC in predicting response to UAE for symptomatic adenomyosis	25 patients undergoing UAE for symptomatic adenomyosis	University Hospital (South Korea)	Patients who visited the study site for symptomatic adenomyosis (menorrhagia, dysmenorrhoea, or bulk-related symptoms)	Patients desiring future pregnancy	Diffuse or focal thickening >12mm of the JZ, an ill-defined, LSI area of the myometrium, or punctate HSI myometrial foci on T2W images	Manufacturer: GE, Signa System: 3.0T Slice Thickness: 4 mm Sequences DWI, T2W, T1W	ADC values, JZ thickness, Adenomyosis type, HSI foci (on T2), Uterine volume	ADC value, JZ thickness, Uterine volume	Lower ADC value associated with better treatment response.
Pelage et al. 2005 (154)	Prospective interventional cohort study	To evaluate the midterm results of UAE for symptomatic adenomyosis	18 women with symptomatic adenomyosis	Referral hospital (France)	Symptoms related to adenomyosis, therapy with progestogen, haemostatic agents, or GnRH agonists had failed	Associated fibroids	Myometrial LSI, diffuse or focal thickening >12mm of the JZ, HSI foci corresponding to myometrial cysts, poor definition of the JZ, and poor definition of lesion borders	Manufacturer: GE, Signa System: 1.5T Slice Thickness: NR Sequences T2W, T1W	JZ Thickness, poor definition JZ, presence of myometrial cysts , presence of HSI foci (on T2), Uterine volume, Adenomyosis volume	JZ thickness, Uterine volume, Adenomyosis volume	Uterine and lesion volume reduced after treatment, as did symptoms. No direct correlation investigated.

Sam et al. 2019 (155)	Multicentre retrospective cohort study	To determine the diagnostic accuracy of commonly described sonographic findings in predicting uterine adenomyosis	649 patients undergoing MRI and ultrasound	3 Teaching hospitals (Canada)	Patients that underwent ultrasound 12 months or more before pelvic MRI, 18 years or older, whose definitive diagnosis for the presence/absence of adenomyosis was documented on the clinical MRI report	Cases involving equivocal diagnosis of adenomyosis on MRI or those in which MRI was not evaluable. Cases in which adenomyosis was detected incidentally	JZ thickness > 12 mm OR JZ thickness 8-12 mm with the presence of at least one of the following: myometrial cysts, JZ Diff >5mm and maximum JZ/Myometrium Ratio >40%	Manufacturer: NR System: 1.5T Slice Thickness: 4-6 mm Sequences T1W, T2W	Uterus volume, JZ thickness, JZ Diff, JZ/Myometrium Ratio, SI of myometrium (on T2)	Uterus volume, JZ thickness, JZ Diff, JZ/Myometrium Ratio,	No
Siskin et al. 2001 (156)	Retrospective cohort study	To evaluate the MRI appearance and clinical response of patients undergoing UAE for the treatment of menorrhagia due to adenomyosis	15 patients with adenomyosis and menorrhagia	University Hospital (USA)	Women visiting the outpatient clinic initially diagnosed with uterine fibroids by their gynaecologists, with signs of adenomyosis on MRI	NR	JZ > 12mm. Presence of myometrial HSI foci was considered ancillary evidence of adenomyosis	Manufacturer: GE, Signa System: 1.5T Slice Thickness: 5 mm Sequences T2W, T1W	JZ Thickness, JZ Max, Adenomyosis type, Uterine volume, Presence of fibroids, Fibroid volume	JZ Thickness, JZ Max, Uterine volume	JZ thickness, Uterine volume and symptoms reduced after treatment. No direct correlation investigated.
Smeets et	Retrospective	To evaluate long-term	40 women with	Regional hospital	Women with adenomyosis	NR	Diffuse or focal JZ	Manufacturer:	JZ Thickness, adenomyosis	JZ thickness	No direct correlation

al. 2012 (59)	intervent ional cohort study	outcomes of UAE in women with adenomyosi s.	adenomyosi s	(Netherl ands)	having undergone UAE		thickness >12mm with myometrial LSI on T2W	NR System: NR Slice Thicknes s: NR Sequen ces T1W, T2W	type, presence of HSI foci (on T1/T2)		between degree of JZ reduction and degree of symptom reduction. However, higher baseline JZ associated with therapy resistance and more symptom severity.
Sofic et al. 2016 (157)	Prospect ive, compar ative study	To define the MRI appearance of disorder in the JZ in women with adenomyosi s compared to those without	Adenomyosi s patients (n=82) vs. Control (n=82)	Universit y Hospital (Bosnia)	Women with adenomyosis on MRI	NR	JZ > 12mm	Manufa cturer: Siemens or GE System: 1.5T Slice Thicknes s: 2 mm Sequen ces T2W, T1W	JZ Thickness, Adenomyosis type, Presence of fibroids or endometriosis	JZ Thickness	No
Song et al. 2011 (158)	Retrospe ctive cohort study	To evaluate the MRI features of uterine adenomyom	7 patients with surgically proven	Universit y Hospital (South Korea)	Patients having undergone surgical removal of adenomyomas,	NR	JZ > 12 mm OR ill-defined LSI myometrial	Manufa cturer: Siemens , Magnet	Lesion size, location, margin, presence of adenomyosis,	Adenomyo ma size, JZ thickness	No

		a in comparison with histopathologic findings.	adenomyomas		with pre-operative MRI		mass with embedded HSI foci on T2W images	om Sonata System: 1.5T Slice Thickness: 4-5 mm Sequences T1W, T2W, T1-CE	Lesion SI, SI pattern of lesion borders (on T1/T2)		
Stoelinga et al. 2014 (159)	Prospective diagnostic evaluation study	To estimate the inter-observer agreement and reproducibility of real-time sono-elastography and real-time gray-scale US in the measurement of uterine and fibroid volumes. To evaluate agreement between real-time gray-scale	Premenopausal women suspected of having fibroids (n=10), adenomyosis (n=10), 10 women without gynaecologic disorders or current complaints	University Hospital (Netherlands)	Premenopausal women: 10 with uterine fibroids, 10 with adenomyosis, 10 with no gynaecologic disorders.	Patients who had started medication or had undergone uterine surgery in the period between US and MRI	JZ >12mm or JZ Diff > 5mm	Manufacturer: Siemens Sonata or Avanto System: 1.5T Slice Thickness: 4mm Sequences T2	JZ Thickness, JZ Diff, Uterine length, width, diameter, Uterine volume, Presence of fibroids, Fibroid volume	JZ thickness, JZ Diff, Uterus volume, Uterine length/width/diameter	No

		US, sono-elastography and MRI with respect to these outcomes. To evaluate the diagnostic accuracy of sono-elastography in the diagnosis of uterine pathology on stored sono-elastography and gray-scale cine loops									
Streuli et al. 2016 (160)	Prospective cross-sectional study	To assess whether serum osteopontin levels are different according to specific MRI phenotypes of adenomyosis and endometriosis	148 non-pregnant women <42 years, undergoing surgery for a benign gynaecological condition and who had a pre-operative pelvic MRI	University Hospital (France)	All non-pregnant women <42 years who underwent a surgical intervention by laparoscopy or laparotomy for a benign gynaecological indication	Women with cancer or borderline tumours, those who did not consent to the study	<u>Diffuse Adenomyosis</u> JZ Max >12 mm and/or JZ /Myometrium Ratio>40% and/or HSI myometrial spots . <u>Focal adenomyosis;</u>	Manufacturer: NR System: NR Slice Thickness: NR Sequences NR	Adenomyosis type, JZ thickness, Myometrial thickness, JZ/myometrium ratio, Presence of HSI foci (on T2)	JZ thickness, JZ Max, myometrial thickness, JZ/Myometrium ratio	Focal adenomyosis associated with best therapy response. Significant uterine volume and symptom reduction after treatment. No direct

							localized, ill-defined, LSI mass in the myometrium				correlation investigated.
Verma et al. 2009 (161)	Retrospective cohort study	to describe the sono-hysterographic features of adenomyosis with MRI correlation	26 women who underwent SHG and MRI with suspected adenomyosis	University Hospital (USA)	Women with suspected adenomyosis undergoing SHG and MRI	NR	One of the following: JZ > 12 mm, JZ cysts, or indistinct JZ margins	Manufacturer: GE, Signa System: 1.5T Slice Thickness: 5-6 mm Sequences T2W, T1W, CE	JZ thickness, JZ irregularity, Adenomyosis type	JZ thickness	No
Wang et al. 2016 (170)	Prospective interventional cohort study	To evaluate the safety and efficacy of UAE for the treatment of adenomyosis.	117 Premenopausal patients diagnosed with adenomyosis	Teaching hospital (China)	Premenopausal patients presenting with adenomyosis with heavy menstrual bleeding and dysmenorrhea	Confirmed pregnancy, active pelvic inflammatory disease, renal insufficiency, undiagnosed pelvic mass, or urogenital infections	NR	Manufacturer: NR System: NR Slice Thickness: NR Sequences	Uterine volume	Uterine volume	Significant decrease in uterine volume after treatment. No relationship to clinical outcomes mentioned.

								NR			
Xia et al. 2014 (162)	Prospective feasibility study	To evaluate the feasibility of energy prediction of percutaneous microwave ablation (PMWA) upon uterine fibroids and adenomyosis by MRI	63 patients (fibroids = 49, adenomyosis=14)	Regional hospital (China)	Patients with uterine fibroids and adenomyosis who had been diagnosed by ultrasonography and CE MRI; Patients who had experienced one of the following symptoms for > 1 year: menorrhagia or metrorrhagia, dysmenorrhoea, lower abdominal pain, bulk pressure or urinary frequency; Pre-menopausal patients > 18. years of age; Patients with no reproductive needs	Menstruating, pregnant or breastfeeding females; Pelvic infection, coagulation disorders, heart or brain disease or malignant tumours	JZ >5mm and lesion size >3 cm	Manufacturer: GE, Signa System: 1.5T Slice Thickness: 5 mm Sequences T1W, T2W, CE	SI of lesion (on T1/T2), Lesion volume, JZ thickness, Fibroid size	Lesion volume, JZ thickness	No
Xiong et al. 2015 (167)	Retrospective cohort study	To compare therapeutic efficacy and adverse effects of USgHIFU	534 patients with adenomyosis	University Hospital (China)	NR	NR	Diffuse or focal thickening of JZ or presence of a LSI	Manufacturer: Siemens, Magnetom	Lesion size, Lesion localisation, Lesion SI, Uterine volume	Uterine volume, Lesion size	No

		treatment for adenomyotic c patients with or without prior abdominal surgical scars					myometrial mass with ill-defined borders	Sympho ny System: 1.5T Slice Thicknes s: 4 mm Sequen ces T1			
Yang et al. 2011 (172)	Retrospe ctive cohort study	To investigate the value of DWI-MRI, especially ADC in the differentiatio n of uterine adenomyosi s and fibroids	39 patients (fibroid n=17, adenomyosi s n=22)	Universit y Hospital (China)	Histopathologic confirmed uterine fibroid or uterine adenomyosis; underwent DWI	Endometrial carcinoma; Leiomyosarcoma of uterus	Histopathol ogical diagnosis, not specified for MRI	Manufa cturer: Siemens , Magnet om Trio System: 3.0T Slice Thicknes s: 5 mm Sequen ces T1W, T2W, DWI	ADC values, SI, presence of HSI foci (on T1/T2)	ADC values	Higher ADC values in adenomyosi s vs. fibroids. No correlation to clinical outcomes investigated.
Yang et al. 2019 (171)	Prospect ive intervent ional	To evaluate the combined efficacy of	466 adenomyosi s patients with	Universit y Hospital (China)	(1) Clinical symptoms of progressive dysmenorrhea	(1) Pregnancy, lactation or menstruation;	Not specified (only	Manufa cturer: NR	Uterine volume, Adenomyosis type	Uterine volume	No specific correlation between MRI

	cohort study	HIFU, GnRH-a) and the (LNGIUS) for the treatment of severe adenomyosis	moderate to severe dysmenorrhoea	and/or menorrhagia and no dyspareunia; (2) A large uterine size > 12 weeks pregnancy, an irregular spherical shape during gynaecological examination or a uterine cavity > 9 cm by hysteroscopy; (3) Enlargement of the uterus, an uneven echo of the myometrium and an unclear myometrium and lesion size by TVUS examination; (4) No use of steroid hormones or GnRHa 6 months before treatment and no contraindications for GnRH-a and an	(2) Acute pelvic inflammation; (3) Suspected gynaecological malignancy; (4) History of radiotherapy; (5) Inability to communicate with doctors during the procedure	based on TVUS)	System: NR Slice Thickness: NR Sequences NR	parameters and symptom reduction investigated.

					intrauterine contraceptive; (5) Refusal for surgery; (6) Normal liver and kidney functions.						
Zhang et al. 2013 (168)	Retrospective cohort study	To evaluate the effects of USgHIFU on adenomyosis	202 Patients with adenomyosis who underwent USgHIFU	University Hospital (China)	Women who underwent USgHIFU for adenomyosis	NR	<u>Diffuse Adenomyosis:</u> JZ thickness >30 mm for diffuse adenomyosis <u>Focal Adenomyosis:</u> Lesion diameter >30 mm	Manufacturer: NR System: NR Slice Thickness: NR Sequences T2W, T1W	Uterine volume, Adenomyosis lesion volume, NPV ratio in adenomyotic lesion	Uterine volume, Adenomyosis lesion volume	More symptom relief in focal adenomyosis.

NR: Not reported, MRI: magnetic resonance imaging, CE: contrast-enhanced, JZ: junctional zone, TVUS: transvaginal ultrasound, SI: signal intensity, LSI: low signal intensity, HSI: high signal intensity, UAE: uterine artery embolization, HIFU: high intensity focused ultrasound, ADC: apparent diffusion coefficient, DWI: diffusion weighted imaging, (HR)QoL: (Health Related) Quality of Life, MRgFUS: MR-guided Focused Ultrasound, LNG-IUS/D: levonorgestrel intrauterine system/device,

2. D Risk of Bias Assessment and Applicability of Diagnostic Accuracy Studies

According to the QUADAS-II Checklist (https://annals.org/aim/fullarticle/474994/quadas-2-revised-tool-quality-assessment-diagnostic-accuracy-studies)

Table 2.S7 Patient Selection: Risk of Bias and Applicability

Author, Year	Method of patient selection	Included patients	Consecutive or random patients enrolled?	Case-control design avoided?	Inappropriate exclusion avoided?	Bias in patient selection process?	Do the included patients match the review question?
Ascher et al. 1994	Prospective	see inclusion criteria	Yes	Yes	Unclear	Low	Yes
Badawy et al. 2014	Prospective	see inclusion criteria	Yes	Yes	Yes	Low	Yes
Bazot et al. 2001	Prospective	see inclusion criteria	Yes	Yes	No (some patients excluded due to difficulty in making contact)	Low	Yes
Bazot et al. 2003	Prospective	see inclusion criteria	Yes	Yes	Yes	Low	Yes
Dueholm et al. 2001	Prospective	see inclusion criteria	Yes	Yes	Yes	Low	Yes
Hamimi et al. 2015	Retrospective	see inclusion criteria	No	Yes	Unclear	High, due to retrospective nature	Yes
Hricak et al .1992	Retrospective	See inclusion criteria	Yes	Yes	Unclear	High, due to retrospective nature	Yes
Masui et al. 2003	Prospective	See inclusion criteria	Yes	Yes	Yes	Low	Yes
Moghadam et al. 2006	Retrospective	See inclusion criteria	Unclear	no	Yes	High, due to retrospective nature	Yes

Phillips et al. 1996	Prospective	See inclusion criteria	Yes	Yes	Yes	Low	Somewhat, only included adenomyoma patients instead of adenomyosis generally
Reinhold et al. 1996	Prospective	see inclusion criteria	Yes	Yes	Yes	Low	Yes
Stamatopoulos et al. 2012	Prospective	see inclusion criteria	Yes	Yes	Yes	Low	Yes
Tellum et al. 2019	Prospective	see inclusion criteria	Yes	Yes	Yes	Low	Yes
Tian et al. 2016	Prospective	see inclusion criteria	Yes	Yes	Yes	Low	Yes

NR: not reported

Table 2.S8 Index Test: Risk of Bias and Applicability

Author, Year	MRI method	MRI interpretation	Evaluation by experienced radiologist?	MRI (re) evaluated in real-time during study procedures?	Blinded to result of histopathology?	Pre-specified definition for adenomyosis on MRI?	Menstrual cycle accounted for?	Potential for bias in MRI interpretation?	Does the application of the MRI match the research question?
Ascher et al. 1994	System: 1.0T or 1.5T Slice Thickness: 5mm Sequences: T2W, T1W, T1 gadolinium CE	(a) a myometrial mass with indistinct margins of primarily LSI with all sequences or (li) diffuse or focal widening of the JZ (>5mm)on T2W, fast T2W SE images, and CE T1W images. The	NR	Yes	Yes, Multiple investigators, not necessarily radiologists	Yes	Yes, only MRI in luteal phase	Low	Yes

		presence HSI foci was used as an ancillary finding							
Badawy et al. 2014	System: 1.5T Slice Thickness: 5mm Sequences: T1W (CE), T2W, STIR	No clear definition of adenomyosis prior to diagnosis	NR	Yes	Unclear	Unclear	NR	High, seemingly no predefined definition	Yes
Bazot et al. 2001	System: 1.5T Slice Thickness: 5mm Sequences: T2W, T1W	(i)large, regular, asymmetric uterus without leiomyoma, (ii) JZ Max>12mm and/or ill-defined LSI myometrial area, (iii) JZ/Myometrium ratio >40%, (iv) HSI foci	Yes	Yes	Yes, 2 blinded observers	Yes	No	Low	Yes
Bazot et al. 2003	T2W TSE		Yes	Yes	Yes	Yes	No	Low	Yes
Dueholm et al. 2001	System: 1.5T Slice Thickness: 4mm Sequences: T2	Diffuse: JZ Max >15 mm, OR, JZ of 12–15 mm with non-uniform, thickened JZ or focal not well-demarcated high or low intensity areas in the myometrium	Yes	Yes	Yes, Single observer, blinded	Yes	NR	Unclear	Yes
Hamimi et al. 2015	System: 1.5T	MRI: Intramyometrial cyst(s). Heterogeneo	Not mentioned	Unclear	Unclear	No	NR	Unclear	Yes

	Slice Thickness: 13mm Sequences: T1, T2, T1 gadolinium CE	us myometrium usually heterogeneously hyperintense. JZ >12mm							
Hricak et al. 1992	Manufacturer: GE Signa System: 1.5T Slice Thickness: 5mm Sequences: T1W, T2W, T1 gadolinium CE	Enlarged uterus with smooth border, presence of HSI foci	Yes	Yes	Yes	Yes	NR	Low	Yes
Masui et al. 2003	Manufacturer: GE Horizon LX Echo Speed System: 1.5T Slice Thickness: 5-6mm Sequences: T2W, T2-FSE, T2-SSFSE	Ill-defined LSI lesions with or without HSI spots or having focal or diffuse thickening of the JZ >12 mm	Yes	NR	Yes	Yes	NR	Low	Yes
Moghadam et al. 2006	System: 1.5T Slice thickness: NR	Focal or diffuse widening of JZ> 12 mm, uterine enlargement, or both, with	Yes	NR	Unclear	Yes	No	Unclear	yes

	Sequences: T2, T1	focal or diffuse LSI myometrial area in T2-weighted images, on CE T1 small HSI myometrial spots were indicative of adenomyosis.							
Phillips et al. 1996	Manufacturer: NR System: NR Slice thickness: NR Sequences: T2W, T1W	Unclear	Yes	Yes	Yes	Yes	No	Low	Somewhat, only adenomyoma
Reinhold et al. 1996	System: 1.5T Slice Thickness: 5mm Sequences: T2W	Subjective impression of localized or diffuse thickening of the uterine JZ (with or without the presence of HSI foci in the JZ) or the presence of a low-SI myometrial mass with ill-defined borders	Yes	Yes	Yes	Yes	No	Low	yes
Stamatopoulos et al. 2012	System: 1.0T Slice Thickness: NR Sequences:	When the JZ > 12 mm, focal not well-demarcated areas were present in the myometrium,	Yes	Yes	Yes	yes	No	Low	Yes

	T1W, T2W	and non-uniform JZ							
Tellum et al. 2019	System: 3.0T or 1.5T Slice Thickness: NR Sequences: T1W, T2W	one or more of JZ Max ≥ 12 mm, myometrial cysts, or adenomyoma which are comprehensively described elsewhere were present	Yes	Yes	Yes	yes	No	Low	yes
Tian et al. 2016	System: NR Slice Thickness: 5mm Sequences: T1W, T2W, DWI	NR	Yes	Yes	Yes	No	No	High, no predefined definition	yes

NR: not reported

Table 2.S9 Reference Standard: Risk of Bias and Applicability

Author, Year	Interpretation of histopathology	Evaluated by experienced pathologist?	Blinded to MRI diagnosis?	Likely to have correctly identify adenomyosis using this method?	Potential for bias in histopathological diagnosis?	Does the application of the histopathological diagnosis match the research question?
Ascher et al. 1994	Endometrial glands and stroma lying deeper than 2.5 mm below the endometrial surface.	Evaluated by pathologists, degree of experience unknown	Unclear	Yes	High, not blinded	Yes
Badawy et al. 2014	NR	NR	Unclear	Unclear	Unclear, not mentioned if blinded	Yes
Bazot et al. 2001	Macroscopic: enlarged uterus and a dense anarchically fasciculated unlimited myometrium with small cavities (5-10mm(. Microscopic: presence of ectopic endometrial tissue within myometrium 2.5mm beyond the endometrial/ myometrial junction.	Yes	Yes, One pathologist, blinded	Yes	Low	Yes
Bazot et al. 2003	Macroscopic: enlarged uterus and a dense anarchically fasciculated unlimited myometrium with small cavities (5-10mm(. Microscopic: presence of ectopic endometrial tissue within myometrium 2.5mm beyond the endometrial/ myometrial junction.	Yes	Yes	Yes	Low	Yes

Dueholm et al. 2001	presence of endometrial glands or stroma deep in the endometrial–myometrial junction and the diagnostic criterion of adenomyosis was satisfied when it exceeded one medium power (3100) field (i.e., ;2 mm deep into the endometrial–myometrial junction)	Yes	Yes, Single observer, blinded	Yes	low	Yes
Hamimi et al. 2015	Not mentioned	Not mentioned	Unclear	Unclear	Unclear, unknown what definition or method was used	Unclear
Hricak et al. 1992	NR	Yes	Yes	Unclear	Unclear	Yes
Masui et al. 2003	NR, but only after hysterectomy	Yes	Yes	Unclear	Unclear, unknown what definition or method was used	Unclear
Moghadam et al. 2006	Not mentioned	Yes	No, retrospective	yes	unclear	yes
Phillips et al. 1996	Myometrial biopsy	Yes	Unclear	Yes	High, biopsy less accurate	Somewhat, as only biopsies were taken.
Reinholdt et al. 1996	Endometrial glands and/or stroma > 1 HPF deep to the endometrial myometrial junction	Yes	Yes	yes	low	yes
Stamatopoulos et al. 2012	Ectopic endometrium >2 mm deep in the myometrium or .1 microscopic field at 10-fold	Unclear	No	yes	High, not blinded	yes

	magnification from the endomyometrial junction; adenomyotic foci circumferentially surrounded by bundles of hypertrophic smooth muscle cells at HE staining; or stromal fibroblasts clearly differed cytologically from the adjacent smooth muscle cells. Diffuse: endometrial glands or stroma were diffusely distributed in the myometrium. Focal: circumscribed nodular aggregates of glands or stroma were found within the myometrium. Adenomyomas: circumscribed mass was found, composed of more than rare glands, predominantly of the endometrial type, and a stromal component that consisted primarily of smooth muscle					
Tellum et al. 2019	presence of ectopic endometrial glands and stroma at 2.5 mm below the endometrial-myometrial junction	Yes	Yes	yes	Low	yes
Tian et al. 2016	NR	Unclear	Unclear	Unclear	Unclear	yes

Table 2.S10 Patient Flow and Timing: Risk of Bias and Applicability

Author, Year	Any patients that did not receive MRI or pathology or excluded from 2 x 2 table?	Interval/intervention between MRI and histopathological diagnosis	Appropriate interval between MRI and histopathology?	All patients received (the same) histopathology diagnosis?	All patients included in analysis?	Potential for bias in patient flow?
Ascher et al. 1994	No.	NR	Unclear	No, some diagnosed by biopsy and others by hysterectomy	Yes	Low
Badawy et al. 2014	No.	NR	Unclear	Yes	Yes	Low
Bazot et al. 2001	No.	NR	Unclear	Yes	Yes	Low
Bazot et al. 2003	No	NR	Unclear	Yes	Yes	Unclear
Dueholm et al. 2001	No	2 weeks	Yes	Yes	Yes	Low
Hamimi et al. 2015	No.	NR	Unclear	No, patients received different methods of reference diagnosis	Yes	Unclear
Hricak et al. 1992	No	NR	Unclear	Unclear	Yes	Unclear
Masui et al. 2003	No	NR	Unclear	Unclear	Yes	Low
Moghadam et al. 2006	Unclear	NR	Unclear	Yes	Yes	Low
Phillips et al. 1996	No	NR	Unclear	No, some had transabdominal biopsy	Yes	Unclear
Reinholdt et al. 1996	No	14 days	Yes	Yes	Yes	Low
Stamatopoulos et al. 2012	NR	NR	Unclear	Yes	Yes	Low
Tellum et al. 2019	No	NR	Unclear	Yes	Yes	Low
Tian et al. 2016	No	NR	Unclear	Yes	Yes	Low

NR: not reported

2E. 2 x 2 Tables and SROC Curves per MRI Parameter

MRI Overall:

Figure 2.S1 RevMan 2 x 2 Tables and Forest Plots

Study	TP	FP	FN	TN	Sensitivity (95% CI)	Specificity (95% CI)
Hricak 1992	17	0	2	16	0.89 [0.67, 0.99]	1.00 [0.79, 1.00]
Ascher 1994	15	0	2	3	0.88 [0.64, 0.99]	1.00 [0.29, 1.00]
Phillips 1996	18	2	0	0	1.00 [0.81, 1.00]	0.00 [0.00, 0.84]
Reinholdt 1996	24	13	4	78	0.86 [0.67, 0.96]	0.86 [0.77, 0.92]
Dueholm 2001	14	12	8	72	0.64 [0.41, 0.83]	0.86 [0.76, 0.92]
Bazot 2001	31	6	9	74	0.78 [0.62, 0.89]	0.93 [0.84, 0.97]
Masui 2003	12	4	6	22	0.67 [0.41, 0.87]	0.85 [0.65, 0.96]
Bazot 2003	18	3	6	29	0.75 [0.53, 0.90]	0.91 [0.75, 0.98]
Moghadam 2006	12	11	19	111	0.39 [0.22, 0.58]	0.91 [0.84, 0.95]
Stamatopoulos 2012	12	0	14	127	0.46 [0.27, 0.67]	1.00 [0.97, 1.00]
Badawy 2014	17	0	0	37	1.00 [0.80, 1.00]	1.00 [0.91, 1.00]
Tian 2016	18	2	3	23	0.86 [0.64, 0.97]	0.92 [0.74, 0.99]
Tellum 2019	41	17	16	19	0.72 [0.58, 0.83]	0.53 [0.35, 0.70]

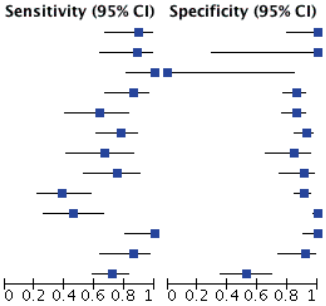

Figure 2.S2 MetaDTA SROC Curve for MRI Overall vs. Histopathology

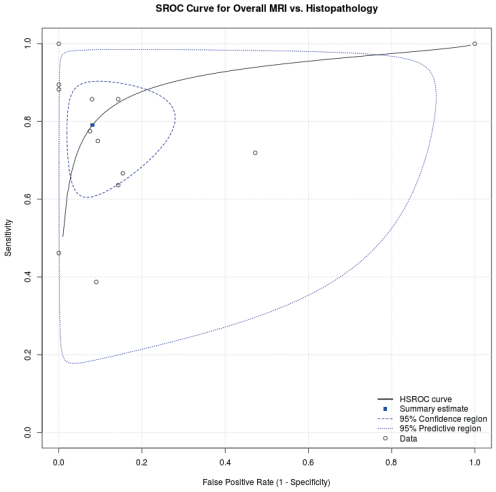

JZ Diameter > 12mm

Figure 2.S3 RevMan Forest Plots for JZ Diameter >12mm

Study	TP	FP	FN	TN	Sensitivity (95% CI)	Specificity (95% CI)
Reinholdt 1996	26	8	2	83	0.93 [0.76, 0.99]	0.91 [0.83, 0.96]
Bazot 2001	25	3	15	77	0.63 [0.46, 0.77]	0.96 [0.89, 0.99]
Hamimi 2015	42	1	3	14	0.93 [0.82, 0.99]	0.93 [0.68, 1.00]
Tellum 2019	30	20	27	16	0.53 [0.39, 0.66]	0.44 [0.28, 0.62]

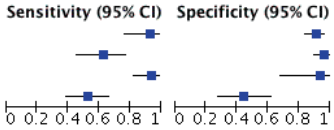

Figure 2.S4 MetaDTA SROC Curve for JZ Diameter >12mm

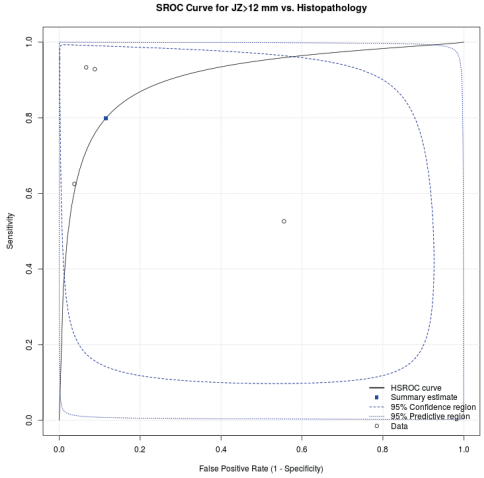

JZ Differential > 5 mm

Figure 2.S5 RevMan 2 x 2 Tables and Forest Plots for JZ Diff >5mm

Study	TP	FP	FN	TN	Sensitivity (95% CI)	Specificity (95% CI)
Dueholm 2001	15	10	7	74	0.68 [0.45, 0.86]	0.88 [0.79, 0.94]
Tellum 2019	30	9	27	27	0.53 [0.39, 0.66]	0.75 [0.58, 0.88]

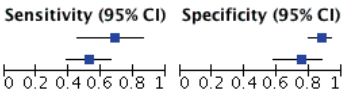

Figure 2.S6 MetaDTA SROC Curve for JZ Diff >5mm

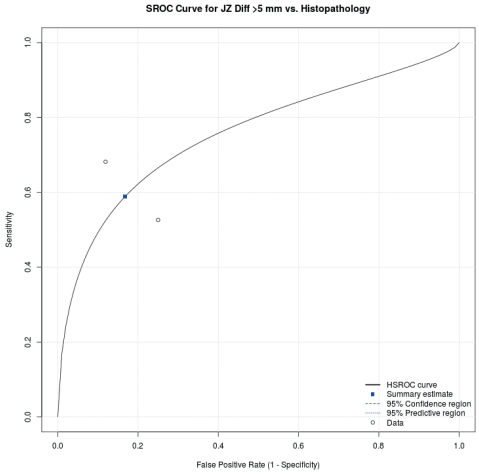

JZ – Myometrium Ratio >40 %

Figure 2.S7 RevMan 2 x 2 Tables and Forest Plots for JZ-Myo Ratio >40%

Study	TP	FP	FN	TN	Sensitivity (95% CI)	Specificity (95% CI)
Bazot 2001	26	6	14	74	0.65 [0.48, 0.79]	0.93 [0.84, 0.97]
Tellum 2019	24	13	15	15	0.62 [0.45, 0.77]	0.54 [0.34, 0.72]

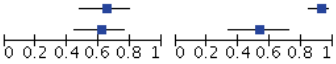

Figure 2.S8 MetaDTA SROC Curve for JZ-Myo Ratio >40%

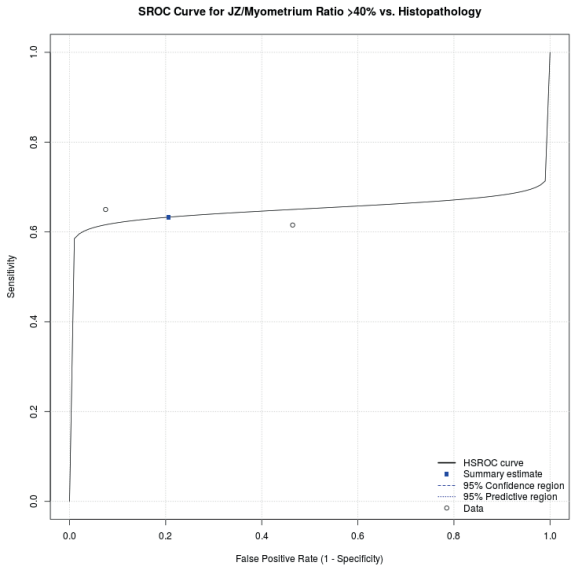

Uterine Enlargement

Figure 2.S9 RevMan 2 x 2 Tables and Forest Plots for Uterine Enlargement

Study	TP	FP	FN	TN	Sensitivity (95% CI)	Specificity (95% CI)
Bazot 2001	9	2	31	78	0.23 [0.11, 0.38]	0.97 [0.91, 1.00]
Tellum 2019	29	10	15	13	0.66 [0.50, 0.80]	0.57 [0.34, 0.77]

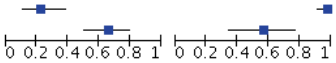

Figure 2.S10 MetaDTA SROC Curve for Uterine Enlargement

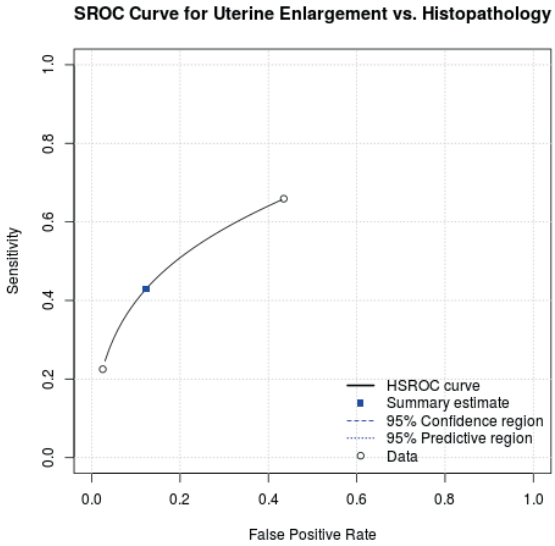

Presence of Myometrial Cysts

Figure 2.S11 RevMan 2 x 2 Tables and Forest Plots for Myometrial Cysts

Study	TP	FP	FN	TN	Sensitivity (95% CI)	Specificity (95% CI)
Bazot 2001	19	1	21	79	0.47 [0.32, 0.64]	0.99 [0.93, 1.00]
Hamimi 2015	20	5	20	15	0.50 [0.34, 0.66]	0.75 [0.51, 0.91]
Tellum 2019	40	4	17	32	0.70 [0.57, 0.82]	0.89 [0.74, 0.97]

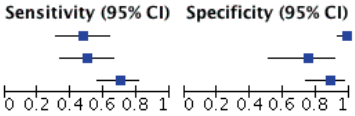

Figure2.S12 MetaDTA SROC Curve for Myometrial Cysts

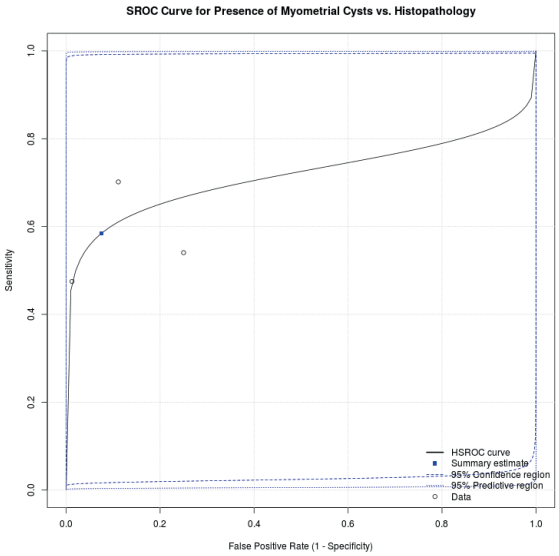

2F. Subjective Measures of Adenomyosis on MRI:

Table 2.S11 Subjective Measures Adenomyosis on MRI

MRI Feature	Definition
Adenomyosis type	- Diffuse - Focal - (Juvenile) Cystic
Adenomyosis localisation	Reported localisation of (focal) adenomyosis - Anterior, Posterior, Fundal etc. - Inner/Outer Myometrium
Irregular Junctional Zone	Subjective reporting of perceived irregularity of JZ
Poor definition of JZ	Measurement accuracy impaired due to unclear JZ borders
Presence of submucosal microcysts	Presence of submucosal high signal intensity foci (on T2W or T1W imaging), corresponding to myometrial cysts
Linear Striations	In combination with HSI foci

2G. Full Reference List of Studies included in the Review

1. Alcalde AM, Martínez-Zamora MÁ, Gracia M, Ros C, Rius M, Castelo-Branco C, et al. Assessment of Quality of Life, Sexual Quality of Life, and Pain Symptoms in Deep Infiltrating Endometriosis Patients With or Without Associated Adenomyosis and the Influence of a Flexible Extended Combined Oral Contraceptive Regimen: Results of a Prospective, Observational Study. J Sex Med. 2022;19(2).
2. Alcalde AM, Martínez-Zamora MÁ, Gracia M, Ros C, Rius M, Nicolás I, et al. Impact of Adenomyosis on Women's Psychological Health and Work Productivity: A Comparative Cross-Sectional Study. J Women's Heal. 2021;30(11).
3. Benagiano G, Brosens I, Carrara S. Adenomyosis: new knowledge is generating new treatment strategies. Womens Health (Lond Engl) [Internet]. 2009 May;5(3):297–311. Available from: https://www.ncbi.nlm.nih.gov/pubmed/19392615
4. Hasdemir PS, Farasat M, Aydin C, Ozyurt BC, Guvenal T, Pekindil G. The Role of Adenomyosis in the Pathogenesis of Preeclampsia. Geburtshilfe Frauenheilkd. 2016;
5. Protopapas A, Grimbizis G, Athanasiou S, Loutradis D. Adenomyosis: Disease, uterine aging process leading to symptoms, or both? Facts, Views Vis ObGyn [Internet]. 2020 Aug 5 [cited 2022 Jun 28];12(2):91. Available from: /pmc/articles/PMC7431194/
6. Peric H, Fraser IS. The symptomatology of adenomyosis. Best Pract Res Clin Obstet Gynaecol [Internet]. 2006 Aug;20(4):547–55. Available from: https://www.ncbi.nlm.nih.gov/pubmed/16515888
7. Struble J, Reid S, Bedaiwy MA. Adenomyosis: A Clinical Review of a Challenging Gynecologic Condition. Journal of Minimally Invasive Gynecology. 2016.
8. Leyendecker G, Bilgicyildirim A, Inacker M, Stalf T, Huppert P, Mall G, et al. Adenomyosis and endometriosis. Re-visiting their association and further insights into the mechanisms of auto-traumatisation. An MRI study. Arch Gynecol Obstet. 2015;
9. Leyendecker G, Wildt L, Mall G. The pathophysiology of endometriosis and adenomyosis: Tissue injury and repair. Arch Gynecol Obstet. 2009;
10. Guo SW. The Pathogenesis of Adenomyosis vis-à-vis Endometriosis. J Clin Med [Internet]. 2020 Feb 10 [cited 2020 Aug 3];9(2):485. Available from: https://www.mdpi.com/2077-0383/9/2/485
11. Marcellin L, Santulli P, Bourdon M, Maignien C, Campin L, Lafay-Pillet MC, et al. Focal adenomyosis of the outer myometrium and deep infiltrating endometriosis severity. Fertil Steril. 2020;114(4).
12. Chapron C, Tosti C, Marcellin L, Bourdon M, Lafay-Pillet MC,

Millischer AE, et al. Relationship between the magnetic resonance imaging appearance of adenomyosis and endometriosis phenotypes. Hum Reprod. 2017;
13. Brosens I, Gordts S, Habiba M, Benagiano G. Uterine Cystic Adenomyosis: A Disease of Younger Women. Vol. 28, Journal of Pediatric and Adolescent Gynecology. 2015.
14. Bourdon M, Oliveira J, Marcellin L, Santulli P, Bordonne C, Maitrot Mantelet L, et al. Adenomyosis of the inner and outer myometrium are associated with different clinical profiles. Hum Reprod. 2021;36(2).
15. Iwasawa T, Takahashi T, Maeda E, Ishiyama K, Takahashi S, Suganuma R, et al. Effects of localisation of uterine adenomyosis on outcome of in vitro fertilisation/intracytoplasmic sperm injection fresh and frozen-thawed embryo transfer cycles: a multicentre retrospective cohort study. Reprod Biol Endocrinol [Internet]. 2021 Dec 1 [cited 2022 Aug 3];19(1):1–11. Available from: https://rbej.biomedcentral.com/articles/10.1186/s12958-021-00764-7
16. Kobayashi H, Matsubara S. A Classification Proposal for Adenomyosis Based on Magnetic Resonance Imaging. Gynecol Obstet Invest. 2020;85(2):118–26.
17. Kishi Y, Suginami H, Kuramori R, Yabuta M, Suginami R, Taniguchi F. Four subtypes of adenomyosis assessed by magnetic resonance imaging and their specification. Am J Obstet Gynecol [Internet]. 2012 Aug;207(2):114.e1-7. Available from: https://www.ncbi.nlm.nih.gov/pubmed/22840719
18. Exacoustos C, Morosetti G, Conway F, Camilli S, Martire FG, Lazzeri L, et al. New Sonographic Classification of Adenomyosis: Do Type and Degree of Adenomyosis Correlate to Severity of Symptoms? J Minim Invasive Gynecol. 2020;27(6).
19. Chapron C, Vannuccini S, Santulli P, Abrão MS, Carmona F, Fraser IS, et al. Diagnosing adenomyosis: An integrated clinical and imaging approach. Hum Reprod Update. 2020;
20. Agarwal SK, Chapron C, Giudice LC, Laufer MR, Leyland N, Missmer SA, et al. Clinical diagnosis of endometriosis: a call to action. Am J Obstet Gynecol. 2019 Apr 1;220(4):354.e1-354.e12.
21. Staal AHJ, Van Der Zanden M, Nap AW. Diagnostic Delay of Endometriosis in the Netherlands. Gynecol Obstet Invest. 2016 Jul 1;81(4):321–4.
22. Tan N, McClure TD, Tarnay C, Johnson MT, Lu DS, Raman SS. Women seeking second opinion for symptomatic uterine leiomyoma: role of comprehensive fibroid center. J Ther ultrasound [Internet]. 2014;2:3. Available from: https://www.ncbi.nlm.nih.gov/pubmed/25512867

23. Kassam Z, Petkovska I, Wang CL, Trinh AM, Kamaya A. Benign Gynecologic Conditions of the Uterus. Magn Reson Imaging Clin N Am [Internet]. 2017 Aug;25(3):577–600. Available from: https://www.ncbi.nlm.nih.gov/pubmed/28668161
24. Valentini AL, Speca S, Gui B, Soglia BG, Miccò M, Bonomo L. Adenomyosis: From the sign to the diagnosis. Imaging, diagnostic pitfalls and differential diagnosis: A pictorial review. Radiologia Medica. 2011.
25. Brucker SY, Huebner M, Wallwiener M, Stewart EA, Ebersoll S, Schoenfisch B, et al. Clinical characteristics indicating adenomyosis coexisting with leiomyomas: A retrospective, questionnaire-based study. Fertil Steril. 2014;101(1).
26. Bourdon M, Santulli P, Marcellin L, Maignien C, Maitrot-Mantelet L, Chapron C. Adenomyosis pathophysiology: An unresolved enigma. Vol. 50, Gynecologie Obstetrique Fertilite et Senologie. 2022.
27. Benagiano G, Brosens I. History of adenomyosis. Vol. 20, Best Practice and Research: Clinical Obstetrics and Gynaecology. 2006.
28. Van Den Bosch T, Dueholm M, Leone FPG, Valentin L, Rasmussen CK, Votino A, et al. Terms, definitions and measurements to describe sonographic features of myometrium and uterine masses: A consensus opinion from the Morphological Uterus Sonographic Assessment (MUSA) group. Ultrasound Obstet Gynecol. 2015;46(3).
29. Tellum T, Nygaard S, Lieng M. Noninvasive Diagnosis of Adenomyosis: A Structured Review and Meta-Analysis of Diagnostic Accuracy in Imaging. J Minim Invasive Gynecol [Internet]. 2019 Nov; Available from: https://www.ncbi.nlm.nih.gov/pubmed/31712162
30. Van den Bosch T, de Bruijn AM, de Leeuw RA, Dueholm M, Exacoustos C, Valentin L, et al. Sonographic classification and reporting system for diagnosing adenomyosis. Ultrasound Obstet Gynecol. 2019 May 1;53(5):576–82.
31. Dueholm M, Hjorth IMD. Structured imaging technique in the gynecologic office for the diagnosis of abnormal uterine bleeding. Best Pract Res Clin Obstet Gynaecol [Internet]. 2017 Apr;40:23–43. Available from: https://www.ncbi.nlm.nih.gov/pubmed/27818130
32. Munro MG. Classification Systems for Adenomyosis. J Minim Invasive Gynecol [Internet]. 2019 Nov; Available from: https://www.ncbi.nlm.nih.gov/pubmed/31785418
33. Agostinho L, Cruz R, Osório F, Alves J, Setúbal A, Guerra A. MRI for adenomyosis: a pictorial review. Insights Imaging [Internet]. 2017 Dec;8(6):549–56. Available from: https://www.ncbi.nlm.nih.gov/pubmed/28980163
34. Bazot M, Daraï E. Role of transvaginal sonography and magnetic

resonance imaging in the diagnosis of uterine adenomyosis. Fertility and Sterility. 2018.
35. Dueholm M. Transvaginal ultrasound for diagnosis of adenomyosis: a review. Best Pract Res Clin Obstet Gynaecol [Internet]. 2006 Aug;20(4):569–82. Available from: https://www.ncbi.nlm.nih.gov/pubmed/16545618
36. Dueholm M, Lundorf E, Hansen ES, Sorensen JS, Ledertoug S, Olesen F. Magnetic resonance imaging and transvaginal ultrasonography for the diagnosis of adenomyosis. 2001;76(3):588-594. Available from: https://www.cochranelibrary.com/central/doi/10.1002/central/CN-00424865/full
37. Champaneria R, Abedin P, Daniels J, Balogun M, Khan KS. Ultrasound scan and magnetic resonance imaging for the diagnosis of adenomyosis: Systematic review comparing test accuracy. Acta Obstetricia et Gynecologica Scandinavica. 2010.
38. Mark AS, Hricak H, Heinrichs LW, Hendrickson MR, Winkler ML, Bachica JA, et al. Adenomyosis and leiomyoma: Differential diagnosis with MR imaging. Radiology. 1987;
39. Vitiello D, McCarthy S. Diagnostic imaging of myomas. Obstetrics and Gynecology Clinics of North America. 2006.
40. Exacoustos C, Manganaro L, Zupi E. Imaging for the evaluation of endometriosis and adenomyosis. Best Pract Res Clin Obstet Gynaecol. 2014;
41. Örs F, Lev-Toaff AS, Bergin D. Cystic adenomyoma: Transvaginal ultrasound and MRI findings. Anatol J Clin Investig. 2009;
42. Takeuchi M, Matsuzaki K. Adenomyosis: Usual and unusual imaging manifestations, pitfalls, and problem-solving MR imaging techniques. Radiographics. 2011;
43. Gordts S, Brosens JJ, Fusi L, Benagiano G, Brosens I. Uterine adenomyosis: A need for uniform terminology and consensus classification. Reprod Biomed Online. 2008;
44. Reinhold C, Tafazoli F, Wang L. Imaging features of adenomyosis. Hum Reprod Update [Internet]. 1998 Jul;4(4):337–49. Available from: https://www.ncbi.nlm.nih.gov/pubmed/9825849
45. Tellum T, Matic G V, Dormagen JB, Nygaard S, Viktil E, Qvigstad E, et al. Diagnosing adenomyosis with MRI: a prospective study revisiting the junctional zone thickness cutoff of 12 mm as a diagnostic marker. Eur Radiol [Internet]. 2019 Dec;29(12):6971–81. Available from: https://www.ncbi.nlm.nih.gov/pubmed/31264010
46. Meylaerts LJ, Wijnen L, Grieten M, Palmers Y, Ombelet W, Vandersteen M. Junctional zone thickness in young nulliparous women according to menstrual cycle and hormonal contraception use. Reprod

Biomed Online. 2017;
47. Novellas S, Chassang M, Delotte J, Toullalan O, Chevallier A, Bouaziz J, et al. MRI characteristics of the uterine junctional zone: From normal to the diagnosis of adenomyosis. American Journal of Roentgenology. 2011.
48. Kido A, Togashi K, Koyama T, Yamaoka T, Fujiwara T, Fujii S. Diffusely enlarged uterus: evaluation with MR imaging. Radiographics [Internet]. 2003 Nov;23(6):1423–39. Available from: https://www.ncbi.nlm.nih.gov/pubmed/14615554
49. Gong C, Yang B, Shi Y, Liu Z, Wan L, Zhang H, et al. Factors influencing the ablative efficiency of high intensity focused ultrasound (HIFU) treatment for adenomyosis: A retrospective study. Int J Hyperth. 2016;
50. Mochimaru A, Aoki S, Oba MS, Kurasawa K, Takahashi T, Hirahara F. Adverse pregnancy outcomes associated with adenomyosis with uterine enlargement. J Obstet Gynaecol Res. 2015;
51. Kissler S, Zangos S, Kohl J, Wiegratz I, Rody A, Gätje R, et al. Duration of dysmenorrhoea and extent of adenomyosis visualised by magnetic resonance imaging. Eur J Obstet Gynecol Reprod Biol. 2008;
52. Keserci B, Duc NM. Magnetic resonance imaging features influencing high-intensity focused ultrasound ablation of adenomyosis with a nonperfused volume ratio of ≥90% as a measure of clinical treatment success: retrospective multivariate analysis. Int J Hyperth. 2018;
53. Froeling V, Scheurig-Muenkler C, Hamm B, Kroencke TJ. Uterine artery embolization to treat uterine adenomyosis with or without uterine leiomyomata: Results of symptom control and health-related quality of life 40 months after treatment. Cardiovasc Intervent Radiol. 2012;
54. Dashottar S, Singh AK, Debnath J, Muralidharan CG, Singh RK, Kumar S. Comparative analysis of changes in MR imaging of pre and post intrauterine progesterone implants in adenomyosis cases. Med journal, Armed Forces India [Internet]. 2015 Apr;71(2):145–51. Available from: https://www.ncbi.nlm.nih.gov/pubmed/25859077
55. Marnach ML, Laughlin-Tommaso SK. Evaluation and Management of Abnormal Uterine Bleeding. Mayo Clin Proc [Internet]. 2019;94(2):326–35. Available from: https://www.ncbi.nlm.nih.gov/pubmed/30711128
56. Pontis A, D'Alterio MN, Pirarba S, de Angelis C, Tinelli R, Angioni S. Adenomyosis: a systematic review of medical treatment. Gynecol Endocrinol [Internet]. 2016 Sep;32(9):696–700. Available from: https://www.ncbi.nlm.nih.gov/pubmed/27379972
57. Streuli I, Dubuisson J, Santulli P, De Ziegler D, Batteux F, Chapron C. An update on the pharmacological management of adenomyosis. Vol.

15, Expert Opinion on Pharmacotherapy. 2014.
58. Benetti-Pinto CL, Mira TAA de, Yela DA, Teatin-Juliato CR, Brito LGO. Pharmacological Treatment for Symptomatic Adenomyosis: A Systematic Review. Rev Bras Ginecol Obstet [Internet]. 2019 Sep;41(9):564–74. Available from: https://www.ncbi.nlm.nih.gov/pubmed/31546278
59. Smeets AJ, Nijenhuis RJ, Boekkooi PF, Vervest HAM, Van Rooij WJ, Lohle PNM. Long-term follow-up of uterine artery embolization for symptomatic adenomyosis. Cardiovasc Intervent Radiol. 2012;
60. Nijenhuis RJ, Smeets AJ, Morpurgo M, Boekkooi PF, Reuwer PJHM, Smink M, et al. Uterine Artery Embolisation for Symptomatic Adenomyosis with Polyzene F-Coated Hydrogel Microspheres: Three-Year Clinical Follow-Up Using UFS–QoL Questionnaire. Cardiovasc Intervent Radiol. 2015;
61. Vannuccini S, Petraglia F. Recent advances in understanding and managing adenomyosis. F1000Research [Internet]. 2019;8. Available from: https://www.ncbi.nlm.nih.gov/pubmed/30918629
62. Osada H, Silber S, Kakinuma T, Nagaishi M, Kato K, Kato O. Surgical procedure to conserve the uterus for future pregnancy in patients suffering from massive adenomyosis. Reprod Biomed Online [Internet]. 2011 Jan;22(1):94–9. Available from: https://www.ncbi.nlm.nih.gov/pubmed/21118751
63. Benagiano G, Brosens I, Habiba M. Adenomyosis: A life-cycle approach. Reproductive BioMedicine Online. 2015.
64. Kunz G, Leyendecker G. Uterine peristaltic activity during the menstrual cycle: characterization, regulation, function and dysfunction. Reprod Biomed Online [Internet]. 2002;4:5–9. Available from: https://www.ncbi.nlm.nih.gov/pubmed/12470555
65. Kunz G, Noe M, Herbertz M, Leyendecker G. Uterine peristalsis during the follicular phase of the menstrual cycle: Effects of oestrogen, antioestrogen and oxytocin. Hum Reprod Update. 1998 Sep;4(5):647–54.
66. De Ziegler D, Bulletti C, Fanchin R, Epiney M, Brioschi PA. Contractility of the nonpregnant uterus: The follicular phase. In: Annals of the New York Academy of Sciences. 2001.
67. Bulletti C, De Ziegler D, Setti PL, Cicinelli E, Polli V, Flamigni C. The patterns of uterine contractility in normal menstruating women: From physiology to pathology. In: Annals of the New York Academy of Sciences. 2004.
68. Ijland MM, Evers JLH, Dunselman GAJ, Hoogland HJ. Subendometrial contractions in the nonpregnant uterus: An ultrasound study. Eur J Obstet Gynecol Reprod Biol. 1996;70(1):23–4.

69. Ijland MM, H Evers JL, J Dunselman GA, van Katwijk C, Lo Henk J Hoogland CR. Endometrial wavelike movements during the menstrual cycle. Am Soc Reprod Med. 1996;65(4).
70. van Gestel I, IJland MM, Evers JLH, Hoogland HJ. Complex endometrial wave-patterns in IVF. Fertil Steril. 2007;
71. Ijland MM, Hoogland HJ, Dunselman GAJ, Lo CR, Evers JLH. Endometrial wave direction switch and the outcome of in vitro fertilization. Fertil Steril. 1999 Mar;71(3):476–81.
72. Kunz G, Herbertz M, Beil D, Huppert P, Leyendecker G. Adenomyosis as a disorder of the early and late human reproductive period. Reprod Biomed Online [Internet]. 2007 Dec;15(6):681–5. Available from: https://www.ncbi.nlm.nih.gov/pubmed/18062865
73. Kido A, Koyama T, Kataoka M, Yamamoto A, Saga T, Turner R, et al. Physiological changes of the human uterine myometrium during menstrual cycle: Preliminary evaluation using BOLD MR imaging. J Magn Reson Imaging. 2007;
74. Shaked S, Jaffa AJ, Grisaru D, Elad D. Uterine peristalsis-induced stresses within the uterine wall may sprout adenomyosis. Biomech Model Mechanobiol. 2015;14(3).
75. Kissler S, Hamscho N, Zangos S, Wiegratz I, Schlichter S, Menzel C, et al. Uterotubal transport disorder in adenomyosis and endometriosis–a cause for infertility. BJOG. 2006 Aug;113(8):902–8.
76. Leyendecker G, Kunz G, Herbertz M, Beil D, Huppert P, Mall G, et al. Uterine peristaltic activity and the development of endometriosis. In: Annals of the New York Academy of Sciences. 2004.
77. Kissler S, Hamscho N, Zangos S, Wiegratz I, Schlichter S, Menzel C, et al. Uterotubal transport disorder in adenomyosis and endometriosis - A cause for infertility. BJOG An Int J Obstet Gynaecol. 2006;
78. Naftalin J, Hoo W, Pateman K, Mavrelos D, Holland T, Jurkovic D. How common is adenomyosis? A prospective study of prevalence using transvaginal ultrasound in a gynaecology clinic. Hum Reprod. 2012;27(12).
79. J. PA, I. O, J. M-S, L. C, C. I, J.A. G-V. High prevalence of adenomyosis in recurrent pregnancy loss and previous ART failure. Hum Reprod. 2014;
80. Puente JM, Fabris A, Patel J, Patel A, Cerrillo M, Requena A, et al. Adenomyosis in infertile women: Prevalence and the role of 3D ultrasound as a marker of severity of the disease. Reprod Biol Endocrinol. 2016;
81. Horton J, Sterrenburg M, Lane S, Maheshwari A, Li TC, Cheong Y. Reproductive, obstetric, and perinatal outcomes of women with adenomyosis and endometriosis: A systematic review and meta-

analysis. Hum Reprod Update. 2019;
82. Campo S, Campo V, Benagiano G. Adenomyosis and infertility. Reprod Biomed Online. 2012 Jan;24(1):35–46.
83. Kuijsters NPM, Methorst WG, Kortenhorst MSQ, Rabotti C, Mischi M, Schoot BC. Uterine peristalsis and fertility: current knowledge and future perspectives: a review and meta-analysis. Reproductive BioMedicine Online. 2017.
84. Harada T, Khine YM, Kaponis A, Nikellis T, Decavalas G, Taniguchi F. The Impact of Adenomyosis on Women's Fertility. Obstet Gynecol Surv. 2016;
85. Vlahos NF, Theodoridis TD, Partsinevelos GA. Myomas and Adenomyosis: Impact on Reproductive Outcome. BioMed Research International. 2017.
86. Sharma S, Bathwal S, Agarwal N, Chattopadhyay R, Saha I, Chakravarty B. Does presence of adenomyosis affect reproductive outcome in IVF cycles? A retrospective analysis of 973 patients. Reprod Biomed Online. 2019;
87. Ballester M, Roman H, Mathieu E, Touleimat S, Belghiti J, Daraï E. Prior colorectal surgery for endometriosis-associated infertility improves ICSI-IVF outcomes: results from two expert centres. Eur J Obstet Gynecol Reprod Biol. 2017;
88. Younes G, Tulandi T. Effects of adenomyosis on in vitro fertilization treatment outcomes: a meta-analysis. Fertil Steril [Internet]. 2017;108(3):483-490.e3. Available from: https://www.ncbi.nlm.nih.gov/pubmed/28865548
89. Vercellini P, Consonni D, Dridi D, Bracco B, Frattaruolo MP, Somigliana E. Uterine adenomyosis and in vitro fertilization outcome: a systematic review and meta-analysis. Hum Reprod [Internet]. 2014 May;29(5):964–77. Available from: https://www.ncbi.nlm.nih.gov/pubmed/24622619
90. Benaglia L, Cardellicchio L, Paffoni A, Leonardi M, Faulisi S, Somigliana E. Adenomyosis does not influence pregnancy rate in women undergoing IVF. Fertil Steril. 2013;
91. Benaglia L, Cardellicchio L, Leonardi M, Faulisi S, Vercellini P, Paffoni A, et al. Asymptomatic adenomyosis and embryo implantation in IVF cycles. Reprod Biomed Online. 2014;
92. Costello MF, Lindsay K, McNally G. The effect of adenomyosis on in vitro fertilisation and intra-cytoplasmic sperm injection treatment outcome. Eur J Obstet Gynecol Reprod Biol. 2011;
93. Mijatovic V, Florijn E, Halim N, Schats R, Hompes P. Adenomyosis has no adverse effects on IVF/ICSI outcomes in women with endometriosis treated with long-term pituitary down-regulation before IVF/ICSI. Eur J

Obstet Gynecol Reprod Biol. 2010;
94. Maheshwari A, Gurunath S, Fatima F, Bhattacharya S. Adenomyosis and subfertility: A systematic review of prevalence, diagnosis, treatment and fertility outcomes. Human Reproduction Update. 2012.
95. Meylaerts LJ, Wijnen L, Ombelet W, Bazot M, Vandersteen M. Uterine junctional zone thickness in infertile women evaluated by MRI. J Magn Reson Imaging. 2017;
96. Maged AM, Ramzy AM, Ghar MA, El Shenoufy H, Gad Allah SH, Wahba AH, et al. 3D ultrasound assessment of endometrial junctional zone anatomy as a predictor of the outcome of ICSI cycles. Eur J Obstet Gynecol Reprod Biol. 2017;
97. Kunz G, Beil D. Characterization of the uterine junctional zone prior to IVF/ICSI: An observational study. Arch Gynecol Obstet. 2010;
98. Maubon A, Faury A, Kapella M, Pouquet M, Piver P. Uterine junctional zone at magnetic resonance imaging: A predictor of in vitro fertilization implantation failure. J Obstet Gynaecol Res. 2010;
99. Piver P. Uterine factors limiting ART coverage. J Gynecol Obstet Biol la Reprod. 2005;
100. Kunz G, Beil D, Huppert P, Noe M, Kissler S, Leyendecker G. Adenomyosis in endometriosis - Prevalence and impact on fertility. Evidence from magnetic resonance imaging. Hum Reprod. 2005;
101. Tamura H, Kishi H, Kitade M, Asai-Sato M, Tanaka A, Murakami T, et al. Clinical outcomes of infertility treatment for women with adenomyosis in Japan. Reprod Med Biol. 2017;
102. Juang CM, Chou P, Yen MS, Twu NF, Horng HC, Hsu WL. Adenomyosis and risk of preterm delivery. BJOG An Int J Obstet Gynaecol. 2007;
103. Shin YJ, Kwak DW, Chung JH, Kim MY, Lee SW, Han YJ. The risk of preterm births among pregnant women with adenomyosis. J Ultrasound Med. 2018;
104. Harada T, Taniguchi F, Amano H, Kurozawa Y, Ideno Y, Hayashi K, et al. Adverse obstetrical outcomes for women with endometriosis and adenomyosis: A large cohort of the Japan Environment and Children's Study. PLoS One. 2019;
105. Scala C, Maggiore ULR, Racca A, Barra F, Vellone VG, Venturini PL, et al. Influence of adenomyosis on pregnancy and perinatal outcomes in women with endometriosis. Ultrasound Obstet Gynecol. 2018;
106. Exacoustos C, Lauriola I, Lazzeri L, De Felice G, Zupi E. Complications during pregnancy and delivery in women with untreated rectovaginal deep infiltrating endometriosis. Fertil Steril. 2016;
107. Bruun MR, Arendt LH, Forman A, Ramlau-Hansen CH. Endometriosis and adenomyosis are associated with increased risk of preterm

delivery and a small-for-gestational-age child: a systematic review and meta-analysis. Acta Obstetricia et Gynecologica Scandinavica. 2018.
108. Hashimoto A, Iriyama T, Sayama S, Nakayama T, Komatsu A, Miyauchi A, et al. Adenomyosis and adverse perinatal outcomes: increased risk of second trimester miscarriage, preeclampsia, and placental malposition. J Matern Neonatal Med. 2018;
109. Kim YM, Kim SH, Kim JH, Sung JH, Choi SJ, Oh S young, et al. Uterine wall thickness at the second trimester can predict subsequent preterm delivery in pregnancies with adenomyosis. Taiwan J Obstet Gynecol. 2019;
110. Yamaguchi A, Kyozuka H, Fujimori K, Hosoya M, Yasumura S, Yokoyama T, et al. Risk of preterm birth, low birthweight and small-for-gestational-age infants in pregnancies with adenomyosis: A cohort study of the Japan Environment and Children's Study. Acta Obstet Gynecol Scand. 2019;
111. Brosens I, Derwig I, Brosens J, Fusi L, Benagiano G, Pijnenborg R. The enigmatic uterine junctional zone: the missing link between reproductive disorders and major obstetrical disorders? Hum Reprod [Internet]. 2010 Mar;25(3):569–74. Available from: https://www.ncbi.nlm.nih.gov/pubmed/20085913
112. Brosens I, Pijnenborg R, Benagiano G. Defective myometrial spiral artery remodelling as a cause of major obstetrical syndromes in endometriosis and adenomyosis. Placenta [Internet]. 2013 Feb;34(2):100–5. Available from: https://www.ncbi.nlm.nih.gov/pubmed/23232321
113. Kang S, Turner DA, Foster GS, Rapoport MI, Spencer SA, Wang JZ. Adenomyosis: specificity of 5 mm as the maximum normal uterine junctional zone thickness in MR images. AJR Am J Roentgenol [Internet]. 1996 May;166(5):1145–50. Available from: https://www.ncbi.nlm.nih.gov/pubmed/8615259
114. Whiting PF, Rutjes AWS, Westwood ME, Mallett S, Deeks JJ, Reitsma JB, et al. Quadas-2: A revised tool for the quality assessment of diagnostic accuracy studies. Annals of Internal Medicine. 2011.
115. Freeman SC, Kerby CR, Patel A, Cooper NJ, Quinn T, Sutton AJ. Development of an interactive web-based tool to conduct and interrogate meta-analysis of diagnostic test accuracy studies: MetaDTA. BMC Med Res Methodol. 2019;
116. Moghadam R, Lathi RB, Shahmohamady B, Saberi NS, Nezhat CH, Nezhat F, et al. Predictive value of magnetic resonance imaging in differentiating between leiomyoma and adenomyosis. JSLS J Soc Laparoendosc Surg [Internet]. 2006 Apr;10(2):216–9. Available from: https://www.ncbi.nlm.nih.gov/pubmed/16882423

117. Hamimi A. What are the most reliable signs for the radiologic diagnosis of uterine adenomyosis? An ultrasound and MRI prospective. Egypt J Radiol Nucl Med. 2015;
118. Badawy ME, Elkholi DGEY, Sherif MF, Hefedah MAE. Magnetic resonance imaging of uterovaginal lesions associated with female infertility. Middle East Fertil Soc J. 2015;
119. Tian T, Zhang G-F, Zhang H, Liu H. Intravoxel incoherent motion diffusion-weighted imaging in differentiating uterine fibroid from focal adenomyosis: initial results. Springerplus [Internet]. 2016;5:9. Available from: https://www.ncbi.nlm.nih.gov/pubmed/26759748
120. Ascher SM, Arnold LL, Patt RH, Schruefer JJ, Bagley AS, Semelka RCR, et al. Adenomyosis: Prospective comparison of MR imaging and transvaginal sonography. Radiology. 1994;
121. Phillips DR, Nathanson HG, Milim SJ, Haselkorn JS. Magnetic resonance imaging for diagnosing adenomyomata. J Am Assoc Gynecol Laparosc [Internet]. 1996 Feb;3(2):245–50. Available from: https://www.ncbi.nlm.nih.gov/pubmed/9050634
122. Dueholm M, Lundorf E, Hansen ES, Sorensen JS, Ledertoug S, Olesen F. Magnetic resonance imaging and transvaginal ultrasonography for the diagnosis of adenomyosis. Fertil Steril. 2001;
123. Andersson J, Khan Z, Gemzell-Danielsson K, Weaver A, Vaughan L, Stewart E. Vaginal Bromocriptine Improves Pain and Bleeding in Women with Adenomyosis. J Minim Invasive Gynecol. 2016;
124. Bazot M, Daraï E, De Givry SC, Boudghène F, Uzan S, Le Blanche AF. Fast breath-hold T2-weighted MR imaging reduces interobserver variability in the diagnosis of adenomyosis. Am J Roentgenol. 2003;
125. Bazot M, Cortez A, Darai E, Rouger J, Chopier J, Antoine JM, et al. Ultrasonography compared with magnetic resonance imaging for the diagnosis of adenomyosis: Correlation with histopathology. Hum Reprod. 2001;
126. Hricak H, Finck S, Honda G, Goranson H. MR imaging in the evaluation of benign uterine masses: Value of gadopentetate dimeglumine-enhanced T1-weighted images. Am J Roentgenol. 1992;
127. Masui T, Katayama M, Kobayashi S, Shimizu S, Nozaki A, Sakahara H. Pseudolesions related to uterine contraction: Characterization with multiphase-multisection T2-weighted MR imaging. Radiology. 2003;
128. Reinhold C, McCarthy S, Bret PM, Mehio A, Atri M, Zakarian R, et al. Diffuse adenomyosis: Comparison of endovaginal US and MR imaging with histopathologic correlation. Radiology. 1996;
129. Stamatopoulos CP, Mikos T, Grimbizis GF, Dimitriadis AS, Efstratiou I, Stamatopoulos P, et al. Value of Magnetic Resonance Imaging in Diagnosis of Adenomyosis and Myomas of the Uterus. J Minim

Invasive Gynecol. 2012;
130. Bae SH, Kim MD, Kim GM, Lee SJ, Park S Il, Won JY, et al. Uterine Artery Embolization for Adenomyosis: Percentage of Necrosis Predicts Midterm Clinical Recurrence. J Vasc Interv Radiol. 2015;
131. Bourdon M, Santulli P, Chouzenoux S, Maignien C, Bailly K, Andrieu M, et al. The Disease Phenotype of Adenomyosis-Affected Women Correlates With Specific Serum Cytokine Profiles. Reprod Sci. 2019;
132. Bragheto AM, Caserta N, Bahamondes L, Petta CA. Effectiveness of the levonorgestrel-releasing intrauterine system in the treatment of adenomyosis diagnosed and monitored by magnetic resonance imaging. Contraception. 2007;
133. Bratby MJ, Walker WJ. Uterine artery embolisation for symptomatic adenomyosis-Mid-term results. Eur J Radiol. 2009;
134. Byun JY, Kim SE, Choi BG, Ko GY, Jung SE, Choi KH. Diffuse and focal adenomyosis: MR imaging findings. Radiographics. 1999;
135. Ferrari F, Arrigoni F, Miccoli A, Mascaretti S, Fascetti E, Mascaretti G, et al. Effectiveness of Magnetic Resonance-guided Focused Ultrasound Surgery (MRgFUS) in the uterine adenomyosis treatment: technical approach and MRI evaluation. Radiol Medica. 2016;
136. Fukunishi H, Funaki K, Sawada K, Yamaguchi K, Maeda T, Kaji Y. Early Results of Magnetic Resonance-guided Focused Ultrasound Surgery of Adenomyosis: Analysis of 20 Cases. J Minim Invasive Gynecol. 2008;
137. Imaoka I, Ascher SM, Sugimura K, Takahashi K, Li H, Cuomo F, et al. MR imaging of diffuse adenomyosis changes after GnRH analog therapy. J Magn Reson Imaging. 2002;
138. Jha RC, Takahama J, Imaoka I, Korangy SJ, Spies JB, Cooper C, et al. Adenomyosis: MRI of the uterus treated with uterine artery embolization. Am J Roentgenol. 2003;
139. Jha RC, Zanello PA, Ascher SM, Rajan S. Diffusion-weighted imaging (DWI) of adenomyosis and fibroids of the uterus. Abdom Imaging. 2014;
140. Jung DC, Kim MD, Oh YT, Won JY, Lee DY. Prediction of early response to uterine arterial embolisation of adenomyosis: Value of T2 signal intensity ratio of adenomyosis. Eur Radiol. 2012;
141. Keserci B, Duc NM. The role of T1 perfusion-based classification in predicting the outcome of magnetic resonance-guided high-intensity focused ultrasound treatment of adenomyosis. Int J Hyperthermia [Internet]. 2018;34(3):306–14. Available from: https://www.ncbi.nlm.nih.gov/pubmed/28540825
142. Khandeparker MS, Jalkote S, Panpalia M, Nellore S, Mehta T, Ganesan K, et al. High-resolution magnetic resonance imaging in the

detection of subtle nuances of uterine adenomyosis in infertility. Glob Reprod Heal. 2018;3(14).
143. Kilickesmez O, Bayramoglu S, Inci E, Cimilli T, Kayhan A. Quantitative diffusion-weighted magnetic resonance imaging of normal and diseased uterine zones. Acta radiol. 2009;
144. Kim KA, Yoon SW, Lee C, Seong SJ, Yoon BS, Park H. Short-term results of magnetic resonance imaging-guided focused ultrasound surgery for patients with adenomyosis: Symptomatic relief and pain reduction. Fertil Steril. 2011;
145. Kim MD, Won JW, Lee DY, Ahn CS. Uterine artery embolization for adenomyosis without fibroids. Clin Radiol. 2004;
146. Kitamura Y, Allison SJ, Jha RC, Spies JB, Flick PA, Ascher SM. MRI of adenomyosis: Changes with uterine artery embolization. Am J Roentgenol. 2006;
147. Krinsky G, DeCorato DR, Rofsky NM, Flyer M, Earls JP, Ambrosino M, et al. Rapid T2-weighted MR imaging of uterine leiomyoma and adenomyosis. Abdom Imaging. 1997;
148. Kunz G, Herbertz M, Beil D, Huppert G, Leyendecker G. Adenomyosis as a disorder of the early and late human reproductive period. Reprod Biomed Online. 2007;
149. Larsen SB, Lundorf E, Forman A, Dueholm M. Adenomyosis and junctional zone changes in patients with endometriosis. Eur J Obstet Gynecol Reprod Biol. 2011;
150. Lohle PNM, De Vries J, Klazen CAH, Boekkooi PF, Vervest HAM, Smeets AJ, et al. Uterine Artery Embolization for Symptomatic Adenomyosis with or without Uterine Leiomyomas with the Use of Calibrated Tris-acryl Gelatin Microspheres: Midterm Clinical and MR Imaging Follow-up. J Vasc Interv Radiol. 2007;
151. Marcellin L, Santulli P, Bortolato S, Morin C, Millischer AE, Borghese B, et al. Anterior Focal Adenomyosis and Bladder Deep Infiltrating Endometriosis: Is There a Link? J Minim Invasive Gynecol. 2018;
152. Parker JD, Leondires M, Sinaii N, Premkumar A, Nieman LK, Stratton P. Persistence of dysmenorrhea and nonmenstrual pain after optimal endometriosis surgery may indicate adenomyosis. Fertil Steril. 2006;
153. Park Y, Kim MD, Jung DC, Lee SJ, Kim G, Park S Il, et al. Can measurement of apparent diffusion coefficient before treatment predict the response to uterine artery embolization for adenomyosis? Eur Radiol. 2015;
154. Pelage J-P, Jacob D, Fazel A, Namur J, Laurent A, Rymer R, et al. Midterm results of uterine artery embolization for symptomatic adenomyosis: initial experience. Radiology [Internet]. 2005 Mar;234(3):948–53. Available from:

https://www.ncbi.nlm.nih.gov/pubmed/15681687
155. Sam M, Raubenheimer M, Manolea F, Aguilar H, Mathew RP, Patel VH, et al. Accuracy of findings in the diagnosis of uterine adenomyosis on ultrasound. Abdom Radiol (New York) [Internet]. 2019 Sep; Available from: https://www.ncbi.nlm.nih.gov/pubmed/31552462
156. Siskin GP, Tublin ME, Stainken BF, Dowling K, Dolen EG. Uterine artery embolization for the treatment of adenomyosis: Clinical response and evaluation with MR imaging. Am J Roentgenol. 2001;
157. Sofic A, Husic-Selimovic A, Carovac A, Jahic E, Smailbegovic V, Kupusovic J. The significance of MRI evaluation of the uterine Junctional zone in the early diagnosis of adenomyosis. Acta Inform Medica. 2016;
158. Song SE, Sung DJ, Park BJ, Kim MJ, Cho SB, Kim KA. MR imaging features of uterine adenomyomas. Abdom Imaging. 2011;
159. Stoelinga B, Hehenkamp WJK, Brölmann HAM, Huirne JAF. Real-time elastography for assessment of uterine disorders. Ultrasound Obstet Gynecol. 2014;
160. Streuli I, Santulli P, Chouzenoux S, Chapron C, Batteux F. Serum Osteopontin Levels Are Decreased in Focal Adenomyosis. Reprod Sci. 2017;
161. Verma SK, Lev-Toaff AS, Baltarowich OH, Bergin D, Verma M, Mitchell DG. Adenomyosis: Sonohysterography with MRI correlation. Am J Roentgenol. 2009;
162. Xia M, Jing Z, Zhi-Yu H, Jian-Ming C, Hong-Yu Z, Rui-Fang X, et al. Feasibility study on energy prediction of microwave ablation upon uterine adenomyosis and leiomyomas by MRI. Br J Radiol. 2014;
163. Gong C, Setzen R, Liu Z, Liu Y, Xie B, Aili A, et al. High intensity focused ultrasound treatment of adenomyosis: The relationship between the features of magnetic resonance imaging on T2 weighted images and the therapeutic efficacy. Eur J Radiol. 2017;
164. Guo Y, Duan H, Cheng J, Zhang Y. Gonadotrophin-releasing hormone agonist combined with high-intensity focused ultrasound ablation for adenomyosis: a clinical study. BJOG An Int J Obstet Gynaecol. 2017;
165. Lee JS, Hong GY, Lee KH, Kim TE. Changes in anti-müllerian hormone levels as a biomarker for ovarian reserve after ultrasound-guided high-intensity focused ultrasound treatment of adenomyosis and uterine fibroid. BJOG An Int J Obstet Gynaecol. 2017;
166. Long L, Chen J, Xiong Y, Zou M, Deng Y, Chen L, et al. Efficacy of high-intensity focused ultrasound ablation for adenomyosis therapy and sexual life quality. Int J Clin Exp Med. 2015;
167. Xiong Y, Yue Y, Shui L, Orsi F, He J, Zhang L. Ultrasound-guided high-intensity focused ultrasound (USgHIFU) ablation for the treatment of

patients with adenomyosis and prior abdominal surgical scars: A retrospective study. Int J Hyperth. 2015;
168. Zhang X, Li K, Xie B, He M, He J, Zhang L. Effective ablation therapy of adenomyosis with ultrasound-guided high-intensity focused ultrasound. Int J Gynecol Obstet. 2014;
169. Kim MD, Kim YM, Kim HC, Cho JH, Kang HG, Lee C, et al. Uterine artery embolization for symptomatic adenomyosis: A new technical development of the 1-2-3 protocol and predictive factors of MR imaging affecting outcomes. J Vasc Interv Radiol. 2011;
170. Wang S, Meng X, Dong Y. The evaluation of uterine artery embolization as a nonsurgical treatment option for adenomyosis. Int J Gynaecol Obstet [Internet]. 2016 May;133(2):202–5. Available from: https://www.ncbi.nlm.nih.gov/pubmed/26868068
171. Yang X, Zhang X, Lin B, Feng X, Aili A. Combined therapeutic effects of HIFU, GnRH-a and LNG-IUS for the treatment of severe adenomyosis. Int J Hyperth. 2019;
172. Yang Q, Zhang LH, Su J, Liu J. The utility of diffusion-weighted MR imaging in differentiation of uterine adenomyosis and leiomyoma. Eur J Radiol. 2011;
173. Takeuchi M, Matsuzaki K, Nishitani H. Diffusion-weighted magnetic resonance imaging of endometrial cancer: differentiation from benign endometrial lesions and preoperative assessment of myometrial invasion. Acta Radiol [Internet]. 2009 Oct;50(8):947–53. Available from: https://www.ncbi.nlm.nih.gov/pubmed/19724949
174. Thum MY, Saso S, Clancy N, Smith JR. Imaging of organ viability during uterine transplantation surgery. Hum Reprod. 2015;30:34–34.
175. He Y, Ding N, Li Y, Li Z, Xiang Y, Jin Z, et al. 3-T diffusion tensor imaging (DTI) of normal uterus in young and middle-aged females during the menstrual cycle: Evaluation of the cyclic changes of fractional anisotropy (FA) and apparent diffusion coefficient (ADC) values. Br J Radiol. 2015;
176. Nakagawa M, Nakaura T, Namimoto T, Iyama Y, Kidoh M, Hirata K, et al. A multiparametric MRI-based machine learning to distinguish between uterine sarcoma and benign leiomyoma: comparison with 18F-FDG PET/CT. Clin Radiol. 2019;
177. Fornazari VAV, Vayego SA, Szejnfeld D, Szejnfeld J, Goldman SM. Functional magnetic resonance imaging for clinical evaluation of uterine contractility. Einstein (Sao Paulo) [Internet]. 2018;16(1):eMD3863. Available from: https://www.ncbi.nlm.nih.gov/pubmed/29694619
178. Nakashima A, Komesu I, Sakumoto T, Hamakawa H, Terada Y, Takayama H, et al. Study of uterine kinetics in nonpregnant women

using cine-mode magnetic resonance imaging. Reprod Med Biol. 2019;
179. Bozkurt DK. Diffusion-weighted and diffusion-tensor imaging of normal and diseased uterus. World J Radiol. 2015;
180. Porpora MG, Vinci V, De Vito C, Migliara G, Anastasi E, Ticino A, et al. The Role of Magnetic Resonance Imaging-Diffusion Tensor Imaging in Predicting Pain Related to Endometriosis: A Preliminary Study. J Minim Invasive Gynecol [Internet]. 2018 Jun;25(4):661–9. Available from: https://www.ncbi.nlm.nih.gov/pubmed/29126882
181. Rees CO, Nederend J, Mischi M, van Vliet HAAM, Schoot BC. Objective measures of adenomyosis on MRI and their diagnostic accuracy—a systematic review & meta-analysis. Acta Obstetricia et Gynecologica Scandinavica. 2021.
182. Van den Bosch T, Van Schoubroeck D. Ultrasound diagnosis of endometriosis and adenomyosis: State of the art. Best Pract Res Clin Obstet Gynaecol [Internet]. 2018 Aug;51:16–24. Available from: https://www.ncbi.nlm.nih.gov/pubmed/29506961
183. Van den Bosch T, de Bruijn AM, de Leeuw RA, Dueholm M, Exacoustos C, Valentin L, et al. Sonographic classification and reporting system for diagnosing adenomyosis. Ultrasound in Obstetrics and Gynecology. 2019.
184. Tellum T, Nygaard S, Skovholt EK, Qvigstad E, Lieng M. Development of a clinical prediction model for diagnosing adenomyosis. Fertil Steril. 2018 Oct 1;110(5):957-964.e3.
185. Andres MP, Borrelli GM, Ribeiro J, Baracat EC, Abrão MS, Kho RM. Transvaginal Ultrasound for the Diagnosis of Adenomyosis: Systematic Review and Meta-Analysis. J Minim Invasive Gynecol. 2018 Feb 1;25(2):257–64.
186. Lazzeri L, Giovanni A Di, Exacoustos C, Tosti C, Pinzauti S, Malzoni M, et al. Preoperative and Postoperative Clinical and Transvaginal Ultrasound Findings of Adenomyosis in Patients With Deep Infiltrating Endometriosis.
187. Gonzales M, Accardo De Matos L, Orlando Da Costa Gonçalves M, Blasbalg R, João A, Dias J, et al. Patients with adenomyosis are more likely to have deep endometriosis.
188. Gambadauro P, Carli V, Hadlaczky G. Depressive symptoms among women with endometriosis: a systematic review and meta-analysis. Vol. 220, American Journal of Obstetrics and Gynecology. Mosby Inc.; 2019. p. 230–41.
189. Von Elm E, Altman DG, Egger M, Pocock SJ, Gøtzsche PC, Vandenbrouckef JP. The Strengthening the Reporting of Observational Studies in Epidemiology (STROBE) Statement: Guidelines for reporting

observational studies. Bull World Health Organ. 2007 Nov;85(11):867–72.
190. Collins GS, Reitsma JB, Altman DG, Moons KGM. Transparent Reporting of a multivariable prediction model for Individual Prognosis Or Diagnosis (TRIPOD): the TRIPOD Statement. 2015; Available from: http://www.annals.org
191. Grant SW, Collins GS, Nashef SAM. Statistical Primer: developing and validating a risk prediction model †. Cardiothorac Surg [Internet]. 2018;54:203–11. Available from: https://academic.oup.com/ejcts/article/54/2/203/4993384
192. Rasmussen CK, Hansen ES, Dueholm M. Inter-rater agreement in the diagnosis of adenomyosis by 2- and 3-dimensional transvaginal ultrasonography. J Ultrasound Med [Internet]. 2019 Mar 1 [cited 2022 Aug 1];38(3):657–66. Available from: https://onlinelibrary.wiley.com/doi/full/10.1002/jum.14735
193. Habiba M, Gordts S, Bazot M, Brosens I, Benagiano G. Exploring the challenges for a new classification of adenomyosis. Reprod Biomed Online. 2020 Apr 1;40(4):569–81.
194. Aleksandrovych V, Basta P, Gil K. Current facts constituting an understanding of the nature of adenomyosis. Advances in Clinical and Experimental Medicine. 2019.
195. Hauth EAM, Jaeger HJ, Libera H, Lange S, Forsting M. MR imaging of the uterus and cervix in healthy women: determination of normal values. Eur Radiol [Internet]. 2007 Mar;17(3):734–42. Available from: https://www.ncbi.nlm.nih.gov/pubmed/16703306
196. Templeman C, Marshall SF, Ursin G, Horn-Ross PL, Clarke CA, Allen M, et al. Adenomyosis and endometriosis in the California Teachers Study. Fertil Steril. 2008 Aug 1;90(2):415–24.
197. Harmsen MJ, Van den Bosch T, Leeuw RA, Dueholm M, Exacoustos C, Valentin L, et al. Consensus on revised definitions of morphological uterus sonographic assessment (MUSA) features of adenomyosis: results of a modified Delphi procedure . Ultrasound Obstet Gynecol. 2021;
198. Harmsen MJ, Trommelen LM, de Leeuw RA, Tellum T, Juffermans LJM, Griffioen AW, et al. Multidisciplinary view on uterine junctional zone in uteri affected by adenomyosis: explaining discrepancies between MRI and transvaginal ultrasound images on a microscopic level . Ultrasound in Obstetrics & Gynecology. 2022. 0–3 p.
199. Tellum T, Munro MG. Classifications of Adenomyosis and Correlation of Phenotypes in Imaging and Histopathology to Clinical Outcomes: a Review. Curr Obstet Gynecol Rep [Internet]. 2022;11(1):1–11. Available from: https://doi.org/10.1007/s13669-021-00320-5

200. Garcia L, Isaacson K. Adenomyosis: Review of the Literature. J Minim Invasive Gynecol. 2011 Jul 1;18(4):428–37.
201. Abbott JA. Adenomyosis and Abnormal Uterine Bleeding (AUB-A)-Pathogenesis, diagnosis, and management. Best Pract Res Clin Obstet Gynaecol [Internet]. 2017 Apr;40:68–81. Available from: https://www.ncbi.nlm.nih.gov/pubmed/27810281
202. Levy G, Dehaene A, Laurent N, Lernout M, Collinet P, Lucot J-P, et al. An update on adenomyosis. Diagn Interv Imaging [Internet]. 2013 Jan;94(1):3–25. Available from: https://www.ncbi.nlm.nih.gov/pubmed/23246186
203. Kishi Y, Shimada K, Fujii T, Uchiyama T, Yoshimoto C, Konishi N, et al. Phenotypic characterization of adenomyosis occurring at the inner and outer myometrium. PLoS One [Internet]. 2017;12(12):e0189522. Available from: https://www.ncbi.nlm.nih.gov/pubmed/29253010
204. Rees CO, van de Wiel M, Nederend J, Huppelschoten A, Mischi M, van Vliet HAAM, et al. Prediction of adenomyosis diagnosis based on MRI. J Endometr Uterine Disord. 2023 Jun 1;2:100028.
205. Donders ART, van der Heijden GJMG, Stijnen T, Moons KGM. Review: A gentle introduction to imputation of missing values. J Clin Epidemiol. 2006 Oct 1;59(10):1087–91.
206. Hajian-Tilaki K. Receiver operating characteristic (ROC) curve analysis for medical diagnostic test evaluation. Casp J Intern Med. 2013;4(2):627–35.
207. Ramspek CL, Jager KJ, Dekker FW, Zoccali C, Van DIepen M. External validation of prognostic models: what, why, how, when and where? Clin Kidney J [Internet]. 2021 Feb 3 [cited 2023 Nov 19];14(1):49–58. Available from: https://dx.doi.org/10.1093/ckj/sfaa188
208. Martínez-Conejero JA, Morgan M, Montesinos M, Fortuño S, Meseguer M, Simón C, et al. Adenomyosis does not affect implantation, but is associated with miscarriage in patients undergoing oocyte donation. Fertil Steril. 2011;
209. Eisenberg VH, Arbib N, Schiff E, Goldenberg M, Seidman DS, Soriano D. Sonographic Signs of Adenomyosis Are Prevalent in Women Undergoing Surgery for Endometriosis and May Suggest a Higher Risk of Infertility. Biomed Res Int. 2017;2017.
210. Vannuccini S, Tosti C, Carmona F, Huang SJ, Chapron C, Guo SW, et al. Pathogenesis of adenomyosis: an update on molecular mechanisms. Reproductive BioMedicine Online. 2017.
211. Maruyama S, Imanaka S, Nagayasu M, Kimura M, Kobayashi H. Relationship between adenomyosis and endometriosis; Different phenotypes of a single disease? Vol. 253, European Journal of Obstetrics and Gynecology and Reproductive Biology. 2020.

212. Imaoka I, Wada A, Matsuo M, Yoshida M, Kitagaki H, Sugimura K. MR Imaging of Disorders Associated with Female Infertility: Use in Diagnosis, Treatment, and Management. Radiographics. 2003.
213. Vergouwe Y, Steyerberg EW, Eijkemans MJC, Habbema JDF. Substantial effective sample sizes were required for external validation studies of predictive logistic regression models. J Clin Epidemiol. 2005 May 1;58(5):475–83.
214. He YL, Ding N, Li Y, Li Z, Xiang Y, Jin ZY, et al. Cyclic changes of the junctional zone on 3 T MRI images in young and middle-aged females during the menstrual cycle. Clin Radiol. 2016 Apr 1;71(4):341–8.
215. Fanchin R, Ayoubi JM. Uterine dynamics: Impacton the human reproduction process. Reproductive BioMedicine Online. 2009.
216. van Gestel I, Ijland MM, Hoogland HJ, Evers JLH. Endometrial wave-like activity in the non-pregnant uterus. Human Reproduction Update. 2003.
217. Bulletti C, De Ziegler D. Uterine contractility and embryo implantation. Current Opinion in Obstetrics and Gynecology. 2006.
218. Kissler S, Zangos S, Vogl TJ, Hamscho N, Gruenwald F, Kohl J, et al. Impaired utero-tubal sperm transport in adenomyosis and endometriosis—a cause for infertility. Int Congr Ser. 2004;
219. Kissler S, Zangos S, Wiegratz I, Kohl J, Rody A, Gaetje R, et al. Utero-tubal sperm transport and its impairment in endometriosis and adenomyosis. In: Annals of the New York Academy of Sciences. 2007.
220. Kuijsters NPM, Sammali F, Rabotti C, Huang Y, Mischi M, Schoot BC. Visual inspection of transvaginal ultrasound videos to characterize uterine peristalsis: an inter-observer agreement study. J Ultrasound. 2020;
221. Sammali F, Kuijsters NPM, Huang Y, Blank C, Rabotti C, Schoot BC, et al. Dedicated Ultrasound Speckle Tracking for Quantitative Analysis of Uterine Motion Outside Pregnancy. IEEE Trans Ultrason Ferroelectr Freq Control. 2019;
222. Huang Y, Sammali F, Kuijsters NPM, Blank C, Schoot BC, Mischi M. Quantitative Motion Analysis of the Uterus by Optical Flow and Two-dimensional Strain Mapping. In: MeMeA 2018 - 2018 IEEE International Symposium on Medical Measurements and Applications, Proceedings. 2018.
223. Sammali F, Blank C, Xu L, Huang Y, Kuijsters NPM, Schoot BC, et al. Experimental setup for objective evaluation of uterine motion analysis by ultrasound speckle tracking. Biomed Phys Eng Express. 2018;
224. Sammali F, Blank C, Huang Y, Kuijsters NPM, Rabotti C, Schoot BC, et al. Quantitative Analysis of Uterine Motion Outside Pregnancy by Dedicated Ultrasound Speckle Tracking. In: IEEE International

Ultrasonics Symposium, IUS. 2018.
225. Sammali F, Blank C, Bakkes TGH, Huang Y, Rabotti C, Schoot BC, et al. Multi-Modal Uterine-Activity Measurements for Prediction of Embryo Implantation by Machine Learning. IEEE Access. 2021;9:47096–111.
226. Blank C, Sammali F, Kuijsters N, Huang Y, Rabotti C, de Sutter P, et al. Assessment of uterine activity during IVF by quantitative ultrasound imaging: a pilot study [Internet]. Reproductive BioMedicine Online. 2020 [cited 2021 Oct 19]. p. 1045–53. Available from: https://www.sciencedirect.com/science/article/pii/S1472648320304399?casa_token=xEVdHOVluqMAAAAA:8nsb2PSMYxuUeR2w1rxl_W0OZwYZVprwug1uz8r3QUKcWQoY2FgH8kL5AIBDgBUE1wHWsSYFId0
227. Sammali F, Blank C, Bakkes THGF, Huang Y, Rabotti C, Schoot BC, et al. Prediction of embryo implantation by machine learning based on ultrasound strain imaging. In: IEEE International Ultrasonics Symposium, IUS. 2019.
228. Huang Y, Sammali F, Blank C, Kuijsters N, Rabotti C, Schoot BC, et al. Quantitative Ultrasound Imaging and Characterization of Uterine Peristaltic Waves. In: IEEE International Ultrasonics Symposium, IUS. 2018.
229. Huang Y, Rees C, Sammali F, Blank C, Schoot D, Mischi M. Characterization of uterine peristaltic waves by ultrasound strain analysis; Characterization of uterine peristaltic waves by ultrasound strain analysis. IEEE Trans Ultrason Ferroelectr Freq Control [Internet]. 2022;PP. Available from: http://www.ieee.org/publications_standards/publications/rights/index.html
230. Hu LY, Fan HY. Inversion formula and Parseval theorem for complex continuous wavelet transforms studied by entangled state representation. Chinese Phys B. 2010;19(7).
231. Kuijsters NPM, Methorst WG, Kortenhorst MSQ, Rabotti C, Mischi M, Schoot BC. Uterine peristalsis and fertility: current knowledge and future perspectives: a review and meta-analysis. Reprod Biomed Online. 2017 Jul 1;35(1):50–71.
232. Leyendecker, Kunz G, Wildt L, Beil D, Deininger H. Uterine hyperperistalsis and dysperistalsis as dysfunctions of the mechanism of rapid sperm transport in patients with endometriosis and infertility [Internet]. Vol. 11, Human Reproduction. 1996. Available from: https://academic.oup.com/humrep/article/11/7/1542/636603
233. Kuijsters NPM, Methorst WG, Kortenhorst MSQ, Rabotti C, Mischi M, Schoot BC. Uterine peristalsis and fertility: current knowledge and

future perspectives: a review and meta-analysis. Reprod Biomed Online. 2017 Jul 1;35(1):50–71.
234. Martinez-Gaudio M, Yoshida T, Bengtsson LP. Propagated and nonpropagated myometrial contractions in normal menstrual cycles. Am J Obstet Gynecol. 1973;
235. Togashi K. Uterine Contractility Evaluated on Cine Magnetic Resonance Imaging. Ann N Y Acad Sci [Internet]. 2007 Apr 1 [cited 2022 Jun 15];1101(1):62–71. Available from: https://onlinelibrary.wiley.com/doi/full/10.1196/annals.1389.030
236. Zhang Y, Qian J, Zaltzhendler O, Bshara M, Jaffa AJ, Grisaru D, et al. Analysis of *in vivo* uterine peristalsis in the non-pregnant female mouse. Interface Focus. 2019 Aug;9(4):20180082.
237. Bulletti C, De Ziegler D, Polli V, Diotallevi L, Del Ferro E, Flamigni C. Uterine contractility during the menstrual cycle. Hum Reprod. 2000;15(SUPPL. 1):81–9.
238. Oki T, Douchi T, Maruta K, Nakamura S, Nagata Y. Changes in endometrial wave-like movements in accordance with the phases of menstrual cycle. J Obstet Gynaecol Res. 2002 Jun;28(3):176–81.
239. Pritts EA, Parker WH, Olive DL. Fibroids and infertility: an updated systematic review of the evidence. Fertil Steril. 2009 Apr 1;91(4):1215–23.
240. Schenken RS, Guzick DS. Revised endometriosis classification: 1996. Fertil Steril. 1997;67(5):815–6.
241. Venetis CA, Papadopoulos SP, Campo R, Gordts S, Tarlatzis BC, Grimbizis GF. Clinical implications of congenital uterine anomalies: a meta-analysis of comparative studies. Reprod Biomed Online. 2014 Dec 1;29(6):665–83.
242. Taylor E, Gomel V. The uterus and fertility. Fertil Steril. 2008 Jan 1;89(1):1–16.
243. Rayyan – Intelligent Systematic Review - [Internet]. [cited 2022 Jun 15]. Available from: https://www.rayyan.ai/
244. Downs SH, Black N. The feasibility of creating a checklist for the assessment of the methodological quality both of randomised and non-randomised studies of health care interventions. J Epidemiol Community Heal [Internet]. 1998;52:377–84. Available from: http://jech.bmj.com/
245. Kido A, Togashi K, Nishino M, Miyake K, Koyama T, Fujimoto R, et al. Cine MR imaging of uterine peristalsis in patients with endometriosis. Eur Radiol. 2007;
246. Kido A, Ascher SM, Hahn W, Kishimoto K, Kashitani N, Jha RC, et al. 3 T MRI uterine peristalsis: Comparison of symptomatic fibroid patients versus controls. Clin Radiol. 2014 May 1;69(5):468–72.

247. Kido A, Ascher SM, Kishimoto K, Hahn W, Jha RC, Togashi K, et al. Comparison of Uterine Peristalsis Before and After Uterine Artery Embolization at 3-T MRI. http://dx.doi.org/102214/AJR105349 [Internet]. 2012 Nov 23 [cited 2022 Jun 15];196(6):1431–5. Available from: www.ajronline.org
248. Yoshino O, Nishii O, Osuga Y, Asada H, Okuda S, Orisaka M, et al. Myomectomy Decreases Abnormal Uterine Peristalsis and Increases Pregnancy Rate. J Minim Invasive Gynecol. 2012 Jan 1;19(1):63–7.
249. Yoshino O, Hayashi T, Osuga Y, Orisaka M, Asada H, Okuda S, et al. Decreased pregnancy rate is linked to abnormal uterine peristalsis caused by intramural fibroids. Hum Reprod [Internet]. 2010; Available from: https://academic.oup.com/humrep/article/25/10/2475/2385697
250. Nishino M, Togashi K, Nakai A, Hayakawa K, Kanao S, Iwasaku K, et al. Uterine contractions evaluated on cine MR imaging in patients with uterine leiomyomas. Eur J Radiol. 2005 Jan 1;53(1):142–6.
251. Adami Vayego Fornazari V, Szejnfeld D, Szejnfeld J, dio Emilio Bonduki C, Adami Vayego S, Menasce Goldman S, et al. Evaluation of Uterine Contractility by Magnetic Resonance Imaging in Women Undergoing Embolization of Uterine Fibroids. Cardiovasc Interv Radiol. 2018;42:186–94.
252. Orisaka M, Kurokawa T, Shukunami KI, Orisaka S, Fukuda MT, Shinagawa A, et al. A comparison of uterine peristalsis in women with normal uteri and uterine leiomyoma by cine magnetic resonance imaging. Eur J Obstet Gynecol Reprod Biol. 2007 Nov;135(1):111–5.
253. Bulletti C, De Ziegler D, Rossi S, Polli V, Massoneau M, Rossi E, et al. Abnormal uterine contractility in nonpregnant women. Ann N Y Acad Sci. 1997;828:223–9.
254. Bulletti C, Ziegler D De, Polli V, Del Ferro E, Palini S, Flamigni C. Characteristics of uterine contractility during menses in women with mild to moderate endometriosis. Fertil Steril. 2002 Jun 1;77(6):1156–61.
255. Szamatowicz J, Laudaǹski T, Bulkszas B, Åkerlund M. Fibromyomas and uterine contractions. Acta Obstet Gynecol Scand [Internet]. 1997 Oct 1 [cited 2022 Jun 15];76(10):973–6. Available from: https://onlinelibrary.wiley.com/doi/full/10.3109/00016349709034912
256. Oliva GC, Fratoni A, Genova M, Romanini C. Uterine motility in patients with bicornuate uterus. Int J Gynecol Obstet [Internet]. 1992 Jan 1 [cited 2022 Jun 15];37(1):7–12. Available from: https://onlinelibrary.wiley.com/doi/full/10.1016/0020-7292%2892%2990971-K

257. Pinto V, Matteo M, Tinelli R, Mitola PC, De Ziegler D, Cicinelli E. Altered uterine contractility in women with chronic endometritis. Fertil Steril. 2015 Apr 1;103(4):1049–52.
258. Qu Y, Xiao Z, Liu LA, Lv FF, Sheng BG, Li J, et al. Uterine Peristalsis Before and After Ultrasound-Guided High-Intensify Focused Ultrasound (USgHIFU) Treatment for Symptomatic Uterine Fibroids. 2019; Available from: https://www.medscimonit.com/abstract/index/idArt/913392
259. Hunt S, Abdallah KS, Ng E, Rombauts L, Vollenhoven B, Mol BW. Impairment of Uterine Contractility Is Associated with Unexplained Infertility. Semin Reprod Med [Internet]. 2020 Jan 1 [cited 2022 Jun 15];38(1):61–73. Available from: http://www.thieme-connect.com/products/ejournals/html/10.1055/s-0040-1716409
260. Sammali F, Kuijsters NPM, Huang Y, Blank C, Rabotti C, Schoot BC, et al. Dedicated Ultrasound Speckle Tracking for Quantitative Analysis of Uterine Motion Outside Pregnancy. IEEE Trans Ultrason Ferroelectr Freq Control. 2019 Mar 1;66(3):581–90.
261. Bulletti C, De Ziegler D. Uterine contractility and embryo implantation. Curr Opin Obstet Gynecol. 2006 Aug;18(4):473–84.
262. Kunz G, Noe M, Herbertz M, Leyendecker G. Uterine peristalsis during the follicular phase of the menstrual cycle: Effects of oestrogen, antioestrogen and oxytocin. In: Human Reproduction Update. 1998.
263. Rees CO, de Boer A, Huang Y, Wessels B, Blank C, Kuijsters N, et al. Uterine contractile activity in healthy women throughout the menstrual cycle measured using a novel quantitative two-dimensional transvaginal ultrasound speckle tracking method. Reprod Biomed Online. 2023 Jan 1;46(1):115–22.
264. Huang Y, Rees C, Sammali F, Blank C, Schoot D, Mischi M. Characterization of Uterine Peristaltic Waves by Ultrasound Strain Analysis. IEEE Trans Ultrason Ferroelectr Freq Control. 2022 Jun 1;69(6):2050–60.
265. Habiba M, Benagiano G, Guo S-W. An Appraisal of the Tissue Injury and Repair (TIAR) Theory on the Pathogenesis of Endometriosis and Adenomyosis. Biomolecules. 2023 Jun 11;13(6):975.
266. de Boer A, Rees CO, Mischi M, Van Vliet H, Huirne J, Schoot BC. The influence of uterine abnormalities on uterine peristalsis in the non-pregnant uterus: A systematic review. J Endometr Uterine Disord [Internet]. 2023;3(June):100038. Available from: https://doi.org/10.1016/j.jeud.2023.100038
267. Sammali F, Kuijsters NPM, Huang Y, Blank C, Rabotti C, Schoot BC, et al. Dedicated Ultrasound Speckle Tracking for Quantitative Analysis of Uterine Motion Outside Pregnancy. IEEE Trans Ultrason Ferroelectr

Freq Control. 2019 Mar 1;66(3):581–90.
268. Lymperi S, Neofytou E, Vaitsopoulou C, Bazioti MG, Kalyvianaki K, Chatzimeletiou K, et al. Oxytocin preprotein and oxytocin receptor mRNA expression is altered in semen samples with abnormal semen parameters. Reprod Biomed Online. 2023 Feb 1;46(2):363–70.
269. Guo SW, Mao X, Ma Q, Liu X. Dysmenorrhea and its severity are associated with increased uterine contractility and overexpression of oxytocin receptor (OTR) in women with symptomatic adenomyosis. Fertil Steril. 2013 Jan 1;99(1):231–40.
270. Zhang Y, Yu P, Sun F, Li TC, Cheng JM, Duan H. Expression of oxytocin receptors in the uterine junctional zone in women with adenomyosis. Acta Obstet Gynecol Scand. 2015;94(4):412–8.
271. Mehasseb MK, Panchal R, Taylor AH, Brown L, Bell SC, Habiba M. Estrogen and progesterone receptor isoform distribution through the menstrual cycle in uteri with and without adenomyosis. Fertil Steril. 2011 Jun 1;95(7):2228-2235.e1.
272. Macer ML, Taylor HS. Endometriosis and Infertility. A Review of the Pathogenesis and Treatment of Endometriosis-associated Infertility. Obstetrics and Gynecology Clinics of North America. 2012.
273. Sammali F, Blank C, Xu L, Huang Y, Kuijsters NPM, Schoot BC, et al. Experimental setup for objective evaluation of uterine motion analysis by ultrasound speckle tracking. Biomed Phys Eng Express. 2018 Mar 13;4(3).
274. Higgins C, Fernandes H, Da Silva Costa F, Martins WP, Vollenhoven B, Healey M. The impact of adenomyosis on IVF outcomes: a prospective cohort study. Hum Reprod Open. 2021;
275. Buggio L, Monti E, Gattei U, Dridi D, Vercellini P. Adenomyosis: Fertility and obstetric outcome. A comprehensive literature review. Minerva Ginecologica. 2018.
276. Brosens J, Verhoeven H, Campo R, Gianaroli L, Gordts S, Hazekamp J, et al. High endometrial aromatase P450 mRNA expression is associated with poor IVF outcome. Hum Reprod. 2004;
277. Tremellen KP, Russell P. The distribution of immune cells and macrophages in the endometrium of women with recurrent reproductive failure. II: adenomyosis and macrophages. J Reprod Immunol [Internet]. 2012 Jan;93(1):58–63. Available from: https://www.ncbi.nlm.nih.gov/pubmed/22209314
278. Campo S, Campo V, Benagiano G. Adenomyosis and infertility. Reproductive BioMedicine Online. 2012.
279. van der Houwen LEE, Lier MCI, Schreurs AMF, van Wely M, Hompes PGA, Cantineau AEP, et al. Continuous oral contraceptives versus long-term pituitary desensitization prior to IVF/ICSI in moderate to severe

endometriosis: study protocol of a non-inferiority randomized controlled trial. Hum Reprod Open. 2019;
280. Graziano A, Lo Monte G, Piva I, Caserta D, Karner M, Engl B, et al. Diagnostic findings in adenomyosis: a pictorial review on the major concerns. Eur Rev Med Pharmacol Sci [Internet]. 2015 Apr;19(7):1146–54. Available from: https://www.ncbi.nlm.nih.gov/pubmed/25912572
281. Nirgianakis K, Kalaitzopoulos DR, Schwartz ASK, Spaanderman M, Kramer BW, Mueller MD, et al. Fertility, pregnancy and neonatal outcomes of patients with adenomyosis: a systematic review and meta-analysis. Reprod Biomed Online. 2021;42(1):185–206.
282. Bourdon M, Santulli P, Bordonne C, Millisher AE, Maitrot-Mantelet L, Maignien C, et al. Presence of adenomyosis at MRI reduces live birth rates in ART cycles for endometriosis. Hum Reprod [Internet]. 2022 Jun 30 [cited 2022 Aug 3];37(7):1470–9. Available from: https://academic.oup.com/humrep/article/37/7/1470/6573229
283. Rees CO, Rupert IAM, Nederend J, Consten D, Mischi M, A.A.M. van Vliet H, et al. Women with combined adenomyosis and endometriosis on MRI have worse IVF/ICSI outcomes compared to adenomyosis and endometriosis alone: A matched retrospective cohort study. Eur J Obstet Gynecol Reprod Biol. 2022 Apr;271:223–34.
284. Coccia ME, Rizzello F, Mariani G, Bulletti C, Palagiano A, Scarselli G. Impact of endometriosis on IVF-ET cycles in young women: a stage dependent interference. Acta Obstet Gynecol Scand. 2011;
285. Brosens JJ, de Souza NM, Barker FG. Uterine junctional zone: function and disease. Lancet (London, England) [Internet]. 1995 Aug;346(8974):558–60. Available from: https://www.ncbi.nlm.nih.gov/pubmed/7658784
286. Dakhly DMR, Abdel Moety GAF, Saber W, Gad Allah SH, Hashem AT, Abdel Salam LOE. Accuracy of Hysteroscopic Endomyometrial Biopsy in Diagnosis of Adenomyosis. J Minim Invasive Gynecol. 2016 Mar 1;23(3):364–71.
287. Pinzauti S, Lazzeri L, Tosti C, Centini G, Orlandini C, Luisi S, et al. Transvaginal sonographic features of diffuse adenomyosis in 18-30-year-old nulligravid women without endometriosis: association with symptoms. Ultrasound Obs Gynecol [Internet]. 2015 [cited 2022 Nov 14];46:730–6. Available from: https://obgyn.onlinelibrary.wiley.com/doi/10.1002/uog.14834
288. Loring M, Chen TY, Isaacson KB. A Systematic Review of Adenomyosis: It Is Time to Reassess What We Thought We Knew about the Disease. J Minim Invasive Gynecol. 2021 Mar 1;28(3):644–55.

289. Leyendecker G, Kunz G, Kissler S, Wildt L. Adenomyosis and reproduction. Best Practice and Research: Clinical Obstetrics and Gynaecology. 2006.
290. Berlanda N, Donati A, Fedele F, Lepri M, Vercellini P. Adenomyosis and Obstetrical Outcome: a Narrative Mini-Review of the Latest Evidence. Curr Obstet Gynecol Reports 2022 [Internet]. 2022 Apr 8 [cited 2022 Aug 3];1–12. Available from: https://link.springer.com/article/10.1007/s13669-021-00316-1
291. Harada T, Taniguchi F, Harada T. Increased risk of obstetric complications in patients with adenomyosis: A narrative literature review. Reprod Med Biol [Internet]. 2022 Jan 1 [cited 2022 Aug 3];21(1):e12473. Available from: https://onlinelibrary.wiley.com/doi/full/10.1002/rmb2.12473
292. Zhang M, Bazot M, Tsatoumas M, Munro MG, Reinhold C. MRI of Adenomyosis: Where Are We Today? https://doi.org/101177/08465371221114197 [Internet]. 2022 Jul 20 [cited 2023 Nov 21];74(1):58–68. Available from: https://journals.sagepub.com/doi/abs/10.1177/08465371221114197
293. Guo SW, Benagiano G, Bazot M. In Search of an Imaging Classification of Adenomyosis: A Role for Elastography? J Clin Med 2023, Vol 12, Page 287 [Internet]. 2022 Dec 30 [cited 2023 Dec 17];12(1):287. Available from: https://www.mdpi.com/2077-0383/12/1/287/htm
294. Chou SY, Chan C, Lee YC, Yu TN, Tzeng CR, Chen CH. Evaluation of adenomyosis after gonadotrophin-releasing hormone agonist therapy using ultrasound post-processing imaging: a pilot study. J Int Med Res [Internet]. 2020 Jun 1 [cited 2023 Dec 17];48(6). Available from: https://journals.sagepub.com/doi/full/10.1177/0300060520920056
295. Zanolli NC, Cline BC, Befera NT, Martin JG. Diagnostic accuracy of clinically reported adenomyosis on pelvic ultrasound and MRI compared to surgical pathology. Clin Imaging. 2022;82.
296. Leyendecker G, Kunz G, Wildt L, Beil D, Deininger H. Uterine hyperperistalsis and dysperistalsis as dysfunctions of the mechanism of rapid sperm transport in patients with endometriosis and infertility. Hum Reprod. 1996;11(7):1542–51.
297. Xie T, Xu X, Yang Y, Wu C, Liu X, Zhou L, et al. The Role of Abnormal Uterine Junction Zone in the Occurrence and Development of Adenomyosis. Reprod Sci [Internet]. 2022 Oct 1 [cited 2023 Dec 12];29(10):2719–30. Available from: https://link.springer.com/article/10.1007/s43032-021-00684-2
298. Barbanti C, Centini G, Lazzeri L, Habib N, Labanca L, Zupi E, et al.

Adenomyosis and infertility: the role of the junctional zone. Gynecol Endocrinol [Internet]. 2021 [cited 2023 Dec 13];37(7):577–83. Available from: https://www.tandfonline.com/doi/abs/10.1080/09513590.2021.1878131

299. Tellum T, Naftalin J, Chapron C, Dueholm M, Guo SW, Hirsch M, et al. Development of a core outcome set and outcome definitions for studies on uterus-sparing treatments of adenomyosis (COSAR): an international multistakeholder-modified Delphi consensus study. Hum Reprod [Internet]. 2022 Aug 25 [cited 2023 Dec 13];37(9):2012–31. Available from: https://dx.doi.org/10.1093/humrep/deac166
300. Benagiano G, Brosens I, Habiba M. Structural and molecular features of the endomyometrium in endometriosis and adenomyosis. Hum Reprod Update [Internet]. 2014 May 1 [cited 2023 Nov 21];20(3):386–402. Available from: https://dx.doi.org/10.1093/humupd/dmt052
301. Maruyama S, Imanaka S, Nagayasu M, Kimura M, Kobayashi H. Relationship between adenomyosis and endometriosis; Different phenotypes of a single disease? Eur J Obstet Gynecol Reprod Biol. 2020 Oct 1;253:191–7.
302. Cozzolino M, Tartaglia S, Pellegrini L, Troiano G, Rizzo G, Petraglia F. The Effect of Uterine Adenomyosis on IVF Outcomes: a Systematic Review and Meta-analysis. Reprod Sci [Internet]. 2022 Nov 1 [cited 2023 Nov 21];29(11):3177–93. Available from: https://link.springer.com/article/10.1007/s43032-021-00818-6
303. Moayed ME, Moini A, Kashani L, Mojtahedi MF, Rezaee T, Tabasizadeh H, et al. Pregnancy outcomes in women with adenomyosis, undergoing artificial endometrial preparation with and without gonadotropin-releasing hormone agonist pretreatment in frozen embryo transfer cycles: An RCT. Int J Reprod Biomed [Internet]. 2023 Jun 1 [cited 2023 Nov 21];21(6):481. Available from: /pmc/articles/PMC10407916/
304. Wu Y, Huang J, Zhong G, Lan J, Lin H, Zhang Q. Long-term GnRH agonist pretreatment before frozen embryo transfer improves pregnancy outcomes in women with adenomyosis. Reprod Biomed Online. 2022 Feb 1;44(2):380–8.
305. Wang Y, Yi YC, Guu HF, Chen YF, Kung HF, Chang JC, et al. Impact of adenomyosis and endometriosis on IVF/ICSI pregnancy outcome in patients undergoing gonadotropin-releasing hormone agonist treatment and frozen embryo transfer. Sci Reports 2023 131 [Internet]. 2023 Apr 25 [cited 2023 Nov 21];13(1):1–8. Available from: https://www.nature.com/articles/s41598-023-34045-7

306. Dashottar S, Singh AK, Debnath J, Muralidharan CG, Singh RK, Kumar S. Comparative analysis of changes in MR imaging of pre and post intrauterine progesterone implants in adenomyosis cases. Med J Armed Forces India. 2015;
307. Kang S, Turner DA, Foster GS, Rapoport MI, Spencer SA, Wang JZ. Adenomyosis: Specificity of 5 mm as the maximum normal uterine junctional zone thickness in MR images. Am J Roentgenol. 1996;

3A. Search Terms for Patient Selection

The following search terms were used for pelvic MRI:

- Magnetic Resonance Imaging
- Magnetic Resonance
- Mri Scan
- MRI
- NMR
- Mriscan
- magnetic Resonance Imaging
- Kernspintomografie

For hysterectomy surgery, the following terms were used:

- Hysterectomie
- Laparoscopische uterus extirpatie met tubae
- lap uterus extirpatie LAVH', 'abd. uterusextirpatie
- laparoscopische uterus extirpatie
- laparoscopische uterus extirpatie LAVH LASH met tubectomie
- abdominale uterusextirpatie met verwijdering van p
- abd. uterus ext. + adnexa
- abd. uterus ext.
- vag. uterus ext. + VW + AW plastiek
- lap uterusextirpatie
- lap uterus extirpatie met tubectomie
- lapsc. uterus ext.
- vag. uterus ext.
- abd-vag. radicale uterusextirpatie + lymfadenectomie
- abdominale uterus extirpatie
- lap uterus extirpatie
- lap uterus extirpatie LAVH LASH
- vaginale uterus extirpatie
- Laparoscopische uterus extirpatie LAVH LASH
- abdominale uterusextirpatie
- V-notes uterus extirpatie

3B. Local Protocol for Pelvic MRI

MRI for Endometriosis Diagnosis:

Patients with suspected or known endometriosis are given an MRI according to the following protocol in our centre. There is a preference for using the 3 Tesla scan, however the 1.5 Tesla scan can also be used.
Scan procedure, in chronological order:

Setting	Sequence	Orientation
T2	TSE	Sagittal
T2	TSE	Transverse
T2	TSE	Coronal
T1 (spiral)	TSE	Transverse

TSE: turbo spin echo
Contrast agent: none.
Medication: Buscopan/Glucagon are given in order to minimise the effect of uterine contractions on the evaluation of the images.

MRI for Adenomyosis Embolisation
Additional MRI's may be carried out in patients with fibroids or (focal) adenomyosis in order to determine the suitability of the lesion for potential uterine artery embolization. There is a preference for using the 3 Tesla scan, however the 1.5 Tesla scan can also be used.

This is carried out using the following protocol (in chronological order):

Setting	Sequence	Orientation
T2W	TSE	Sagittal
T1W	TSE	Transverse
T1W	TSE	Sagittal
Injection of contrast agent		
T2W	TSE	Transverse
T1W	TSE	Sagittal

*T2W: T2 weighted TSE: turbo spin echo
Contrast agent: Gadolinium pentate

- Dosage
    - 1.5T: 0,2mg/kg
    - 3T: 0,1 mg/kg

3C. MRI Parameters Measured

Table 3.S1: Overview of Assessed MRI parameters

MRI characteristic	Definition	Unit (stratification)
Mean JZ thickness	Mean of JZ at six points of the uterus: anterior fundus, posterior fundus, anterior mid-corpus, posterior mid-corpus, anterior isthmus, posterior isthmus	Millimetres
Maximal JZ thickness (JZ Max)	Maximal diameter of JZ, out of all imaging planes	Millimetres (≥12)
Minimal JZ thickness (JZ Min)	Minimal diameter of JZ	Millimetres
JZ differential (JZ Diff)	Measure of JZ irregularity, difference between maximal and minimal JZ thickness	Millimetres (≥5)
JZ asymmetry (JZ Asym)	Absolute difference between anterior and posterior JZ thickness (based on measurements at six points of the uterus as previously described)	Millimetres
Uterine length	Measured from cervix to fundus in sagittal orientation	Millimetres
Uterine volume	Volume of the uterus in three orientations: sagittal, transversal and coronal	Millimetres^3
Mean uterine wall thickness	Measured from endometrium to myometrium at six points of the uterus as previously described	Millimetres
Mean uterine wall asymmetry	Absolute difference between anterior and posterior uterine wall thickness	Millimetres
JZ to myometrium ratio (JZ/MYO)	Ratio of JZ to full myometrium thickness (based on measurements at six points of the uterus as previously described)	Percentage (>40)
High signal intensity foci (HSI Foci)	Presence of high signal intensity myometrial foci on T2 or T1 imaging	
Signal intensity ratio	Signal intensity ratio of adenomyotic tissue compared to that of the rectus muscle on T2 imaging	Unitless

MRI = Magnetic Resonance Imaging. JZ = Junctional Zone

3D. STROBE Statement for Cohort Studies

	Item No	Recommendation	Page No
Title and abstract	1	(*a*) Indicate the study's design with a commonly used term in the title or the abstract (*b*) Provide in the abstract an informative and balanced summary of what was done and what was found	1 – 3
Introduction			
Background /rationale	2	Explain the scientific background and rationale for the investigation being reported	4
Objectives	3	State specific objectives, including any prespecified hypotheses	4
Methods			
Study design	4	Present key elements of study design early in the paper	5
Setting	5	Describe the setting, locations, and relevant dates, including periods of recruitment, exposure, follow-up, and data collection	5
Participants	6	(*a*) Give the eligibility criteria, and the sources and methods of selection of participants. Describe methods of follow-up (*b*) For matched studies, give matching criteria and number of exposed and unexposed	5
Variables	7	Clearly define all outcomes, exposures, predictors, potential confounders, and effect modifiers. Give diagnostic criteria, if applicable	8
Data sources/ measurement	8*	For each variable of interest, give sources of data and details of methods of assessment (measurement). Describe comparability of assessment methods if there is more than one group	5, 6
Bias	9	Describe any efforts to address potential sources of bias	6, 7
Study size	10	Explain how the study size was arrived at	8
Quantitative variables	11	Explain how quantitative variables were handled in the analyses. If applicable, describe which groupings were chosen and why	7, 8
Statistical methods	12	(*a*) Describe all statistical methods, including those used to control for confounding (*b*) Describe any methods used to examine subgroups and interactions (*c*) Explain how missing data were addressed (*d*) If applicable, explain how loss to follow-up was addressed (*e*) Describe any sensitivity analyses	7, 8
Results			
Participants	13*	(a) Report numbers of individuals at each stage of study—eg numbers potentially eligible, examined for eligibility, confirmed eligible, included in the study, completing follow-up, and analysed (b) Give reasons for non-participation at each stage	8, 9

		(c) Consider use of a flow diagram	
Descriptive data	14*	(a) Give characteristics of study participants (eg demographic, clinical, social) and information on exposures and potential confounders (b) Indicate number of participants with missing data for each variable of interest (c) Summarise follow-up time (eg, average and total amount)	8, 9
Outcome data	15*	Report numbers of outcome events or summary measures over time	9, 10
Main results	16	(a) Give unadjusted estimates and, if applicable, confounder-adjusted estimates and their precision (eg, 95% confidence interval). Make clear which confounders were adjusted for and why they were included	9-11
		(b) Report category boundaries when continuous variables were categorized	8
		(c) If relevant, consider translating estimates of relative risk into absolute risk for a meaningful time period	
Other analyses	17	Report other analyses done—eg analyses of subgroups and interactions, and sensitivity analyses	9-11

Discussion

Key results	18	Summarise key results with reference to study objectives	11
Limitations	19	Discuss limitations of the study, taking into account sources of potential bias or imprecision. Discuss both direction and magnitude of any potential bias	12, 13
Interpretation	20	Give a cautious overall interpretation of results considering objectives, limitations, multiplicity of analyses, results from similar studies, and other relevant evidence	12, 13
Generalisability	21	Discuss the generalisability (external validity) of the study results	13

Other information

Funding	22	Give the source of funding and the role of the funders for the present study and, if applicable, for the original study on which the present article is based	1

3E. TRIPOD Statement

Section/Topic		Checklist Item	Page
Title and abstract			
Title	1	Identify the study as developing and/or validating a multivariable prediction model, the target population, and the outcome to be predicted.	1
Abstract	2	Provide a summary of objectives, study design, setting, participants, sample size, predictors, outcome, statistical analysis, results, and conclusions.	2
Introduction			
Background and objectives	3a	Explain the medical context (including whether diagnostic or prognostic) and rationale for developing or validating the multivariable prediction model, including references to existing models.	4
	3b	Specify the objectives, including whether the study describes the development or validation of the model or both.	4, 5
Methods			
Source of data	4a	Describe the study design or source of data (e.g., randomized trial, cohort, or registry data), separately for the development and validation data sets, if applicable.	5
	4b	Specify the key study dates, including start of accrual; end of accrual; and, if applicable, end of follow-up.	5
Participants	5a	Specify key elements of the study setting (e.g., primary care, secondary care, general population) including number and location of centres.	5
	5b	Describe eligibility criteria for participants.	5
	5c	Give details of treatments received, if relevant.	5
Outcome	6a	Clearly define the outcome that is predicted by the prediction model, including how and when assessed.	5
	6b	Report any actions to blind assessment of the outcome to be predicted.	5
Predictors	7a	Clearly define all predictors used in developing or validating the multivariable prediction model, including how and when they were measured.	5, 6
	7b	Report any actions to blind assessment of predictors for the outcome and other predictors.	6
Sample size	8	Explain how the study size was arrived at.	5
Missing data	9	Describe how missing data were handled (e.g., complete-case analysis, single imputation, multiple imputation) with details of any imputation method.	7
Statistical analysis methods	10a	Describe how predictors were handled in the analyses.	7, 8
	10b	Specify type of model, all model-building procedures (including any predictor selection), and method for internal validation.	7, 8
	10d	Specify all measures used to assess model performance and, if relevant, to compare multiple models.	8
Risk groups	11	Provide details on how risk groups were created, if done.	-
Results			

Participants	13a	Describe the flow of participants through the study, including the number of participants with and without the outcome and, if applicable, a summary of the follow-up time. A diagram may be helpful.	8
	13b	Describe the characteristics of the participants (basic demographics, clinical features, available predictors), including the number of participants with missing data for predictors and outcome.	8, 9
Model development	14a	Specify the number of participants and outcome events in each analysis.	8, 9
	14b	If done, report the unadjusted association between each candidate predictor and outcome.	9-11
Model specification	15a	Present the full prediction model to allow predictions for individuals (i.e., all regression coefficients, and model intercept or baseline survival at a given time point).	11
	15b	Explain how to the use the prediction model.	12
Model performance	16	Report performance measures (with CIs) for the prediction model.	9-11
Discussion			
Limitations	18	Discuss any limitations of the study (such as nonrepresentative sample, few events per predictor, missing data).	12-13
Interpretation	19b	Give an overall interpretation of the results, considering objectives, limitations, and results from similar studies, and other relevant evidence.	12-13
Implications	20	Discuss the potential clinical use of the model and implications for future research.	13
Other information			
Supplementary information	21	Provide information about the availability of supplementary resources, such as study protocol, Web calculator, and data sets.	-
Funding	22	Give the source of funding and the role of the funders for the present study.	1

3F. Details of MRI Measurement Consensus and Discrepancies between Investigators

Table 3.S2. Specification of Discrepancies between Assessments of two Researchers

Assessment	**Discrepancies (n)**	**Conclusion after Reassessment (n)**	**Effect on Multivariate Analysis**	
			Odds Ratio with corresponding 95% CI and *p* value before reassessment	Odds Ratio with corresponding 95% CI and *p* value after reassessment
Presence of HSI Foci	31	HSI Foci Present (n=31)	11.702 (2.384-57.447, *p* .002)	4.650 (.1.857-11.648, *p* .001)
JZ Measurements	15	Overestimation JZ (n=4)	Mean JZ: 1.137 (.980-1.318, *p* .089)	Mean JZ: 1.203 (1.040-1.392, *p* .013)
		Underestimation JZ (n=6)	JZ/MYO>.4: .193 (.060-.618, *p* .006)	JZ/MYO >.4: .194 (.060-.621, *p* .006)
		JZ not measurable (n=1)		
JZ Max/JZ Min	4	Overestimation JZ Max (2)	JZ Diff ≥ 5 mm: 1.900 (.537-6.716, *p* .319)	JZ Diff ≥ 5: 1.535 (.441-5.351, *p* .501)
		Underestimation JZ Max (1)		
		Underestimation JZ Max + Overestimation JZ Min (1)		
Presence of Focal Adenomyosis	7	Focal Adenomyosis Present (7)	Not applicable	Not applicable
Presence of Cystic Adenomyosis	1	Consult pelvic Radiologist (1)	Not applicable	Not applicable

CI = Confidence Interval. HSI = High Signal Intensity. JZ = Junctional Zone. JZ/MYO = Junctional Zone to Myometrium Ratio. JZ Max = Maximal Junctional Zone thickness. JZ Min = Minimal Junctional Zone thickness. JZ Diff = Junctional Zone Differential.

3G. Diagnostic Accuracy of Readers (CR and MvdW) versus Radiologist

Table 3.S3: Diagnostic accuracy between Radiology Report and Reader Detection.

	Radiology Report						
	Sensitivity	Specificity	PPV	NPV	PLR	NLR	Overall accuracy
Reader detection	90.2%	57.8%	61.1%	88.9%	2.1	0.2	71.5%

PPV = Positive Predictive Value. NPV = Negative Predictive Value. PLR = Positive Likelihood Ratio. NLR = Negative Likelihood Ratio.

CHAPTER 4:

4A. Search terms CTcue

For hysterectomy surgery, the following terms were used:

- Hysterectomie
- Laparoscopische uterusextirpatie met tubae
- Laparoscopische uterusextirpatie LAVH', 'abdominale uterusextirpatie
- Laparoscopische uterusextirpatie
- Laparoscopische uterusextirpatie LAVH LASH met tubectomie
- Abdominale uterusextirpatie met verwijdering van p
- Abdominale uterusextirpatie + adnexa
- Abdominale uterusextirpatie
- Vaginale uterusextirpatie. + VW + AW plastiek
- Laparoscopische uterusextirpatie
- Laparoscopische uterusextirpatie met tubectomie
- Vaginale uterusextirpatie
- Abd-vag. radicale uterusextirpatie + lymfadenectomie
- Abdominale uterusextirpatie
- Lap uterusextirpatie
- Lap uterusextirpatie LAVH LASH
- Vaginale uterusextirpatie
- Laparoscopische uterusextirpatie LAVH LASH
- Abdominale uterusextirpatie
- V-notes uterusextirpatie

CHAPTER 6:

6A. Results of intra- and inter-observer variability Analysis

As reported in Huang et al. 2022 (229), an inter- intra-observer analysis was conducted for analysis of the novel introduced features of velocity and coordination.

Feature name	ICC	95 % Confidence Interval	
		Lower Bound	Upper Bound
Velocity C2F	0.918	0.689	0.979
Velocity F2C	0.961	0.798	0.991
Coordination by CC	0.950	0.771	0.988
Coordination by MSE	0.914	0.673	0.978
Coordination by Hd	0.899	0.602	0.975

Figure 6.S1 Intra-observer reproducibility test of contraction velocity and coordination features extracted from TVUS recordings from 10 patients, with 95% confidence interval

Feature name	ICC	
	Intra-observer variability	Inter-observer variability
Velocity C2F	0.969 (0.910 - 0.992)	0.953 (0.866 - 0.987)
Velocity F2C	0.921 (0.762 - 0.979)	0.965 (0.899 - 0.990)
Coordination by CC	0.853 (0.589 - 0.960)	0.752 (0.318 - 0.931)
Coordination by MSE	0.841 (0.553 - 0.956)	0.762 (0.353 - 0.934)
Coordination by Hd	0.863 (0.616 - 0.963)	0.785 (0.409 - 0.940)

Figure 6.S13 Inter- and Intra-observer variability for contraction velocity and coordination for 10 patients

6B: STROBE Checklist

	Item No.	Recommendation	Page No.	Relevant text from manuscript
Title and abstract	1	(*a*) Indicate the study's design with a commonly used term in the title or the abstract		1
		(*b*) Provide in the abstract an informative and balanced summary of what was done and what was found		1, 2
Introduction				
Background/rationale	2	Explain the scientific background and rationale for the investigation being reported		3
Objectives	3	State specific objectives, including any prespecified hypotheses		4
Methods				
Study design	4	Present key elements of study design early in the paper		4
Setting	5	Describe the setting, locations, and relevant dates, including periods of recruitment, exposure, follow-up, and data collection		4
Participants	6	(*a*) C*ohort study*—Give the eligibility criteria, and the sources and methods of selection of participants. Describe methods of follow-up *Case-control study*—Give the eligibility criteria, and the sources and methods of case ascertainment and control selection. Give the rationale for the choice of cases and controls *Cross-sectional study*—Give the eligibility criteria, and the sources and methods of selection of participants		4
		(*b*) C*ohort study*—For matched studies, give matching criteria and number of exposed and unexposed *Case-control study*—For matched studies, give matching criteria and the number of controls per case		
Variables	7	Clearly define all outcomes, exposures, predictors, potential confounders, and effect modifiers. Give diagnostic criteria, if applicable		7
Data sources/ measurement	8*	For each variable of interest, give sources of data and details of methods of assessment (measurement). Describe comparability of assessment methods if there is more than one group		4, 5
Bias	9	Describe any efforts to address potential sources of bias		
Study size	10	Explain how the study size was arrived at		

6C. Additional coordination parameters:

	Menstrual	Early Follicular	Periovulatory	Early Luteal	Late Luteal	P-value*
Correlation (Mean, SD)	0.08 (0.31)	0.11 (0.24)	0.04 (0.29)	0.05 (0.21)	0.02 (0.27)	0.981
MSE (Mean, SD)	0.15 (0.04)[b]	0.25 (0.10)	0.26 (0.13)[a,c]	0.20 (0.08)	0.18 (0.07)	0.027
HD (Mean, SD)	1.88 (0.50)	1.97 (0.37)	1.99 (0.48)	1.94 (0.30)	1.81 (0.34)	0.711

Three indices were defining assessing the uterine contraction coordination depending on the adopted similarity measure: mean square error (MSE), cross correlation (CC) and Hausdorff distance (HD). Again, full details on the technical background of these units has been published elsewhere (229). For the MSE and HD indices, a lower value reflected increased contraction coordination. Conversely, for the CC index, a higher value reflected increased contraction coordination.

CHAPTER 7:

7A: Literature search

Search in PubMed

Search	Query op January 12th, PUBMED	Items found
#1	peristalsis[MeSH Terms] AND uterus[MeSH Terms]	37
#2	"uterine contraction" [MeSH Terms]	7,650
#3	(uterine [Title/Abstract] AND (peristal* [Title/Abstract] OR contract* [Title/Abstract] OR wave [Title/Abstract])) OR (uterus [Title/Abstract] AND (peristal* [Title/Abstract] OR contract* [Title/Abstract] OR wave [Title/Abstract])) OR (junctional zone [Title/Abstract] AND (peristal* [Title/Abstract] OR contract* [Title/Abstract] OR wave [Title/Abstract])) OR (endometrial [Title/Abstract] AND (peristal* [Title/Abstract] OR contract* [Title/Abstract] OR wave [Title/Abstract])) OR (subendometrial [Title/Abstract] AND (peristal* [Title/Abstract] OR contract* [Title/Abstract] OR wave [Title/Abstract])) OR (sub endometrial [Title/Abstract] AND (peristal* [Title/Abstract] OR contract* [Title/Abstract] OR wave [Title/Abstract]))	10,403
#4	#1 OR #2 OR #3	14,031
#5	"Uterus/abnormalities"[Mesh] OR leiomyoma[MeSH Terms] OR adenomyosis[MeSH Terms] OR endometritis[MeSH Terms] OR congenital uterine abnormal*[Title/Abstract]	30,469
#6	#4 AND #5	208

Search in the Cochrane Library

Search	Query op 12 januari, Cochrane Library	Items found
#1	MeSH descriptor: [Peristalsis] explode all trees	175
#2	MeSH descriptor: [Uterus] explode all trees	2855
#3	#1 AND #2	0
#4	MeSH descriptor: [Uterine Contraction] explode all trees	378
#5	(peristal*):ti,ab,kw	810
#6	(contract*):ti,ab,kw	19066
#7	(wave):ti,ab,kw	12148
#8	(uterine):ti,ab,kw16	16333
#9	(uterus):ti,ab,kw	5659
#10	(junctional zone):ti,ab,kw	21
#11	(endometrial):ti,ab,kw	6412
#12	(subendometrial):ti,ab,kw	62
#13	(sub endometrial)ti,ab,kw	97
#14	(#8 AND (#5 OR #6 OR #7)) OR (#9 AND (#5 OR #6 OR #7)) OR (#10 AND (#5 OR #6 OR #7)) OR (#11 AND (#5 OR #6 OR #7)) OR (#12 AND (#5 OR #6 OR #7)) OR (#13 AND (#5 OR #6 OR #7))	1908
#15	#3 OR #4 OR #14	1908
#16	(abnormal*)ti,ab,kw	36255
#17	#16 AND (#8 OR #9)	1891
#18	MeSH descriptor: [Leiomyoma] explode all trees	693
#19	MeSH descriptor: [Adenomyosis] explode all trees	40
#20	MeSH descriptor: [Endometritis] explode all trees	284
#21	MeSH descriptor: [Congenital Abnormalities] explode all trees	6099
#22	#21 AND (#8 OR #9)	39
#23	#17 OR #18 OR #19 OR #20 OR #22	2856
#24	#15 AND #23	212

Search in Embase

Search	Query op 12 januari, Embase	Items found
#1	**'peristalsis'**/exp AND **'uterus'**/exp	214
#2	**'uterus contraction'**/exp	10,383
#3	**uterine**:ti,ab,kw AND (**peristal***:ti,ab,kw OR **contract***:ti,ab,kw OR **wave**:ti,ab,kw) OR (**uterus**:ti,ab,kw AND (**peristal***:ti,ab,kw OR **contract***:ti,ab,kw OR **wave**:ti,ab,kw)) OR (**junctional** AND **zone**:ti,ab,kw AND (**peristal***:ti,ab,kw OR **contract***:ti,ab,kw OR **wave**:ti,ab,kw)) OR (**endometrial**:ti,ab,kw AND (**peristal***:ti,ab,kw OR **contract***:ti,ab,kw OR **wave**:ti,ab,kw)) OR (**subendometrial**:ti,ab,kw AND (**peristal***:ti,ab,kw OR **contract***:ti,ab,kw OR **wave**:ti,ab,kw)) OR (**sub** AND **endometrial**:ti,ab,kw AND (**peristal***:ti,ab,kw OR **contract***:ti,ab,kw OR **wave**:ti,ab,kw))	13,718
#4	#1 OR #2 OR #3	18,983
#5	**uterus** AND **'abnormalities'**/exp OR **'leiomyoma'**/exp OR **'adenomyosis'**/exp OR **'endometritis'**/exp OR (**'congenital'**/exp AND **'uterine'**/exp AND **abnormal***:ti,ab,kw)	33,186
#6	#4 AND #5	290

7B. Extensive risk of bias assessment

		Max. obtainable score	Bulletti et al. (1997)	Bulletti et al. (2002)	Fornazari et al. (2019)	Kido et al. (2007)	Kido et al. (2011)	Kido et al. (2014)	Kissler et al. (2007)	Leyendecker et al. (1996)	Nishino et al. (2005)	Oliva et al. (1992)	Orisaka et al. (2007)	Pinto et al. (2015)	Qu et al. (2019)	Szamatowicz et al. (1997)	Yoshino et al. (2010)	Yoshino et al. (2012)
Reporting																		
1	Hypothesis / aim/ objective clearly described	**1**	1	1	1	1	1	1	0	1	1	0	1	1	1	1	1	1
2	Main outcomes in introduction or methods section	**1**	1	1	1	1	1	1	0	1	1	0	1	1	1	1	1	1
3	Patient characteristics clearly described	**1**	1	1	1	1	1	1	0	1	1	0	1	1	1	0	1	1
4	Interventions of interest clearly described	**1**	N/A	0	1	N/A	1	N/A	N/A	N/A	N/A	1	N/A	N/A	1	1	N/A	1
5	Distributions of principal confounders clearly described	**2**	0	1	2	1	1	1	0	1	1	0	1	1	2	0	2	2
6	Main findings clearly described	**1**	1	1	1	1	1	1	1	1	1	1	1	0	1	1	1	1
7	Estimates of random variability provided for main outcomes	**1**	1	1	0	1	0	0	0	1	0	0	0	0	1	1	1	1
8	All adverse	**1**	N/A	0	0	N/A	0	N/A	N/A	N/A	N/A	0	N/A	N/A	0	0	N/A	0

	events as consequence of intervention reported																	
9	Characteristics of patients lost to follow-up described	1	N/A	0	1	N/A	1	N/A	0	N/A	N/A	0	N/A	N/A	1	1	0	1
10	Exact probability values reported for main outcomes	1	0	0	1	1	0	0	1	0	N/A	N/A	N/A	0	0	1	0	1
External validity																		
11	Subjects asked to participate were representative of source population	1	UTD	0	UTD	UTD	UTD	UTD	UTD	UTD	1	UTD	UTD	UTD	UTD	UTD	1	UTD
12	Subjects prepared to participate were representative of source population	1	0	1	1	UTD	0	0	UTD	UTD	1	UTD	UTD	UTD	UTD	UTD	UTD	UTD
13	Location of study intervention was representative of source population	1	N/A	1	0	N/A	1	N/A	N/A	N/A	N/A	N/A	N/A	N/A	UTD	1	1	1
Internal validity – bias																		
14	Study participants blinded to intervention	1	N/A	N/A	N/A	N/A	N/A	N/A	N/A	N/A	N/A	N/A	N/A	N/A	N/A	N/A	N/A	N/A

15	Blinded outcome assessment	1	N/A	N/A	N/A	N/A	N/A	N/A	N/A	N/A	N/A	N/A	N/A	N/A	N/A	N/A	N/A	N/A
16	Data dredging clearly described, if any	1	1	1	1	1	1	1	1	1	1	1	1	1	1	1	1	1
17	Analyses adjust for differing lengths of follow-up	1	N/A	N/A	1	N/A	0	N/A	N/A	N/A	N/A	1	N/A	N/A	0	1	0	0
18	Appropriate statistical tests used	1	1	1	1	1	1	1	UTD	1	N/A	N/A	N/A	1	1	UTD	1	UTD
19	Compliance with interventions was reliable	1	N/A	1	1	N/A	1	N/A	N/A	N/A	N/A	1	N/A	N/A	1	1	1	1
20	Outcome measures were used accurate	1	1	1	1	1	1	1	1	1	1	1	1	1	1	1	1	1
Internal validity - confounding (selection bias)																		
21	All participants recruited from the same source population	1	1	1	N/A	0	N/A	0	UTD	UTD	1	UTD	0	1	N/A	N/A	1	N/A
22	All participants recruited over the same time period	1	UTD	UTD	N/A	0	N/A	UTD	UTD	UTD	1	UTD	UTD	1	N/A	N/A	1	N/A
23	Participants randomzied to intervention(s)	1	N/A	N/A	N/A	N/A	N/A	N/A	N/A	N/A	N/A	N/A	N/A	N/A	N/A	N/A	N/A	N/A
24	Allocation of intervention concealed from	1	N/A	N/A	N/A	N/A	N/A	N/A	N/A	N/A	N/A	N/A	N/A	N/A	N/A	N/A	N/A	N/A

	investigators and participants																	
25	Adequate adjustment for confounding	**1**	0	0	1	0	0	0	0	0	0	0	0	0	1	0	0	0
26	Losses to follow-up taken into account	**1**	N/A	UTD	1	N/A	1	N/A	UTD	N/A	N/A	0	N/A	N/A	1	UTD	UTD	1
Power																		
27	Sample sizes have been calculated	**1**	0	0	0	0	0	0	0	0	0	0	0	0	0	0	0	0
Obtained score			9	13	17	10	13	8	4	9	11	6	7	9	15	12	15	15
Maximum obtainable score		28	17	23	22	17	22	17	19	17	15	21	15	17	22	22	22	22
Percentage obtained (%)		100	53	57	77	59	59	47	21	53	73	29	47	53	68	55	68	68
Overall quality assessment (colour coded) ● Poor ● Fair ● Good ● Excellent			●	●	●	●	●	●	●	●	●	●	●	●	●	●	●	●

CHAPTER 8:

8A. STROBE Statement

STROBE Statement—checklist of items that should be included in reports of observational studies

	Item No.	Recommendation	Page No.	Relevant text from manuscript
Title and abstract	1	(*a*) Indicate the study's design with a commonly used term in the title or the abstract		1
		(*b*) Provide in the abstract an informative and balanced summary of what was done and what was found		3
Introduction				
Background/rationale	2	Explain the scientific background and rationale for the investigation being reported		*4, 5*
Objectives	3	State specific objectives, including any prespecified hypotheses		*5*
Methods				
Study design	*4*	Present key elements of study design early in the paper		*5*
Setting	*5*	Describe the setting, locations, and relevant dates, including periods of recruitment, exposure, follow-up, and data collection		*5*
Participants	6	(*a*) C*ohort study*—Give the eligibility criteria, and the sources and methods of selection of participants. Describe methods of follow-up *Case-control study*—Give the eligibility criteria, and the sources and methods of case ascertainment and control selection. Give the rationale for the choice of cases and controls *Cross-sectional study*—Give the eligibility criteria, and the sources and methods of selection of participants		*5*
		(*b*) C*ohort study*—For matched studies, give matching criteria and number of exposed and unexposed *Case-control study*—For matched studies, give matching criteria and the number of controls per case		

Variables	7	Clearly define all outcomes, exposures, predictors, potential confounders, and effect modifiers. Give diagnostic criteria, if applicable	7
Data sources/ measurement	8*	For each variable of interest, give sources of data and details of methods of assessment (measurement). Describe comparability of assessment methods if there is more than one group	6, 7, 8. 9
Bias	9	Describe any efforts to address potential sources of bias	
Study size	10	Explain how the study size was arrived at	5

Quantitative variables	11	Explain how quantitative variables were handled in the analyses. If applicable, describe which groupings were chosen and why	
Statistical methods	12	(a) Describe all statistical methods, including those used to control for confounding	9
		(b) Describe any methods used to examine subgroups and interactions	9
		(c) Explain how missing data were addressed	
		(d) Cohort study—If applicable, explain how loss to follow-up was addressed Case-control study—If applicable, explain how matching of cases and controls was addressed Cross-sectional study—If applicable, describe analytical methods taking account of sampling strategy	
		(e) Describe any sensitivity analyses	
Results			
Participants	13*	(a) Report numbers of individuals at each stage of study—eg numbers potentially eligible, examined for eligibility, confirmed eligible, included in the study, completing follow-up, and analysed	10
		(b) Give reasons for non-participation at each stage	10
		(c) Consider use of a flow diagram	10, Fig 2
Descriptive data	14*	(a) Give characteristics of study participants (eg demographic, clinical, social) and information on exposures and potential confounders	10
		(b) Indicate number of participants with missing data for each variable of interest	10,11
		(c) Cohort study—Summarise follow-up time (eg, average and total amount)	
Outcome data	15*	Cohort study—Report numbers of outcome events or summary measures over time	11, 12

		Case-control study—Report numbers in each exposure category, or summary measures of exposure	
		Cross-sectional study—Report numbers of outcome events or summary measures	
Main results	16	(a) Give unadjusted estimates and, if applicable, confounder-adjusted estimates and their precision (eg, 95% confidence interval). Make clear which confounders were adjusted for and why they were included	10, 11, 12
		(b) Report category boundaries when continuous variables were categorized	
		(c) If relevant, consider translating estimates of relative risk into absolute risk for a meaningful time period	

Other analyses	17	Report other analyses done—eg analyses of subgroups and interactions, and sensitivity analyses	
Discussion			
Key results	18	Summarise key results with reference to study objectives	12, 13
Limitations	19	Discuss limitations of the study, taking into account sources of potential bias or imprecision. Discuss both direction and magnitude of any potential bias	14, 15
Interpretation	20	Give a cautious overall interpretation of results considering objectives, limitations, multiplicity of analyses, results from similar studies, and other relevant evidence	13, 14, 15
Generalisability	21	Discuss the generalisability (external validity) of the study results	14, 15, 16
Other information			
Funding	22	Give the source of funding and the role of the funders for the present study and, if applicable, for the original study on which the present article is based	1

CHAPTERS NINE and TEN:

10A. : Local Protocol for Pelvic MRI

MRI for Endometriosis Diagnosis:

Patients with suspected or known endometriosis are given an MRI according to the following protocol in our centre. There is a preference for using the 3 Tesla scan, however the 1.5 Tesla scan can also be used.

Scan procedure, in chronological order

Table10.S1 MRI Scan Procedure, in chronological order

Setting	Sequence	Orientation
T2	TSE	Sagittal
T2	TSE	Transverse
T2	TSE	Coronal
T1 (spiral)	TSE	Transverse

TSE: turbo spin echo

Contrast agent: none.

Medication: Buscopan/Glucagon (muscle relaxants) are given in order to minimise the effect of uterine contractions on the evaluation of the images.

MRI for Adenomyosis Embolisation

Additional MRI's may be carried out in patients with fibroids or (focal) adenomyosis in order to determine the suitability of the lesion for potential uterine artery embolization. There is a preference for using the 3 Tesla scan, however the 1.5 Tesla scan can also be used.

This is carried out using the following protocol (in chronological order):

Table 10.S2 MRI Scanning protocol, in chronological order

Setting	Sequence	Orientation
T2W	TSE	Sagittal
T1W	TSE	Transverse
T1W	TSE	Sagittal
Injection of contrast agent		
T2W	TSE	Transverse
T1W	TSE	Sagittal

*T2W: T2 weighted TSE: turbo spin echo

Contrast agent: Gadolinium pentate

- Dosage
    - 1.5T: 0,2mg/kg
    - 3T: 0,1 mg/kg

10B. Local eligibility requirements for fertility treatment

A couple or woman seeking fertility treatment can be referred to our centre either via a general practitioner, from another hospital, or by another specialist within our hospital (for example a urologist). Generally, they include the following groups of patients:

- A couple that has not had a previous pregnancy
- A couple that has had a previous pregnancy using assisted reproductive technology (ART)
- A couple that has undergone initial fertility treatment at another centre and requires IVF

Couples that meet the following criteria are then considered eligible for fertility treatment and further investigation in the case of the following criteria:

- No spontaneous pregnancy after 1 year of ovulation-led unprotected intercourse, with a regular menstrual cycle
- Confirmed dysovulation
- Indication for tubal defects or endometriosis
- Severe sperm abnormalities
- Previous pregnancy using ART

At the start of the fertility treatment process, the following standard investigations are carried out:

Male:

- Sperm analysis for volume, concentration, motility, morphology and presence of atypical cells
- Further specific analysis is done if the initial analysis proves abnormal

Female

- Detailed medical and reproductive history (including family history)
    - If there is an irregular menstrual cycle, cycle monitoring will be implemented
- Pelvic exam, including TVUS

    - In the case of a family history of premature ovarian insufficiency: AMH and antral follicle count will be assessed
- Laboratory tests: Chlamydia antigen test and thyroid function (TSH), and virusscreening (Hepatitis B & C, HIV, HTLV)
    - In case of oligo- or a-menorrhoea: LH, FSH, Prolactin, Testosterone, progesterone, oestradiol
- A hysterosalpingography will be carried out in the case of positive history (or active) chlamydia or pelvic inflammatory disease (PID) , or absence of pregnancy with unexplained fertility

Based on the results of these tests and investigations, if possible, a likely cause for infertility will be found, which will influence further treatment. In the case of unexplained infertility, a Hunault score will be calculated in decide management.
For a couple to be eligible specifically for IVF or ICSI treatment, the following criteria must be met:

- Maternal age under 42
- Women with unexplained fertility <38 years, with a minimum of 6 failed IUI's
- Women with unexplained fertility >38 years regardless of number of IUI attempts
- Severe male factor (VCM score <3)
- HSG-confirmed tubal infertility
- An- or Dys-ovulation
- No contraindication for IVF treatment of pregnancy
    - Including moral/ethical contraindications

10C. Local protocol for embryo quality assessment

Table 10.S3 Local Embryo Quality Assessment Protocol: Embryo quality is based on the appearance of the embryos on day 1, 2 and 3. A final embryo quality assessment is given on day 3

Day	Criterion	Super	Good	Fair	Moderate	Poor
1	Type pn*	2pn^{a} 2pn^{b} /0pn →	2pn^{a} 2pn^{b}/0pn →	2pn^{a}	2pn^{a} / 2pn^{b} / 0pn/ 1pn with IVF	2pn^{a} / 2pn^{b} / 0pn / 1pn
		No vacuoles	Some small vacuoles	Some small vacuoles	N.a.	N.a.
2	Number of Cells	4 Cells	4/5 Cells	2-5 Cells	≥2 Cells	≥ 2 Cells
	Fragmentation	≤20% (score 1+2*)	≤20% (score1+2)	≤50% (score 1+2+3)	≤50% (score 1+2+3)	N.a.
	Blastomere Uniformity	Uniform	Uniform/Somewhat uneven	N.a.	N.a.	N.a.
	Mulitnuclear blastomeres (MNB)	None	None	None	MNB's ≤25 %	N.a.
	Vacuoles/Irregularities	None	None	Some vacuoles	N.a.	N.a.
	Clarity	Clear	Clear	N.a.	N.a.	N.a.
3	Number of Cells	8/9 Cells	7-10 cells / starting. Morula	6-10 cells / starting Morula	≥ 4 cells	≥ 4 cells
	Fragmentation	≤20% (score1+2)	≤20% (score 1+2)	≤20% (score 1+2)	≤50% (score 1+2+3)	N.a.
	Blastomere Uniformity	Uniform/Somewhat uneven	Uniform/Somewhat uneven	N.a.	N.a.	N.a.
	Mulitnuclear blastomeres	None	None	Some vacuoles	N.a.	N.a.
	Vacuoles/Irregularities	Clear	Clear	N.a.	N.a.	N.a.

2pn^{b} → If the embryo has a lower 2pn score (a instead of b), the overall quality will decrease by one level. There should be progression between days 2 and 3, or there should be at least 2 blastomeres present for an embryo to have a quality score of 'II'. If this is not the case, the embryo is automatically scored as having a quality of III.

Criteria for choice of Fresh ET Embryo:

- For ET, the embryos of the highest available quality are chosen.
- Super > Good > Fair > Moderate > Poor
- When multiple embryos of equal final quality are available, the choice depends on how the embryo(s) were on **day 2**,. Whereby: 4 cell > 2 cell > 3 cell
- IN the case of continued division from day 2 to day 3, priority is given to the embryo that is dividing 'on schedule'.
- In the case of fragmentation, concentrated pockets of fragmentation are preferred to diffuse fragmentation
- If there are no embryo dividing 'on schedule' preference is given to embryos with higher uniformity
- $2pn^a > 2pn^b > 0pn > 1pn$
- Embryos >24 hours behind the expected stage of development are not eligible for ET.

*In the case of stagnation between days 2 and 3 (**without** deterioration in quality), ET is potentially possible.*

10D: Sub-analysis of IVF/ICSI Outcomes

Table 10.S4: Sub-analysis for Adenomyosis patients with and without pregnancies after IVF/ICSI based on MRI-timing

		Pregnancy (N=31)	No Pregnancy (N=93)	P-value*
MRI prior to IVF/ICSI treatment	Yes	12 (38.7%)	34 (36.6%)	0.830
	No	19 (61.3%)	59 (63.4%)	
MRI within 5 years of fertility treatment	Yes	21 (67.7%)	62 (66.7%)	0.912
	No	10 (32.3%)	31 (33.3%)	

*chi-squared analysis

Table 10.S5: Sub-analysis for IVF/ICSI Outcomes for Adenomyosis Patients versus Male Infertility Controls with only Fair-to-Super Embryos

	Adenomyosis Patients (N=95)	**Control Group (N=717)**	**P-value**
Biochemical Pregnancy	25 (26.3%)	290 (40.4%)	0.010
Ongoing Pregnancy	16 (17.2%)	234 (32.6%)	0.002
Live Birth	14 (15.2%)	206 (28.7%)	0.014

Table 10.S6 Full IVF/ICSI Outcomes for MRI Markers for Adenomyosis/Endometriosis Patients versus Male Infertility Controls:

IVF/ICSI Outcome	***Adenomyosis Patients Overall (N=124)***		***Control Group (N=889)***	**P-value**
Biochemical Pregnancy	31 (25%)		323 (36.3%)	0.013
Ongoing Pregnancy	19 (15.6%)		261 (29.4%)	0.001
Live Birth	17 (14.0%)		233 (26.8%)	0.009
	Adenomyosis Patients without Myometrial Cysts (N=63)	*Adenomyosis Patients with Myometrial Cysts (N=60)*	*Control Group (N=889)*	P-value*
Biochemical Pregnancy	15 (23.8%)	15 (25.0%)	323 (36.3%)	0.033
Ongoing Pregnancy	10 (16.4%)	9 (15.0%)	261 (29.4%)	0.007
Live Birth	10 (16.1%)	7 (12.1%)	233 (26.8%)	0.052
	Adenomyosis Patients with Mean JZ<12mm (N= 103)	*Adenomyosis Patients with Mean JZ>12mm (N= 20)*	*Control Group (N=889)*	
Biochemical Pregnancy	28 (27.2%)	3 (15.0%)	323 (36.3%)	0.031
Ongoing Pregnancy	17 (16.7%)	2 (10.5%)[a]	261 (29.4%)	0.006
Live Birth	15 (15.0%)	2 (10.5%)	233 (26.8%)	0.053
	Adenomyosis Patients with JZ-Diff <5mm (N=13)	*Adenomyosis Patients with JZ-Diff>5mm (N= 110)*	*Control Group (N=889)*	
Biochemical Pregnancy	2 (15.4%)	29 (26.4%)	323 (36.3%)	0.039
Ongoing Pregnancy	1 (7.7%)	18 (16.7%)[a]	261 (29.4%)	0.005
Live Birth	1 (7.7%)	16 (15.0%)	233 (26.8%)	0.051
	Adenomyosis Patients with JZ-Myometrium <40% (N=31)	*Adenomyosis Patients with JZ-Myometrium Ratio >40% (N=92)*	*Control Group (N=889)*	
Biochemical Pregnancy	9 (29.0%)	22 (23.9%)	323 (36.3%)	0.046
Ongoing Pregnancy	6 (19.4%)	13 (14.4%)[a]	261 (29.4%)	0.006

Live Birth	5 (16.7%)	12 (13.3%)[a]	233 (26.8%)	0.055
	Diffuse Adenomyosis (N=31)	*Focal Adenomyosis (N=58)*	*Control Group (n=889)*	
Biochemical Pregnancy	10 (32.3%)	12 (20.7%)	323 (36.3%)	0.117
Ongoing Pregnancy	5 (17.2%)	9 (15.5%)	261 (29.4%)	0.047
Live Birth	5 (16.7%)	9 (15.5%)	233 (26.8%)	0.446
	Adenomyosis Alone (n=31)	*Adenomyosis and Endometriosis (n=93)*	*Control Group (n=889)*	
Biochemical Pregnancy	9 (29.0%)	22 (23.7%)	323 (36.3%)	0.040
Ongoing Pregnancy	6 (20.0%)	12 (14.1%)	261 (29.4%)	0.005
Live Birth	5 (17.2%)	12 (14.1%)	233 (26.8%)	0.049
	Adenomyosis without DIE (n=98)	*Adenomyosis with DIE (n=26)*	*Control Group (n=889)*	
Biochemical Pregnancy	27 (27.6%)	4 (15.4%)	323 (36.3%)	0.024
Ongoing Pregnancy	17 (17.7%)[a]	2 (7.7%)[a]	261 (29.4%)	0.004
Live Birth	15 (15.8%)	2 (7.7%)	233 (26.8%)	0.039

*Chi-squared analysis with Bonferroni correction. a: denotes statistical significance vs. control group

Table10. S7: Adjusted Odds Ratio IVF/ICSI Outcomes versus Controls

IVF/ICSI Outcome	***Adjusted Odds Ratio (95% CI) vs Control Group****	
	Adenomyosis Patients Overall (N=124)	
Biochemical Pregnancy	0.683 (0.411-1.138)	
Ongoing Pregnancy	0.501 (0.276-0.909)	
Live Birth	0.484 (0.259-0.905)	
	Adenomyosis Patients without Myometrial Cysts (N=63)	*Adenomyosis Patients with Myometrial Cysts (N=60)*
Biochemical Pregnancy	0.612 (0.314-1.195)	0.708 (0.367-1.365)
Ongoing Pregnancy	0.513 (0.237-1.112)	0.500 (0.229-1.090)
Live Birth	0.556 (0.255-1.214)	0.420 (0.177-0.997)
	Adenomyosis Patients with Mean JZ<12mm (N= 103)	*Adenomyosis Patients with Mean JZ>12mm (N= 20)*
Biochemical Pregnancy	0.746 (0.436-1.270)	0.407 (0.113-1.465)
Ongoing Pregnancy	0.531 (0.285-0.990)	0.363(0.079-2.659)

Live Birth	0.510 (0.264-0.985)	0.374 (0.082-1.700)
	Adenomyosis Patients with JZ-Diff <5mm (N=13)	*Adenomyosis Patients with JZ-Diff>5mm (N= 110)*
Biochemical Pregnancy	0.396 (0.084-1.856)	0.729 (0.431-1.234)
Ongoing Pregnancy	0.232 (0.293-1.856)	0.543 (0.295-1.001)
Live Birth	0.255 (0.032-2.041)	0.519 (0.273-0.990)
	Adenomyosis Patients with JZ-Myometrium <40% (N=31)	*Adenomyosis Patients with JZ-Myometrium Ratio >40% (N=92)*
Biochemical Pregnancy	0.878 (0.379-2.033)	0.633 (0.357-1.122)
Ongoing Pregnancy	0.665 (0.255-1.738)	0.454 (0.255-1.738)
Live Birth	0.598 (0.212-1.683)	0.453 (0.222-0.921)
	Diffuse Adenomyosis (N=31)	*Focal Adenomyosis (N=58)*
Biochemical Pregnancy	0.943 (0.417-2.131)	0.497 (0.297-1.035)
Ongoing Pregnancy	0.552 (0.198-1.542)	0.476 (0.210-1.078)
Live Birth	0.583 (0.209-1.201)	0.525 (0.230-1.626)
	Adenomyosis Alone (n=31)	*Adenomyosis and Endometriosis (n=93)*
Biochemical Pregnancy	0.854 (0.362-2.011)	0.635 (0.361-1.117)
Ongoing Pregnancy	0.738 (0.274-1.985)	0.440 (0.225-0.861)
Live Birth	0.652 (0.225-1.889)	0.440 (0.219-0.886)
	Adenomyosis without DIE (n=98)	*Adenomyosis with DIE (n=26)*
Biochemical Pregnancy	0.764 (0.445-1.310)	0.399 (0.130-1.226)
Ongoing Pregnancy	0.574 (0.307-1.074)	0.244 (0.055-1.084)
Live Birth	0.542 (0.280-1.050)	0.272 (0.061-1.212)

*Multivariate logistic regression adjusted for: age at time of IVF, IVF or ICSI treatment, embryo quality, year of IVF treatment and number of transferred embryos,

CHAPTER 11

11A. Full list of Outcomes with Definitions:

Table 11.S1: *Obstetric Outcomes collected from Perined; the Dutch national perinatal registry*

	Obstetric Outcomes
Maternal Mortality	(yes/no), with cause of death
Termination of pregnancy	(yes/no), with number of gestational weeks
Pregnancy complications overall	(Gestational) Diabetes Hypertensive Disorder of Pregnancy (HDP) - Gestational hypertension , (pre) eclampsia, HELLP Dysmaturity (Birthweight <10th percentile) Macrosomia (Birthwright >95th percentile) Antepartum Blood loss (with trimester) (P)PROM Imminent premature birth Placenta praevia
Fetal Growth Restriction	Fetal biometry <p10 or more than 20 percentile reduction in abdominal circumference
Preterm Birth	Gestational Age <37 weeks at delivery
Threatened Prematurity	Composite outcome including diagnosis during pregnancy of: - Premature contraction requiring admission <37 weeks gestational age - Cervical insufficiency/incompetency during pregnancy - PPROM
Proteinuria during pregnancy	Yes/no, with mg/L
Highest diastolic BP	Mm/Hg During pregnancy Hypertension defined as : >140/90 mm/Hg
Duration of ruptured membranes	Hours, days PPROM (Premature Preterm Rupture of Membranes), <37 weeks gestational age PROM (Premature Rupture of Membranes)
Start of labour	Induction (with indication) Spontaneous Elective CS Emergency CS
Interventions during Labour	None Stimulation with Oxytocin
Pain relief during labour	None Sedation Non-opioid analgesics Opioid analgesics

	Epidural during labour Epidural at CS Spinal at CS General anaesthesia at CS Unknown
Labor complications	Presence of meconium in amniotic fluid Foetal distress (as an indication for operative delivery or caesarean section_ Prolonged labour (rupture of membranes >24h) Shoulder dystocia
Failure to Progress	Stagnation/Slow progress of labor, as reported as an indication for operative delivery or caesarean section, stratified to: - Primary phase of labor - Secondary phase of labor
Foetal position/presentation	Cephalic Shoulder Breech
Duration of cervical dilatation	<6 hours 6-12 hours 12-24 hours >24 hours
Duration of active pushing during labour	<1 hour 1-2 hours 2-4 hours >4 hours Unknown
Mode of Delivery	Spontaneous vaginal Forceps/Vacuum extraction Breech delivery Emergency CS (with indication) Elective CS (with indication) Unknown
Post-partum complications	None PPH >1000mL Placental Retention Puerperal fever/Endometritis Other
Location of delivery	Home or primary care centre (with midwife) Secondary/Tertiary Hospital (with gynaecologist)
Maternal hospital admission	Yes/no, with duration
	Neonatal Outcomes
Neonatal Mortality	Yes/No, with cause(s) of death (including pathology report) Antepartum Durante partum 24 hours post-partum Day 2 – 7 Day 8 – 28 >28 days of age Unclear
Stillbirth (Antepartum)	Yes/no, with gestational age
Gestational age at delivery	In weeks/days

Prematurity/Preterm Birth	Gestational age at delivery of <37 weeks Stratified: <28 weeks, <34 weeks, <37 weeks
Birthweight	Grammes
Birthweight percentile	%, according to the Dutch average (Hoftiezer percentiles) Stratified: <10% (Small for gestational Age) and >95% (Large for Gestational Age)
Small-for-gestational age	Birthweight percentile <p10 at delivery
Apgar Score	At 1 and 5 minutes Stratified: Apgar <7 and >7 at 5 minutes
Umbilical artery pH <7.00	Yes/no
Congenital abnormality	Yes/no, with details
Paediatric consult required	Yes/no, with reason(s)
NICU Admission required	Yes/no, with reason(s)

CS: caesarean section; (P)PROM: (Preterm) Premature Rupture Of Membranes; HDP: hypertensive disorders of pregnancy;

Table 11.S12 Overview of Additional Outcomes with Definitions

Characteristics	Units/Definition
Demographic Characteristics	
Age	In years At time of delivery At time of pathological adenomyosis diagnosis
Timing of adenomyosis diagnosis	Stratified to: - <5 years after registered pregnancy - >5 years after registered pregnancy
Ethnicity	E.g. Dutch, Turkish, Surinamese etc.
Socioeconomic Status	Low income area yes/no
Medical History	Previous surgery, known gynaecological conditions, other chronic diseases/conditions (including depression or mental illness)
Chronic medication Use	Any medication used chronically or regularly (during pregnancy)
Obstetric Characteristics	
Gravidity	n
Parity	n Stratified to: Nulliparous Multiparous
Multiple gestation in current pregnancy	Yes/No
Previous Abortions/Miscarriages	Number
Mode of Conception	Spontaneous Assisted (IUI, IVF, ovulation stimulation) Other
Previous pregnancy complications	Premature birth, dysmaturity, abortion/miscarriage, HDP, vacuum extraction, Caesarean section, post-partum haemorrhage
Gestational age at start of antenatal care	In weeks

IUI: intra-uterine insemination; IVF: in-vitro fertilisation; HDP: hypertensive disorders of pregnancy;

11B: Search Strategy PALGA Database

Search terms: (Adenomyose (code M76510) OR Adenomyoom (code M90130)) AND ('uterus')
Retrieval terms: None
Years: 1995 – 2018
Material: Histology
Gender: Female
Age category: 18 – 50
Number of search results with these parameters: *37,415 samples*.

11C: Variables Collected from Perined Database:

Requested from 1995 onwards.

Table 11.S3: Available variables in Perined; the Dutch national perinatal registry

Variable	Label
ABORTUS	Zwschap afgebroken?
ACHTERST	Achterstand
AMDDD	Zwangerschapsduur (dg)
AMWW	Zwangerschapsduur (wk)
AMWW1OND	Zw.weken bij 1e onderzk
AOI5_IGZ1	Adverse outcome (IGZ)-Mort (dp of pp)
AOI5_IGZ2	Adverse outcome (IGZ)-Lage Apgar
AOI5_IGZ3	Adverse outcome (IGZ)-NICU opname (37w+)
AOI5_IGZ4	Adverse outcome (IGZ)-Ernstige ruptuur
AOI5_IGZ5	Adverse outcome (IGZ)-Fluxus
APGAR5	Apgar 5 min
BB_DETAIL	Begin baring detail
CONCEP	Conceptiewijze
CGA_ERNST	Cong.afw. (ernst)
CONGAFW1	Congenitale afwijkingen-Zenuwstelsel en zintuigen
CONGAFW2	Congenitale afwijkingen-Hart en bloedvaten
CONGAFW3	Congenitale afwijkingen-Tractus digestivus
CONGAFW4	Congenitale afwijkingen-Tractus respiratorius
CONGAFW5	Congenitale afwijkingen-Tractus urogenitalis
CONGAFW6	Congenitale afwijkingen-Huid en buikwand
CONGAFW7	Congenitale afwijkingen-Skelet en spierstelsel
CONGAFW8	Congenitale afwijkingen-Multipele/syndromale afw.
CONGAFW9	Congenitale afwijkingen-Overige congenitale afw.
CONGAFW10	Congenitale afwijkingen-Geboortetrauma
DDAT	Aterme datum
DDGEB	Geb.datum kind
DDGEBM	Geb.datum moeder
DUUR_GVL	Duur gebroken vliezen
DUUR_UITDR	Uitdrijvingsduur
EB_DETAIL	Einde baring detail
EPI	Episiotomie

ETNIC	Etniciteit
GESL	Geslacht
GEW	Geboortegewicht
GEWp50	Norm gewicht
GEWPCTLA	Gewichtspercentiel
GRAV	Graviditeit
HOFTIEZER	Hoftiezer pctl
HPP	Bloedverlies
JAAR	Registratiejaar
KIND_MORBID1	Morbiditeit-Prematuur
KIND_MORBID2	Morbiditeit-Apgar < 7
KIND_MORBID3	Morbiditeit-SGA (Gew < P10)
KIND_MORBID4	Morbiditeit-Cong. afwijking
KIND_MORT	Kind overleden
LEVENSVTBR	Levensvatbaar?
LFT	Leeftijd moeder
LIGGING	Ligging
MATMORT	Moeder overleden
MC	Meerlingnummer
NICUopname	NICU opname
OMV	Omvang meerling
PAR	Pariteit
PEDIATER	Pediatrische betrokkenheid
PLTSECHT	Plaats bevalling
PROBL_BA1	Problemen bij baring-Meconium
PROBL_BA2	Problemen bij baring-Foetale nood
PROBL_BA3	Problemen bij baring-Langd gebr vliezen
PROBL_BA4	Problemen bij baring-Onvold vorderen
PROBL_IA1	Anamnese problemen-Abortus/miskraam
PROBL_IA2	Anamnese problemen-Eclampsie/HELLP/toxicose
PROBL_IA3	Anamnese problemen-Vroeggeboorte
PROBL_IA4	Anamnese problemen-Dysmaturiteit
PROBL_IA5	Anamnese problemen-Kunstverlossing
PROBL_IA6	Anamnese problemen-Sectio
PROBL_IA7	Anamnese problemen-HPP
PROBL_IA8	Anamnese problemen-MPV
PROBL_IA9	Anamnese problemen-Totaalruptuur

PROBL_IA10	Anamnese problemen-Problematisch kind
PROBL_ZW1	Zwangerschap problemen-Diabetes
PROBL_ZW2	Zwangerschap problemen-Hypertensie/toxicose
PROBL_ZW3	Zwangerschap problemen-(Pre-)eclampsie
PROBL_ZW4	Zwangerschap problemen-Neg. Dyscongruentie
PROBL_ZW5	Zwangerschap problemen-Pos. dyscongruentie
PROBL_ZW6	Zwangerschap problemen-Bloedverlies
PROBL_ZW7	Zwangerschap problemen-Vruchtwater verlies
PROBL_ZW10	Zwangerschap problemen-Dreigende vroeggeboorte
RESP_BB	Zorg begin baring
RESP_EB	Zorg einde baring
RESP_ZW	Zorg begin zwangerschap
RUPT	Ruptuur
SECTIO_I_A	Sectio in anamnese?
SES	SES
TELLING1	Telling-Zwangerschappen
TELLING2	Telling-Alle partus
TELLING3	Telling-1e kind v partus
TELLING4	Telling-Laatste kind
TELLING5	Telling-Alle kinderen
TELLING6	Telling-Alle casus
TYPEBARING	Type baring
URBAN	Urbanisatiegraad
N_APGAR_1	Apgar na 1 min
N_APGAR_5	Apgar na 5 min
N_ASFYXIE_VERDENKING_ONTSLAG	Asfyxie verdenking?
N_BEH1	Behandelingen
N_BEH2	Behandelingen
N_BEH3	Behandelingen
N_BEH4	Behandelingen
N_BEH5	Behandelingen
N_BEH6	Behandelingen
N_BEH7	Behandelingen
N_BEH8	Behandelingen
N_BEH9	Behandelingen
N_BEH10	Behandelingen
N_BEH11	Behandelingen

N_BEH12	Behandelingen
N_BEH13	Behandelingen
N_BEH14	Behandelingen
N_BEH15	Behandelingen
N_BEH16	Behandelingen
N_BEH17	Behandelingen
N_BEH18	Behandelingen
N_BEH19	Behandelingen
N_BEH20	Behandelingen
N_BEH21	Behandelingen
N_BEH22	Behandelingen
N_BEH23	Behandelingen
N_BEH24	Behandelingen
N_BEH25	Behandelingen
N_BEH26	Behandelingen
N_BEH27	Behandelingen
N_BEH28	Behandelingen
N_BEH29	Behandelingen
N_BEH30	Behandelingen
N_BLOEDGROEP_KIND	Bloedgroep kind
N_BLOEDGROEP_VROUW	Bloedgroep moeder
N_CGMA1	Cong. afw. (detail)
N_CGMA2	Cong. afw. (detail)
N_CGMA3	Cong. afw. (detail)
N_CGMA4	Cong. afw. (detail)
N_CGMA5	Cong. afw. (detail)
N_CGMA6	Cong. afw. (detail)
N_CGMA7	Cong. afw. (detail)
N_CGMA8	Cong. afw. (detail)
N_CGMA9	Cong. afw. (detail)
N_CGMA10	Cong. afw. (detail)
N_CGMA11	Cong. afw. (detail)
N_CGMA12	Cong. afw. (detail)
N_CGMA13	Cong. afw. (detail)
N_CGMA14	Cong. afw. (detail)
N_CGMA15	Cong. afw. (detail)
N_CGMA16	Cong. afw. (detail)

N_CGMA17	Cong. afw. (detail)
N_CGMA18	Cong. afw. (detail)
N_CGMA19	Cong. afw. (detail)
N_CGMA20	Cong. afw. (detail)
N_CPAPDG	dagen CPAP
N_DDBEGINZORG	Opname datum
N_DDEINDEZORG	Ontslag datum
N_DDMORT	Sterftedatum
N_DIAGD1	Spijsverteringskanaal stoornis
N_DIAGD2	Spijsverteringskanaal stoornis
N_DIAGD3	Spijsverteringskanaal stoornis
N_DIAGD4	Spijsverteringskanaal stoornis
N_DIAGD5	Spijsverteringskanaal stoornis
N_DIAGD6	Spijsverteringskanaal stoornis
N_DIAGR1	Respiratoire problemen
N_DIAGR2	Respiratoire problemen
N_DIAGR3	Respiratoire problemen
N_DIAGR4	Respiratoire problemen
N_DIAGR5	Respiratoire problemen
N_DIAGR6	Respiratoire problemen
N_DIAGC1	Circulatoire problemen
N_DIAGC2	Circulatoire problemen
N_DIAGC3	Circulatoire problemen
N_DIAGC4	Circulatoire problemen
N_DIAGC5	Circulatoire problemen
N_DIAGC6	Circulatoire problemen
N_DIAGZ1	Zenuw/zintuig stoornissen
N_DIAGZ2	Zenuw/zintuig stoornissen
N_DIAGZ3	Zenuw/zintuig stoornissen
N_DIAGZ4	Zenuw/zintuig stoornissen
N_DIAGZ5	Zenuw/zintuig stoornissen
N_DIAGZ6	Zenuw/zintuig stoornissen
N_DIAGG1	Geboortetrauma
N_DIAGG2	Geboortetrauma
N_DIAGG3	Geboortetrauma
N_DIAGG4	Geboortetrauma
N_DIAGG5	Geboortetrauma

N_DIAGG6	Geboortetrauma
N_DIAGA1	Diagnosen (detail)
N_DIAGA2	Diagnosen (detail)
N_DIAGA3	Diagnosen (detail)
N_DIAGA4	Diagnosen (detail)
N_DIAGA5	Diagnosen (detail)
N_DIAGA6	Diagnosen (detail)
N_DIAGA7	Diagnosen (detail)
N_DIAGA8	Diagnosen (detail)
N_DIAGA9	Diagnosen (detail)
N_DIAGA10	Diagnosen (detail)
N_DIAGA11	Diagnosen (detail)
N_DIAGA12	Diagnosen (detail)
N_DIAGA13	Diagnosen (detail)
N_DIAGA14	Diagnosen (detail)
N_DIAGA15	Diagnosen (detail)
N_DIAGA16	Diagnosen (detail)
N_DIAGA17	Diagnosen (detail)
N_DIAGA18	Diagnosen (detail)
N_DIAGA19	Diagnosen (detail)
N_DIAGA20	Diagnosen (detail)
N_DIAGA21	Diagnosen (detail)
N_DIAGA22	Diagnosen (detail)
N_DIAGA23	Diagnosen (detail)
N_DIAGA24	Diagnosen (detail)
N_DIAGA25	Diagnosen (detail)
N_DIAGA26	Diagnosen (detail)
N_DIAGA27	Diagnosen (detail)
N_DIAGA28	Diagnosen (detail)
N_DIAGA29	Diagnosen (detail)
N_DIAGA30	Diagnosen (detail)
N_DIAGH1	Hematologische stoornissen
N_DIAGH2	Hematologische stoornissen
N_DIAGH3	Hematologische stoornissen
N_DIAGH4	Hematologische stoornissen
N_DIAGH5	Hematologische stoornissen
N_DIAGH6	Hematologische stoornissen

N_DIAGI1	Infecties
N_DIAGI2	Infecties
N_DIAGI3	Infecties
N_DIAGI4	Infecties
N_DIAGI5	Infecties
N_DIAGI6	Infecties
N_DIAGI7	Infecties
N_DIAGI8	Infecties
N_DIAGI9	Infecties
N_DIAGI10	Infecties
N_DIAG1	Diagnosen (overview)
N_DIAG2	Diagnosen (overview)
N_DIAG3	Diagnosen (overview)
N_DIAG4	Diagnosen (overview)
N_DIAG5	Diagnosen (overview)
N_DIAG6	Diagnosen (overview)
N_DIAG7	Diagnosen (overview)
N_DIAG8	Diagnosen (overview)
N_DIAGM1	Metabolische stoornissen
N_DIAGM2	Metabolische stoornissen
N_DIAGM3	Metabolische stoornissen
N_DIAGM4	Metabolische stoornissen
N_DIAGM5	Metabolische stoornissen
N_DIAGM6	Metabolische stoornissen
N_HCDG	dagen HC
N_ICDG	dagen IC
N_ICHCDG	dagen post ICHC
N_IND_SECTIO_A	Indicatie sectio-Niet vorderende ontsluiting
N_IND_SECTIO_B	Indicatie sectio-Niet vorderende uitdrijving
N_IND_SECTIO_C	Indicatie sectio-Levensgevaar kind
N_IND_SECTIO_D	Indicatie sectio-Levensgevaar moeder
N_IND_SECTIO_E	Indicatie sectio-Overig, medische reden
N_IND_SECTIO_F	Indicatie sectio-Overig, niet-medische reden
N_IND_SECTIO_Z	Indicatie sectio-Onbekend
N_LENGTE	Lengte bij geboorte
N_MORT	Kind overleden?
N_MORT_VRL_OORZAAK1	Doodsoorzaak

N_MORT_VRL_OORZAAK2	Doodsoorzaak
N_MORT_VRL_OORZAAK3	Doodsoorzaak
N_OPNAME_IND_A	Opname indicaties-Zwangerschapsduur
N_OPNAME_IND_B	Opname indicaties-Geboortegewicht
N_OPNAME_IND_C	Opname indicaties-Problemen partus
N_OPNAME_IND_D	Opname indicaties-Kunstverlossing
N_OPNAME_IND_E	Opname indicaties-Liggingsafwijking
N_OPNAME_IND_F	Opname indicaties-Langdurig gebroken vliezen
N_OPNAME_IND_H	Opname indicaties-Klinische conditie kind
N_OPNAME_IND_I	Opname indicaties-Meconiumhoudend vruchtwater
N_OPNAME_IND_J	Opname indicaties-Icterus neonatorum
N_OPNAME_IND_K	Opname indicaties-Voedingsproblemen
N_OPNAME_IND_L	Opname indicaties-Infectieverdenking
N_OPNAME_IND_M	Opname indicaties-Verdenking op hartafwijking
N_OPNAME_IND_N	Opname indicaties-Overige klinische condities
N_OPNAME_IND_O	Opname indicaties-Overige indicaties
N_OPNAME_IND_P	Opname indicaties-Maternale medicatie of maternale anamnese
N_OPNAME_IND_Z	Opname indicaties-Onbekend
N_OPNDUUR	Opnameduur (dg)
N_PA_AANMELDING	PA aanmelding
N_PHAUMBILICALIS	pH bepaald?
N_PH_WAARDE	pH waarde
N_TYPE_DRUGS_ZWSCHAP_1	Drugsgebruik-Cannabis/marihuana
N_TYPE_DRUGS_ZWSCHAP_2	Drugsgebruik-Cocaine
N_TYPE_DRUGS_ZWSCHAP_3	Drugsgebruik-Crack/Base coke
N_TYPE_DRUGS_ZWSCHAP_4	Drugsgebruik-XTC
N_TYPE_DRUGS_ZWSCHAP_5	Drugsgebruik-Amfetamine/speed
N_TYPE_DRUGS_ZWSCHAP_6	Drugsgebruik-Heroine
N_TYPE_DRUGS_ZWSCHAP_7	Drugsgebruik-Methadon
N_TYPE_DRUGS_ZWSCHAP_8	Drugsgebruik-GHB
N_TYPE_DRUGS_ZWSCHAP_9	Drugsgebruik-Poppers
N_TYPE_DRUGS_ZWSCHAP_10	Drugsgebruik-LSD
N_TYPE_DRUGS_ZWSCHAP_11	Drugsgebruik-Paddo's/ecodrugs
N_TYPE_DRUGS_ZWSCHAP_98	Drugsgebruik-Overige
g_AANTKIND	Aantal kinderen bij deze partus
g_ABO	Aantal abortus/EUG/mola
N_REDOVPL	Reden overpl naar NICU

g_BIJZONDER1	Bijzonderheden
g_BIJZONDER2	Bijzonderheden
g_BIJZONDER3	Bijzonderheden
g_BIJZONDER4	Bijzonderheden
g_BIJZONDER5	Bijzonderheden
g_BIJZONDER6	Bijzonderheden
g_BIJZONDER7	Bijzonderheden
g_BIJZONDER8	Bijzonderheden
g_BIJZONDER9	Bijzonderheden
g_BIJZONDER10	Bijzonderheden
g_GESL	Geslacht
g_GVLCAT	Categorie duur gebroken vliezen
g_HER	Type vrouw
g_HLP1	Hulp bij de baring
g_HLP2	Hulp bij de baring
g_INDBEG	Indicatie inleiding/primaire sectio
g_INDHLP	Indicatie hulp/secundaire sectio
g_INTBEG	Interventies begin baring
g_INTEIND	Interventies einde baring
g_IUVD1	IUV bij 1e onderzoek
g_NAGEB1	Nageboortetijdperk
g_NAGEB2	Nageboortetijdperk
g_NAGEB_	Nageboorte behandeling
g_PERI1	Perineum/Ruptuur
g_PERI2	Perineum/Ruptuur
g_PIJN1	Pijnbestrijding
g_PIJN2	Pijnbestrijding
g_PROT	Proteinurie
g_PROT_MG	Aantal mg/l proteinurie
g_REDOV1	Reden overname
g_REDOV2	Reden overname
g_REDOV3	Reden overname
g_REDOV4	Reden overname
g_STIMUL_BARING	Bijstimulatie
g_TEN	Hoogste diastolische tensie
g_UITCAT	Categorie uitdrijvingsduur
g_UUPERS	Begin aktief meepersen (u)

g_VERVOLG	LVR2 vervolgrecords
g_VERBLMOE	Verblijfsduur moeder pp
v_ABO	Aantal abortus
v_ABORTUS	Abortus deze zwschap
g_ZEK	Zekerheid a terme datum
v_BIJZ1	Bijzonderheden
v_BIJZ2	Bijzonderheden
v_BIJZ3	Bijzonderheden
v_CONSKA	Consult kinderarts
v_HER_	Herkomst moeder
v_JAAR	Registratiejaar
v_LCONSGYN	Laatste consult gyn
v_LYN2RED1	Reden zorg 2e lijn
v_LYN2RED2	Reden zorg 2e lijn
v_MEDICPP	Medicatie na geb kind
v_MORT1_	Kind overleden 1e lijn
v_MORT2_	Kind overleden 2e lijn
v_OND1	Onderzoek/verrichting
v_OND2	Onderzoek/verrichting
v_OND3	Onderzoek/verrichting
v_PERI1	Perineum/vulva
v_PERI2	Perineum/vulva
v_PERI3	Perineum/vulva
v_PLTSPLAN	Geplande plaats bevalling
v_PROBK1	Problemen kind
v_PROBK2	Problemen kind
v_PROBK3	Problemen kind
v_PROBMOE1	Problemen moeder
v_PROBMOE2	Problemen moeder
v_PROBMOE3	Problemen moeder
v_REDCON1	Reden consult gyn
v_REDCON2	Reden consult gyn
v_REDCON3	Reden consult gyn
v_REDCONKA	Reden consult kinderarts
v_REDOVD1	Reden overdracht/einde
v_REDOVD2	Reden overdracht/einde
v_REDOVD3	Reden overdracht/einde

v_REDOVDKA	Reden overdr kinderarts
v_REDOVLG	Reden overleg
v_UITDR	Uitdrijvingsduur
v_UUPERS	Uur begin meepersen
v_UUVLIES	Uur breken vliezen
v_VERVOLG	LVR1 vervolgrecords
v_VRWAT	Kleur vruchtwater

11D: Search Results

Table 11.S4: Search results from PALGA and Perined

	PALGA	Perined
Total number of patients extracted from PALGA search	36,168	5,156,730
Able to be linked using national statistics bureau (CBS)	19,252	4,097,353
Obstetric Outcomes available in Perined		7,925

Table 11.S5 PALGA Registry Characteristics of Patients Diagnosed with Adenomyosis after Hysterectomy from 1995-2018

	Total Number of Adenomyosis Patients (n=36,168)	**Adenomyosis Patients with Obstetric Outcomes** (n=7,925)	**p-value***
Age at Hysterectomy (in years, Mean, (SD))	43.66 (4·60)	42.42 (4·86)	P= 0·001
Year of hysterectomy (year, Median, IQR)	2006 (IQR 12)	2014 (IQR 5)	P <0·001
Time between registered pregnancy and hysterectomy (In years, Mean (SD))	n/a	13.22 (4·99) Within 5 years of pregnancy: 1,396 (16·0%)	n/a

*P-value calculated using Chi^2 analysis for dichotomous outcomes, Independent T-test for normally distributed continuous variables and Mann-Whitney U test for abnormally distributed continuous variables.

11E. Univariate Logistic Regression Analysis

Table 11.S6: Odds Ratio for Adverse Obstetric Outcomes for Adenomyosis Patients versus General Population

Outcome	OR (95% CI)
Miscarriage	OR 1.22 (1.166 – 1.283)
Prematurity	OR 0.658 (95% 0.613-0.706)
Small for Gestational Age	OR: 1.32 (95% CI 1.23-1.40)
Hypertensive Disorders of Pregnancy	OR: 1.73 (95% CI 1.61 – 1.86)
Postpartum Haemorrhage	OR 1.058 (95% 0.971 – 1.152)
Placental Issues (Composite)	OR 1.144 (1.1016 – 1.287)
Placenta Praevia	OR 1.335 (95% CI 0.894-1.993)
Placental Abruption	OR 1.565 (95% CI 0.957-2.557)
Placental Retention	OR 1,102 (95% CI 0.971-1.251)
Emergency CS	OR 1.670 (95% CI 1.559-1.788)
Neonatal Death	OR 1.161 (95% CI 0.851-1.585)
Intra-Uterine Foetal Death	OR 0.749 (95% CI 0.587-0.956)
Low Apgar (<7 at 5min)	OR 1.001 (95% 0.863-1.162)
NICU admission	OR 0.938 (95% CI 0.884-0.996)
Threatened Prematurity	OR 1.837 (95% CI 1.658-2.035)
Foetal Distress	OR 1.219 (95% CI 1.131-1.313)
Non-vertex Lie	OR 1.420 (95% CI 1.337-1.509)
Hyperemesis Gravidarum	OR 2.055 (95% OR 1.560-2.708)
Pain Relief during Labour	OR 1.136 (95% CI 1.080-1.195)
Failure to progress	OR 1.540 (1.460-1.623)
Endometritis:	OR 2.479 (95% CI 1.492-4.119)
Caesarean Section	OR 1.564 (95% CI 1.479-1.653)

11F: Multivariate Regression Analysis

Table 11.S7. Outcomes of multivariate regression analysis:

MULTIVARIATE LOGISTIC REGRESSION ANALYSIS	
Miscarriage	OR 1.525 (95% 1.440-1.616)
Prematurity	OR 0.761 (95% CI 0.692-0.836)
Small for Gestational Age	OR 1.15 (95% CI 1.067-1.248)
Hypertensive Disorders of Pregnancy	OR 1.370 (95% CI 1.25-1.498)
Placental Issues (Composite)	OR 1.350 (95% CI 1.176-1.550)
Placenta Praevia	OR 2.129 (95% CI 1.355 - 3.344)
Placental Abruption	OR 1.341 (95% CI 0.777-2.314)
Placental Retention	OR 1.278 (95% CI 1.101 -1.484)
Threatened Prematurity	OR 1.597 (95% CI 1.427 – 1.787)
Emergency CS	OR 1.538 (95% CI 1.410 – 1.679)
Foetal Distress	OR 1.126 (95% CI 1.029-1.232)
Non-vertex Lie	OR 1.367 (95% CI 1.270-1.473)
Hyperemesis Gravidarum	OR 2.071 (95% CI 1.521-2.820)
Pain Relief during Labour	OR 1.381 (95% CI 1.295-1.473)
Failure to progress	OR 1.156 (95% CI 1.084-1.233)
Failure to progress in first stage of labour	OR 0.972 (95% CI 0.864 – 1.094)
Failure to progress in second stage of labour	OR 1.242 (95% CI 1.124 – 1.373)
Oxytocin Stimulation	OR 1.040 (95% CI 0.947 – 1.143)
Endometritis	OR 1.696 (95% CI 1.020-2.820)
Caesarean Section	OR 1.725 (95% CI 1.606 – 1.853)
Postpartum Haemorrhage	OR 1.232 (95% CI 1.098-1.383)

Instrumental delivery	OR 0.994 (95% CI 0.848-1.165)
Prolonged rupture of membranes	OR 1.355 (95% CI 1.238-1.483)
PPROM	OR 1.411 (95% CI 1.161-1.716)
Preeclampsia	OR 1.373 (95% CI 1.248-1.510)
HELLP	OR 0.991 (95% CI 0.662-1.484)
PIH	OR 1.378 (95% CI 1.258-1.509)

Corrected for: Parity, Age, Year of Birth, Multiple gestation, Induction of Labour, Low-income area, Ethnicity, Gestational Diabetes, History of Hypertensive disorder

OR: Odds ratio; CS: caesarean section; PPROM: Preterm premature rupture of membranes; PIH: pregnancy induced hypertension

11G: STROBE Checklist

STROBE Statement—Checklist of items that should be included in reports of ***cohort studies***

	Item No	Recommendation	Page Number
Title and abstract	1	(*a*) Indicate the study's design with a commonly used term in the title or the abstract	1
		(*b*) Provide in the abstract an informative and balanced summary of what was done and what was found	2
Introduction			
Background/rationale	2	Explain the scientific background and rationale for the investigation being reported	3
Objectives	3	State specific objectives, including any prespecified hypotheses	3, 4
Methods			
Study design	4	Present key elements of study design early in the paper	4
Setting	5	Describe the setting, locations, and relevant dates, including periods of recruitment, exposure, follow-up, and data collection	4
Participants	6	(*a*) Give the eligibility criteria, and the sources and methods of selection of participants. Describe methods of follow-up	4
		(*b*) For matched studies, give matching criteria and number of exposed and unexposed	
Variables	7	Clearly define all outcomes, exposures, predictors, potential confounders, and effect modifiers. Give diagnostic criteria, if applicable	4, Appendix
Data sources/ measurement	8*	For each variable of interest, give sources of data and details of methods of assessment (measurement). Describe comparability of assessment methods if there is more than one group	4, 5
Bias	9	Describe any efforts to address potential sources of bias	-
Study size	10	Explain how the study size was arrived at	4
Quantitative variables	11	Explain how quantitative variables were handled in the analyses. If applicable, describe which groupings were chosen and why	5
Statistical methods	12	(*a*) Describe all statistical methods, including those used to control for confounding	5
		(*b*) Describe any methods used to examine subgroups and interactions	-
		(c) Explain how missing data were addressed	-
		(*d*) If applicable, explain how loss to follow-up was addressed	-
		(e) Describe any sensitivity analyses	-

Results			
Participants	13*	(a) Report numbers of individuals at each stage of study—eg numbers potentially eligible, examined for eligibility, confirmed eligible, included in the study, completing follow-up, and analysed	5, 6
		(b) Give reasons for non-participation at each stage	5
		(c) Consider use of a flow diagram	6
Descriptive data	14*	(a) Give characteristics of study participants (eg demographic, clinical, social) and information on exposures and potential confounders	5, 6
		(b) Indicate number of participants with missing data for each variable of interest	-
		(c) Summarise follow-up time (eg, average and total amount)	-
Outcome data	15*	Report numbers of outcome events or summary measures over time	7-13
Main results	16	(a) Give unadjusted estimates and, if applicable, confounder-adjusted estimates and their precision (eg, 95% confidence interval). Make clear which confounders were adjusted for and why they were included	7-13
		(b) Report category boundaries when continuous variables were categorized	5, 7-13
		(c) If relevant, consider translating estimates of relative risk into absolute risk for a meaningful time period	-
Other analyses	17	Report other analyses done—eg analyses of subgroups and interactions, and sensitivity analyses	-
Discussion			
Key results	18	Summarise key results with reference to study objectives	15
Limitations	19	Discuss limitations of the study, taking into account sources of potential bias or imprecision. Discuss both direction and magnitude of any potential bias	15, 16
Interpretation	20	Give a cautious overall interpretation of results considering objectives, limitations, multiplicity of analyses, results from similar studies, and other relevant evidence	16
Generalisability	21	Discuss the generalisability (external validity) of the study results	16
Other information			
Funding	22	Give the source of funding and the role of the funders for the present study and, if applicable, for the original study on which the present article is based	1